THERAPEUTIC DRUG MONITORING AND CLINICAL TOXICOLOGY OF ANTI-CANCER DRUGS

EDITED BY: Miao Yan, Yao Liu and Jennifer Martin

PUBLISHED IN: Frontiers in Oncology and Frontiers in Pharmacology

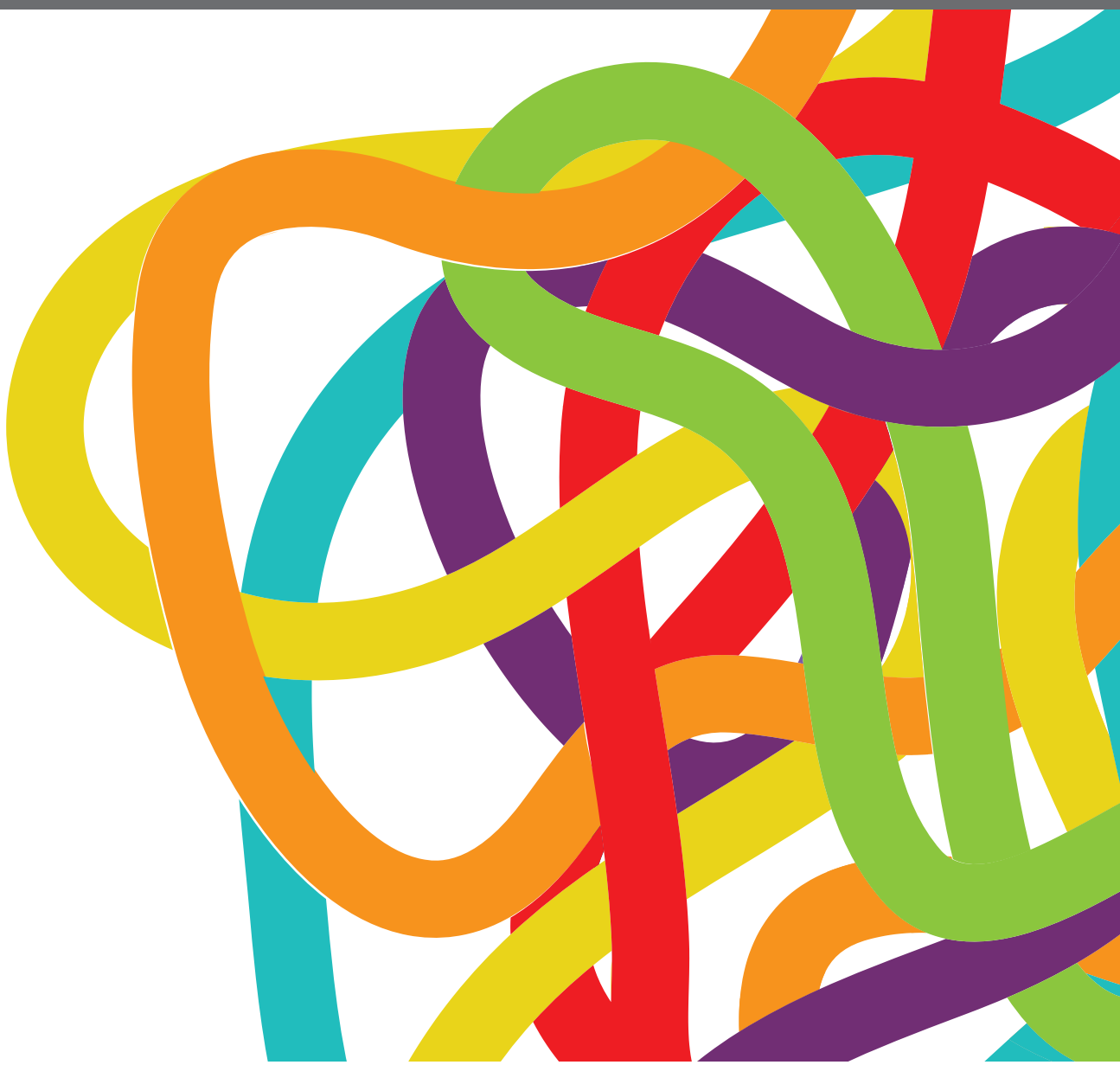

frontiers Research Topics

ISSN 1664-8714
ISBN 978-2-83250-108-5
DOI 10.3389/978-2-83250-108-5

About Frontiers

Frontiers is more than just an open-access publisher of scholarly articles: it is a pioneering approach to the world of academia, radically improving the way scholarly research is managed. The grand vision of Frontiers is a world where all people have an equal opportunity to seek, share and generate knowledge. Frontiers provides immediate and permanent online open access to all its publications, but this alone is not enough to realize our grand goals.

Frontiers Journal Series

The Frontiers Journal Series is a multi-tier and interdisciplinary set of open-access, online journals, promising a paradigm shift from the current review, selection and dissemination processes in academic publishing. All Frontiers journals are driven by researchers for researchers; therefore, they constitute a service to the scholarly community. At the same time, the Frontiers Journal Series operates on a revolutionary invention, the tiered publishing system, initially addressing specific communities of scholars, and gradually climbing up to broader public understanding, thus serving the interests of the lay society, too.

Dedication to Quality

Each Frontiers article is a landmark of the highest quality, thanks to genuinely collaborative interactions between authors and review editors, who include some of the world's best academicians. Research must be certified by peers before entering a stream of knowledge that may eventually reach the public - and shape society; therefore, Frontiers only applies the most rigorous and unbiased reviews.
Frontiers revolutionizes research publishing by freely delivering the most outstanding research, evaluated with no bias from both the academic and social point of view. By applying the most advanced information technologies, Frontiers is catapulting scholarly publishing into a new generation.

What are Frontiers Research Topics?

Frontiers Research Topics are very popular trademarks of the Frontiers Journals Series: they are collections of at least ten articles, all centered on a particular subject. With their unique mix of varied contributions from Original Research to Review Articles, Frontiers Research Topics unify the most influential researchers, the latest key findings and historical advances in a hot research area! Find out more on how to host your own Frontiers Research Topic or contribute to one as an author by contacting the Frontiers Editorial Office: frontiersin.org/about/contact

THERAPEUTIC DRUG MONITORING AND CLINICAL TOXICOLOGY OF ANTI-CANCER DRUGS

Topic Editors:
Miao Yan, Central South University, China
Yao Liu, Daping Hospital, China
Jennifer Martin, The University of Newcastle, Australia

Citation: Yan, M., Liu, Y., Martin, J., eds. (2022). Therapeutic Drug Monitoring and Clinical Toxicology of Anti-Cancer Drugs. Lausanne: Frontiers Media SA. doi: 10.3389/978-2-83250-108-5

Table of Contents

frontiers | Frontiers in Oncology

TYPE Editorial
PUBLISHED 25 October 2022
DOI 10.3389/fonc.2022.1053211

OPEN ACCESS

EDITED AND REVIEWED BY
Olivier Feron,
Université catholique de Louvain,
Belgium

*CORRESPONDENCE
Miao Yan
yanmiao@csu.edu.cn

SPECIALTY SECTION
This article was submitted to Pharmacology of Anti-Cancer Drugs, a section of the journal Frontiers in Oncology

RECEIVED 25 September 2022
ACCEPTED 03 October 2022
PUBLISHED 25 October 2022

CITATION
Liu Y, Martin JH and Yan M (2022) Editorial: Therapeutic drug monitoring and clinical toxicology of anti-cancer drugs.
Front. Oncol. 12:1053211.
doi: 10.3389/fonc.2022.1053211

Editorial: Therapeutic drug monitoring and clinical toxicology of anti-cancer drugs

Yao Liu[1], Jennifer H. Martin[2] and Miao Yan[3,4,5]*

[1]Department of Pharmacy, Daping Hospital of Army Medical University, ChongQing, China, [2]School of Medicine and Public Health, University of Newcastle, Newcastle, NSW, Australia, [3]Department of Pharmacy, the Second Xiangya Hospital of Central South University, ChangSha, Hunan, China, [4]Hunan Provincial Center for Poison Information and Treatment, ChangSha, Hunan, China, [5]International Research Center for Precision Medicine, Transformative Technology and Software Services, Hunan, China

KEYWORDS

therapeutic drug monitoring, clinical toxicology, anti-cancer drugs, editorial, precision medicine

Editorial on the Research Topic
Therapeutic drug monitoring and clinical toxicology of anti-cancer drugs

Introduction

Cancer incidence in China is currently the highest in the world, and the demand for antineoplastic drugs is thus also growing. In the context of precision medicine and precision pharmaceutical services, anti-tumor drugs have transitioned from traditional chemotherapy drugs to combined use with molecular targeted drugs and immunosuppressants. Many of these have come into clinical practice rapidly, with recommendations to use a single dose despite significant inter-individual variability in achieved exposure between patients.

In addition, most of these antineoplastic drugs have the characteristics of a narrow therapeutic window, large individual differences in drug metabolism, nonlinear pharmacokinetic characteristics and obvious organ toxicity particularly when exposure is above recommended target exposure ranges. Further, in order to achieve personalized medicine and precision medicine, factors such as the patient's genes, enzymes, diseases, drug sensitivity to tumors, multi-drug combinations and patient characteristics need to be considered. (1–3). Therefore, along with research into cancer biology and into the effects of these agents in different cancer genotypes or phenotypes, studies on therapeutic drug monitoring (TDM) and population pharmacokinetics (PPK)/pharmacodynamics (PD) for anti-cancer drugs play a crucial part in the optimization of antineoplastic regimens and precise drug treatment. These tools can minimize drug-induced toxicity and maximize the treatment outcome. In addition, although antitumor drugs have changed from conventional chemotherapeutic drugs with low selectivity and high toxicity to molecular targeted drugs

with high selectivity and low toxicity, the related adverse events (AEs) involving vital organs, such as related cardiotoxicity, endocrine, gut and liver toxicity, cause significant morbidity and sometimes death (4–7). The in-depth toxicological research of these newer therapies in the clinical setting is vital to better understand the factors contributing to toxic effects and provide guidance for improved drug use.

In this special issue, 24 manuscripts, including nine review articles and fifteen original research articles providing a wide discussion of TDM and clinical toxicology of antineoplastic agents in different clinical settings. This special issue thus aims to both provide guidance on more individualized drug administration plans for treatment using TDM and PPK/PD research and to understand the potential mechanism of antitumor drugs therapeutic and toxic side effects.

Firstly, there were some articles and reviews that explored and provided an update on research progress of PPK, PD and TDM in the response and toxicity of anti-tumor drugs. Wen et al. systematically reviewed the recent progress of PK-PD modeling in predicting cardiovascular adverse reactions and how to manage this in the clinical setting. He et al. summarized the existing evidence of the clinical PK variation of dasatinib concentration-response relationships and advice on development of methods for individualizing the dosage of administration. In addition, Barnett et al. provided a summary of current research using TDM in pediatric cancer and implementing TDM-based dosing recommendations. And Huang et al. built a new PK model of busulfan (BU) providing guidance for patients of Chinese descent to achieve individualized and optimal dosage regimens.

Then, plasma obtained by conventional venous blood sampling is usually standard matrix for TDM of antineoplastic drugs, with LC-MS/MS the conventional method of choice for measuring TDM. As an update, to measure 6-thioguanine and 6-methylmercaptopurine in red blood cells, Bajaj et al. used a LC-MS/MS method, evaluating the association between TM concentrations, thiopurine-S-methyltransferase (TPMT) phenotype and genotype testing. This provided a new approach for thiopurine TDM to minimize myelosuppression and the risk of hepatotoxicity. In addition, Guo et al. used HPLC-HG-AFS to analyze the concentrations of inorganic arsenic, methyl methacrylate (MMA) and nitrosodimethylamine (DMA) and used this to discuss features of intrauterine arsenic concentration, the permeability of the placenta to arsenic trioxide (ATO) and its metabolites and provided the first risk evaluation of ATO in pregnant women with acute promyelocytic leukemia. Verougstraete et al. summarized various analysis measuring methods of kinase inhibitors based on emerging dried blood microsample technique, which is minimally invasive and considered convenient and simple.

Third, there are also several systematic reviews and meta-analysis highlighting the toxicity and response of antineoplastic drugs. Zhang et al. identified the effectiveness and risk of adding capecitabine to the chemotherapy for triple negative breast cancer through a meta-analysis. Song et al. and Zhang et al. conducted both systematic review and meta-analysis to analyse the effects of genetic polymorphisms on the toxicity and response of high-dose methotrexate (HD-MTX) and response in tumor. In addition, Yang et al. conducted a pharmacovigilance study showing enfortumab vedotin (EV) was associated with severe skin toxicities. Meanwhile, based on the information from Henan Province's spontaneous reporting system database, Jiao et al. analyzed potential organ toxicities in Chinese pediatric subjects, an area with a previous dearth of data. What's more, Zhao et al. showed PARP inhibitors may induce myelodysplastic syndrome (MDS) and acute myeloid leukemia (AML), with some at higher risk than others. Yu et al. ***via*** a post-marketing surveillance research evaluated the risk of oxaliplatin (OXA) in 3687 Chinese cancer patients. Zhu et al. found SOAT1 can be a prospective prognostic indicator in gastric cancer and may help the clinical dosing regimen.

Besides, He et al. attempted to build a risk scoring model based on gene polymorphisms to predict adverse drug reactions caused by HD-MTX in children (age ≤ 16 years) especially hepatotoxicity based on various relevant indicators. This model informed the MTX regimen and using it reduced toxicity. Han et al. used retrospective and multicenter clinical data to establish a risk scoring system through machine learning methods for predicting liver injury with tyrosine kinase inhibitors. In general, by measuring drug exposure, pharmacological indexes or pharmacodynamic indicators in tumor patients, using technologies such as PPK, PD, TDM and databases to achieve individualized drug treatment these studies have provided individualized dosing regimens.

Meanwhile, in our special issue, 5 manuscripts described and summarized the potential molecular regulatory mechanisms of anti-tumor drugs to exert therapeutic effects and produce toxic side effects. Li et al. detailed the molecular pathways of kinase inhibitors induced EGFR-skin toxicity, strategies to attenuate severe skin toxicity, and provided information to manage such skin reactions. Yang et al. systematically reviewed the probable mechanisms, clinical features, diagnostic method, intervention measures and the most recent advancements in cardiotoxicity of ErbB2-targeting drugs, providing guidance for clinical practice. Han et al reviewed the current epidemiology, risk indicators, molecular regulation mechanisms, prevention and management of irinotecan-induced steatohepatitis, and Guo et al. showed that the kinase inhibitors crizotinib and sunitinib induced hepatotoxicity *via* oxidative stress and mitochondrial apoptosis pathways, suggesting Nrf2 might be a therapeutic target. Du et al. found that the inhibition of PRR could attenuate RAC1-NOX4 pathway and reduce ROS accumulation to weaken doxorubicin-induced heart failure, thus providing a prospective approach to the management of DOX-triggered heart failure. In general, these studies above have indicated the research actuality of anti-tumor drug-induced diseases and potential molecular regulatory mechanisms of toxicity.

Finally, in our special issue, there were also two manuscripts that explored risk management and effectiveness of PD-1/PD-L1

inhibitors. A case report (Tu et al.) showed that the use of avatrombopag in two cases of anti-PD-1 antibody-caused acquired megakaryocytic thrombocytopenia was successful, proposing a promising therapeutic option for this disease. Zhang et al. comprehensively summarized the molecular regulatory mechanisms of immune-related adverse events, the risk and therapeutic effect of PD-1/PD-L1 inhibitors administration in AID subjects, the prevention and control of organ toxicity and provides several promising treatment methods.

Taken together, this Research Topic contributes an update of the current clinical research into TDM and clinical toxicology of antineoplastic drugs to improve use of anti-tumor therapy, guiding clinical dose adjustment, and promoting the development of precision medicine.

Author contributions

All authors listed have made a substantial, direct and intellectual contribution to the work, and approved it for publication.

Funding

MY is supported by the National Natural Science Foundation of China, grant number 81974532 and 81803830, the Natural Science Foundation of Hunan Province, China, grant number 2020JJ4130.

Acknowledgments

We wish to thank all the authors contributing to this Frontiers Research Topic and all the reviewers and invited editors who have helped to make it solid.

Conflict of interest

The authors declare that the research was conducted in the absence of any commercial or financial relationships that could be construed as a potential conflict of interest.

Publisher's note

References

1. Gao B, Yeap S, Clements A, Balakrishnar B, Wong M, Gurney H. Evidence for therapeutic drug monitoring of targeted anticancer therapies. *J Clin Oncol* (2012) 30(32):4017–25. doi: 10.1200/JCO.2012.43.5362

2. Groenland SL, Verheijen RB, Joerger M, Mathijssen RHJ, Sparreboom A, Beijnen JH, et al. Precision dosing of targeted therapies is ready for prime time. *Clin Cancer Res* (2021) 27(24):6644–52. doi: 10.1158/1078-0432.CCR-20-4555

3. Widmer N, Bardin C, Chatelut E, Paci A, Beijnen J, Levêque D, et al. Review of therapeutic drug monitoring of anticancer drugs part two–targeted therapies. *Eur J Cancer* (2014) 50(12):2020–36. doi: 10.1016/j.ejca.2014.04.015

4. Di MM, Basch E, Bryce J, Perrone F. Patient-reported outcomes in the evaluation of toxicity of anticancer treatments. *Nat Rev Clin Oncol* (2016) 13 (5):319–25. doi: 10.1038/nrclinonc.2015.222

5. Porta C, Cosmai L, Gallieni M, Pedrazzoli P, Malberti F. Renal effects of targeted anticancer therapies. *Nat Rev Nephrol* (2015) 11(6):354–70. doi: 10.1038/nrneph.2015.15

6. Peeraphatdit TB, Wang J, Odenwald MA, Hu S, Hart J, Charlton MR. Hepatotoxicity from immune checkpoint inhibitors: A systematic review and management recommendation. *Hepatology* (2020) 72(1):315–29. doi: 10.1002/hep.31227

7. Scott JM, Nilsen TS, Gupta D, Jones LW. Exercise therapy and cardiovascular toxicity in cancer. *Circulation* (2018) 137(11):1176–91. doi: 10.1161/CIRCULATIONAHA.117.024671

frontiers in Pharmacology

ORIGINAL RESEARCH
published: 29 September 2021
doi: 10.3389/fphar.2021.726229

A Risk Scoring Model for High-Dose Methotrexate-Induced Liver Injury in Children With Acute Lymphoblastic Leukemia Based on Gene Polymorphism Study

Xia He[1,2†], Pingli Yao[3†], Mengting Li[1,2], Hong Liang[1,2], Yilong Liu[2], Shan Du[1,2], Min Zhang[4], Wenzhuo Sun[5], Zeyuan Wang[6], Xin Hao[7], Ze Yu[6], Fei Gao[6], Xinxia Liu[1,2] and Rongsheng Tong[1,2]**

[1]Department of Pharmacy, Sichuan Academy of Medical Sciences and Sichuan Provincial People's Hospital, Chengdu, China, [2]Personalized Drug Therapy Key Laboratory of Sichuan Province, School of Medicine, University of Electronic Science and Technology of China, Chengdu, China, [3]Ya'an Polytechnic College, Ya'an, China, [4]Hospital of Chengdu University of Traditional Chinese Medicine, Chengdu, China, [5]Xi'an Jiaotong-liverpool University, Xi'an, China, [6]Beijing Medicinovo Technology Co. Ltd., Beijing, China, [7]Dalian Medicinovo Technology Co. Ltd., Dalian, China

OPEN ACCESS

Edited by:
Miao Yan,
Central South University, China

Reviewed by:
Sandeep Kumar Yadav,
University of Texas MD Anderson Cancer Center, United States
Lei Cui,
Beijing Children's Hospital, Capital Medical University, China

***Correspondence:**
Rongsheng Tong
2207132448@qq.com
Xinxia Liu
cupflysea@163.com

[†]These authors have contributed equally to this work

Specialty section:
This article was submitted to Pharmacology of Anti-Cancer Drugs, a section of the journal Frontiers in Pharmacology

Received: 16 June 2021
Accepted: 23 August 2021
Published: 29 September 2021

Citation:
He X, Yao P, Li M, Liang H, Liu Y, Du S, Zhang M, Sun W, Wang Z, Hao X, Yu Z, Gao F, Liu X and Tong R (2021) A Risk Scoring Model for High-Dose Methotrexate-Induced Liver Injury in Children With Acute Lymphoblastic Leukemia Based on Gene Polymorphism Study. Front. Pharmacol. 12:726229. doi: 10.3389/fphar.2021.726229

A study on 70 acute lymphoblastic leukemia (ALL) children (age ≤16 years) treated with high-dose methotrexate (HD-MTX) in Sichuan Provincial People's Hospital was conducted. The aim of the study was to establish a risk-scoring model to predict HD-MTX-induced liver injury, considering gene polymorphisms' effects. Data screening was performed through *t*-test, chi-square test, and ridge regression, and six predictors were identified: age, *MTRR_AA, MTRR_AG, SLCO1B1_11045879_CC*, albumin_1 day before MTX administration, and IBIL_1 day before MTX administration ($p < 0.1$). Then, the risk-scoring model was established by ridge regression and evaluated the prediction performance. In a training cohort ($n = 49$), the area under the curve (AUC) was 0.76, and metrics including accuracy, precision, sensitivity, specificity, positive predictive value, and negative predictive value were promising (0.86, 0.81, 0.76, 0.91, 0.81, 0.88, respectively). In a test cohort ($n = 21$), the AUC was 0.62 and negative predictive value was 0.80; other evaluation metrics were not satisfactory, possibly due to the limited sample size. Ultimately, the risk scores were stratified into three groups based on their distributions: low- (≤48), medium- (49–89), and high-risk (>89) groups. This study could provide knowledge for the prediction of HD-MTX-induced liver injury and reference for the clinical medication.

Keywords: acute lymphoblastic leukemia, high-dose methotrexate, liver injury, gene polymorphism, ridge regression model, children

INTRODUCTION

Acute lymphoblastic leukemia (ALL) is a malignancy with high incidence in children aged between 1 and 5 years, which needs a long course of treatment (Preethi, 2014). In China, about 12,000 children aged below 16 are newly diagnosed with acute leukemia annually (Tang et al., 2008). Fortunately, due to the development of new drugs and precise chemotherapy, the outcome of pediatric ALL has been

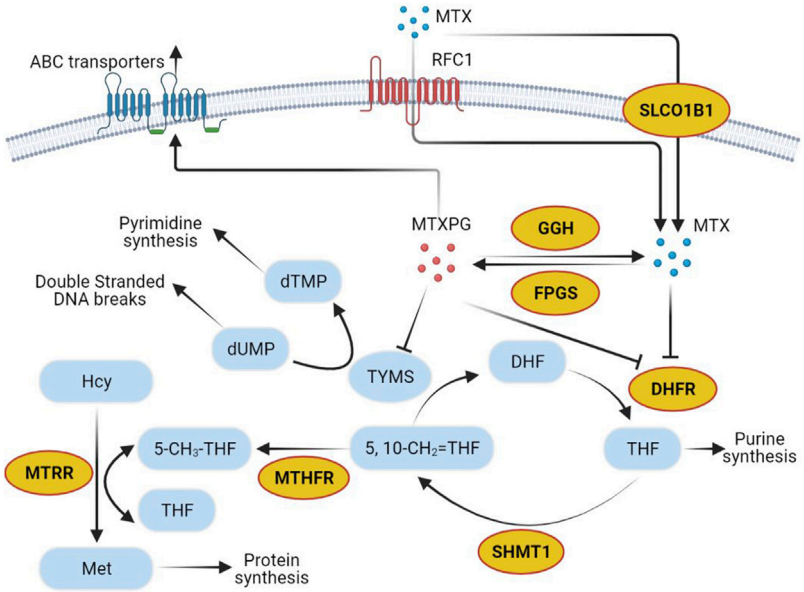

FIGURE 1 | Methotrexate pathway. Yellow circles show genes selected in the present study. Abbreviations: MTX, methotrexate; RFC1, reduced folate carrier-1; SLCO1B1, solute carrier organic anion transporter family member 1B1; dTMP, deoxythymidine monophosphate; dUMP, deoxyuridine monophosphate; TYMS, thymidylate synthetase; MTXPG, the polyglutamated forms of MTX; GGH, gamma-glutamyl hydrolase; FPGS, folylpolyglutamate synthetase; Hcy, homocysteine; MTRR, methionine synthase reductase; Met, Methionine; 5-CH3-THF, 5-methyltetrahydrofolate; THF, tetrahydrofolate; MTHFR, methylenetetrahydrofolate reductase; 5,10-CH2 = THF, 5,10-methylenetetrahydrofolate; DHF, dihydrofolate; DHFR, dihydrofolate reductase; SHMT1, serine hydroxymethyl transferase 1.

improved significantly over the past years; the 5-years survival rate is expected to increase up to 90% (Imanishi et al., 2007; Yang et al., 2012). High-dose methotrexate (HD-MTX) treatment during the consolidation phase is a major component in ALL treatment protocols (Erčulj et al., 2012). MTX is a folate reductase inhibitor and is stored in cells as polyglutamates (Fotoohi and Albertioni, 2008; Elbarbary et al., 2016). Being a result of long-term MTX treatment, the polyglutamates accumulate to higher levels, leading to a longer intracellular presence of the drug (Elbarbary et al., 2016). Previous reports demonstrate a variety of toxic reactions caused by HD-MTX, and liver injury is one of the serious adverse events (ADEs) (Schmiegelow, 2009; Conway and Carey, 2017). MTX-induced liver injury has been studied in patients aged >18 years with rheumatoid arthritis (RA); for instance, Japanese researchers investigated the risk factors for abnormal hepatic enzyme elevation by MTX in adult RA patients (Hakamata et al., 2018). However, the influencing factors of HD-MTX and its risk prediction model for ALL children have not been sufficiently explored.

Most ADEs of MTX treatment show individual differences, which can be partly explained by the gene sequence variation of proteins or transporters during the metabolism or excretion of MTX (Schmiegelow, 2009; Mikkelsen et al., 2011; Csordas et al., 2014; Moriyama et al., 2015). Recently, polymorphisms in genes are believed important to MTX pharmacokinetics, affecting MTX toxicity by altering the expression and activities of folate pathway enzymes (Csordas et al., 2014). Several genes play key roles in the MTX metabolism and transport pathway (**Figure 1**). MTX can be transformed into MTX polyglutamic (MTXPGs) with higher activity and toxicity, which is mediated by folylpolyglutamate synthetase (FPGS) and gamma-glutamyl hydrolase (GGH) (Fotoohi and Albertioni, 2008). Both MTX and MTXPGs combine with dihydrofolate reductase (DHFR) that blocks the reduction of dihydrofolate to tetrahydrofolate competitively (Fotoohi and Albertioni, 2008). As an intermediate metabolite, tetrahydrofolate can be changed into methylenetetrahydrofolate and methyltetrahydrofolate via serine hydroxymethyl transferase 1 (SHMT1) and methylenetetrahydrofolate reductase (MTHFR), correlating to MTX hepatic toxicity (Schmiegelow, 2009). There are also reports indicating that certain polymorphisms in methionine synthase reductase (MTRR) can decrease homocysteine levels and increase folate and cobalamin levels (Lv et al., 2018). Additionally, solute carrier organic anion transporter 1B1 (SLCO1B1) has been described as a membrane transporter involved in the clearance of MTX (Lopez-Lopez et al., 2011; Niemi et al., 2011). Clarifying the relationship between gene polymorphisms and HD-MTX-induced liver injury will be helpful for risk prediction and individualized optimal therapy (Kantar et al., 2009).

METHODS

Study Population

A total of 70 hospitalized Chinese Han children aged 1–16 years were enrolled in this study and were diagnosed with ALL and treated in Sichuan Provincial People's Hospital from October 2015 to August 2018. The specific diagnostic criteria and ALL risk classification were administered according to the Recommendations for Diagnosis and Treatment of Childhood

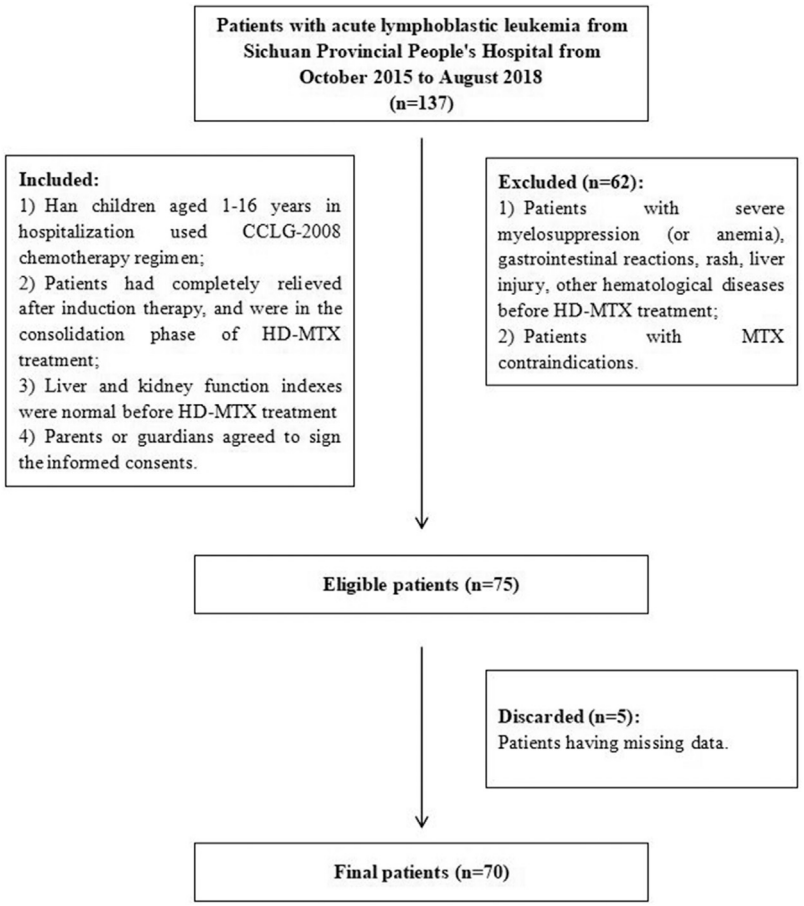

FIGURE 2 | Flowchart of patient inclusion. Abbreviations: CCLG-2008, Chinese Children's Leukemia Group-2008 protocols; MTX, methotrexate; HD-MTX, high-dose methotrexate.

Acute Lymphoblastic Leukemia (Version 4.0). Pediatric ALL patients received regimens referring to the widely used Chinese Children's Leukemia Group (CCLG)-ALL 2008 protocols (Cui et al., 2018).

The inclusion criteria were 1) Han children aged 1–16 years who were hospitalized and used the CCLG-2008 chemotherapy regimen; 2) all patients were completely relieved after induction therapy and were in the consolidation phase of HD-MTX treatment; 3) their liver and kidney function indexes were normal before HD-MTX treatment; 4) parents or guardians agreed to sign the informed consent. Among all candidates, those with severe myelosuppression (or anemia), gastrointestinal reactions, rash, liver injury, other hematological diseases before HD-MTX treatment and MTX contraindications were excluded. The workflow of selecting eligible patients is displayed in **Figure 2**. The study population was randomly divided into training and test cohorts (7:3). All patients were followed up for clinical and laboratory parameters because they received HD-MTX treatment for the first time to assess the development of liver injury. All demographic, clinical, laboratory, and medication data were obtained as the input variables.

This study was approved by the Ethics Committee of Sichuan Provincial People's Hospital. In all cases, informed consent was obtained from the parents or guardians of each participant in advance. Our study is registered in the Clinical Trial Management Public Platform (ChiCTR1800015307).

MTX Treatment and Toxicity Assessment

According to the Recommendations for Diagnosis and Treatment of Childhood Acute Lymphoblastic Leukemia (Version 4.0), MTX for injection (Jiangsu Hengrui Pharmaceutical Co., LTD., National Drug Approval Number H32026197, 1g/dose) was given at 5.0 g/m^2 to the patients in the medium- and high-risk grades, dosage of MTX was 2.0 g/m^2 in the low-risk group, and both were calculated by body surface area. One tenth of the total MTX dose was administered as an assault dose in the first 30 min at a rapid intravenous drip, and the remaining dose was administered at a constant intravenous drip in the following 23.5 h. After HD-MTX administration, leucovorin (Jiangsu Hengrui Pharmaceutical Co., LTD., National Drug Approval Number H32022391, 100 mg/dose) was administered at 15 mg/m^2 per time as rescue therapy to reduce the toxicity at 42, 48, and 54 h, respectively, until MTX blood concentration was

≤0.1 mol/L. If patients had delayed elimination, leucovorin at the same dose was given 1–3 times (Q6h) as supplements. Hydration and alkalinization were required 3 days before and after HD-MTX treatment. The venous blood was collected in the anticoagulant tube at 48 and 72 h after intravenous infusion of MTX. The plasma concentration of MTX was determined by homogeneous enzyme amplification immunoassay (Viva-E, Siemens).

The identification of liver injury used alanine transaminase (ALT) and/or aspartate aminotransferase (AST) as indexes. The normal value of both ALT and AST is 0–40 U/L. According to the National Cancer Institute Common Terminology Criteria for Adverse Events (NCI-CTCAE v4.03) scale, hepatic toxicity of severity grade 2 and above (grade 2, medium; grade 3, severe; grade 4, life-threatening; and grade 5, fatal) is considered as liver injury (National Institute of Can, 2009). To be specific, hepatotoxicity over grade 2 is defined as the levels of ALT and/or AST over the upper limit of the normal value (40 U/L) by three to five times with no symptoms or exceeding the upper limit of the normal value by three times with aggravated symptoms, such as fatigue, nausea, vomiting, pain or tenderness in the upper right abdomen, fever, rash, and eosinophilia (National Institute of Can, 2009). ALT and AST were measured 1 day before and 3 and 7 days after HD-MTX administration (Beckman AU5800).

Variable Selection

Genotyping Analysis

Because of the prominent contribution to MTX toxicity among individuals, we analyzed up to 10 polymorphisms in seven genes (*MTHFR, MTRR, SLCO1B1, FPGS, GGH, SHMT1,* and *DHFR*) from the MTX metabolism and transport pathway.

In this study, real-time fluorescence quantitative polymerase chain reaction (PCR) was used to detect the gene analysis of patients. First, the blood genome column small volume extraction kit (Beijing Kangwei Century Biotechnology Co., LTD.) was used to extract the peripheral blood DNA of the children in strict accordance with its instructions. The concentration and purity of DNA were detected by NanoDrop 2000 (Thermo Fisher Scientific, United States) [DNA concentration was 10–30 ng/μl; purity ($A_{260\ nm}/A_{280\ nm}$) was 1.6–2.0]. The PCR instrument was ABI 7500 real-time quantitative PCR (Thermo Fisher Scientific, United States). MTHFR rs1801133, 1801131, MTRR rs1801394, SLCO1B1 rs2806283, and rs4149056 used gene test kits as follows: *MTHFR (C677T)* gene test kit (National instrument Approval Word 20173401322), *MTRR* and *MTHFR (A1298C)* gene test kit (Hubei Food and Drug Supervision Equipment Production License 20120580), *SLCO1B1* and *ApoE* gene test kit (National Instrument Approval License 20153400245; Wuhan Youzhiyou Medical Technology Co., LTD.). Primers and probes were designed and synthesized by Wuhan Youzhiyou Medical Technology Co., LTD., which is illustrated in **Supplementary Table S1**. PCR reaction system (25 μl): DNA template 1 μl and amplification reagent 24 μl (including PCR buffer, dNTPs, specific primer and probe, internal primer and probe, Taq enzyme, UNG enzyme); reaction conditions: pretreatment at 37°C for 10 min, predenaturation at 95°C for 5 min, denaturation at 95°C for 15 s, annealing at 60°C for 60 s (*MTHFR* and *MTRR*)/45s (*SLCO1B1*), a total of 40 cycles. We purchased TaqMan™ single nucleotide polymorphism (SNP) Genetyping Assays to detect loci: *SLCO1B1 rs11045879* (ID: C_31106904_10), *FPGS rs11545078* (ID: C_25623170_10), *GGHS rs11545078* (ID: C_25623170_10), *SHMT1 rs1979277* (ID: C_3063127_10), *DHFR rs408626* (ID: C_921,481_20). Reaction system (total 25 μl): DNA template 1 μl, Master Mix 12.5 μl, 20×TaqMan SNP Genotyping Assay working fluid 1.25 μl, supplemented with ddH2O 25 μl; reaction conditions: pretreatment at 60°C for 20 s, predenaturation at 95°C for 5 min, denaturation at 95°C for 5 s, annealing at 60°C for 60 s, a total of 40 cycles; extended at 60°C for 5 min.

Nongenetic Analysis

There are some nongenetic factors relating to hepatotoxicity. In addition to demographic factors (age, gender, height, weight, BMI, and body surface), some laboratory indexes were included for screening, such as complete blood counts, hemoglobin, albumin, bilirubin, ALT, AST, alkaline phosphatase (ALP) and gamma glutamyl transferase (GGT). The indicators for renal function were taken into consideration as well, including creatinine (Cr), blood urea nitrogen (BUN), urine protein, and urine pH. MTX dosage and plasma concentration at 48 and 72 h were also influencing factors of MTX toxicity.

Model Construction and Evaluation

Ridge regression was applied to construct the model, which is a parameter estimation method and can address the collinearity problem for multiple linear regressions without reducing variables from the original data set (Mcdonald, 2010). On the other side, to achieve better estimation of the model coefficients, ridge regression can eliminate the bias of the correlations between variables. The regression coefficient β_i of each variable in ridge regression was weighted through the following formula:

$$\hat{\beta}_i = round\left(\frac{\beta_i}{\min\left(\left|\beta_{1,\ldots,K}\right|\right)}/2\right)$$

After weighting the regression coefficient for each predictor, we got the risk-score calculation formula for liver injury. The cumulative risk score for each patient was calculated from the formula by summation of these weightings for respective predictors. Higher score indicates greater risk of liver injury. Risk groups for liver injury were stratified according to the distribution of patients' total risk scores. On this basis, we set the score less than the lower quartile as low-risk (LR) level, score between the lower and upper quartile as medium-risk (MR) level, and score higher than the upper quartile as high-risk (HR) level. Model performance was evaluated through the receiver operating characteristic (ROC) curve and the value of area under the curve (AUC), which represent the overall ability of classification and prediction. Additional statistics, such as accuracy, sensitivity, specificity, positive predictive value, and negative predictive value were obtained.

Statistical Analysis

Based on the significant variables after preliminary screening, the categorical variables were binarized with one-hot encoding. Univariate analysis was performed through two independent sample *t*-tests on continuous variables and a chi-square test on categorical variables with significance level at $p < 0.1$. After that, the

TABLE 1 | Baseline characteristics of study population.

Variable	Value
Target variable	
Liver injury, n (%)	23 (32.9%)
Demographic information	
Age, year, median (IQR)	7.5 (4–12)
Gender, n (%)	
Male	45 (64.3%)
Female	25 (35.7%)
Height, cm, median (IQR)	119.5 (99.3–154.5)
Weight, kg, median (IQR)	24.8 (15.0–40.8)
Body surface area, m^2, median (IQR)	0.9 (0.6–1.3)
BMI, kg/m^2, median (IQR)	16.8 (15.7–18.8)
MTX information	
Dose, g, median (IQR)	4.0 (2.5–5.0)
C_{48h}, umol/l, median (IQR)	0.39 (0.25–0.64)
C_{48h} after dose correction, umol/l, median (IQR)	0.13 (0.08–0.28)
$C_{72h} \leq 0.1$ μmol/L, n%	37 (52.9%)
$C_{72h} > 0.1$ μmol/L, n%	33 (47.1%)
ALL information	
Immunophenotype, n (%)	
B-cell	45 (64.3%)
T-cell	12 (17.1%)
Others	13 (18.6%)
Risk grade	
LR	3 (4.3%)
MR	18 (25.7%)
HR	49 (70.0%)
Assay index	
WBC count_1 day before MTX administration, 10^9/L, median (IQR)	3.3 (2.3–5.5)
NEU count_1 day before MTX administration, 10^9/L, median (IQR)	1.5 (0.8–2.7)
LYM count_1 day before MTX administration, 10^9/L, median (IQR)	1.2 (0.8–1.6)
EOS count_1 day before MTX administration, 10^9/L, median (IQR)	0.019 (0.000–0.078)
BASO count_1 day before MTX administration, 10^9/L, median (IQR)	0.010 (0.000–0.030)
RBC count_1 day before MTX administration, 10^{12}/L, median (IQR)	3.2 (2.7–3.7)
PLT count_1 day before MTX administration, 10^9/L, median (IQR)	239.5 (176.3–408.0)
Hb_1 day before MTX administration, g/L, median (IQR)	98.0 (83.3–107.0)
ALT_1 day before MTX administration, U/L, median (IQR)	22.0 (14.0–36.8)
AST_1 day before MTX administration, U/L, median (IQR)	32.0 (23.0–38.0)
Cr_1 day before MTX administration, μmol/L, median (IQR)	26.2 (20.8–37.5)
BUN_1 day before MTX administration, mmol/L, median (IQR)	3.8 (2.7–4.6)
Albumin_1 day before MTX administration, g/L, median (IQR)	41.9 (38.7–44.9)
Globin_1 day before MTX administration, g/L, median (IQR)	20.2 (17.9–23.8)
TP_1 day before MTX administration, g/L, median (IQR)	62.6 (59.0–57.5)
Globin/Albumin_1 day before MTX administration, median (IQR)	2.1 (1.7–2.4)
ALP_1 day before MTX administration, U/L, median (IQR)	155.0 (115.0–212.0)
GGT_1 day before MTX administration, U/L, median (IQR)	21.0 (13.0–40.0)
Urine protein_1 day before MTX administration, g, median (IQR)	0 (0–0)
Urine pH_1 day before MTX administration, median (IQR)	7.5 (7.5–8.0)
TBIL_1 day before MTX administration, μmol/L, median (IQR)	9.6 (6.7–15.8)
DBIL_1 day before MTX administration, μmol/L, median (IQR)	3.1 (2.3–4.3)
IBIL_1 day before MTX administration, μmol/L, median (IQR)	7.0 (4.3–10.8)

***Abbreviation**: BMI, body mass index; MTX, methotrexate; ALL, acute lymphoblastic leukemia; C48h, 48-h blood concentration; C72h, 72-h blood concentration; LR, low-risk; MR, medium-risk; HR, high-risk; WBC, white blood cells; NEU, neutrophil; LYM, lymphocyte; EOS, eosnophils; BASO, basophils; RBC, red blood cells; PLT, platelet; Hb, hemoglobin; ALT, alanine transaminase; AST, aspartate aminotransferase; Cr, creatinine; BUN, blood urea nitrogen; A/G, the ratio of albumin to globin; TP, total protein; ALP, alkaline phosphatase; GGT, gamma glutamyl transpeptidase; TBIL, total bilirubin; DBIL, direct bilirubin; IBIL, indirect bilirubin.*

important variables were further selected by ridge regression with a ranking of importance scores. Subsequently, the random forest (RF) method was used to fill in the missing values. RF shows the ability of imputing missing data into the given data set with high accuracy and less computation time (Pantanowitz and Marwala, 2009). Then, *t*-tests and chi-square tests were applied to verify the differences between variable characteristics of the training and test cohorts. Ridge regression was used to establish the risk scoring model. Ultimately, the distribution of three risk groups was given, and intergroup differences were assessed by chi-square test.

Data were collected, coded, and entered to the Statistical Package for the Social Sciences software version 22.0 and Python 3.7.0.

RESULTS

Baseline Information

A total of 70 children with ALL were enrolled in our study, including 45 males (64.3%) and 25 females (35.7%), and the median age was 7.5 in a range between 1 and 16 years. The ratio of patients with to those without liver injury was about 1:2. In total, we collected 45 variables from clinical data and genotypes; the basic characteristics are listed in **Tables 1**, **2**. The majority of patients had B-cell ALL (64.3%), and 67 patients were classified as MR or HR grade (95.7%). The median MTX dose administered for patients was 4 [interquartile range (IQR) 2.5–5.0] g, the median MTX concentration measured at 48 h was 0.39 (IQR 0.25–0.64) umol/l, and 33 patients (47.1%) had MTX concentration measured at 72 h > 0.1 umol/l. The detailed MTX plasma concentration values are shown in **Supplementary Table S2**. The median ALT and AST tested 1 day before HD-MTX treatment were 22.0 (IQR 14.0–36.8) U/L and 32.0 (IQR 23.0–38.0) U/L, respectively. After starting the MTX therapy regimen, liver injury occurred in 32.9% (n = 23) of the patients. The basic genotype information and distribution are shown in **Table 2**. According to the calculated results, the polymorphisms included in the model were in Hardy–Weinberg equilibrium, which means samples in our study are representative.

Selected Variables

The outcome of univariate analysis through *t*-tests and chi-square tests is illustrated in **Table 3**, which demonstrates the relationships of all variables to the liver injury. After data screening, seven variables were identified to make statistically significant contributions to liver injury ($p < 0.1$), including age, *MTRR_AA, MTRR_AG, SLCO1B1_11045879_CC*, lymphocyte (LYM) count_1 day before MTX administration, albumin_1 day before MTX administration, and indirect bilirubin (IBIL)_1 day before MTX administration with p values of 0.091, 0.003, 0.001, 0.096, 0.019, 0.094, and 0.068, respectively (shown in **Table 3**). Subsequently, importance scores of the seven variables were calculated and ranked through ridge regression, which were *MTRR_AG* (1.349), *SLCO1B1_11045879_CC* (0.963), albumin_1 day before MTX administration (0.730), *MTRR_AA* (0.558), age (0.443), IBIL_1 day before MTX administration (0.348), and LYM count_1 day before MTX administration (0.032) in descending order. Because LYM count_1 day before MTX administration had the lowest importance score that differed greatly from other variables and for the purpose of

TABLE 2 | Basic information and distribution of genotypes.

Genes (RS no.)	Genotype	N (%)	Allele	Frequency	Hardy–Weinberg equilibrium	
					X^2	*p*
MTHFR (rs1801133)	CC	25 (35.7%)	C	0.62	1.07	0.59
	CT	37 (52.9%)	C[a]	0.71		
	TT	8 (11.4%)	T	0.38		
			T[a]	0.29		
MTHFR (rs1801131)	AA	38 (54.3%)	A	0.74	0.15	0.93
	AC	28 (40.0%)	A[a]	0.84		
	CC	4 (5.7%)	C	0.26		
			C[a]	0.16		
SLCO1B1 (rs11045879)	CC	10 (14.3%)	C	0.41	0.63	0.73
	CT	37 (52.9%)	C[a]	0.45		
	TT	23 (32.9%)	T	0.59		
			T[a]	0.55		
SLCO1B1 (rs2306283)	AA	2 (2.9%)	A	0.20	0.36	0.84
	AG	24 (34.3%)	A[a]	0.21		
	GG	44 (62.9%)	G	0.80		
			G[a]	0.80		
SLCO1B1 (rs4149056)	TT	54 (77.1%)	T	0.86	6.3	0.04
	CT	12 (17.1%)	T[a]	0.88		
	CC	4 (5.7%)	C	0.14		
			C[a]	0.12		
FPGS (rs1544105)	CC	10 (14.3%)	C	0.32	2.3	0.32
	CT	25 (35.7%)	C[a]	0.31		
	TT	35 (50.0%)	T	0.68		
			T[a]	0.70		
GGH (rs11545078)	GG	65 (92.9%)	G	0.96	0.1	0.95
	AG	5 (7.1%)	G[a]	0.92		
	AA	0 (0.0%)	A	0.04		
			A[a]	0.08		
SHMT1 (rs1979277)	GG	59 (84.3%)	G	0.92	0.51	0.78
	AG	11 (15.7%)	G[a]	0.95		
	AA	0 (0.0%)	A	0.08		
			A[a]	0.05		
DHFR (rs408626)	TT	4 (5.7%)	T	0.32	3.14	0.21
	CT	37 (52.9%)	T[a]	0.35		
	CC	29 (41.4%)	C	0.68		
			C[a]	0.65		
MTRR (rs1801394)	AA	31 (44.3%)	A	0.67	0.09	0.96
	AG	32 (45.7%)	A[a]	0.73		
	GG	7 (10.0%)	G	0.33		
			G[a]	0.27		

[a]*Reference allele, data from the PharmGKB Drug Genome Library of the East Asian, a sample of over 3,000 people, https:/www.pharmgkb.org.*

[b]p > .05 *showed data was accord with the Hardy–Weinberg equilibrium.*

Abbreviations: RS, reference single nucleotide polymorphism.

model simplicity, it was excluded as the final predictor. The top six variables were applied as predictors for liver injury, including age, *MTRR_AA, MTRR_AG, SLCO1B1_11045879_CC*, albumin_1 day before MTX administration, and IBIL_1 day before MTX administration. After interpolation of missing values via RF, a comparison of important variable characteristics between training and test cohorts was established (**Table 4**). At the confidence level of 0.05, there was no significant difference between the characteristics of each variable in the training and test cohorts.

Model Construction and Evaluation

The model of predictors for liver injury achieved good discrimination and reached the AUC of 0.76 and 0.62 in the training and test cohorts, respectively, as depicted in **Figure 3**. Additional statistics representing model performance are illustrated in **Table 5**. The model had remarkable accuracy and precision in the training cohort (0.86 and 0.81, respectively), demonstrating its adequate capacity to predict risks accurately and precisely. The value of specificity in the training cohort was high (0.91), showing a good ability to reduce false positives. Of all metrics, the majority in the test cohort had relatively low values, possibly due to the small sample size. Nevertheless, the negative predictive value was good (0.80), indicating low likelihood that no disease was found in negative subjects.

The Risk-Scoring Model

In the ridge regression model, the regression coefficient βi of each predictor was weighted and estimated. After that, the risk-score calculation formula for liver injury was obtained as follows:

TABLE 3 | Significance analysis of the influencing variables of liver injury.

Variable	*t* statistics	χ^2 statistics	*p*-value	Odds ratio (95% CI)
Age	−1.71	—	0.091	
Gender	—	0.17	0.676	1.246 (0.444–3.496)
Height	−0.43	—	0.671	
Weight	−0.52	—	0.606	
Body surface area	−0.48	—	0.630	
BMI	−0.80	—	0.426	
Dosage	−1.45	—	0.150	
C_{48h}	−0.187	—	0.852	
C_{48h} after dose correction	0.471	—	0.639	
C_{72h}	—	0.88	0.348	0.616 (0.223–1.698)
Immunophenotype	—			
B-cell	—	0.01	0.909	1.063 (0.374–3.019)
T-cell	—	0.001	0.969	1.026 (0.274–3.840)
Others	—	0.03	0.859	0.889 (0.242–3.262)
Risk grade	—			
LR	—	1.53	0.216	
MR	—	0.28	0.594	0.726 (0.223–2.362)
HR	—	1.11	0.291	1.852 (0.582–5.927)
MTHFR_C677T	—			
CC	—	0.01	0.909	0.941 (0.331–2.674)
CT	—	0.19	0.667	1.246 (0.457–3.398)
TT	—	0.25	0.615	0.651 (0.121–3.508)
MTHFRA1298C	—			
AA	—	0.06	0.804	0.881 (0.324–2.395)
AC	—	0.17	0.678	1.239 (0.450–3.412)
CC	—	0.12	0.730	0.667 (0.065–6.786)
MTRR	—			
AA	—	8.87	0.003	4.876 (1.657–14.350)
AG	—	11.07	0.001	0.143 (0.042–0.487)
GG	—	0.35	0.553	1.613 (0.329–7.893)
SLCO1B1_11045879	—			
CC	—	2.76	0.096	0.192 (0.023–1.618)
CT	—	2.10	0.147	2.131 (0.759–5.979)
TT	—	0.09	0.763	0.848 (0.290–2.480)
*SLCO1B1*1b (rs2306283_A > G)*	—			
AA	—	1.01	0.316	0.957 (0.901–1.017)
AG	—	0.004	0.951	1.033 (0.362–2.950)
GG	—	0.08	0.775	1.164 (0.411–3.294)
*SLCO1B1*5 (rs4149056_T > C)*	—			
TT	—	0.58	0.446	1.629 (0.461–5.752)
TC	—	0.001	0.969	1.026 (0.274–3.840)
CC	—	2.08	0.150	0.915 (0.838–0.998)
FPGS (rs1544105_C > T)	—			
CC	—	0.04	0.835	0.857 (0.200–3.673)
CT	—	0.17	0.676	1.246 (0.444–3.496)
TT	—	0.07	0.799	0.878 (0.324–2.384)
GGH (rs11545078_A > G)	—	0.40	0.525	0.489 (0.051–4.639)
SHMT1 (rs1979277_A > G)	—	1.27	0.259	0.402 (0.079–2.036)
DHFR (rs408626_T > C)	—			
TT	—	0.12	0.730	0.667 (0.065–6.786)
TC	—	1.21	0.271	0.570 (0.208–1.560)
CC	—	1.63	0.202	1.925 (0.700–5.294)
WBC count_1 day before MTX administration	−0.2	—	0.842	
NEU count_1 day before MTX administration	0.07	—	0.949	
LYM count_1 day before MTX administration	0.10	—	0.019	
EOS count_1 day before MTX administration	1.07	—	0.289	
BASO count_1 day before MTX administration	−1.16	—	0.251	
RBC count_1 day before MTX administration	−0.93	—	0.363	
PLT count_1 day before MTX administration	0.06	—	0.954	
Hb_1 day before MTX administration	−0.01	—	0.995	
ALT_1 day before MTX administration	−0.69	—	0.494	
AST_1 day before MTX administration	−0.91	—	0.364	
Cr_1 day before MTX administration	0.88	—	0.385	
BUN_1 day before MTX administration	0.73	—	0.465	

(Continued on following page)

TABLE 3 | (*Continued*) Significance analysis of the influencing variables of liver injury.

Variable	*t* statistics	χ^2 statistics	*p*-value	Odds ratio (95% CI)
Albumin_1 day before MTX administration	1.70	—	0.094	
Globin_1 day before MTX administration	−0.06	—	0.953	
TP_1 day before MTX administration	1.28	—	0.206	
A/G_1 day before MTX administration	0.64	—	0.526	
ALP_1 day before MTX administration	0.24	—	0.808	
GGT_1 day before MTX administration	−0.81	—	0.429	
Urine protein_1 day before MTX administration	−0.56	—	0.584	
Urine pH_1 day before MTX administration	−0.07	—	0.942	
TBIL_1 day before MTX administration	−1.58	—	0.128	
DBIL_1 day before MTX administration	−1.45	—	0.164	
IBIL_1 day before MTX administration	−1.86	—	0.068	

Abbreviations*: CI, confidence interval; BMI, body mass index; MTX, methotrexate; ALL, acute lymphoblastic leukemia; C48h, 48-h blood concentration; C72h, 72-h blood concentration; LR, low-risk; MR, medium-risk; HR, high-risk; MTHFR, methylenetetrahydrofolate reductase; SLCO1B1, solute carrier organic anion transporter 1B1; FPGS, folypolyglutamate synthetase; GGH, gamma-glutamyl hydrolase; DHFR, dihydrofolate reductase; SHMT1, serine hydroxymethyl transferase 1; MTRR, methionine synthase reductase; WBC, white blood cells; NEU, neutrophil; LYM, lymphocyte; EOS, eosinophils; BASO, basophils; RBC, red blood cells; PLT, platelet; Hb, hemoglobin; ALT, alanine transaminase; AST, aspartate aminotransferase; Cr, creatinine; BUN, blood urea nitrogen; A/G, the ratio of albumin to globin; TP, total protein; ALP, alkaline phosphatase; GGT, gamma glutamyl transpeptidase; TBIL, total bilirubin; DBIL, direct bilirubin; IBIL, indirect bilirubin.*

TABLE 4 | Comparison of significant variable characteristics between training and test cohorts.

Variable	Training cohort (n = 49)	Test cohort (n = 21)	*p*-value
Liver injury, n%			0.617
0	32 (65.3%)	15 (71.4%)	
	17 (34.7%)	6 (28.6%)	
Age, median (IQR)	8 (4–12)	7 (4–11)	0.191
MTRR_AA, n%			0.875
0	27 (55.1%)	12 (57.1%)	
1	22 (44.9%)	9 (42.9%)	
MTRR_AG, n%			0.173
0	24 (49.0%)	14 (66.7%)	
1	25 (51.0%)	7 (33.3%)	
SLCO1B1_11045879_CC, n%			0.456
0	43 (87.8%)	17 (81.0%)	
1	6 (12.2%)	4 (19.0%)	
Albumin_1 day before MTX administration, median (IQR)	41.9 (39.0–44.5)	42.7 (40.1–44.2)	0.102
IBIL_1 day before MTX administration, median (IQR)	7.2 (4.4–10.7)	5.4 (4.3–8.0)	0.096

Risk score = 1*age - 1*albumin_1 day before MTX administration +1 *IBIL_1 day before MTX administration - 25**MTRR_AA*- 61**MTRR_AG* - 44**SLCO1B1_11045879_CC* + 140.

The data of patients in the training cohort were substituted into the formula, and the patients' total scores were calculated, showing the score distribution with a range from 10 to 128 (**Table 6**). According to the upper and lower quartile levels of total risk scores, we stratified the risk scores into three groups, representing the LR (≤48), MR (48–89), and HR (>89) groups. The distribution of patients with liver injury among different risk groups in the training and test cohorts is displayed in **Figure 4**. We can see an ascending trend that liver injury occurred from LR to HR groups in both cohorts, and the intergroup differences of LR-HR and MR-HR in the training cohort were significant ($p < 0.01$), indicating that the model had good differentiating ability between LR-HR and MR-HR levels. However, there was no significant difference between groups in the test cohort, probably due to the limited amount of the test sample. The distribution of patients with liver injury among different risk groups was that, in the training cohort, there was one patient in the LR group, seven patients in the MR group, and nine patients in the HR group; in the test group, there were zero patients in the LR group, three patients in the MR group, and three patients in the HR group.

DISCUSSION

The present study focuses on investigating the associations between clinical, genetic, and laboratory factors and HD-MTX-induced liver injury in pediatric ALL patients in China, constructing a risk-scoring model and endeavoring to achieve a balance between the efficacy and toxicity of HD-MTX treatment.

The identification of important factors is crucial, and multiple covariates have demonstrated their significance in previous studies. A population pharmacokinetic model was constructed for ALL children, finding age and total body weight as significant influencing factors in MTX clearance (Aumente et al., 2006). It illustrates an inverse relationship between MTX clearance and patient age, which means younger patients show faster

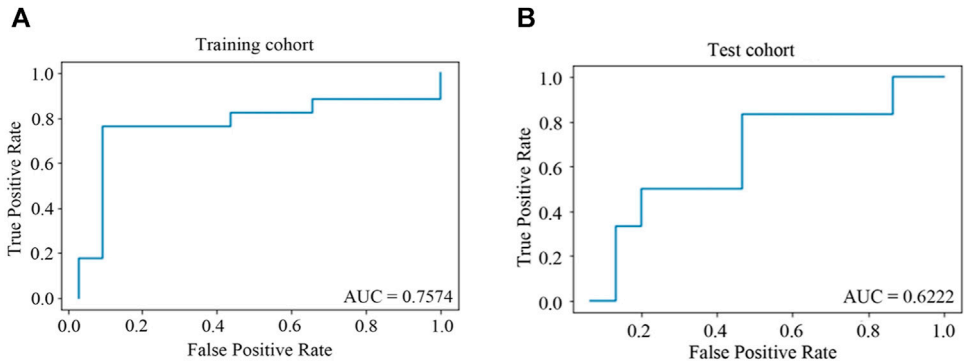

FIGURE 3 | ROC curves for predictors of HD-MTX-induced liver injury in ridge regression model. **(A)** ROC curve in training cohort; **(B)** ROC curve in test cohort. When the value of AUC is closer to one, the classification effect of the model is better.

TABLE 5 | Performance of the ridge regression model.

Metric	Training cohort	Test cohort
Accuracy	0.86	0.57
Precision	0.81	0.36
Sensitivity	0.76	0.67
Specificity	0.91	0.53
Positive predictive value	0.81	0.36
Negative predictive value	0.88	0.80

TABLE 6 | Risk score description in training and test cohorts.

Risk score	Training cohort	Test cohort
Average	67.36	74.80
SD	26.38	31.61
Minimum value	10.30	0.80
Lower quartile	47.50	51.00
Median	57.90	78.20
Upper quartile	88.65	98.60
Maximum value	128.20	126.50

***Abbreviation**: SD, standard deviation.*

elimination of HD-MTX, leading to maximum treatment effect without elevating toxicity (Aumente et al., 2006). Based on the predictor coefficients in our risk-scoring formula, age is positively related to the risk of hepatotoxicity caused by HD-MTX, which is consistent with former perspectives. In terms of other nongenetic factors, the elevation of ALT and AST could indicate potential damaged liver structural integrity (Seidel et al., 1994; Elbarbary et al., 2016; Hakamata et al., 2018). ALP and GGT are common markers of cholestatic problems induced by liver injury (Hawkey et al., 2012). However, these transaminases were not included in the final model; likewise, kidney function indexes, including Cr, urine protein, urine pH, and BUN, were not selected as predictors, possibly due to the initial exclusion of patients with abnormal liver and/or kidney function. In addition, serum bilirubin is related to the excretion of anions and formation of bile, and albumin has an impact on protein synthesis (Limdi and Hyde, 2003). HD-MTX is proven to increase the concentration of serum bilirubin while decreasing albumin concentration, corresponding to our findings that the HD-MTX-induced liver injury risk was positively correlated to IBIL and negatively to albumin (Moghadam et al., 2015).

Of all risk factors for MTX toxicity, the role of gene polymorphisms is indubitable, leading to various responses to MTX toxicity among ALL children. We analyzed seven genes from MTX metabolism, some of which have had their impacts on MTX-induced toxic reactions illustrated in previous reports; these include that *MTHFR_C677T* can significantly increase the risk of MTX toxicity, the low activity of *GGH* may lead to increased intracellular cytotoxicity of MTX in leukemic cells, the inhibition of *DHFR* can be definitively responsible for the exertion of MTX cytotoxicity, and *SHMT1* can affect enzymatic activity, which is associated with liver toxicity during MTX therapy (Fotoohi and Albertioni, 2008; Schmiegelow, 2009; Lopez-Lopez et al., 2011; Yang et al., 2012). In the final results, *MTRR* and *SLCO1B1* polymorphisms occupied a critical position in the risk-score formula with significantly greater weightings than other predictors, and their negative coefficients represent an inverse relationship between *MTRR* and *SLCO1B1* polymorphisms and liver injury risks. In other words, patients with *MTRR_AA*, *MTRR_AG*, and/or *SLCO1B1_11045879_CC* could have lower risk of liver injury. The present work provides a novel perspective about the effect of *MTRR* polymorphisms on the HD-MTX toxicity in ALL children. In terms of the *SLCO1B1* gene, it was deemed to be associated with MTX clearance, and the significant correlations between its polymorphisms (*rs11045879* and *rs4149056*) and the levels of serum MTX are proven in other studies (Faganel Kotnik et al., 2011; Niemi et al., 2011; Moriyama et al., 2015).

There are studies pointing out that some gene polymorphisms involved in the MTX pathway that are not investigated in our study may have associations with MTX toxicity as well. A polymorphism in reduced folate carrier (*RFC1*), *C3435T* in the multidrug-resistance protein (*ABCB1*), and *C421A* in the breast cancer resistance protein (*ABCG2*) are reported to have associations with hepatic, gastrointestinal, and nervous system toxicities (Lopez-Lopez et al., 2011; Mikkelsen et al., 2011). However, there is an adverse viewpoint from Lopez et al. with a research population of 115 ALL children,

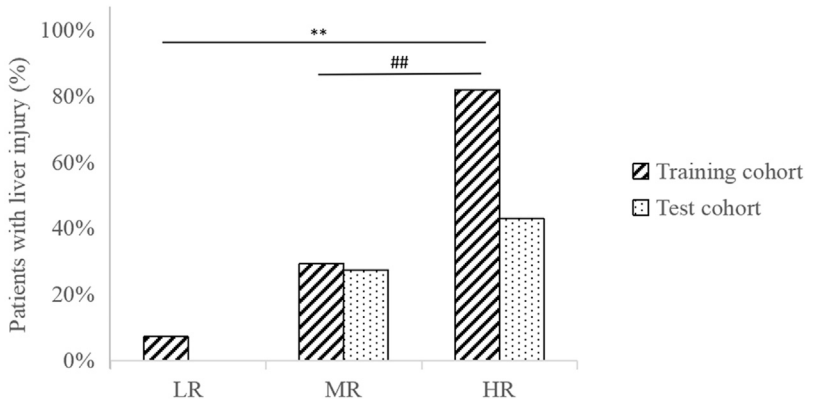

FIGURE 4 | Distribution of patients with liver injury among different risk groups in training and test cohorts. $^{**}p < 0.01$, indicating significant differences between LR-HR groups in the training cohort. $^{\#\#}p < 0.01$, indicating significant differences between MR-HR groups in the training cohort.

who claimed that *MTHFR* (*C677T* and *A1298C*), *TYMS* (*28 bp* and *6 bp-del*), *SHMT1* (*C1420T*), *ABCB1* (*C3435T*), *ABCG2* (*C421A*), *RFC1* (*G80A*), and *SLCO1B1* (*rs4149081*) were not available to show relationships with MTX toxicity in childhood ALL (Lopez-Lopez et al., 2011). They believe that the associations between polymorphisms in enzymes or transporter genes and MTX proven in the former literature could be attributed to the small or unhomogeneous sample size, nonobjective toxicity markers, or different treatment protocols (Lopez-Lopez et al., 2011). Herein, we analyzed as many as 10 polymorphisms in seven genes, which provides a comprehensive analysis of the associations between genotypes and HD-MTX-induced liver injury, to provide an optimized therapy regimen based on individual diversity. Moreover, we chose quantifiable markers of toxicity, ALT, and AST levels to objectively analyze HD-MTX-induced hepatotoxicity. However, we were aware that one drawback in this study was the inadequate sample size; thus further research with larger populations and clinical practice are necessary.

In summary, we explored the relationship between multiple risk factors and HD-MTX-induced liver injury and established a risk-scoring model based on the identified predictors. Besides liver injury, the modeling process in present study can be applied to predict the risks of other MTX-induced ADEs caused by MTX. This study provides knowledge of risk prediction for HD-MTX hepatotoxicity in pediatric ALL patients that few studies have investigated, which could be used as a reference for clinical medication.

DATA AVAILABILITY STATEMENT

The raw data supporting the conclusions of this article will be made available by the authors, without undue reservation.

ETHICS STATEMENT

The studies involving human participants were reviewed and approved by the Ethics Committee of Sichuan Provincial People's Hospital, Sichuan Academy of Medical Sciences (Number: Ethic Audit 2015.52th). Written informed consent to participate in this study was provided by the participants' legal guardian/next of kin.

AUTHOR CONTRIBUTIONS

XiaH, RT and ZY designed the study. XiaH, XL, SD, ZY and FG performed the research. XiaH, PY and YL performed pharmacogenetic analysis. XL, MZ, PY and YL collected the data. WS and ZW were responsible for statistical analysis. XiaH, XinH, ML, HL, XL and YL wrote the manuscript. All authors contributed to data interpretation. All authors read and approved the final manuscript for publishing.

FUNDING

This work was supported by National key R&D Program of China (2020YFC2005500) and Key Research and Development Program of Science and Technology Department of Sichuan Province (2019YFS0514) and Sichuan Medical Association (S16068) and Sichuan Provincial People's Hospital (2020LY06) for RT. This work was also supported by Sichuan Provincial People's Hospital (2015QN08) and Health and Family Planning Commission of Sichuan Province (16PJ480) for XH. This work was also supported by The Science and Technology Project of Health and Family Planning Commission of Sichuan Province (19PJ269) and Research Fund for the Doctoral Program of Sichuan Academy of Medical Sciences and Sichuan Provincial People's Hospital (2015BS04) for XL.

SUPPLEMENTARY MATERIAL

The Supplementary Material for this article can be found online at: https://www.frontiersin.org/articles/10.3389/fphar.2021.726229/full#supplementary-material

REFERENCES

Aumente, D., Buelga, D. S., Lukas, J. C., Gomez, P., Torres, A., and García, M. J. (2006). Population Pharmacokinetics of High-Dose Methotrexate in Children with Acute Lymphoblastic Leukaemia. *Clin. Pharmacokinet.* 45 (12), 1227–1238. doi:10.2165/00003088-200645120-00007

Conway, R., and Carey, J. J. (2017). Risk of Liver Disease in Methotrexate Treated Patients. *World J. Hepatol.* 9 (26), 1092–1100. doi:10.4254/wjh.v9.i26.1092

Csordas, K., Lautner-Csorba, O., Semsei, A. F., Harnos, A., Hegyi, M., Erdelyi, D. J., et al. (2014). Associations of Novel Genetic Variations in the Folate-Related and ARID5B Genes with the Pharmacokinetics and Toxicity of High-Dose Methotrexate in Paediatric Acute Lymphoblastic Leukaemia. *Br. J. Haematol.* 166, 410–420. doi:10.1111/bjh.12886

Cui, L., Li, Z. G., Chai, Y. H., Yu, Y., Gao, J., Zhu, X. F., et al. (2018). Outcome of Children with Newly Diagnosed Acute Lymphoblastic Leukemia Treated with CCLG-ALL 2008: The First Nationwide Prospective Multicenter Study in China[J]. *Am. J. Hematol.*

Elbarbary, N. S., Ismail, E. A. R., Farahat, R. K., and El-Hamamsy, M. (2016). ω-3 Fatty Acids as an Adjuvant Therapy Ameliorates Methotrexate-Induced Hepatotoxicity in Children and Adolescents with Acute Lymphoblastic Leukemia: A Randomized Placebo-Controlled Study. *Nutrition* 32 (1), 41–47. doi:10.1016/j.nut.2015.06.010

Erčulj, N., Kotnik, B. F., Debeljak, M., Jazbec, J., and Dolžan, V. (2012). Influence of Folate Pathway Polymorphisms on High-Dose Methotrexate-Related Toxicity and Survival in Childhood Acute Lymphoblastic Leukemia[J]. *Leuk. Lymphoma* 53 (6), 1096–1104.

Faganel Kotnik, B., Grabnar, I., Bohanec Grabar, P., Dolžan, V., and Jazbec, J. (2011). Association of Genetic Polymorphism in the Folate Metabolic Pathway with Methotrexate Pharmacokinetics and Toxicity in Childhood Acute Lymphoblastic Leukaemia and Malignant Lymphoma. *Eur. J. Clin. Pharmacol.* 67 (10), 993–1006. doi:10.1007/s00228-011-1046-z

Fotoohi, A. K., and Albertioni, F. (2008). Mechanisms of Antifolate Resistance and Methotrexate Efficacy in Leukemia Cells. *Leuk. Lymphoma* 49 (3), 410–426. doi:10.1080/10428190701824569

Hakamata, J., Hashiguchi, M., Kaneko, Y., Yamaoka, K., Shimizu, M., Maruyama, J., et al. (2018). Risk Factors for Abnormal Hepatic Enzyme Elevation by Methotrexate Treatment in Patients with Rheumatoid Arthritis: A Hospital Based-Cohort Study. *Mod. Rheumatol.* 28 (3), 611–620. doi:10.1080/14397595.2017.1414765

Hawkey, C. J., Bosch, J., Richter, J. E., Garcia-Tsao, G., and Chan, F. K. L. (2012). "Abnormal Liver Function Tests," in *Textbook of Clinical Gastroenterology and Hepatology* (Wiley-Blackwell). doi:10.1002/9781118321386

Imanishi, H., Okamura, N., Yagi, M., Noro, Y., Moriya, Y., Nakamura, T., et al. (2007). Genetic Polymorphisms Associated with Adverse Events and Elimination of Methotrexate in Childhood Acute Lymphoblastic Leukemia and Malignant Lymphoma. *J. Hum. Genet.* 52 (2), 166–171. doi:10.1007/s10038-006-0096-z

Kantar, M., Kosova, B., Cetingul, N., Gumus, S., Toroslu, E., Zafer, N., et al. (2009). Methylenetetrahydrofolate Reductase C677T and A1298C Gene Polymorphisms and Therapy-Related Toxicity in Children Treated for Acute Lymphoblastic Leukemia and Non-hodgkin Lymphoma. *Leuk. Lymphoma* 50, 912–917. doi:10.1080/10428190902893819

Limdi, J. K., and Hyde, G. M. (2003). Evaluation of Abnormal Liver Function Tests. *Postgrad. Med. J.* 79 (932), 307–312. doi:10.1136/pmj.79.932.307

Lopez-Lopez, E., Martin-Guerrero, I., Ballesteros, J., Piñan, M. A., Garcia-Miguel, P., Navajas, A., et al. (2011). Polymorphisms of the SLCO1B1 Gene Predict Methotrexate-Related Toxicity in Childhood Acute Lymphoblastic Leukemia. *Pediatr. Blood Cancer* 57 (4), 612–619. doi:10.1002/pbc.23074

Lv, S., Fan, H., Li, J., Yang, H., Huang, J., Shu, X., et al. (2018). Genetic Polymorphisms of TYMS, MTHFR, ATIC, MTR, and MTRR Are Related to the Outcome of Methotrexate Therapy for Rheumatoid Arthritis in a Chinese Population. *Front. Pharmacol.* 9, 1390. doi:10.3389/fphar.2018.01390

Mcdonald, G. C . (2010). Ridge Regression[J]. *Wiley Interdiplinary Rev. Comput. Stats* 1 (1), 93–100.

Mikkelsen, T. S., Thorn, C. F., Yang, J. J., Ulrich, C. M., French, D., Zaza, G., et al. (2011). PharmGKB Summary: Methotrexate Pathway. *Pharmacogenet Genomics* 21, 679–686. doi:10.1097/FPC.0b013e328343dd93

Moghadam, A. R., Tutunchi, S., Namvaran-Abbas-Abad, A., Yazdi, M., Bonyadi, F., Mohajeri, D., et al. (2015). Pre-administration of Turmeric Prevents Methotrexate-Induced Liver Toxicity and Oxidative Stress. *BMC Complement. Altern. Med.* 15 (1), 246. doi:10.1186/s12906-015-0773-6

Moriyama, T., Relling, M. V., and Yang, J. J. (2015). Inherited Genetic Variation in Childhood Acute Lymphoblastic Leukemia. *Blood* 125, 3988–3995. doi:10.1182/blood-2014-12-580001

National Institute of Cancer (2009). *Common Terminology Criteria for Adverse Events (CTCAE) v4.0[J]*. National Institute of Health and Center for Biomedical Informatics and Information Technology. Available at: http://evs.nci.nih.gov/ftp1/CTCAE/About.html

Niemi, M., Pasanen, M. K., and Neuvonen, P. J. (2011). Organic Anion Transporting Polypeptide 1B1: a Genetically Polymorphic Transporter of Major Importance for Hepatic Drug Uptake. *Pharmacol. Rev.* 63, 157–181. doi:10.1124/pr.110.002857

Pantanowitz, A., and Marwala, T. (2009). Missing Data Imputation through the Use of the Random Forest Algorithm. *Adv. Comput. Intelligence* 116, 53–62. doi:10.1007/978-3-642-03156-4_6

Preethi, C. R. (2014). Clinico Haematological Study of Acute Lymphoblastic Leukemia[J]. *Glob. J. Med. Res.*

Schmiegelow, K. (2009). Advances in Individual Prediction of Methotrexate Toxicity: a Review. *Br. J. Haematol.* 146 (5), 489–503. doi:10.1111/j.1365-2141.2009.07765.x

Seidel, H., Moe, P. J., Nygaard, R., Nygaard, K., Brede, W., and Borsi, J. D. (1994). Evaluation of Serious Adverse Events in Patients Treated with Protocols Including Methotrexate Infusions. *Pediatr. Hematol. Oncol.* 11 (2), 165–172. doi:10.3109/08880019409141652

Tang, Y., Xu, X., Song, H., Yang, S., Shi, S., and Wei, J. (2008). Long-term Outcome of Childhood Acute Lymphoblastic Leukemia Treated in China. *Pediatr. Blood Cancer* 51 (3), 380–386. doi:10.1002/pbc.21629

Yang, L., Hu, X., and Xu, L. (2012). Impact of Methylenetetrahydrofolate Reductase (MTHFR) Polymorphisms on Methotrexate-Induced Toxicities in Acute Lymphoblastic Leukemia: a Meta-Analysis. *Tumour Biol.* 33 (5), 1445–1454. doi:10.1007/s13277-012-0395-2

Conflict of Interest: ZW, ZY, and FG are employed by Beijing Medicinovo Technology Co. Ltd. XH is employed by Dalian Medicinovo Technology Co. Ltd.

The remaining authors declare that the research was conducted in the absence of any commercial or financial relationships that could be construed as a potential conflict of interest.

frontiers in Oncology

MINI REVIEW
published: 11 October 2021
doi: 10.3389/fonc.2021.754891

Irinotecan-Induced Steatohepatitis: Current Insights

Jun Han[1,2], *Jing Zhang*[3] *and Chengliang Zhang*[1*]

[1] Tongji Hospital, Tongji Medical College, Huazhong University of Science and Technology, Wuhan, China, [2] Department of Pharmacy, Affiliated Hospital of Jianghan University, Wuhan, China, [3] Wuhan Red Cross Hospital, Wuhan, China

The hepatotoxicity of irinotecan is drawing wide concern nowadays due to the widespread use of this chemotherapeutic against various solid tumors, particularly metastatic colorectal cancer. Irinotecan-induced hepatotoxicity mainly manifests as transaminase increase and steatosis with or without transaminase increase, and is accompanied by vacuolization, and lobular inflammation. Irinotecan-induced steatohepatitis (IIS) increases the risk of morbidity and mortality in patients with colorectal cancer liver metastasis (CRCLM). The major risks and predisposing factors for IIS include high body mass index (BMI) or obesity, diabetes, and high-fat diet. Mitochondrial dysfunction and autophagy impairment may be involved in the pathogenesis of IIS. However, there is currently no effective preventive or therapeutic treatment for this condition. Thus, the precise mechanisms underlying the pathogenesis of IIS should be deciphered for the development of therapeutic drugs. This review summarizes the current knowledge and research progress on IIS.

Keywords: irinotecan, chemotherapy, hepatotoxicity, hepatic steatosis, steatohepatitis

OPEN ACCESS

Edited by:
Miao Yan,
Central South University, China

Reviewed by:
Yves Horsmans,
Cliniques Universitaires Saint-Luc, Belgium
Pegah Varamini,
The University of Sydney, Australia

****Correspondence:***
Chengliang Zhang
clzhang@tjh.tjmu.edu.cn

Specialty section:
This article was submitted to Pharmacology of Anti-Cancer Drugs, a section of the journal Frontiers in Oncology

Received: *07 August 2021*
Accepted: *23 September 2021*
Published: *11 October 2021*

Citation:
Han J, Zhang J and Zhang C (2021) Irinotecan-Induced Steatohepatitis: Current Insights. Front. Oncol. 11:754891. doi: 10.3389/fonc.2021.754891

INTRODUCTION

Irinotecan, also termed as CPT-11 or 7-ethyl-10-[4-(1-piperidino)-1-piperidino]-carbonyloxycamptothecine (**Figure 1**), is an inhibitor of DNA topoisomerase I and has been used for 27 years since it was first approved in Japan in 1994 (1). As a crucial chemotherapeutic agent, it is widely used either alone or in combination against various solid tumors, particularly for the treatment of metastatic colorectal cancer, as recommended by the guidelines of the National Comprehensive Cancer Network and the European Society for Medical Oncology (1, 2). Notably, irinotecan-based neoadjuvant chemotherapy has improved the five-year survival rate in colorectal cancer liver metastasis (CRCLM) with unresectable tumors by approximately 58% (3, 4). However, there is a growing realization that irinotecan-induced hepatotoxicity, such as hepatic steatosis and steatohepatitis, can increase the risk of morbidity and mortality in patients with CRCLM (5, 6). Although irinotecan-induced steatohepatitis (IIS) has been known to be a clinicopathological

Abbreviations: BMI, body mass index; CASH, chemotherapy-associated steatohepatitis; CRCLM, colorectal cancer liver metastasis; IIS, irinotecan-induced steatohepatitis; NAFLD, non-alcoholic fatty liver disease; PUFA, polyunsaturated fatty acids; ROS, reactive oxygen species; UGT1A1, uridine diphosphate-glucuronosyl transferase 1A1.

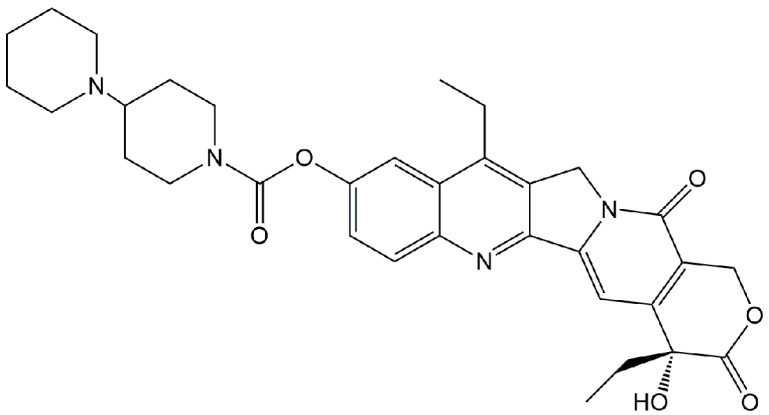

FIGURE 1 | The structure of irinotecan.

symptom of irinotecan for decades, the mechanisms underlying this adverse effect are not exactly known. This review provides current insights into the clinical understanding of the epidemiology, risk factors, possible causal mechanisms, as well as preventive and therapeutic approaches regarding IIS.

BRIEF DESCRIPTION OF IRINOTECAN

Irinotecan, which is a semi-synthetic and water-soluble camptothecin-derivative cytotoxic drug (2). It inhibits the DNA-topoisomerase I complex and causes DNA double-strand breaks, thereby inducing cytotoxicity (7, 8). As a prodrug, irinotecan is metabolized to the active metabolite SN-38, also termed as 7-ethyl-10-hydroxycamptothecin, in the blood and liver mainly by human carboxylesterase 2 (1, 9). Compared with irinotecan, SN-38 is a stronger inhibitor of DNA topoisomerase I (10, 11) and can induce lethal DNA double-strand breaks and eventually cell death (9, 11). SN-38 is inactivated upon its conversion into SN-38G (β-glucuronide conjugate) by uridine diphosphate-glucuronosyl transferase 1A1 (UGT1A1) in the liver. SN-38G can be converted back into SN-38 by bacterial β-glucuronidase in the intestinal tract, and the resulting SN-38 is absorbed into the systemic circulation, whereby the anti-tumor effect of irinotecan is extended (9, 12).

Unfortunately, irinotecan can non-specifically damage any rapidly proliferating cell, including both tumor cells and non-tumor cells, such as bone-marrow cells and intestinal basal cells, as well as the commensal bacteria in the body (1). Consequently, hematotoxicity (neutropenia) and gastrointestinal toxicity (diarrhea) are common irinotecan-induced toxicities (8), with a large inter-individual variation (1). In recent years, an increasing body of evidence has demonstrated that irinotecan-induced hepatotoxicity, including hepatic steatosis and steatohepatitis can increase the risk of morbidity and mortality in patients with CRCLM (6). Therefore, IIS is nowadays drawing increasing attention in clinical practice.

EPIDEMIOLOGY OF IIS

Long-term or high-dose administration of irinotecan may impair the liver parenchyma, thus leading to hepatotoxicity with or without transaminase increase (7, 13–16). There are numerous epidemiological reports on IIS, which mainly focus on patients with CRCLM. However, there are significant differences in IIS incidence among these studies. Morris-Stiff et al. summarized that up to 50% of patients with CRCLM who receive neoadjuvant irinotecan develop IIS (17). In a prospective study involving 45 patients with CRCLM who underwent hepatic resection, Gomez-Ramirez et al. observed that four out of the seven patients (57.2%) who had received neoadjuvant irinotecan developed IIS (18). Pawlik and colleagues analyzed 153 patients with CRCLM and reported that moderate or severe hepatic steatosis was dramatically more frequent in the patients who had received neoadjuvant irinotecan (n = 15, 27.3%) than in those without any chemotherapy (n = 2, 3.4%) or with 5-FU (n = 10, 14.9%) or oxaliplatin (n = 3, 9.6%) monotherapy (19). A meta-analysis found that one in every twelve patients with CRCLM under irinotecan-based regimens will ultimately develop IIS (20). By analyzing 406 patients with CRCLM who had undergone hepatic resection, Vauthey and co-workers showed that irinotecan is related to IIS (20.2% vs. 4.4% of the patients without chemotherapy) (21). Moreover, although liver biopsy, which is the gold standard in diagnosing steatosis or steatohepatitis (6), is recommended to diagnose IIS (22), sampling error and observational variations among pathologists can affect the diagnosis (23).

IIS is associated with the disruption of lipid homeostasis and with inflammation in hepatic cells. It may progressively increase the risk of fibrosis, cirrhosis and liver failure (24, 25), because irinotecan-based regimens have potentially harmful effects on liver parenchyma and associated with impaired liver regeneration (17, 26). Vauthey et al. found that IIS remarkably increased the 90-day mortality of patients with CRCLM (14.7% vs. 1.6% of those with no IIS) (21). The presence of IIS is more

concerning than simple steatosis when undergoing major liver resection and has been demonstrated to be associated with increased surgical morbidity and mortality after resection of colorectal liver metastases. Morris-Stiff and colleagues found that IIS is related to increased morbidity and possibly to increased mortality in patients with CRCLM following hepatectomy because of the development of liver failure (17). The detrimental effect of hepatic steatosis in patients undergoing liver resection was also demonstrated in a meta-analysis by Robinson et al. (20). Therefore, it is crucial to emphasize that careful consideration needs to be given when performing extensive procedures on patients with IIS.

RISK FACTORS FOR IIS

Multiple studies have found that confounding factors could impact the development of chemotherapy-associated steatohepatitis (CASH) (including IIS) (26–28). High body mass index (BMI) or obesity is closely related to an increased risk of CASH (14, 29). Patients with BMI ≥ 25 kg/m^2 under irinotecan-based chemotherapy have a 2.03-fold risk of IIS compared with those with BMI < 25 kg/m^2 (21). Another report by Ryan et al. noted that both IIS and hepatic steatosis are correlated with a BMI of ≥ 30 kg/m^2 (30). In a small cohort study, patients with a high BMI who had undergone irinotecan-based chemotherapy were found to be associated with a high IIS score according to the Brunt System (29). Fernandez et al. demonstrated that severe IIS is related to neoadjuvant irinotecan in patients, particularly obese patients, with CRCLM who had undergone hepatic resection (22). Animal experiments have shown that the decreased hepatic UGT1A1 and increased fecal β-glucuronidase levels in diet-induced obese mice compared with the levels in lean mice are responsible for the prolonged retention of SN-38, consequently increasing the occurrence of IIS, in these obese mice (31).

Diabetes may be another important risk factor for IIS. Wolf et al. demonstrated that hepatic steatosis or IIS is more common in diabetic patients treated with irinotecan-based regimens as neoadjuvant chemotherapy before hepatic resection of CRCLM (27). Moreover, a diet with high-fat content may also accelerate the development of IIS. A dietary study by Mallick et al. demonstrated that, upon irinotecan treatment, mice on a high-fat diet, such as lard, develop steatosis more easily than those on a regular diet (32). Although these reports are based on retrospective analyses or animal studies, the results indicate that, upon irinotecan-based chemotherapy, patients on a high-fat diet or with baseline obesity or diabetes may have a higher risk of developing IIS than non-diabetic and non-obese patients on a regular diet. However, this possibility should be verified *via* prospective controlled trials.

MECHANISMS UNDERLYING IIS

The exact mechanisms underlying IIS have not been fully elucidated. However, mitochondrial dysfunction and autophagy impairment have been proposed to be involved in the pathogenesis of IIS (**Figure 2**).

Mitochondrial Dysfunction

Hepatocytes are rich in mitochondria, which are vulnerable to chemotherapeutic agents (33–35). In general, inhibition of β-oxidation of fatty acids, oxidative phosphorylation, and mitochondrial respiration primarily contributes to mitochondrial dysfunction (7). Irinotecan causes accumulation of lipids in hepatocytes *via* inhibiting the β-oxidation of fatty acids, which is one of the main pathways of the lipid metabolism, in the mitochondria of hepatocytes (7, 25). Moreover, irinotecan induces oxidative stress by uncoupling oxidative phosphorylation, restraining mitochondrial respiration, and facilitating the mitochondrial release of reactive oxygen species (ROS) in

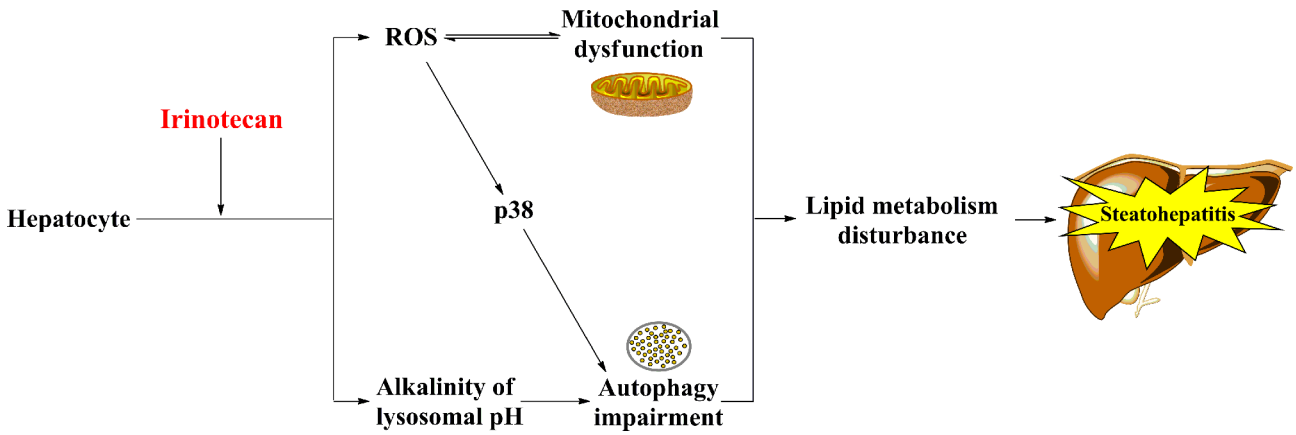

FIGURE 2 | The potential mechanisms of IIS. Irinotecan-caused mitochondrial dysfunction and autophagy impairment result in lipid metabolism disturbance ultimately, which may involve in the pathogenesis of IIS.

hepatocytes (7, 36). Interestingly, Bao et al. demonstrated that SN-38 upregulated ROS in cells derived from primary human hepatocytes but not in cancer cells (MDA-MB-231 and T47D) *in vitro* (8). Upregulation of ROS causes mitochondrial dysfunction (37) and stimulates the pathogenesis of IIS (14). It is worth noting that mitochondrial dysfunction usually improves when the chemotherapy is terminated (25).

Autophagy Impairment

Autophagy is a lysosome-mediated intracellular protein-degradation mechanism. It also regulates the lipid metabolism by metabolizing intracellular lipid droplets (triglycerides), which are the main form of lipid storage in the cell (38). Thus, impairment of this mechanism causes multiple metabolic diseases, such as obesity and hepatic steatosis (39). Mahli et al. found that irinotecan can weaken the autophagic flux by increasing the lysosomal pH to alkalinity, thereby contributing to lipid accumulation and steatosis in primary human hepatocytes (40). Furthermore, irinotecan impairs mitochondrial function and indirectly activates p38, thus inhibiting autophagosome formation (41, 42).

POTENTIAL PREVENTIVE AND THERAPEUTIC APPROACHES AGAINST IIS

In general, there is still a lack of effective preventive and therapeutic strategies against IIS due to its complex mechanism of pathogenesis. However, several preclinical studies for IIS have suggested potential interventional drugs or measures, as described below.

Silymarin

Silymarin is a hepatoprotective agent, and it is derived from the seeds of *Silybum marianum* (43). As a natural flavonoid, silymarin has antioxidative effects and can decrease the oxidative stress in the liver (44). A study by Marcolino et al. about the effect of silymarin on IIS in mice reported that silymarin has a dual effect; low-dosage (1.5 mg/kg) of silymarin prevents irinotecan-induced hepatic injury, such as steatosis, vacuolization, lobular inflammation, and fibrosis, by suppressing the inflammatory factors and oxidative stress in the liver, whereas high-dosage (150 mg/kg) of silymarin exacerbates IIS and increases the mortality (45). Thus, the mechanisms whereby silymarin at different dosages result in different effects remain to be explored, and the specific clinical effects need to be confirmed, in future studies.

Pioglitazone

Pioglitazone is a thiazolidinedione antidiabetic agent. It modulates the lipid metabolism and ameliorates the glycemic control in patients with type-2 diabetes *via* activating the peroxisome proliferator-activated receptor (46, 47). A study in rats demonstrated that pioglitazone has a hepatoprotective effect against chemotherapy (irinotecan and 5-fluorouracil)-induced steatohepatitis, but no effect on histopathological changes (24). Therefore, the hepatoprotective effect of pioglitazone against IIS should be further explored.

Sorafenib

Sorafenib, a multityrosine-kinase inhibitor, is used for the treatment of unresectable hepatocellular carcinoma and advanced renal cell carcinoma (48). Mahli and co-workers reported that sorafenib has a protective effect against IIS by decreasing irinotecan-induced ERK activation and pro-inflammatory gene expression in hepatocytes and murine models of IIS (40). Nevertheless, the hepatoprotective effect of sorafenib against IIS should be confirmed in patients *via* clinical studies.

Glycine

Glycine is a nonessential amino acid with remarkable protective effects against liver injury (49, 50). Mikalauskas et al. found that glycine markedly reduces the levels of transaminases and microvesicular steatosis in rats treated with FOLFIRI, presumably by inhibiting the activation of Kupffer cells and enhancing the hepatic microcirculation (51).

Grain-Based Chow Diet

Phytoestrogens (especially isoflavones) and polyunsaturated fatty acids (PUFA) in diet may be effective in suppressing non-alcoholic fatty liver disease (NAFLD) or IIS. Isoflavones can be beneficial against NAFLD by reducing the lipogenesis, lipolysis, and fat deposition in adipocytes (52, 53). PUFA can decrease hepatic storage of triglycerides and has a significant protective effect against hepatic steatosis (54). A dietary study by Mallick et al. reported that a grain-based chow diet, which included a low level of fat (vegetable-based, such as soybean oil, which is especially rich in PUFA) and high levels of carbohydrate (fiber), phytoestrogen, and protein, had a notably protective effect against irinotecan-induced mixed hepatic steatosis (micro & macrovesicular) in mice (32). Thus, similar dietary studies involving specific ingredients should be performed on cancer patients undergoing irinotecan treatment.

CONCLUSIONS

Overall, IIS is a crucial adverse effect of irinotecan and can increase the risk of morbidity and mortality in patients with CRCLM. The major risks and predisposing factors for IIS include high BMI or obesity, diabetes, and high-fat diet. Although mitochondrial dysfunction and autophagy impairment may be involved in the pathogenesis of IIS, the exact causal mechanisms of IIS have not been fully elucidated. Till now, liver biopsy is the gold standard in diagnosing hepatotoxicity, including IIS, but it is a highly invasive, complex, and painful operation. Thus, biomarkers of IIS, are urgently needed to precisely evaluate irinotecan-induced hepatotoxicity. Besides, we should explore more risk factors for the development of IIS which can help oncologists to identify the patients at risk. Furthermore, effective preventive and therapeutic approaches are still lacking. Potential interventional drugs or measures have been reported in multiple preclinical studies and the medications susceptible to be active in steatosis such as fibroblast growth factor 21 agonists, obeticholic acid or glucagon-like peptide-1 agonists deserve considerations. Thus, further investigations involving humans, especially clinical trials, are required to develop feasible preventive and therapeutic approaches against IIS.

AUTHOR CONTRIBUTIONS

CZ designed this work. JH and JZ wrote this manuscript. All authors contributed to the article and approved the submitted version.

FUNDING

This work was supported by grants from the scientific research project of Wuhan NO.6 hospital (No. LX19013 to JH).

REFERENCES

1. Bailly C. Irinotecan: 25 Years of Cancer Treatment. *Pharmacol Res* (2019) 148:104398. doi: 10.1016/j.phrs.2019.104398
2. Kciuk M, Marciniak B, Kontek R. Irinotecan-Still an Important Player in Cancer Chemotherapy: A Comprehensive Overview. *Int J Mol Sci* (2020) 21 (14):4919. doi: 10.3390/ijms21144919
3. Choti MA, Sitzmann JV, Tiburi MF, Sumetchotimetha W, Rangsin R, Schulick RD, et al. Trends in Long-Term Survival Following Liver Resection for Hepatic Colorectal Metastases. *Ann Surg* (2002) 235(6):759–66. doi: 10.1097/00000658-200206000-00002
4. Fernandez FG, Drebin JA, Linehan DC, Dehdashti F, Siegel BA, Strasberg SM. Five-Year Survival After Resection of Hepatic Metastases From Colorectal Cancer in Patients Screened by Positron Emission Tomography With F-18 Fluorodeoxyglucose (FDG-PET). *Ann Surg* (2004) 240(3):438–47; discussion 447-50. doi: 10.1097/01.sla.0000138076.72547.b1
5. Chun YS, Laurent A, Maru D, Vauthey JN. Management of Chemotherapy-Associated Hepatotoxicity in Colorectal Liver Metastases. *Lancet Oncol* (2009) 10(3):278–86. doi: 10.1016/S1470-2045(09)70064-6
6. Cai Z, Yang J, Shu X, Xiong X. Chemotherapy-Associated Hepatotoxicity in Colorectal Cancer. *J BUON* (2014) 19(2):350–6.
7. Schumacher JD, Guo GL. Mechanistic Review of Drug-Induced Steatohepatitis. *Toxicol Appl Pharmacol* (2015) 289(1):40–7. doi: 10.1016/j.taap.2015.08.022
8. Bao X, Wu J, Kim S, LoRusso P, Li J. Pharmacometabolomics Reveals Irinotecan Mechanism of Action in Cancer Patients. *J Clin Pharmacol* (2019) 59(1):20–34. doi: 10.1002/jcph.1275
9. Mathijssen RH, Loos WJ, Verweij J, Sparreboom A. Pharmacology of Topoisomerase I Inhibitors Irinotecan (CPT-11) and Topotecan. *Curr Cancer Drug Targets* (2002) 2(2):103–23. doi: 10.2174/1568009023333890
10. Li F, Jiang T, Li Q, Ling X. Camptothecin (CPT) and Its Derivatives Are Known to Target Topoisomerase I (Top1) as Their Mechanism of Action: Did We Miss Something in CPT Analogue Molecular Targets for Treating Human Disease Such as Cancer? *Am J Cancer Res* (2017) 7(12):2350–94.
11. Liu LF, Desai SD, Li TK, Mao Y, Sun M, Sim SP. Mechanism of Action of Camptothecin. *Ann N Y Acad Sci* (2000) 922:1–10. doi: 10.1111/j.1749-6632.2000.tb07020.x
12. Hasegawa Y, Ando Y, Ando M, Hashimoto N, Imaizumi K, Shimokata K. Pharmacogenetic Approach for Cancer Treatment-Tailored Medicine in Practice. *Ann N Y Acad Sci* (2006) 1086:223–32. doi: 10.1196/annals.1377.020
13. Pessaux P, Chenard MP, Bachellier P, Jaeck D. Consequences of Chemotherapy on Resection of Colorectal Liver Metastases. *J Visc Surg* (2010) 147(4):e193–201. doi: 10.1016/j.jviscsurg.2010.06.004
14. European Association for the Study of the Liver. Electronic address, C. Clinical Practice Guideline Panel, m. Panel and E. G. B. representative. EASL Clinical Practice Guidelines: Drug-Induced Liver Injury. *J Hepatol* (2019) 70(6):1222–61. doi: 10.1016/j.jhep.2019.02.014
15. Okusaka T, Ikeda M, Fukutomi A, Ioka T, Furuse J, Ohkawa S, et al. Phase II Study of FOLFIRINOX for Chemotherapy-Naive Japanese Patients With Metastatic Pancreatic Cancer. *Cancer Sci* (2014) 105(10):1321–6. doi: 10.1111/cas.12501
16. Chung MJ, Kim YJ, Park JY, Bang S, Song SY, Chung JB, et al. Prospective Phase II Trial of Gemcitabine in Combination With Irinotecan as First-Line Chemotherapy in Patients With Advanced Biliary Tract Cancer. *Chemotherapy* (2011) 57(3):236–43. doi: 10.1159/000328021
17. Morris-Stiff G, Tan YM, Vauthey JN. Hepatic Complications Following Preoperative Chemotherapy With Oxaliplatin or Irinotecan for Hepatic Colorectal Metastases. *Eur J Surg Oncol* (2008) 34(6):609–14. doi: 10.1016/j.ejso.2007.07.007
18. Gomez-Ramirez J, Martin-Perez E, Amat CG, Sanz IG, Bermejo E, Rodriguez A, et al. Influence of Pre-Surgical Chemotherapy on Liver Parenchyma and Post-Surgical Outcome of Patients Subjected to Hepatectomy Due to Colorectal Carcinoma Metastases. *Cir Esp* (2010) 88(6):404–12. doi: 10.1016/j.ciresp.2010.09.005
19. Pawlik TM, Olino K, Gleisner AL, Torbenson M, Schulick R, Choti MA. Preoperative Chemotherapy for Colorectal Liver Metastases: Impact on Hepatic Histology and Postoperative Outcome. *J Gastrointest Surg* (2007) 11(7):860–8. doi: 10.1007/s11605-007-0149-4
20. Robinson SM, Wilson CH, Burt AD, Manas DM, White SA. Chemotherapy-Associated Liver Injury in Patients With Colorectal Liver Metastases: A Systematic Review and Meta-Analysis. *Ann Surg Oncol* (2012) 19(13):4287–99. doi: 10.1245/s10434-012-2438-8
21. Vauthey JN, Pawlik TM, Ribero D, Wu TT, Zorzi D, Hoff PM, et al. Chemotherapy Regimen Predicts Steatohepatitis and an Increase in 90-Day Mortality After Surgery for Hepatic Colorectal Metastases. *J Clin Oncol* (2006) 24(13):2065–72. doi: 10.1200/JCO.2005.05.3074
22. Fernandez FG, Ritter J, Goodwin JW, Linehan DC, Hawkins WG, Strasberg SM. Effect of Steatohepatitis Associated With Irinotecan or Oxaliplatin Pretreatment on Resectability of Hepatic Colorectal Metastases. *J Am Coll Surg* (2005) 200(6):845–53. doi: 10.1016/j.jamcollsurg.2005.01.024
23. Fiorini RN, Kirtz J, Periyasamy B, Evans Z, Haines JK, Cheng G, et al. Development of an Unbiased Method for the Estimation of Liver Steatosis. *Clin Transplant* (2004) 18(6):700–6. doi: 10.1111/j.1399-0012.2004.00282.x
24. Celik S, Kartal K, Ozseker H, Hayran M, Hamaloglu E. Hepatoprotective Effect of Pioglitazone in Cases of Chemotherapy Induced Steatohepatitis. *Chirurgia (Bucur)* (2015) 110(1):49–55.
25. Meunier L, Larrey D. Chemotherapy-Associated Steatohepatitis. *Ann Hepatol* (2020) 19(6):597–601. doi: 10.1016/j.aohep.2019.11.012
26. Bower M, Wunderlich C, Brown R, Scoggins CR, McMasters KM, Martin RC. Obesity Rather Than Neoadjuvant Chemotherapy Predicts Steatohepatitis in Patients With Colorectal Metastasis. *Am J Surg* (2013) 205(6):685–90. doi: 10.1016/j.amjsurg.2012.07.034
27. Wolf PS, Park JO, Bao F, Allen PJ, DeMatteo RP, Fong Y, et al. Preoperative Chemotherapy and the Risk of Hepatotoxicity and Morbidity After Liver Resection for Metastatic Colorectal Cancer: A Single Institution Experience. *J Am Coll Surg* (2013) 216(1):41–9. doi: 10.1016/j.jamcollsurg.2012.08.030
28. Pathak S, Tang JM, Terlizzo M, Poston GJ, Malik HZ. Hepatic Steatosis, Body Mass Index and Long Term Outcome in Patients Undergoing Hepatectomy for Colorectal Liver Metastases. *Eur J Surg Oncol* (2010) 36(1):52–7. doi: 10.1016/j.ejso.2009.09.004
29. Zorzi D, Laurent A, Pawlik TM, Lauwers GY, Vauthey JN, Abdalla EK. Chemotherapy-Associated Hepatotoxicity and Surgery for Colorectal Liver Metastases. *Br J Surg* (2007) 94(3):274–86. doi: 10.1002/bjs.5719
30. Ryan P, Nanji S, Pollett A, Moore M, Moulton CA, Gallinger S, et al. Chemotherapy-Induced Liver Injury in Metastatic Colorectal Cancer: Semiquantitative Histologic Analysis of 334 Resected Liver Specimens Shows That Vascular Injury But Not Steatohepatitis Is Associated With Preoperative Chemotherapy. *Am J Surg Pathol* (2010) 34(6):784–91. doi: 10.1097/PAS.0b013e3181dc242c
31. Mallick P, Shah P, Gandhi A, Ghose R. Impact of Obesity on Accumulation of the Toxic Irinotecan Metabolite, SN-38, in Mice. *Life Sci* (2015) 139:132–8. doi: 10.1016/j.lfs.2015.08.017
32. Mallick P, Shah P, Ittmann MM, Trivedi M, Hu M, Gao S, et al. Impact of Diet on Irinotecan Toxicity in Mice. *Chem Biol Interact* (2018) 291:87–94. doi: 10.1016/j.cbi.2018.06.018
33. Begriche K, Massart J, Robin MA, Borgne-Sanchez A, Fromenty B. Drug-Induced Toxicity on Mitochondria and Lipid Metabolism: Mechanistic Diversity and Deleterious Consequences for the Liver. *J Hepatol* (2011) 54 (4):773–94. doi: 10.1016/j.jhep.2010.11.006
34. Degli Esposti D, Hamelin J, Bosselut N, Saffroy R, Sebagh M, Pommier A, et al. Mitochondrial Roles and Cytoprotection in Chronic Liver Injury. *Biochem Res Int* (2012) 2012:387626. doi: 10.1155/2012/387626

35. McWhirter D, Kitteringham N, Jones RP, Malik H, Park K, Palmer D. Chemotherapy Induced Hepatotoxicity in Metastatic Colorectal Cancer: A Review of Mechanisms and Outcomes. *Crit Rev Oncol Hematol* (2013) 88 (2):404–15. doi: 10.1016/j.critrevonc.2013.05.011
36. Labbe G, Pessayre D, Fromenty B. Drug-Induced Liver Injury Through Mitochondrial Dysfunction: Mechanisms and Detection During Preclinical Safety Studies. *Fundam Clin Pharmacol* (2008) 22(4):335–53. doi: 10.1111/j.1472-8206.2008.00608.x
37. Fromenty B, Robin MA, Igoudjil A, Mansouri A, Pessayre D. The Ins and Outs of Mitochondrial Dysfunction in NASH. *Diabetes Metab* (2004) 30 (2):121–38. doi: 10.1016/S1262-3636(07)70098-8
38. Saito T, Kuma A, Sugiura Y, Ichimura Y, Obata M, Kitamura H, et al. Autophagy Regulates Lipid Metabolism Through Selective Turnover of Ncor1. *Nat Commun* (2019) 10(1):1567. doi: 10.1038/s41467-019-08829-3
39. Khawar MB, Gao H, Li W. Autophagy and Lipid Metabolism. *Adv Exp Med Biol* (2019) 1206:359–74. doi: 10.1007/978-981-15-0602-4_17
40. Mahli A, Saugspier M, Koch A, Sommer J, Dietrich P, Lee S, et al. ERK Activation and Autophagy Impairment Are Central Mediators of Irinotecan-Induced Steatohepatitis. *Gut* (2018) 67(4):746–56. doi: 10.1136/gutjnl-2016-312485
41. Corcelle E, Djerbi N, Mari M, Nebout M, Fiorini C, Fenichel P, et al. Control of the Autophagy Maturation Step by the MAPK ERK and P38: Lessons From Environmental Carcinogens. *Autophagy* (2007) 3(1):57–9. doi: 10.4161/auto.3424
42. Wu D, Cederbaum AI. Inhibition of Autophagy Promotes CYP2E1-Dependent Toxicity in Hepg2 Cells via Elevated Oxidative Stress, Mitochondria Dysfunction and Activation of P38 and JNK MAPK. *Redox Biol* (2013) 1:552–65. doi: 10.1016/j.redox.2013.10.008
43. Tvrdy V, Pourova J, Jirkovsky E, Kren V, Valentova K, Mladenka P. Systematic Review of Pharmacokinetics and Potential Pharmacokinetic Interactions of Flavonolignans From Silymarin. *Med Res Rev* (2021) 41 (4):2195–246. doi: 10.1002/med.21791
44. Ghiasian M, Nafisi H, Ranjbar A, Mohammadi Y, Ataei S. Antioxidative Effects of Silymarin on the Reduction of Liver Complications of Fingolimod in Patients With Relapsing-Remitting Multiple Sclerosis: A Clinical Trial Study. *J Biochem Mol Toxicol* (2021) 35(8):e22800. doi: 10.1002/jbt.22800
45. Marcolino Assis-Junior E, Melo AT, Pereira VBM, Wong DVT, Sousa NRP, Oliveira CMG, et al. Dual Effect of Silymarin on Experimental non-Alcoholic Steatohepatitis Induced by Irinotecan. *Toxicol Appl Pharmacol* (2017) 327:71–9. doi: 10.1016/j.taap.2017.04.023
46. Leclercq IA, Lebrun VA, Starkel P, Horsmans YJ. Intrahepatic Insulin Resistance in a Murine Model of Steatohepatitis: Effect of Ppargamma Agonist Pioglitazone. *Lab Invest* (2007) 87(1):56–65. doi: 10.1038/labinvest.3700489
47. Laplante M, Festuccia WT, Soucy G, Gelinas Y, Lalonde J, Berger JP, et al. Mechanisms of the Depot Specificity of Peroxisome Proliferator-Activated Receptor Gamma Action on Adipose Tissue Metabolism. *Diabetes* (2006) 55 (10):2771–8. doi: 10.2337/db06-0551
48. Abdelgalil AA, Alkahtani HM, Al-Jenoobi FI. Sorafenib. *Profiles Drug Subst Excip Relat Methodol* (2019) 44:239–66. doi: 10.1016/bs.podrm.2018.11.003
49. Zhong Z, Wheeler MD, Li X, Froh M, Schemmer P, Yin M, et al. L-Glycine: A Novel Antiinflammatory, Immunomodulatory, and Cytoprotective Agent. *Curr Opin Clin Nutr Metab Care* (2003) 6(2):229–40. doi: 10.1097/00075197-200303000-00013
50. Luntz SP, Unnebrink K, Seibert-Grafe M, Bunzendahl H, Kraus TW, Buchler MW, et al. HEGPOL: Randomized, Placebo Controlled, Multicenter, Double-Blind Clinical Trial to Investigate Hepatoprotective Effects of Glycine in the Postoperative Phase of Liver Transplantation [ISRCTN69350312]. *BMC Surg* (2005) 5:18. doi: 10.1186/1471-2482-5-18
51. Mikalauskas S, Mikalauskiene L, Bruns H, Nickkholgh A, Hoffmann K, Longerich T, et al. Dietary Glycine Protects From Chemotherapy-Induced Hepatotoxicity. *Amino Acids* (2011) 40(4):1139–50. doi: 10.1007/s00726-010-0737-6
52. Torre-Villalvazo I, Tovar AR, Ramos-Barragan VE, Cerbon-Cervantes MA, Torres N. Soy Protein Ameliorates Metabolic Abnormalities in Liver and Adipose Tissue of Rats Fed a High Fat Diet. *J Nutr* (2008) 138(3):462–8. doi: 10.1093/jn/138.3.462
53. Lephart ED, Porter JP, Lund TD, Bu L, Setchell KD, Ramoz G, et al. Dietary Isoflavones Alter Regulatory Behaviors, Metabolic Hormones and Neuroendocrine Function in Long-Evans Male Rats. *Nutr Metab (Lond)* (2004) 1(1):16. doi: 10.1186/1743-7075-1-16
54. Levy JR, Clore JN, Stevens W. Dietary N-3 Polyunsaturated Fatty Acids Decrease Hepatic Triglycerides in Fischer 344 Rats. *Hepatology* (2004) 39 (3):608–16. doi: 10.1002/hep.20093

Conflict of Interest: The authors declare that the research was conducted in the absence of any commercial or financial relationships that could be construed as a potential conflict of interest.

Publisher's Note: All claims expressed in this article are solely those of the authors and do not necessarily represent those of their affiliated organizations, or those of the publisher, the editors and the reviewers. Any product that may be evaluated in this article, or claim that may be made by its manufacturer, is not guaranteed or endorsed by the publisher.

frontiers in Oncology

ORIGINAL RESEARCH
published: 21 October 2021
doi: 10.3389/fonc.2021.757196

Edited by:
Miao Yan,
Central South University, China

Reviewed by:
Xianglin Du,
University of Texas Health Science Center at Houston, United States
Biswajit Dubashi,
Jawaharlal Institute of Postgraduate Medical Education and Research (JIPMER), India

***Correspondence:**
Chengliang Zhang
clzhang@tjh.tjmu.edu.cn
Dong Liu
ld2069@outlook.com

†These authors have contributed equally to this work and share first authorship

Specialty section:
This article was submitted to Pharmacology of Anti-Cancer Drugs, a section of the journal Frontiers in Oncology

Received: *11 August 2021*
Accepted: *06 October 2021*
Published: *21 October 2021*

Citation:
Yu Z, Huang R, Zhao L, Wang X, Shangguan X, Li W, Li M, Yin X, Zhang C and Liu D (2021) Safety Profile of Oxaliplatin in 3,687 Patients With Cancer in China: A Post-Marketing Surveillance Study. Front. Oncol. 11:757196. doi: 10.3389/fonc.2021.757196

Safety Profile of Oxaliplatin in 3,687 Patients With Cancer in China: A Post-Marketing Surveillance Study

Zaoqin Yu[1†], Rui Huang[2†], Li Zhao[3], Ximin Wang[1], Xiaofang Shangguan[2], Wei Li[1], Min Li[1], Xianguo Yin[3], Chengliang Zhang[1] and Dong Liu[1*]*

[1] Department of Pharmacy, Tongji Hospital, Tongji Medical College, Huazhong University of Science and Technology, Wuhan, China, [2] School of Pharmacy, Tongji Medical College, Huazhong University of Science and Technology, Wuhan, China, [3] Hubei Center for Adverse Drug Reaction Monitoring, Wuhan, China

Background: Oxaliplatin (OXA), a third-generation platinum derivative, has become one of the main chemotherapeutic drugs for colorectal cancer and other cancers, but reports of adverse reactions are also increasing with the extensive application of OXA. In this study, post-marketing surveillance was carried out to investigate the safety profile of OXA in a real-world setting in Chinese cancer patients to provide a reference for the rational application of OXA.

Methods: All patients with cancer who received OXA-based chemotherapy in 10 tertiary hospitals in Hubei Province, China, between May 2016 and November 2016 were enrolled. A central registration method was used to document patients' demographics, clinical use, and any incidence of adverse reactions to OXA. All adverse drug reactions (ADRs) were collected and analyzed to assess causality, severity, treatment, and outcome.

Results: In total, 3687 patients were enrolled in this study. Approximately 64.6% of the patients were male, and 68.8% were aged 50-70 years, with a mean age of 55.3 years. The proportions of patients diagnosed with colorectal and gastric cancers were 59.3% and 31.6%, respectively. In this study, the overall incidence of ADRs and serious ADRs was 42.7% and 1.3%, respectively. The most common ADRs were gastrointestinal disorders (25.7%), blood disorders (21.1%), and peripheral nervous system disorders

(8.0%). The serious ADRs identified were hypersensitivity reactions, thrombocytopenia, abnormal hepatic function, and leukopenia/neutropenia. The median onset of gastrointestinal toxicity, myelosuppression, peripheral neurotoxicity, and abnormal hepatic function was 1 d, 5 d, 1 d, and 14 d, respectively. The majority (84.7%) of hypersensitivity reactions were mild to moderate, and the median time to onset of these reactions was within the first 20 min of OXA infusion. Almost 88.0% of patients who experienced ADRs recovered or improved with treatment.

Conclusion: Our data suggest that OXA-induced ADRs are very common in Chinese patients with cancer; however, more attention should be paid to hypersensitivity reactions caused by OXA. This study provides a valuable reference regarding the safe application of OXA in a real-world setting.

Keywords: oxaliplatin, cancer, post-marketing surveillance, safety, Chinese

INTRODUCTION

Oxaliplatin (OXA) is a third-generation platinum-based anti-tumor drug that inhibits DNA and protein synthesis by forming intra- and inter-strand DNA platinum adducts, leading to tumor growth inhibition and apoptosis (1). OXA has better efficacy and lower toxicity than cisplatin and carboplatin (2) and is extensively used in various tumors, including colorectal, gastroesophageal, pancreatic, biliary, gynecologic malignancies, lung cancer and head and neck cancers (3–5). Studies have demonstrated that OXA combined with 5-fluorouracil (5-FU) and leucovorin increases survival and reduces the risk of recurrence in patients with colorectal cancer (CRC) (6, 7). Nowadays, OXA combined with 5-FU and leucovorin (FOLFOX) or with capecitabine (XELOX) has emerged as the standard regimen of adjuvant chemotherapy for stage III CRC and stage II CRC with high-risk factors and as the first-line regimen for metastatic CRC (8, 9).

With the extensive clinical application of OXA, adverse reactions towards OXA have also been reported in recent years, mainly including gastrointestinal side effects, hematologic toxicities, and dose-limiting peripheral neurotoxicity (10–12). Moreover, the reports on OXA-related hypersensitivity reactions (HSRs) are increasing gradually (13). Although OXA has been on the market for over 20 years, and there have been a few reports on its side effects, comprehensive safety profiles of OXA in large-scale populations in the real world have rarely been produced. The MOSAIC trial, a large randomized multi-institution randomized trial, only included over 1,100 patients who were receiving adjuvant FOLFOX chemotherapy for colorectal cancer (14). Thus, it is necessary to evaluate the post-marketing safety of OXA further to strengthen pharmacovigilance. In this article, a multicenter prospective study was carried out in 10 tertiary hospitals in Hubei province, China, to evaluate the post-marketing safety profile of OXA. We aimed to investigate the clinical use of OXA, the incidence of adverse reactions, time to onset, clinical manifestations, treatments, and outcomes to provide a reference for medical decision-making and the rational application of OXA.

METHODS

Study Design and Patients

This multicenter observational study was conducted in 10 tertiary hospitals in Hubei Province, China, between May 2016 and November 2016. All patients with malignant tumors treated with OXA were enrolled in this study. All patients were prospectively registered upon initiation of OXA treatment by documenting the patients' demographics, clinical application, and adverse reactions of OXA using a central monitor method.

The investigators received unified and standardized project training according to research work manual and case report forms (CRF) (**Supplementary Table 1**) before the study to ensure complete registration and quality data. Meanwhile, each subcenter designated special personnel (including one oncologist and one clinical pharmacist) responsible for the collection and filing of CRF. This study was conducted in accordance with the Drug Reevaluation Regulations and Guiding Principles from the Drug Evaluation Center of the State Food and Drug Administration and was approved by the Ethics Committee of Tongji Medical College, Huazhong University of Science and Technology (No.TJIRB20160504). All participants were briefed and have provided written informed consent before completing the survey.

Safety Assessment

OXA-induced ADRs were collected through patients' self-reports (especially some symptoms such as rash, cough, nausea, vomiting, abdominal pain, numbness and dizziness) during ward round and patient education as well as lab results (such as vital signs, blood routine, liver and kidney function) from HIS system, and the frequency was usually 3 times a week. The investigators needed to report all adverse reactions that occurred after OXA treatment, concomitant medications used, time to onset, symptoms, administered treatments, and outcomes. All reported ADRs were recorded according to the Provisions of Adverse Drug Reaction Reporting and Monitoring with the clinical pharmacists' assessment of causality.

This adverse reaction can be submitted only when the ADR correlation evaluation with OXA is possible or above. The severity of OXA-induced ADRs was classified according to the National Cancer Institute Common Criteria (NCI-CTCAE v5.0), and grade 3 and above adverse reactions were defined as serious ADRs. ADRs were classified using the preferred terms and system organ classes from the World Health Organization (WHO) Glossary of Adverse Drug Reactions. Additional information, such as the results of laboratory tests, was also recorded for serious ADRs.

Statistical Analysis

More than 3000 patients receiving OXA were enrolled to detect an ADR in one out of every 1000 patients with a probability of ≥95%. The collected data were verified and encoded by special personnel. All data analyses were performed using SPSS version 24.0 (SPSS Inc. Chicago, IL, USA). Descriptive analysis was used to evaluate patients' demographics (such as sex and age), clinical characteristics such as Karnofsky performance status (KPS), diagnosis, clinical use of OXA, and the incidence of adverse reactions, time to onset, symptoms, administered treatments, and outcomes.

RESULTS

Patient Demographics

A total of 3775 case report forms were enrolled between May 1, 2016, and November 31, 2016. Eighty-eight reports were excluded due to duplication; thus, 3687 patients were enrolled for this safety study. **Table 1** describes the patient demographics and clinical characteristics. Nearly 64.6% of patients were male, and most patients were between 40 and 70 years old (86.5%), with a mean (SD) age of 55.3 (± 10.6) years. Most patients had KPS scores of 80 (40.4%) and 90 (36.7%). Almost all (96.2%) patients were diagnosed with gastrointestinal cancer, with 59.3% and 31.6% of these patients diagnosed with colorectal and gastric cancer, respectively. Nearly two-thirds (61.7%) of the patients used the FOLFOX regimen, followed by the XELOX (19.5%) and SOX (S-1 plus OXA) (7.5%) regimens. About 25.5% of the patients had other diseases such as hypertension, hyperlipidemia, diabetes, coronary heart disease, kidney stones, and tuberculosis. Only 0.8% of the patients had a history of allergies, and 5.9% had a previous history of ADRs, mainly caused by antibiotics.

Incidence of ADRs and Serious ADRs

Of the 3687 patients, ADRs were reported in 1575 patients, giving an incidence rate of 42.7%. Most ADRs were grade 1 and 2, with grade 1 ADR reported in 562 patients (15.2%) and grade 2 ADR reported in 965 patients (26.2%). Serious ADRs (grade≥3) were reported in 48 patients (1.3%), showed in **Figure 1**. The majority (88.0%) of patients who developed ADR were healed and improved, and about 11.0% were unknown.

The most commonly reported ADRs fell into the general categories of gastrointestinal disorders (25.7%), blood disorders (21.1%), and peripheral nervous system disorders (8.0%) (**Table 2**). Other ADRs, such as respiratory, cardiac and eye disorders, had a low incidence rate and low severity (**Table 2**). However, systemic disorders such as hypersensitivity reactions occurred in 118 of the patients (3.2%), with related serious ADRs accounting for 0.5% of all cases. In addition, hepatic function abnormalities were reported in 186 patients (5.1%), with serious ADRs of this nature accounting for 0.2% of all cases (**Table 2**).

Most Frequently-Occurring ADRs

The OXA-linked ADRs with the highest frequency were nausea (20.3%), leukopenia (17.3%), neutropenia (12.1%), vomiting (9.8%), anemia (7.0%), thrombocytopenia (5.6%), and peripheral paresthesia or dysesthesia of hands and feet (5.7%). Meanwhile, the most frequent serious ADRs recorded were hypersensitivity reactions, leukopenia, neutropenia, thrombocytopenia, abnormal hepatic function, and vomiting (0.5%, 0.2%, 0.2%, 0.2%, 0.2%, 0.1%, respectively) (**Table 3**). Thus, gastrointestinal disorders, blood disorders, peripheral nervous system disorders, hypersensitivity reactions, and hepatic function abnormalities were regarded as the major ADRs caused by OXA.

Time to Onset, Management, and Outcome of Major ADRs

The median time from the start of OXA administration to the occurrence of gastrointestinal disorders, blood system disorders, peripheral nervous system disorders, and hepatic function abnormalities were 1 d, 5 d, 1 d, and 14 d, respectively. For hypersensitivity reactions, the median time from start to occurrence was much shorter, at only 20 min. In addition, the above 5 ADRs occurred in a median cycle of OXA chemotherapy of 3, 4, 4, 4 and 6, respectively. More than 90% of those who experienced gastrointestinal toxicity, myelosuppression, and peripheral neurotoxicity continued OXA therapy. Of those that experienced hypersensitivity reactions, approximately 85% suspended OXA administration and received the corresponding treatment (**Table 4**). Overall, most of these ADRs recovered and improved, and ADRs that had sequelae occurred in 11 patients who experienced hepatic dysfunction and 12 patients with myelosuppression.

OXA-Related Hypersensitivity Reactions

The manifestation of OXA-related HSRs is shown in **Table 5**. The most common events were cutaneous symptoms such as flushing (48.3%), itching (48.3%), and rashes (22.9%). For most patients (84.7%), the symptoms were grade 1 or 2, while hypersensitivity symptoms with grade ≥ 3 were reported in 18 patients (15.2%). Of these 18 patients, six experienced anaphylactic shock, characterized by wheezing, dizziness, abdominal pain, or loss of consciousness with hypotension.

The time between OXA infusion to the appearance of HSRs is shown in **Figure 2**, with most reactions occurring within the first hour. The time to onset varied between mild and severe cases: the median time to onset of grade 1 HSRs was 60 min, while grade 2, 3, and 4 events occurred mainly within the first 20 min after OXA infusion (**Table 5**). Most patients who experienced hypersensitivity (84.7%) were managed *via* discontinuation of

TABLE 1 | Patient demographics and baseline characteristics.

Characteristics	n = 3687 n (%)
Sex	
Male	2382 (64.6)
Female	1305 (35.4)
Age (years)	
20-29	112 (3.0)
30-39	185 (5.0)
40-49	651 (17.7)
50-59	1326 (36.0)
60-69	1211 (32.8)
≥70	202 (5.5)
KPS score	
100	379 (10.3)
95	17 (0.5)
90	1352 (36.7)
85	324 (8.8)
80	1490 (40.4)
70	94 (2.5)
60	11 (0.3)
Missing and wrong entry	4 (0.1)
Histology or cytology	
Colorectal cancer	2187 (59.3)
Gastric cancer	1166 (31.6)
Liver cancer	114 (3.1)
Esophageal cancer	56 (1.5)
Pancreatic cancer	24 (0.7)
other	140 (3.8)
Complication	
Yes	940 (25.5)
No	2747 (74.5)
OXA- based chemotherapy	
FOLFOX	2274 (61.7)
FOLFOXIRI	10 (0.3)
XELOX	718 (19.5)
GEMOX	39 (1.1)
SOX	278 (7.5)
EOX	2 (0.1)
Others	366 (9.3)
History of Allergy	
Yes	31 (0.8)
No	3656 (99.2)
Previous history of ADRs	
Yes	219 (5.9)
No	2915 (79.1)
Unknown	553 (15.0)

treatment with OXA and the administration of hypersensitivity treatments, including dexamethasone (61.0%), histamine-receptor 1 antagonist (51.7%), oxygen (28.8%), and epinephrine (8.5%). All patients recovered or improved after the corresponding symptomatic treatment (**Table 4**).

DISCUSSION

According to the 2018 Global Cancer Statistics, colorectal and gastric cancer incidence rates rank third and fourth among malignancies in China, and their mortality rate is placing fifth and second respectively (15). OXA, a third-generation platinum derivative, has become one of the mainstay chemotherapeutic drugs in gastrointestinal malignancies. The most common adverse reactions reported with this drug are gastrointestinal tract reactions, myelosuppression, peripheral neurotoxicity, and hypersensitivity reactions (14, 16). Hence, a multicenter observational study was carried out to investigate the safety profile of OXA in a real-world setting to provide a reference for the rational use of OXA.

In this study, 3687 patients who received OXA were enrolled. As far as we can confirm, at present, this is the largest real-world post-marketing safety evaluation of OXA in China. The majority (64.6%) of enrolled patients were male, within the age bracket of 50 to 69 years old. Epidemiology shows that the incidence rate of colorectal and gastric cancer in males is higher than in females, and most of these occur in middle-aged and older people (17). Thus, the characteristics of patients enrolled were consistent with previous epidemiological studies of colorectal and gastric cancer in China.

Moreover, this study showed that patients receiving OXA were mainly diagnosed with colorectal and gastric cancer (59.3% and 31.6%, respectively), and FOLFOX was the most commonly used chemotherapy regimen (61.7%), followed by XELOX (19.5%) and SOX (7.5%). According to NCCN guidelines of colorectal and gastric cancer (18, 19), FOLFOX and XELOX are the most popular chemotherapy regimens in colorectal cancer, which are widely used in neoadjuvant chemotherapy, adjuvant chemotherapy, and advanced palliative chemotherapy; XELOX and SOX are also frequently used chemotherapy regimens in gastric cancer. These suggest that the clinical application of OXA is in line with the recommendations described in these above guidelines.

Regarding the safety results, the overall incidence rate of ADRs was 42.7%, and that of serious ADRs was 1.3%. The most common reported ADRs of OXA in this study were gastrointestinal disorders (25.7%), blood disorders (21.1%), and peripheral nervous system disorders (8.0%), which were consistent with the results of other studies (14, 16, 20, 21).

Nausea, vomiting, and diarrhea were the most common gastrointestinal side effects of OXA, with a median time of onset of 1.6 d, and most patients recovered or improved quickly. Nausea and vomiting are usually mild to moderate and are readily controlled with the prophylactic administration of standard antiemetics such as dexamethasone or 5-HT3 receptor antagonists (22). Grade 1 and 2 diarrhea has been reported in OXA-treated patients with advanced colorectal cancer. The incidence of this ADR is usually higher with a protracted continuous infusion or with very high infusion doses (23). In practice, prophylaxis is not required, and the OXA dose should only be reduced in subsequent cycles if diarrhea becomes severe.

In general, hematological side effects caused by OXA include leukopenia, neutropenia, thrombocytopenia, and anemia (24). In our study, the prevalence of OXA-induced myelosuppression was 21.1%. Leukopenia (17.3%), neutropenia (12.1%), anemia (7.0%), and thrombocytopenia (5.6%) were also common hematological side effects of OXA treatment. Therefore, any patient treated with OXA should closely monitor their WBC count, platelet levels, hemoglobin levels, and absolute

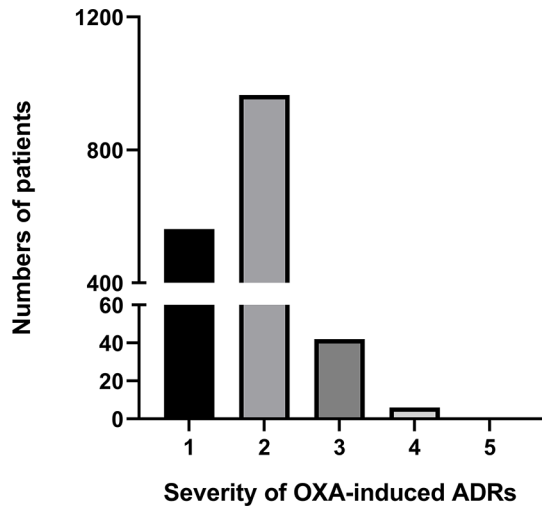

FIGURE 1 | Severity classification of OXA induced ADRs.

neutrophil count (ANC). Moreover, this study showed that thrombocytopenia was a common serious ADR, with an incidence of 0.2%, and the median time of onset from OXA treatment to this event was 4.7 d. Studies have demonstrated that thrombocytopenia was a prominent side effect of OXA-related myelosuppression (25, 26). Although thrombocytopenia of grades 3 and 4 was noted in only 3%-4% of patients exposed to OXA, its toxicity tends to increase with repeated exposures and may limit the benefits of OXA (25, 27). Recently, mechanisms of OXA-induced thrombocytopenia have emerged, including bone marrow suppression, immune-dependent mechanism, and splenic sequestration of platelets due to portal hypertension related to liver sinusoidal injury (11). However, in our study, it was difficult to determine the specific mechanism involved in OXA-induced thrombocytopenia; thus, this condition needs further study. Therefore, medical practitioners should be vigilant about thrombocytopenia caused by splenomegaly after long-term exposure to OXA and be aware of allergy-induced acute thrombocytopenia (28).

A major dose-limiting side-effect of OXA treatment is its peripheral neurotoxicity. Our study showed that OXA-induced peripheral neurotoxicity (OIPN) was reported in 266 patients (8.0%), mainly including paresthesias or dysesthesias of the hands and feet. Most reported OIPN cases were mild, and 96.6% of patients recovered or improved, with the median time to onset of 1 d. OXA induces two clinically distinct forms of peripheral neuropathy. The first is acute OIPN, which is transient, appearing only during or shortly after infusion of OXA, and can be triggered by cold stimulation. The other form, chronic OIPN, is associated with a cumulative dose of OXA and appears after administration of OXA at a total dose of 540-850 mg/m^2 (12). Acute OIPN consists mainly of sensory symptoms in the form of paresthesias or dysesthesias in the distal or perioral regions and are related to the dosage and infusion rate of OXA. These symptoms are generally mild, short-lived, and completely reversible within a few hours or days (29). Thus, oncologists can prolong the duration of OXA infusion up to 6 h and request that their patients avoid cold liquids for several days after OXA therapy, which may prevent the development of acute OIPN.

While not as common as the previously discussed ADRs, hepatotoxicity also represents a serious ADR that warrants further investigation. There is evidence that the most common type of hepatotoxicity associated with OXA administration is hepatic sinusoidal injury. It is histologically characterized by sinusoidal dilatation, hepatocyte necrosis, and obliteration of hepatic venules due to sinusoidal endothelial cell damage (30–32). OXA-induced hepatic sinusoidal obstruction syndrome (HSOS) has been demonstrated in up to 77% of colorectal cancer patients with liver metastasis following OXA-based chemotherapy (33). Studies have reported that preoperative OXA was associated with HSOS and that this increased postoperative morbidity after partial hepatectomy with colorectal cancer liver metastasisn (34, 35). OXA-induced HSOS frequently presents with ascites, jaundice, right

TABLE 2 | Incidence of ADRs and serious ADRs in patients receiving OXA (N = 3687).

System Organ Class	ADRs n (%)	Serious ADRs n (%)
Total	1575 (42.7)	48 (1.3)
Gastrointestinal disorders	949 (25.7)	10 (0.3)
Blood system disorders	779 (21.1)	18 (0.5)
Peripheral and Central Nervous system disorders	296 (8.0)	2 (0.0)
Systemic disorders and administration-site conditions	168 (4.5)	18 (0.5)
Hepatobiliary disorders	186 (5.1)	6 (0.2)
Respiratory disorders	11 (0.3)	2 (0.0)
Cardiac disorders	9 (0.2)	1 (0.0)
Eye disorders	4 (0.1)	0 (0.0)
Skin and subcutaneous tissue disorders	4 (0.1)	0 (0.0)
Musculoskeletal and connective tissue disorders	4 (0.1)	0 (0.0)
Renal and urinary disorders	3 (0.1)	0 (0.0)
Infections and infestations	1 (0.0)	1 (0.0)

TABLE 3 | Incidence and severity of most frequently-occurring ADRs.

Major ADRs	ADRs n (%)	Serious ADRs n (%)
Gastrointestinal disorders		
Nausea	748 (20.3)	1 (0.0)
Vomiting	362 (9.8)	5 (0.1)
Diarrhea	71 (1.9)	2 (0.0)
Blood system disorders		
Leukopenia	637 (17.3)	8 (0.2)
Neutropenia	445 (12.1)	9 (0.2)
Anemia	258 (7.0)	2 (0.0)
Thrombocytopenia	207 (5.6)	6 (0.2)
Peripheral nervous system disorders		
Paresthesia or disesthesia (hands and feet)	211 (5.7)	0 (0.0)
Abnormal hepatic function	186 (5.1)	6 (0.2)
Hypersensitivity reactions	118 (3.2)	18 (0.5)

upper quadrant pain, splenomegaly with subsequent thrombocytopenia, and portal hypertension. Systemic elevation of liver enzymes is often not significant, especially in the early stage (30). We found that the incidence of abnormal hepatic function was only 5.1%; however, our study only measured hepatic biochemical parameters such as the levels of transaminases, aspartate aminotransferase, and bilirubin. Without the results of histopathological examinations, it is difficult to give a definitive diagnosis of HSOS, leading to an underestimation of the hepatotoxicity of OXA. Therefore, OXA-induced HSOS should be specially studied and evaluated in patients with metastatic colorectal cancer who received OXA-based neoadjuvant chemotherapy after hepatectomy.

OXA-related HSRs are another major problem associated with the extensive use of the drug, the occurrence of which may lead to therapy delay, discontinuation of treatment, and even death (36). The reported frequency of HSR in patients undergoing OXA-based chemotherapy ranges from less than 2% to 25% (37–42), while the prevalence of severe HSRs is 0.5-2% (38, 43). Our study reported OXA-related HSRs in 118 out of 3687 Chinese patients, giving an incidence rate of 3.2% and a severe hypersensitivity rate of 0.5%. The clinical manifestations of HSRs involve multiple systems, such as cutaneous, digestive, neurologic, and respiratory systems. This study found that the most common events were cutaneous symptoms with severities of grades 1 and 2, which corroborates the findings of our previous study (44). Events of grade 3 and above are less common, but six patients developed life-threatening cases of severe anaphylactic shock. These results align with other studies that reported OXA-induced HSRs being potentially severe and life-threatening (45). In this study, however, patients who developed HSRs were managed with the corresponding treatments, and eventually, all patients recovered or improved. This suggests that OXA-induced HSRs are controllable through close monitoring, comprehensive evaluation, and the provision of timely and effective treatment. Hence, medical staff should pay close attention to the signs of potential HSRs and inform patients to closely monitor any symptoms that may arise.

Previous studies have noted that OXA-induced hypersensitivity reactions usually occur within the first 30 min of infusion (46, 47). In our study, the median time to onset of HSRs was 20 min, but the time to onset of different grades of HSRs varied. The median time to onset of grade 1 HSRs was 60 min, while grade 2 to 4 events occurred mainly within the first 20 min of OXA infusion. Our previous retrospective analysis also demonstrated that HSRs caused by OXA might occur at any time within a cycle of therapy but were mainly observed at the first 20 min of OXA infusion (44). Thus, patients should be closely monitored for HSRs, but especially within the first 20 min after the start of an OXA infusion.

TABLE 4 | Time to onset, cycle, management and outcome of major ADRs.

Major ADRs	Median time to onset, days (range)	Median cycle of OXA chemotherapy (range)	Management of OXA-induced ADRs, % (n)		ADRs that recovered or improved, % (n)
			Continued	Suspended	
Gastrointestinal toxicity	1 (0–8)	3 (1–15)	94.2 (894)	3.2 (30)	94.8 (900)
Myelosuppression	5 (1–39)	4 (1–12)	92.8 (723)	3.6 (28)	82.5 (643)
Peripheral neurotoxicity	1 (0–7)	4 (1–15)	91.0 (242)	1.5 (4)	96.6 (257)
Abnormal hepatic function	14 (2–33)	4 (1–11)	95.9 (178)	3.2 (6)	77.5 (144)
Hypersensitivity reactions	20min (2-1440min)	6 (1–18)	14.4 (17)	85.6 (101)	100 (118)

TABLE 5 | Manifestations of OXA-induced hypersensitivity reactions.

Subjects (total=118)			N (%)
Symptom	Cutaneous		
		Flushing	57 (48.3)
		Itching	57 (48.3)
		Rash/Urticaria	27 (22.9)
	Digestive		
		Nausea	35 (29.7)
		Vomiting	21 (17.8)
		Others	15 (12.7)
	Neurologic		
		Dizziness	7 (5.9)
		Numb	24 (20.3)
		Laryngeal abnormal	8 (6.8)
		Loss of consciousness	4 (3.4)
	Respiratory		
		Dyspnea	5 (4.2)
		Chest discomfort	45 (38.1)
		Wheezing	15 (12.7)
		Cough	2 (1.7)
	Generalized		
		Sweating	27 (22.9)
		Chills	3 (2.5)
		Fever	3 (2.5)
	Cardiovascular		
		Hypotension	13 (11.0)
		Tachycardia	21 (17.8)
	Vision		
		Blurred vision	2 (1.7)
		Conjunctival congestion	3 (2.5)
	Anaphylaxis		6 (5.1)
	Others		7 (5.9)
Grade of severity			
		1	24 (20.3)
		2	76 (64.4)
		3	12 (10.2
		4	6 (5.1)
The median time of hypersensitivity Reactions in different grades (min)			
		1	60 (10–1440)
		2	19 (2–180)
		3	10 (5–120)
		4	22 (2–60)
Management			
	Discontinuation of oxaliplatin administration		100 (84.7)
	Histamine-receptor 1 antagonist		61 (51.7)
	Dexamethasone		72 (61.0)
	Oxygen		34 (28.8)
	Subcutaneous adrenaline		10 (8.5)

However, this study can still be further expanded. First, this was a non-interventional observational study that aimed to observe the safety profile of OXA with no control group, and there was a short observation period of only 6 months and lack of follow-up. Hence, the OXA efficacy in these patients was unknown, and some delayed ADRs such as chronic OIPN may not be immediately reported and were underestimated. Second, patients treated with OXA was the only inclusion criteria implemented, and a comparison of safety accounting for the effects of different diseases and treatment regimens was not performed. In addition, although the researchers have identified OXA-related ADRs, the effects of other drugs cannot be completely excluded because OXA is often used in combination with other chemotherapeutic drugs. Further investigation is also required to identify the risk factors that affect the incidence of OXA-induced ADRs to provide a reference for the rational application of OXA.

CONCLUSIONS

In conclusion, this large post-marketing surveillance study conducted in more than 3000 Chinese patients preliminarily explored the incidence, characteristics, cycle, occurrence time and outcome of OXA induced ADRs. Overall, OXA induced adverse reactions were very prevalent. Our results showed that gastrointestinal toxicity,

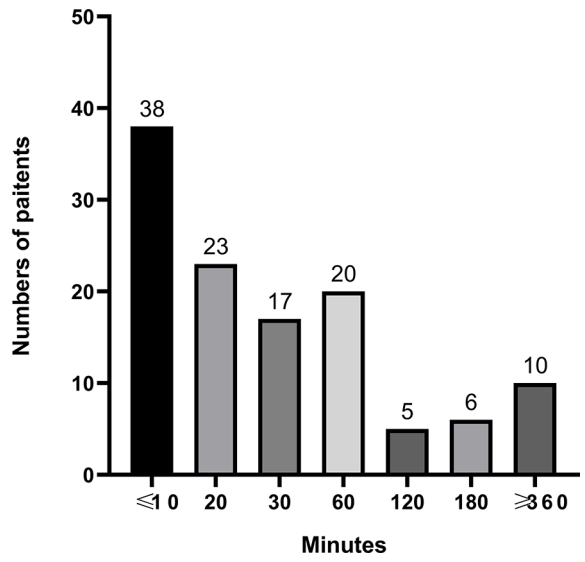

FIGURE 2 | Occurrence time of HSR from the start of OXA infusion.

hematotoxicity, peripheral neurotoxicity, HSRs and abnormal liver function were the main common ADRs of OXA, in which the latter two had unique characteristics, need more attention, and warrant close monitoring during OXA infusion. Although further studies are still required, this study provides valuable reference for the rational use of OXA and has great guidance for the management of OXA-induced ADRs in routine clinical practice.

DATA AVAILABILITY STATEMENT

The original contributions presented in the study are included in the article/**Supplementary Material**. Further inquiries can be directed to the corresponding authors.

ETHICS STATEMENT

The studies involving human participants were reviewed and approved by the Ethics Committee of Tongji Medical College, Huazhong University of Science and Technology (No.TJIRB20160504). The patients/participants provided their written informed consent to participate in this study.

AUTHOR CONTRIBUTIONS

ZY and RH, first authors, contributed to the data analysis and writing of manuscript. LZ and XY contributed to organization, management, and supervision of the project. XW and XS contributed to data collection, data curation, analysis, and validation. WL and ML contributed to contributed to the editing and submission of the article. CZ and DL, the corresponding authors, involved in conception of the project, performing data analysis, review of manuscript and provision of feedback and comments to first author. All authors contributed to the article and approved the submitted version.

FUNDING

This work was supported by the National Natural Science Foundation of China (No: 7187040708), Hubei Center for Adverse drug reaction Monitoring (No: 20160422), Funding for research-oriented clinician plan of Tongji Medical College, Huazhong University of Science and Technology (No: 5001540076); Clinical toxicology foundation of Chinese Society of Toxicology (CST2020CT107).

ACKNOWLEDGMENTS

The authors would like to thank all investigators and collaborators for the contributions to the conduct of this study, and we also thank Hubei Center for adverse drug reaction monitoring for assistance in the development of this study.

SUPPLEMENTARY MATERIAL

The Supplementary Material for this article can be found online at: https://www.frontiersin.org/articles/10.3389/fonc.2021.757196/full#supplementary-material

REFERENCES

1. Grothey A, Goldberg RM. A Review of Oxaliplatin and its Clinical Use in Colorectal Cancer. *Expert Opin Pharmacother* (2004) 5:2159–70. doi: 10.1517/14656566.5.10.2159
2. Huang J, Zhao Y, Xu Y, Zhu Y, Huang J, Liu Y, et al. Comparative Effectiveness and Safety Between Oxaliplatin-Based and Cisplatin-Based Therapy in Advanced Gastric Cancer: A Meta-Analysis of Randomized Controlled Trials. *Oncotarget* (2016) 7(23):34824–31. doi: 10.18632/oncotarget.9189
3. Ajani JA, D'Amico TA, Bentrem DJ, Chao J, Corvera C, Das P, et al. Esophageal and Esophagogastric Junction Cancers, Version 2.2019, NCCN Clinical Practice Guidelines in Oncology. *J Natl Compr Canc Netw* (2019) 17 (7):855–83. doi: 10.6004/jnccn.2019.0033
4. Tempero MA. NCCN Guidelines Updates: Pancreatic Cancer. *J Natl Compr Canc Netw* (2019) 17(5.5):603–5. doi: 10.6004/jnccn.2019.5007
5. Taylor SE, Beck TL, Krivak TC, Zorn KK, Kelley JL, Edwards RP. Oxaliplatin Salvage for Recurrent Ovarian Cancer: A Single Institution's Experience in Patient Populations With Platinum Resistant Disease or a History of Platinum Hypersensitivity[J]. *Gynecol Oncol* (2014) 134(1):68–72. doi: 10.1016/j.ygyno.2014.04.039
6. André T, Boni C, Mounedji-Boudiaf L, Navarro M, Tabernero J, Hickish T, et al. Oxaliplatin, Fluorouracil and Leukovorin as Adjuvant Treatment for Colon Cancer. *N Engl J Med* (2004) 350(23):2343–51. doi: 10.1056/NEJMoa032709

7. Nielsen DL, Palshof JA, Larsen FO, Jensen BV, Pfeiffer P. A Systematic Review of Salvage Therapy to Patients With Metastatic Colorectal Cancer Previously Treated With Fuorouracil, Oxaliplatin and Irinotecan +/- Targeted Therapy. *Cancer Treat Rev* (2014) 40(6):701–15. doi: 10.1016/j.ctrv.2014.02.006
8. Volovat SR, Volovat R, Negru SM, Danciu M, Scripcariu V. The Efficacy and Safety of Hepatic Arterial Infusion of Oxaliplatin Plus Intravenous Irinotecan, Leucovorin and Fuorouracil in Colorectal Cancer With Inoperable Hepatic Metastasis. *J Chemother* (2016) 28(3):235–41. doi: 10.1179/1973947815Y.0000000042
9. Ohta H, Hayashi T, Murai S, Shiouchi H, Ando Y, Kumazawa S, et al. Comparison Between Hypersensitivity Reactions to Cycles of Modified FOLFOX6 and XELOX Therapies in Patients With Colorectal Cancer. *Cancer Chemoth Pharm* (2017) 79(5):1021–9. doi: 10.1007/s00280-017-3294-9
10. Abu-Sbeih H, Mallepally N, Goldstein R, Chen E, Tang T, Dike UK, et al. Gastrointestinal Toxic Effects in Patients With Cancer Receiving Platinum-Based Therapy. *J Cancer* (2020) 11(11):3144–50. doi: 10.7150/jca.37777
11. Erdem GU, Dogan M, Demirci NS, Zengin N. Oxaliplatin-Induced Acute Thrombocytopenia. *J Cancer Res Ther* (2016) 12(2):509–14. doi: 10.4103/0973-1482.154056
12. Kang L, Tian Y, Xu S, Chen H. Oxaliplatin–induced Peripheral Neuropathy: Clinical Features, Mechanisms, Prevention and Treatment. *J Neurol* (2021) 268(9):3269–82. doi: 10.1007/s00415-020-09942-w
13. Aroldi F, Prochilo T, Bertocchi P, Zaniboni A. Oxaliplatin-Induced Hypersensitivity Reaction: Underlying Mechanisms and Management. *J Chemother* (2015) 27(2):63–6. doi: 10.1179/1973947814Y.0000000204
14. Andre T, Boni C, Navarro M, Tabernero J, Hickish T, Topham C, et al. Improved Overall Survival With Oxaliplatin, Fuorouracil, and Leucovorin as Adjuvant Treatment in Stage II or III Colon Cancer in the MOSAIC Trial. *J Clin Oncol* (2009) 27(19):3109–16. doi: 10.1200/JCO.2008.20.6771
15. Bray F, Ferlay J, Soerjomataram I, Siegel RL, Torre LA, Jemal A. Global Cancer Statistics 2018: GLOBOCAN Estimates of Incidence and Mortality Worldwide for 36 Cancers in 185 Countries. *CA Cancer J Clin* (2018) 68(6):394–424. doi: 10.3322/caac.21492
16. Hoff PM, Saad ED, Costa F, Coutinho AK, Caponero R, Prolla G, et al. Literature Review and Practical Aspects on the Management of Oxaliplatin-Associated Toxicity. *Clin Colorectal Cancer* (2012) 11(2):93–100. doi: 10.1016/j.clcc.2011.10.004
17. Chen W, Zheng R, Baade PD, Zhang S, Zeng H, Bray F, et al. Cancer Statistics in China, 2015. *CA Cancer J Clin* (2016) 66(2):115–32. doi: 10.3322/caac.21338
18. Messersmith WA. NCCN Guidelines Updates: Management of Metastatic Colorectal Cancer. *J Natl Compr Cancer Netw* (2019) 17(5.5):599–601. doi: 10.6004/jnccn.2019.5014
19. Ajani JA, D'Amico TA, Almhanna K, Bentrem DJ, Chao J, Das P, et al. Gastric Cancer, Version 3.2016, NCCN Clinical Practice Guidelines in Oncology. *J Natl Compr Canc Netw* (2016) 14(10):1286–312. doi: 10.6004/jnccn.2016.0137
20. Cassidy J, Misset JL. Oxaliplatin-Related Side Effects:Characteristics and Management. *Semin Oncol* (2002) 29(5 Suppl 15):11–20. doi: 10.1053/sonc.2002.35524
21. Oun R, Moussa YE, Wheate NJ. The Side Effects of Platinum-Based Chemotherapy Drugs: A Review for Chemists. *Dalton Trans* (2018) 47 (19):6645–53. doi: 10.1039/c8dt00838h
22. Berger MJ, Ettinger DS, Aston J, Barbour S, Bergsbaken J, Bierman PJ, et al. NCCN Guidelines Insights: Antiemesis, Version 2.2017. *J Natl Compr Canc Netw* (2017) 15(7):883–93. doi: 10.6004/jnccn.2017.0117
23. Xu N, Fang WJ, Zhang XC, Yu LF, Bao HY, Shi GM, et al. A Phase II Trial of Oxaliplatin, Folinic Acid, and 5-Fluorouracil (FOLFOX4) as First-Line Chemotherapy in Advanced Colorectal Cancer: A China Single-Center Experience. *Cancer Investig* (2007) 25(7):599–605. doi: 10.1080/07357900701470739
24. Kamimura K, Matsumoto Y, Zhou Q, Moriyama M, Saijo Y. Myelosuppression by Chemotherapy in Obese Patients With Gynecological Cancers. *Cancer Chemother Pharmacol* (2016) 78(3):633–41. doi: 10.1007/s00280-016-3119-2
25. Jardim DL, Rodrigues CA, Novis YA, Rocha VG, Hoff PM. Oxaliplatin-Related Thrombocytopenia. *Ann Oncol* (2012) 23(8):1937–42. doi: 10.1093/annonc/mds074
26. Phull P, Quillen K, Hartshorn KL. Acute Oxaliplatin-Induced Hemolytic Anemia, Thrombocytopenia, and Renal Failure: Case Report and a Literature Review. *Clin Colorectal Canc* (2016) S1533-0028(16):30259-6. doi: 10.1016/j.clcc.2016.11.005
27. Polyzos A, Tsavaris N, Gogas H, Souglakos J, Vambakas L, Vardakas N, et al. Clinical Features of Hypersensitivity Reactions to Oxaliplatin: A 10-Year Experience. *Oncology* (2009) 76(1):36–41. doi: 10.1159/000178163
28. Bautista MA, Stevens WT, Chen CS, Curtis BR, Aster RH, Hsueh CT. Hypersensitivity Reaction and Acute Immunemediated Thrombocytopenia From Oxaliplatin:Two Case Reports and a Review of the Literature. *J Hematol Oncol* (2010) 3:12. doi: 10.1186/1756-8722-3-12
29. Gebremedhn EG, Shortland PJ, Mahns DA. The Incidence of Acute Oxaliplatin-Induced Neuropathy and its Impact on Treatment in the First Cycle: A Systematic Review. *BMC Cancer* (2018) 18(1):410. doi: 10.1186/s12885-018-4185-0
30. Rubbia-Brandt L, Lauwers GY, Wang H, Majno PE, Tanabe K, Zhu AX, et al. Sinusoidal Obstruction Syndrome and Nodular Regenerative Hyperplasia are Frequent Oxaliplatin-Associated Liver Lesions and Partially Prevented by Bevacizumab in Patients With Hepatic Colorectal Metastasis. *Histopathology* (2010) 56(4):430–9. doi: 10.1111/j.1365-2559.2010.03511.x
31. Lu QY, Zhao AL, Deng W, Li ZW, Shen L. Hepatic Histopathology and Postoperative Outcome After Preoperative Chemotherapy for Chinese Patients With Colorectal Liver Metastases. *World J Gastrointest Surg* (2013) 5(3):30–6. doi: 10.4240/wjgs.v5.i3.30
32. Liu F, Cao X, Ye J, Pan XL, Kan XF, Song YH. Oxaliplatin-Induced Hepatic Sinusoidal Obstruction Syndrome in a Patient With Gastric Cancer: A Case Report. *Mol Clin Oncol* (2018) 8(3):453–6. doi: 10.3892/mco.2017.1540
33. van Mierlo KM, Zhao J, Kleijnen J, Rensen SS, Schaap FG, Dejong CH, et al. The Influence of Chemotherapy-Associated Sinusoidal Dilatation on Short-Term Outcome After Partial Hepatectomy for Colorectal Liver Metastases: A Systematic Review With Meta-Analysis. *Surg Oncol* (2016) 25(3):298–307. doi: 10.1016/j.suronc.2016.05.030
34. Zhao J, van Mierlo KMC, Gómez-Ramírez J, Kim H, Pilgrim CHC, Pessaux P, et al. Systematic Review of the Influence of Chemotherapy-Associated Liver Injury on Outcome After Partial Hepatectomy for Colorectal Liver Metastases. *Br J Surg* (2017) 104(8):990–1002. doi: 10.1002/bjs.10572
35. Hisaka T, Ishikawa H, Sakai H, Kawahara R, Goto Y, Nomura Y, et al. Sinusoidal Obstruction Syndrome and Postoperative Complications Resulting From Preoperative Chemotherapy for Colorectal Cancer Liver Metastasis. *Anticancer Res* (2019) 39(8):4549–54. doi: 10.21873/anticanres.13632
36. Bano N, Najam R, Qazi F, Mateen A. Clinical Features of Oxaliplatin Induced Hypersensitivity Reactions and Therapeutic Approaches. *Asian Pac J Cancer Prev* (2016) 17(4):1637–41. doi: 10.7314/apjcp.2016.17.4.1637
37. Brandi G, Pantaleo MA, Galli C, Falcone A, Antonuzzo A, Mordenti P, et al. Hypersensitivity Reactions Related to Oxaliplatin (OHP). *Br J Cancer* (2003) 89(3):477–81. doi: 10.1038/sj.bjc.6601155
38. Shibata Y, Ariyama H, Baba E, Takii Y, Esaki T, Mitsugi K, et al. Oxaliplatin-Induced Allergic Reaction in Patients With Colorectal Cancer in Japan. *Int J Clin Oncol* (2009) 14(5):397–401. doi: 10.1007/s10147-009-0883-6
39. Parel M, Ranchon F, Nosbaum A, You B, Vantard N, Schwiertz V, et al. Hypersensitivity to Oxaliplatin: Clinical Features and Risk Factors. *BMC Pharmacol Toxicol* (2014) 15:1. doi: 10.1186/2050-6511-15-1
40. Okayama T, Ishikawa T, Sugatani K, Yoshida N, Kokura S, Matsuda K, et al. Hypersensitivity Reactions to Oxaliplatin: Identifying the Risk Factors and Judging the Efficacy of a Desensitization Protocol. *Clin Ther* (2015) 37 (6):1259–69. doi: 10.1016/j.clinthera.2015.03.012
41. Yamauchi H, Goto T, Takayoshi K, Sagara K, Uoi M, Kawanabe C, et al. A Retrospective Analysis of the Risk Factors for Allergic Reactions Induced by the Administration of Oxaliplatin. *Eur J Cancer Care* (2015) 24(1):111–6. doi: 10.1111/ecc.12156
42. Shao YY, Hu FC, Liang JT, Chiu WT, Cheng AL, Yang CH. Characteristics and Risk Factors of Oxaliplatin-Related Hypersensitivity Reactions. *J Formos Med Assoc* (2010) 109(5):362–8. doi: 10.1016/S0929-6646(10)60064-2

43. Kim BH, Bradley T, Tai J, Budman DR. Hypersensitivity to Oxaliplatin: An Investigation of Incidence and Risk Factors, and Literature Review. *Oncology* (2009) 76(4):231–8. doi: 10.1159/000205263
44. Li M, Jiang C, Yang JY, Yu ZQ, Li W, Zhao L, et al. Clinical Features of Oxaliplatin-Related Hypersensitivity Reactions in Chinese Patients: A Retrospective Multicenter Analysis. *Curr Med Sci* (2021) 41(4):827–31. doi: 10.1007/s11596-021-2387-1
45. Wang JH, King TM, Chang MC, Hsu CW. Oxaliplatin-Induced Severe Anaphylactic Reactions in Metastatic Colorectal Cancer:Case Series Analysis. *World J Gastroenterol* (2012) 18(38):5427–33. doi: 10.3748/wjg.v18.i38.5427
46. Siu SW, Chan RT, Au GK. Hypersensitivity Reactions to Oxaliplatin: Experience in a Single Institute. *Ann Oncol* (2006) 17(2):259–61. doi: 10.1093/annonc/mdj042
47. Nozawa H, Muto Y, Yamada Y. Desensitization to Oxaliplatin With Two Stages of Premedication in a Patient With Metastatic Rectal Cancer. *Clin Ther* (2008) 30(6):1160–5. doi: 10.1016/j.clinthera.2008.06.007

Conflict of Interest: The authors declare that the research was conducted in the absence of any commercial or financial relationships that could be construed as a potential conflict of interest.

frontiers in Pharmacology

SYSTEMATIC REVIEW
published: 21 October 2021
doi: 10.3389/fphar.2021.757464

The Role of Genetic Polymorphisms in High-Dose Methotrexate Toxicity and Response in Hematological Malignancies: A Systematic Review and Meta-Analysis

Zaiwei Song[1,2,3], *Yang Hu*[1,2,3,4], *Shuang Liu*[1,2,3], *Dan Jiang*[1,2,3,4], *Zhanmiao Yi*[1,2,3], *Mason M. Benjamin*[5] *and Rongsheng Zhao*[1,2,3]*

[1]*Department of Pharmacy, Peking University Third Hospital, Beijing, China,* [2]*Institute for Drug Evaluation, Peking University Health Science Center, Beijing, China,* [3]*Therapeutic Drug Monitoring and Clinical Toxicology Center, Peking University, Beijing, China,* [4]*Department of Pharmacy Administration and Clinical Pharmacy, School of Pharmaceutical Sciences, Peking University, Beijing, China,* [5]*Department of Pharmaceutical Sciences, College of Pharmacy, University of Michigan, Ann Arbor, MI, United States*

OPEN ACCESS

Edited by:
Yao Liu,
Daping Hospital, China

Reviewed by:
Lana Nezic,
University of Banja Luka, Bosnia and Herzegovina
Hamed Barabadi,
Shahid Beheshti University of Medical Sciences, Iran

***Correspondence:**
Rongsheng Zhao
zhaorongsheng@bjmu.edu.cn

Specialty section:
This article was submitted to Pharmacology of Anti-Cancer Drugs, a section of the journal Frontiers in Pharmacology

Received: *12 August 2021*
Accepted: *08 September 2021*
Published: *21 October 2021*

Citation:
Song Z, Hu Y, Liu S, Jiang D, Yi Z, Benjamin MM and Zhao R (2021) The Role of Genetic Polymorphisms in High-Dose Methotrexate Toxicity and Response in Hematological Malignancies: A Systematic Review and Meta-Analysis. Front. Pharmacol. 12:757464. doi: 10.3389/fphar.2021.757464

Objective: High-dose methotrexate (HDMTX) is a mainstay therapeutic agent for the treatment of diverse hematological malignancies, and it plays a significant role in interindividual variability regarding the pharmacokinetics and toxicity. The genetic association of HDMTX has been widely investigated, but the conflicting results have complicated the clinical utility. Therefore, this systematic review aims to determine the role of gene variants within the HDMTX pathway and to fill the gap between knowledge and clinical practice.

Methods: Databases including EMBASE, PubMed, Cochrane Central Register of Controlled Trials (CENTRAL), and the Clinical Trials.gov were searched from inception to November 2020. We included twelve single-nucleotide polymorphisms (SNPs) within the HDMTX pathway, involving *RFC1*, *SLCO1B1*, *ABCB1*, *FPGS*, *GGH*, *MTHFR*, *DHFR*, *TYMS*, and *ATIC*. Meta-analysis was conducted by using Cochrane Collaboration Review Manager software 5.3. The odds ratios (ORs) or hazard ratios (HRs) with 95% confidence interval (95% CI) were analyzed to evaluate the associations between SNPs and clinical outcomes. This study was performed according to the PRISMA guideline.

Results: In total, 34 studies with 4102 subjects were identified for the association analysis. Nine SNPs involving *MTHFR*, *RFC1*, *ABCB1*, *SLCO1B1*, *TYMS*, *FPGS*, and *ATIC* genes were investigated, while none of studies reported the polymorphisms of *GGH* and *DHFR* yet. Two SNPs were statistically associated with the increased risk of HDMTX toxicity: *MTHFR 677C>T* and hepatotoxicity (dominant, OR=1.52, 95% CI=1.03-2.23; recessive, OR=1.68, 95% CI=1.10–2.55; allelic, OR=1.41, 95% CI=1.01–1.97), mucositis (dominant, OR=2.11, 95% CI=1.31–3.41; allelic, OR=1.91, 95% CI=1.28–2.85), and renal toxicity (recessive, OR=3.54, 95% CI=1.81–6.90; allelic, OR=1.89, 95% CI=1.18–3.02); *ABCB1 3435C>T* and hepatotoxicity (dominant, OR=3.80, 95% CI=1.68-8.61), whereas a tendency toward the decreased risk of HDMTX toxicity was present in three SNPs: *TYMS 2R>3R* and mucositis

(dominant, OR=0.66, 95% CI=0.47–0.94); *RFC1 80A>G* and hepatotoxicity (recessive, OR=0.35, 95% CI=0.16–0.76); and *MTHFR 1298A>C* and renal toxicity (allelic, OR=0.41, 95% CI=0.18–0.97). Since the data of prognosis outcomes was substantially lacking, current studies were underpowered to investigate the genetic association.

Conclusions: We conclude that genotyping of *MTHFR* and/or *ABCB1* polymorphisms prior to treatment, *MTHFR 677C>T* particularly, is likely to be potentially useful with the aim of tailoring HDMTX therapy and thus reducing toxicity in patients with hematological malignancies.

Keywords: methotrexate, pharmacogenetics, polymorphism, toxicity, hematological malignancies

INTRODUCTION

Acute lymphoblastic leukemia (ALL) is the most common neoplasm in children, accounting for about 30 percent of all pediatric malignancies (Coluzzi et al., 2020). High-dose methotrexate (HDMTX) is commonly defined as an intravenous dose greater than 500 mg/m^2 (Howard et al., 2016), and HDMTX is recommended as an essential component of chemotherapy for ALL and non-Hodgkin lymphoma (NHL) in clinical guidelines (National Comprehensive Cancer Network, 2021a; b; c). Although breakthroughs have been made in the complex treatment of hematological malignancies, HDMTX still plays a key role and is established as the first-line drug (Gervasini and Mota-Zamorano, 2019). However, patients differ largely in their response to treatment regarding HDMTX pharmacokinetics and toxicities, even when given the identical dose (Schmiegelow, 2009; Giletti and Esperon, 2018). Serious and life-threatening toxicity can occur in patients, leading to treatment interruption and discontinuation, dose reduction, poor prognosis, and even death (Howard et al., 2016; Purkayastha et al., 2018).

The interindividual diversity in the response to HDMTX can be partially explained by genetic variations involved in the MTX pathway, including cellular transport, drug metabolism, and target (Giletti and Esperon, 2018). Regarding transcellular transport, the cellular influx and efflux are mainly mediated by the reduced folate carrier 1 (RFC1/SLC19A1) (Zhao et al., 2011) and ATP-binding cassette transporters (ABC, predominantly ABCB1) (Assaraf, 2006), respectively. In some tissues, the influx process is related to organic anion transporting polypeptides (OATP/SLCO) (Wang et al., 2019). Regarding the polyglutamation pathway, MTX is converted into polyglutamate forms (PGMTX) by the enzyme folylpolyglutamate synthetase (FPGS) once inside the cell, and this process can be reversed by the enzyme gamma-glutamyl hydrolase (GGH) (Giletti and Esperon, 2018). Regarding the target, dihydrofolate reductase (DHFR), thymidylate synthase (TYMS/TS), and 5-aminoimidazole-4-carboxamide ribonucleotide transformylase (ATIC) are main therapeutic targets of HDMTX. And it has an indirect effect on methylenetetrahydrofolate reductase (MTHFR) (Giletti and Esperon, 2018). The cellular metabolic pathway and targets of HDMTX are summarized in **Figure 1**.

In recent years, pharmacogenetics of MTX has become a wide clinical concern and research focus. Numerous pharmacogenetic studies have evaluated the associations of HDMTX genetic polymorphism and outcomes (Avivi et al., 2014; Yang et al., 2017; Kotur et al., 2020), whereas the conflicting and contrasting evidence complicates the clinical utility. Six systematic reviews focusing on hematological malignancies have also been published and reported inconsistent findings (Yang et al., 2012; Lopez-Lopez et al., 2013; He et al., 2014; Zhao et al., 2016; Oosterom et al., 2018; Yao et al., 2019). However, most of systematic reviews did not set strict restrictions on the high dose (HDMTX) (Yang et al., 2012; Lopez-Lopez et al., 2013; He et al., 2014; Zhao et al., 2016; Yao et al., 2019), although the side effect profile of MTX varies markedly as its dose changes, and the pharmacogenetic associations may differ. Obviously, studies included in the latest systematic review (Yao et al., 2019) were published before January 2018, and the included data might be out of date. For example, four recent cohort studies (Chae et al., 2020; Esmaili et al., 2020; Kotur et al., 2020; Chang et al., 2021) investigating HDMTX pharmacogenetics were published in 2020. In addition, previous systematic reviews only included individual polymorphisms, focusing on toxicity but not prognosis outcomes (He et al., 2014; Zhao et al., 2016; Oosterom et al., 2018). Currently, there still exists gap between pharmacogenetic research and genetic testing in clinical practice. Predicting the toxic effects and tailoring HDMTX doses still remain an unmet clinical need in HDMTX therapy.

Thus, we conducted a systematic review to assess the association between gene polymorphisms within the HDMTX pathway and HDMTX toxicity or response in patients with hematological malignancies, aiming to provide applicable evidence for further personalized medications and fill the gap between knowledge and clinical practice.

METHODS

This study was performed according to the Preferred Reporting Items for Systematic Reviews and Meta-Analysis (PRISMA) statement (Moher et al., 2009). The PRISMA checklist was included in **Supplementary Material I** (**Supplementary Table S1**). The protocol for this systematic review has been registered in

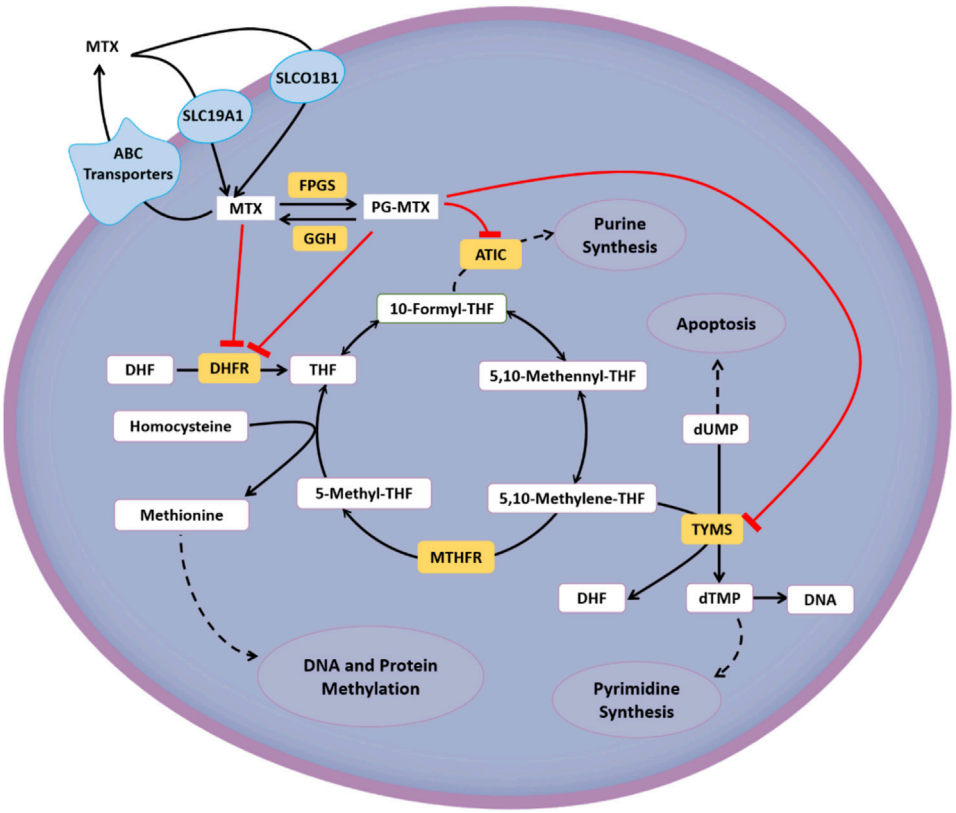

FIGURE 1 | Cellular metabolic pathway and targets of HDMTX.

the International Prospective Register of Systematic Reviews (PROSPERO, No. CRD42018096986).

Eligibility Criteria

Studies were considered eligible if they satisfied all of the following inclusion criteria: 1) type of studies: cohort study; 2) type of subject: patients with ALL, NHL, and other hematological malignancies receiving HDMTX chemotherapy, with no restrictions on ethnicity, gender, or age; 3) classification of exposure: patients were grouped by wild or mutant genotype of included genes within the HDMTX pathway (**Table 1**). There were 12 genetic polymorphisms in total, including but not limited to genes involved in the Pharmacogenomics Knowledge Base (PharmGKB, https://www.pharmgkb.org/guidelineAnnotations), which contains recommendations from the Clinical Pharmacogenetics Implementation Consortium (CPIC) and other national association of pharmacogenomics; and 4) types of outcomes measured: HDMTX-related toxicity and prognosis outcomes. The toxicity outcomes included the rate of hepatic toxicity, renal toxicity, oral mucositis, gastrointestinal (GI) toxicity, neurotoxicity, dermal toxicity, overall toxicity, and therapeutic interference due to toxicity. The toxicity outcomes were identified by the Common Terminology Criteria for Adverse Events established by American National Cancer Institute (NCI-CTC) or Toxicity Grading Scale for Determining the Severity of Adverse Events of Chemotherapeutic Drugs established by the World Health Organization (WHO) or other common criteria. Grade 3 to 4 (G3-4) indicates severe toxicity. The prognosis outcomes included overall survival (OS), progression-free survival (PFS), disease-free survival (DFS), event-free survival (EFS), relapse-free survival (RFS), and relapse/death. The exclusion criteria were as follows: duplicate publications; abstracts without available full texts; unqualified data; and studies not in accordance with the Hardy–Weinberg

TABLE 1 | Genetic polymorphisms within the HDMTX pathway

Gene	SNP	Polymorphisms	Remark
Transcellular transport			
RFC1/SLC19A1	rs1051266	80A>G	Research focus
SLCO1B1	rs4149056	521T>C	
ABCB1	rs1045642	3435C>T	Research focus
Polyglutamation pathway			
FPGS	rs10106	1994A>G	
FPGS	rs1544105	2752G>A	
GGH	rs3758149	401C>T	
Targets			
MTHFR	rs1801133	677C>T	Research focus
MTHFR	rs1801131	1298A>C	Research focus
DHFR	rs408626	317A>G	
DHFR	rs442767	680C>A	
TYMS/TS	rs34743033	2R/3R	
ATIC	rs2372536	347C>G	

equilibrium (HWE) (Trikalinos et al., 2006) or not reporting the genotype distribution.

Search Strategy

Electronic databases including PubMed, Embase, Cochrane Central Register of Controlled Trials (CENTRAL), and Clinical Trials.gov were searched for potentially relevant studies from inception to November 11, 2020. Specific search strategies were developed for each database. The combination of keywords ("Methotrexate") AND ("Hematologic neoplasms" OR Hematologic malignancy" OR "Leukemia" OR "Lymphoma") AND ("Gene" OR "Polymorphism" OR "Pharmacogenetics" OR "Polymorphism, single nucleotide") were used to search the title and abstract of queried literature (**Supplementary Material II**). No restrictions were placed on study design or language. The reference lists of previous systematic reviews and included literature were searched manually.

Study Selection

Two authors (ZS and YH) independently assessed the eligibility of all studies based on the aforementioned inclusion and exclusion criteria after reviewing the study title, abstract, and full text in succession. Studies were included in only the systematic review (but not the meta-analysis) if their findings were relevant to the research question, but data were not available for quantitative analysis. Any disagreement among authors was discussed and reconciled by the corresponding author (RZ).

Data Extraction

Two authors (ZS and YH) independently extracted data based on a predesigned standardized extraction form, including the first author and publication year, country, ethnicity, diagnosis, sample size and genotype distribution, gender (female/male), age (years), MTX dose, calculated *p*-value for HWE, outcomes, and individual results of the single study. Study authors were contacted for missing data.

Quality Assessment/Risk of Bias

Two authors (ZS and YH) independently assessed the quality of studies under the Newcastle–Ottawa Scale (NOS) (Stang, 2010), as recommended in the Cochrane Handbook. The NOS attributes a maximum of 9 points to studies based on methodological design and formal reporting, involving "selection of cohorts," "comparability of cohorts," and "assessment of outcome." NOS scores ranging from 7 to 9 points indicate high quality, 5 to 6 indicate medium quality, and 0 to 4 indicate low quality. Disagreements regarding data extraction and quality assessment were resolved by consensus or, when necessary, by consulting the corresponding author (RZ).

Statistical Analyses

A chi-square test was performed to verify genotype distributions using SPSS version 25.0. A *p*-value greater than 0.05 would indicate accordance with the HWE. Before conducting the meta-analysis, clinical heterogeneity was estimated by comparing the diagnosis, efficacy or toxicity criteria, and other clinical features among studies. If two or more studies reported the same outcome and obvious clinical heterogeneity was not observed, meta-analysis was performed to quantitatively integrate outcomes by using the Cochrane Collaboration review manager software 5.3 (RevMan 5.3). Otherwise, only a descriptive analysis was performed.

The meta-analysis was performed as follows: 1) odds ratios (ORs) and hazard ratios (HRs) were calculated to evaluate the genetic association of toxicity or prognosis outcomes, respectively. And if the corresponding 95% confidence intervals (95% CIs) of the OR value (HR value) did not overlap with the value of 1 and the *p*-value was less than 0.05, the association was considered statistically significant. 2) The pooled OR or HR was calculated under the dominant model (MM/Mm vs mm), recessive model (MM vs Mm/mm), and allelic model (M vs m), where M is the mutant allele such that the G allele at *RFC1 80A>G*, C allele at *SLCO1B1 521T>C*, T allele at *ABCB1 3435C>T*, and so on; m is the wild allele, such that the A allele at *RFC1 80A>G*, T allele at *SLCO1B1 521T>C*, C allele at *ABCB1 3435C>T*, and so on. 3) The fixed-effect model was used initially, and the random-effects model was adopted when unidentified significant heterogeneity was detected. 4) The heterogeneity across the studies was assessed using a chi-square-based Q-test and I^2 statistics. $P_{heterogeneity}$ (P_{het}) values <0.05 and I^2 values >50% were considered to indicate significant heterogeneity (Sedgwick, 2015), and in these cases, the source of heterogeneity was investigated by examining the steps taken to check data and perform the subgroup analysis and sensitivity analysis. If the potential sources of heterogeneity remained unclear, the random-effects model was used, or the descriptive analysis was performed. 5) Subgroup analyses were performed based on patients' age. Age subgroups were defined as pediatric, adult, and mixed-age. $P_{subgroup}$ (P_{sub}) <0.05 indicated a statistically significant difference across subgroups.

Sensitivity Analyses and Publication Bias Assessment

Sensitivity analyses were conducted to assess the impact of individual studies on the pooled estimates and the stability of the pooled estimates. A pooled OR (HR) was recalculated after removing each single primary study one by one and replacing the statistical model of meta-analysis. Publication bias was assessed by inspecting the funnel plot visually, and it was considered to be valid when 10 or more studies were included (Sedgwick and Marston, 2015).

RESULTS

Electronic Searches and Study Selection

A total of 4395 candidate references were identified in electronic database searches, and no additional reference was identified using a manual search. Of the total 4395 candidates, 441 duplicate references were removed and then 3904 were excluded after careful review of the titles and abstracts. Only 50 references were recognized as relevant and then we assessed all full texts. The PRISMA 2020 flow diagram is shown in **Figure 2**. Of the

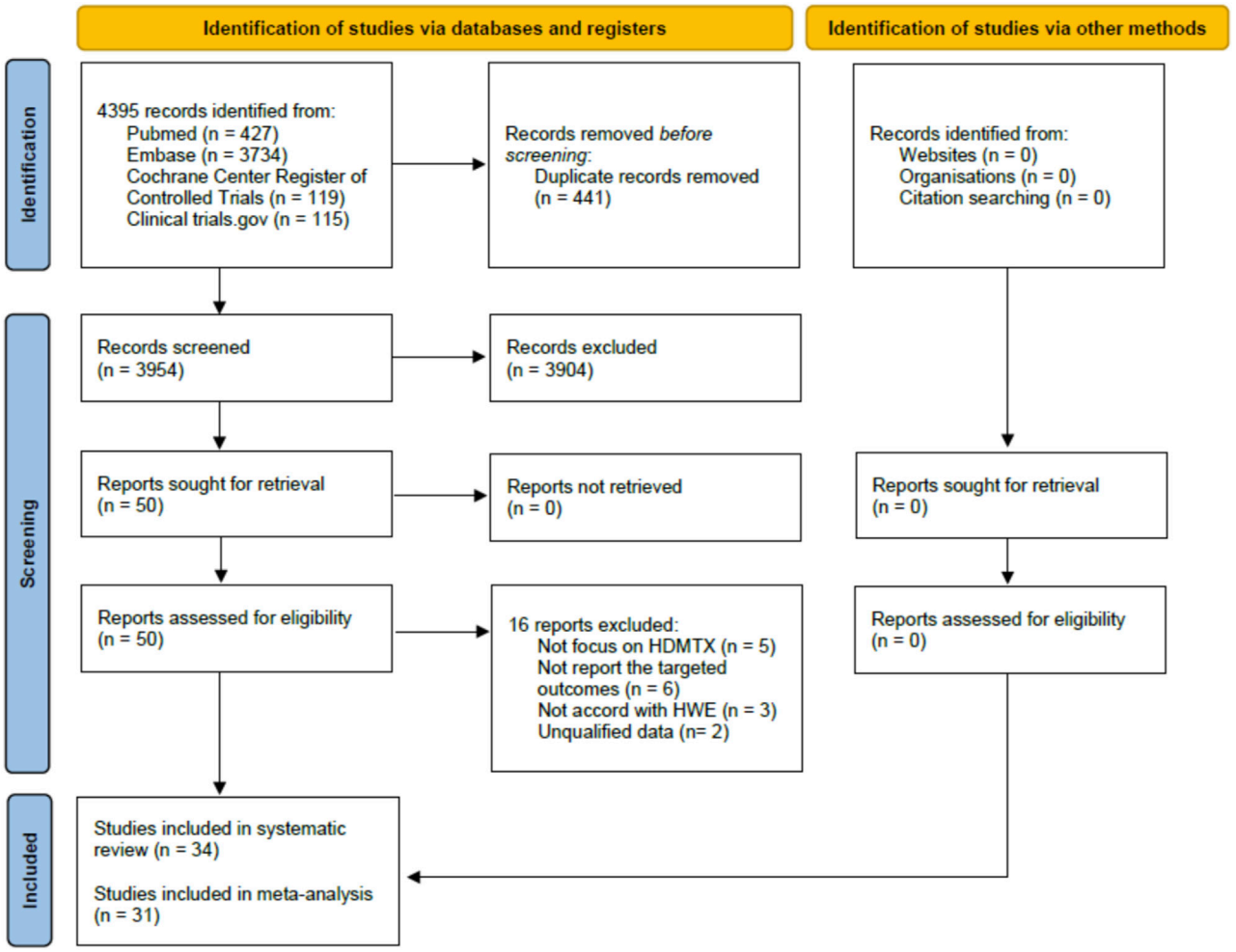

FIGURE 2 | PRISMA 2020 flow diagram of studies selection for the systematic review and meta-analysis.

total 50 references, five did not focus on HDMTX, six did not report the targeted outcomes, three did not accord with HWE, and two did not have qualified data. Finally, according to the aforementioned inclusion and exclusion criteria, 34 studies were included in our systematic review. Of the 34 studies (Laverdière et al., 2002; Kishi et al., 2003; Seidemann et al., 2006; Shimasaki et al., 2006; Imanishi et al., 2007; Ruiz-Argüelles et al., 2007; Ashton et al., 2009; Faganel Kotnik et al., 2010; D'Angelo et al., 2011; Faganel Kotnik et al., 2011; Liu et al., 2011; Chiusolo et al., 2012; Erčulj et al., 2012; Haase et al., 2012; Fukushima et al., 2013; Radtke et al., 2013; Yanagimachi et al., 2013; Avivi et al., 2014; Erculj et al., 2014; Suthandiram et al., 2014; den Hoed et al., 2015; Ma et al., 2015; Huang et al., 2016; Tsujimoto et al., 2016; Choi et al., 2017; Giletti et al., 2017; Liu et al., 2017; Yang et al., 2017; Yazıcıoğlu et al., 2017; Oosterom et al., 2018; Chae et al., 2020; Esmaili et al., 2020; Kotur et al., 2020; Chang et al., 2021) included, 31 studies were included in the meta-analysis and three studies were only included for the descriptive analysis since the meta-analysis was infeasible.

Study Characteristics and Quality Assessment

In total, 34 studies involving 4102 patients were included for investigating the associations between genetic polymorphisms and HDMTX outcomes. Of the studies included, 14 studies reported the polymorphisms of *RFC1 (rs1051266)*, six studies *SLCO1B1 (rs4149056)*, seven studies *ABCB1 (rs1045642)*, one study *FPGS (rs10106)*, one study *FPGS (rs1544105)*, 26 studies *MTHFR (rs1801133)*, 17 studies *MTHFR (rs1801131)*, six studies *TYMS (rs34743033)*, and one study *ATIC (rs2372536)*. None of studies reported the polymorphisms of *GGH (rs3758149)* and *DHFR (rs408626, rs442767)* yet. Among included studies, 20 and 14 studies were conducted in the ethnicity of Caucasian and Asian, respectively. Patients' diagnosis included ALL, acute myeloid leukemia (AML), diffuse large B-cell lymphoma (DLBCL), primary CNS lymphoma (PCNSL), and other NHL. A total of 25 studies included pediatric patients only, 8 studies included adult patients only, and one study did not impose restrictions on patient age. All the studies were in accord with

the HWE. And 30 studies reported toxicities outcomes, while prognosis outcomes were involved in 14 studies. Regarding quality assessment, 2 studies earned a full NOS score of 9 points, 19 studies earned 8 points, and 11 studies earned 7 points, varying mainly in presentation of the outcomes at the start of study and outcome follow-up. The average NOS score of all studies was 7.6 points, indicating a relatively high quality of overall methodology. The main characteristics and NOS scores of the studies included are summarized in **Table 2**. And the detailed NOS scores of the studies included are given in **Supplemental Material III** (**Supplementary Table S2**).

Overall Findings

The overall findings are summarized in **Table 3**. Regarding the cellular transport and metabolism, *RFC1 (rs1051266)* was associated with a reduced risk of hepatic toxicity and overall toxicity (in pediatric), while *ABCB1 (rs1045642)* was associated with an increased risk of hepatic toxicity. No association was observed in other toxicities outcomes and genetic polymorphisms. According to findings of prognostic outcomes from individual studies, *RFC1 (rs1051266)* was associated with worse 2y-OS and 2y-PFS (in adult), and *SLCO1B1 (rs4149056)* was associated with worse 5y-EFS (in pediatric). However, *FPGS (rs1544105)* was associated with better 2y-OS (in adult). No association was observed in other outcomes of relapse.

Regarding the target, the polymorphisms of *MTHFR* were the most extensively investigated genes. *MTHFR (rs1801133)* was associated with an increased risk of hepatic toxicity, renal toxicity, mucositis, and therapeutic interference (in pediatric). In contrast, *MTHFR (rs1801133)*, *MTHFR (rs1801131)*, and *TYMS (rs34743033)* were associated with a reduced risk of G3-4 hepatic toxicity, renal toxicity, and mucositis, respectively. Only one study investigated the polymorphisms of *ATIC (rs2372536)*, and it reported the lack of association of the neurotoxicity. According to findings of prognostic outcomes from individual studies, no association was observed.

Meta-Analysis of Genetic Polymorphisms Within the Cellular Transport and Metabolism

The Association Between *RFC1* (rs1051266) and Toxicities and Prognosis Outcomes

The pooled OR (HR) of the associations for each outcome under three genetic models is summarized in **Figure 3** and **Supplementary Table S3**. Regarding toxicity outcomes, significant associations were found in the outcomes of hepatotoxicity and overall toxicity. The pooled OR (95% CI) of hepatotoxicity was dominant, 0.62 (0.33–1.16); recessive, 0.35 (0.16–0.76) (**Supplementary Figure S1**); and allelic, 0.77 (0.48–1.21). The pooled OR of renal toxicity under three genetic models was 0.93 (0.41–2.10), 0.73 (0.21–2.56), and 0.91 (0.49–1.70), respectively. The pooled OR (95% CI) of mucositis under three genetic models was 0.91 (0.54–1.52), 0.99 (0.60–1.61), and 0.90 (0.61–1.32), respectively. Besides, a single study of pediatric patients (Laverdière et al., 2002) reported *RFC1* was associated with a reduced risk of overall toxicity (GG vs GA/AA: $p < 0.05$). Neither significant heterogeneity nor significant subgroup difference was detected in most comparisons. A moderate heterogeneity was only found in hepatotoxicity under the dominant model ($P_{het} = 0.02$, $I^2 = 65\%$). Regarding prognosis outcomes, qualitative analysis was performed since meta-analysis was unfeasible. Significant associations were found between *RFC1* and worse 2y-OS and 2y-PFS (GG vs GA/AA: $p < 0.05$), but the association was not observed in the outcome of relapse.

The Association Between *SLCO1B1* (rs4149056) and Toxicities and Prognosis Outcomes

The pooled OR (HR) of the associations for each outcome under three genetic models is summarized in **Figure 3** and **Supplementary Table S4**. Regarding toxicity outcomes, no significant association was found in the outcomes of hepatic toxicity, renal toxicity, mucositis, and other toxicities. A considerable heterogeneity was detected in hepatotoxicity under the dominant model ($P_{het} = 0.0008$, $I^2 = 91\%$), which was partially related to significant differences among pediatric and adult subgroups (**Supplementary Table S4**). The pooled OR (95% CI) of pediatric and adult patients was 0.31 (0.13–0.76) and 3.05 (1.12–8.32), respectively. Regarding prognosis outcomes, qualitative analysis was performed since meta-analysis was unfeasible. Significant associations were found between *SLCO1B1 (rs4149056)* and worse 5y-EFS (CC vs TC/TT: $p < 0.05$), but the association was not observed in the outcomes of relapse.

The Association Between *ABCB1* (rs1045642) and Toxicities and Prognosis Outcomes

The pooled OR (HR) of the associations for *each outcome* under three genetic models is summarized in **Figure 3** and **Supplementary Table S5**. Regarding toxicity outcomes, the pooled OR (95% CI) of hepatotoxicity was dominant, 3.80 (1.68–8.61) (**Supplementary Figure S2**); recessive, 1.91 (0.89–4.09); and allelic, 1.61 (0.89–2.90). Remarkably, for adult patients, the pooled OR (95% CI) of hepatotoxicity under the recessive model was 3.38 (1.07–10.68), which was inconsistent with the overall results of general population. However, neither significant heterogeneity nor significant subgroup difference was detected in all meta-analyses. Regarding prognosis outcomes, two studies (Ma et al., 2015; Esmaili et al., 2020) with conflicting results reported the outcome of EFS, so the association still remained ambiguous.

The Association Between *FPGS* (rs10106, rs1544105) and Toxicities and Prognosis Outcomes

The pooled OR (HR) of the associations is summarized at **Supplementary Tables S6, S7**. One study (Yang et al., 2017) reported no association of *FPGS (rs10106)* and the risk of hepatic toxicity in adults (GG vs AG/AA: OR = 0.60, 95% CI = 0.27–1.32). Conversely, another study (Huang et al., 2016) reported the association of *FPGS (rs1544105)* and better 2y-OS in adults, with the HR (95% CI) = 0.45 (0.24–0.84) under the recessive model.

TABLE 2 | Main characteristics and NOS scores of the studies included

Author-year	Country	Ethnicity	No. of cases	F/M	Age (y)	HWE	Outcome	*RFC1/ SLC19A1*	*SLCO1B1*	*ABCB1*	*FPGS*	*MTHFR*	*MTHFR*	*TYMS/MS*	*ATIC*	NOS score
								80 A>G rs1051266	*521 T>C rs4149056*	*3435 C>T rs1045642*	*2752 G > A, rs1544105; 1994 A>G, rs10106*	*677 C>T rs1801133*	*1298 A>C rs1801131*	*2R>3R rs34743033*	*347 C>G rs2372536*	
Esmaili M A-2020	Iran	Caucasian	74	28/46	Median 5, pediatric	Yes	Tox[a], Prog[b]	AG↗ Tox		T↘ Prog		TT↘ Prog	AC↘ Tox			7
Kotur N-2020	Serbia	Caucasian	148	54/94	Median 5.5 (0.9–17.6)	Yes	Tox	G↘ Tox	NS[c]			NS	NS			7
Liu S G-2017	China	Asian	322	NR	Median 4 (1.0–15.0)	Yes	Tox, Prog	NS	CC↘ Prog	NS						7
Den Hoed M-2014	Netherlands	Caucasian	134	64/70	Median 5.3 (1.4–18.1)	Yes	Tox	NS	NS			NS	NS			8
Suthandiram S-2014	Malaysia	Asian	71	35/36	36.6 ± 14.2	Yes	Tox	G↘ Tox		T↗ Tox		TT↗ Tox	NS			8
Yanagimachi M-2013	Japan	Asian	51	25/26	Median 5.9 (1–15)	Yes	Tox	NS				NS	NS			6
Chiusolo P-2012	Italy	Caucasian	54	25/29	Median 52 (15–78)	Yes	Tox, Prog	GG↘ Prog				NS	C↘ Tox			8
Faganel K B-2011	Slovenia	Caucasian	64	38/26	Median 5 (1.6–16.8)	Yes	Tox	NS		NS		T↗ Tox	NS	3R↘ Tox		8
Faganel K B-2010	Slovenia	Caucasian	60	37/23	Pediatric	Yes	Tox, Prog	NS								8
Ashton L J-2009	Australia	Caucasian	170	NR	Pediatric	Yes	Prog	GG↘ Prog				NS				8
Imanishi H-2007	Japan	Asian	26	10/16	6.7 ± 4.7	Yes	Tox	NS				NS				8
Shimasaki N-2006	Japan	Asian	15	9/6	Median 6 (1–14)	Yes	Tox	G↗ Tox				NS				8
Kishi S-2003	America	Caucasian	53	23/30	Median 6 (0–18)	Yes	Tox	NS				NS				7
Laverdiere C-2002	Canada	Caucasian	204	92/112	Pediatric	Yes	Tox, Prog	GG↘ Tox, GG↗ Prog								7
Yang L-2017	China	Asian	105	33/72	42.5 ± 17.9	Yes	Tox		C↗ Tox		1994 A>G NS					8
Avivi I-2014	Israel	Caucasian	69	20/49	Median 56 (25–83)	Yes	Tox		C↘ Tox	NS		NS	NS			9
Fukushima H-2013	Japan	Asian	103	41/62	Median 7.43 (0.2–19.2)	Yes	Tox, Prog		NS			T↗ Tox	C↗ Prog, C↗ Tox			8
Tsujimoto S-2016	Japan	Asian	56	27/29	Median 5 (0–15)	Yes	Tox			NS		NS			NS	8
Ma C X-2015	China	Asian	178	72/106	Median 30 (18–59)	Yes	Tox, Prog			T↗ Tox						8

(Continued on following page)

TABLE 2 | (*Continued*) Main characteristics and NOS scores of the studies included

Author-year	Country	Ethnicity	No. of cases	F/M	Age (y)	HWE	Outcome	*RFC1/ SLC19A1*	*SLCO1B1*	*ABCB1*	*FPGS*	*MTHFR*	*MTHFR*	*TYMS/MS*	*ATIC*	NOS score
								80 A>G rs1051266	*521 T>C rs4149056*	*3435 C>T rs1045642*	*2752 G > A, rs1544105; 1994 A>G, rs10106*	*677 C>T rs1801133*	*1298 A>C rs1801131*	*2R>3R rs34743033*	*347 C>G rs2372536*	
Chae H-2020	Korea	Asian	117	35/82	Median 9 (5–13)	Yes	Tox					TT↗Tox	NS			8
Chang X-2021	China	Asian	32	11/21	≥14	Yes	Tox					TT↗Tox				8
Giletti-2017	Uruguayan	Caucasian	41	12/29	36 ± 13.9	Yes	Tox					NS				7
Yazicioglu B-2017	Turkey	Caucasian	106	39/67	Median 5 (1–17)	Yes	Tox, Prog					NS	NS	NS		7
Choi Y J-2016	Korea	Asian	111	53/58	Median 60 (17–86)	Yes	Tox					T↗Tox				8
Erculj N-2014	Slovenia	Caucasian	29	4/25	Median 11 (1–8)	Yes	Tox					T↗Tox	NS	NS		8
Erculj, N-2012	Slovenia	Caucasian	167	87/80	Median 4.7 (0.3–18)	Yes	Tox, Prog					NS	NS	NS		8
Haase R-2012	Germany	Caucasian	34	17/17	7.1 ± 4.8	Yes	Tox					NS	NS			7
D'Angelo V-2011	Italy	Caucasian	151	48/103	Pediatric	Yes	Prog					TT↘Prog	NS			7
Liu S G-2011	China	Asian	181	66/115	5.7 ± 3.6	Yes	Tox					NS	C↘Tox			8
Ruiz-Arg elles G J-2007	Mexico	Caucasian	28	7/21	Mean 16.5 (0–40)	Yes	Tox					NS				6
Seidemann-2006	Austria, Germany, Switzerland	Caucasian	484	144/340	Pediatric	Yes	Prog					NS				7
Huang Z-2016	China	Asian	57	26/31	5.9 ± 4.3	Yes	Prog				2752 AA↗Prog					9
Oosterom N-2017	Netherlands	Caucasian	108	49/59	Median 5.7 (1–18)	Yes	Tox							NS		7
Radkte S-2013	Germany	Caucasian	499	204/295	6.4 ± 4.0	Yes	Tox, Prog						CC↘Prog	3R↘Tox		8

Note: ↗: increase; ↘: reduce.

Abbreviation:

[a]*Tox: toxicity.*

[b]*Prog: prognosis.*

[c]*NS: no significant association between the genetic polymorphisms and the outcomes.*

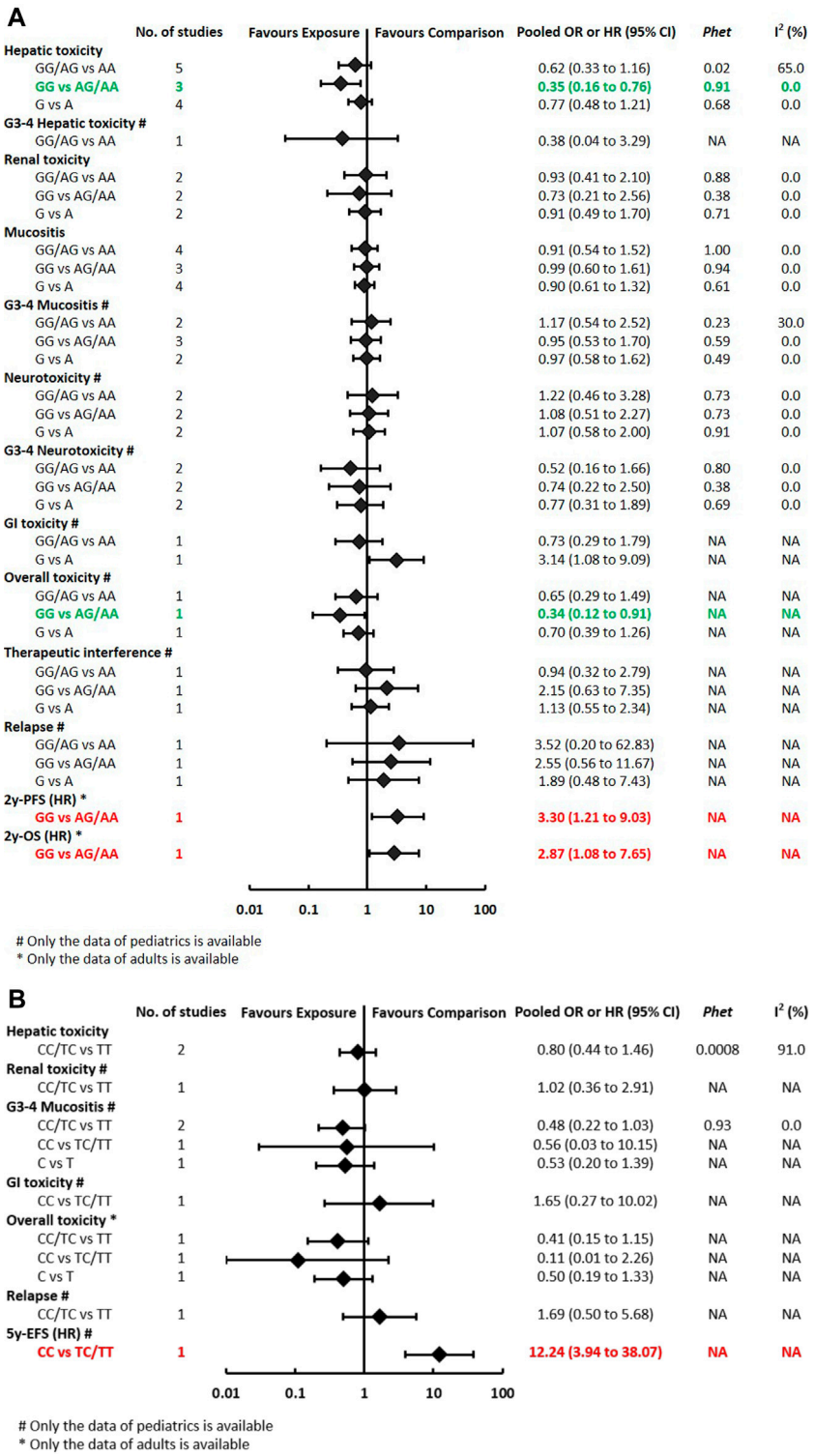

FIGURE 3A-B | (A) Findings of the association between *RFC1 (rs1051266)* and HDMTX-related outcomes under three genetic models. **(B)** Findings of the association between *SLCO1B1 (rs4149056)* and HDMTX-related outcomes under three genetic models.

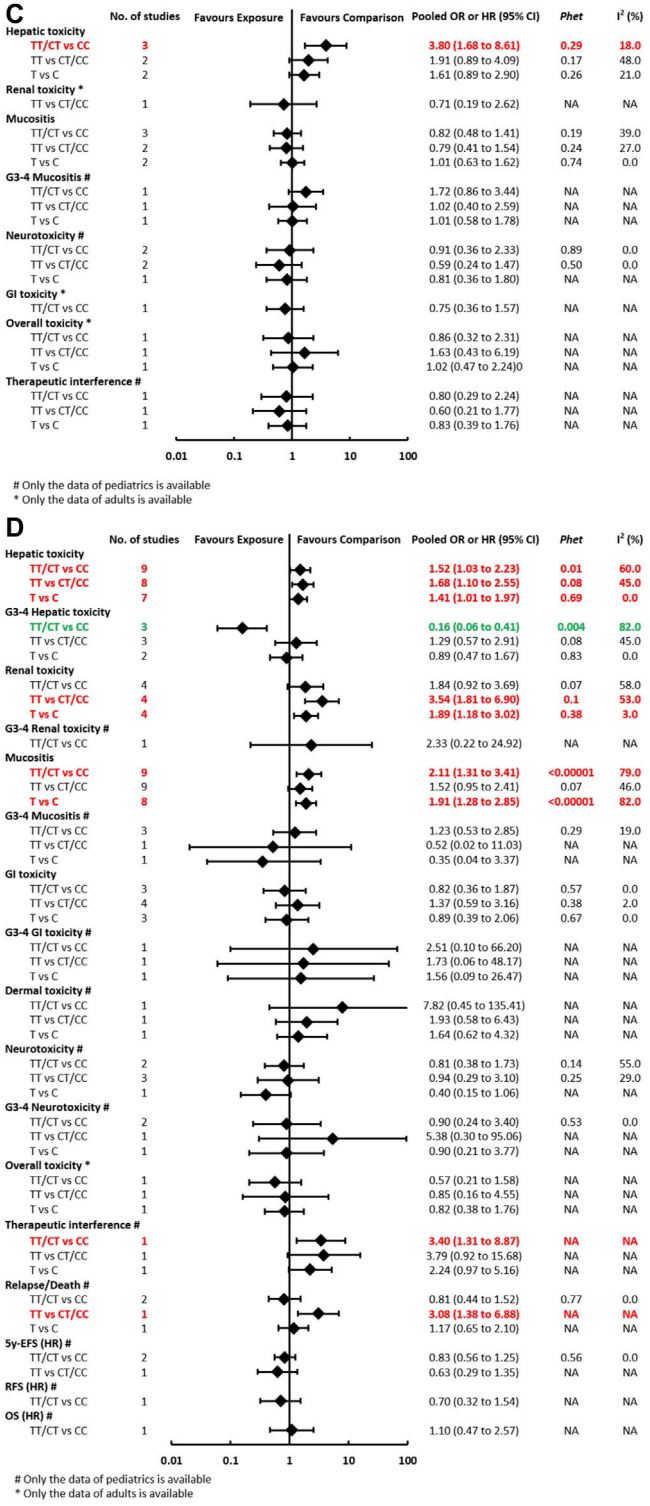

FIGURE 3C-D | (C) Findings of the association between *ABCB1 (rs1045642)* and HDMTX-related outcomes under three genetic models. **(D)** Findings of the association between *MTHFR (rs1801133)* and HDMTX-related outcomes under three genetic models.

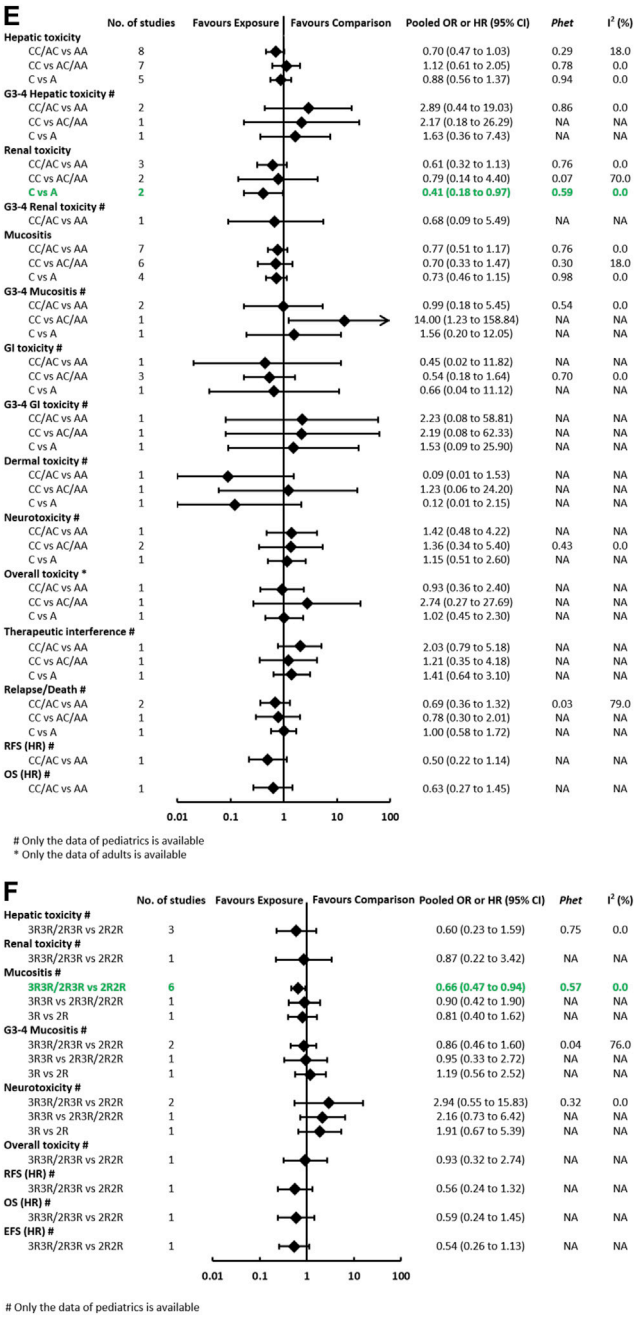

FIGURE 3E-F | (E) Findings of the association between *MTHFR (rs1801131)* and HDMTX-related outcomes under three genetic models. **(F)** Findings of the association between *TYMS (rs34743033)* and HDMTX-related outcomes under three genetic models.

Meta-Analysis of Genetic Polymorphisms Within the Drug Targets

The Association Between *MTHFR* (rs1801133) and Toxicities and Prognosis Outcomes

The pooled OR (HR) of the associations for each outcome under three genetic models is summarized at **Figure 3** and **Supplementary Table S8**. Regarding toxicity outcomes, significant associations were found in the outcomes of hepatotoxicity, G3-4 hepatotoxicity, renal toxicity, and mucositis. The pooled OR (95% CI) of hepatotoxicity was dominant, 1.52 (1.03–2.23) (**Supplementary Figure S3**); recessive, 1.68 (1.10–2.55); and allelic, 1.41 (1.01–1.97). On the contrary, the pooled OR (95% CI) of G3-4 hepatotoxicity under the dominant model was 0.16 (0.06–0.41). The pooled OR of renal toxicity under three genetic models was 1.84 (0.92–3.69), 3.54 (1.81–6.90), and 1.89 (1.18–3.02), respectively. The pooled

OR (95% CI) of mucositis under three genetic models was 2.11 (1.31–3.41), 1.52 (0.95–2.41), and 1.91 (1.28–2.85), respectively. Significant heterogeneity was detected in several positive results, which can be explained partially by significant differences between pediatric and adult subgroups. Remarkably, the associations of hepatic toxicity or renal toxicity were observed in adults but not pediatric patients. However, the associations of mucositis were observed in pediatric but not adult patients (**Supplementary Table S8**). Regarding prognosis outcomes, significant association was found between *MTHFR (rs1801133)* and an increased risk of relapse/death (TT vs CT/CC: $p < 0.05$) in pediatric patients in a single study (D'Angelo et al., 2011), but the association was not observed in other outcomes of OS, RFS, and 5y-EFS.

The Association Between *MTHFR* (rs1801131) and Toxicities and Prognosis Outcomes

The pooled OR (HR) of the associations for each outcome under three genetic models is summarized at **Figure 3** and **Supplementary Table S9**. Regarding toxicity outcomes, significant association was only found in the outcome of renal toxicity. The pooled OR (95% CI) of hepatotoxicity under three genetic models was 0.70 (0.47–1.03), 1.12 (0.61–2.05), and 0.88 (0.56–1.37), respectively. Notably, the association of hepatic toxicity was observed in pediatric (AC/CC vs AA: OR=0.59, 95% CI=0.37–0.92) but not adult patients. The pooled OR of renal toxicity under three genetic models was 0.61 (0.32–1.13), 0.79 (0.14–4.40), and 0.41 (0.18–0.97), respectively. The pooled OR (95% CI) of mucositis under three genetic models was 0.77 (0.51–1.17), 0.70 (0.33–1.47), and 0.73 (0.46–1.15), respectively. Neither significant heterogeneity nor significant subgroup difference was detected in all comparisons (**Supplementary Table S9**). Regarding prognosis outcomes in pediatric patients, two studies (Erčulj et al., 2012; Fukushima et al., 2013) with conflicting results reported the outcome of EFS, so the association still remained ambiguous. No association was observed in other prognosis outcomes of relapse/death, OS, and RFS.

The Association Between *TYMS* (rs34743033) and Toxicities and Prognosis Outcomes

The pooled OR (HR) of the associations for each outcome under three genetic models is summarized at **Figure 3** and **Supplementary Table S10**. A meta-analysis of four studies showed that *TYMS (rs34743033)* was marginally associated with a reduced risk of mucositis under the dominant model (OR = 0.66, 95% CI = 0.47–0.94) (**Supplementary Figure S4**). No association was observed in the outcomes of hepatotoxicity, renal toxicity, neurotoxicity, and overall toxicity. Regarding prognosis outcomes, meta-analysis was unfeasible since only single study (Erčulj et al., 2012) reported the same outcomes, and no association was found in outcomes of OS, EFS, and RFS.

The Association Between *ATIC* (rs2372536) and Toxicities

The pooled OR of the associations is summarized at **Supplementary Table S11**. Only one study (Tsujimoto et al., 2016) investigated the relationship between *ATIC (rs2372536)* and neurotoxicity in pediatric patients and did not report the presence of an association.

Sensitivity Analyses

To assess the impact of individual studies on the overall pooled estimate and explore potential sources of heterogeneity, sensitivity analyses were conducted by removing each study one by one for each comparison. In a total of 66 meta-analyses in this study, substantial changes were indicated in a small proportion of comparisons. For the meta-analysis of *RFC1 (rs1051266)*, the outcome of hepatotoxicity under the dominant model changed to OR = 0.39 with 95% CI = 0.19–0.80 after excluding Esmali 2020 (Esmaili et al., 2020). For the *MTHFR (rs1801133)*, the statistically significant result of hepatotoxicity under the dominant model changed substantially after excluding Chang 2021 (Chang et al., 2021) or Suthandiram 2014 (Suthandiram et al., 2014) or Fukushima 2013 (Fukushima et al., 2013) or switching into the random-effects model (**Figure 4**). Similarly, the substantial changes of pooled OR (95% CI) were detected in the following comparisons of *MTHFR (rs1801133)*: the result of hepatotoxicity under recessive and allelic models after excluding Chang 2021 (Chang et al., 2021) or Suthandiram 2014 (Suthandiram et al., 2014); the renal toxicity under recessive and allelic models after excluding Chang 2021 (Chang et al., 2021); the mucositis under dominant and allelic models after excluding Faganel 2011 (Faganel Kotnik et al., 2011); and the mucositis under the recessive model after excluding Suthandiram 2014 (Suthandiram et al., 2014). However, the pooled estimate of all the other comparisons did not change significantly when different data were used, indicating that the conclusions of this study had a certain degree of reliability.

Publication Bias Assessment

Publication bias was evaluated by analyzing the funnel plots visually. Serious publication bias was not indicated in any of the outcomes. For instance, the funnel plot (**Supplementary Figure S5**) does not suggest any serious bias for hepatotoxicity under the dominant model of *MTHFR (rs1801133)*. However, it is notable that publication bias for some outcomes could not be excluded entirely by visual inspection of the funnel plots.

DISCUSSION

General Findings and Trends

Recently, investigations into the HDMTX response from the perspective of genetic variation have been relatively recent and wide in scope. In this study, we conducted a systematic review aiming to identify and summarize present evidence evaluating the associations between genetic polymorphisms with HDMTX toxicity and prognosis outcomes. With the aim of identifying relevant variants that could be implemented in clinical prediction, we reviewed and investigated genetic polymorphisms within the whole pathway of drug metabolism and targets in this study. As HDMTX is far more toxic than low-dose MTX (Schmiegelow, 2009), patients with malignant cancer receiving HDMTX are

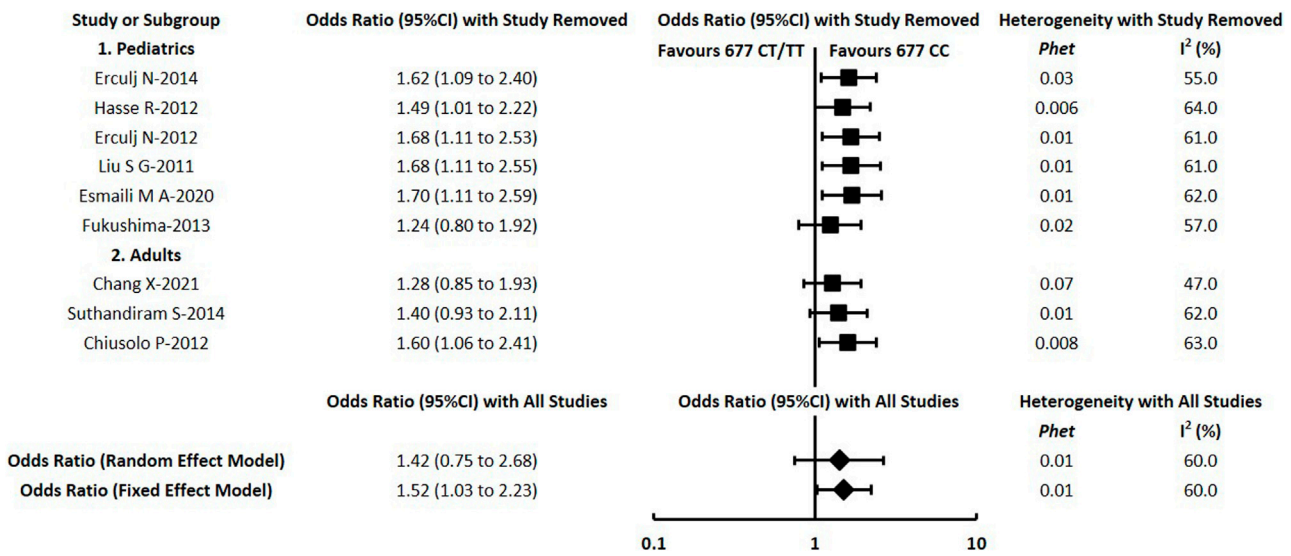

FIGURE 4 | Sensitivity analysis for meta-analysis of the association between *MTHFR (rs1801133)* and hepatotoxicity under the dominant model.

more easily associated with serious toxic responses than those with rheumatoid arthritis. Besides, the dosage and infusion regimens of HDMTX vary greatly in the treatment of hematological malignancies and osteosarcoma (Ramsey et al., 2018), so toxic responses can be markedly different in the two malignant cancers. Therefore, we pay more attention to patients with hematological malignancies in this present study.

The polymorphisms of *RFC1 (rs1051266)*, *ABCB1 (rs1045642)*, and *MTHFR (rs1801133*, *rs1801131)* were the research focus in current pharmacogenetic studies of HDMTX. The most investigated clinical outcomes were hepatic toxicity and mucositis, followed by renal toxicity, while prognostic outcomes were reported by a small proportion of studies (14/34). Generally speaking, our study confirmed that the *MTHFR 677C>T (rs1801133)* has a significant effect on the increased risk of HDMTX toxicities (including hepatotoxicity, mucositis, and renal toxicity), and the *ABCB1 3435C>T (rs1045642)* has a significant effect on the increased risk of hepatotoxicity, which corresponds to the findings in previous studies (Yang et al., 2012; Zhao et al., 2016; Zhu et al., 2018; Yao et al., 2019; Maagdenberg et al., 2021), whereas we found a tendency toward reduced risk of hepatotoxicity in carriers of *RFC1 80GG* and toward reduced risk of mucositis in those with *TYMS 3R3R or 2R3R* genotypes. Also, a tendency toward reduced risk of renal toxicity was observed in carriers with the *MTHFR 1298 variant C allele*, which was similar to the results of mucositis and GI toxicity (Zhao et al., 2016) and dermal toxicity (Yang et al., 2012). In other words, a protective effect of some genetic polymorphisms on developing individual toxicities is suggestive in our study. It is worth mentioning that Lopez-Lopez 2013 (Lopez-Lopez et al., 2013) reported no association between *MTHFR 677C>T* and MTX toxicity in pediatric ALL (recessive model), and Oosterom 2018 (Oosterom et al., 2018) reported no association between *TYMS 2R>3R* and MTX toxicity in pediatric ALL (dominant model), which were contrary to our findings. The inconsistent patient's age and MTX dosage may explain the discrepancy in different findings. With regard to descriptive analysis, limited evidence from single studies showed significant associations in the following prognosis outcomes: *RFC1 (rs1051266)* and worse 2y-PFS and 2y-OS; *SLCO1B1 (rs4149056)* and worse 5y-EFS; and *FPGS (rs1544105)* and better 2y-OS. Besides, a lack of association was observed in other outcomes investigated in our review.

Since HDMTX-related tolerance and toxicities might be influenced by patients' age in the real clinical practice (Zhu et al., 2018), subgroup analysis was conducted to explore the difference. Significant differences were suggestive in the following outcomes: hepatotoxicity (*SLCO1B1 rs4149056*; *MTHFR rs1801133)*, renal toxicity (*MTHFR rs1801133)*, and mucositis (*MTHFR rs1801133)*. It is worth mentioning that in the meta-analysis of *MTHFR (rs1801133)*, the aforementioned subgroup differences can explain the heterogeneity of those outcomes with positive findings (hepatotoxicity, renal toxicity, and mucositis) to a certain extent. And patients' age is possibly identified as a potential contributor to the association with some certain toxicities.

Review of Previous Meta-Analysis

As the associations between genetic variations and HDMTX toxicities have become a wide clinical concern, some systematic reviews or meta-analyses have been researched earlier. Initially, we conducted an umbrella review of systematic reviews about the pharmacogenetics of MTX toxicity in patients with osteosarcoma or hematological malignancies in 2019 (Song et al., 2019a). After performing an update search and review in July 2021, we found six similar meta-analyses (Yang et al., 2012; Lopez-Lopez et al., 2013; He et al., 2014; Zhao et al., 2016; Oosterom et al., 2018; Yao et al., 2019) had a discussion on this issue in patients with hematological malignancies. Besides, three meta-analyses (Hagleitner et al.,

2014; Zhu et al., 2018; Maagdenberg et al., 2021) included cancer patients and did not distinguish between hematological malignancies and osteosarcoma, although the dosage and infusion regimens of HDMTX vary greatly in the two diseases (**Table 4**).

To the best of our knowledge, there have not been any previous meta-analysis to address the following points: 1) investigated 12 genetic polymorphisms within the whole HDMTX pathway and performed analysis on prognosis outcomes, while most previous studies did not discuss these issues (Yang et al., 2012; Lopez-Lopez et al., 2013; Hagleitner et al., 2014; He et al., 2014; Zhao et al., 2016; Oosterom et al., 2018; Zhu et al., 2018); 2) set strict restrictions on hematological malignancies (specified diseases) and HDMTX (specified dose ranges), since the side effect profile of MTX varies markedly as its dose changes in clinical practice; 3) set strict restrictions on the HWE of included pharmacogenetic research, since HWE is crucial for genetic research; 4) analyzed the associations under the dominant model, recessive model, and allelic model, since the genetic models of HDMTX toxicities remain incompletely understood and need validation, whereas most studies only assumed one genetic model; 5) removed restrictions on patient age and ethnicity, which enabled this review to include a greater number of studies and populations than previous studies. The main characteristics of our review and previous meta-analysis are summarized in **Table 4**. Consequently, our review has provided a comprehensive and up-to-date synthesis of present evidence, and a more reliable conclusion of the association could be reached.

Biological Mechanisms

Currently, the biological mechanisms linking genetic polymorphisms to HDMTX toxicities still remain incompletely understood. In theory, the delayed MTX clearance or prolonged and elevated exposure of MTX can potentially lead to an increased risk of MTX-induced toxicities. But what is interesting, in one study (Yanagimachi et al., 2013), although an association with higher MTX plasma levels was observed, a genetic association with renal toxicity could not be established, which reminds us that other clinical and genetic factors may play a role together.

The enzyme MTHFR plays a critical role in the folate metabolism by catalyzing the conversion of 5,10-methylene-tetrahydrofolate (THF) to 5-methyl-THF. This is the primary circulating form of folate, which is needed to reduce the toxic homocysteine to methionine. Through this process, folate is an important donor of methyl groups for all intracellular methylation processes (Taylor et al., 2021). The mutation *677C>T* (*rs1801133)* causes a change of alanine to valine in the protein, and the mutation *1298A>C (rs1801131)* causes the replacement of glutamate by valine, resulting in decreased enzyme activity of MTHFR(Robien and Ulrich, 2003). Therefore, the mutations lead to the reduction of folate and then might exert an influence in HDMTX-related toxicities. MTX is extruded by cells using different transporters including ABC family members, and P-glycolprotein (P-gp) is a representative cell membrane protein encoded by the gene *ABCB1* (Castaldo et al., 2011). The *ABCB1* 3435C>T *(rs1045642)* mutations can affect the activity of P-gp and thus may play a role in HDMTX toxicities.

Limitations and Future Perspective

Several limitations should be considered for our review. First, the outcome measures we investigated were clinical outcomes of HDMTX-related toxicities or prognosis and not the plasma concentration or other pharmacokinetic outcomes of MTX, since the relationships of clinical outcomes and plasma concentration still remain to be verified. And notably, a recent systematic review has discussed on pharmacogenetic factors influencing HDMTX pharmacokinetics (Taylor et al., 2021). Second, data of prognosis outcomes was substantially lacking, which made the quantitative analysis unfortunately impossible for the most prognosis outcomes. Therefore, the genetic associations with prognostic outcomes still remain inconclusive in this study. Third, the sample size of some studies is too small (most are less than 200), and thus, its statistical power might be limited. Furthermore, in addition to the positive findings in the *MTHFR rs1801133* and the *TYMS rs34743033*, statistically significant results of other genetic polymorphisms are only confirmed by meta-analysis of two to three studies. The fact that a meta-analysis of two studies reveals the association between *MTHFR rs1801131* and a decreased risk of renal toxicity (allelic model) means that the trend may not reflect the actual situation, and the results should be cautiously explained. Last but not least, although overall heterogeneity was not observed, the baseline characteristics varied among studies included, including diverse treatment protocols, infusion hours of HDMTX, leucovorin rescue, and other therapy-related factors which might contribute to the associations observed in these studies.

The aforementioned limitations warrant future larger validation studies into genetic association of HDMTX-related clinical outcomes. In line with the research gaps, we would recommend that further studies pay more attention to prognosis outcomes and the genetic polymorphisms of *FPGS (rs10106*, *rs1544105)*, *GGH (rs3758149)*, *DHFR (rs408626*, *rs442767)*, and *ATIC (rs2372536).* And the validation studies are encouraged to calculate the sample size, establish analysis strategies, and prospectively collect data of toxicity and prognosis. With the aim to construct clinically relevant prediction models, the future studies should not focus on the individual effect of single polymorphisms but take into account other polymorphisms within the whole pharmacokinetic and targets/folate pathway. Besides, the prospective cohort studies are encouraged to confirm the clinical benefits of genetic testing by comparing the differences between patients performing genetic testing and those who have not carried out testing.

Recommendation for Clinical Practice

In light of the findings in this study, associations between genetic variations and the increased/decreased risk of HDMTX toxicities are observed, whereas the association of prognosis outcomes still remains inconclusive due to lacking data. From a clinician or pharmacist's point of view, we focus more on the role of genetic testing in predicting increased toxicity to tailor MTX therapy,

TABLE 3 | Overall findings

	Dominant model	Recessive model	Allelic model	Other findings of prognosis[a]
***RFC1* A80G (rs1051266)**	GG/AG vs AA	GG vs AG/AA	G vs A	
Hepatotoxicity	=	↘	=	
G3-4 hepatotoxicity (pediatric)	=	No data	No data	
Renal toxicity	=	=	=	
Mucositis	=	=	=	
G3-4 mucositis (pediatric)	=	=	=	
Neurotoxicity (pediatric)	=	=	=	
G3-4 neurotoxicity (pediatric)	=	=	=	
GI[b] toxicity (pediatric)	=	No data	=	
Overall toxicity (pediatric)	=	↘	=	
Therapeutic interference (pediatric)	=	=	=	
Relapse (pediatric)	=	=	=	
2y-PFS (adult)	No data	↘	No data	NR[c]
2y-OS (adult)	No data	↘	No data	NR
5y-EFS (pediatric)	No data	=	No data	NR
***SLCO1B1* T521C (rs4149056)**	**CC/TC vs TT**	**CC vs TC/TT**	**C vs T**	
Hepatotoxicity	=	No data	No data	
Renal toxicity (pediatric)	=	No data	No data	
G3-4 mucositis (pediatric)	=	=	=	
GI toxicity (pediatric)	No data	=	No data	
Overall toxicity (adult)	=	=	=	
Relapse (pediatric)	=	No data	No data	
5y-EFS (pediatric)	No data	↘	No data	NR
***ABCB1* C3435T (rs1045642)**	**TT/CT vs CC**	**TT vs CT/CC**	**T vs C**	
Hepatotoxicity	↗	=	=	
Renal toxicity (adult)	No data	=	No data	
Mucositis	=	=	=	
G3-4 Mucositis (pediatric)	=	=	=	
Neurotoxicity (pediatric)	=	=	=	
GI toxicity (adult)	=	No data	No data	
Overall toxicity (adult)	=	=	=	
Therapeutic interference (pediatric)	=	=	=	
EFS	= **or**↘	No data	No data	NR
***FPGS* A1994G (rs10106)**	**GG/AG vs AA**	**GG vs AG/AA**	**G vs A**	
Hepatotoxicity (adult)	No data	=	No data	
***FPGS* G2752A (rs1544105)**	**AA/GA vs GG**	**AA vs GA/AA**	**A vs G**	
2y-OS (adult)	No data	↗	No data	NR
***MTHFR* C677T (rs1801133)**	**TT/CT vs CC**	**TT vs CT/CC**	**T vs C**	
Hepatotoxicity	↗	↗	↗	
G3-4 hepatotoxicity	↘	=	=	
Renal toxicity	=	↗	↗	
G3-4 renal toxicity (pediatric)	=	No data	No data	
Mucositis	↗	=	↗	
G3-4 mucositis (pediatric)	=	=	=	
G3-4 GI toxicity (pediatric)	=	=	=	
Dermal toxicity (pediatric)	=	=	=	
Neurotoxicity (pediatric)	=	=	=	
Overall toxicity (adult)	=	=	=	
Therapeutic interference (pediatric)	↗	=	=	
Relapse/death (pediatric)	=	↗	=	
5y-EFS (pediatric)	=	=	No data	**(TT vs CT vs CC)** =
RFS (pediatric)	=	No data	No data	NR
OS (pediatric)	=	No data	No data	NR
***MTHFR* A1298C (rs1801131)**	**CC/AC vs AA**	**CC vs AC/AA**	**C vs A**	
Hepatotoxicity	=	=	=	
G3-4 Hepatotoxicity (Pediatric)	=	=	=	
Renal toxicity	=	=	↘	
G3-4 renal toxicity (pediatric)	=	No data	No data	
Mucositis	=	=	=	
G3-4 mucositis (pediatric)	=	=	=	
GI toxicity (pediatric)	=	=	=	
G3-4 GI toxicity (pediatric)	=	=	=	
Dermal toxicity (pediatric)	=	=	=	
Neurotoxicity (pediatric)	=	=	=	
Overall toxicity (adult)	=	=	=	

(Continued on following page)

TABLE 3 | (*Continued*) Overall findings

	Dominant model	Recessive model	Allelic model	Other findings of prognosis[a]
Therapeutic interference (pediatric)	=	=	=	
Relapse/death (pediatric)	=	=	=	
EFS (pediatric)	= or↗	No data	No data	**(AC vs CC vs AA)** = **(CC vs AA)** ↘
RFS (pediatric)	=	No data	No data	NR
OS (pediatric)	=	No data	No data	NR
***TYMS*/*MS* 2R>3R (rs34743033)**	**3R3R/2R3R vs 2R2R**	**3R3R vs 2R3R/2R2R**	**3R vs 2R**	
Hepatotoxicity (pediatric)	=	No data	No data	
Renal toxicity (pediatric)	=	No data	No data	
Mucositis (pediatric)	↘	=	=	
G3-4 mucositis (pediatric)	=	=	=	
Neurotoxicity (pediatric)	=	=	=	
Overall toxicity (pediatric)	=	No data	No data	
RFS (pediatric)	=	No data	No data	NR
OS (pediatric)	=	No data	No data	NR
EFS (pediatric)	=	No data	No data	**(2R3R vs 3R3R vs 2R2R)** =
***ATIC* 347C>G (rs2372536)**	**GG/CG vs CC**	**GG vs CG/CC**	**G vs C**	
Neurotoxicity (pediatric)	=	=	No data	

Note: *↗: increase; ↘: reduce; =: no association between the genetic polymorphism and the outcome; = or↗: no association or increase; = or↘: no association or reduce.*
[a]*Several included studies reported outcomes of prognosis in other genetic models, and we also included these results for narrative analysis in the present review.*
[b]*GI: gastrointestinal.*
[c]*NR: not reported.*

TABLE 4 | Main characteristics of our review and previous meta-analysis

	Present review	Maagdenberg et al. (2021)	Yao et al. (2019)	Oosterom et al. (2018)	Zhu et al. (2018)	Zhao et al. (2016)	He et al. (2014)	Hagleitner et al. (2014)	Lopez-Lopez et al. (2013)	Yang et al. (2012)
Gene	*RFC1*, *SLCO1B1*, *ABCB1*, *GGH*, *FPGS*, *DHFR*, *MTHFR*, *TYMS*, *ATIC*	*RFC1*, *SLCO1B1*, *DHFR*, *MTHFR*, *TYMS*, *MTRR*, *ABCC2*, *andetc*	*MTHFR*	*TYMS*	*MTHFR*	*MTHFR*	*RFC1*	*MTHFR*	*MTHFR*	*MTHFR*
Population	HM[a]	HM, OS[b]	HM	ALL[c]	HM, OS	HM	ALL	HM, OS	ALL	ALL
Age	No restriction	No restriction	No restriction	Pediatric	Pediatric	Adult	Pediatric	No restriction	Pediatric	No restriction
Outcomes	Toxicity, Prognosis	Mucositis	Toxicity, Prognosis	Mucositis	Toxicity	Toxicity	Toxicity	Hepatotoxicity	Toxicity	Toxicity
Dose of MTX	HDMTX	No restriction	No restriction	HDMTX	HDMTX	No restriction	No restriction	No restriction	No restriction	No restriction
HWE restriction	Yes	Yes	No restriction	Yes	No restriction	No restriction	No restriction	No restriction	No restriction	No restriction
Genetic models	Dom[d],Rec[e],Alle[f]	Dom, Rec, Alle, Overdom[g]	Dom	Dom	Dom, Rec, Homo[h]	Dom, Rec, Alle, Homo, Het[i]	Dom	Alle	Rec	Dom, Rec, Alle, Homo
Date of search	Dec 2020	Aug 2019	Jan 2018	Oct 2017	Aug 2016	Sep 2015	Sep 2013	Dec 2010	Nov 2011	Sep 2011
Studies included	34	57	17	8	14	6	15	7	24	14

Abbreviation:
[a]*HM: hematological malignancies.*
[b]*OS: osteosarcoma.*
[c]*ALL: acute lymphoblastic leukemia.*
[d]*Dom: dominant model*
[e]*Rec: recessive model.*
[f]*Alle: allelic model.*
[g]*Overdom: overdominant model.*
[h]*Homo: homozygote model.*
[i]*Het: heterozygote model.*

while the data of the potentially protective effect may be less meaningful clinically. With regard to clinical implementation of pharmacogenomics (PGx), the certainty and reliability of supporting evidence are important factors to consider. For instance, the associations between *MTHFR 677C>T (rs1801133)* and an increased risk of hepatotoxicity and mucositis are demonstrated by meta-analysis of nine studies, while the associations between *ABCB1 3435C>T (rs1045642)* and hepatotoxicity are supported by meta-analysis of only three studies.

With the aim to provide practical recommendations, we also reviewed drug instructions of MTX, clinical guidelines or expert consensus of HDMTX, CPIC, and several other pharmacogenetics guidelines. The French National Network of Pharmacogenetics (RNPGx) states that methotrexate pharmacogenetic tests are potentially useful in cancer patients (Quaranta and Thomas, 2017). The evidence-based practice guideline of HDMTX medication of the Chinese Pharmacological Society (Wang et al., 2021) states that the genotyping of *MTHFR 677C>T* and *1298A>C* polymorphisms can be considered for patients with hematological malignancies (weak recommendation, moderate quality evidence), and the genotyping of *ABCB1 3435C>T* may be considered under certain conditions (weak recommendation, low-quality evidence). Further combining the PGx implementation of HDMTX from Chinese perspective (Song et al., 2019b), we would recommend clinicians to consider genetic testing of *MTHFR* polymorphisms when necessary, and *ABCB1* 3435C>T can also be a potential candidate gene. Since patients with gene mutations (*MTHFR 677C>T* particularly) are at the risk of increased hepatotoxicity and/or mucositis, a relatively lower dose and closer monitoring of plasma MTX concentrations are advisable to these patients.

It is worth mentioning that although PGx research has been advanced rapidly in recent years, the clinical implementation of PGx has a long way to go (Guo et al., 2021). To reduce HDMTX-related toxicities and improve outcomes, in addition to the role of genetic polymorphisms, renal function evaluation prior to treatment, co-medications, hydration and urinary alkalization, therapeutic drug monitoring (TDM), and leucovorin rescue might be taken into full consideration. Renal toxicity is one of the most feared side effects of MTX, since the renal dysfunction significantly delays MTX clearance and may cause other toxicities (Schmiegelow, 2009). So far, there is no proven useful approach to predict the individual risk of acute renal failure from the perspective of genetic variation. However, the implementation of standardized hydration and urinary alkalinization and TDM during HDMTX therapy contributes a lot to prevent renal toxicity and maintain MTX elimination.

CONCLUSION

In conclusion, the available evidence confirms the associations between the genes *MTHFR* and *ABCB1* and the increased risk of HDMTX toxicity. And a tendency of the genes *RFC1* and *TYMS* toward the decreased toxicity is suggestive in this systematic review. However, current evidence does not support the presence of the associations of the gene *SLCO1B1*. Current studies are often underpowered and unfit to investigate the genetic association of prognosis outcomes. We conclude that genotyping of *MTHFR* and/or *ABCB1* polymorphisms prior to treatment, *MTHFR 677C>T* particularly, is likely to be potentially useful with the aim of tailoring HDMTX therapy and thus reducing toxicity in patients with hematological malignancies. Future larger validation studies into genetic association of HDMTX are still needed.

DATA AVAILABILITY STATEMENT

The original contributions presented in the study are included in the article/**Supplementary Material**; further inquiries can be directed to the corresponding author.

AUTHOR CONTRIBUTIONS

ZS, RZ conceived and designed the study. ZS, YH, and SL collected, analyzed the data, and performed the statistical analysis. ZS wrote the article. ZS, YH, and DJ prepared the pictures and tables. RZ, ZY, and MB provided suggestions and participated in the revision of the article. All authors read and approved the final manuscript.

FUNDING

This work was supported by the National Natural Science Foundation of China (NSFC) (72074005) and the National Key R&D Program of China (2020YFC2008305).

ACKNOWLEDGMENTS

The authors acknowledge the Division of TDM, Chinese Pharmacological Society for launching and approving the project of Medication Therapy of High-Dose Methotrexate: An Evidence-Based Practice Guideline, in which this study was designed to answer clinical problems about genetic testing. The authors thank the anonymous peer reviewers for constructive criticism and suggested additions, which have all been addressed and have significantly improved this article.

SUPPLEMENTARY MATERIAL

The Supplementary Material for this article can be found online at: https://www.frontiersin.org/articles/10.3389/fphar.2021.757464/full#supplementary-material

REFERENCES

Ashton, L. J., Gifford, A. J., Kwan, E., Lingwood, A., Lau, D. T., Marshall, G. M., et al. (2009). Reduced Folate Carrier and Methylenetetrahydrofolate Reductase Gene Polymorphisms: Associations with Clinical Outcome in Childhood Acute Lymphoblastic Leukemia. *Leukemia* 23 (7), 1348–1351. doi:10.1038/leu.2009.67

Assaraf, Y. G. (2006). The Role of Multidrug Resistance Efflux Transporters in Antifolate Resistance and Folate Homeostasis. *Drug Resist. Updat* 9 (4–5), 227–246. doi:10.1016/j.drup.2006.09.001

Avivi, I., Zuckerman, T., Krivoy, N., and Efrati, E. (2014). Genetic Polymorphisms Predicting Methotrexate Blood Levels and Toxicity in Adult Non-hodgkin Lymphoma. *Leuk. Lymphoma* 55 (3), 565–570. doi:10.3109/10428194.2013.789506

Castaldo, P., Magi, S., Nasti, A. A., Arcangeli, S., Lariccia, V., Alesi, N., et al. (2011). Clinical Pharmacogenetics of Methotrexate. *Curr. Drug Metab.* 12 (3), 278–286. doi:10.2174/138920011795101840

Chae, H., Kim, M., Choi, S. H., Kim, S. K., Lee, J. W., Chung, N. G., et al. (2020). Influence of Plasma Methotrexate Level and MTHFR Genotype in Korean Paediatric Patients with Acute Lymphoblastic Leukaemia. *J. Chemother.* 32 (5), 251–259. doi:10.1080/1120009x.2020.1764280

Chang, X., Guo, Y., Su, L., Zhang, Y., Hui, W., Zhao, H., et al. (2021). Influence of MTHFR C677T Polymorphism on High-Dose Methotrexate-Related Toxicity in Patients with Primary Central Nervous System Diffuse Large B-Cell Lymphoma. *Clin. Lymphoma Myeloma Leuk.* 21 (2), 91–96. doi:10.1016/j.clml.2020.08.020

Chiusolo, P., Giammarco, S., Bellesi, S., Metafuni, E., Piccirillo, N., De Ritis, D., et al. (2012). The Role of MTHFR and RFC1 Polymorphisms on Toxicity and Outcome of Adult Patients with Hematological Malignancies Treated with High-Dose Methotrexate Followed by Leucovorin rescue. *Cancer Chemother. Pharmacol.* 69 (3), 691–696. doi:10.1007/s00280-011-1751-4

Choi, Y. J., Park, H., Lee, J. S., Lee, J. Y., Kim, S., Kim, T. W., et al. (2017). Methotrexate Elimination and Toxicity: MTHFR 677C>T Polymorphism in Patients with Primary CNS Lymphoma Treated with High-Dose Methotrexate. *Hematol. Oncol.* 35 (4), 504–509. doi:10.1002/hon.2363

Coluzzi, F., Rocco, M., Green Gladden, R., Persiani, P., Thur, L. A., and Milano, F. (2020). Pain Management in Childhood Leukemia: Diagnosis and Available Analgesic Treatments. *Cancers (Basel)* 12 (12), 3671. doi:10.3390/cancers12123671

D'Angelo, V., Ramaglia, M., Iannotta, A., Crisci, S., Indolfi, P., Francese, M., et al. (2011). Methotrexate Toxicity and Efficacy during the Consolidation Phase in Paediatric Acute Lymphoblastic Leukaemia and MTHFR Polymorphisms as Pharmacogenetic Determinants. *Cancer Chemother. Pharmacol.* 68 (5), 1339–1346. doi:10.1007/s00280-011-1665-1

den Hoed, M. A., Lopez-Lopez, E., te Winkel, M. L., Tissing, W., de Rooij, J. D., Gutierrez-Camino, A., et al. (2015). Genetic and Metabolic Determinants of Methotrexate-Induced Mucositis in Pediatric Acute Lymphoblastic Leukemia. *Pharmacogenomics J.* 15 (3), 248–254. doi:10.1038/tpj.2014.63

Erčulj, N., Kotnik, B. F., Debeljak, M., Jazbec, J., and Dolžan, V. (2012). Influence of Folate Pathway Polymorphisms on High-Dose Methotrexate-Related Toxicity and Survival in Childhood Acute Lymphoblastic Leukemia. *Leuk. Lymphoma* 53 (6), 1096–1104. doi:10.3109/10428194.2011.639880

Erculj, N., Kotnik, B. F., Debeljak, M., Jazbec, J., and Dolzan, V. (2014). The Influence of Folate Pathway Polymorphisms on High-Dose Methotrexate-Related Toxicity and Survival in Children with Non-hodgkin Malignant Lymphoma. *Radiol. Oncol.* 48 (3), 289–292. doi:10.2478/raon-2013-0076

Esmaili, M. A., Kazemi, A., Faranoush, M., Mellstedt, H., Zaker, F., Safa, M., et al. (2020). Polymorphisms within Methotrexate Pathway Genes: Relationship between Plasma Methotrexate Levels, Toxicity Experienced and Outcome in Pediatric Acute Lymphoblastic Leukemia. *Iran J. Basic Med. Sci.* 23 (6), 800–809. doi:10.22038/ijbms.2020.41754.9858

Faganel Kotnik, B., Dolzan, V., Grabnar, I., and Jazbec, J. (2010). Relationship of the Reduced Folate Carrier Gene Polymorphism G80A to Methotrexate Plasma Concentration, Toxicity, and Disease Outcome in Childhood Acute Lymphoblastic Leukemia. *Leuk. Lymphoma* 51 (4), 724–726. doi:10.3109/10428191003611402

Faganel Kotnik, B., Grabnar, I., Bohanec Grabar, P., Dolžan, V., and Jazbec, J. (2011). Association of Genetic Polymorphism in the Folate Metabolic Pathway with Methotrexate Pharmacokinetics and Toxicity in Childhood Acute Lymphoblastic Leukaemia and Malignant Lymphoma. *Eur. J. Clin. Pharmacol.* 67 (10), 993–1006. doi:10.1007/s00228-011-1046-z

Fukushima, H., Fukushima, T., Sakai, A., Suzuki, R., Nakajima-Yamaguchi, R., Kobayashi, C., et al. (2013). Polymorphisms of MTHFR Associated with Higher Relapse/Death Ratio and Delayed Weekly MTX Administration in Pediatric Lymphoid Malignancies. *Leuk. Res. Treat.* 2013, 238528. doi:10.1155/2013/238528

Gervasini, G., and Mota-Zamorano, S. (2019). Clinical Implications of Methotrexate Pharmacogenetics in Childhood Acute Lymphoblastic Leukaemia. *Curr. Drug Metab.* 20 (4), 313–330. doi:10.2174/1389200220666190130161758

Giletti, A., and Esperon, P. (2018). Genetic Markers in Methotrexate Treatments. *Pharmacogenomics J.* 18 (6), 689–703. doi:10.1038/s41397-018-0047-z

Giletti, A., Vital, M., Lorenzo, M., Cardozo, P., Borelli, G., Gabus, R., et al. (2017). Methotrexate Pharmacogenetics in Uruguayan Adults with Hematological Malignant Diseases. *Eur. J. Pharm. Sci.* 109, 480–485. doi:10.1016/j.ejps.2017.09.006

Guo, C., Hu, B., Guo, C., Meng, X., Kuang, Y., Huang, L., et al. (2021). A Survey of Pharmacogenomics Testing Among Physicians, Pharmacists, and Researchers from China. *Front. Pharmacol.* 12, 682020. doi:10.3389/fphar.2021.682020

Haase, R., Elsner, K., Merkel, N., Stiefel, M., Mauz-Körholz, C., Kramm, C. M., et al. (2012). High Dose Methotrexate Treatment in Childhood ALL: Pilot Study on the Impact of the MTHFR 677C>T and 1298A>C Polymorphisms on MTX-Related Toxicity. *Klin Padiatr* 224 (3), 156–159. doi:10.1055/s-0032-1304623

Hagleitner, M. M., Coenen, M. J., Aplenc, R., Patiño-Garcia, A., Chiusolo, P., Gemmati, D., et al. (2014). The Role of the MTHFR 677C>T Polymorphism in Methotrexate-Induced Liver Toxicity: a Meta-Analysis in Patients with Cancer. *Pharmacogenomics J.* 14 (2), 115–119. doi:10.1038/tpj.2013.19

He, H. R., Liu, P., He, G. H., Dong, W. H., Wang, M. Y., Dong, Y. L., et al. (2014). Association between Reduced Folate Carrier G80A Polymorphism and Methotrexate Toxicity in Childhood Acute Lymphoblastic Leukemia: a Meta-Analysis. *Leuk. Lymphoma* 55 (12), 2793–2800. doi:10.3109/10428194.2014.898761

Howard, S. C., McCormick, J., Pui, C. H., Buddington, R. K., and Harvey, R. D. (2016). Preventing and Managing Toxicities of High-Dose Methotrexate. *Oncologist* 21 (12), 1471–1482. doi:10.1634/theoncologist.2015-0164

Huang, Z., Tong, H. F., Li, Y., Qian, J. C., Wang, J. X., Wang, Z., et al. (2016). Effect of the Polymorphism of Folylpolyglutamate Synthetase on Treatment of High-Dose Methotrexate in Pediatric Patients with Acute Lymphocytic Leukemia. *Med. Sci. Monit.* 22, 4967–4973. doi:10.12659/msm.899021

Imanishi, H., Okamura, N., Yagi, M., Noro, Y., Moriya, Y., Nakamura, T., et al. (2007). Genetic Polymorphisms Associated with Adverse Events and Elimination of Methotrexate in Childhood Acute Lymphoblastic Leukemia and Malignant Lymphoma. *J. Hum. Genet.* 52 (2), 166–171. doi:10.1007/s10038-006-0096-z

Kishi, S., Griener, J., Cheng, C., Das, S., Cook, E. H., Pei, D., et al. (2003). Homocysteine, Pharmacogenetics, and Neurotoxicity in Children with Leukemia. *J. Clin. Oncol.* 21 (16), 3084–3091. doi:10.1200/jco.2003.07.056

Kotur, N., Lazic, J., Ristivojevic, B., Stankovic, B., Gasic, V., Dokmanovic, L., et al. (2020). Pharmacogenomic Markers of Methotrexate Response in the Consolidation Phase of Pediatric Acute Lymphoblastic Leukemia Treatment. *Genes (Basel)* 11 (4), 468. doi:10.3390/genes11040468

Laverdière, C., Chiasson, S., Costea, I., Moghrabi, A., and Krajinovic, M. (2002). Polymorphism G80A in the Reduced Folate Carrier Gene and its Relationship to Methotrexate Plasma Levels and Outcome of Childhood Acute Lymphoblastic Leukemia. *Blood* 100 (10), 3832–3834. doi:10.1182/blood.V100.10.3832

Liu, S. G., Gao, C., Zhang, R. D., Zhao, X. X., Cui, L., Li, W. J., et al. (2017). Polymorphisms in Methotrexate Transporters and Their Relationship to Plasma Methotrexate Levels, Toxicity of High-Dose Methotrexate, and Outcome of Pediatric Acute Lymphoblastic Leukemia. *Oncotarget* 8 (23), 37761–37772. doi:10.18632/oncotarget.17781

Liu, S. G., Li, Z. G., Cui, L., Gao, C., Li, W. J., and Zhao, X. X. (2011). Effects of Methylenetetrahydrofolate Reductase Gene Polymorphisms on Toxicities during Consolidation Therapy in Pediatric Acute Lymphoblastic Leukemia in a Chinese Population. *Leuk. Lymphoma* 52 (6), 1030–1040. doi:10.3109/10428194.2011.563883

Lopez-Lopez, E., Martin-Guerrero, I., Ballesteros, J., and Garcia-Orad, A. (2013). A Systematic Review and Meta-Analysis of MTHFR Polymorphisms in Methotrexate Toxicity Prediction in Pediatric Acute Lymphoblastic Leukemia. *Pharmacogenomics J.* 13 (6), 498–506. doi:10.1038/tpj.2012.44

Ma, C. X., Sun, Y. H., and Wang, H. Y. (2015). ABCB1 Polymorphisms Correlate with Susceptibility to Adult Acute Leukemia and Response to High-Dose Methotrexate. *Tumour Biol.* 36 (10), 7599–7606. doi:10.1007/s13277-015-3403-5

Maagdenberg, H., Oosterom, N., Zanen, J., Gemmati, D., Windsor, R. E., Heil, S. G., et al. (2021). Genetic Variants Associated with Methotrexate-Induced Mucositis in Cancer Treatment: A Systematic Review and Meta-Analysis. *Crit. Rev. Oncol. Hematol.* 161, 103312. doi:10.1016/j.critrevonc.2021.103312

Moher, D., Liberati, A., Tetzlaff, J., and Altman, D. G. (2009). Preferred Reporting Items for Systematic Reviews and Meta-Analyses: the PRISMA Statement. *Bmj* 339, b2535. doi:10.1136/bmj.b2535

National Comprehensive Cancer Network (2021a). NCCN Clinical Practice Guidelines in Oncology: Acute Lymphoblastic Leukemia. Version 2, 2021. Available at: http://nccn.org/ Accessed August 12021.

National Comprehensive Cancer Network (2021b). NCCN Clinical Practice Guidelines in Oncology: B-Cell Lymphomas. Version 4, 2021. Available at: http://nccn.org/ Accessed August 12021.

National Comprehensive Cancer Network (2021c). NCCN Clinical Practice Guidelines in Oncology: Central Nervous System Cancers. Version 1, 2021. Available at: http://nccn.org/ Accessed August 12021.

Oosterom, N., Berrevoets, M., den Hoed, M. A. H., Zolk, O., Hoerning, S., Pluijm, S. M. F., et al. (2018). The Role of Genetic Polymorphisms in the Thymidylate Synthase (TYMS) Gene in Methotrexate-Induced Oral Mucositis in Children with Acute Lymphoblastic Leukemia. *Pharmacogenet Genomics* 28 (10), 223–229. doi:10.1097/fpc.0000000000000352

Purkayastha, A., Pathak, A., Guleria, B., Rathore, A., Viswanath, S., and Gupta, A. (2018). High Dose Methotrexate in Oncological Practice: A Review and Update on Recent Trends in Administration and Management of Toxicity. *Cancer Clin. J.* 1 (1), 1001.

Quaranta, S., and Thomas, F. (2017). Pharmacogenetics of Anti-cancer Drugs: State of the Art and Implementation - Recommendations of the French National Network of Pharmacogenetics. *Therapie* 72 (2), 205–215. doi:10.1016/j.therap.2017.01.005

Radtke, S., Zolk, O., Renner, B., Paulides, M., Zimmermann, M., Möricke, A., et al. (2013). Germline Genetic Variations in Methotrexate Candidate Genes Are Associated with Pharmacokinetics, Toxicity, and Outcome in Childhood Acute Lymphoblastic Leukemia. *Blood* 121 (26), 5145–5153. doi:10.1182/blood-2013-01-480335

Ramsey, L. B., Balis, F. M., O'Brien, M. M., Schmiegelow, K., Pauley, J. L., Bleyer, A., et al. (2018). Consensus Guideline for Use of Glucarpidase in Patients with High-Dose Methotrexate Induced Acute Kidney Injury and Delayed Methotrexate Clearance. *Oncologist* 23 (1), 52–61. doi:10.1634/theoncologist.2017-0243

Robien, K., and Ulrich, C. M. (2003). 5,10-Methylenetetrahydrofolate Reductase Polymorphisms and Leukemia Risk: a HuGE Minireview. *Am. J. Epidemiol.* 157 (7), 571–582. doi:10.1093/aje/kwg024

Ruiz-Argüelles, G. J., Coconi-Linares, L. N., Garcés-Eisele, J., and Reyes-Núñez, V. (2007). Methotrexate-induced Mucositis in Acute Leukemia Patients Is Not Associated with the MTHFR 677T Allele in Mexico. *Hematology* 12 (5), 387–391. doi:10.1080/10245330701448479

Schmiegelow, K. (2009). Advances in Individual Prediction of Methotrexate Toxicity: a Review. *Br. J. Haematol.* 146 (5), 489–503. doi:10.1111/j.1365-2141.2009.07765.x

Sedgwick, P., and Marston, L. (2015). How to Read a Funnel Plot in a Meta-Analysis. *Bmj* 351, h4718. doi:10.1136/bmj.h4718

Sedgwick, P. (2015). Meta-analyses: what Is Heterogeneity?. *Bmj* 350, h1435. doi:10.1136/bmj.h1435

Seidemann, K., Book, M., Zimmermann, M., Meyer, U., Welte, K., Stanulla, M., et al. (2006). MTHFR 677 (C-->T) Polymorphism Is Not Relevant for Prognosis or Therapy-Associated Toxicity in Pediatric NHL: Results from 484 Patients of Multicenter Trial NHL-BFM 95. *Ann. Hematol.* 85 (5), 291–300. doi:10.1007/s00277-005-0072-2

Shimasaki, N., Mori, T., Samejima, H., Sato, R., Shimada, H., Yahagi, N., et al. (2006). Effects of Methylenetetrahydrofolate Reductase and Reduced Folate Carrier 1 Polymorphisms on High-Dose Methotrexate-Induced Toxicities in Children with Acute Lymphoblastic Leukemia or Lymphoma. *J. Pediatr. Hematol. Oncol.* 28 (2), 64–68. doi:10.1097/01.mph.0000198269.61948.90

Song, Z., Huang, Z., and Zhao, R. (2019a). Investigation of Willingness on Individualized Medication of High-Dose Methotrexate in Patients with Osteosarcoma or Hematological Malignancy. *Chin. J. Evidence-Based Med.* 19 (6), 639–644. doi:10.7507/1672-2531.201901094

Song, Z., Huang, Z., and Zhao, R. (2019b). Pharmacogenetics of Methotrexate Toxicity in Patients with Osteosarcoma or Hematological Malignancy: an Umbrella Review of Systematic Reviewa. *Chin. J. Clin. Pharmacol.* 35 (9), 896–899. doi:10.13699/j.cnki.1001-6821.2019.09.020

Stang, A. (2010). Critical Evaluation of the Newcastle-Ottawa Scale for the Assessment of the Quality of Nonrandomized Studies in Meta-Analyses. *Eur. J. Epidemiol.* 25 (9), 603–605. doi:10.1007/s10654-010-9491-z

Suthandiram, S., Gan, G. G., Zain, S. M., Bee, P. C., Lian, L. H., Chang, K. M., et al. (2014). Effect of Polymorphisms within Methotrexate Pathway Genes on Methotrexate Toxicity and Plasma Levels in Adults with Hematological Malignancies. *Pharmacogenomics* 15 (11), 1479–1494. doi:10.2217/pgs.14.97

Taylor, Z. L., Vang, J., Lopez-Lopez, E., Oosterom, N., Mikkelsen, T., and Ramsey, L. B. (2021). Systematic Review of Pharmacogenetic Factors that Influence High-Dose Methotrexate Pharmacokinetics in Pediatric Malignancies. *Cancers (Basel)* 13 (11), 2837. doi:10.3390/cancers13112837

Trikalinos, T. A., Salanti, G., Khoury, M. J., and Ioannidis, J. P. (2006). Impact of Violations and Deviations in Hardy-Weinberg Equilibrium on Postulated Gene-Disease Associations. *Am. J. Epidemiol.* 163 (4), 300–309. doi:10.1093/aje/kwj046

Tsujimoto, S., Yanagimachi, M., Tanoshima, R., Urayama, K. Y., Tanaka, F., Aida, N., et al. (2016). Influence of ADORA2A Gene Polymorphism on Leukoencephalopathy Risk in MTX-Treated Pediatric Patients Affected by Hematological Malignancies. *Pediatr. Blood Cancer* 63 (11), 1983–1989. doi:10.1002/pbc.26090

Wang, G., Song, Z., Hu, Y., Zhang, X., Zhai, S., Du, G., et al. (2021). Recommendations of Practical Guidelines for Clinical Medication of High-Dose Methotrexate Based upon the Delphi Method. *Chin. J. Hosp. Pharm.* 41 (11), 1085–1090. doi:10.13286/j.1001-5213.2021.11.01

Wang, Z., Zhang, N., Chen, C., Chen, S., Xu, J., Zhou, Y., et al. (2019). Influence of the OATP Polymorphism on the Population Pharmacokinetics of Methotrexate in Chinese Patients. *Curr. Drug Metab.* 20 (7), 592–600. doi:10.2174/1389200220666190701094756

Yanagimachi, M., Goto, H., Kaneko, T., Naruto, T., Sasaki, K., Takeuchi, M., et al. (2013). Influence of Pre-hydration and Pharmacogenetics on Plasma Methotrexate Concentration and Renal Dysfunction Following High-Dose Methotrexate Therapy. *Int. J. Hematol.* 98 (6), 702–707. doi:10.1007/s12185-013-1464-z

Yang, L., Hu, X., and Xu, L. (2012). Impact of Methylenetetrahydrofolate Reductase (MTHFR) Polymorphisms on Methotrexate-Induced Toxicities in Acute Lymphoblastic Leukemia: a Meta-Analysis. *Tumour Biol.* 33 (5), 1445–1454. doi:10.1007/s13277-012-0395-2

Yang, L., Wu, H., Gelder, T. V., Matic, M., Ruan, J. S., Han, Y., et al. (2017). SLCO1B1 Rs4149056 Genetic Polymorphism Predicting Methotrexate Toxicity in Chinese Patients with Non-hodgkin Lymphoma. *Pharmacogenomics* 18 (17), 1557–1562. doi:10.2217/pgs-2017-0110

Yao, P., He, X., Zhang, R., Tong, R., and Xiao, H. (2019). The Influence of MTHFR Genetic Polymorphisms on Adverse Reactions after Methotrexate in Patients with Hematological Malignancies: a Meta-Analysis. *Hematology* 24 (1), 10–19. doi:10.1080/10245332.2018.1500750

Yazıcıoğlu, B., Kaya, Z., Güntekin Ergun, S., Perçin, F., Koçak, Ü., Yenicesu, İ., et al. (2017). Influence of Folate-Related Gene Polymorphisms on High-Dose Methotrexate-Related Toxicity and Prognosis in Turkish Children with Acute Lymphoblastic Leukemia. *Turk J. Haematol.* 34 (2), 143–150. doi:10.4274/tjh.2016.0007

Zhao, M., Liang, L., Ji, L., Chen, D., Zhang, Y., Zhu, Y., et al. (2016). MTHFR Gene Polymorphisms and Methotrexate Toxicity in Adult Patients with Hematological Malignancies: a Meta-Analysis. *Pharmacogenomics* 17 (9), 1005–1017. doi:10.2217/pgs-2016-0004

Zhao, R., Diop-Bove, N., Visentin, M., and Goldman, I. D. (2011). Mechanisms of Membrane Transport of Folates into Cells and across Epithelia. *Annu. Rev. Nutr.* 31, 177–201. doi:10.1146/annurev-nutr-072610-145133

Zhu, C., Liu, Y. W., Wang, S. Z., Li, X. L., Nie, X. L., Yu, X. T., et al. (2018). Associations between the C677T and A1298C Polymorphisms of MTHFR and the Toxicity of Methotrexate in Childhood Malignancies: a Meta-Analysis. *Pharmacogenomics J.* 18 (3), 450–459. doi:10.1038/tpj.2017.34

Conflict of Interest: The authors declare that the research was conducted in the absence of any commercial or financial relationships that could be construed as a potential conflict of interest.

Publisher's Note: All claims expressed in this article are solely those of the authors and do not necessarily represent those of their affiliated organizations, or those of the publisher, the editors, and the reviewers. Any product that may be evaluated in this article, or claim that may be made by its manufacturer, is not guaranteed or endorsed by the publisher.

frontiers in Pharmacology

ORIGINAL RESEARCH
published: 01 November 2021
doi: 10.3389/fphar.2021.769647

SOAT1 Promotes Gastric Cancer Lymph Node Metastasis Through Lipid Synthesis

Tingting Zhu[1†], Zhangding Wang[1†], Tianhui Zou[2†], Lei Xu[1†], Shu Zhang[1], Yali Chen[3], Chen Chen[3], Weijie Zhang[4], Shouyu Wang[3,5,6]*, Qingqing Ding[7]* and Guifang Xu[1]**

[1]Department of Gastroenterology, The Affiliated Drum Tower Hospital of Nanjing University Medical School, Nanjing, China, [2]Division of Gastroenterology and Hepatology, Renji Hospital, Shanghai Jiao-Tong University School of Medicine, Shanghai Institute of Digestive Disease, Key Laboratory of Gastroenterology and Hepatology, Ministry of Health, Shanghai, China, [3]Jiangsu Key Laboratory of Molecular Medicine, Medical School of Nanjing University, Nanjing, China, [4]Department of Thyroid and Breast Surgery, The Affiliated Drum Tower Hospital of Nanjing University Medical School, Nanjing, China, [5]Department of Hepatobiliary Surgery, The Affiliated Drum Tower Hospital of Nanjing University Medical School, Nanjing, China, [6]Center for Public Health Research, Medical School of Nanjing University, Nanjing, China, [7]Department of Gerontology, The First Affiliated Hospital of Nanjing Medical University, Nanjing, China

Emerging evidences demonstrate that metabolic reprogramming is a hallmark of malignancies, including gastric cancer (GC). Abnormal expression of metabolic rate-limiting enzymes, as the executive medium of energy metabolism, drives the occurrence and development of cancer. However, a comprehensive model of metabolic rate-limiting enzymes associated with the development and progression of GC remains unclear. In this research, we identified a rate-limiting enzyme, sterol O-acyltransferase 1 (SOAT1), was highly expressed in cancerous tissues, which was associated with advanced tumor stage and lymph node metastasis, leading to the poor prognosis of GC. It was shown that knockdown of SOAT1 or pharmacological inhibition of SOAT1 by avasimibe could suppress GC cell proliferation, cholesterol ester synthesis, and lymphangiogenesis. However, overexpression of SOAT1 promoted these biological processes. Mechanistically, SOAT1 regulated the expression of cholesterol metabolism genes SREBP1 and SREBP2, which could induce lymphangiogenesis via increasing the expression of VEGF-C. In conclusion, our results indicated that SOAT1 promotes gastric cancer lymph node metastasis through lipid synthesis, which suggested that it may be a promising prognostic biomarker for guiding clinical management and treatment decisions.

Keywords: rate-limiting enzymes, lipid metabolism, gastric cancer, lymphangiogenesis, lymph node metastasis

OPEN ACCESS

Edited by:
Yao Liu,
Daping Hospital, China

Reviewed by:
Tran Ngoc Nguyen,
Vingroup Big Data Institute, Vietnam
Wenxia Xu,
Zhejiang University, China
Marco Falasca,
Curtin University, Australia

****Correspondence:***
Weijie Zhang
zhangweijie1616@163.com
Shouyu Wang
sywang@nju.edu.cn
Qingqing Ding
dingqingqing@jsph.org.cn
Guifang Xu
xuguifang@njglyy.com

[†]These authors have contributed equally to this work

Specialty section:
This article was submitted to Pharmacology of Anti-Cancer Drugs, a section of the journal Frontiers in Pharmacology

Received: *02 September 2021*
Accepted: *19 October 2021*
Published: *01 November 2021*

Citation:
Zhu T, Wang Z, Zou T, Xu L, Zhang S, Chen Y, Chen C, Zhang W, Wang S, Ding Q and Xu G (2021) SOAT1 Promotes Gastric Cancer Lymph Node Metastasis Through Lipid Synthesis. Front. Pharmacol. 12:769647. doi: 10.3389/fphar.2021.769647

INTRODUCTION

Gastric cancer (GC) has the fifth highest morbidity and third highest mortality among malignancies worldwide (Sung et al., 2021). Over the last decades, improved treatments have improved the prognosis of patients with early gastric cancer. Unfortunately, GC is always diagnosed at an advanced stage with malignant proliferation and metastasis, leading to the poor prognosis of GC patients (Digklia and Wagner, 2016; Smyth et al., 2020). Therefore, it is urgent to explore novel therapeutic targets and molecular mechanisms responsible for the progression of GC.

The emerging view of cancer is that metabolic reprogramming evolves as tumors progress from precancerous lesions to locally invasive cancer to metastatic tumors (Faubert et al., 2020).

Dysregulated metabolic activities can be exploited to diagnose, monitor, and treat malignancies. One of the main features of these metabolic alterations is the enhanced glycolysis and decreased mitochondrial aerobic respiration even in the presence of abundant oxygen (Warburg effect), which is a driving force of cancer cell survival, growth and aggressiveness (Vander Heiden et al., 2009; Liberti and Locasale, 2016). In addition, numerous studies have highlighted the intricate relationship between oncogenic signaling and lipid metabolism reprogramming (Snaebjornsson et al., 2020). Enhanced synthesis and uptake of lipids contribute to tumor formation and progression, dysregulation of Sterol regulatory element-binding proteins (SREBPs) plays a central role in these processes (Cheng et al., 2015). Collectively, a comprehensive understanding of the molecular mechanisms of metabolic reprogramming is essential for developing more prognostic biomarkers and therapeutic strategies.

Metabolic rate-limiting enzymes are the executive agents of energy metabolism, and abnormal changes in metabolic enzymes drive the progression of tumors. Recently, several metabolic rate-limiting enzymes in glycolysis, glutamine metabolism and fatty acid oxidation (FAO) have been identified as biomarkers and drug targets (Tong et al., 2009; Roberts and Miyamoto, 2015; Menendez and Lupu, 2017). In these processes, a critical regulatory role is played by Sterol O-acyltransferase 1 (SOAT1), one of rate-limiting enzymes of the mevalonate pathway, main function is converting excess cholesterol into cholesterol esters and stored in cytosolic lipid droplets (Cheng et al., 2018). Recent studies showed that SOAT1 is highly upregulated in malignancies and correlates inversely with patient prognosis (Geng et al., 2016; Jiang et al., 2019; Xu et al., 2020). In addition, numerous inhibitors targeting rate-limiting enzymes are in preclinical and clinical studies for different human cancers have been found to simultaneously suppress tumor growth and metastasis (Vander Heiden and DeBerardinis, 2017). However, the abnormal alterations and biological functions of rate-limiting enzymes in GC are unintelligible. Therefore, systematic identification of enzymes from metabolic rate-limiting enzyme databases may provide more potential novel anticancer treatments for GC.

In this study, we identified SOAT1 as a critical biomarker of gastric cancer, it was markedly upregulated in gastric cancer tissues, which was significantly associated with the clinicopathological characteristics and prognosis of gastric cancer patients. SOAT1 overexpression enhanced the ability of proliferation, migration and invasion of GC cells. Furthermore, SOAT1 induced SREBP1 and SREBP2 expression participated in the pro-lymphangiogenic process via promoting VEGFC expression and ultimately contributed to gastric cancer lymphangiogenesis. Importantly, pharmacological inhibition of SOAT1 by avasimibe suppressed these processes in a dose-dependent manner. Overall, our study identified the biological roles of SOAT1 in GC and uncovered that SOAT1 may be a novel biomarker and therapeutic target for GC lymph mode metastasis.

RESULTS

Identification of SOAT1 as a Biomarker in GC Based on Database Analysis

To investigate changes in metabolic rate-limiting enzymes in GC, we systematically screened the transcriptome profiles of 111 rate-limiting enzymes between tumor and adjacent normal tissues from a database reported previously (Wang et al., 2019). All these genes were listed in the **Supplementary Table S1**. A total of 29 differentially expressed transcripts were identified ($p < 0.05$): 21 upregulated and 8 downregulated transcripts (**Figure 1A**). We then utilized Cox regression analysis with the LASSO algorithm to determine the effects of these transcripts on clinical prognosis, and five genes (SOAT1, GNE, UCK2, DCK, and GAD1) were selected according to the minimum criteria and the regression coefficients (**Figure 1B**). Based on the expression levels of the five genes, the following formula was derived to calculate the risk score for predicting the prognosis of each patient: Risk score = (0.0360 × expression value of SOAT1) + (−0.0006 × expression value of GNE) + (−0.0052 × expression value of UCK2) + (−0.0087 × expression value of DCK) + (−0.0700 × expression value of GAD1) (**Figure 1C**). By the risk score formula, the patients were divided into the low-risk ($n = 152$) and high-risk ($n = 151$) subgroups based on the mean risk score. The expression level of SOAT1 was higher in the high-risk group, while the expression levels of the other four genes were higher in the low-risk group. In addition, the high-risk group patients often had a more advanced TNM stage ($p = 0.021$), higher tumor grade ($p = 0.016$), and higher incidence of lymph node metastasis (LNM) ($p = 0.025$) (**Figure 1D**). Moreover, the patients in the high-risk group had shorter overall survival (OS) time than those in the low-risk group (**Figure 1E**). Among the five genes, high expression level of SOAT1 was significantly correlated with poor prognosis in GC patients, and the expression of the other four genes was not associated with the survival of GC patients (**Figure 1F**; **Supplementary Figures S1A–D**). Furthermore, Kaplan-Meier plotter data also confirmed that high level of SOAT1 was associated with poor survival in patients with gastric adenocarcinoma patients (**Supplementary Figure S1E**). Moreover, the expression level of SOAT1 was significantly associated with clinicopathological features, such as TNM stage ($p < 0.001$) and LNM ($p < 0.001$) (**Figures 1G,H**). However, SOAT1 expression had no statistically significant association with tumor grade, invasion depth or distant metastasis status (**Supplementary Figures S1F–H**). Taken together, these results revealed that the expression of SOAT1 was upregulated in GC and it might be an independent prognostic risk factor in GC patients.

SOAT1 Is Overexpressed and Associated With Poor Prognosis in GC Patients

To further confirm the expression of SOAT1 in GC, we first examined the SOAT1 expression levels in 34 GC cancerous tissues and paired adjacent noncancerous tissues. We found that the mRNA levels of SOAT1 were significantly higher in cancerous tissues (**Figure 2A**) and the protein levels of SOAT1

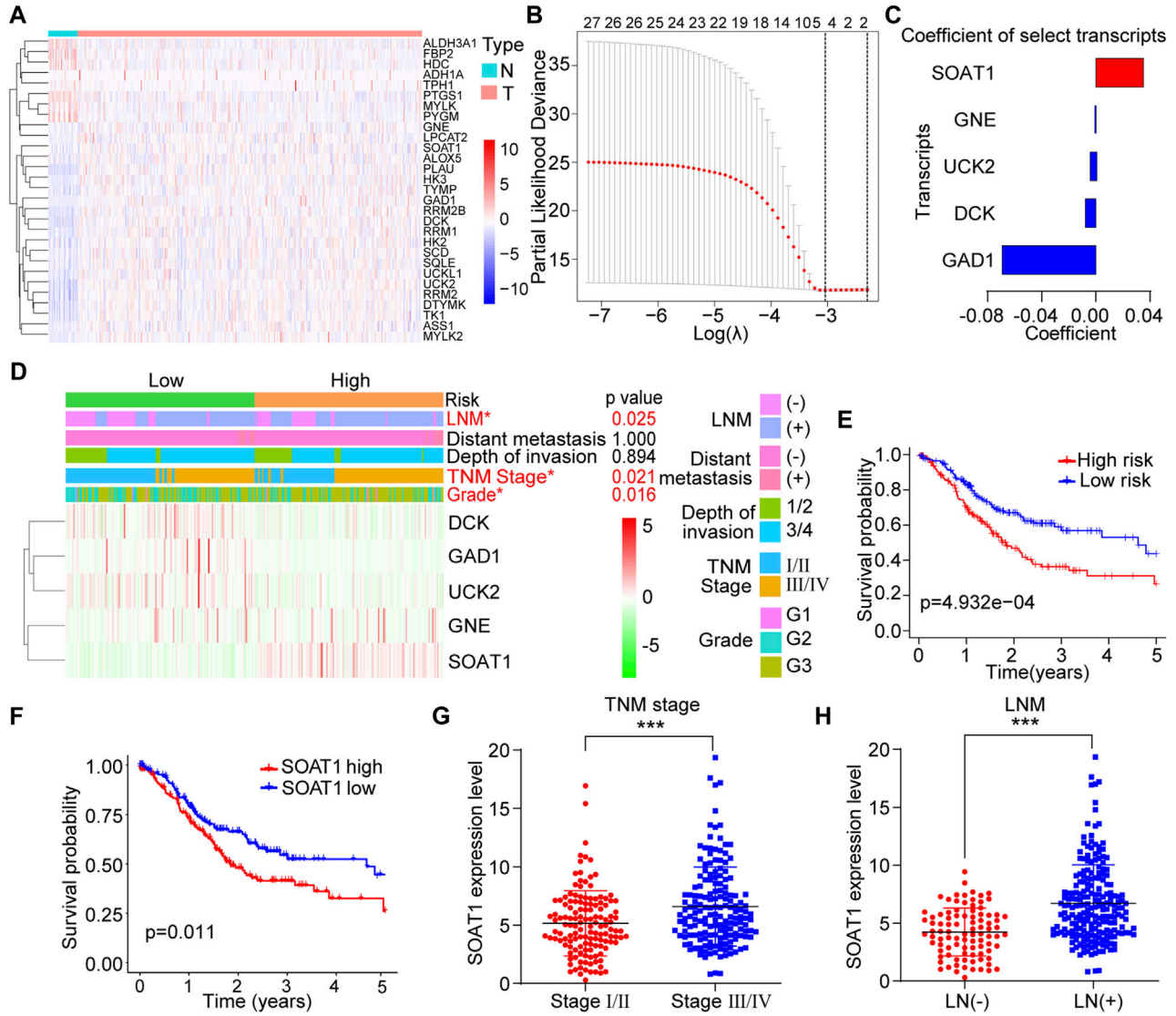

FIGURE 1 | Identification of SOAT1 as a biomarker in GC from 111 rate-limiting enzymes based on TCGA database. **(A)** Heatmap of differentially expressed rate-limiting enzymes between GC tumor (n = 375) and normal tissues (n = 32) in TCGA. **(B)** The coefficients were calculated by multivariate Cox regression using the LASSO method. **(C)** Coefficients of the five selected genes. **(D)** The expression levels of the five selected genes in high- and low-risk GC patients. **(E)** Kaplan–Meier overall survival (OS) curve for GC patients assigned to the high- and low-risk groups. **(F)** Kaplan–Meier OS curve of GC patients stratified by SOAT1 expression. **(G,H)** Correlation of SOAT1 expression with TNM stage **(G)** and LNM **(H)** in GC tissues based on TCGA data.

were significantly higher in 9/10 (90%) cancerous tissues than the corresponding noncancerous tissues (**Figure 2B**). We then utilized an independent validation cohort to further investigate SOAT1 expression and its relationship with clinical outcome using immunohistochemistry (IHC) staining in a GC tissue microarray (TMA). Similarly, these results showed that the expression of SOAT1 was significantly increased in cancerous tissues compared with the matched normal tissues (n = 160, p < 0.01; **Figures 2C,D**, **Supplementary Figure S2B**). Furthermore, the protein expression of SOAT1 in the GC cohort was significantly correlated with LNM status (p = 0.001), TNM stage (p = 0.029) and differentiation degree (p = 0.006); however, SOAT1 expression had no statistically significant correlation with depth of invasion (p = 0.195), distant metastasis (p = 0.328), tumor diameter (p = 0.697) or histological type (p = 0.366) (**Supplementary Table S2**). Moreover, SOAT1 protein expression was greatly increased in advanced-stage and LNM-positive patients (**Figures 2E,F**). Kaplan-Meier survival analysis showed that GC patients with high level of SOAT1 had worse OS (p = 6.558e-04) (**Figure 2G**). Simultaneously, univariate Cox regression analysis revealed that TNM stage (HR = 5.817, 95% CI: 3.114–10.836), depth of invasion (HR = 2.499, 95% CI: 1.808–3.454), LNM (HR = 2.832, 95% CI: 2.189–3.665) and SOAT1 (HR = 2.437, 95% CI: 1.567–3.791) were significantly associated with the survival in patients with GC (**Supplemental Figure S2A**). Furthermore,

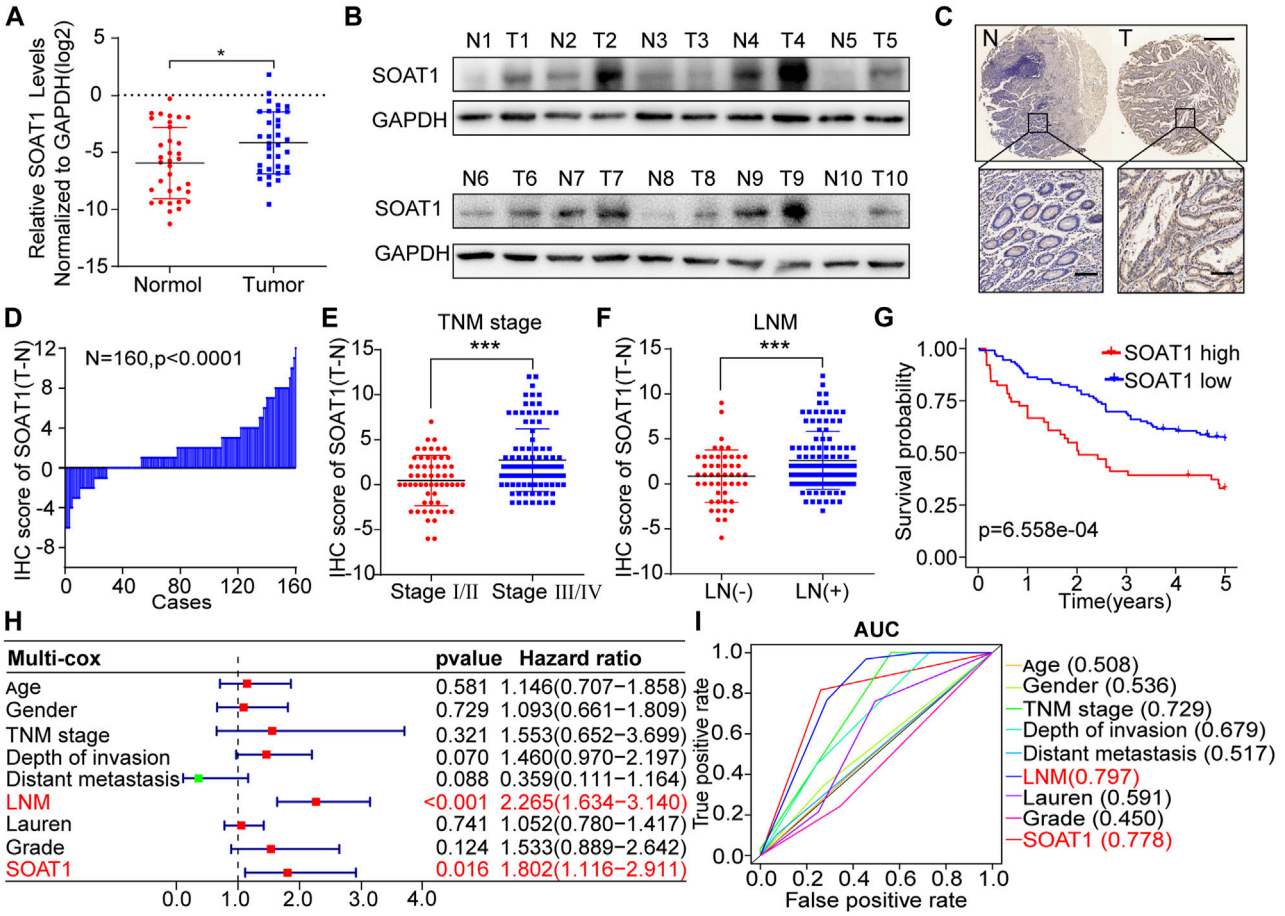

FIGURE 2 | SOAT1 expression is elevated in GC and correlates with poor prognosis in GC patients. **(A)** The relative RNA expression level of SOAT1 in GC and corresponding noncancerous tissues was measured by qRT-PCR (n = 34). **(B)** The protein level of SOAT1 was measured by western blot assay in GC tissues and the corresponding noncancerous tissues (n = 10). **(C)** Representative IHC images of the TMA probed with the anti-SOAT1 antibody (scale bars = 200 and 50 μm, respectively) were shown. **(D)** The distribution of the differences in the immunoreactivity score (IRS) for SOAT1 staining was available for 160 pairs of GC tissues and the corresponding noncancerous tissues (ΔIRS = IRST-IRSN). **(E,F)** Correlation of SOAT1 expression with TNM stage **(E)** and LNM **(F)** in GC tissues based on TMA data. **(G)** Kaplan-Meier OS analysis of GC patients stratified by the relative SOAT1 expression level. **(H)** Multivariate analyses were performed with the above-mentioned GC patients, and all bars correspond to 95% confidence intervals (CIs) and hazard ratios (HRs). **(I)** Receiver operating characteristic (ROC) analysis of the risk factors in the above-mentioned GC patients.

by using multivariate Cox regression analysis, we found that SOAT1 was one of the independent predictors of the prognosis of GC patients HR = 1.802 (1.116–2.911) (**Figure 2H**). To further evaluate the predictive ability of the SOAT1 expression level, we conducted receiver operating characteristic curve (ROC) analysis, and the area under the curve (AUC) of SOAT1 and LNM were 0.778 and 0.797, respectively (**Figure 2I**). Collectively, these data revealed that SOAT1 expression level was significantly increased in GC tissues and that SOAT1 might be an independent prognostic risk factor for GC.

SOAT1 Promotes GC Cells Proliferation, Migration and Invasion

To elucidate the function of SOAT1 in GC cells, we first investigated SOAT1 expression in GC cell lines and normal gastric mucosal cells (GES-1) by western blot, and it was shown that its expression was higher in most of GC cells than GES-1 cells (**Figure 3A**). Subsequently, we established stable SOAT1-overexpressing GC cells in AGS cells with relative low expression of SOAT1 (AGS-SOAT1) (**Figure 3B**). As shown in **Figure 3C**, overexpression of SOAT1 significantly increased the colony formation efficiency of AGS cells. We also knocked down SOAT1 by two specific siRNAs in MGC-803 and BGC-823 cells and confirmed that both the mRNA and protein levels of SOAT1 were markedly reduced after transfection for 72 h (**Figures 3D,E**; **Supplementary Figures S3A–B**). As expected, knockdown of SOAT1 obviously decreased the colony formation efficiency (**Figure 3F**; **Supplementary Figure S3C**). All these results confirmed that SOAT1 promoted the proliferative ability of GC cells.

In addition, transwell analysis was performed to determine the role of SOAT1 in GC cell migration and invasion. The results showed that over expression of SOAT1 promoted the migration and invasion of AGS cells (**Figure 3G**). Conversely, knockdown

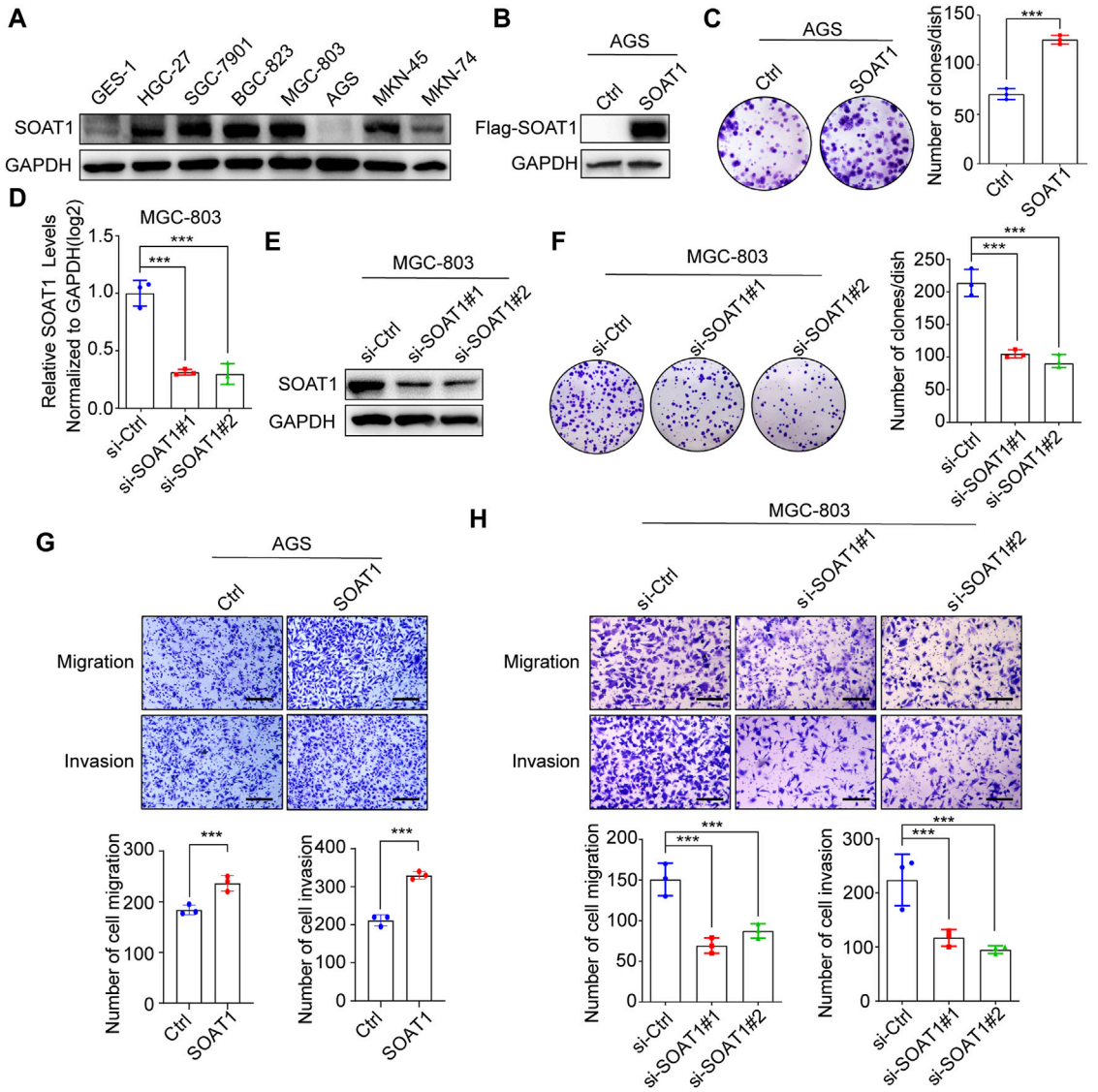

FIGURE 3 | SOAT1 promotes GC cell proliferation, migration and invasion. **(A)** The protein level of SOAT1 in GES-1 cells and GC cell lines were analyzed by western blot. **(B)** The overexpression efficiencies were verified at the protein level in AGS by western blot. **(C)** Representative images of colony formation assay in AGS after overexpression of SOAT1 (left panel), the right panel shows the quantitative results. **(D,E)** The knockdown efficiency was verified at the mRNA and protein levels by qRT-PCR **(D)** and western blot assay **(E)**, respectively. **(F)** Representative images of colony formation assay in MGC-803 after knockdown of SOAT1 (left panel), and the quantitative data were shown (right panel). **(G)** Transwell assays in SOAT1 overexpression AGS cells. Representative images of migrated and invaded GC cells in each group were shown in the upper panel, and quantitative results were shown in the lower panel. **(H)** Transwell assay in MGC-803 cells after knockdown of SOAT1. Representative images of migrated and invaded GC cells in each group were shown in the left panel, and the quantitative results were shown in the right panel. Scale bars: 100 μm.

of SOAT1 in MGC-803 and BGC-823 cells exerted the opposite effects (**Figure 3H**; **Supplementary Figure S3D**). Collectively, these data indicate the critical role of SOAT1 in promoting GC cell proliferation, migration and invasion.

Inhibitory Effects of Avasimibe on the Proliferation and Metastasis of GC Cells

Avasimibe, a potent small molecule inhibitor of SOAT1 (**Figure 4A**), has been proven to exert anticancer effects against many tumors, including glioblastoma (GBM), hepatocellular carcinoma (HCC) and prostate cancer (PCa) (Tardif et al., 2004; Bemlih et al., 2010; Jiang et al., 2019; Liu et al., 2021). Herein, we investigated whether avasimibe has an inhibitory effect on GC cells. As shown by the cell viability curve, avasimibe inhibited the proliferation of GC cell lines in a dose-dependent manner. The IC50 values of avasimibe in MGC-803 and BGC-823 cells at 24 h were 13.489 and 25.377 μM, respectively. In addition, the respective IC50 values at 48 h were 8.811 and 14.208 μM (**Figures 4B,C**; **Supplementary Figures S4A,B**). Consistent with the CCK-8 assay results, avasimibe also decreased the colony-forming

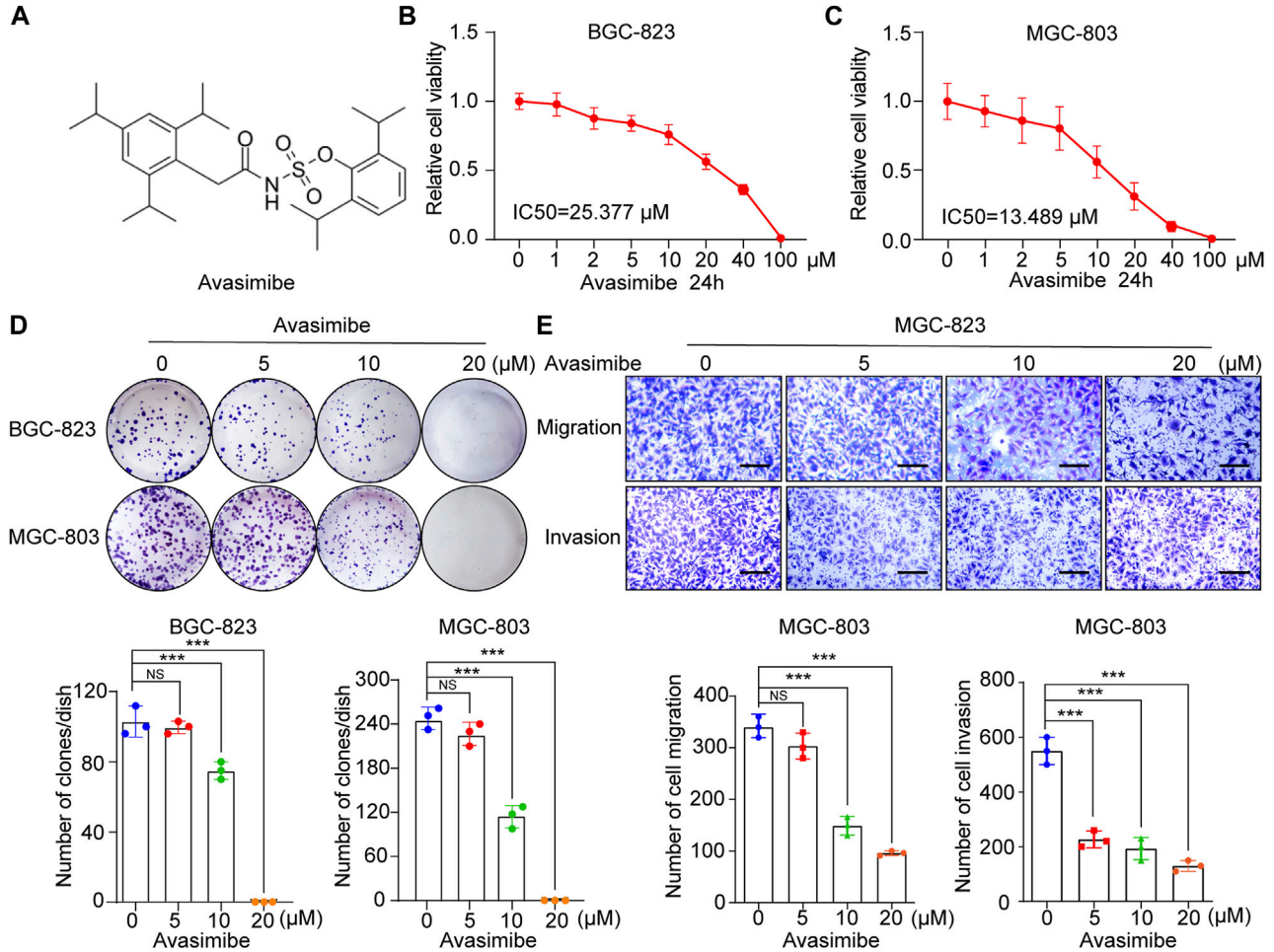

FIGURE 4 | Avasimibe inhibits GC cell growth and metastasis. **(A)** Molecular structure of avasimibe. **(B,C)** Relative cell viability was measured by CCK-8 assay after avasimibe treatment for 24 h at multiply concentrations (0, 1, 2, 5, 10, 20, 40, and 100 μM). **(D)** Representative images of colony formation assay in BGC-823 and MGC-803 cells after avasimibe treatment (upper panel); the quantitative results were shown (lower panel). **(E)** Transwell assay in MGC-803 cells after avasimibe treatment. Representative images of migrated and invaded GC cells in each group were shown in the left panel, and the quantitative results were shown in the right panel. Scale bars: 100 μm.

capacity of GC cells in a dose-dependent manner (**Figure 4D**).

Next, we explored the effects of avasimibe treatment on the cell metastasis ability in GC cell lines. The wound healing assay showed that avasimibe significantly reduced the migration capability of BGC-823 cells (**Supplementary Figure S4C**). In addition, we performed a transwell assay, which showed significant dose-dependent decreases in the numbers of migrated and invaded MGC-803 and BGC-823 cells after treatment with avasimibe (**Figure 4E**; **Supplementary Figure S4D**). Collectively, these results indicated the critical inhibitory effect of avasimibe on GC cell proliferation and metastasis.

SOAT1 Accelerates Lipid Metabolism in GC Cells

It has been reported that SOAT1 can convert excess free cholesterol into cholesteryl esters for storage in lipid droplets (Xu et al., 2020). We first detected the level of cholesterol in GC cells, and the results showed that esterified cholesterol was significantly reduced in SOAT1 knocked-down GC cells or avasimibe treatment (**Figures 5A,B**). In addition, we evaluated whether the inhibition of SOAT1 affected the formation of lipid droplets by Nile red and oil red O staining. The results showed that knocking down SOAT1 could significantly reduce the number of lipid droplets in GC cells (**Figure 5C**, **Supplementary Figures S5A,B**), and avasimibe treatment had a similar effect (**Figures 5D–G**).

To further confirm that SOAT1 regulates lipid biosynthesis and catabolism, we examined the expression levels of a panel of lipid metabolism-related genes in SOAT1-knockdown and avasimibe-treated GC cells. Intriguingly, both SOAT1 knockdown and avasimibe treatment reduced the expression of cholesterol metabolism genes (HMGCR, SREBP1, and SREBP2) and fatty acid biosynthesis genes (FASN, ACC, and SCD1) (**Figures 5H,I**; **Supplementary Figures S5C,D**). In

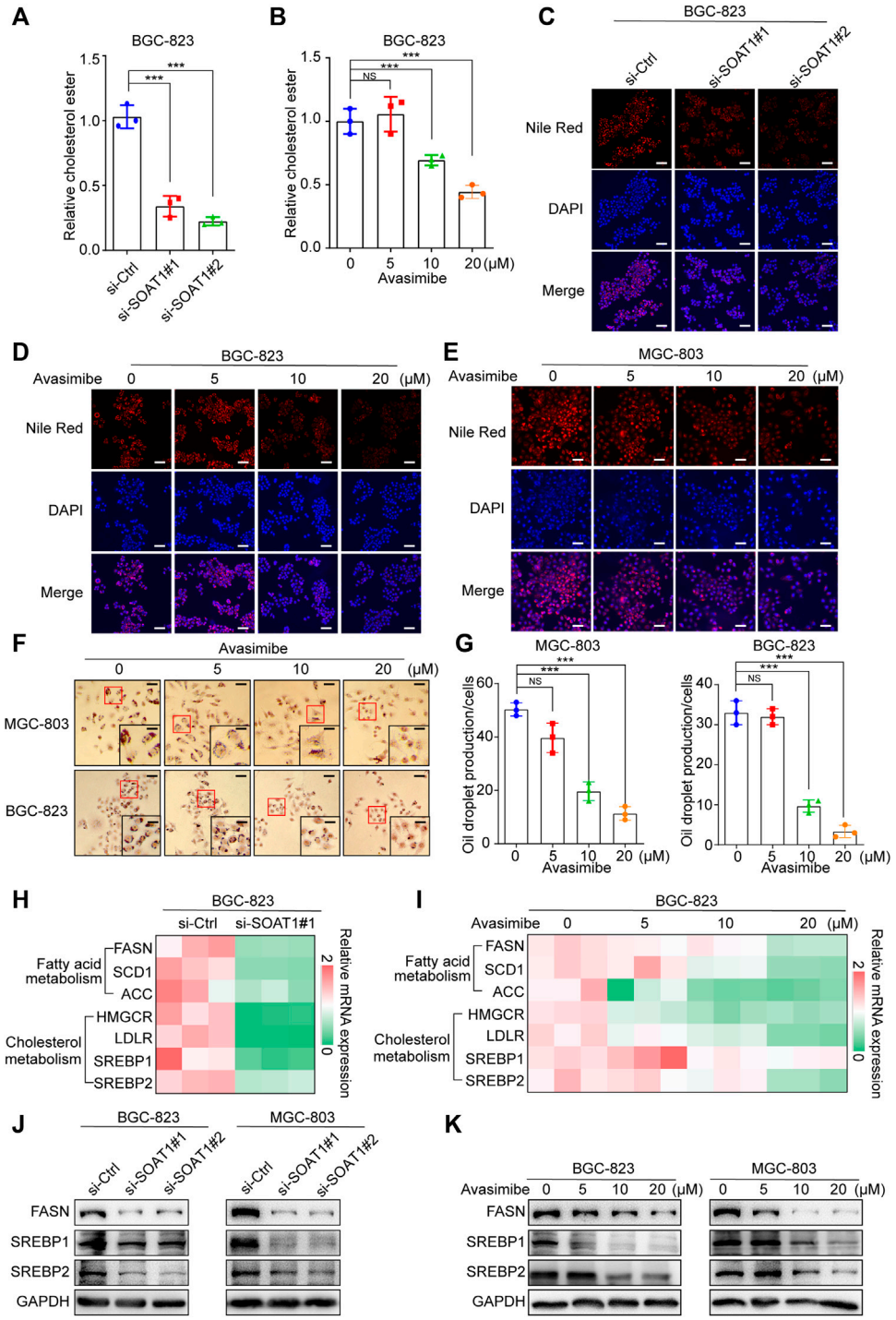

FIGURE 5 | Inhibition of SOAT1 decreases the level of lipid synthesis in GC cells. **(A,B)** Cholesterol ester assays for BGC-823 cells after knockdown of SOAT1 **(A)** or avasimibe treatment **(B)**. **(C)** Representative images of Nile red stanning assay in BGC-823 cells after knockdown of SOAT1. Scale bars: 100 μm. **(D, E)** Representative images of Nile red stanning assay in BGC-823 **(D)** and MGC-803 **(E)** cells after avasimibe treatment. Scale bars: 100 μm. **(F)** Representative images of Oil red O staining in BGC-823 and MGC-803 cells after avasimibe treatment. **(G)** Quantitative data for lipid synthesis were shown. Scale bars: 100 and 50 μm, respectively. **(H,I)** Heatmap generated from the qRT-PCR results showed the gene expression levels of cholesterol metabolism and fatty acid biosynthesis-related genes in BGC-823 cells after knockdown of SOAT1 **(H)** or avasimibe treatment **(I)**. **(J,K)** FASN, SREBP1, and SREBP2 protein expression were measured by western blot assay after knockdown of SOAT1 **(J)** or avasimibe treatment **(K)**.

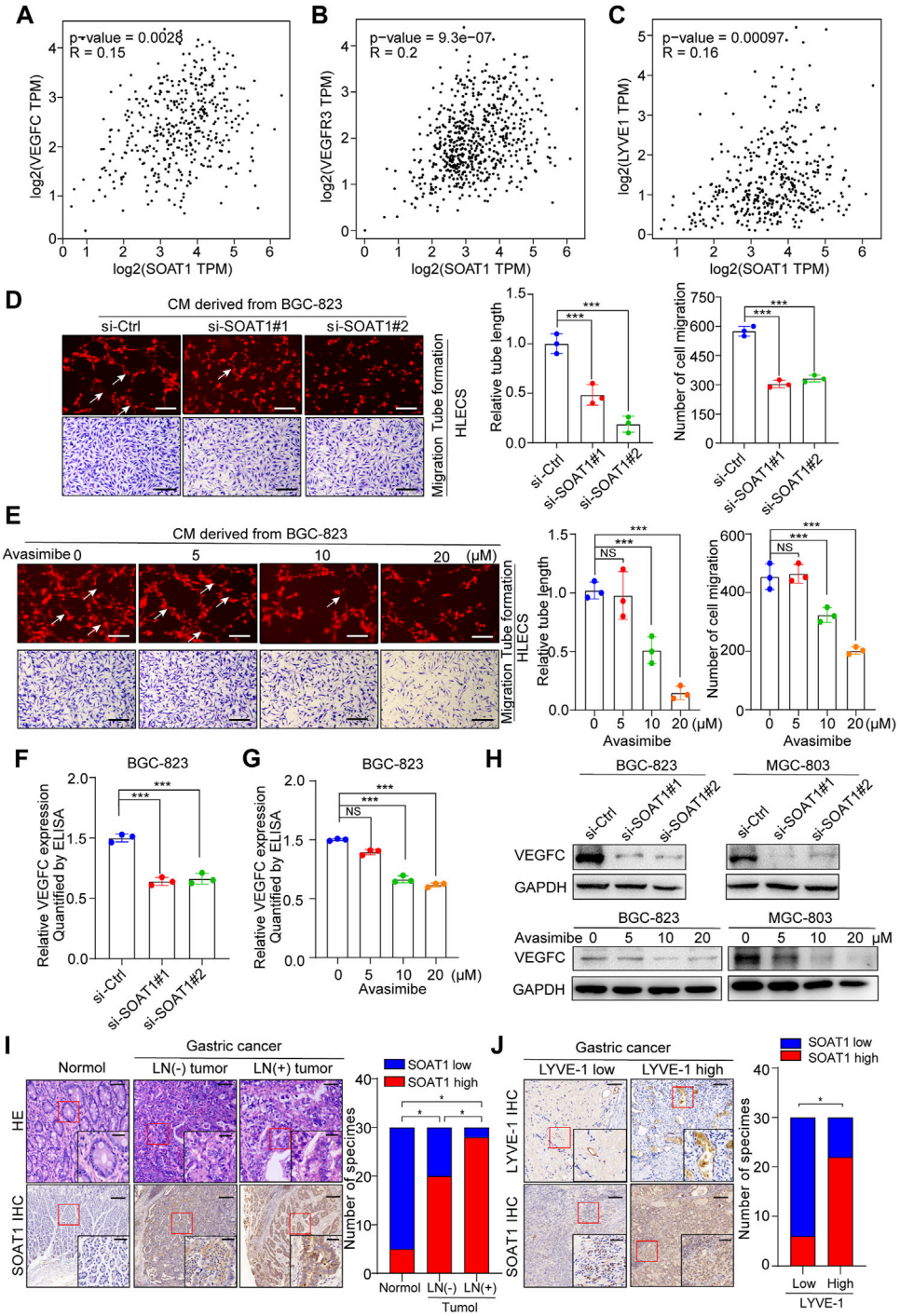

FIGURE 6 | SOAT1 promotes lymphangiogenesis and lymph node metastasis in GC. **(A–C)** The correlation of SOAT1 expression with VEGFC, VEGFR3, and LYVE-1 were analyzed via online bioinformatics tool (http://gepia.cancer-pku.cn/). **(D,E)** Representative images (left panel) and quantitative analysis (right panel) of tube formation and transwell migration assays of HLECs cultured with conditioned medium collected from SOAT1-knockdown **(D)** or avasimibe-treated **(E)** BGC-823 cells. Scale bars: 100 μm **(F,G)** ELISA assay of VEGFC expression in conditioned medium collected from the SOAT1 knockdown or avasimibe treated BGC-823 cells. **(H)** VEGFC expression at the protein level in BGC-823 and MGC-803 cells were measured by western blot assay after knockdown of SOAT1 or avasimibe treatment. **(I)** Representative images (left panel) and quantitative analysis (right panel) of SOAT1 IHC staining in paraffin-embedded paired normal tissues, sections of tumors with or without LNM from patients with GC. Scale bars: 200 μm and 50 μm, respectively. **(J)** Representative images (left panel) and quantitative analysis (right panel) of SOAT1 IHC staining in high or low levels of LYVE-1-positive microvessels in the GC tissues. Scale bars: 200 μm and 50 μm, respectively.

addition, the expression of SREBP1, SREBP2, and FASN were strikingly reduced at the protein level (**Figures 5J–K**). Taken together, these results suggested that dysregulated SOAT1 accelerates the esterification of cholesterol and the synthesis of lipids in GC cells.

SOAT1 Is Related to Lymph Node Metastasis in GC Patients and Promotes Lymphangiogenesis

It has been demonstrated that lipids are required as energy sources and cellular signaling molecules, which are crucial for cancer lymphangiogenesis and lymph node metastasis (Ma Y. et al., 2018; Lee et al., 2019). In addition, the bioinformatic analysis using TCGA and our TMA data suggested that the expression level of SOAT1 was significantly higher in LNM-positive GC tissues (**Figures 1H**, **2F**). Thus, we speculated whether SOAT1 could promote lymph node metastasis of GC cells. VEGFC, VEGFR3, and LYVE-1, which play key role in lymph node metastasis of multiple malignancies, therefore we used online bioinformatics tools (http://gepia.cancer-pku.cn/) to study the relationship between SOAT1 and VEGFC, VEGFR3, and LYVE-1 expression. The results showed that the expression level of SOAT1 was significantly positively correlated with VEGFC, VEGFR3, and LYVE-1 (**Figures 6A–C**). Next, we further examined whether SOAT1 has an effect on tumor-induced lymphangiogenesis. As shown in **Figures 6D,E** and **Supplementary Figures S6A,B**, HLECs treated with conditioned medium (CM) derived from SOAT1-knockdown or avasimibe treatment GC cells significantly reduced the lymphatic capillary formation and the migratory capability of HLECs compared with CM derived from the corresponding vector cells. In addition, compared with CM from the control group, CM from SOAT1-overexpressing GC cells significantly promoted these biological processes (**Supplementary Figure S6C**). As expected, qRT-PCR data showed that the mRNA levels of VEGFC and VEGFD were significantly decreased in both SOAT1-knockdown and avasimibe-treated GC cells (**Supplementary Figures S6D–G**). Furthermore, we evaluated the secretion level of VEGFC using ELISA, and found that the VEGFC protein levels were significantly decreased in conditioned medium collected from GC cells which knockdown of SOAT1 or treated with avasimibe compared to conditioned medium from the corresponding control cells (**Figures 6F,G**; **Supplementary Figures S6H,I**). In addition, the expression of VEGFC were also decreased at the protein levels (**Figure 6H**). Intriguingly, the IHC staining results showed that the expression of SOAT1 was scarcely detected in adjacent noncancerous tissues, slightly increased in LNM-negative GC tissues and strongly upregulated in LNM-positive GC tissues, and positively correlated with the density of microlymphatic vessels, as indicated by the number of LYVE-1-positive microvessels (**Figures 6I,J**). Taken together, these findings indicated that inhibition of SOAT1 suppresses lymphangiogenesis and that avasimibe has the potential therapeutic effect for GC patients with lymph node metastasis.

SOAT1 Accelerates the Lymphangiogenesis by Activating SREBP1 and SREBP2

SREBP1 and SREBP2 are both important signaling molecules that relate to tumor lymph node metastasis (Heo et al., 2020; Li et al., 2020). To investigate whether SREBP1 and SREBP2 involved in SOAT1-mediated lymphangiogenesis and VEGFC production, we pharmacologically inhibited SREBP1 and SREBP2 by fatostatin, which displays antitumor activity in cancers by downregulating SREBP- mediated metabolic pathways (Li et al., 2014). As shown by the cell viability curve, fatostatin inhibited the proliferation of AGS cells in a dose-dependent manner and the IC50 value is 30.822 μM (**Figure 7A**). Intriguingly, the results showed that fatostatin could significantly reversed the promoting effects of SOAT1 overexpression on the migration and the lymphatic tube formation of GC cells (**Figures 7B–D**). In addition, ELISA and qRT-PCR results suggested that the expression of VEGFC were recovered after treated with fatostatin (**Figures 7E,F**). Collectively, these results indicating that blocking SREBP1 and SREBP2 pathway inhibits SOAT1-mediated lymphangiogenesis in gastric cancer.

DISCUSSION

Recently, accumulating investigations have confirmed that metabolic reprogramming plays a significant role in malignant processes in various cancers (Li et al., 2019). Rate-limiting enzymes play a vital role in malignant processes, and cancer cells tend to have a robust metabolism and increase their energy consumption by changing these rate-limiting enzymes (Faubert et al., 2020; Xu et al., 2020). For instance, Hexokinase 2 (HK-2), the rate-limiting enzyme in glycolysis, decreases mTORC1 activity and regulates autophagy through direct phosphorylation of ULK1 (Roberts et al., 2014; Roberts and Miyamoto, 2015). Renal glutaminase (GLS1) provides the antioxidants glutathione (GSH) and nicotinamide adenine dinucleotide phosphate (NADPH) for tumor cell metabolism, and promotes tumor cell growth by reducing reactive oxygen species (ROS) (Tong et al., 2009). High HMGCR activation decreases the growth-inhibitory effect of atorvastatin on TGF-β-treated epithelial cancer cells (Warita et al., 2021). We systematically screened the expression of 111 rate-limiting enzymes in TCGA database, and identified SOAT1 expression level is significantly increased in cancer tissues and closely associated with the poor outcome of GC patients. Subsequently, our TMA data also confirmed that SOAT1 expression is associated with the clinicopathological characteristic and prognosis in patients. More importantly, SOAT1 expression level have a powerful predictive ability of clinical risk scores. Thus, SOAT1 could be used as an effective potential predictive biomarker and therapeutic target for GC.

SOAT1, localized in the endoplasmic reticulum, catalyzes the formation of cholesterol esters (Chang et al., 2006; Chang et al., 2009). SOAT1 is frequently upregulated in multiple cancers, including GBM, HCC and PCa (Geng et al., 2016; Gu et al.,

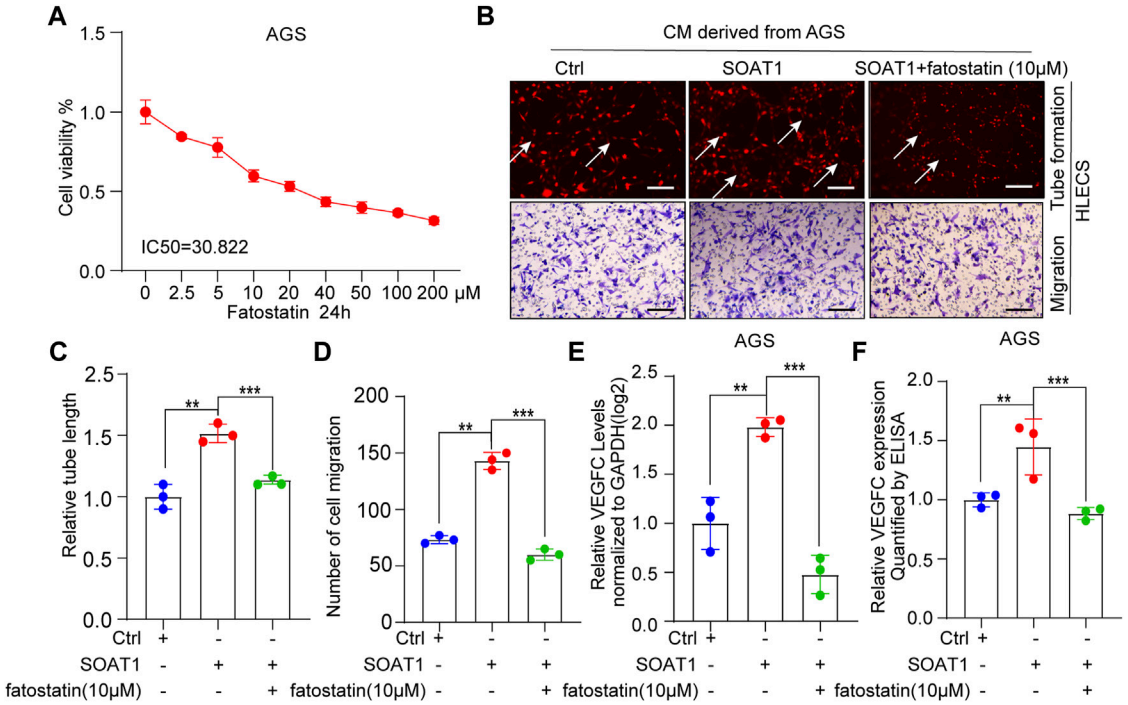

FIGURE 7 | SOAT1 accelerates GC lymphangiogenesis by upregulating the activity of SREBP1 and SREBP2. **(A)** Relative cell viability was measured by CCK-8 assay after fatostatin treatment for 24 h at multiply concentrations (0, 2.5, 5, 10, 20, 40, 100, and 200 μM). **(B–D)** Representative images **(A)** and quantification results **(C,D)** of the tube formation and transwell migration assays of HLECs cultured with conditioned medium collected from SOAT1-overexpressing AGS cells treated with fatostatin or the corresponding controls. **(E)** The expression level of VEGFC was measured by qRT-PCR in SOAT1-overexpressing AGS cells treated with fatostatin or their corresponding controls. **(F)** ELISA assay of VEGFC expression in conditioned medium collected from the SOAT1-overexpressing AGS cells treated with fatostatin or their corresponding controls.

2020; Liu et al., 2021). Previous research demonstrated that SOAT1 promotes lipid metabolism and tumor growth (Jiang et al., 2019; Gu et al., 2020). In addition, Oni et al. (2020) reported that SOAT1 promotes organoid growth and tumor metastasis in pancreatic carcinoma mouse model by activating the mevalonate pathway and disrupting the negative feedback of cholesterol. However, the biological function of SOAT1 and its regulatory mechanisms in GC remain elusive. Our experiment data demonstrated that SOAT1 overexpression elevated GC cell proliferation, migration and invasion ability, highlighting the role of SOAT1 in GC progression. We also showed that inhibition of SOAT1 decreases the synthesis of cholesterol eater and the formation of lipid droplets. Mechanically, we also confirmed that inhibition of SOAT1 downregulating these genes related to numerous aspects of cholesterol metabolism and fatty acid biosynthesis.

Notably, numerous studies have demonstrated that cancer cells undergo metabolic changes during the progression of lymph node metastasis, dysregulated lipid metabolism plays an indispensable role in this process. The metabolism of cholesterol, bile acid and fatty acid are critical in the proliferation and differentiation of lymphatic endothelial cells (Wong et al., 2017). In addition, lymph node metastasis requires that tumor cells undergo a metabolic transition toward fatty acid oxidation (Wong et al., 2017; Lee et al., 2019). SOAT1 catalyzes the conversion of excess cholesterol into cholesterol esters for storage in lipid droplets, and high expression of SOAT1 in tumors may disrupt the balance between free cholesterol and cholesterol esters (Oelkers et al., 1998; Li et al., 2006). Our statistical analysis revealed that the expression level of SOAT1 was higher in LN-metastatic tumors and was positively correlated with the expression level of VEGFC, VEGFR3 and LYVE-1, which are lymphangiogenic growth factors (Ji et al., 2014; Stacker et al., 2014; Ma C. et al., 2018). We also found that inhibition of SOAT1 effectively reduced tumor-associated lymphangiogenesis and the migratory ability of HLECs. Additionally, the expression of VEGFC was dramatically decreased in GC cells after knockdown of SOAT1. Intriguingly, the promoting effect of SOAT1 on lymphangiogenesis was restored by fatostatin. Taken together, these data demonstrate that SOAT1 inhibition leads to suppression of lipid synthesis and GC lymph node metastasis by SREBP1 and SREBP2 pathway.

Rate-limiting enzymes are considered as rational targets for antitumor drug development, and inhibitors of these enzymes have applicated in the clinical trial as promising methods for malignancies, such as statins, perhexiline and trimetazidine (Tong et al., 2009; Ma Y. et al., 2018). Recently, several SOAT1 inhibitors have been discovered, including K-604, nevanimibe, and avasimibe. K-604 has been confirmed an inhibitory effect in glioblastoma cells by downregulated the activation of Akt and extracellular signal-regulated kinase (Ohmoto et al., 2015). Nevanimibe shows the significant

suppresses effect in metastatic adrenocortical carcinoma (ACC) (Smith et al., 2020). Among these agents, avasimibe is a notable anticancer drug that significantly reduces cholesteryl ester storage by inhibits vesicular transport, integrin and TGF-β pathways (Jiang et al., 2019). In the current study, we first found that avasimibe notably suppressed the proliferation, migration and invasion of GC cells in a dose-dependent manner. Subsequently, avasimibe induce a decrease in cholesterol ester synthesis and lipid droplet formation in GC cells. Importantly, our data indicated that HLECs tube formation and migration ability were significantly inhibited by avasimibe. Our further investigation showed that avasimibe significantly decreased the expression and secretion of VEGFC in gastric cancer cells. These results provide that avasimibe may serve as a potential chemical inhibitor for the treatment of lymph node metastasis of gastric cancer.

In summary, our results reveal for the first time the role for SOAT1 as a biomarker for GC development and lymph node metastasis, and the antitumor effect of avasimibe on GC cells. These findings suggest that SOAT1 may be a potential predictor and therapeutic approach for the development of gastric cancer.

MATERIALS AND METHODS

Cell Culture

Human GC cell lines AGS cells were purchased from the American Type Culture Collection (ATCC). HLECs, HEK-293T, BGC-823, HGC-27, MGC-803, SGC-7901, MKN-74, and MKN-45 were obtained from the Type Culture Collection of the Chinese Academy of Sciences (Shanghai, China). HEK-293T cells were cultured in DMEM (Biological Industries, Cromwell, CT, United States), AGS cells were cultured in F12K medium (Biological Industries, Cromwell, CT, United States), and the other cells were cultured in RPMI-1640 medium (Biological Industries, Cromwell, CT, United States). All cells were cultured with 10% fetal bovine serum (FBS; Biological Industries, Cromwell, CT, United States), 100 U/ml penicillin (Invitrogen), 100 μg/ml streptomycin (Invitrogen) and incubated in 5% CO_2 at 37°C.

Patients and Specimens

A total of 34 pathologically confirmed GC tissues and the corresponding adjacent noncancerous fresh frozen tissues were collected from patients treated with radical gastrectomy at the Nanjing Drum Tower Hospital, the Affiliated Hospital of Nanjing University Medical School (Nanjing, Jiangsu, China). All patients provided written informed consent, and all these tissues were obtained for further qRT-PCR, western blot and immunohistochemistry assay.

Immunohistochemistry

A total of 160 pathologically confirmed GC patient tissues from Nanjing Drum Tower Hospital were obtained for TMA construction, and the expression of SOAT1 was detected by IHC staining. The chips were stained and scanned by Servicebio (Wuhan, Hubei, China) according to a standard protocol. Stanning of SOAT1 was scored by the two pathologists blind to the clinical data by applying a semi-quantitative immunoreactivity score (IRS), IRS of 0–6 and IRS of 8–12 were classified as low and high expression of SOAT1, respectively.

SiRNAs and Plasmids

SOAT1 si-RNAs were designed and synthesized by RiboBio (Guangzhou, China), and the sequence was showed as follows: si-SOAT1#1: 5′-TAATGGTCGAATTGACATAA-3′; si-SOAT1#2: 5′-TTGAACTCAAGTACCAGCCTTC-3′. The vector expressing SOAT1 (pcDNA3.1-SOAT1) as well as the blank pcDNA3.1-vector were purchased from Hanbio Biotechnology Company (Shanghai, China). SiRNA and plasmid were transfected with DharmaFECT4 (GE Healthcare) and Lipofectamine 3000 (Invitrogen, Carlsbad, CA, United States). Virus-containing supernatant was collected 48 h after transfection and was added to cell when confluence reached 70%, 48 h later, transduced cells were selected with 1 μg/ml puromycin.

RNA Extraction and qRT-PCR Assay

Total RNAs were extracted from human GC tissues and associated non-cancerous tissues using TRIzol reagent (Invitrogen, Carlsbad, CA, United States) according to the manufacturer's instructions. The reverse transcription reaction (RT) was performed with Reverse Transcription kit (Vazyme, Nanjing, China). The RT-PCR reactions were performed with a SYBR Green PCR Kit (Vazyme, Nanjing, China), measured in triplicate and performed on an Applied Biosystems 7900HT sequence detection system (Applied Biosystems). GAPDH was used as an internal control for mRNA. The relative expression levels of the target genes were calculated using the comparative 2−ΔΔCt method. All primers used in this study were listed in **Supplementary Table S3**. All results were obtained from three independent experiments performed in duplicate.

Western Blot Assay

The Western blot protocol was performed as previously described(Wang et al., 2020). The antibodies used were listed as follows: anti-SOAT1 (Immunoway, YN1370); anti-SOAT1 (Abcam, ab39327); anti-VEGFC (Proteintech, 14517-1-AP); anti-FASN (Proteintech, 10624-2-AP); anti-SREBP1 (Proteintech, 66875-1-AP); anti-SREBP2 (Proteintech, 28212-1-AP); and anti-GAPDH (Proteintech, 60004-1-Ig). Phenylmethylsulfonyl fluoride was purchased from Selleck (Houston, TX, United States).

Proliferation Assay

The antiproliferative effect of avasimibe and fatostatin (MedChemExpress, Shanghai, China) was evaluated with a Cell Counting Kit-8 kit (CCK-8, Vazyme, Nanjing, China). One day before avasimibe treatment, GC cells were seeded in 96-well plates (5,000 cells/well). The cells were treated with avasimibe for 24 h or 48 h. After the indicated time, 10 μL per well of CCK-8 solution was added and incubated at 37°C for 1 h. Absorbance was recorded at 450 nm, and five independent assays were carried out.

For the plate colony formation assay, GC cells were seeded in 6-well plates or 12-well plates (1,000 cells/well in 6-well plates and 500 cells/well in 12-well plates) and incubated for 10–14 days. The medium with or without avasimibe was changed every other day. Then, the cells were fixed with 4% paraformaldehyde for 15 min and stained with crystal violet for 1 h. Images were acquired with a digital camera, and three independent assays were carried out.

Oil Red O Staining and Nile Red Staining

GC cells were seeded in 12-well plates, following by 0.2 μM oil acid (OA) (Sigma, United States) for 24 h. Then the cells were fixed with 4% paraformaldehyde solution. For Oil red O staining, cells were incubated with 60% isopropanol for 15 min before stanning by Oil red O working solution. The Oil red O working solution was prepared by diluting the Oil red O stock solution with distilled water at a ratio of 3:2, followed by filtration. For Nile red staining, cells were sequentially stained with 0.05 μg/ml Nile red (Sigma, United States), washed with PBS twice and then stained with DAPI (Beyotime, Shanghai, China). Images of the cells were acquired by fluorescence microscopy. All the operations were performed in a dark environment.

HLECs Tube Formation and Transwell Assays

HLECs were seeded in 96-well plates (2×10^4/well, precoated with 50 μL of Matrigel, Corning Life Sciences, Bedford, MA, United States), containing medium obtained from tumor cells and cultured for 12 h. Images of lymphatic tubes were acquired using a fluorescence microscope and quantified by measuring the number and area of the completed tubule structures.

Cell migration and invasion abilities were evaluated by transwell chambers (Corning Life Sciences, Bedford, MA, United States). Briefly, a total of 5×10^4 GC cells suspended in media without FBS were seeded in the upper chambers coated with or without 50 μL of Matrigel (BD Biosciences). Then, 600 μL of culture medium containing 10% FBS was added to the lower chambers. After incubation at 37°C for 12 h, the cells in the lower chambers were fixed with 4% paraformaldehyde for 30 min, stained with crystal violet (Beyotime, Shanghai, China) for 30 min. Finally, three random fields were microscopically examined, and the number of cells was determined by photoshop software.

Wound Healing Assay

GC cells were seeded into six-well plates and grown to 90% confluence. The cell layer was scrapping with a 10-μL sterile pipette tip and washed with three times with PBS to remove the floating and detached cells, then cultured in 1% FBS medium and images were acquired under a microscope at multiple time points (0, 6, 12, and 24 h).

Enzyme-Linked Immunosorbent Assay

The cell culture supernatant was collected, secreted VEGFC was quantified using the Human VEGFC Quantikine ELISA Kit (Cat. No. E-EL-H1600c, elabacience) according to the manufacturer's instructions. Briefly, GC cells seeded in 6-well culture plates were cultured in the growth medium until 90% confluence. The cells were washed three times with phosphate-buffered saline (PBS) and cultured in serum-free medium for 24 h. The cell culture supernatant or VEGFC standards were added to the 96-well plates coated with polyclonal antibody specific for human VEGFC in triplicate and incubated for 1.5 h at 37°C. Then, the Biotinylated detection Ab working fluid was added to each well and incubated for 1 h at 37°C. Afterwards, the well was washed five times, HRP conjugate working solution was added and incubated for 30 min at 37°C. Then, substrate solution was added to each well, and incubated for 30 min at 37°C in the dark. Then, the stop solution was added to each well. Absorbance was determined at 450 nm. All assays were performed in triplicate.

Cholesterol Assay

Cells were collected by centrifugation for 10 min (4°C, 1,000×*g*) and resuspended in 200 μL extracting solution, then ultrasonic crushing in an ice bath was performed for 30 s. Supernatants were combined and centrifuged for 20 min at 10,000 × *g* (4°C) and placed on ice for measurement. Total cholesterol and unesterified cholesterol were quantitated using the manufacturer's protocol of a Total Cholesterol and Cholesterol ester Fluorescence Determination Kit (Cat. No. E-BC-F032, elabacience). Amount of cholesterol ester were determined by subtracting the amount of unesterified cholesterol from total cholesterol.

Statistical Analysis

A total of 111 human rate-limiting metabolic enzymes were obtained from the rate-limiting enzyme database according to a previous study (Wang et al., 2019). The RNA expression data and clinical information of GC patients were obtained from TCGA (https://tcga-data.nci.nih.gov/tcga/). Differentially expressed genes were screened with the R package "limma." The expression level of prognostic associated rate-limiting metabolic enzymes between cancerous and normal samples was displayed via package "heatmap" and "ggplot," respectively. Univariate Cox regression analysis was performed to identify prognostic associated rate-limiting metabolic enzymes. Package "glmnet" was used to perform LASSO Cox regression model to select optimal weighting coefficients via penalized maximum likelihood and build a prognostic signature. The formula of the risk score for the prediction of GC patients' prognosis was as follows: risk score = the sum of the multivariate Cox regression coefficient ratio of each mRNA multiplied by the expression level of each mRNA. For survival analysis, overall survival was defined as the time from first treatment to death for any cause, Kaplan-Meier method and log-rank test were used to detect potential prognostic factors. For clarify relationship of SOAT1, clinicopathological characteristics, and prognosis, univariate Cox regression analysis was performed to find out the independent factors correlated with OS. AUC was employed to demonstrate the sensitivity and specificity of different variables by risk estimation. The "pROC" package was used to perform ROC curve and analyze AUC. All

statistical tests were two sided and $p < 0.05$ were significant and each experiment was carried out in at least triplicate.

DATA AVAILABILITY STATEMENT

The original contributions presented in the study are included in the article/**Supplementary Material**, further inquiries can be directed to the corresponding authors.

ETHICS STATEMENT

The studies involving human participants were reviewed and approved by Nanjing Drum Tower Hospital, the Affiliated Hospital of Nanjing University Medical School. The patients/participants provided their written informed consent to participate in this study.

AUTHOR CONTRIBUTIONS

TZ, ZW, SW, and GX designed the project. TZ performed the experiments. ZW collected and analyzed the TCGA data. TZ, CC, and YC evaluated the IHC of TMA. TZ, LX, WZ, SZ and QD provided clinical samples and collected clinical information. TZ drafted the manuscript. ZW, SW, QD and GX revised this manuscript. All authors read and approved the final manuscript.

FUNDING

This work was supported by the National Natural Science Foundation of China (82103373, 82073114, 82102984, 82170548, 81773383, and 82002622), the natural science foundation of Jiangsu Province (BK20200132), the Project funded by China Postdoctoral Science Foundation (2020M681562), the Nanjing Medical Science and Technology Development Program (Nos. YKK12072, YKK15061, and YKK16078). This work was also part of a C-class sponsored research project of the Jiangsu Provincial Six Talent Peaks (WSN-078) and the Young Scholars Project of Shanghai Municipal Health Commission (20194Y0096).

SUPPLEMENTARY MATERIAL

The Supplementary Material for this article can be found online at: https://www.frontiersin.org/articles/10.3389/fphar.2021.769647/full#supplementary-material

REFERENCES

Bemlih, S., Poirier, M. D., and El Andaloussi, A. (2010). Acyl-coenzyme A: Cholesterol Acyltransferase Inhibitor Avasimibe Affect Survival and Proliferation of Glioma Tumor Cell Lines. *Cancer Biol. Ther.* 9 (12), 1025–1032. doi:10.4161/cbt.9.12.11875

Chang, C., Dong, R., Miyazaki, A., Sakashita, N., Zhang, Y., Liu, J., et al. (2006). Human Acyl-CoA:cholesterol Acyltransferase (ACAT) and its Potential as a Target for Pharmaceutical Intervention against Atherosclerosis. *Acta Biochim. Biophys. Sin (Shanghai)* 38 (3), 151–156. doi:10.1111/j.1745-7270.2006.00154.x

Chang, T. Y., Li, B. L., Chang, C. C., and Urano, Y. (2009). Acyl-coenzyme A: cholesterol Acyltransferases. *Am. J. Physiol. Endocrinol. Metab.* 297 (1), E1–E9. doi:10.1152/ajpendo.90926.2008

Cheng, C., Geng, F., Cheng, X., and Guo, D. (2018). Lipid Metabolism Reprogramming and its Potential Targets in Cancer. *Cancer Commun. (Lond)* 38 (1), 27. doi:10.1186/s40880-018-0301-4

Cheng, C., Ru, P., Geng, F., Liu, J., Yoo, J. Y., Wu, X., et al. (2015). Glucose-Mediated N-Glycosylation of SCAP Is Essential for SREBP-1 Activation and Tumor Growth. *Cancer Cell* 28 (5), 569–581. doi:10.1016/j.ccell.2015.09.021

Digklia, A., and Wagner, A. D. (2016). Advanced Gastric Cancer: Current Treatment Landscape and Future Perspectives. *World J. Gastroenterol.* 22 (8), 2403–2414. doi:10.3748/wjg.v22.i8.2403

Faubert, B., Solmonson, A., and DeBerardinis, R. J. (2020). Metabolic Reprogramming and Cancer Progression. *Science* 368 (6487), eaaw5473. doi:10.1126/science.aaw5473

Geng, F., Cheng, X., Wu, X., Yoo, J. Y., Cheng, C., Guo, J. Y., et al. (2016). Inhibition of SOAT1 Suppresses Glioblastoma Growth via Blocking SREBP-1-Mediated Lipogenesis. *Clin. Cancer Res.* 22 (21), 5337–5348. doi:10.1158/1078-0432.Ccr-15-2973

Gu, L., Zhu, Y., Lin, X., Tan, X., Lu, B., and Li, Y. (2020). Stabilization of FASN by ACAT1-Mediated GNPAT Acetylation Promotes Lipid Metabolism and Hepatocarcinogenesis. *Oncogene* 39 (11), 2437–2449. doi:10.1038/s41388-020-1156-0

Heo, M. J., Kang, S. H., Kim, Y. S., Lee, J. M., Yu, J., Kim, H. R., et al. (2020). UBC12-Mediated SREBP-1 Neddylation Worsens Metastatic Tumor Prognosis. *Int. J. Cancer* 147 (1), 2550–2563. doi:10.1002/ijc.33113

Ji, H., Cao, R., Yang, Y., Zhang, Y., Iwamoto, H., Lim, S., et al. (2014). TNFR1 Mediates TNF-α-Induced Tumour Lymphangiogenesis and Metastasis by Modulating VEGF-C-VEGFR3 Signalling. *Nat. Commun.* 5, 4944. doi:10.1038/ncomms5944

Jiang, Y., Sun, A., Zhao, Y., Ying, W., Sun, H., Yang, X., et al. (2019). Proteomics Identifies New Therapeutic Targets of Early-Stage Hepatocellular Carcinoma. *Nature* 567 (7747), 257–261. doi:10.1038/s41586-019-0987-8

Lee, C. K., Jeong, S. H., Jang, C., Bae, H., Kim, Y. H., Park, I., et al. (2019). Tumor Metastasis to Lymph Nodes Requires YAP-dependent Metabolic Adaptation. *Science* 363 (6427), 644–649. doi:10.1126/science.aav0173

Li, B. L., Chang, T. Y., Chen, J., Chang, C. C., and Zhao, X. N. (2006). Human ACAT1 Gene Expression and its Involvement in the Development of Atherosclerosis. *Future Cardiol.* 2 (1), 93–99. doi:10.2217/14796678.2.1.93

Li, C., Peng, X., Lv, J., Zou, H., Liu, J., Zhang, K., et al. (2020). SREBP1 as a Potential Biomarker Predicts Levothyroxine Efficacy of Differentiated Thyroid Cancer. *Biomed. Pharmacother.* 123, 109791. doi:10.1016/j.biopha.2019.109791

Li, X., Chen, Y. T., Hu, P., and Huang, W. C. (2014). Fatostatin Displays High Antitumor Activity In Prostate Cancer By Blocking SREBP-Regulated Metabolic Pathways And Androgen Receptor Signaling. *Mol. Cancer Ther.* 13 (4), 855–866. doi:10.1158/1535-7163.Mct-13-0797

Li, X., Wenes, M., Romero, P., Huang, S. C., Fendt, S. M., and Ho, P. C. (2019). Navigating Metabolic Pathways to Enhance Antitumour Immunity and Immunotherapy. *Nat. Rev. Clin. Oncol.* 16 (7), 425–441. doi:10.1038/s41571-019-0203-7

Liberti, M. V., and Locasale, J. W. (2016). The Warburg Effect: How Does it Benefit Cancer Cells?. *Trends Biochem. Sci.* 41 (3), 211–218. doi:10.1016/j.tibs.2015.12.001

Liu, Y., Wang, Y., Hao, S., Qin, Y., and Wu, Y. (2021). Knockdown of Sterol O-Acyltransferase 1 (SOAT1) Suppresses SCD1-Mediated Lipogenesis and Cancer Procession in Prostate Cancer. *Prostaglandins Other Lipid Mediat* 153, 106537. doi:10.1016/j.prostaglandins.2021.106537

Ma, C., Luo, C., Yin, H., Zhang, Y., Xiong, W., Zhang, T., et al. (2018a). Kallistatin Inhibits Lymphangiogenesis and Lymphatic Metastasis of Gastric Cancer by Downregulating VEGF-C Expression and Secretion. *Gastric Cancer* 21 (4), 617–631. doi:10.1007/s10120-017-0787-5

Ma, Y., Temkin, S. M., Hawkridge, A. M., Guo, C., Wang, W., Wang, X. Y., et al. (2018b). Fatty Acid Oxidation: An Emerging Facet of Metabolic Transformation in Cancer. *Cancer Lett.* 435, 92–100. doi:10.1016/j.canlet.2018.08.006

Menendez, J. A., and Lupu, R. (2017). Fatty Acid Synthase (FASN) as a Therapeutic Target in Breast Cancer. *Expert Opin. Ther. Targets* 21 (11), 1001–1016. doi:10.1080/14728222.2017.1381087

Oelkers, P., Behari, A., Cromley, D., Billheimer, J. T., and Sturley, S. L. (1998). Characterization of Two Human Genes Encoding Acyl Coenzyme A: cholesterol Acyltransferase-Related Enzymes. *J. Biol. Chem.* 273 (41), 26765–26771. doi:10.1074/jbc.273.41.26765

Ohmoto, T., Nishitsuji, K., Yoshitani, N., Mizuguchi, M., Yanagisawa, Y., Saito, H., et al. (2015). K604, a Specific acyl-CoA:cholesterol A-cyltransferase 1 I-nhibitor, S-uppresses P-roliferation of U251-MG G-lioblastoma C-ells. *Mol. Med. Rep.* 12 (4), 6037–6042. doi:10.3892/mmr.2015.4200

Oni, T. E., Biffi, G., Baker, L. A., Hao, Y., Tonelli, C., Somerville, T. D. D., et al. (2020). SOAT1 Promotes Mevalonate Pathway Dependency in Pancreatic Cancer. *J. Exp. Med.* 217 (9), e20192389. doi:10.1084/jem.20192389

Roberts, D. J., and Miyamoto, S. (2015). Hexokinase II Integrates Energy Metabolism and Cellular protection: Akting on Mitochondria and TORCing to Autophagy. *Cell Death Differ* 22 (2), 364. doi:10.1038/cdd.2014.208

Roberts, D. J., Tan-Sah, V. P., Ding, E. Y., Smith, J. M., and Miyamoto, S. (2014). Hexokinase-II Positively Regulates Glucose Starvation-Induced Autophagy through TORC1 Inhibition. *Mol. Cel* 53 (4), 521–533. doi:10.1016/j.molcel.2013.12.019

Smith, D. C., Kroiss, M., Kebebew, E., Habra, M. A., Chugh, R., Schneider, B. J., et al. (2020). A Phase 1 Study of Nevanimibe HCl, a Novel Adrenal-specific Sterol O-Acyltransferase 1 (SOAT1) Inhibitor, in Adrenocortical Carcinoma. *Invest. New Drugs* 38 (5), 1421–1429. doi:10.1007/s10637-020-00899-1

Smyth, E. C., Nilsson, M., Grabsch, H. I., van Grieken, N. C., and Lordick, F. (2020). Gastric Cancer. *Lancet* 396 (10251), 635–648. doi:10.1016/s0140-6736(20)31288-5

Snaebjornsson, M. T., Janaki-Raman, S., and Schulze, A. (2020). Greasing the Wheels of the Cancer Machine: The Role of Lipid Metabolism in Cancer. *Cell Metab* 31 (1), 62–76. doi:10.1016/j.cmet.2019.11.010

Stacker, S. A., Williams, S. P., Karnezis, T., Shayan, R., Fox, S. B., and Achen, M. G. (2014). Lymphangiogenesis and Lymphatic Vessel Remodelling in Cancer. *Nat. Rev. Cancer* 14 (3), 159–172. doi:10.1038/nrc3677

Sung, H., Ferlay, J., Siegel, R. L., Laversanne, M., Soerjomataram, I., Jemal, A., et al. (2021). Global Cancer Statistics 2020: GLOBOCAN Estimates of Incidence and Mortality Worldwide for 36 Cancers in 185 Countries. *CA Cancer J. Clin.* 71 (3), 209–249. doi:10.3322/caac.21660

Tardif, J. C., Grégoire, J., L'Allier, P. L., Anderson, T. J., Bertrand, O., Reeves, F., et al. (2004). Effects of the Acyl Coenzyme A:cholesterol Acyltransferase Inhibitor Avasimibe on Human Atherosclerotic Lesions. *Circulation* 110 (21), 3372–3377. doi:10.1161/01.Cir.0000147777.12010.Ef

Tong, X., Zhao, F., and Thompson, C. B. (2009). The Molecular Determinants of De Novo Nucleotide Biosynthesis in Cancer Cells. *Curr. Opin. Genet. Dev.* 19 (1), 32–37. doi:10.1016/j.gde.2009.01.002

Vander Heiden, M. G., Cantley, L. C., and Thompson, C. B. (2009). Understanding the Warburg Effect: the Metabolic Requirements of Cell Proliferation. *Science* 324 (5930), 1029–1033. doi:10.1126/science.1160809

Vander Heiden, M. G., and DeBerardinis, R. J. (2017). Understanding the Intersections between Metabolism and Cancer Biology. *Cell* 168 (4), 657–669. doi:10.1016/j.cell.2016.12.039

Wang, X., Liu, R., Zhu, W., Chu, H., Yu, H., Wei, P., et al. (2019). UDP-glucose Accelerates SNAI1 mRNA Decay and Impairs Lung Cancer Metastasis. *Nature* 571 (7763), 127–131. doi:10.1038/s41586-019-1340-y

Wang, Z., Wang, Q., Xu, G., Meng, N., Huang, X., Jiang, Z., et al. (2020). The Long Noncoding RNA CRAL Reverses Cisplatin Resistance via the miR-505/CYLD/AKT axis in Human Gastric Cancer Cells. *RNA Biol.* 17 (11), 1576–1589. doi:10.1080/15476286.2019.1709296

Warita, K., Ishikawa, T., Sugiura, A., Tashiro, J., Shimakura, H., Hosaka, Y. Z., et al. (2021). Concomitant Attenuation of HMGCR Expression and Activity Enhances the Growth Inhibitory Effect of Atorvastatin on TGF-β-Treated Epithelial Cancer Cells. *Sci. Rep.* 11 (1), 12763. doi:10.1038/s41598-021-91928-3

Wong, B. W., Wang, X., Zecchin, A., Thienpont, B., Cornelissen, I., Kalucka, J., et al. (2017). The Role of Fatty Acid β-oxidation in Lymphangiogenesis. *Nature* 542 (7639), 49–54. doi:10.1038/nature21028

Xu, H., Zhou, S., Tang, Q., Xia, H., and Bi, F. (2020). Cholesterol Metabolism: New Functions and Therapeutic Approaches in Cancer. *Biochim. Biophys. Acta Rev. Cancer* 1874 (1), 188394. doi:10.1016/j.bbcan.2020.188394

Conflict of Interest: The authors declare that the research was conducted in the absence of any commercial or financial relationships that could be construed as a potential conflict of interest.

Publisher's Note: All claims expressed in this article are solely those of the authors and do not necessarily represent those of their affiliated organizations, or those of the publisher, the editors and the reviewers. Any product that may be evaluated in this article, or claim that may be made by its manufacturer, is not guaranteed or endorsed by the publisher.

GLOSSARY

GC Gastric cancer
SOAT1 Sterol O-acyltransferase 1
LNM Lymph node metastasis
NADPH Nicotinamide adenine dinucleotide phosphate
GSH Glutathione
FAO Fatty acid oxidation
FASN Fatty acid synthase
KGA Kidney-type glutaminase
EMT Epithelial–mesenchymal transition
HLECs Human lymphatic endothelial cells
TCGA The cancer genome atlas
GNE Glucosamine
UCK2 Uridine-cytidine kinase 2
DCK Deoxycytidine kinase
GAD1 Glutamate decarboxylase 1
OS Overall survival
IHC Immunohistochemistry
TMA Tissue microarray
HR Hazard ratio
CI Confidence interval
ROC Receiver operating characteristic curve
AUC Area under the curve
GBM Glioblastoma
HCC Hepatocellular carcinoma
PCa Prostate cancer
IC50 Half-inhibitory concentration
OA Oil acid
HMGCR 3-Hydroxy-3-Methylglutaryl-CoA Reductase
SREBP1 Sterol regulatory element binding transcription factor 1
SREBP2 Sterol regulatory element binding transcription factor 2
ACC Acetyl-CoA carboxylase 1
SCD1 Stearoyl-CoA desaturase 2
VEGFC Vascular endothelial growth factor C
VEGFD Vascular endothelial growth factor D
VEGFR3 Vascular endothelial growth factor receptor 3
LYVE-1 Lymphatic vessel endothelial hyaluronan receptor 1
CM Conditioned medium
qRT-PCR Real-time quantitative reverse transcription
HK-2 Hexokinase 2
mTORC1 mammalian target of rapamycin
Ulk1 Unc-51 like autophagy activating kinase 1
GLS1 Glutaminase 1
ROS Reactive oxygen species
LECs Lymphatic endothelial cells
TGF-β Transforming growth factor beta 1.

frontiers in Pharmacology

REVIEW
published: 01 November 2021
doi: 10.3389/fphar.2021.741451

Cardiotoxicity of Epidermal Growth Factor Receptor 2-Targeted Drugs for Breast Cancer

ZiYan Yang[1†], Wei Wang[2†], Xiaojia Wang[3] and ZhiQuan Qin[1]**

[1]Department of Oncology Center, Oncology, Zhejiang Provincial People's Hospital, People's Hospital of Hangzhou Medical College, Hangzhou, China, [2]Graduate School of Bengbu Medical College, Bengbu, China, [3]Department of Breast Medical Oncology, Cancer Hospital of the University of Chinese Academy of Sciences (Zhejiang Cancer Hospital), Hangzhou, China

Breast cancer is the most common form of cancer in women and its incidence has been increasing over the years. Human epidermal growth factor receptor 2 (HER2 or ErbB2) overexpression is responsible for 20 to 25% of invasive breast cancers, and is associated with poor prognosis. HER2-targeted therapy has significantly improved overall survival rates in patients with HER2-positive breast cancer. However, despite the benefits of this therapy, its cardiotoxicity is a major concern, especially when HER2-targeted therapy is used in conjunction with anthracyclines. At present, the mechanism of this cardiotoxicity is not fully understood. It is thought that HER2-targeting drugs inhibit HER2/NRG 1 dimer formation, causing an increase in ROS in the mitochondria of cardiomyocytes and inhibiting the PI3K/Akt and Ras/MAPK pathways, resulting in cell apoptosis. Antioxidants, ACE inhibitors, angiotensin II receptor blockers, β-blockers, statins and other drugs may have a cardioprotective effect when used with ErbB2-targeting drugs. NT-proBNP can be used to monitor trastuzumab-induced cardiotoxicity during HER2-targeted treatment and may serve as a biological marker for clinical prediction of cardiotoxicity. Measuring NT-proBNP is non-invasive, inexpensive and reproducible, therefore is worthy of the attention of clinicians. The aim of this review is to discuss the potential mechanisms, clinical features, diagnostic strategies, and intervention strategies related to cardiotoxicity of ErbB2-targeting drugs.

Keywords: cardiotoxicity, ErbB2, targeting drugs, breast cancer, therapy

OPEN ACCESS

Edited by:
Yao Liu,
Daping Hospital, China

Reviewed by:
Samrein B. M. Ahmed,
University of Sharjah, United Arab Emirates
Angelique Nyinawabera,
L.E.A.F. Pharmaceuticals, United States

****Correspondence:***
ZhiQuan Qin
qzq66@126.com
Xiaojia Wang
wxiaojia0803@163.co

[†]These authors have contributed equally to this work

Specialty section:
This article was submitted to Pharmacology of Anti-Cancer Drugs, a section of the journal Frontiers in Pharmacology

Received: *14 July 2021*
Accepted: *08 October 2021*
Published: *01 November 2021*

Citation:
Yang Z, Wang W, Wang X and Qin Z (2021) Cardiotoxicity of Epidermal Growth Factor Receptor 2-Targeted Drugs for Breast Cancer. Front. Pharmacol. 12:741451. doi: 10.3389/fphar.2021.741451

1 INTRODUCTION

Breast cancer is the most common cancer among women worldwide, and its incidence has been increasing yearly (Bray et al., 2018). Chemotherapy is one of the main treatments for breast cancer (Piccart-Gebhart and Sotiriou, 2007). Human epidermal growth factor receptor 2 (HER2), also known as erythroblast leukemia virus oncogene homolog 2 (ErbB2), is overexpressed in 20–25% of breast cancers. This transmembrane receptor promotes abnormal cell growth and proliferation in human breast cancer, leading to tumor cell invasion and poor prognosis (Slamon et al., 1987). HER2/ErbB2 are potential targets in chemotherapy of HER2-positive (HER2+) breast cancer. The 2021 ASCO Guidelines indicated that ErbB2-targeting drugs significantly improved survival rates and more patients were included in the range of drug (Korde et al., 2021). Unfortunately, target drugs is often discontinued once cardiotoxicity occurs during clinical (Perez and Rodeheffer, 2004). Cardiotoxicity is mainly caused by the reversible decrease of ejection fraction, but also severe heart failure and even fatal (Jerusalem et al., 2019).

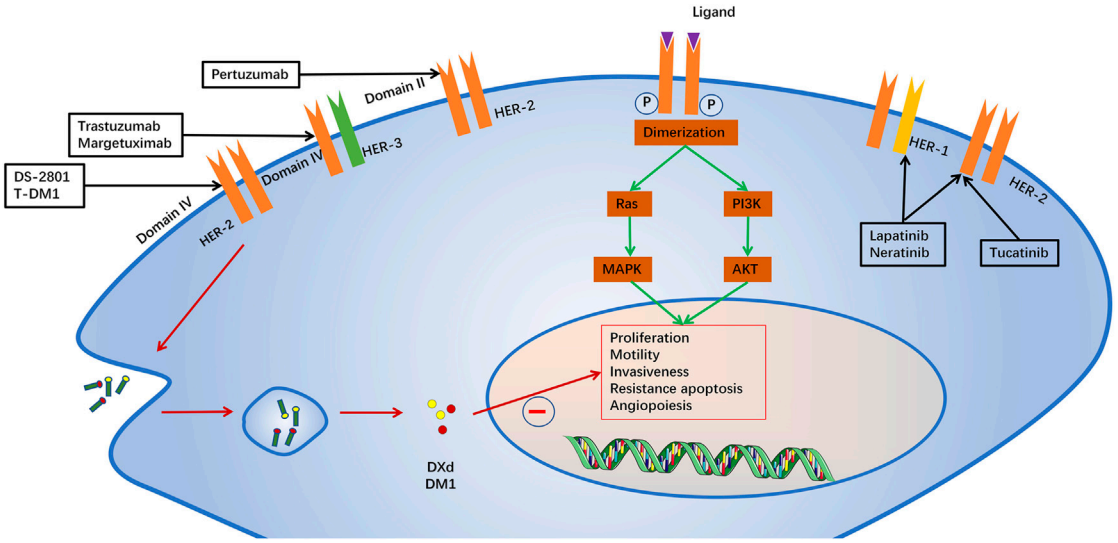

FIGURE 1 | Mechanism of action of ErbB2-targeted drugs.

HER2 belongs to a family of receptor tyrosine kinases with four members: HER1 (EGFR), HER2, HER3 and HER4. When activated, the HER proteins homodimerize or heterodimerize and subsequently activate intricate cellular signalling cascades, including the PI3K/AKT and RAS/MAPK (ERK) pathways, which regulate cell proliferation and survival, as well as the metastasis of tumour cells (Slamon et al., 1987). ErbB2-targeted drugs include monoclonal antibodies, antibody drug conjugates and tyrosine kinase inhibitors (Godeau et al., 2021). Monoclonal antibodies mainly include trastuzumab, pertuzumab and margetuximab. Trastuzumab, a humanized monoclonal antibody against ErbB2 domain IV was the first immunotherapeutic agent for HER2(+) breast cancer (Jerian and Keegan, 1999). Margetuximab is a novel anti-HER2 antibody that has a higher affinity with the Fc receptor and stronger antibody-dependent cell-mediated antitumor cytotoxicity (ADCC) (Kaplon and Reichert, 2021). Pertuzumab is another humanized monoclonal antibody that binds to ErbB2 domain II and inhibits its dimerization (Capelan et al., 2013). Trastuzumab emtansine(T-DM1) and Trastuzumab deruxtecan (DS-2801,Enhertu) are antibo-cytotoxic drug conjugates composed of trastuzumab with the microtubule toxin DM1 and topoisomerase I inhibitor, a potent mitotic inhibitor (Zhao et al., 2020; Andrikopoulou et al., 2021). T-DM1 is currently a second-line treatment for patients with metastatic HER2(+) breast cancer (Verma et al., 2012). The Tyrosine kinase inhibitors include lapatinib, Neratinib and Tucatinib (Chaar et al., 2018). Lapatinib is an oral tyrosine kinase inhibitor that reverses ErbB2 and endothelium growth factor receptor (EGFR orErbB1) signaling (Moy et al., 2007). Neratinib is an irreversible small molecule inhibitor of HER1, HER2 and HER4 tyrosine kinases, approved for the extended adjuvant treatment of women with early-stage and metastatic HER2 + breast cancer (Oh and Bang, 2020). Tucatinib, a newly approved tyrosine kinase inhibitor, is characterized by its high selectivity for HER2/ErbB2 (Corti and Criscitiello, 2021). In order to better understand the cardiotoxicity of ErbB2-targeted drugs, we have systematically reviewed recently published papers on the potential mechanisms, clinical manifestations, diagnostic strategies, intervention strategies, and the latest progress in ErbB2-targeted drug cardiotoxicity. We summarized the potential mechanism and intervention strategies with ErbB2/nauregulin 1 (NRG1) pathway causing cardiac dysfunction reported to date, to provide more evidence for clinical practice (**Figure 1**).

2 MECHANISM OF CARDIOTOXICITY

The ErbB receptor is a transmembrane receptor tyrosine kinase that regulates cell physiological responses including cell growth, division, differentiation, adhesion, function, and apoptosis (Linggi and Carpenter., 2006). ErbB signaling in the heart is critical for the normal development of the fetal heart (Gassmann et al., 1995). In mutant mice with a deletion of the ErbB2 gene, abnormal ventricular trabeculae resulted in fetal death (Lee et al., 1995; Meyer and Birchmeier, 1995). In addition, ErbB2 plays an important role in adult cardiomyocytes growth (Zhao et al., 1998). ErbB2 mutant mice showed decreased ErbB2 expression and impaired ventricular dilation and contraction, and histology of the myocardium revealed ultrastructural changes (Ozcelik et al., 2002). Trastuzumab and pertuzumab reduced the dimerization of ErbB2/4 in rat and human cardiomyocytes (Fedele et al., 2012a). The NRG-1/ErbB2/ErbB4 complex controls cardiomyocyte survival and myofibrillary disorders in cardiomyocytes (Kuramochi et al., 2006). NRG-1 activation directly promotes cardiomyocyte survival through the ErbB2/ERBB4 heterodimer (De Keulenaer et al., 2010). NRG1 activates PI3-kinase/Akt and MAPK/Erk1/2 pathways through ErbB2 phosphorylation

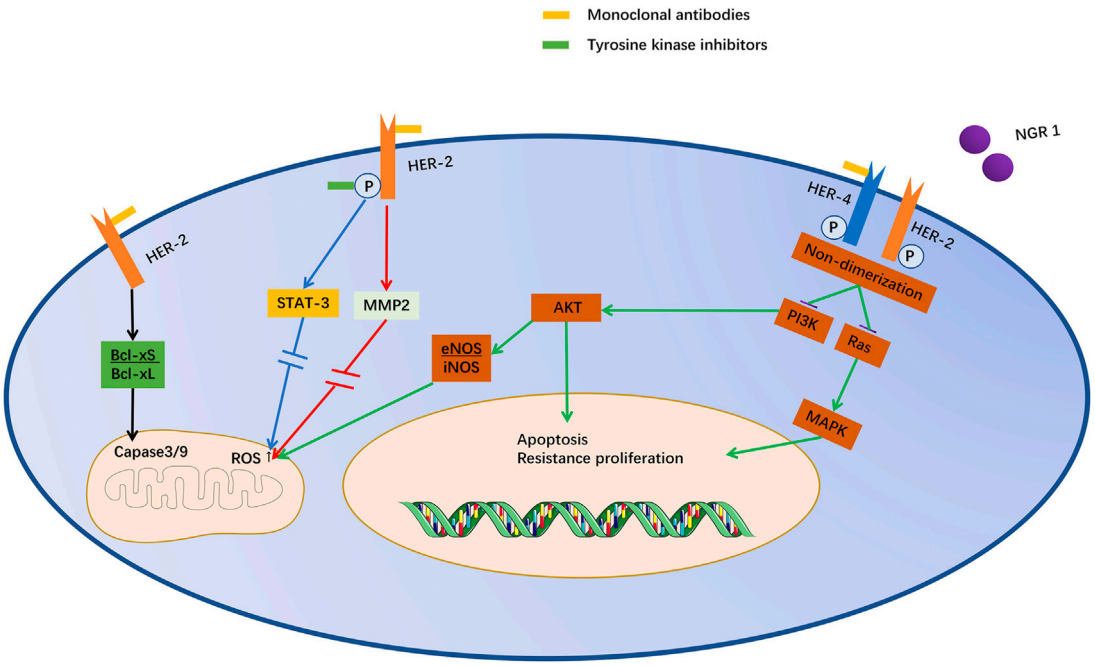

FIGURE 2 | Potential mechanism of cardiotoxicity induced by anti-ErbB-targeted drugs. Trastuzumab and T-DM1 act on the same epitope of ErbB2, and pertuzumab also acts on similar epitopes. They inhibit ErbB2/4 dimerization induced by NRG1. Lapatinib acts directly on the phosphorylation site of ErbB2. Inhibition of ErbB2 can inhibit STAT3 through MAPK/ERK1/2, leading to mitochondrial dysfunction and promoting cell death. Moreover, Akt expression can decrease iNOS and increase eNOS, which leads to the accumulation of ROS in mitochondria. Moreover, the increase in the Bcl-XS/Bcl-XL ratio directly stimulates caspase 3/9 and promotes cell apoptosis.

(Lemmens et al., 2004). Silencing or down-regulation of ErbB2 expression attenuated NRG-1-induced intracellular Akt and ERK1/2 phosphorylation (Hsu et al., 2018).

NRG1 is a ligand of the epidermal growth factor family, which can bind to ErbB3 or ErbB4 monomers and induce the formation of homodimers (ErbB4/4) and heterodimers (ErbB2/3 or ErbB2/4) (Lemmens et al., 2007). The NRG1 stimulates glucose uptake and protein synthesis in cardiomyocytes. (Cote et al., 2005). ErbB2 inhibition decreased expression of endothelial nitric oxide synthase (eNOS) and increased inducible nitric oxide synthase(iNOS), leading to produce more reactive oxygen species (ROS) (Timolati et al., 2006). NRG1 reduces contraction without impairing diastole by upregulating NOS and reducing the effect of β-adrenergic stimulation (Lemmens et al., 2004). STAT-3 is a transcription factor that is activated by tyrosine phosphorylation in response to certain ligand, such as interferon and epidermal growth factor (Tkach et al., 2013). It plays a key role in cell growth and differentiation, leading to ultrastructural changes in cardiomyocytes (Kabel and Elkhoely, 2017). ErbB2 inhibition can lead to increased Bcl-xS/Bcl-xL ratio, activation of mitochondrial caspase-9 and caspase-3, and causing apoptosis (Rohrbach et al., 2005). ErbB2 inhibition has also been reported to alter Bcl-x splicing, induce endogenous apoptotic signaling (Grazette et al., 2004; De Lorenzo et al., 2018). Besides, Matrix metalloproteinase-2 (MMP2) mRNA is elevated in trastuzumab cardiotoxicity, accompanied by an increase in ROS (Riccio et al., 2018). Lapatinib can affect cardiac function and fibrosis in mice (Fedele et al., 2012b). Lapatinib can directly inhibit ErbB2 phosphorylation (Sawyer et al., 2002). Although lapatinib did not affect NOS expression and basal mitochondrial respiration, it impaired the standby oxygen consumption rate (Hsu et al., 2018). Cardiotoxicity caused by the inhibition of ErbB2 may be due to the adaptation of the heart to stress reactions. There is evidence that trastuzumab, pertuzumab, and lapatinib reduce cell viability in a concentration-dependent manner (Fedele et al., 2012a). Furthermore, ErbB2 inhibition increased ROS production and impaired mitochondrial function in a concentration-dependent manner (Pentassuglia et al., 2007) (**Figure 2**).

3 CLINICAL FEATURES OF CARDIOTOXICITY

3.1 Monoclonal Antibody

The main reason for discontinuation of ErbB2-targeted therapy is cardiotoxicity (Martín et al., 2009). Trastuzumab was the first ErbB2-targeting drug to be used in HER + breast cancer, therefore, trastuzumab-associated cardiotoxicity is the most well-studied cardiotoxicity of the cardiotoxicities associated with Erb2-targeting drugs (Herrmann, 2020). Trastuzumab-associated cardiotoxicity is usually characterized by an asymptomatic decrease in left ventricular ejection fraction (LVEF), which can be reversed after drug discontinuation (Perez and Rodeheffer, 2004). However, a prospective study showed that 48.53% of patients with available cardiac

TABLE 1 | Summary of studies for development of clinical HER-2 target drugs.

Author/Date	Trial type	Population studies	Number	Methods	Significant	References
Jacquinot et al. (2018)	Prospective study	Patients who received 12 months of trastuzumab	1631	LVEF performed every 3 months; every 6 months (patients received trastuzumab and after completion of treatment over the first 2 years)	48.53% of patients with available measures did not fully recover their baseline LVEF value	Jacquinot et al. (2018)
Yoon et al. (2019)	Retrospective study	Patients with trastuzumab-induced left ventricular dysfunction (LVD)	243	Major adverse clinical events (MACEs) were compared in non-recovered LVD and recovered LVD.	Non-recovered LVD was associated with MACEs. Decreased LVEF, enlarged LV size, pulmonary hypertension, and anaemia were independent predictors of LV-functional non-recovery	Yoon et al. (2019)
Nowsheen et al. (2018)	Retrospective study	Patients with reduced left ventricular ejection fraction during using trastuzumab	428	A retrospective study of women treated with trastuzumab for human epidermal growth factor receptor 2 breast cancer at Mayo Clinic Rochester between January 1, 2000 and August 31, 2015 with pre- and on-therapy echocardiograms available for review	Impaired baseline cardiac function experience no higher risk of LVEF decline, but more frequently develop symptomatic heart failure	Nowsheen et al. (2018)
Hussain et al. (2019)	Retrospective study	Patients with reduced left ventricular ejection fraction during using trastuzumab	160	Retrospectively studied 160 patients with breast cancer receiving trastuzumab in the adjuvant (n = 129) as well as metastatic (n = 31) settings in our institution from 2006 to 2015. During the median follow-up of 3.5 years	Lower LVEF before trastuzumab independently predicted subsequent development of TRC	Hussain et al. (2019)
Kaboré et al. (2019)	Prospective study	Patients with stage I–III BC treated with anthracycline and/or trastuzumab	929	Analyzed associations between BMI and cardiotoxicity using multivariate logistic regression	The obese group was more prone to cardiotoxicity than the normal-weight group. Obesity and administration of trastuzumab were independently associated with c ardiotoxicity	Kaboré et al. (2019)
Keramida et al. (2019)	Prospective study	Patients with consecutive receiving trastuzumab for 12 months	101	Comprehensive two-dimensional echocardiography with speckle tracking imaging of LV and RV global longitudinal strain (GLS) and RV free wall longitudinal strain (FWLS) analyses were performed at baseline and every 3 months up to treatment completion	Deformation mechanics of both the left and right ventricle follow similar temporal pattern and degree of impairment, confirming the global and uniform effect of trastuzumab on myocardial function	Keramida et al. (2019)

TABLE 2 | Summary of studies for toxicities of HER-2 target drugs.

ERBb2-Targeted drugs		Toxicities	References
Monoclonal antibody	Trastuzumab	LVEF decreased, HF happened, Arrhythmia	Romond et al. (2012), Bayar et al. (2015), Serrano et al. (2015), Jacquinot et al. (2018), Nowsheen et al. (2018), Hussain et al. (2019), Keramida et al. (2019), Yoon et al. (2019), Upshaw et al. (2020)
	Pertuzumab	Neutropenia and diarrhoea	van Ramshorst et al. (2016), Tan et al. (2021)
	Margetuximab	Diarrhoea, nausea, anaemia and pyrexia	Markham (2021)
Antibody–drug conjugates	T-DM1	Transient LVEF decreased	(Krop et al. (2014), Pondé et al. (1990), Perez et al. (2017), von Minckwitz et al. (2019)
	DS-8201	Anaemia, neutropenia, thrombocytopenia, leukopenia, and interstitial lung disease or pneumonia	Modi et al. (2020)
Tyrosine kinase inhibitors	Lapatinib	Mild diarrhoea and rash	Bilancia et al. (2007), de Azambuja et al. (2014), Eiger et al. (2020)
	Neratinib	Diarrhoea	Awada et al. (2016), Chan et al. (2016), Martin et al. (2017)
	Tucatinib	Diarrhoea and hepatotoxicity	Lee (2020), Shah et al. (2021)

LVEF, left ventricular ejection fraction; HF, heart failure; T-DM1, Trastuzumab emtansine; DS-8201, Trastuzumab deruxtecan.

TABLE 3 | Summary of intervening measure. Current interventions are mainly antioxidants, ACER/AEB/BB and new material combination drugs. Antioxidants are made up of Probucol, Ranolazine, flaxseed (FLX), alpha-linolenic acid (ALA), secoisolariciresinol diglucoside (SDG), the antioxidant coenzyme Q (10) and nanoemulsion (NES). The possible mechanism is mainly antioxidant effect. The drugs mainly affected reactive oxygen species (ROS) accumulation to inhibit of cell death.

Types	Drugs	Test subjects	Function	References
Antioxidant	Probucol	Rats	ROS↓/Myocardial remodeling↓	PMID:21353471
	Ranolazine	Mice	MMP2/Capase3↓	PMID:29467663
	FLX/ALA/SDG	Mice	Antioxidant	PMID: 32510147
	Q(10)+NEs	Humans	LTB4/NF-κB/IL-6↓	PMID: 32764923
ACER/ARB/BB	ACEI/ARB	—	RASS↓/Myocardial remodeling↓	PMID: 32777728
	BB	—	Sympathetic nervous↓	PMID: 32777728
	BB	Mice	Sirtuin-3↓/ROS↓	PMID: 33529501
	Statin	—	GS-SG↓/ROS↓	PMID: 28622591
	Lipidosome	Cells/Humans	Cardiotoxicity↓	PMID: 26759238

ultrasound measurements (379 out of 781 patients) did not fully recover baseline LVEF (Jacquinot et al., 2018). Nonetheless, more than 30% of the people in the study were 60 years old. Therefore, the failure to exclude elderly patients with heart diseases from the study may have caused bias. Unfortunately, the study did not conduct a follow up, so long-term LVEF recovery results were not available. However, Yoon et al. found that non-recovery of trastuzumab-induced left ventricular dysfunction (LVD) had an impact on the clinical outcome of breast cancer. The survival rates of the group without left ventricular hypertrophy were significantly lower than those of the group with left ventricular hypertrophy. Increased left ventricular volume, pulmonary hypertension, and anemia were found to be contributing factors (Yoon et al., 2019). A recent study indicated that patients with reduced baseline cardiac function undergoing trastuzumab therapy for breast cancer developed symptomatic heart failure more frequently than patients with normal cardiac function, but did not experience a higher risk of LVEF decline (Nowsheen et al., 2018). These results contradict a previous study by Romond et al. (2012), that detected LVEF decline during trastuzumab treatment. However, the latter study tracked patients for up to 5 years and this may be the main reason for the opposing results. The development of diastolic dysfunction after treatment with anthracyclines alone, or anthracycline plus trastuzumab, is common (Serrano et al., 2015). However, the development of diastolic dysfunction was not observed with trastuzumab alone (Upshaw et al., 2020). Trastuzumab may cause right heart failure and right ventricular dysfunction and its effect on myocardial function was global and uniform (Bayar et al., 2015; Keramida et al., 2019). Hussain et al. found that patients with asymptomatic LVEF decline to <50% continued to use trastuzumab, who are expected to benefit from additional anti-HER2 therapy (Hussain et al., 2019).

Pertuzumab, in combination with other drugs, mostly causes neutropenia and diarrhoea. Significant cardiac toxicity is rare with both regimens, and overall toxicity is manageable (van Ramshorst et al., 2016). Tan et al. (2021) obtained the same result and the occurrence of cardiotoxic events was less than 1%. Lynce et al. (2019) observed no statistical difference in the incidence of adverse cardiac events between pertuzumab combined with trastuzumab and trastuzumab alone. This was consistent with the results of two previous prospective studies (von Minckwitz et al., 2017). Pertuzumab may only inhibit ErbB2/3 dimerization but does not block the ErbB2/4 signalling pathway in cardiomyocytes (Franklin et al., 2004).

The safety of margetuximab combined with chemotherapy was considered to be acceptable, and margetuximab improved primary progression-free survival (PFS) compared with trastuzumab, with a 24% relative risk reduction (Rugo et al., 2021). In December 2020, margetuximab was approved by the United States Food and Drug Administration (FDA) for use in combination with chemotherapy for metastatic HER2+ breast cancer (Markham, 2021). Treatment was well-tolerated, with toxicities mostly consisting of constitutional symptoms such as diarrhea, nausea, anemia, and pyrexia. A phase I study found no LVEF reduction to <50% or symptomatic heart failure with the use of margetuximab (Bang et al., 2017). Primary analysis of results of the phase III Sophia trial, reported that the incidence of LVEF of any grade was lower in the margetuximab group, than in the trastuzumab group (Rugo et al., 2019).

3.2 Antibody–Drug Conjugates

The incidence of cardiac events (CEs) was low in patients treated with trastuzumab emtansine (T-DM1) (Krop et al., 2014). The latest meta-analysis included individual patient-level data of 1,961 patients exposed to T-DM1 from seven trials. Multivariate analysis showed age ≥65 years (OR 3.0; 95% CI, 1.77–5.14; $p < 0.001$) and baseline LVEF <55% (OR 2.62; 95% CI, 1.29–5.32; $p = 0.008$) as risk factors. The majority (79%) of patients had CE resolution after discontinuation of treatment (Pondé et al., 1990). The Phase III Marianne trial compared T-DM1 to T-DM1 + pertuzumab and trastuzumab + taxane, and both T-DM1-containing regimens (0.8 and 2.5%, respectively) had a lower incidence of LVEF reduction than the trastuzumab regimen (4.5%) (Perez et al., 2017). In the Katherine trial, cardiac adverse events were very rare overall (0.3%), but the incidence of T-DM1 (1 in 740) was still lower than that of trastuzumab (4 per 720) (von Minckwitz et al., 2019).

Trastuzumab deruxtecan (DS-8201) was approved by the FDA for the treatment of unresectable or metastatic HER2-positive breast cancer in December 2019 (Narayan et al., 2021). Trastuzumab deruxtecan rarely causes cardiotoxic events, and the most common adverse effects are hematological, including

anemia, neutropenia, thrombocytopenia, and leukopenia. Other adverse effects include interstitial lung disease and pneumonia (Modi et al., 2020).

3.3 Tyrosine Kinase Inhibitors

Lapatinib is well tolerated and has a low incidence of cardiotoxicity, with mild diarrhea and rash being the most common toxic effects (Bilancia et al., 2007; de Azambuja et al., 2014). Eiger et al. (2020) discovered that compare trastuzumab (T) with galapatinib (L) dual HER2-blocking treatment to trastuzumab, CE was observed in 363 (8.6%) and 166 (7.9%) patients in the T + L arm versus 197 (9.3%) in the T arm (OR = 0.85; [95% CI, 0.68–1.05]).

Neratinib had a bigger problem—diarrhoea in clinical (Chan et al., 2016). In the Nefert-T study, the incidence of grade 3 or higher cardiotoxicity was 1.3% in the neratinib/paclitaxel group and 3.0% in the trastuzumab/paclitaxel group (Awada et al., 2016). In the Extenet trial, and no long-term cardiovascular toxicity was observed. Although cardiotoxicity is negligible, other obvious adverse events, such as diarrhea, require clinician attention (Martin et al., 2017).

Diarrhea and hepatotoxicity were reported as the major adverse events of tucatinib (Lee, 2020). On April 2020, the FDA approved tucatinib in combination with trastuzumab and capecitabine for the treatment of patients with advanced unresectable or metastatic HER2-positive breast cancer, including patients with brain metastases (Shah et al., 2021). In the HER2CLIMB phase III trial, cardiotoxicity was less than 1% in both groups of participants (Murthy et al., 2020).

The latest individual patient data level pooled analysis of HERA, NSBAP B-31, and NCCTG 9831 (Alliance Trials) revealed baseline risk factors that were significantly associated with the development of CE. These factors were baseline LVEF <60%, hypertension, body mass index > 25, age ≥ 60 years, and non-Caucasian ethnicity (de Azambuja et al., 2020). In addition, Jones et al. (2018) found that cardiac function in the first 3 months after trastuzumab treatment had an impact on the long-term assessment of heart failure (6–24 months after treatment), and patients with no significant decrease in EF at 3 months tended to have better long-term assessment of heart failure. The French national multicentre prospective CANTO (CANcer TOxicities) study showed that obesity appears to be associated with an important increase in risk-related cardiotoxicity, which is consistent with the results of meta-analysis (Kaboré et al., 2019) (**Tables 1**,**2**).

4 DIAGNOSTIC STRATEGIES

4.1 Imaging

Cardiac ultrasonography is the main method to detect heart failure caused by cardiotoxicity (Fallah-Rad et al., 2011). Impairment of the left ventricular diastolic function before treatment is an independent predictor of trastuzumab cardiotoxicity, and assessment of diastolic function before administration predicts cardiotoxicity risk (Cochet et al., 2011). Moreover, diastolic dysfunction was more sensitive than left ventricular ejection fraction on radiographic examination (Cao et al., 2015). Global longitudinal strain (GLS) analysis can detect cardiac changes earlier and more comprehensively (Lorenzini et al., 2017). A retrospective study showed that anthracycline trastuzumab treatment resulted in early worsening of left ventricle GLS, peripheral strain, and systolic strain rate and the right ventricle GLS and strain rate are also affected. However, early changes in GLS are a good predictor of cardiotoxicity (Arciniegas Calle et al., 2018). GLS based on the 3-apex viewpoint is the preferred technique for detecting cardiac toxicity (Ben Kridis et al., 2020). The latest meta-analysis, including 21 studies comprising of 1782 patients treated with anthracyclines with or without trastuzumab, found the high-risk cut-off values ranged from −21.0 to −13.8%, with worse GLS associated with a higher cancer therapy-related cardiac dysfunction (CTRCD) risk (odds ratio, 12.27; 95% CI, 7.73–19.47; area under the HSROC, 0.86; 95% CI, 0.83–0.89) (Oikonomou et al., 2019). Patients with persistent worsening in diastolic function while taking breast cancer chemotherapeutic agents have a small risk of subsequent systolic dysfunction (Upshaw et al., 2020). There are two new prospective studies comparing variability of echocardiography and cardiovascular magnetic resonance (CMR) in detecting cardiac dysfunction associated with cancer chemotherapy, but the results of these studies are inconclusive (Lambert et al., 2020; Houbois et al., 2021). Therefore, 2D-GLS appears to be the most suitable for clinical applications in individual patients.

4.2 Biological Markers

With increasing research, the detection of cardiotoxicity is not limited to imaging, and the use of biological markers is becoming more common in clinical practice (Upshaw, 2020). Placental growth factor (PLGF), growth differentiation factor 15 (GDF-15), high-sensitivity C-reactive protein (hs-CRP), myeloperoxidase (MPO), and troponin I (TnI) can predict decreased LVEF and are promising biomarkers for detecting cardiac function (Onitilo et al., 2012; Bonnie et al., 2014; Putt et al., 2015). A sub-study of the NEOALTTO trial suggested troponin T (TnT) and the amino-terminal fragment of brain natriuretic peptide (NT-proBNP) do not provide an early predictor of cardiac toxicity (Ponde et al., 2018). Besides, a meta-analysis found that an increase in the average BNP/NT-proBNP level of patients after treatment cannot predict left ventricle dysfunction (Michel et al., 2020). But, the latest prospective study, the NEOALTTO trial, fifty newly diagnosed human epidermal growth factor receptor 2-positive BC women received or did not receive anthracycline followed by taxus and trastuzumab for 15 months of follow-up, found NT-pro-BNP measured at the completion of anthracyclines are useful in the prediction of subsequent TIC (Ben Kridis et al., 2020). The NEOALTTO trial had only 11 study patients and receiving trastuzumab and lapatinib two targeted therapies may be the factors. Moreover, the meta-analysis research object is all tumor patients, not just breast cancer and BNP is more susceptible compared to NT-proBNP. The circulating level of NT-proBNP is increased in the unselected cancer patient population, which is related to the increase of myocardial performance index (MPI)

value, and is closely related to all-cause mortality (Yildirim et al., 2013; Pavo et al., 2015). GeparOcto-GBG 84 Trial also found a small but significant increase in early NT-proBNP levels in patients with cardiotoxic reactions. NT-proBNP and haemoglobin were significantly associated with cardiotoxicity in patients receiving dose-intensive chemotherapy for early-stage breast cancer, whereas hypersensitive cardiac troponin T was not (Rüger et al., 2020). This may be because direct necrosis of the heart tissue results in more cardiomyocyte dysfunction, as well as the short half-life of TnI and systematic errors caused by experimental design and detection technology. Andersson et al. (2021) found the sensitivity and specificity of NT-proBNP in the detection of trastuzumab induced cardiotoxicity (TIC) were 100 and 95% and changes in NT-proBNP may be used to monitor TIC in patients receiving trastuzumab treatment. They also provide a prognostic value (Pudil et al., 2020). Therefore, NT-proBNP level is an indicator worthy of clinical attention.

5 PREVENTIVE MEASURES

5.1 Antioxidants

ErbB2-targeting drugs are widely used and an increasing measures for prevention and treatment of cardiotoxicity are being investigated (Dias et al., 2016). Prophylaxis of the antioxidant Probucol (Prob) resulted in a 50% reduction in trastuzumab-treated mice with no significant reduction in left ventricular size or contraction parameters (Walker et al., 2011). In addition, renorizine can also inactivate the cardiotoxicity of trastuzumab by inhibiting the accumulation of ROS through redox-mediated mechanisms. Renolazine also reduced the side effects of pertuzumab and TDM1 (De Lorenzo et al., 2018). Surprisingly, dietary supplementation of flaxseed (FLX), alpha-linolenic acid (ALA), and secoisolariciresinol diglucoside (SDG) also appeared to have cardioprotective effects (Asselin et al., 2020). Similarly, the incorporation of the antioxidant coenzyme Q (10) into nanoemulsion (NES) reduced the expression of leukotriene B4 and p65/nuclear factor-kappa B (NF-κB) and the production of interleukin-1β and interleukin-6 to protect the heart (Quagliariello et al., 2020).

5.2 ACEIs/ARBs and BB

The combination of ACEIs/ARBs and BB (ACE inhibitors, angiotensin II receptor blockers and beta-blockers) with trastuzumab adjuvant therapy is beneficial for LVEF recovery (Oliva et al., 2012). ACEI/ARB can change the neurohumoral renin-angiotensin-aldosterone system (RAAS) pathway and prevent heart remodelling. Beta-blockers reduce sympathetic dysfunction (Elghazawy et al., 2020). However, metoprolol had no effect on the overall decline in LVEF (Gulati et al., 2016). It cannot prevent the decrease in LVEF, nor can it prevent severe heart atrophy, heart necrosis, or heart remodelling caused by chemotherapy (Nicol et al., 2021). Beta-1 adrenergic blockade may inhibit sirtuin-3 activation and promote oxidative stress, reducing the protective effect of the sirtuin-3 pathway on mitochondrial function and fibrosis (Guglin et al., 2019). Lisinopril or carvedilol was used to minimize the interruption of trastuzumab. Further prospective studies are required to verify whether this prophylaxis prevents trastuzumab-related cardiac toxicity.

5.3 Statins

Statins reduce the risk of heart failure due to anthracycline (Seicean et al., 2012). A recent retrospective study found that statins also reduced the decline in LVEF caused by trastuzumab. A total of 129 patients with HER2-positive breast cancer were treated with desuximab. Forty-three patients were treated with statins during the cancer treatment. The median trastuzumab exposure time was 11.8 months (range, 11–12 months). Compared with the control group, the adjusted final LVEF was lower during a median cardiac follow-up of 11 months (IQR 9–18 months) (61.2 versus 64.6%, $p = 0.034$) (Calvillo-Argüelles et al., 2019). Statins reduce the risk of heart failure after chemotherapy for early breast cancer (including anthracyclines), but the risk associated with the use of statins after trastuzumab treatment remains unclear. Currently, the mechanism underlying the effect of statins on ErbB2-targeted cardiotoxicity remains unclear (Abdel-Qadir et al., 2021). However, one trial found that rosuvastatin inactivates the deterioration of left ventricular function and the production of reactive oxygen species (ROS) and glutathione. Therefore, the pleiotropic effects of HMG-CoA reductase inhibitors may be related (Kabel and Elkhoely, 2017).

5.4 Others

In addition, various other methods have been reported to reduce cardiotoxicity. Cardiac monitoring in patients receiving ErbB2-targeted therapy should be a priority (Henry et al., 2018). Monitoring of LVEF for 3 months was considered mandatory (Visser et al., 2016). Strict adherence to guidelines is necessary to avoid serious cardiovascular events. SAFE-HEaRt, a long-term follow-up study, found that continued multidisciplinary care of patients with cancer and heart disease was essential to improve patient outcomes (Khoury et al., 2021). In addition, there was no significant difference in the incidence of adverse events between subcutaneous and intravenous administration, and it was safe and tolerable in HER2-positive early/locally advanced breast cancer (EBC/LABC) (Zambetti et al., 1990; De Sanctis et al., 2021). Surprisingly, moderate-intensity exercise training in patients prevented LVEF and loss of strength (Hojan et al., 13797) (**Table 3**).

6 DISCUSSION

ErbB2-targeted drugs cause cardiac dysfunction that is exacerbated when combined with anthracycline chemotherapy for HER2-positive breast cancer. Although cardiotoxicity causes ultrastructural damage to the myocardium, the death of cardiomyocytes was found pathologically. Currently, the mechanism of cardiotoxicity remains unclear. However, the targeted drugs lead to an increase in mitochondrial ROS, activation of endogenous apoptotic procedures, and inhibition of NGR1/HER-2

affecting downstream PI3K/Akt and Ras/MAPK pathways which provide possible explanations for the clinical protective effect of antioxidant drugs. MMP2 is a newly discovered target, which is mainly related to apoptosis. This is similar to the previous discovery of the BCL pathway. Myocardial toxicity and cell apoptosis deserve further study. These molecular structures may be potential therapeutic targets. Current interventions mainly include antioxidants, ACER/ARB/BB, and new material combination drugs. This protective effect may be achieved by reducing the accumulation of mitochondrial ROS. They have been shown to reduce the risk of cardiotoxicity in clinical and animal studies as antioxidants, but there is no further evidence of their roles in the ErbB2-induced pathway. More experiments are needed to verify whether these drugs act on the ErbB2-induced pathway. The main clinical symptom is decreased LVEF, but right ventricular dysfunction has also been reported, and the type of damage caused by cardiotoxicity to cardiomyocytes still further investigation. Risk factors significantly associated with the development of cardiac events were baseline LVEF <60%, hypertension, body mass index >25, age ≥60, and non-Caucasian ethnicity. They are the easiest and most significant indicators for assessing cardiotoxicity before the use of targeted drugs. Whether used alone or in combination, trastuzumab has more severe cardiotoxicity in ErbB2-targeted drugs than other drugs. While pertuzumab, margetuximab, antibody-drug conjugates, and tyrosine kinase inhibitors show less cardiotoxicity, other side effects like diarrhoea, rashes, and blood problems can also be a barrier to taking the medicine. Of course, high cost is also one of the factors that keeps patients away. The cardiotoxicity of trastuzumab combined with pertuzumab is low, but the cardiotoxicity of trastuzumab combined with lapatinib is higher. It is possible that lapatinib directly inhibits ErbB2 phosphorylation, while trastuzumab and pertuzumab have similar ErbB2 epitope-binding sites. Routine detection of LVEF and early presentation of GLS with ErbB2-targeted therapy can predict the development of cardiotoxicity. NT-proBNP has always been a hot marker in the predictive diagnosis of myocardial toxicity. Although there are still contradictory results in all tumor myocardial toxicity studies, it has good specificity and sensitivity in the treatment of breast cancer resulting in myocardial toxicity. NT-proBNP may be used to monitor TIC during treatment and has a predictive effect on TIC prognosis. It is non-invasive, inexpensive, reproducible, and worthy of the attention of clinicians. NT-proBNP may serve as a biological marker for clinical prediction of the occurrence of cardiotoxicity.

AUTHOR CONTRIBUTIONS

ZY supervised the writing of the manuscript; WW and ZY prepared the manuscript and wrote the draft together; WW prepared the figures and tables. WW and ZY contributed equally to this work. All authors have read and agreed to the published version of the manuscript.

ACKNOWLEDGMENTS

The authors thank all of the individuals who participated in the investigations.

REFERENCES

Abdel-Qadir, H., Bobrowski, D., Zhou, L., Austin, P. C., Calvillo-Argüelles, O., Amir, E., et al. (2021). Statin Exposure and Risk of Heart Failure after Anthracycline- or Trastuzumab-Based Chemotherapy for Early Breast Cancer: A Propensity Score–Matched Cohort Study. *J. Am. Heart Assoc.* 10 (2), e018393. doi:10.1161/JAHA.119.018393

Andersson, A. E., Linderholm, B., and Giglio, D. (2021). Delta NT-proBNP Predicts Cardiotoxicity in HER2-Positive Breast Cancer Patients Treated with Trastuzumab. *Acta Oncologica* 60, 475–481. doi:10.1080/0284186X.2020.1842904

Andrikopoulou, A., Zografos, E., Liontos, M., Koutsoukos, K., Dimopoulos, M. A., and Zagouri, F. (2021). Trastuzumab Deruxtecan (DS-8201a): The Latest Research and Advances in Breast Cancer. *Clin. Breast Cancer* 21 (3), e212–e219. doi:10.1016/j.clbc.2020.08.006

Arciniegas Calle, M. C., Sandhu, N. P., Xia, H., Cha, S. S., Pellikka, P. A., Ye, Z., et al. (2018). Two-dimensional Speckle Tracking Echocardiography Predicts Early Subclinical Cardiotoxicity Associated with Anthracycline-Trastuzumab Chemotherapy in Patients with Breast Cancer. *BMC cancer* 18, 1037. doi:10.1186/s12885-018-4935-z

Asselin, C. Y., Lam, A., Cheung, D. Y. C., Eekhoudt, C. R., Zhu, A., Mittal, I., et al. (2020). The Cardioprotective Role of Flaxseed in the Prevention of Doxorubicin- and Trastuzumab-Mediated Cardiotoxicity in C57BL/6 Mice. *J. Nutr.* 150 (9), 2353–2363. doi:10.1093/jn/nxaa144

Awada, A., Colomer, R., Inoue, K., Bondarenko, I., Badwe, R. A., Demetriou, G., et al. (2016). Neratinib Plus Paclitaxel vs Trastuzumab Plus Paclitaxel in Previously Untreated Metastatic ERBB2-Positive Breast Cancer: The NEfERT-T Randomized Clinical Trial. *JAMA Oncol.* 2, 1557–1564. doi:10.1001/jamaoncol.2016.0237

Bang, Y. J., Giaccone, G., Im, S. A., Oh, D. Y., Bauer, T. M., Nordstrom, J. L., et al. (2017). First-in-human Phase 1 Study of Margetuximab (MGAH22), an Fc-Modified Chimeric Monoclonal Antibody, in Patients with HER2-Positive Advanced Solid Tumors. *Ann. Oncol.* 28 (4), 855–861. doi:10.1093/annonc/mdx002

Bayar, N., Küçükseymen, S., Göktaş, S., and Arslan, Ş. (2015). Right Ventricle Failure Associated Wıth Trastuzumab. *Ther. Adv. Drug Saf.* 6 (3), 98–102. doi:10.1177/2042098615582162

Ben Kridis, W., Charfeddine, S., Toumi, N., Daoud, J., Kammoun, S., and Khanfir, A. (2020). A Prospective Study about Trastuzumab-Induced Cardiotoxicity in HER2-Positive Breast Cancer. *Am. J. Clin. Oncol.* 43 (7), 510–516. doi:10.1097/COC.0000000000000699

Bilancia, D., Rosati, G., Dinota, A., Germano, D., Romano, R., and Manzione, L. (2007). Lapatinib in Breast Cancer. *Ann. Oncol.* 18 Suppl 6 (Suppl. 6), vi26–30. doi:10.1093/annonc/mdm220

Bonnie, Ky., Putt, M., Sawaya, H., French, B., Januzzi, J. L., Sebag, I. A., et al. (2014). Early Increases in Multiple Biomarkers Predict Subsequent Cardiotoxicity in Patients with Breast Cancer Treated with Doxorubicin, Taxanes, and Trastuzumab. *J. Am. Coll. Cardiol.* 63, 809–816. doi:10.1016/j.jacc.2013.10.061

Bray, F., Ferlay, J., Soerjomataram, I., Siegel, R. L., Torre, L. A., and Jemal, A. (2018). Global Cancer Statistics 2018: GLOBOCAN Estimates of Incidence and Mortality Worldwide for 36 Cancers in 185 Countries. *CA Cancer J. Clin.* 68 (6), 394–424. doi:10.3322/caac.21492

Calvillo-Argüelles, O., Michalowska, M., Billia, F., Suntheralingam, S., Amir, E., and Thavendiranathan, P. (2019). Cardioprotective Effect of Statins in Patients

with HER2-Positive Breast Cancer Receiving Trastuzumab Therapy. *Can. J. Cardiol.* 35 (2), 153–159. doi:10.1016/j.cjca.2018.11.028

Cao, L., Cai, G., Chang, C., Miao, A. Y., Yu, X. L., Yang, Z. Z., et al. (2015). Diastolic Dysfunction Occurs Early in HER2-Positive Breast Cancer Patients Treated Concurrently with Radiation Therapy and Trastuzumab. *Oncologist* 20 (6), 605–614. doi:10.1634/theoncologist.2014-0299

Capelan, M., Pugliano, L., De Azambuja, E., Bozovic, I., Saini, K. S., Sotiriou, C., et al. (2013). Pertuzumab: new hope for Patients with HER2-Positive Breast Cancer. *Ann. Oncol.* 24 (2), 273–282. doi:10.1093/annonc/mds328

Chaar, M., Kamta, J., and Ait-Oudhia, S. (2018). Mechanisms, Monitoring, and Management of Tyrosine Kinase Inhibitors-Associated Cardiovascular Toxicities. *Onco Targets Ther.* 11, 6227–6237. doi:10.2147/OTT.S170138

Chan, A., Delaloge, S., Holmes, F. A., Moy, B., Iwata, H., Harvey, V. J., et al. (2016). Neratinib after Trastuzumab-Based Adjuvant Therapy in Patients with HER2-Positive Breast Cancer (ExteNET): a Multicentre, Randomised, Double-Blind, Placebo-Controlled, Phase 3 Trial. *Lancet Oncol.* 17 (3), 367–377. doi:10.1016/S1470-2045(15)00551-3

Cochet, A., Quilichini, G., Dygai-Cochet, I., Touzery, C., Toubeau, M., Berriolo-Riedinger, A., et al. (2011). Baseline Diastolic Dysfunction as a Predictive Factor of Trastuzumab-Mediated Cardiotoxicity after Adjuvant Anthracycline Therapy in Breast Cancer. *Breast Cancer Res. Treat.* 130 (3), 845–854. doi:10.1007/s10549-011-1714-9

Corti, C., and Criscitiello, C. (2021). Tucatinib Approval by EMA Expands Options for HER2-Positive Locally Advanced or Metastatic Breast Cancer. *ESMO open* 6 (2), 100063. doi:10.1016/j.esmoop.2021.100063

Cote, G. M., Miller, T. A., Lebrasseur, N. K., Kuramochi, Y., and Sawyer, D. B. (2005). Neuregulin-1alpha and Beta Isoform Expression in Cardiac Microvascular Endothelial Cells and Function in Cardiac Myocytes *In Vitro*. *Exp. Cel Res* 311, 135–146. doi:10.1016/j.yexcr.2005.08.017

de Azambuja, E., Holmes, E., Di Cosimo, S., Swaby, R. F., Untch, M., Jackisch, C., et al. (2014). Lapatinib with Trastuzumab for HER2-Positive Early Breast Cancer (NeoALTTO): Survival Outcomes of a Randomised, Open-Label, Multicentre, Phase 3 Trial and Their Association with Pathological Complete Response. *Lancet Oncol.* 15, 1137–1146. doi:10.1016/S1470-2045(14)70320-1

de Azambuja, E., Procter, N., Rastogi, P., Cecchini, R. S., Lambertini, M., Ballman, K., et al. (2020). A Pooled Analysis of the Cardiac Events in the Trastuzumab Adjuvant Trials. *Breast Cancer Res. Treat.* 179 (1), 161–171. doi:10.1007/s10549-019-05453-z

De Keulenaer, G. W., Doggen, K., and Lemmens, K. (2010). The Vulnerability of the Heart as a Pluricellular Paracrine Organ: Lessons from Unexpected Triggers of Heart Failure in Targeted ErbB2 Anticancer Therapy. *Circ. Res.* 106, 35–46. doi:10.1161/CIRCRESAHA.109.205906

De Lorenzo, C., Riccio, G., Rea, D., Barbieri, A., Coppola, C., and Maurea, N. (2018). Cardiotoxic Effects of the Novel Approved Anti-ErbB2 Agents and Reverse Cardioprotective Effects of Ranolazine. *Onco Targets Ther.* 11, 2241–2250. doi:10.2147/OTT.S157294

De Sanctis, R., D'Antonio, F., Agostinetto, E., Marinello, A., Guiducci, D., Masci, G., et al. (2021). Clinical Predictors of Cardiac Toxicity in HER2-Positive Early Breast Cancer Patients Treated with Adjuvant s.C. Versus i.V. Trastuzumab. *The Breast* 57, 80–85. doi:10.1016/j.breast.2021.03.004

Dias, A., Claudino, W., Sinha, R., Perez, C. A., and Jain, D. (2016). Human Epidermal Growth Factor Antagonists and Cardiotoxicity-A Short Review of the Problem and Preventative Measures. *Crit. Rev. Oncol. Hematol.* 104, 42–51. doi:10.1016/j.critrevonc.2016.04.015

Eiger, D., Pondé, N. F., Agbor-Tarh, D., Moreno-Aspitia, A., Piccart, M., Hilbers, F. S., et al. (2020). Long-term Cardiac Outcomes of Patients with HER2-Positive Breast Cancer Treated in the Adjuvant Lapatinib And/or Trastuzumab Treatment Optimization Trial. *Br. J. Cancer* 122 (10), 1453–1460. doi:10.1038/s41416-020-0786-x

Elghazawy, H., Venkatesulu, B. P., Verma, V., Pushparaji, B., Monlezun, D. J., Marmagkiolis, K., et al. (2020). The Role of Cardio-Protective Agents in Cardio-Preservation in Breast Cancer Patients Receiving Anthracyclines ± Trastuzumab: a Meta-Analysis of Clinical Studies. *Crit. Rev. Oncol. Hematol.* 153, 103006. doi:10.1016/j.critrevonc.2020.103006

Fallah-Rad, N., Lytwyn, M., Bohonis, S., Fang, T., Tian, G., Kirkpatrick, I. D., et al. (2011). The Utility of Cardiac Biomarkers, Tissue Velocity and Strain Imaging, and Cardiac Magnetic Resonance Imaging in Predicting Early Left Ventricular Dysfunction in Patients with Human Epidermal Growth Factor Receptor II-Positive Breast Cancer Treated with Adjuvant Trastuzumab Therapy. *J. Am. Coll. Cardiol.* 57 (22), 2263–2270. doi:10.1016/j.jacc.2010.11.063

Fedele, C., Riccio, G., Coppola, C., Barbieri, A., Monti, M. G., Arra, C., et al. (2012). Comparison of Preclinical Cardiotoxic Effects of Different ErbB2 Inhibitors. *Breast Cancer Res. Treat.* 133 (2), 511–521. doi:10.1007/s10549-011-1783-9

Fedele, C., Riccio, G., Malara, A. E., D'Alessio, G., and De Lorenzo, C. (2012). Mechanisms of Cardiotoxicity Associated with ErbB2 Inhibitors. *Breast Cancer Res. Treat.* 134 (2), 595–602. doi:10.1007/s10549-012-2103-8

Franklin, M. C., Carey, K. D., Vajdos, F. F., Leahy, D. J., de Vos, A. M., and Sliwkowski, M. X. (2004). Insights into ErbB Signaling from the Structure of the ErbB2-Pertuzumab Complex. *Cancer cell* 5 (4), 317–328. doi:10.1016/s1535-6108(04)00083-2

Gassmann, M., Casagranda, F., Orioli, D., Simon, H., Lai, C., Klein, R., et al. (1995). Aberrant Neural and Cardiac Development in Mice Lacking the ErbB4 Neuregulin Receptor. *Nature* 378, 390–394. doi:10.1038/378390a0

Godeau, D., Petit, A., Richard, I., Roquelaure, Y., and Descatha, A. (2021). Return-to-work, Disabilities and Occupational Health in the Age of COVID-19. *Scand. J. Work Environ. Health* 47 (5), 408–409. doi:10.5271/sjweh.3960

Grazette, L. P., Boecker, W., Matsui, T., Semigran, M., Force, T. L., Hajjar, R. J., et al. (2004). Inhibition of ErbB2 Causes Mitochondrial Dysfunction in Cardiomyocytes: Implications for Herceptin-Induced Cardiomyopathy. *J. Am. Coll. Cardiol.* 44, 2231–2238. doi:10.1016/j.jacc.2004.08.066

Guglin, M., Krischer, J., Tamura, R., Fink, A., Bello-Matricaria, L., McCaskill-Stevens, W., et al. (2019). Randomized Trial of Lisinopril versus Carvedilol to Prevent Trastuzumab Cardiotoxicity in Patients with Breast Cancer. *J. Am. Coll. Cardiol.* 73 (22), 2859–2868. doi:10.1016/j.jacc.2019.03.495

Gulati, G., Heck, S. L., Ree, A. H., Hoffmann, P., Schulz-Menger, J., Fagerland, M. W., et al. (2016). Prevention of Cardiac Dysfunction during Adjuvant Breast Cancer Therapy (PRADA): a 2 × 2 Factorial, Randomized, Placebo-Controlled, Double-Blind Clinical Trial of Candesartan and Metoprolol. *Eur. Heart J.* 37, 1671–1680. doi:10.1093/eurheartj/ehw022

Henry, M. L., Niu, J., Zhang, N., Giordano, S. H., and Chavez-MacGregor, M. (2018). Cardiotoxicity and Cardiac Monitoring Among Chemotherapy-Treated Breast Cancer Patients. *JACC Cardiovasc. Imaging* 11, 1084–1093. doi:10.1016/j.jcmg.2018.06.005

Herrmann, J. (2020). Adverse Cardiac Effects of Cancer Therapies: Cardiotoxicity and Arrhythmia. *Nat. Rev. Cardiol.* 17 (8), 474–502. doi:10.1038/s41569-020-0348-1

Hojan, K., Procyk, D., Horyńska-Kęstowicz, D., Leporowska, E., and Litwiniuk, M. (1379). The Preventive Role of Regular Physical Training in Ventricular Remodeling, Serum Cardiac Markers, and Exercise Performance Changes in Breast Cancer in Women Undergoing Trastuzumab Therapy-An REH-HER Study. *J. Clin. Med.* 9, 5. doi:10.3390/jcm9051379

Houbois, C. P., Nolan, M., Somerset, E., Shalmon, T., Esmaeilzadeh, M., Lamacie, M. M., et al. (2021). Serial Cardiovascular Magnetic Resonance Strain Measurements to Identify Cardiotoxicity in Breast Cancer: Comparison with Echocardiography. *JACC Cardiovasc. Imaging* 14 (5), 962–974. doi:10.1016/j.jcmg.2020.09.039

Hsu, W. T., Huang, C. Y., Yen, C. Y. T., Cheng, A. L., and Hsieh, P. C. H. (2018). The HER2 Inhibitor Lapatinib Potentiates Doxorubicin-Induced Cardiotoxicity through iNOS Signaling. *Theranostics* 8, 3176–3188. doi:10.7150/thno.23207-

Hussain, Y., Drill, E., Dang, C. T., Liu, J. E., Steingart, R. M., and Yu, A. F. (2019). Cardiac Outcomes of Trastuzumab Therapy in Patients with HER2-Positive Breast Cancer and Reduced Left Ventricular Ejection Fraction. *Breast Cancer Res. Treat.* 175 (1), 239–246. doi:10.1007/s10549-019-05139-6

Jacquinot, Q., Paget-Bailly, S., Fumoleau, P., Romieu, G., Pierga, J. Y., Espié, M., et al. (2018). Fluctuation of the Left Ventricular Ejection Fraction in Patients with HER2-Positive Early Breast Cancer Treated by 12 Months of Adjuvant Trastuzumab. *Breast* 41, 1–7. doi:10.1016/j.breast.2018.06.001

Jerian, S., and Keegan, P. (1999). Cardiotoxicity Associated with Paclitaxel/trastuzumab Combination Therapy. *J. Clin. Oncol.* 17 (5), 1647–1648. doi:10.1200/jco.1999.17.5.1644e

Jerusalem, G., Lancellotti, P., and Kim, S. B. (2019). HER2+ Breast Cancer Treatment and Cardiotoxicity: Monitoring and Management. *Breast Cancer Res. Treat.* 177 (2), 237–250. doi:10.1007/s10549-019-05303-y

Jones, D. N., Jordan, J. H., Meléndez, G. C., Lamar, Z., Thomas, A., Kitzman, D. W., et al. (2018). Frequency of Transition from Stage A to Stage B Heart Failure after Initiating Potentially Cardiotoxic Chemotherapy. *JACC Heart Fail.* 6, 1023–1032. doi:10.1016/j.jchf.2018.08.005

Kabel, A. M., and Elkhoely, A. A. (2017). Targeting Proinflammatory Cytokines, Oxidative Stress, TGF-B1 and STAT-3 by Rosuvastatin and Ubiquinone to Ameliorate Trastuzumab Cardiotoxicity. *Biomed. Pharmacother.* 93, 17–26. doi:10.1016/j.biopha.2017.06.033

Kaboré, E. G., Guenancia, C., Vaz-Luis, I., Di Meglio, A., Pistilli, B., Coutant, C., et al. (2019). Association of Body Mass index and Cardiotoxicity Related to Anthracyclines and Trastuzumab in Early Breast Cancer: French CANTO Cohort Study. *Plos Med.* 16, e1002989. doi:10.1371/journal.pmed.1002989

Kaplon, H., and Reichert, J. M. (2021). Antibodies to Watch in 2021. *mAbs* 13 (1), 1860476. doi:10.1080/19420862.2020.1860476

Keramida, K., Farmakis, D., Bingcang, J., Sulemane, S., Sutherland, S., Bingcang, R. A., et al. (2019). Longitudinal Changes of Right Ventricular Deformation Mechanics during Trastuzumab Therapy in Breast Cancer Patients. *Eur. J. Heart Fail.* 21 (4), 529–535. doi:10.1002/ejhf.1385

Khoury, K., Lynce, F., Barac, A., Geng, X., Dang, C., Yu, A. F., et al. (2021). Long-term Follow-Up Assessment of Cardiac Safety in SAFE-HEaRt, a Clinical Trial Evaluating the Use of HER2-Targeted Therapies in Patients with Breast Cancer and Compromised Heart Function. *Breast Cancer Res. Treat.* 185, 863–868. doi:10.1007/s10549-020-06053-y

Korde, L. A., Somerfield, M. R., Carey, L. A., Crews, J. R., Denduluri, N., Hwang, E. S., et al. (2021). Neoadjuvant Chemotherapy, Endocrine Therapy, and Targeted Therapy for Breast Cancer: ASCO Guideline. *Jco* 39 (13), 1485–1505. doi:10.1200/JCO.20.03399

Krop, I. E., Kim, S. B., González-Martín, A., LoRusso, P. M., Ferrero, J. M., Smitt, M., et al. (2014). Trastuzumab Emtansine versus Treatment of Physician's Choice for Pretreated HER2-Positive Advanced Breast Cancer (TH3RESA): a Randomised, Open-Label, Phase 3 Trial. *Lancet Oncol.* 15 (7), 689–699. doi:10.1016/S1470-2045(14)70178-0

Kuramochi, Y., Guo, X., and Sawyer, D. B. (2006). Neuregulin Activates erbB2-dependent Src/FAK Signaling and Cytoskeletal Remodeling in Isolated Adult Rat Cardiac Myocytes. *J. Mol. Cel Cardiol* 41 (2), 228–235. doi:10.1016/j.yjmcc.2006.04.007

Lambert, J., Lamacie, M., Thampinathan, B., Altaha, M. A., Esmaeilzadeh, M., Nolan, M., et al. (2020). Variability in Echocardiography and MRI for Detection of Cancer Therapy Cardiotoxicity. *Heart* 106 (11), 817–823. doi:10.1136/heartjnl-2019-316297

Lee, A. (2020). Tucatinib: First Approval. *Drugs* 80 (10), 1033–1038. doi:10.1007/s40265-020-01340-w

Lee, K. F., Simon, H., Chen, H., Bates, B., Hung, M. C., and Hauser, C. (1995). Requirement for Neuregulin Receptor erbB2 in Neural and Cardiac Development. *Nature* 378, 394–398. doi:10.1038/378394a0

Lemmens, K., Doggen, K., and De Keulenaer, G. W. (2007). Role of neuregulin-1/ErbB Signaling in Cardiovascular Physiology and Disease: Implications for Therapy of Heart Failure. *Circulation* 116, 954–960. doi:10.1161/CIRCULATIONAHA.107.690487

Lemmens, K., Fransen, P., Sys, S. U., Brutsaert, D. L., and De Keulenaer, G. W. (2004). Neuregulin-1 Induces a Negative Inotropic Effect in Cardiac Muscle: Role of Nitric Oxide Synthase. *Circulation* 109 (3), 324–326. doi:10.1161/01.CIR.0000114521.88547.5E

Linggi, B., and Carpenter., G. (2006). ErbB Receptors: New Insights on Mechanisms and Biology. *Trends Cel Biol* 16, 649–656. doi:10.1016/j.tcb.2006.10.008

Lorenzini, C., Lamberti, C., Aquilina, M., Rocca, A., Cortesi, P., and Corsi, C. (2017)., 30. official publication of the American Society of Echocardiography, 1103–1110. doi:10.1016/j.echo.2017.06.025Reliability of Left Ventricular Ejection Fraction from Three-Dimensional Echocardiography for Cardiotoxicity Onset Detection in Patients with Breast Cancer*J. Am. Soc. Echocardiogr*

Lynce, F., Barac, A., Geng, X., Dang, C., Yu, A. F., Smith, K. L., et al. (2019). Prospective Evaluation of the Cardiac Safety of HER2-Targeted Therapies in Patients with HER2-Positive Breast Cancer and Compromised Heart Function: the SAFE-HEaRt Study. *Breast Cancer Res. Treat.* 175 (3), 595–603. doi:10.1007/s10549-019-05191-2

Markham, A. (2021). Margetuximab: First Approval. *Drugs* 81 (5), 599–604. doi:10.1007/s40265-021-01485-2

Martín, M., Esteva, F. J., Alba, E., Khandheria, B., Pérez-Isla, L., García-Sáenz, J. A., et al. (2009). Minimizing Cardiotoxicity while Optimizing Treatment Efficacy with Trastuzumab: Review and Expert Recommendations. *Oncologist* 14, 1–11. doi:10.1634/theoncologist.2008-0137

Martin, M., Holmes, F. A., Ejlertsen, B., Delaloge, S., Moy, B., Iwata, H., et al. (2017). Neratinib after Trastuzumab-Based Adjuvant Therapy in HER2-Positive Breast Cancer (ExteNET): 5-year Analysis of a Randomised, Double-Blind, Placebo-Controlled, Phase 3 Trial. *Lancet Oncol.* 18, 1688–1700. doi:10.1016/S1470-2045(17)30717-9

Meyer, D., and Birchmeier, C. (1995). Multiple Essential Functions of Neuregulin in Development. *Nature* 378, 386–390. doi:10.1038/378386a0

Michel, L., Mincu, R. I., Mahabadi, A. A., Settelmeier, S., Al-Rashid, F., Rassaf, T., et al. (2020). Troponins and Brain Natriuretic Peptides for the Prediction of Cardiotoxicity in Cancer Patients: a Meta-Analysis. *Eur. J. Heart Fail.* 22 (2), 350–361. doi:10.1002/ejhf.1631

Modi, S., Saura, C., Yamashita, T., Park, Y. H., Kim, S. B., Tamura, K., et al. (2020). Trastuzumab Deruxtecan in Previously Treated HER2-Positive Breast Cancer. *N. Engl. J. Med.* 382 (7), 610–621. doi:10.1056/NEJMoa1914510

Moy, B., Kirkpatrick, P., Kar, S., and Goss, P. (2007). Lapatinib. *Nat. Rev. Drug Discov.* 6, 431–432. doi:10.1038/nrd2332

Murthy, R. K., Loi, S., Okines, A., Paplomata, E., Hamilton, E., Hurvitz, S. A., et al. (2020). Tucatinib, Trastuzumab, and Capecitabine for HER2-Positive Metastatic Breast Cancer. *N. Engl. J. Med.* 382 (7), 597–609. doi:10.1056/NEJMoa1914609

Narayan, P., Osgood, C. L., Singh, H., Chiu, H.-J., Ricks, T. K., Chiu Yuen Chow, E., et al. (2021). FDA Approval Summary: Fam-Trastuzumab Deruxtecan-Nxki for the Treatment of Unresectable or Metastatic HER2-Positive Breast Cancer, 22 Mar. 2021. *Clin. Cancer Res.* 27, 4478–4485. clincanres. doi:10.1158/1078-0432.CCR-20-4557

Nicol, M., Sadoune, M., Polidano, E., Launay, J. M., Samuel, J. L., Azibani, F., et al. (2021). Doxorubicin-induced and Trastuzumab-Induced Cardiotoxicity in Mice Is Not Prevented by Metoprolol. *ESC Heart Fail.* 8 (2), 928–937. doi:10.1002/ehf2.13198

Nowsheen, S., Aziz, K., Park, J. Y., Lerman, A., Villarraga, H. R., Ruddy, K. J., et al. (2018). Trastuzumab in Female Breast Cancer Patients with Reduced Left Ventricular Ejection Fraction. *J. Am. Heart Assoc.* 7 (15), e008637. doi:10.1161/JAHA.118.008637

Oh, D. Y., and Bang, Y. J. (2020). HER2-targeted Therapies - a Role beyond Breast Cancer. *Nat. Rev. Clin. Oncol.* 17 (1), 33–48. doi:10.1038/s41571-019-0268-3

Oikonomou, E. K., Kokkinidis, D. G., Kampaktsis, P. N., Amir, E. A., Marwick, T. H., Gupta, D., et al. (2019). Assessment of Prognostic Value of Left Ventricular Global Longitudinal Strain for Early Prediction of Chemotherapy-Induced Cardiotoxicity: A Systematic Review and Meta-Analysis. *JAMA Cardiol.* 4, 1007–1018. doi:10.1001/jamacardio.2019.2952

Oliva, S., Cioffi, G., Frattini, S., Simoncini, E. L., Faggiano, P., Boccardi, L., et al. (2012). Administration of Angiotensin-Converting Enzyme Inhibitors and β-blockers during Adjuvant Trastuzumab Chemotherapy for Nonmetastatic Breast Cancer: Marker of Risk or Cardioprotection in the Real World?. *Oncologist* 17 (7), 917–924. doi:10.1634/theoncologist.2011-0445

Onitilo, A. A., Engel, J. M., Stankowski, R. V., Liang, H., Berg, R. L., and Doi, S. A. (2012). High-sensitivity C-Reactive Protein (Hs-CRP) as a Biomarker for Trastuzumab-Induced Cardiotoxicity in HER2-Positive Early-Stage Breast Cancer: a Pilot Study. *Breast Cancer Res. Treat.* 134, 291–298. doi:10.1007/s10549-012-2039-z

Ozcelik, C., Erdmann, B., Pilz, B., Wettschureck, N., Britsch, S., Hübner, N., et al. (2002). Conditional Mutation of the ErbB2 (HER2) Receptor in Cardiomyocytes Leads to Dilated Cardiomyopathy. *Proc. Natl. Acad. Sci. U S A.* 99, 8880–8885. doi:10.1073/pnas.122249299

Pavo, N., Raderer, M., Hülsmann, M., Neuhold, S., Adlbrecht, C., Strunk, G., et al. (2015). Cardiovascular Biomarkers in Patients with Cancer and Their Association with All-Cause Mortality. *Heart* 101, 1874–1880. doi:10.1136/heartjnl-2015-307848

Pentassuglia, L., Timolati, F., Seifriz, F., Abudukadier, K., Suter, T. M., and Zuppinger, C. (2007). Inhibition of ErbB2/neuregulin Signaling Augments

Paclitaxel-Induced Cardiotoxicity in Adult Ventricular Myocytes. *Exp. Cel Res* 313, 1588–1601. doi:10.1016/j.yexcr.2007.02.007

Perez, E. A., Barrios, C., Eiermann, W., Toi, M., Im, Y. H., Conte, P., et al. (2017). Trastuzumab Emtansine with or without Pertuzumab versus Trastuzumab Plus Taxane for Human Epidermal Growth Factor Receptor 2-Positive, Advanced Breast Cancer: Primary Results from the Phase Iii Marianne Study. *J. Clin. Oncol.* 35 (2), 141–148. doi:10.1200/JCO.2016.67.4887

Perez, E. A., and Rodeheffer, R. (2004). Clinical Cardiac Tolerability of Trastuzumab. *J. Clin. Oncol.* 22 (2), 322–329. doi:10.1200/JCO.2004.01.120

Piccart-Gebhart, M. J., and Sotiriou, C. (2007). Adjuvant Chemotherapy-Yes or No? Prognostic Markers in Early Breast Cancer. *Ann. Oncol.* 18 Suppl 12 (Suppl. 12), xii2–7. doi:10.1093/annonc/mdm532

Pondé, N., Ameye, L., Lambertini, M., Paesmans, M., Piccart, M., and de Azambuja, E. (1990). Trastuzumab Emtansine (T-Dm1)-Associated Cardiotoxicity: Pooled Analysis in Advanced HER2-Positive Breast Cancer. *Eur. J. Cancer* 126 (2020), 65–73. Oxford, England. doi:10.1016/j.ejca.2019.11.023

Ponde, N., Bradbury, I., Lambertini, M., Ewer, M., Campbell, C., Ameels, H., et al. (2018). Cardiac Biomarkers for Early Detection and Prediction of Trastuzumab And/or Lapatinib-Induced Cardiotoxicity in Patients with HER2-Positive Early-Stage Breast Cancer: a NeoALTTO Sub-study (BIG 1-06). *Breast Cancer Res. Treat.* 168, 631–638. doi:10.1007/s10549-017-4628-33

Pudil, R., Mueller, C., Čelutkienė, J., Henriksen, P. A., Lenihan, D., Dent, S., et al. (2020). Role of Serum Biomarkers in Cancer Patients Receiving Cardiotoxic Cancer Therapies: a Position Statement from the Cardio-Oncology Study Group of the Heart Failure Association and the Cardio-Oncology Council of the European Society of Cardiology. *Eur. J. Heart Fail.* 22, 1966–1983. doi:10.1002/ejhf.2017

Putt, M., Hahn, V. S., Januzzi, J. L., Sawaya, H., Sebag, I. A., Plana, J. C., et al. (2015). Longitudinal Changes in Multiple Biomarkers Are Associated with Cardiotoxicity in Breast Cancer Patients Treated with Doxorubicin, Taxanes, and Trastuzumab. *Clin. Chem.* 61 (9), 1164–1172. doi:10.1373/clinchem.2015.241232

Quagliariello, V., Vecchione, R., De Capua, A., Lagreca, E., Iaffaioli, R. V., Botti, G., et al. (2020). Nano-Encapsulation of Coenzyme Q10 in Secondary and Tertiary Nano-Emulsions for Enhanced Cardioprotection and Hepatoprotection in Human Cardiomyocytes and Hepatocytes during Exposure to Anthracyclines and Trastuzumab. *Int. J. Nanomedicine* 15, 4859–4876. doi:10.2147/IJN.S245170

Riccio, G., Antonucci, S., Coppola, C., D'Avino, C., Piscopo, G., Fiore, D., et al. (2018). Ranolazine Attenuates Trastuzumab-Induced Heart Dysfunction by Modulating ROS Production. *Front. Physiol.* 9. doi:10.3389/fphys.2018.00038

Rohrbach, S., Muller-Werdan, U., Werdan, K., Koch, S., Gellerich, N. F., and Holtz, J. (2005). Apoptosis-modulating Interaction of the neuregulin/erbB Pathway with Anthracyclines in Regulating Bcl-xS and Bcl-xL in Cardiomyocytes. *J. Mol. Cel Cardiol* 38 (3), 485–493. doi:10.1016/j.yjmcc.2004.12.013

Romond, E. H., Jeong, J. H., Rastogi, P., Swain, S. M., Geyer, C. E., Ewer, M. S., et al. (2012). Seven-year Follow-Up Assessment of Cardiac Function in NSABP B-31, a Randomized Trial Comparing Doxorubicin and Cyclophosphamide Followed by Paclitaxel (ACP) with ACP Plus Trastuzumab as Adjuvant Therapy for Patients with Node-Positive, Human Epidermal Growth Factor Receptor 2-positive Breast Cancer. *J. Clin. Oncol.* 30, 3792–3799. doi:10.1200/JCO.2011.40.0010

Rüger, A. M., Schneeweiss, A., Seiler, S., Tesch, H., van Mackelenbergh, M., Marmé, F., et al. (2020). Cardiotoxicity and Cardiovascular Biomarkers in Patients with Breast Cancer: Data from the GeparOcto-GBG 84 Trial. *J. Am. Heart Assoc.* 9 (23), e018143. doi:10.1161/JAHA.120.018143

Rugo, H. S., Im, S. A., Cardoso, F., Cortés, J., Curigliano, G., Musolino, A., et al. (2021). Efficacy of Margetuximab vs Trastuzumab in Patients with Pretreated ERBB2-Positive Advanced Breast Cancer: A Phase 3 Randomized Clinical Trial. *JAMA Oncol.* 7 (4), 573–584. doi:10.1001/jamaoncol.2020.7932

Rugo, H. W. G., Seock-Ah, I., et al. (2019). Sophia Primary Analysis: A Phase 3 (P3) Study of Margetuximab (M) + Chemotherapy (C) versus Trastuzumab (T) + C in Patients (Pts) with HER2+ Breast Cancer Research and Treatment 13 Metastatic (Met) Breast Cancer (MBC) after Prior Anti-HER2 Therapies (Tx). *J. Clin. Onc* 37 (15), 1000. doi:10.1200/jco.2019.37.15_suppl.1000

Sawyer, D. B., Zuppinger, C., Miller, T. A., Eppenberger, H. M., and Suter, T. M. (2002). Modulation of Anthracycline-Induced Myofibrillar Disarray in Rat Ventricular Myocytes by Neuregulin-1beta and Anti-erbB2: Potential Mechanism for Trastuzumab-Induced Cardiotoxicity. *Circulation* 105, 1551–1554. doi:10.1161/01.cir.0000013839.41224.1c

Seicean, S., Seicean, A., Plana, J. C., Budd, G. T., and Marwick, T. H. (2012). Effect of Statin Therapy on the Risk for Incident Heart Failure in Patients with Breast Cancer Receiving Anthracycline Chemotherapy: an Observational Clinical Cohort Study. *J. Am. Coll. Cardiol.* 60, 2384–2390. doi:10.1016/j.jacc.2012.07.067

Serrano, J. M., González, I., Del Castillo, S., Muñiz, J., Morales, L. J., Moreno, F., et al. (2015). Diastolic Dysfunction Following Anthracycline-Based Chemotherapy in Breast Cancer Patients: Incidence and Predictors. *Oncologist* 20 (8), 864–872. doi:10.1634/theoncologist.2014-0500

Shah, M., Wedam, S., Cheng, J., Fiero, M. H., Xia, H., Li, F., et al. (2021). FDA Approval Summary: Tucatinib for the Treatment of Patients with Advanced or Metastatic HER2-Positive Breast Cancer. *Clin. Cancer Res.* 27 (5), 1220–1226. doi:10.1158/1078-0432.CCR-20-2701

Slamon, D. J., Clark, G. M., Wong, S. G., Levin, W. J., Ullrich, A., and McGuire, W. L. (1987). Human Breast Cancer: Correlation of Relapse and Survival with Amplification of the HER-2/neu Oncogene. *Science* 235, 177–182. doi:10.1126/science.3798106

Tan, A. R., Im, S. A., Mattar, A., Colomer, R., Stroyakovskii, D., Nowecki, Z., et al. (2021). Fixed-dose Combination of Pertuzumab and Trastuzumab for Subcutaneous Injection Plus Chemotherapy in HER2-Positive Early Breast Cancer (FeDeriCa): a Randomised, Open-Label, Multicentre, Non-inferiority, Phase 3 Study. *Lancet Oncol.* 22 (1), 85–97. doi:10.1016/S1470-2045(20)30536-2

Thavendiranathan, P., Negishi, T., Coté, M. A., Penicka, M., Massey, R., Cho, G. Y., et al. (2018). Single versus Standard Multiview Assessment of Global Longitudinal Strain for the Diagnosis of Cardiotoxicity during Cancer Therapy. *JACC Cardiovasc. Imaging* 11, 1109–1118. doi:10.1016/j.jcmg.2018.03.003

Timolati, F., Ott, D., Pentassuglia, L., Giraud, M. N., Perriard, J. C., Suter, T. M., et al. (2006). Neuregulin-1 Beta Attenuates Doxorubicin-Induced Alterations of Excitation-Contraction Coupling and Reduces Oxidative Stress in Adult Rat Cardiomyocytes. *J. Mol. Cel Cardiol* 41 (5), 845–854. doi:10.1016/j.yjmcc.2006.08.002

Tkach, M., Rosemblit, C., Rivas, M. A., Proietti, C. J., Díaz Flaqué, M. C., Mercogliano, M. F., et al. (2013). p42/p44 MAPK-Mediated Stat3Ser727 Phosphorylation Is Required for Progestin-Induced Full Activation of Stat3 and Breast Cancer Growth. *Endocr. Relat. Cancer* 20, 197–212. 22 Mar. 2013. doi:10.1530/ERC-12-0194

Upshaw, J. N. (2020). Cardioprotective Strategies to Prevent Cancer Treatment-Related Cardiovascular Toxicity: a Review. *Curr. Oncol. Rep.* 22 (7 72), 72. doi:10.1007/s11912-020-00923-w

Upshaw, J. N., Finkelman, B., Hubbard, R. A., Smith, A. M., Narayan, H. K., Arndt, L., et al. (2020). Comprehensive Assessment of Changes in Left Ventricular Diastolic Function with Contemporary Breast Cancer Therapy. *JACC Cardiovasc. Imaging* 13 (1 Pt 2), 198–210. doi:10.1016/j.jcmg.2019.07.018

van Ramshorst, M. S., van Werkhoven, E., Honkoop, A. H., Dezentjé, V. O., Oving, I. M., Mandjes, I. A., et al. (2016). Toxicity of Dual HER2-Blockade with Pertuzumab Added to Anthracycline versus Non-anthracycline Containing Chemotherapy as Neoadjuvant Treatment in HER2-Positive Breast Cancer: The TRAIN-2 Study. *Breast* 29, 153–159. doi:10.1016/j.breast.2016.07.017

Verma, S., Miles, D., Gianni, L., Krop, I. E., Welslau, M., Baselga, J., et al. (2012). Trastuzumab Emtansine for HER2-Positive Advanced Breast Cancer. *N. Engl. J. Med.* 367, 1783–1791. doi:10.1056/NEJMoa1209124

Visser, A., van de Ven, E. M., Ruczynski, L. I., Blaisse, R. J., van Halteren, H. K., Aben, K., et al. (2016). Cardiac Monitoring during Adjuvant Trastuzumab Therapy: Guideline Adherence in Clinical Practice. *Acta Oncol.* 55 (4), 423–429. doi:10.3109/0284186X.2015.1068444

von Minckwitz, G., Huang, C. S., Mano, M. S., Loibl, S., Mamounas, E. P., Untch, M., et al. (2019). Trastuzumab Emtansine for Residual Invasive HER2-Positive Breast Cancer. *N. Engl. J. Med.* 380 (7), 617–628. doi:10.1056/NEJMoa1814017

von Minckwitz, G., Procter, M., de Azambuja, E., Zardavas, D., Benyunes, M., Viale, G., et al. (2017). Adjuvant Pertuzumab and Trastuzumab in Early HER2-Positive Breast Cancer. *N. Engl. J. Med.* 377 (2), 122–131. doi:10.1056/NEJMoa1703643

Walker, J. R., Sharma, A., Lytwyn, M., Bohonis, S., Thliveris, J., Singal, P. K., et al. (2011). The Cardioprotective Role of Probucol against Anthracycline and Trastuzumab-Mediated Cardiotoxicity. *J. Am. Soc. Echocardiogr* 24, 699–705. official publication of the American Society of Echocardiography. doi:10.1016/j.echo.2011.01.018

Yildirim, A., Tunaoglu, F. S., Kambur, K., and Pinarli, F. G. (2013). The Utility of NT-proBNP and Various Echocardiographic Methods in the Determination of Doxorubicin Induced Subclinical Late Cardiotoxicity. *Kardiol Pol.* 71 (1), 40–46.

Yoon, H. J., Kim, K. H., Kim, H. Y., Park, H., Cho, J. Y., Hong, Y. J., et al. (2019). Impacts of Non-recovery of Trastuzumab-Induced Cardiomyopathy on Clinical Outcomes in Patients with Breast Cancer. *Clin. Res. Cardiol.* 108 (8), 892–900. doi:10.1007/s00392-019-01417-x

Zambetti, M., Montemurro, F., Morandi, P., Zamagni, C., Brandes, A. A., Bisagni, G., et al. (1990). Safety Profile of Subcutaneous Trastuzumab for the Treatment of Patients with HER2-Positive Early or Locally Advanced Breast Cancer: Primary Analysis of the SCHEARLY Study. *Eur. J. Cancer* 105 (2018), 61–70. Oxford, England. doi:10.1016/j.ejca.2018.09.034

Zhao, P., Zhang, Y., Li, W., Jeanty, C., Xiang, G., and Dong, Y. (2020). Recent Advances of Antibody Drug Conjugates for Clinical Applications. *Acta Pharm. Sin B* 10 (9), 1589–1600. doi:10.1016/j.apsb.2020.04.012

Zhao, Y. Y., Sawyer, D. R., Baliga, R. R., Opel, D. J., Han, X., Marchionni, M. A., et al. (1998). Neuregulins Promote Survival and Growth of Cardiac Myocytes. Persistence of ErbB2 and ErbB4 Expression in Neonatal and Adult Ventricular Myocytes. *J. Biol. Chem.* 273, 10261–10269. doi:10.1074/jbc.273.17.10261

Conflict of Interest: The authors declare that the research was conducted in the absence of any commercial or financial relationships that could be construed as a potential conflict of interest.

Publisher's Note: All claims expressed in this article are solely those of the authors and do not necessarily represent those of their affiliated organizations, or those of the publisher, the editors and the reviewers. Any product that may be evaluated in this article, or claim that may be made by its manufacturer, is not guaranteed or endorsed by the publisher.

frontiers in Pharmacology

SYSTEMATIC REVIEW
published: 15 November 2021
doi: 10.3389/fphar.2021.771839

The Clinical Value of Chemotherapy Combined With Capecitabine in Triple-Negative Breast Cancer—A Meta-Analysis

Zilin Zhang[1], *Kai Ma*[1], *Jing Li*[2], *Yeneng Guan*[1], *Chaobo Yang*[1], *Aqin Yan*[1] *and Hongda Zhu*[1]*

[1]*Key Laboratory of Fermentation Engineering (Ministry of Education), Hubei Key Laboratory of Industrial Microbiology, National "111" Center for Cellular Regulation and Molecular Pharmaceutics, School of Food and Biological Engineering, Hubei University of Technology, Wuhan, China,* [2]*Pharmaceutical Department, Hubei Cancer Hospital, Tongji Medical College, Huazhong University of Science and Technology, Wuhan, China*

Purpose: Triple-negative breast cancer (TNBC) is the most dangerous subtype of breast cancer with high rates of metastasis and recurrence. The efficacy of capecitabine in chemotherapy for TNBC is still controversial. This study evaluated the efficacy and safety of capecitabine combining with standard, adjuvant or neoadjuvant chemotherapy for TNBC.

Methods: We systematically searched clinical studies through PubMed, Cochrane library, Embase, Wanfang Database, China Academic Journals (CNKI), and American Society of Clinical Oncology's (ASCO) annual conference report. Studies were assessed for design and quality by the Cochrane risk of bias tool. A meta-analysis was performed using Review Manager to quantify the effect of capecitabine combined with standard, adjuvant or neoadjuvant chemotherapy on the disease-free survival (DFS) rate and overall survival (OS) rate of TNBC patients. Furthermore, safety analysis was performed to evaluate the adverse events.

Results: Twelve randomized controlled clinical trials involving totally 4854 TNBC patients were included, of which 2,214 patients received chemotherapy as control group, and 2,278 patients received capecitabine combining with chemotherapy. The results indicated that capecitabine could significantly improve the DFS [hazard ratio (HR) 0.80, 95% confidence interval (CI) 0.71–0.90, P = 0.0003] and OS (HR 0.83, 95% CI 0.74–0.93, P = 0.001). In subgroup analysis, the combination of capecitabine and cyclophosphamide exhibited a significant benefit in all outcomes (DFS HR 0.75, 95% CI 0.63–0.90, P = 0.002; OS HR 0.65, 95% CI 0.52–0.80, p < 0.0001). Additionally, defferent dose of capecitabine subgroup showed same significant effect on the results. Safety analysis showed that the addition of capecitabine was associated with a much higher risk of hand-foot syndrome, diarrhea and mucositis or stomatitis.

Conclusion: The results showed that adjuvant capecitabine could bring significant benefits on DFS and OS to unselected TNBC patients, the combination of capecitabine and cyclophosphamide could improve the survival rate of patients,

OPEN ACCESS

Edited by:
Yao Liu,
Daping Hospital, China

Reviewed by:
Lawrence Panasci,
Segal Cancer Centre, Canada
Chunsong Yang,
Sichuan University, China
Lingli Zhang,
Sichuan University, China

****Correspondence:***
Hongda Zhu
bszzhuhongda@yeah.net

Specialty section:
This article was submitted to Pharmacology of Anti-Cancer Drugs, a section of the journal Frontiers in Pharmacology

Received: *07 September 2021*
Accepted: *29 October 2021*
Published: *15 November 2021*

Citation:
Zhang Z, Ma K, Li J, Guan Y, Yang C, Yan A and Zhu H (2021) The Clinical Value of Chemotherapy Combined With Capecitabine in Triple-Negative Breast Cancer—A Meta-Analysis. Front. Pharmacol. 12:771839. doi: 10.3389/fphar.2021.771839

although the addition of capecitabine could bring significant side effects such as hand foot syndrome (HFS) and diarrhea.

Keywords: chemotherapy, triple-negative breast cancer, capecitabine, meta-analysis, safety

INTRODUCTION

Triple-negative breast cancer (TNBC) (10–20% of breast cancer) is a subtype of breast cancer with high rates of metastasis and recurrence and lacks of expression of estrogen receptor (ER), progesterone receptor (PR) and human epidermal growth factor receptor 2 (HER2), which cannot be treated with traditional hormone therapy and Her2-targeted therapy (Li et al., 2018) (Mouh et al., 2016). According to the NCCN (National Comprehensive Cancer Network) guidelines, standard therapeutic strategy for TNBC includes a combination of chemotherapy, surgery, and radiation therapy based on the clinic-pathological features of the disease (Waks and Winer, 2019). Although immunotherapies such as programmed cell death 1 (PD1), programmed cell death ligand 1 (PD-L1) inhibitor have been shown to be effective in the neoadjuvant phase, chemotherapy is the major approved treatment strategy of TNBC (Lebert et al., 2018; Wu et al., 2021). The standard chemotherapy, adjuvant or neoadjuvant chemotherapy methods for TNBC include anthracyclines, taxanes, doxorubicin, and cyclophosphamide, platinum compounds (Lebert et al., 2018; Li et al., 2018), but even with these recognized effective treatments, the risk of relapse of TNBC in 10-years is still up to 20–40% (Howard and Olopade, 2021). Therefore, it is important to explore new adjuvant and neoadjuvant treatment.

Capecitabine is an oral prodrug of fluorouracil, which is converted into the active substance 5-fluorouracil (5-FU) by the higher level of thymidine phosphorylase (TP) in the tumor, it may provide better efficacy and safety due to non-cytotoxic of capecitabine and its intermediates (Ishitsuka et al., 1999). Capecitabine has been approved for the treatment of colorectal cancer, gastric cancer and breast cancer so far (Walko and Lindley, 2005; Iqbal and Pan, 2016). Although capecitabine is still controversial in the treatment of breast cancer, it is one of the widely treatment drug in TNBC neoadjuvant and postoperative adjuvant therapy (Steger et al., 2014; Zhang et al., 2017). Twelve meta-analyses summarized the function of capecitabine in the treatment of breast cancer, most of which included all subtypes of breast cancer. Some analyses showed that capecitabine had no significant effect on breast cancer (Martin et al., 2015; Muss et al., 2019; Lluch et al., 2020), and some randomized controlled trials (RCTs) showed that the addition of capecitabine to chemotherapy could improve the survival rate (Zhang et al., 2015; Joensuu et al., 2017; Masuda et al., 2017; Zhang et al., 2017; Li J. et al., 2020; Wang et al., 2021). At the same time, some analyses showed that the addition of capecitabine couldn't affect DFS but improve OS (Natori et al., 2017). Two meta-analyses focused on the role of capecitabine in the treatment of TNBC, the results confirmed that the addition of capecitabine could improve DFS and OS in TNBC patients (Li Y. et al., 2020; Huo et al., 2021). However, these meta-analyses were short of the latest updates of relevant clinical trials, and did not show further subgroup analysis such as the effect of capecitabine dose or combination with other chemotherapeutic drugs. It is necessary to enlarge the sample size and refine the subgroup analysis to make the conclusion more robust.

This study evaluated the efficacy and safety of the addition of capecitabine with standard chemotherapy, adjuvant or neoadjuvant chemotherapy for TNBC treatment through meta-analysis, so as to determine whether it could improve the clinical efficacy and reduce adverse reactions. Furthermore, subgroup analysis was conducted to explore the potential benefits of combined cyclophosphamide and capecitabine dose on the clinical efficacy of capecitabine.

METHODS

Search Criteria

Using "breast cancer" or "triple-negative breast cancer" and "capecitabine" or "Xeloda" as the terms, we searched online databases from inception to October 2021 including PubMed, CNKI, Embase, Wanfang Database and the Cochrane library. The annual conference presentations from American Society of Clinical Oncology (ASCO) were also searched. No language restrictions. The specific search strategy for each database was presented in **Supplementary Material S1**.

Inclusion and Exclusion Criteria

Type of Studying

Phase II and Phase III clinical randomized controlled trials (RCTs) were included. Observational studies were excluded. These RCTs reported the hazard ratio (HR) and its 95% confidence interval (CI) for DFS and/or OS.

Type of Participant

The research subjects were patients with breast cancer (including the TNBC subgroup) or TNBC patients. Eligible patients were females ≥18 years old and confirmed to be TNBC by pathology. There were not any restrictions on other factors of the participants.

Type of Interventions

One arm received standard, adjuvant or neoadjuvant chemotherapy, and the other arm received capecitabine in addition to standard, adjuvant or neoadjuvant chemotherapy. Standard chemotherapy or adjuvant or neoadjuvant chemotherapy is defined as chemotherapy with cyclophosphamide, methotrexate, anthracycline, platinum,

or taxanes. There were no restrictions on the type, order and dosage of chemotherapy drugs and capecitabine.

Type of Comparisons
Based on the definitions of standard, adjuvant and neoadjuvant chemotherapy, capecitabine group and capecitabine-free group were compared in data analysis.

Type of Outcome Measures
Primary result: DFS and/or OS and its 95% CIs.
Adverse events: Any adverse events of any grade.

Data Collection and Analysis
Study Selection
Two researchers independently collected and evaluated all literatures and data. Any disagreement shall be resolved through negotiation or with a third party.

Data Extraction
The following data were collected from the included study, including author name, publication time, baseline patient characteristics, treatment plan, DFS, OS and their HRs, 95% CIs, and adverse events. For the same RCT with different authors and different publication years, the most recently published literature data was used. Due to the lack of DFS or OS HR information in some documents, we used Engauge software (version 10.8) and the data processing table provided by Jayne F Tierney to generate survival data based on the survival curve in the report (Tierney et al., 2007).

Risk of Bias Assessment
The quality and potential bias of twelve studies was assessed using Cochrane's bias risk tool. Visualization of results was used by Review Manager software.

Statistical Analysis
HR and 95% CIs of the extracted efficacy indicators, and adverse events were incorporated into the meta-analysis. Heterogeneity was assessed using Chi-square test and I^2 test statistics. If $p < 0.1$ or $I^2 > 50\%$, indicating significant heterogeneity, the random effects model was utilized to merge the studies, otherwise the fixed effects model was used. All trials are two-sided, and the statistical significance is $p < 0.05$. All statistical analysis is performed using Review Manager 5.2 software.

Subgroup Analysis
The effect of different treatment regimens was compared in subgroup analysis, for example, whether cyclophosphamide was used or not and the effect of the dose of capecitabin in treatment regimen.

Sensitivity Analysis
Sensitivity analysis was evaluated by re-analyzing after excluded individual studies one by one or changing the statistical model to determine the reliability of the results. The results of sensitivity analysis could be discovered in **Supplementary Material S2**.

Publication Bias
Publication bias was analyzed by the Review Manager and presented in the form of a funnel chart.

RESULTS
Search Results
After preliminary search through the databases and looking at the title and abstract, unqualified studies and repeated studies were excluded based on PRISMA (Preferred Reporting Items for Systematic Reviews and Meta-Analyses). After excluding studies of lower quality and unable to obtain the required data, a total of 12 studies were included in the meta-analysis. The PRISMA flow diagram was shown in **Figure 1**.

Characteristics of Included Studies
Twelve relevant RCTs were identified after the initial search. The characteristics were summarized in **Table1**. The included RCTs comprised of 4 whole cohorts and eight subgroups. A total of 4854 TNBC patients were involved, of which 2,214 patients received standard chemotherapy, adjuvant or neoadjuvant chemotherapy and 2,278 received capecitabine basing on standard chemotherapy, adjuvant or neoadjuvant chemotherapy. The Gepar TRIO trial did not provide a specific number of patients in the TNBC subgroup receiving different treatment modalities (von Minckwitz et al., 2013a). Some experiments only provide OS data or DFS data.

Risk of Bias Assessment
This meta-analysis was clearly defined through evidence-based medicine methods and PICOS principles. The overall risk of bias for all trials in this study was average. The results of risk of bias were shown in **Supplementary Figures S1, S2**. Detailed information on the risk of bias assessment was provided in **Supplementary Material S3**. None of the randomized controlled trials included in this study mentioned clear allocation hiding, blinding of participants and personnel, and blinding of result evaluation, which might affect the results and should be treated with caution.

Efficacy and Subgroup Analysis
DFS
The heterogeneity test ($Chi^2 = 14.69$, $P = 0.10$, $I^2 = 39\%$) indicated low statistical heterogeneity between studies. A fixed effects model was applied to calculate the combined HR and 95% CI as 0.80 (0.71–0.90), $P = 0.0003$, indicating a statistically significant difference between capecitabine group and capecitabine-free group (**Figure 2**). This demonstrated that capecitabine could significantly improve DFS in TNBC patients when combined with chemotherapy, which was consistent with the conclusions of two recent meta-analyses about the role of capecitabine for TNBC treatment (Li Y. et al., 2020; Huo et al., 2021).

Whereas, the addition of capecitabine in the treatment of TNBC still had some negative results and significant side effects (Natori et al., 2017). In order to affirm the potential benefits of capecitabine to TNBC treatment, subgroup analysis was

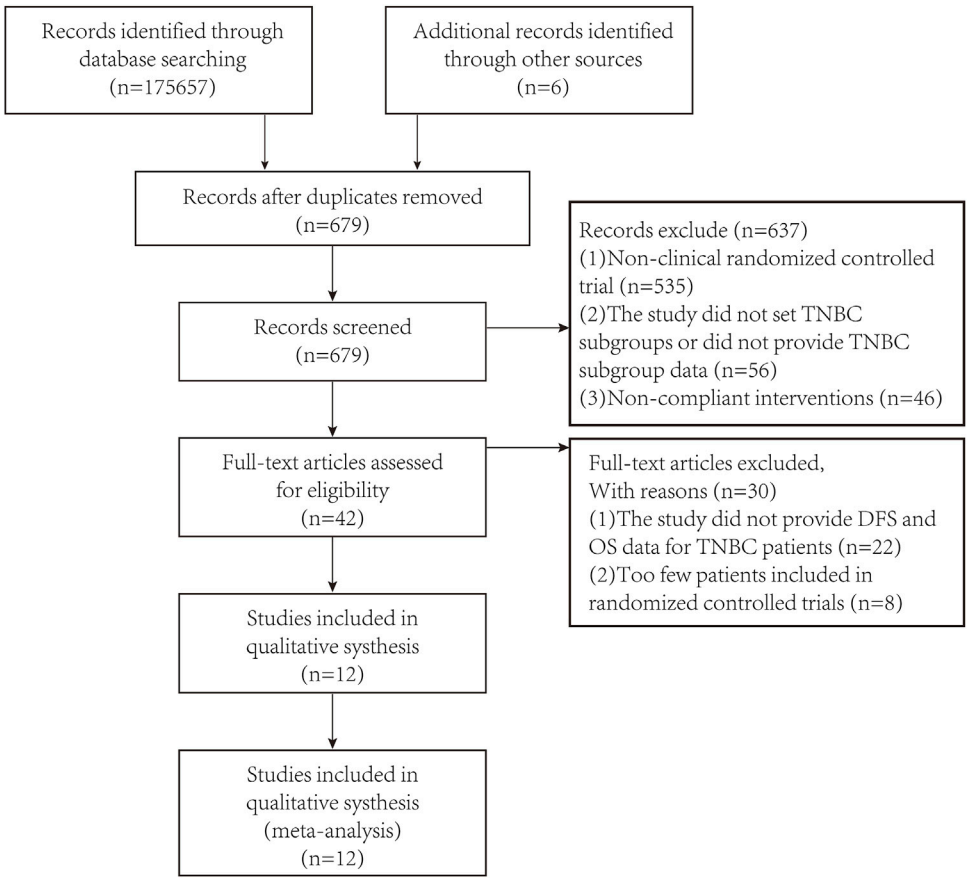

FIGURE 1 | Flow diagram summarizing all study assessment processes.

performed based on whether cyclophosphamide was added to adjuvant chemotherapy or the effect of capecitabine dose on adjuvant chemotherapy. Our results showed that a significant improvement in DFS was observed in the combination capecitabine and cyclophosphamide treatment subgroup (HR 0.76, 95% CI 0.65–0.89, P = 0.0005), but not in the cyclophosphamide free capecitabine treatment subgroup (HR 0.85, 95% CI 0.68–1.06, P = 0.16) (**Figure 3**). The effect of capecitabine dose on the DFS showed that low dose (<1,000 mg/m^2) capecitabine had the same significant effect as high dose (>1,000 mg/m^2) (**Figure 4**).

OS

Ten RCTs were assessed for OS, there was no heterogeneity between the capecitabine group and the capecitabine-free group (Chi^2 = 10.92, P = 0.28, I^2 = 18%), so a fixed effects model was used to calculate the combined HR and 95% CI as 0.83 (0.74–0.93), P = 0.001 (**Figure 5**). The results suggested that adding capecitabine had a significant improvement in OS. Consistent with the results of DFS subgroup analysis, significant improvement was observed in OS when cyclophosphamide was used (HR 0.65, 95% CI 0.52–0.80, p < 0.0001) (**Figure 6**). Different doses of capecitabine had the same significant improvement in OS (**Figure 7**).

Safety and Tolerability

Safety and tolerability analysis of patients with breast cancer included in twelve RCTs was performed. It was found statistically that hand foot syndrome (HFS), neutropenia, mucositis or stomatitis, diarrhea and fatigue were common adverse events with high incidence. Since all adverse reactions between the capecitabine group and the non-capecitabine group were significantly heterogeneous (p < 0.05 and I^2 > 50%), a random effects model was used. The results indicated that capecitabine caused much higher incidence of HFS (OR 25.57, 95% CI 10.44–62.65, p < 0.00001), mucositis or stomatitis (OR 1.88, 95% CI 1.06–3.32, p = 0.03) and diarrhea (OR 3.66, 95% CI 2.11–6.34, p < 0.00001) (**Table 2**).

DISCUSSION

The Results of Meta-Analysis

The evaluation of the efficacy of capecitabine in breast cancer chemotherapy, including TNBC, has attracted wide attention. For example, the efficacy of two adjuvant chemotherapy regimens, TX + CEX (docetaxel plus capecitabine, cyclophosphamide, epirubicin, and capecitabine) and T + CEF (docetaxel, cyclophosphamide, epirubicin, and fluorouracil), were

TABLE 1 | Characteristics of the included studies.

Study	Year	Author	Trial phase	Region	TNBC, N (X/control)	Age	Capecitabine arm	Control arm	Dose of X	Median follow-up (years)	DFS HR/95% CI	OS HR/95% CI	TNBC in study
FinXX Joensuu et al. (2017)	2017	Joensuu Heikki	III	America-Europe	93/109	26–65	3TX→3CEX	3T→3CEF	900 mg/m^2	10.3	0.53 0.31–0.92	0.55 0.31–0.96	Subgroup
GEICAM-2003–10 Martin et al. (2015)	2015	Miguel Martín	III	America-Europe	95/71	25–73	4ET→4X	4EC→4T	1,250 mg/m^2	6.6	1.19 0.70–2.04	NA	Subgroup
CREATE–X Masuda et al. (2017)	2017	N. Masuda	III	Asia	139/147	25–74	standard[1] + 6 – 8X	Standard[1]	1,250 mg/m^2	3.6	0.53 0.31–0.92	0.55 0.31–0.96	Subgroup
CBCSG010 Li et al. (2020a)	2020	Junjie Li	III	Asia	297/288	18–70	3TX→3CEX	3T→3CEF	1,000 mg/m^2	5.6	0.66 0.44–0.99	0.67 0.37–1.22	Whole cohort
Zhang et al. Zhang et al. (2015)	2015	Xiaohui Zhang	II	Asia	140/140	25–74	4AX	4AC	1,000 mg/m^2	4.0	1.23 0.41–3.70	0.78 0.20–3.10	Subgroup
USO 01062 O'Shaughnessy et al. (2015)	2015	Joyce O'Shaughnessy	III	America-Europe	396/384	26–72	4AC→4TX	4AC→4T	825 mg/m^2	6.4	0.81 0.57–1.15	0.62 0.41–0.94	Subgroup
GEICAM/2003–11_CIBOMA/2004–01 Lluch et al. (2020)	2019	Lluch Ana	III	America-Europe	448/428	20–82	8X	None	2,000 mg/m^2	7.3	0.77 0.59–1.00	0.86 0.63–1.20	Whole cohort
CALGB 49907 Muss et al. (2019)	2019	Muss Hyman B	III	America-Europe	76/78	≥65	6X	6CMF/4AC	2,000 mg/m^2	2.4	NA	0.82 0.53–1.25	Subgroup
SYSUCC-001 Wang et al. (2021)	2020	Xi Wang	III	Asia	221/213	24–70	Standard[2] → X	Standard[2]	650 mg/m^2	5.1	0.64 0.42–0.95	0.75 0.47–1.19	Whole cohort
Gepar TRIO von Minckwitz et al. (2013a)	2013	Gunter von Minckwitz	III	America-Europe	362	≤36	2TAC→4NX	2TAC→4/6TAC	1,000 mg/m^2	5.2	0.87 0.61–1.25	NA	Subgroup
GAIN von Minckwitz et al. (2013b)	2013	Gunter von Minckwitz	III	America-Europe	213/208	≤65	4EC→4TX	4ETC	2000 mg/m^2	3.2	0.97 0.68–1.38	0.81 0.54–1.20	Subgroup
ECOG-ACRIN EA1131 Mayer et al. (2021)	2021	Ingrid A. Mayer	III	America-Europe	160/148	26–76	6X	4Platinum	1,000 mg/m^2	1.7	NA	0.98 0.81–1.18	Whole cohort

X capecitabine, T docetaxel, C cyclophosphamide, E epirubicin, F fluorouracil, A pirarubicin, M methotrexate, N vinorelbine.

Standard[1], Sequential anthracycline and taxane or concurrent anthracycline and taxane or anthracycline-containing chemotherapy only or docetaxel and cyclophosphamide only or fluorouracil plus anthracycline.

Standard[2], anthracyclines or taxanes based or anthracyclines and taxanes based.

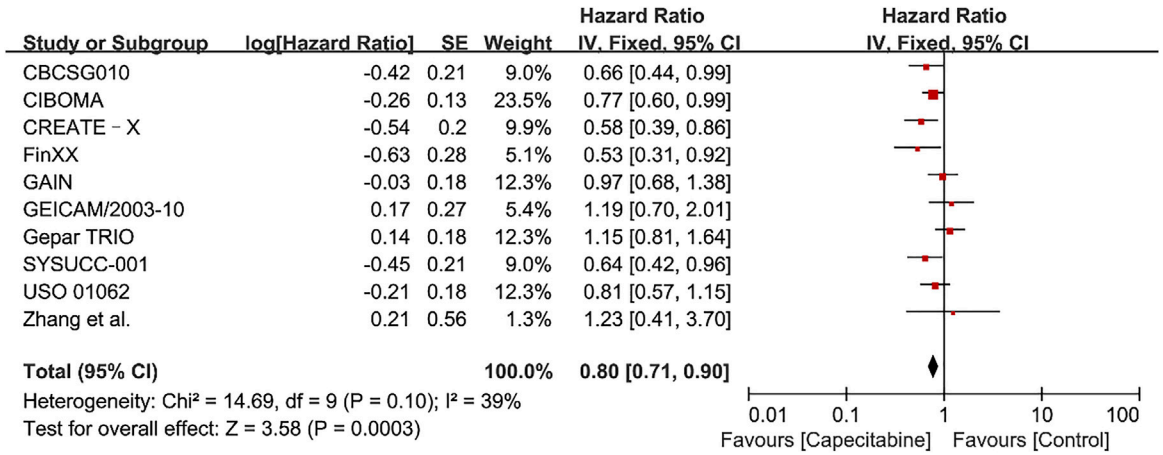

FIGURE 2 | Forest plots for the disease-free survival (DFS) rate in the comparison between chemotherapy with capecitabine group vs. capecitabine-free group in TNBC patients.

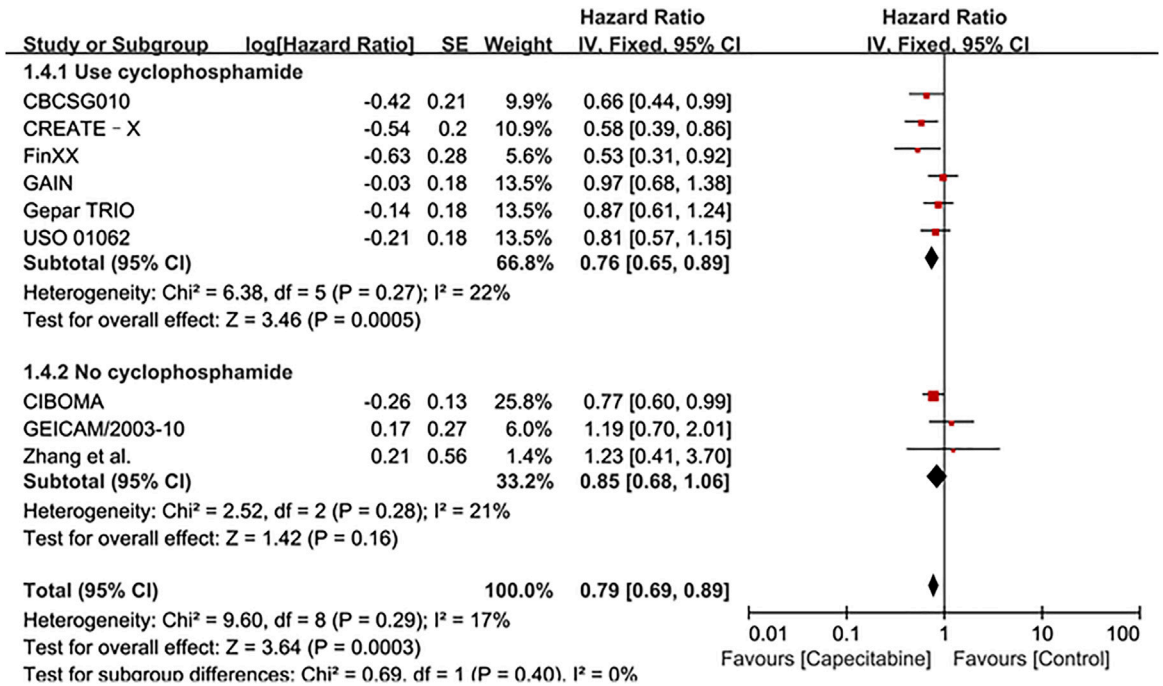

FIGURE 3 | Subgroup analysis of the effect of capecitabine and cyclophosphamide combined with chemotherapy on DFS in TNBC patients.

compared in the FinXX and CBCSG010 trials. The results showed the priority of TX + CEX regimen in DFS (Joensuu et al., 2017; Li J. et al., 2020). Similarly, positive results of DFS and OS were also observed with capecitabine for TNBC patients in the CREATE-X and the USO 01062 trials (O'Shaughnessy et al., 2015; Masuda et al., 2017). The reason might be that nonbasal phenotype tumors with lower value-added index were more sensitive to capecitabine (Lluch et al., 2020). However, for undifferentiated triple-negative patients, the capecitabine group had no improvement in DFS and OS compared with the observation group in the CIBOMA trial. The GEICAM/2003-10 trial showed that capecitabine-free group had the superiority for DFS in lymph node-positive patients (Martin et al., 2015). Similarly, the addition of capecitabine reduced the benefit of lymph node-positive patients in the subgroup analysis of the CIBOMA trial. On the contrary, the different results were obtained in the CBCSG010 trial (Li J. et al., 2020; Lluch et al., 2020). The reason for the different results might be the dose reduction caused

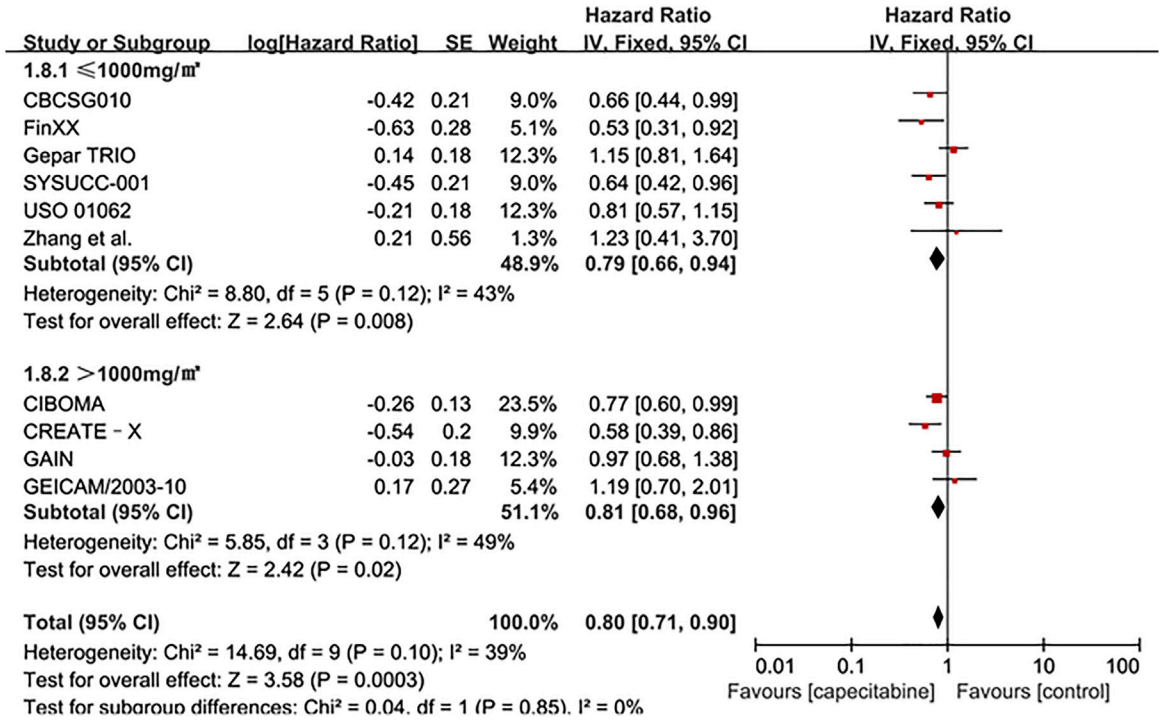

FIGURE 4 | Subgroup analysis of the effect of capecitabine adjuvant chemotherapy dose on DFS in TNBC patients.

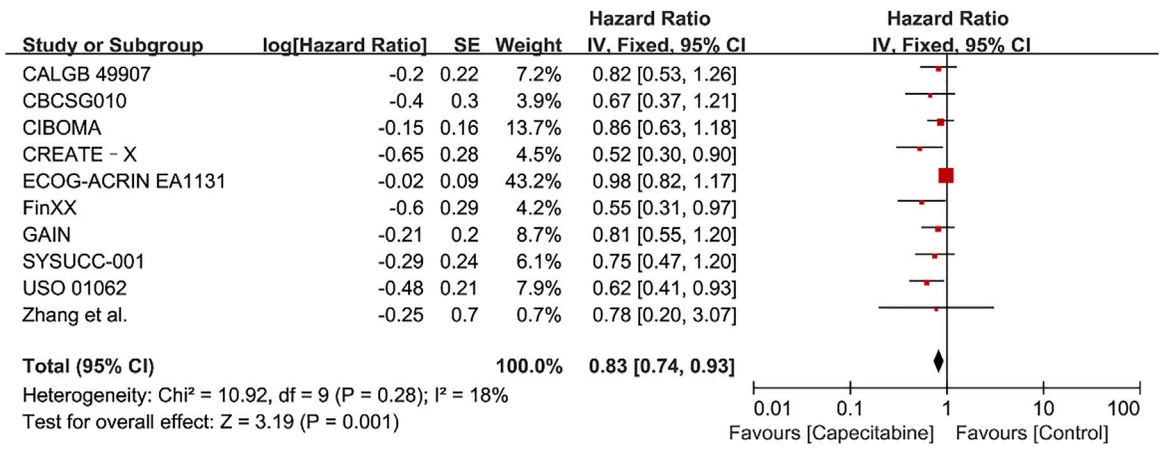

FIGURE 5 | Forest plots for the overall survival (OS) rate in the comparison between chemotherapy with capecitabine group vs. capecitabine-free group in TNBC patients.

by the ethnic difference or the higher risk of recurrence in Asians (Li J. et al., 2020; Lluch et al., 2020), which was similar to the results of the meta-analysis by Li Y et al. (2020). In order to evaluate the efficacy and safety of capecitabine combined with standard chemotherapy, adjuvant chemotherapy or neoadjuvant chemotherapy in the treatment of TNBC, it is necessary to enlarge the sample size and refine the subgroup analysis, so as to make the conclusion more reliable.

Herein, a meta-analysis was performed to evaluate the potential benefits of the clinical efficacy of capecitabine for TNBC. Twelve RCTs were retrieved and included for analysis according to evidence-based medicine methods and PICOS principles. The research was evaluated by bias risk assessment and the overall level of the included studies was average. The results showed that adjuvant capecitabine could bring significant benefits on DFS and OS to unselected TNBC patients, the

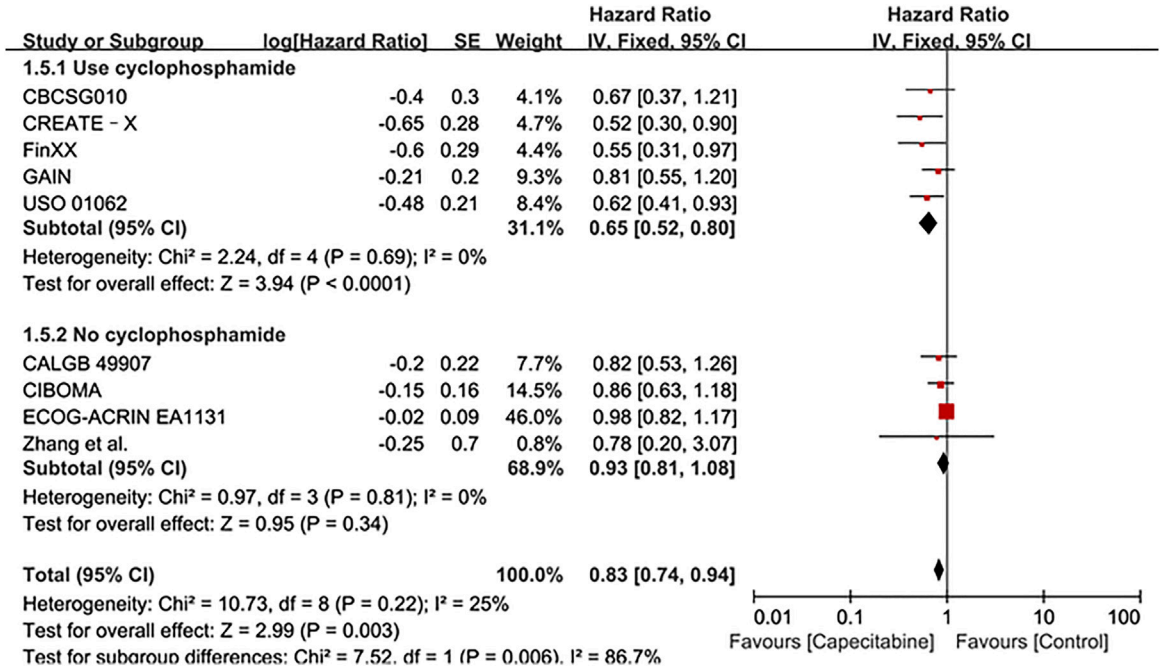

FIGURE 6 | Subgroup analysis of the effect of capecitabine and cyclophosphamide combined with chemotherapy on OS in TNBC patients.

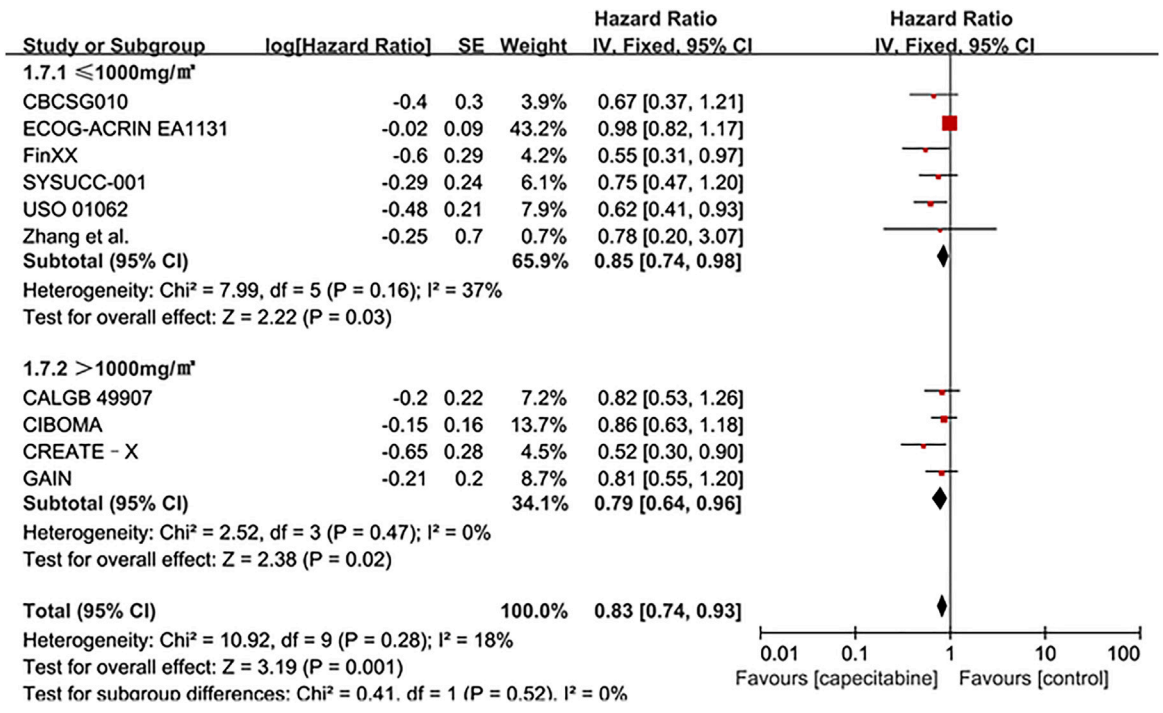

FIGURE 7 | Subgroup analysis of the effect of capecitabine adjuvant chemotherapy dose on OS in TNBC patients.

combination of capecitabine and cyclophosphamide could improve the survival rate of patients, although the addition of capecitabine could bring significant side effects such as HFS and diarrhea. Taxanes and cyclophosphamide as first-line drugs for breast cancer chemotherapy can up-regulate the activity of thymidine phosphorylase (TP) in the tumor (Kurosumi et al.,

TABLE 2 | Analysis of grade adverse events.

Adverse events	Control n/N	Capecitabine n/N	Odds ratio (95% CI)	*p*
Hand-foot syndrome	82/4,407	834/4,473	25.57 (10.44–62.65)	<0.00001
Neutropenia	1,508/3,769	1,471/3,816	0.85 (0.58–1.24)	0.40
Mucositis or stomatitis	116/3,842	203/3,897	1.88 (1.06–3.32)	0.03
Diarrhea	96/4,407	293/4,473	3.66 (2.11–6.34)	<0.00001
Fatigue	308/4,267	318/4,333	1.02 (0.77–1.35)	0.88

2000). Cyclophosphamide in standard, adjuvant or neoadjuvant chemotherapy regimens including capecitabine may up-regulate ThdPase to promote the conversion of capecitabine to fluorouracil and improve the efficacy of capecitabine (Khodeer et al., 2020; Refaie et al., 2020).

The dose of capecitabine or the duration of capecitabine treatment, and even the discontinuation of capecitabine due to early toxicity is one of the influencing factors. The SYSUCC-001 trial showed that adding low-dose capecitabine as maintenance therapy after standard adjuvant therapy significantly improved disease-free survival (Wang et al., 2021). However, two randomized controlled trials were designed with the same dose of capecitabine (1000 mg/m^2, twice a day), the former had six cycles and the latter had eight cycles. Although the proportion of patients in the capecitabine group who reduced the dose was similar in the two trials (39.1 vs. 36.9%), the former reduced the dose less and the proportion of patients who completed the complete planned cycle was greater (84.9 vs. 75.2%). The results proved that the duration of capecitabine treatment might have a significant impact on the results (Wang et al., 2021). The addition of high-dose capecitabine in the CALGB 49907 elderly breast cancer trial showed negative results. It not only brought a lower survival rate, but also induced more obvious side effects. Most deaths were caused by non-breast cancer, which might be related to other competing death factors caused by age and obvious side effects (Muss et al., 2019). Since there was no more rigorous distinction between baseline characteristics such as age and ethnicity, which might affect the patient's dose, there might be some deviations in the results. In spite of different dose of capecitabine subgroup analysis showed same significant effect in our analysis (**Figures 4**, **7**), the addition of capecitabine was associated with higher adverse events such as hand-foot syndrome, diarrhea and mucositis or stomatitis (**Table 2**). Our analysis suggested that low dose (<1,000 mg/m^2) capecitabine combined with cyclophosphamide was more beneficial for TNBC patients.

Some research reports indicated that specific TNBC subgroups, including specific genes related to anti-tumor immunity, immune response, and capecitabine activation might gain greater improvement from the addition of capecitabine (Asleh et al., 2020). In the ABCSG-24 trial, preoperative use of capecitabine increased pathologic complete response (pCR) rates. For the TNBC subgroup, this improvement was more significant (Steger et al., 2014). For some patients with special baseline characteristics, the benefits of capecitabine may be more obvious according to more clinical data and more rigorous analysis. The positive efficacy of adding capecitabine might depend on patient's race, age and different clinical characteristics of patients (Zhang et al., 2016; Li Y. et al., 2020; Huo et al., 2021).

Compared to other meta-analysis, we included more data and performed other subgroup analysis including the effect of capecitabine and cyclophosphamide in combination and the influence of capecitabine dose on adjuvant chemotherapy (Zhang et al., 2016; Natori et al., 2017; Li Y. et al., 2020; Huo et al., 2021). The meta-analysis by Yan Li et al. focused on the role of adjuvant capecitabine in standard chemotherapy, the influence of region and treatment period on the effect of capecitabine were analyzed in the subgroup. The results showed that capecitabine improved the survival of TNBC patients regardless of the region. Longer treatment cycle had a significant improvement for DFS but did not affect OS (Li Y. et al., 2020). The meta-analysis by Huo et al. analyzed the effects of capecitabine in adjuvant and neoadjuvant chemotherapy and different lymph node status on the effect of capecitabine (Huo et al., 2021). The results showed that the addition of capecitabine, lymph node positive and adjuvant chemotherapy were beneficial for DFS, which might be related to the anti-angiogenesis of capecitabine and the inhibition of tumor immune escape (Pasquier et al., 2010). The ECOG-ACRIN EA1131 trial compared the effects of platinum preparations and capecitabine after neoadjuvant chemotherapy (Mayer et al., 2021). The results showed that there was no significant difference between the effects of platinum preparations and capecitabine, and platinum preparations brought more serious toxicity.

Heterogeneity of Research and Publication Bias

The subtypes of triple-negative breast cancer, the diversity of treatment options, and other baseline characteristics of patients were the main reasons for heterogeneity of the included studies, the results were inevitably. Most of I^2 in our analysis was less than 50%, indicating low heterogeneity of results between studies. The publication bias was displayed in the form of a funnel diagram with small sample size and a certain publication bias (**Figure 8**).

Limitation

We have tried our best to ensure the reliability of the results in our research, but there were still some limitations inevitably. Firstly, many randomized controlled trials were not included due to lack of enough data, and the quality of the included studies was average. Secondly, the intervention measures of the randomized controlled trials included in the analysis and the

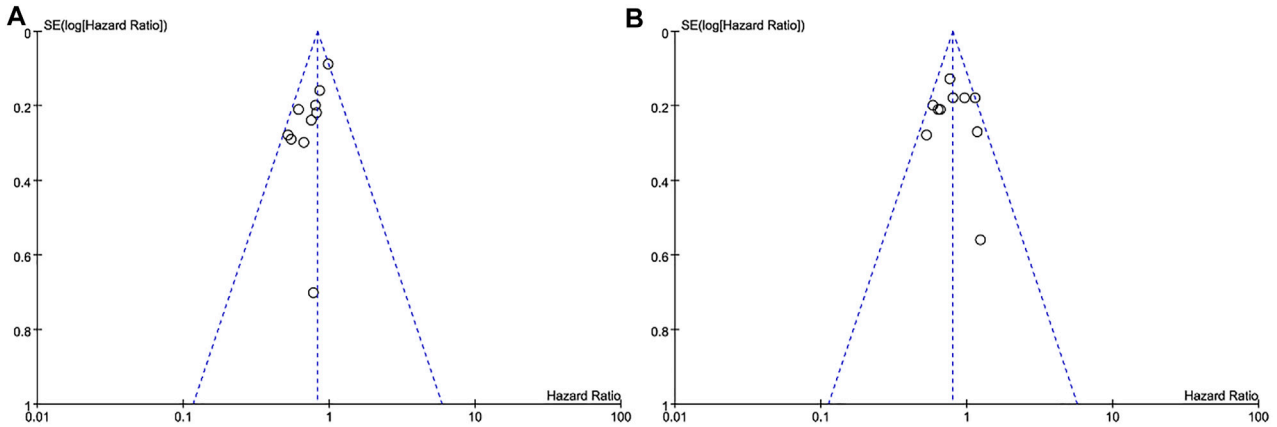

FIGURE 8 | Funnel chart of publication bias. **(A)** DFS. **(B)** OS.

baseline characteristics of patients were inconsistent, which might affect the results. Expand the sample size and refine the subgroup analysis will make the conclusion more reliable.

DATA AVAILABILITY STATEMENT

The original contributions presented in the study are included in the article/**Supplementary Material**, further inquiries can be directed to the corresponding authors.

AUTHOR CONTRIBUTIONS

HZ, ZZ, KM, YG, CY, and AY contributed to the research. HZ provides method support. ZZ and KM carried out article screening, data extraction and statistical analysis. HZ, ZZ, and JL wrote drafts of the article. YG, CY, and AY contributed to the supervision of the research. All authors reviewed and revised the main content, and approved the final version of the article before submission. All authors contributed to this article and approved the submitted version.

FUNDING

This work was supported by Key Laboratory of Fermentation Engineering (Ministry of Education) and Chinese Society of Clinical Oncology (CSCO) supported by Jiangsu Hengrui Cancer Research Foundation (No: Y-HR2019-0325).

SUPPLEMENTARY MATERIAL

The Supplementary Material for this article can be found online at: https://www.frontiersin.org/articles/10.3389/fphar.2021.771839/full#supplementary-material

REFERENCES

Asleh, K., Brauer, H. A., Sullivan, A., Lauttia, S., Lindman, H., Nielsen, T. O., et al. (2020). Predictive Biomarkers for Adjuvant Capecitabine Benefit in Early-Stage Triple-Negative Breast Cancer in the FinXX Clinical Trial. *Clin. Cancer Res.* 26 (11), 2603–2614. doi:10.1158/1078-0432.CCR-19-1945

Howard, F. M., and Olopade, O. I. (2021). Epidemiology of Triple-Negative Breast Cancer. *Cancer J.* 27 (1), 8–16. doi:10.1097/ppo.0000000000000500

Huo, X., Li, J., Zhao, F., Ren, D., Ahmad, R., Yuan, X., et al. (2021). The Role of Capecitabine-Based Neoadjuvant and Adjuvant Chemotherapy in Early-Stage Triple-Negative Breast Cancer: a Systematic Review and Meta-Analysis. *BMC Cancer* 21 (1), 78. doi:10.1186/s12885-021-07791-y

Iba, T., Kidokoro, A., Fukunaga, M., Sugiyama, K., Aihara, N., and Suda, M. (2004). The Efficacy of Long-Term Oral Chemotherapy with 5'-Deoxy-5-Fluorouridine and Cyclophosphamide for Recurrent Breast Cancer. *Int. J. Clin. Oncol.* 9 (5), 383–387. doi:10.1007/s10147-004-0420-6

Iqbal, H., and Pan, Q. (2016). Capecitabine for Treating Head and Neck Cancer. *Expert Opin. Investig. Drugs* 25 (7), 851–859. doi:10.1080/13543784.2016.1181747

Ishitsuka, H., Shimma, N., and Horii, I. (1999). Discovery and Development of Novel Anticancer Drug Capecitabine. *Yakugaku Zasshi* 119 (12), 881–897. doi:10.1248/yakushi1947.119.12_881

Joensuu, H., Kellokumpu-Lehtinen, P. L., Huovinen, R., Jukkola-Vuorinen, A., Tanner, M., Kokko, R., et al. (2017). Adjuvant Capecitabine in Combination with Docetaxel, Epirubicin, and Cyclophosphamide for Early Breast Cancer: The Randomized Clinical FinXX Trial. *JAMA Oncol.* 3 (6), 793–800. doi:10.1001/jamaoncol.2016.6120

Khodeer, D. M., Mehanna, E. T., Abushouk, A. I., and Abdel-Daim, M. M. (2020). Protective Effects of Evening Primrose Oil against Cyclophosphamide-Induced Biochemical, Histopathological, and Genotoxic Alterations in Mice. *Pathogens* 9 (2), 1. doi:10.3390/pathogens9020098

Kurosumi, M., Tabei, T., Suemasu, K., Inoue, K., Kusawake, T., Sugamata, N., et al. (2000). Enhancement of Immunohistochemical Reactivity for Thymidine Phosphorylase in Breast Carcinoma Cells after Administration of Docetaxel as a Neoadjuvant Chemotherapy in Advanced Breast Cancer Patients. *Oncol. Rep.* 7 (5), 945–948. doi:10.3892/or.7.5.945

Lebert, J. M., Lester, R., Powell, E., Seal, M., and McCarthy, J. (2018). Advances in the Systemic Treatment of Triple-Negative Breast Cancer. *Curr. Oncol.* 25 (Suppl. 1), S142–S150. doi:10.3747/co.25.3954

Li, J., Yu, K., Pang, D., Wang, C., Jiang, J., Yang, S., et al. (2020a). Adjuvant Capecitabine with Docetaxel and Cyclophosphamide Plus Epirubicin for

Triple-Negative Breast Cancer (CBCSG010): An Open-Label, Randomized, Multicenter, Phase III Trial. *J. Clin. Oncol.* 38 (16), 1774–1784. doi:10.1200/JCO.19.02474

Li, Y., Zhou, Y., Mao, F., Lin, Y., Zhang, X., Shen, S., et al. (2020b). Adjuvant Addition of Capecitabine to Early-Stage Triple-Negative Breast Cancer Patients Receiving Standard Chemotherapy: a Meta-Analysis. *Breast Cancer Res. Treat.* 179 (3), 533–542. doi:10.1007/s10549-019-05513-4

Li, Z., Qiu, Y., Lu, W., Jiang, Y., and Wang, J. (2018). Immunotherapeutic Interventions of Triple Negative Breast Cancer. *J. Transl Med.* 16 (1), 147. doi:10.1186/s12967-018-1514-7

Lluch, A., Barrios, C. H., Torrecillas, L., Ruiz-Borrego, M., Bines, J., Segalla, J., et al. (2020). Phase III Trial of Adjuvant Capecitabine after Standard Neo-/Adjuvant Chemotherapy in Patients with Early Triple-Negative Breast Cancer (GEICAM/2003-11_CIBOMA/2004-01). *J. Clin. Oncol.* 38 (3), 203–213. doi:10.1200/JCO.19.00904

Martín, M., Ruiz Simón, A., Ruiz Borrego, M., Ribelles, N., Rodríguez-Lescure, Á., Muñoz-Mateu, M., et al. (2015). Epirubicin Plus Cyclophosphamide Followed by Docetaxel versus Epirubicin Plus Docetaxel Followed by Capecitabine as Adjuvant Therapy for Node-Positive Early Breast Cancer: Results from the GEICAM/2003-10 Study. *J. Clin. Oncol.* 33 (32), 3788–3795. doi:10.1200/JCO.2015.61.9510

Masuda, N., Lee, S. J., Ohtani, S., Im, Y. H., Lee, E. S., Yokota, I., et al. (2017). Adjuvant Capecitabine for Breast Cancer after Preoperative Chemotherapy. *N. Engl. J. Med.* 376 (22), 2147–2159. doi:10.1056/NEJMoa1612645

Mayer, I. A., Zhao, F., Arteaga, C. L., Symmans, W. F., Park, B. H., Burnette, B. L., et al. (2021). Randomized Phase III Postoperative Trial of Platinum-Based Chemotherapy versus Capecitabine in Patients with Residual Triple-Negative Breast Cancer Following Neoadjuvant Chemotherapy: ECOG-ACRIN EA1131. *J. Clin. Oncol.* 39 (23), 2539–2551. doi:10.1200/JCO.21.00976

Mouh, F. Z., Mzibri, M. E., Slaoui, M., and Amrani, M. (2016). Recent Progress in Triple Negative Breast Cancer Research. *Asian Pac. J. Cancer Prev.* 17 (4), 1595–1608. doi:10.7314/apjcp.2016.17.4.1595

Muss, H. B., Polley, M. C., Berry, D. A., Liu, H., Cirrincione, C. T., Theodoulou, M., et al. (2019). Randomized Trial of Standard Adjuvant Chemotherapy Regimens versus Capecitabine in Older Women with Early Breast Cancer: 10-Year Update of the CALGB 49907 Trial. *J. Clin. Oncol.* 37 (26), 2338–2348. doi:10.1200/JCO.19.00647

Natori, A., Ethier, J. L., Amir, E., and Cescon, D. W. (2017). Capecitabine in Early Breast Cancer: A Meta-Analysis of Randomised Controlled Trials. *Eur. J. Cancer* 77, 40–47. doi:10.1016/j.ejca.2017.02.024

O'Shaughnessy, J., Koeppen, H., Xiao, Y., Lackner, M. R., Paul, D., Stokoe, C., et al. (2015). Patients with Slowly Proliferative Early Breast Cancer Have Low Five-Year Recurrence Rates in a Phase III Adjuvant Trial of Capecitabine. *Clin. Cancer Res.* 21 (19), 4305–4311. doi:10.1158/1078-0432.CCR-15-0636

Pasquier, E., Kavallaris, M., and André, N. (2010). Metronomic Chemotherapy: New Rationale for New Directions. *Nat. Rev. Clin. Oncol.* 7 (8), 455–465. doi:10.1038/nrclinonc.2010.82

Refaie, M. M. M., Shehata, S., El-Hussieny, M., Abdelraheem, W. M., and Bayoumi, A. M. A. (2020). Role of ATP-Sensitive Potassium Channel (KATP) and eNOS in Mediating the Protective Effect of Nicorandil in Cyclophosphamide-Induced Cardiotoxicity. *Cardiovasc. Toxicol.* 20 (1), 71–81. doi:10.1007/s12012-019-09535-8

Steger, G. G., Greil, R., Lang, A., Rudas, M., Fitzal, F., Mlineritsch, B., et al. (2014). Epirubicin and Docetaxel with or without Capecitabine as Neoadjuvant Treatment for Early Breast Cancer: Final Results of a Randomized Phase III Study (ABCSG-24). *Ann. Oncol.* 25 (2), 366–371. doi:10.1093/annonc/mdt508

Tierney, J. F., Stewart, L. A., Ghersi, D., Burdett, S., and Sydes, M. R. (2007). Practical Methods for Incorporating Summary Time-To-Event Data into Meta-Analysis. *Trials* 8, 16. doi:10.1186/1745-6215-8-16

von Minckwitz, G., Blohmer, J. U., Costa, S. D., Denkert, C., Eidtmann, H., Eiermann, W., et al. (2013a). Response-guided Neoadjuvant Chemotherapy for Breast Cancer. *J. Clin. Oncol.* 31 (29), 3623–3630. doi:10.1200/JCO.2012.45.0940

von Minckwitz, G., Möbus, V., Schneeweiss, A., Huober, J., Thomssen, C., Untch, M., et al. (2013b). German Adjuvant Intergroup Node-Positive Study: a Phase III Trial to Compare Oral Ibandronate versus Observation in Patients with High-Risk Early Breast Cancer. *J. Clin. Oncol.* 31 (28), 3531–3539. doi:10.1200/JCO.2012.47.2167

Waks, A. G., and Winer, E. P. (2019). Breast Cancer Treatment: A Review. *JAMA* 321 (3), 288–300. doi:10.1001/jama.2018.19323

Walko, C. M., and Lindley, C. (2005). Capecitabine: a Review. *Clin. Ther.* 27 (1), 23–44. doi:10.1016/j.clinthera.2005.01.005

Wang, X., Wang, S. S., Huang, H., Cai, L., Zhao, L., Peng, R. J., et al. (2021). Effect of Capecitabine Maintenance Therapy Using Lower Dosage and Higher Frequency vs Observation on Disease-free Survival Among Patients with Early-Stage Triple-Negative Breast Cancer Who Had Received Standard Treatment: The SYSUCC-001 Randomized Clinical Trial. *JAMA* 325 (1), 50–58. doi:10.1001/jama.2020.23370

Wu, Q., Siddharth, S., and Sharma, D. (2021). Triple Negative Breast Cancer: A Mountain yet to Be Scaled Despite the Triumphs. *Cancers* 13 (15), 3697. doi:10.3390/cancers13153697

Zhang, J., Fu, F., Lin, Y., Chen, Y., Lu, M., Chen, M., et al. (2017). Evaluating the Benefits and Adverse Effects of an Enthracycline-Taxane-Capecitabine Combined Regimen in Patients with Early Breast Cancer. *Oncotarget* 8 (46), 81636–81648. doi:10.18632/oncotarget.20386

Zhang, X., Zhou, Y., Mao, F., Lin, Y., Guan, J., and Sun, Q. (2015). Efficacy and Safety of Pirarubicin Plus Capecitabine versus Pirarubicin Plus Cyclophosphamide in Chinese Node-Negative Breast Cancer Patients: a 4-year Open-Label, Randomized, Controlled Study. *Med. Oncol.* 32 (10), 240. doi:10.1007/s12032-015-0686-8

Zhang, Z. C., Xu, Q. N., Lin, S. L., and Li, X. Y. (2016). Capecitabine in Combination with Standard (Neo)Adjuvant Regimens in Early Breast Cancer: Survival Outcome from a Meta-Analysis of Randomized Controlled Trials. *PloS one* 11 (10), e0164663. doi:10.1371/journal.pone.0164663

Conflict of Interest: The authors declare that the research was conducted in the absence of any commercial or financial relationships that could be construed as a potential conflict of interest.

Publisher's Note: All claims expressed in this article are solely those of the authors and do not necessarily represent those of their affiliated organizations, or those of the publisher, the editors and the reviewers. Any product that may be evaluated in this article, or claim that may be made by its manufacturer, is not guaranteed or endorsed by the publisher.

frontiers in Pharmacology

REVIEW
published: 06 December 2021
doi: 10.3389/fphar.2021.797881

Therapeutic Drug Monitoring and Individualized Medicine of Dasatinib: Focus on Clinical Pharmacokinetics and Pharmacodynamics

Shiyu He[1,2], Jialu Bian[1,2], Qianhang Shao[1], Ying Zhang[1], Xu Hao[1], Xingxian Luo[3], Yufei Feng[1] and Lin Huang[1]**

[1]Department of Pharmacy, People's Hospital of Peking University, Beijing, China, [2]Department of Pharmacy Administration and Clinical Pharmacy, School of Pharmaceutical Sciences, Peking University, Beijing, China, [3]School of Pharmaceutical Sciences, Tsinghua University, Beijing, China

Dasatinib is an oral second-generation tyrosine kinase inhibitor known to be used widely in Philadelphia chromosome-positive (Ph^+) chronic myeloid leukemia (CML) and Ph^+ acute lymphoblastic leukemia (ALL). Notably, although a high pharmacokinetic variability in patients and an increased risk of pleural effusion are attendant, fixed dosing remains standard practice. Retrospective studies have suggested that dasatinib exposure may be associated with treatment response (efficacy/safety). Therapeutic drug monitoring (TDM) is gradually becoming a practical tool to achieve the goal of individualized medicine for patients receiving targeted drugs. With the help of TDM, these patients who maintain response while have minimum adverse events may achieve long-term survival. This review summaries current knowledge of the clinical pharmacokinetics variation, exposure-response relationships and analytical method for individualized dosing of dasatinib, in particular with respect to therapeutic drug monitoring. In addition, it highlights the emerging insights into several controversial issues in TDM of dasatinib, with the aim of presenting up-to-date evidence for clinical decision-making and insights for future studies.

Keywords: dasatinib, pharmacokinetics, exposure-response relationships, analytical method, therapeutic drug monitoring, individualized medicine

OPEN ACCESS

Edited by:
Miao Yan,
Central South University, China

Reviewed by:
Masatomo Miura,
Akita University Hospital, Japan
Takero Shindo,
Kyoto University Hospital, Japan

****Correspondence:***
Yufei Feng
fenyufei@126.com
Lin Huang
huanglin@pkuph.edu.cn

Specialty section:
This article was submitted to Pharmacology of Anti-Cancer Drugs, a section of the journal Frontiers in Pharmacology

Received: *19 October 2021*
Accepted: *11 November 2021*
Published: *06 December 2021*

Citation:
He S, Bian J, Shao Q, Zhang Y, Hao X, Luo X, Feng Y and Huang L (2021) Therapeutic Drug Monitoring and Individualized Medicine of Dasatinib: Focus on Clinical Pharmacokinetics and Pharmacodynamics. Front. Pharmacol. 12:797881. doi: 10.3389/fphar.2021.797881

1 INTRODUCTION

Dasatinib is an oral second-generation dual Src-Abl1 kinase inhibitor indicated for the treatment of adults and children with Philadelphia chromosome-positive (Ph^+) chronic myeloid leukemia (CML) and Ph^+ acute lymphoblastic leukemia (ALL) with resistance or intolerance to prior therapy including imatinib, and has become the first-line treatment for CML (Lindauer and Hochhaus, 2018). Dasatinib is 325 times as potent as imatinib in inhibiting unmutated BCR-ABL kinase *in vitro*, and has inhibitory activity against the majority of imatinib-resistant BCR-ABL mutants (Lombardo et al., 2004). Besides, dasatinib has activity in multiple other kinases, including c-KIT, PDGFRβ, and ephrin receptor kinases (Lindauer and Hochhaus, 2018).

Dasatinib has showed an association between exposure and response. As pharmacokinetic (PK) exposure of dasatinib varies highly among patients, some patients may be exposed to the risk of therapeutically relevant toxicity due to high exposure, while others may suffer from suboptimal efficacy resulted from low exposure (Verheijen et al., 2017). Additionally, dose reduction has become

a target for further treatment in some patients with CML having achieved cytogenetic and hematological responses, which can not only reduce the incidence and severity of toxicities, but also lighten the financial burden on patients. However, after the responses have been achieved, we do not have a clear indicator to guide reduction for achieving maximum benefits under minimum dose. Although dasatinib has showed satisfactory efficacy, it still has problems worried us.

Therapeutic drug monitoring (TDM) is an effective tool aimed at optimizing a patient's drug regimen based on biological fluids concentrations of the drug. Several pieces of evidence suggest potential benefits of TDM for the treatment of cancer with tyrosine kinase inhibitors (TKIs). For the treatment dilemma that dasatinib is currently facing, TDM is likely to be an effective assistant strategy to contribute to the solution of problems in clinical practice. Nevertheless, no consensus has been reached on the TDM of dasatinib, including whether it is carried out routinely, monitoring indicators, target ranges and feasibility, etc. The focus of this review is to discuss the problems above in terms of factors affecting exposure of dasatinib, exposure-response relationships for dasatinib in previous studies, as well as analytical method.

2 PHARMACOKINETICS VARIABILITY

Very high interpatient variability of dasatinib exposure was observed on maximum plasma drug concentration (C_{max}), 70–80%, and on area under the plasma concentration-time curve (AUC), 40–54% (Wang et al., 2013; Ishida et al., 2016; Chandani et al., 2017). Moreover, one study suggested that the variability in exposure of dasatinib was greater within subjects than between subjects (Dai et al., 2008). Many factors that lead to the high variability of dasatinib by influencing the PK process of dasatinib need to be considered.

2.1 Absorption

Dasatinib is rapidly absorbed following oral administration with time to C_{max} (T_{max}) ranging from 0.5 to 6 h (European Medicines Agency, 2006). With the emergence of more studies, T_{max} values observed among subjects ranged from 0.28 to 6.3 h (Horinkova et al., 2019). The oral bioavailability was rather low in preclinical studies with values ranging from 45 to 51% (Luo et al., 2006a), whereas other studies showed bioavailability from 14 to 34% (Kamath et al., 2008b). Although a high-fat meal increases the mean AUC of dasatinib by 14% after a single dose of 100 mg (Bristol-Myers Squibb, 2017), the change is not clinically significant.

The most important factor impacting dasatinib absorption is gastric pH. Dasatinib (pK_a = 3.1, 6.8, and 10.8) is a weak base drug and dissolves better in an acidic environment and precipitates in the small intestine (Tsume et al., 2015) (BCS/BDDCS II) (Budha et al., 2012). An extremely low AUC (54.1 ng·h/mL) and C_{max} (8.3 ng/ml) were reported in a patient with a history of total gastrectomy surgery, showing that the influence of gastric pH on reduced absorption of dasatinib through total gastrectomy surgery for the first time (Iwamoto et al., 2019). An *in vivo* study had shown that the elevated gastric pH range of 4.0–6.0 would significantly reduce the solubility of dasatinib (Tsume et al., 2015). Due to the pH-dependent solubility, all co-administration agents regulating gastric pH may have a great impact on the oral bioavailability of dasatinib, including proton pump inhibitors (PPIs), H_2-receptor antagonists (H_2RAs), antacids, pentagastrin and betaine HCl (**Table 1**).

PPIs (omeprazole, lansoprazole, rabeprazole and esomeprazole) which cancer patients often take for palliation of the gastroesophageal reflux, dyspepsia, and gastritis, have the effect of decreasing dasatinib exposure, which has been demonstrated in several studies. In study of Budha et al., after 4 days administration of omeprazole (40 mg/d), dasatinib (100 mg/d) was administered concomitantly with omeprazole on the next day. The C_{max}, AUC from time zero extrapolated to infinite time (AUC_{inf}) and relative bioavailability (F_R) of dasatinib in healthy subjects were reduced by 42, 43 and ~40%, respectively (Wang et al., 2008; Budha et al., 2012). In another study, 6 healthy subjects who began with a pretreatment of 20 mg rabeprazole twice daily for 3 days, were given a morning dose on the morning of the fourth study day before 100 mg dasatinib, and significant reductions in dasatinib C_{max} and AUC_{inf} of 78 and 84% were observed (Yago et al., 2014). One case report has also indicated that after esomeprazole discontinuation for 4 days, C_{max} and the estimated $AUC_{0\text{-}6.5}$ increased from 23.1 to 52.0 ng/ml and from 89.6 to 130.6 ng·h/mL, respectively (Pape et al., 2016).

H_2RAs significantly reduce dasatinib exposure both in animals and human. In the preclinical study, when the rats were given 3.4 mg of dasatinib (equal to 50 mg in human) along with famotidine (10 mg/kg) injected 2 h prior to dasatinib dosing, the AUC_{inf} of dasatinib approximately declined 4.5-fold compared with the control group (Lubach et al., 2013). In healthy subjects, a dramatic decrease in C_{max} and $AUC_{0\text{-}12}$ of dasatinib of 63 and 61%, respectively, was observed even though they were taking famotidine 10 h earlier than dasatinib (Eley et al., 2009). Same trend was also noticed in a patient with Ph^+ ALL (Matsuoka et al., 2012). On the contrary, famotidine taken 2 h post dasatinib had no effect on the PK of dasatinib, suggesting that administration of famotidine 2 h following dasatinib mitigated the interaction between these two drugs (Eley et al., 2009).

Similarly, when healthy subjects received 30 ml of aluminum hydroxide/magnesium hydroxide–containing antacid (Maalox) co-administered with dasatinib, the $AUC_{0\text{-}12}$ and C_{max} of dasatinib were decreased drastically by 55 and 58%, respectively. Whereas the antacid Maalox, taken 2 h before dasatinib, showed no significant change (Eley et al., 2009).

Interestingly, pentagastrin, which is well-known to stimulate acid secretion in mammals, was found to reduce exposure of dasatinib in rats. A reasonable explanation may be that dasatinib is probably fully dissolved in the stomach because of the high solubility at low pH (below ~4), indicating that as the drug passes through the intestinal tract (pH increases to 5–7), systemic absorption of dasatinib decreases owing to rapid supersaturation in the gut and possible precipitation. In this study, the gastric juice of fasted rats was highly acidic, with a

TABLE 1 | Effect of gastric acid pH modulators on the oral absorption of dasatinib.

Dasatinib (dose regimen)	Gastric acid pH modulator (dose)	Subject (N)	Change		Comment	References
			AUC	C_{max}		
100 mg, QD	Day 1: dasatinib; Days 2–5: omeprazole (40 mg); Day 6: dasatinib and omeprazole (40 mg)	Healthy subjects (N = 13)	↓ 43%	↓ 42%	AUC_{inf}; C_{max}	Clinicaltrials.gov, (2009); Budha et al., (2012)
50 mg, Q12H	Famotidine (40 mg) 2 h after the evening dose of dasatinib	Healthy subjects (N = 21, crossover study)	No significant change		AUC_{0-12}; C_{max}	Eley et al. (2009)
	Famotidine (40 mg) 10 h before the morning dose of dasatinib		↓ 61%	↓ 63%		
	Maalox[a] (30 ml) 2 h prior to dasatinib		↑ 5%[b]	↑ 26%		
	Maalox[a] (30 ml) co-administered with dasatinib		↓ 55%	↓ 58%		
20–140 mg, Q12H	Lansoprazole (30 mg) or famotidine (20–40 mg/d) or nizatidine (300 mg/d)	CML or Ph^+ ALL (N = 12)	Median: ↓ 58%[b]	Median: ↓ 72%[b]	AUC_{0-4}ss; C_2ss	Takahashi et al. (2012a)
70 mg, BID	Famotidine (20 mg)	Ph^+ ALL (N = 1)	↓ 72%[b]	/	AUC_{0-12}	Matsuoka et al. (2012)
3.4 ± 0.1 mg, QD (based on a 50 mg human dose)	Famotidine (10 mg/kg, iv) 2 h prior to dasatinib	Rats (N = 5)	↓ 78%	↓ 82%	AUC_{inf}; C_{max}	Lubach et al. (2013)
	Pentagastrin (0.25 mg/kg, ih) 2 h prior to dasatinib	Rats (N = 5)	↓ 29%	↓ 43%		
100 mg, QD	Pretreatment: Rabeprazole (20 mg, BID) for 3 days; Rabeprazole (20 mg), gastric pH ≥ 4 for at least 15 min before dasatinib	Healthy subjects (N = 12, crossover study)	↓ 78%	↓ 92%	AUC_{inf}; C_{max}	Yago et al. (2014)
	Betaine HCl (1,500 mg) 5 min prior to dasatinib		↑ 5%	↑ 21%		
50 mg, QD	Esomeprazole (40 mg)	Ph^+ ALL (N = 1)	↓ 32%	↓ 56%	$AUC_{0-6.5}$; C_{max}	Pape et al. (2016)

QD, once daily; BID, twice daily; Q12H, every 12 h; N, number of subjects; iv, intravenous injection; ih, hypodermic injection; ss, steady state.
[a]*Maalox, Aluminum hydroxide/magnesium hydroxide–containing antacid.*
[b]*Calculated from the data in the reference; /, unmentioned in the reference.*

pH around 2, which is close to the value of the pentagastrin pretreatment group (Lubach et al., 2013). That means patients had better not take dasatinib with a prolonged fast, although food has no effect on the absorption of dasatinib.

In order to mitigate the interaction between PPIs and dasatinib, two studies reported the effects of betaine HCl and acidic beverages. Patients pretreated with rabeprazole received betaine HCl (1,500 mg) 5 min pre-dasatinib and it was able to restore dasatinib AUC_{inf} and C_{max} to 1.05, and 1.21-fold of the control treatment with dasatinib alone. That means that the reduced exposure to dasatinib induced by rabeprazole can be reversed through coadministration with betaine HCl (Yago et al., 2014). Furthermore, it was found that the effect of concomitant strong acid-reducing agents on ketoconazole, posaconazole, and erlotinib absorption may be offset by coadministration of acidic beverages such as glutamic acid, dilute hydrochloric acid, or carbonated beverages (e.g., cola). Since both dasatinib and these drugs require an acidic environment for optimal absorption, thus, Knoebel et al. suggest that coadministration of acidic beverages such as cola with dasatinib may be a rational option for patients who require potent acid-reducing agents, especially for PPIs (Knoebel and Larson, 2018).

2.2 Distribution

Approximately 96% of dasatinib (93% of its active metabolite) is bound to human plasma proteins (mainly to albumin) *in vitro* (Bristol-Myers Squibb, 2017). And the apparent volume of distribution is 2505 L (Bristol-Myers Squibb, 2017), demonstrating that dasatinib is well distributed into tissues. As we learned, drugs with moderate to high affinity for the same binding sites can have an effect on free drug serum concentrations by competing protein binding sites. For instance, aspirin, displaced valproate from protein binding sites and the free fraction of valproate increased significantly (Orr et al., 1982). Regrettably, no study on the protein binding of dasatinib was found. In addition, there was a negative correlation between the amount of albumin and valproate concentration (Lai et al., 2020). Additional attention should be paid to patients with low albumin levels due to complicated cirrhosis or hypoproteinemia on account of the high binding of dasatinib to plasma proteins.

The cellular uptake of dasatinib is not dependent on drug transporters. The intracellular uptake and retention (IUR) of dasatinib was linear over the range of drug concentrations tested at 4 and 37°C temperatures, suggesting that the cellular uptake is mainly a passive process (Giannoudis et al., 2008; Hiwase et al., 2008). Accordingly, dasatinib uptake is not dependent on hOCT1 (hOCT2 and hOCT3, too (Kamath et al., 2008a)) in contrast to imatinib, even if dasatinib is a substrate for hOCT1 (Giannoudis et al., 2008).

The cellular efflux of dasatinib is partially regulated by drug transporters, which has been confirmed by studies both *in vivo* and *in vitro*. The effects of several efflux proteins belonging to the ATP-binding cassette transporter family on dasatinib diffusion have been reported in multiple studies, including ABCB1 (MDR1/P-gp), ABCG2 (BCRP) and ABCC6 (MRP6). It had been shown that dasatinib was a substrate for both P-gp and BCRP by cell models (Giannoudis et al., 2008; Hiwase et al., 2008) as well as directly measuring intracellular dasatinib levels (Chen

et al., 2009; Hegedus et al., 2009). Overexpression of ABCB1 or ABCG2 protein reduced dasatinib IUR, resulting in an increase in the IC_{50} of dasatinib, which could be modulated with inhibitors (Hiwase et al., 2008; Chen et al., 2009). Likewise, a study conducted in BCR-ABL1$^+$ cell lines indicated that inhibition of ABCC6 reduced dasatinib efflux, leading to a significant decrease in IC_{50} of dasatinib (Eadie et al., 2018).

The central nervous system (CNS) delivery of dasatinib is predominantly subject to the limitations of P-gp and BCRP. *In vivo*, there was no difference in brain accumulation of dasatinib between *Abcg2*$^{-/-}$ mice and wild-type (WT) mice, but it was 3.6-fold and 13.2-fold increase in *Abcb1a/1b*$^{-/-}$ and *Abcb1a/1b;Abcg2*$^{-/-}$ mice, respectively (Lagas et al., 2009), which was confirmed in study by Chen et al. (2009) These results show that P-gp likely exerts a leading role in limiting CNS delivery of dasatinib, whereas BCRP alone shows no such effect on CNS transport of dasatinib. Notably, similar results were reported for imatinib and lapatinib. It suggests that there appears to be a "synergistic" activity of P-gp and BCRP, with the highest efflux activity exhibited by the combination of these two transporters (Bihorel et al., 2007; Chen et al., 2009; Lagas et al., 2009; Polli et al., 2009). The CNS concentration in patients was rarely examined and mostly was undetectable, even if the samples were collected in the absorptive phase (Porkka et al., 2008). In 7 patients with CML or Ph$^+$ ALL (including adult and pediatric), the brain-to-plasma concentration (B/P) ratio was detected (0.01, 0.03, 0.03, 0.04, 0.05, 0.08, and 0.28) (Porkka et al., 2008; Zhou et al., 2013). And the B/P ratios of AUC_{0-24} in 2 pediatric patients with diffuse intrinsic pontine glioma were 0.028 and 0.016 (Broniscer et al., 2013). The finding that P-gp and BCRP have a combined effect on CNS delivery of drug may have significant implications for the treatment of CNS leukemia.

PPIs are substrates and inhibitors of P-gp (Pauli-Magnus et al., 2001). High concentrations of pantoprazole and esomeprazole (1 and 2 mM) resulted in a significant increase of dasatinib IUR in ABCB1 overexpressing cells (Hiwase et al., 2010), which was probably due to the fact that PPIs inhibited the function of P-gp to pump the dasatinib out of the target cells. However, this concentrations at clinically relevant doses is much lower than that of 1 and 2 mM and thus does not achieve the effect of P-gp inhibition. There are other P-gp inhibitors which also have no *in vitro* and *in vivo* data, including cyclosporine, itraconazole, calcium antagonists, antiarrhythmic drugs and macrolides antibiotics. More care still should be taken if co-administered with these drugs.

2.3 Metabolism

Dasatinib is metabolized in humans, primarily by CYP3A4, and flavin-containing monooxygenase 3 (FMO-3) and uridine diphosphate-glucuronosyltransferase (UGT) enzymes are also involved in the formation of dasatinib metabolites (Bristol-Myers Squibb, 2017). Routes of metabolism include hydroxylation, N-dealkylation, N-oxidation, alcohol oxidation and direct glucuronide or sulphate conjugation (Horinkova et al., 2019). There are five phase I circulating metabolites: M4, M5, M6, M20 and M24, among which M20 and M24 represent 45 and 25% of the AUC_{0-24} of dasatinib, respectively. The primary active metabolite, M4 (N-dealkylated) whose antiproliferative activity *in vitro* is similar to that of dasatinib represents only 5% of dasatinib AUC(Leveque et al., 2020).

The coadministration of CYP3A4 inhibitors or inducers lead to varying degrees of fluctuation in dasatinib plasma concentrations. The mean C_{max} and AUC of dasatinib increased by 4-fold and 5-fold, respectively, when used in combination with ketoconazole (strong CYP3A4 inhibitor) (Bristol-Myers Squibb, 2017). Similarly, other moderate or strong CYP3A4 inhibitors used frequently in patients with CML may have the same effect, such as, aprepitan, grapefruit juice, macrolides antibiotics (clarithromycin and erythromycin), azole antifungal agents (itraconazole, voriconazole, and posaconazole) and so on. In opposite, the coadministration of rifampin (strong CYP3A4 inducer) decreased the mean C_{max} and AUC of dasatinib by 81 and 82%, respectively (Bristol-Myers Squibb, 2017). Other CYP3A4 inducers include antiepileptic drugs, dexamethasone and herbal preparations such as St John's wort (known as *hypericum perforatum* in China) and ginseng (Leveque et al., 2020).

The data from European public assessment reports (EPARs) show a high degree of absorption of dasatinib with the fraction of the dose absorbed (f_{abs}) of at least 70%. However, due to the low absolute bioavailability (34%), a considerable amount of first-pass metabolism can be predictably expected. So if CYP3A4 has a 50% or greater contribution to the overall clearance of dasatinib, then a phenotype analysis might be essential for dose adjustment to enable individualized medicine (Mikus and Isabelle Foerster, 2017).

2.4 Excretion

Elimination is primarily via the feces. Besides, the bile also plays a role. Following a single radiolabeled dose of oral dasatinib, 4% of the administered radioactivity was recovered in the urine and 85% in the feces within 10 days, and unchanged dasatinib was in the minority. The mean terminal half-life of dasatinib is 3–5 h (Bristol-Myers Squibb, 2017).

The gut microbiome has been recognized as the second human genome. So, it's not surprising that large interpatient variability of the gut ecosystem has been found. Additional data has become available showing that except liver, the gut microbiome can also directly influence an individual's response to a specific drug by enzymatically transforming the drug's structure and altering its bioavailability, bioactivity or toxicity (Doestzada et al., 2018; Weersma et al., 2020). As the majority of dasatinib is excreted out of body through feces, it is worthy of further investigation for a complex interaction of dasatinib with the gut microbiome.

2.5 Pharmacogenetics

The pharmacogenetics of dasatinib are rarely reported. Although to date we have not found any evidence of a relationship between *CYP3A4* gene polymorphisms and dasatinib PK, the effects of *CYP3A4* gene polymorphisms and its regulation and expression on PK of drugs have been extensively investigated. The *CYP3A4*1G* allele with high frequency in Asians was suggested to decrease CYP3A activity and fentanyl consumption (Wei et al., 2010). Additionally, in clinic observation of kidney transplantation, *CYP3A4*22* carriers

required less Tacrolimus dose to achieve the target exposure compared with *CYP3A4*1/*1* carriers (Yu et al., 2018).

The 3 most relevant *ABCB1* gene polymorphisms are: 1236C > T, 2677G > T/A, and 3435C > T. One study reported *ABCB1* TTT haplotype (1236T, 2677T, 3435T) led to significantly lower intracellular accumulation of dasatinib (Skoglund et al., 2013). Moreover, an *in vitro* study reported that the *ABCB1* 1199A variant was associated to a higher ABCB1 efflux activity, particularly toward imatinib and dasatinib (Dessilly et al., 2016).

Taken together, all these results suggest that polymorphisms of metabolic enzymes and transporters may have a potential impact on dasatinib exposure in plasma and further studies with large sample size are needed to confirm this.

2.6 Special Populations

Age (15–86 years old), sex, and renal impairment (creatinine clearance 21.6 ml/min to 342.3 ml/min as estimated by Cockcroft Gault) have no clinically relevant effect on the PK of dasatinib, according to the prescribing information (Bristol-Myers Squibb, 2017).

2.6.1 Pediatric Patients

The PK of pediatric is very similar to that of adults. In pediatric patients with a dosing regimen of 60 mg/m^2, the model simulated geometric mean (coefficient of variation, CV%) steady-state plasma average concentrations of dasatinib were 14.7 (64.6%) ng/mL (for 2 to <6 years old), 16.3 (97.5%) ng/mL (for 6 to <12 years old), and 18.2 (67.7%) ng/mL (for 12 years and older). Because of the difficulty in swallowing tablets, some prefer dispersed tablets, which have an estimated 36% lower bioavailability than intact tablets (Bristol-Myers Squibb, 2017).

2.6.2 Patients With Hepatic Impairment

Compared to subjects with normal liver function, patients with moderate hepatic impairment (Child-Pugh B) had decreases in mean C_{max} by 47% and mean AUC by 8%. Patients with severe hepatic impairment (Child-Pugh C) had decreases in mean C_{max} by 43% and in mean AUC by 28% compared to the subjects with normal liver function (Bristol-Myers Squibb, 2017). No dose adjustment for patients with hepatic impairment is currently recommended.

3 EXPOSURE-RESPONSE RELATIONSHIPS

3.1 Exposure-Efficacy

In preclinical studies (both *in vivo* and *in vitro*), it was suggested that the efficacy of kinase inhibition correlated with dasatinib exposure. In BCR-ABL-positive cell lines exposed to gradient concentrations of dasatinib (from 0.5 to 150 nM), phospho-BCR-ABL/phospho-CrkL (p-CrkL) levels were considerably diminished and apoptosis levels were increased with elevated concentrations of dasatinib (Copland et al., 2006; Shah et al., 2008b; Snead et al., 2009; O'hare et al., 2013), which was also shown in SRC-expressing cells (Luo et al., 2008). Results of validation in primary CML cells from CML patients were similar to those of cell lines (Shah et al., 2008b; Luo et al., 2008; Snead et al., 2009). In a phase I study using peripheral blood mononuclear cells (PBMC) obtained from 5 dasatinib-treated CML patients, p-CrKL decreased in a dose-dependent manner after 4 h of the initial dose but was largely recovered after 8 h, coinciding with the decline in dasatinib serum levels measured in these same patients (Talpaz et al., 2006).

Besides, in tumors from mice bearing human tumor xenografts, tumoral phospho-BCR-ABL/phospho-SRC was dose-dependently inhibited (a single oral dose ranging from 1.25 to 50 mg/kg), and directly related to the plasma concentrations of dasatinib (Luo et al., 2006b; Luo et al., 2008). Notably, two studies reported that practically undetectable p-CrkL levels (O'hare et al., 2013) or near-maximal apoptosis levels (Snead et al., 2009) were observed when exposed to 100 nM (~48.8 ng/ml) dasatinib. What's more, Shah et al. found that 100 nM dasatinib exposure killed about 90% of the cells as short as 20 min, even for imatinib-resistant (except for T315I) (Shah et al., 2008b). These results suggest that transient potent inhibition (>50 ng/ml) is sufficient to commit CML cells to apoptosis.

To the best of our knowledge, few clinical studies have shown that there is some certain link between exposure and efficacy. Plasma concentration at 2 h (C_2), C_{max} and $AUC_{0\text{-}4}$ detected in patients with T315I were significantly lower than those without. The median C_{max} in patients with T315I and without were 43.8 ng/ml and 112.4 ng/ml, respectively ($p = 0.0242$) (Takahashi et al., 2012b). As a consequence, a low exposure to dasatinib may be associated with the emergence of BCR-ABL mutations, including T315I. In a prospective cohort study of 10 CML patients receiving dasatinib 100 mg once daily, analysis by Iwamoto et al. revealed that the cut-off value of dasatinib AUC and C_{max} for achieving major molecular response (MMR) within 6 months were 336.1 ng·h/ml and 69.2 ng/ml, respectively, and the accuracy ratio to predict MMR was 88.9% for the AUC, and 77.8% for the C_{max} (Iwamoto et al., 2019). It is worth noting that the monitoring of AUC cannot be generalized in clinical practice because of its operational complexity, although it is the best PK parameter to characterize dasatinib exposure. Compared with AUC, C_{max} is a more applicable parameter for prediction of efficacy.

The study by Wang et al. using data from 567 Ph$^+$ CML subjects indicated that achieving major cytogenetic response (MCyR) was most closely related to increasing $wC_{avg}ss$, so from the perspective of this study, the most significant predictor of MCyR was $wC_{avg}ss$ (Wang et al., 2013). Despite $wC_{avg}ss$ suggested to predict efficacy, TDM based on $wC_{avg}ss$ is not feasible clinically (Yu et al., 2014).

In aggregate, it is important that transient potent dasatinib concentration of 100 nM achieves inhibition of BCR-ABL and the effect can last for several hours, that's why dasatinib is taken once daily in spite of the short half-life. In addition, although continuous low-level exposure can achieve a similar efficacy of BCR-ABL inhibition, a relatively high exposure is needed for reducing the risk of developing BCR-ABL point mutations. Vainstein et al. found higher inhibitory potential at peak concentration (IPP), which integrated IC_{50}, slope, and C_{max}, correlated with improved complete cytogenetic response

TABLE 2 | Overview of outcomes for patients administrated different oral dose of dasatinib.

Study	Dose	Patient (N)	Efficacy, %					Safety, %
			OHR	CHR	MaHR	CCyR	MCyR	Pleural effusion (all grades)
Cortes et al. (2007)	70 mg, BID	CML-BC (N = 116)	47	26	33	33	38	23
Guilhot et al. (2007)	70 mg, BID	CML-AP (N = 107)	81	39	64	24	33	23
Hochhaus et al. (2007)	70 mg, BID	CML-CP (N = 186)	/	90	/	/	52	19
Kantarjian et al. (2007)	70 mg, BID	CML-CP (N = 101)	/	93	/	40	52	17
Shah et al. (2010)	100 mg, QD	CML-CP (N = 167)	/	92	37	50	63	14
	50 mg, BID	CML-CP (N = 168)	/	92	38	50	61	23
	140 mg, QD	CML-CP (N = 167)	/	87	38	50	63	25
	70 mg, BID	CML-CP (N = 168)	/	88	38	54	61	23

/, unmentioned in the reference.

OHR, overall hematologic response; CHR, complete hematologic response; MaHR, major hematologic response; CCyR, complete cytogenetic response; MCyR, major cytogenetic response; QD, once daily; BID, twice daily; BC, blast crisis; CP, chronic-phase; AP, accelerated-phase.

(CCyR) rates in CML patients treated with dasatinib (Vainstein et al., 2013), which confirmed the importance of C_{max} laterally. A study has proved that the C_2 concentration, not concentration at 1 h (C_1) or 4 h (C_4), had a higher correlation with the measured AUC_{0-4} of dasatinib using 34 PK profiles ($r = 0.9419$, $p < 0.0001$) (Takahashi et al., 2012a). The monitoring of C_2 concentration is easily achieved clinically to predict whether an enough C_{max} will be obtained.

On the whole, the monitoring of dasatinib C_{max}/C_2 level does make sense. It is generally accepted that a relatively high C_{max} level should be maintained to ensure the clinical efficacy and to reduce the risk of dasatinib resistance. Based on current limited evidence, it is recommended to maintain C_2 concentration at least ≥50 ng/ml.

Additionally, dasatinib showed the special capacity to induce immunomodulation. The present *in vitro* studies indicated that dasatinib dose-dependently inhibited the proliferation and function of $CD4^+CD25^+$ regulatory T cells (Tregs) (Fei et al., 2009), meanwhile it enhanced the expansion of large granular lymphocytes [LGLs, mono- or oligoclonal $CD8^+$T cells, γδT cells, and natural killer (NK) cells] (Uchiyama et al., 2013). This effect was also confirmed using a collection of 37 leukemia patients that the blood counts closely mirrored dasatinib plasma concentrations (Mustjoki et al., 2013). Importantly, most of the dasatinib discontinuation trials showed that increased LGLs levels and reduced immune suppressive Treg levels in dasatinib treatment interrupted patients were linked to better prognosis and treatment-free remission (TFR) successes (Hughes and Yong, 2017; Climent and Plana, 2019). Therefore, we reasonably speculate that the exposure of dasatinib is closely related to TFR. However, no studies currently have been conducted to determine whether dasatinib exposure levels correlate with successful TFR. But it is highly worthy of investigation and discussion, and we expect that such research will emerge in the future.

3.2 Exposure-Safety

Reviewing data from several clinical studies, it was found that pleural effusion (PE), an adverse event, was intimately associated with dasatinib treatment, and was the primary reason for discontinuation. In DASISION study, fluid retention (all grades) occurred more frequently with imatinib than with dasatinib (42 vs. 19%), yet it's a remarkable fact that PE was reported only in the dasatinib group: 26 patients (10%) (Kantarjian et al., 2010). Subsequently, it was also identified that the incidence of PE was related to the dasatinib dose regimens, with the lowest of the 100 mg once daily regimen (Shah et al., 2008a; Shah et al., 2016) (**Table 2**).

A phase II study (OPTIM) reported that after CML patients with a trough plasma concentration (C_0) value ≥3 nmol/L (about 1.5 ng/ml) were randomly assigned between the continuation of dasatinib 100 mg/d (control arm: $n = 42$) and a dose reduction strategy (TDM arm: $n = 38$), the TDM arm had a significantly lower cumulative incidence of PE (12 vs. 39%) and discontinuation rates (21 vs. 36%) compared to the control arm by 36 months. It was encouraging that molecular responses evaluated during 3 years were found to be similar in both arms (Rousselot et al., 2021). In study by Mizuta et al. (2018), CML patients administered dasatinib once daily at a dose of 100 mg ($n = 27$) or 50 mg ($n = 5$) had a median C_0 of dasatinib of 1.4 ng/ml, with no significance in PE rate between high C_0 group (≥1.4 ng/ml) and low C_0 group (<1.4 ng/ml) (31 vs. 19%). Nonetheless, after adjusting for dasatinib dose (g) and body weight (kg) (C_0/D/W), higher median C_0 was correlated with the incidence of the dasatinib interruption/reduction in treatment. These results suggest that dose optimization by C_0 assessment using TDM, a valuable "PE prediction tool" (Rousselot et al., 2021), reduces the risk of exposure to PE while ensuring the efficacy.

Wang et al. (2013) also found that patients with 100 mg once daily schedule had the lowest PE rate (11%) and steady-state C_0 of dasatinib (2.61 ng/ml). And the C_0 was identified as the most significant predictor of PE in the Cox proportional hazards model (hazard increased 1.22-fold for every 1 ng/ml increase in C_0). Based on Wang et al.'s study (Wang et al., 2008), Yu et al. (2014) defined a dose interruption rate of about 50% as a non-acceptable cut-off, then the C_0 should not exceed 2.5 ng/ml in chronic phase CML patients. However, this cut-off value should be interpreted with caution in the clinic, as it is derived from a mixed dosing regimen ($n = 567$). What's more, the analysis by Verheijen et al. (2017)

TABLE 3 | Overview of LC–MS/MS analytical methods of dasatinib in human plasma in recent 5 years.

References	Analtye	Analytical column	Internal standard	Calibration range, ng/mL	LLOQ, ng/mL	Extraction
Huynh et al. (2017)	Dasatinib, other 13 TKIs	Acquity UPLC BEH C18 column (2.1 mm × 50 mm; 1.9 μm)	$^{2}H_{8}$-dasatinib	1–500	0.75	PPT
Wojnicz et al. (2017)	Dasatinib, imatinib, nilotinib	Poroshell 120 EC-C18 column (2.1 mm × 75 mm, 2.7 μm)	D_{8}-dasatinib	0.75–400	0.75	SPE
Zeng et al. (2017)	Dasatinib, imatinib, nilotinib	Xtimate Phenyl column (2.1 mm × 150 mm, 3 μm)	/	2–490	2	LLE
Maher et al. (2018)	Dasatinib	Acquity UPLC BEH C18 column (1.0 mm × 100 mm, 1.7 μm)	Erlotinib	1–500	1	SPE
Merienne et al. (2018)	Dasatinib, other 16 TKIs and 2 metabolites	CORTECS UPLC C18 column (2.1 × 50 mm, 1.6 μm)	$^{13}C_{6}$-dasatinib	0.1–200	0.1	SPE
Ezzeldin et al. (2020)	Dasatinib, other 6 TKIs	Acquity UPLC BEH C18 column (2.1 mm × 100 mm, 1.7 μm)	Quizartinib	5–1000	5	PPT
Koller et al. (2020)	Dasatinib, other 10 TKIs	Poroshell 120 EC-C18 column (2.1 mm × 75 mm, 2.7 μm)	D_{8}-dasatinib	0.38–400	0.38	PPT; SPE
Mukai et al. (2020)	Dasatinib, other 4 TKIs and 3 active metabolites	L-column3 C18 (2.1 mm × 50 mm, 3 μm)	D_{8}-dasatinib	0.5–150	0.5	SLE
Hirasawa et al. (2021)	Dasatinib, other 4 TKIs	Triart C18 MetalFree column (2.1 mm × 50 mm, 3 μm)	$^{2}H_{8}$-dasatinib	0.1–200	0.1	PPT
Llopis et al. (2021)	Dasatinib, other 8 TKIs, 2 active metabolites and 2 AAs	Acquity UPLC T3 HSS C18 column (2.1 × 100 mm, 1.8 μm)	$^{2}H_{8}$-dasatinib	1–500	1	PPT
Sumimoto et al. (2021)	Dasatinib, other 4 TKIs and 2 active metabolites	Acquity BEH C18 column (2.1 mm × 50 mm, 1.7 μm)	D_{8}-dasatinib	0.2–200	0.2	SPE
Verougstraete et al. (2021)	Dasatinib, other 7 TKIs	Acquity UPLC BEH C18 column (2.1 mm× 100 mm, 1.7 μm)	D_{8}-dasatinib	0.5–450	0.5	PPT

/, unmentioned in the reference.

PPT, protein precipitation; SPE, solid-phase extraction; LLE, liquid-liquid extraction; SLE, supported liquid extraction method using an ISOLUTE SLE+ column; LC–MS/MS, liquid chromatography/electrospray ionization–tandem mass spectrometry; AAs, antiandrogen drugs.

indicated that across all kinase inhibitors, the target exposure fitted 81.7% of the population exposure and supported the argument that in the absence of a definitive TDM target, the geometric mean C_0 of dasatinib [2.61 ng/ml for 100 mg once daily, n = 146 (Wang et al., 2013)], representing the CML population average, could be an alternative. There was an additional viewpoint from Mirua et al. who suggested the C_0 cut-off value of 4.33 ng/ml (median) from the regression model studied by Wang et al. (2013) be determined as the minimum toxic concentration (MTC) to avoid PE (Miura and Takahashi, 2019). On balance, the above recommendations on the target range for dasatinib C_0 are derived from single data source (all based on Wang et al.' study), and as such need to be supported by additional evidence.

Age was a major risk factor for PE, which was confirmed in several studies (Wang et al., 2013; Mizuta et al., 2018; Rousselot et al., 2021). And it was found that this effect was driven by PK parameters (Wang et al., 2013). Patients with high median age had a higher level of C_0, and so did a higher incidence of PE. As a result, the therapeutic window of elderly patients may be narrower relative to younger patients, and these patients may need more intensive monitoring.

All things considered, the relationship between C_0 of dasatinib and the occurrence of PE in patients has been basically established, i. e., maintaining a relatively low level of C_0 can reduce the risk of PE. Meanwhile, the threshold of dasatinib C_0 from some experts' suggestions is concentrated at 2–5 ng/ml, despite lack of hard evidence to support it. Consequently, it is necessary to monitor C_0 of dasatinib, but the target range needs to be further explored and confirmed.

4 ANALYTICAL METHOD

Because of the low steady-state blood concentration of dasatinib, the currently preferred analytical method for measuring concentrations of dasatinib is liquid chromatography-tandem mass spectrometry (LC-MS/MS), which has a high sensitivity for quantifying unchanged dasatinib in biological fluids. **Table 3** shows studies on the LC-MS/MS analytical method of dasatinib published in recent 5 years (**Table 3**). Recently, some studies have reported other methods used for dasatinib, such as sequential spectrophotometric-based univariate methods (Abdelhameed et al., 2021). Most studies determined dasatinib levels with a lower limit of quantification (LLOQ) of 1 ng/ml (Couchman et al., 2012; Furlong et al., 2012; Birch et al., 2013), while the method of Bouchet et al. (2011) determined dasatinib levels with a lower LLOQ of 0.1 ng/mL. A study found that about 4.7% of the available dasatinib concentration measurements (contained 4044 measurements) were below the LLOQ of 1.0 ng/ml (Wang et al., 2013; Miura and Takahashi, 2016), suggesting that lower LLOQ of less than 1.0 ng/ml was a necessity.

Currently, the monitoring of dasatinib uses plasma samples, which contain both free and bound fractions. However, only free drug in equilibrium with cells can exert pharmacological effects.

Simultaneously, pharmacologically active free fraction may undergo significant changes due to variations in the concentration, conformation, and/or other physicochemical properties of plasma proteins (Haouala et al., 2013). Hence, free dasatinib concentration should be in consideration because of its high protein binding rate (Widmer et al., 2014). There was a study measured free and total imatinib concentrations and predicted imatinib free concentrations by an established model based on total concentrations and plasma proteins measurements (Haouala et al., 2013).

Plasma samples are collected in tubes using heparin or EDTA as anticoagulant by immediate centrifugation. Different sample preparation methods, such as protein precipitation (PPT) (Haouala et al., 2009; Huynh et al., 2017), solid-phase extraction (SPE) (Bouchet et al., 2011; Furlong et al., 2012; Wojnicz et al., 2017; Koller et al., 2020) and liquid-liquid extraction (LLE) (Couchman et al., 2012; Birch et al., 2013), have been used for TKIs. PPT, however, is at most risk of causing ion suppression in electrospray ionization (ESI), since it does not remove all endogenous compounds that interfere with ESI-LC-MS/MS analysis (Koller et al., 2020). In particular, samples will be diluted by the addition of protein precipitator, resulting in a lower concentration of the drug to be measured. Therefore, it is not suitable for samples with low concentration like C_0 of dasatinib. LLE is characterized by clean extraction, of which multiple extraction steps are required to improve the recovery of analytes. SPE is less time-consuming and requires less solvent volume (Koller et al., 2020), which is a more costly method compared with LLE (Zeng et al., 2017). Moreover, Mukai et al. employed a supported liquid extraction method using an ISOLUTE SLE+ column which was more convenient compared to SPE (Mukai et al., 2020). Another proper alternative to SPE is thin-film solid-phase microextraction (TF-SPME) whose distinctive characteristics are high sensitivity, large extraction capacity, and minimum requisite sample pre-treatment (Khodayari et al., 2021).

5 CONCLUSION AND PROSPECT

The findings presented in this review demonstrate that TDM of dasatinib is essential and feasible, and the clinical benefits of dasatinib TDM in individualized medicine have also been initially shown. Based on the evidence currently available, scholars suggest that maintain a relatively high level of C_2 or C_{max} to obtain sufficient efficacy and reduce the risk of BCR-ABL mutations, and a relatively low level of C_0 to reduce the risk of exposure to PE. Moreover, age is a factor with more attention and elderly patients may need regular monitoring compared with young patients.

At present, there is a real need to identify the range of the monitoring target and high-quality controlled studies need to be performed to confirm its appropriateness, especially for C_0. Accordingly, with the progressing of the research, a classification refinement of dasatinib TDM is likely needed, such as diseases, ages, races and so on. Following the launch of targeted drugs with safety and efficacy, more and more patients are achieving responses, accompanied by increasing demands for dose reduction. Extending the existing knowledge with additional studies in the field of individualized medicine will open up the era of guiding reduction by TDM and implementing it into clinical practice in the foreseeable future to improve patients' quality of life. Additionally, to facilitate clinical application, there is an inevitable need to advance technologies for feasible and accurate monitoring of drug concentrations. For example, the determination of free concentration or the free concentration modelled predicted can more accurately reflect the exposure of pharmacologically active free fraction. Overall, the strategy of TDM will help overcome difficulties of dasatinib in treatment and bring further survival benefit and a better quality of life for patients in the future.

AUTHOR CONTRIBUTIONS

LH and YF contributed to conception and design of the study. SH, JB and XH helped with the literature search and organization. QS and YZ contributed to data extraction. SH wrote the manuscript. XL drew the tables. All authors contributed to manuscript revision. All authors read and approved the final manuscript.

FUNDING

This work was supported by the Beijing Municipal Natural Science Foundation (grant number 7192218).

ACKNOWLEDGMENTS

We would like to thank Prof. Qian Jiang for valuable clinical comments on this review.

REFERENCES

Abdelhameed, A. S., Hassan, E. S., Attwa, M. W., Al-Shakliah, N. S., Alanazi, A. M., and Alrabiah, H. (2021). Simple and Efficient Spectroscopic-Based Univariate Sequential Methods for Simultaneous Quantitative Analysis of Vandetanib, Dasatinib, and Sorafenib in Pharmaceutical Preparations and Biological Fluids. *Spectrochim Acta A. Mol. Biomol. Spectrosc.* 260, 119987. doi:10.1016/j.saa.2021.119987

Bihorel, S., Camenisch, G., Lemaire, M., and Scherrmann, J. M. (2007). Influence of Breast Cancer Resistance Protein (Abcg2) and P-Glycoprotein (Abcb1a) on the Transport of Imatinib Mesylate (Gleevec) across the Mouse Blood-Brain Barrier. *J. Neurochem.* 102, 1749–1757. doi:10.1111/j.1471-4159.2007.04808.x

Birch, M., Morgan, P. E., Handley, S., Ho, A., Ireland, R., and Flanagan, R. J. (2013). Simple Methodology for the Therapeutic Drug Monitoring of the Tyrosine Kinase Inhibitors Dasatinib and Imatinib. *Biomed. Chromatogr.* 27, 335–342. doi:10.1002/bmc.2796

Bouchet, S., Chauzit, E., Ducint, D., Castaing, N., Canal-Raffin, M., Moore, N., et al. (2011). Simultaneous Determination of Nine Tyrosine Kinase Inhibitors by 96-well Solid-phase Extraction and Ultra Performance LC/MS-MS. *Clin. Chim. Acta* 412, 1060–1067. doi:10.1016/j.cca.2011.02.023

Bristol-Myers Squibb (2017). Sprycel: Full Prescribing Information. *E. coli*. Available at: https://packageinserts.bms.com/pi/pi_sprycel.pdf (Accessed September 29, 2021).

Broniscer, A., Baker, S. D., Wetmore, C., Pai Panandiker, A. S., Huang, J., Davidoff, A. M., et al. (2013). Phase I Trial, Pharmacokinetics, and Pharmacodynamics of

Vandetanib and Dasatinib in Children with Newly Diagnosed Diffuse Intrinsic Pontine Glioma. *Clin. Cancer Res.* 19, 3050–3058. doi:10.1158/1078-0432.CCR-13-0306

Budha, N. R., Frymoyer, A., Smelick, G. S., Jin, J. Y., Yago, M. R., Dresser, M. J., et al. (2012). Drug Absorption Interactions between Oral Targeted Anticancer Agents and PPIs: Is pH-dependent Solubility the Achilles Heel of Targeted Therapy? *Clin. Pharmacol. Ther.* 92, 203–213. doi:10.1038/clpt.2012.73

Chandani, R., He, J., and Trabelsi, F. (2017). "Atypical Pharmacokinetic Profiles Observed with Dasatinib Reference Listed Drug Product in Bioequivalence Studies," in Conference presentation (San Diego, CA, United States: AAPS Annual Meeting). Available at: http://www.BioPharmaServices.com.

Chen, Y., Agarwal, S., Shaik, N. M., Chen, C., Yang, Z., and Elmquist, W. F. (2009). P-glycoprotein and Breast Cancer Resistance Protein Influence Brain Distribution of Dasatinib. *J. Pharmacol. Exp. Ther.* 330, 956–963. doi:10.1124/jpet.109.154781

Climent, N., and Plana, M. (2019). Immunomodulatory Activity of Tyrosine Kinase Inhibitors to Elicit Cytotoxicity against Cancer and Viral Infection. *Front. Pharmacol.* 10, 1232. doi:10.3389/fphar.2019.01232

Clinicaltrials.gov (2009). The Effect of Omeprazole on the Pharmacokinetics of Dasatinib (BMS-354825) in Healthy Subjects. *E. coli*. Available at: https://clinicaltrials.gov/ct2/show/results/NCT00655746?term=NCT00655746&draw=2&rank=1 (Accessed September 29, 2021).

Copland, M., Hamilton, A., Elrick, L. J., Baird, J. W., Allan, E. K., Jordanides, N., et al. (2006). Dasatinib (BMS-354825) Targets an Earlier Progenitor Population Than Imatinib in Primary CML but Does Not Eliminate the Quiescent Fraction. *Blood* 107, 4532–4539. doi:10.1182/blood-2005-07-2947

Cortes, J., Rousselot, P., Kim, D. W., Ritchie, E., Hamerschlak, N., Coutre, S., et al. (2007). Dasatinib Induces Complete Hematologic and Cytogenetic Responses in Patients with Imatinib-Resistant or -intolerant Chronic Myeloid Leukemia in Blast Crisis. *Blood* 109, 3207–3213. doi:10.1182/blood-2006-09-046888

Couchman, L., Birch, M., Ireland, R., Corrigan, A., Wickramasinghe, S., Josephs, D., et al. (2012). An Automated Method for the Measurement of a Range of Tyrosine Kinase Inhibitors in Human Plasma or Serum Using Turbulent Flow Liquid Chromatography-Tandem Mass Spectrometry. *Anal. Bioanal. Chem.* 403, 1685–1695. doi:10.1007/s00216-012-5970-2

Dai, G., Pfister, M., Blackwood-Chirchir, A., and Roy, A. (2008). Importance of Characterizing Determinants of Variability in Exposure: Application to Dasatinib in Subjects with Chronic Myeloid Leukemia. *J. Clin. Pharmacol.* 48, 1254–1269. doi:10.1177/0091270008320604

Dessilly, G., Elens, L., Panin, N., Karmani, L., Demoulin, J. B., and Haufroid, V. (2016). ABCB1 1199G>A Polymorphism (Rs2229109) Affects the Transport of Imatinib, Nilotinib and Dasatinib. *Pharmacogenomics* 17, 883–890. doi:10.2217/pgs-2016-0012

Doestzada, M., Vila, A. V., Zhernakova, A., Koonen, D. P. Y., Weersma, R. K., Touw, D. J., et al. (2018). Pharmacomicrobiomics: a Novel Route towards Personalized Medicine? *Protein Cell* 9, 432–445. doi:10.1007/s13238-018-0547-2

Eadie, L. N., Dang, P., Goyne, J. M., Hughes, T. P., and White, D. L. (2018). ABCC6 Plays a Significant Role in the Transport of Nilotinib and Dasatinib, and Contributes to TKI Resistance *In Vitro*, in Both Cell Lines and Primary Patient Mononuclear Cells. *PLoS One* 13, e0192180. doi:10.1371/journal.pone.0192180

Eley, T., Luo, F. R., Agrawal, S., Sanil, A., Manning, J., Li, T., et al. (2009). Phase I Study of the Effect of Gastric Acid pH Modulators on the Bioavailability of Oral Dasatinib in Healthy Subjects. *J. Clin. Pharmacol.* 49, 700–709. doi:10.1177/0091270009333854

European Medicines Agency (2006). Sprycel: EPAR – Scientific Discussion. *E. coli*. Available at: http://www.ema.europa.eu (Accessed September 29, 2021).

Ezzeldin, E., Iqbal, M., Herqash, R. N., and Elnahhas, T. (2020). Simultaneous Quantitative Determination of Seven Novel Tyrosine Kinase Inhibitors in Plasma by a Validated UPLC-MS/MS Method and its Application to Human Microsomal Metabolic Stability Study. *J. Chromatogr. B Analyt Technol. Biomed. Life Sci.* 1136, 121851. doi:10.1016/j.jchromb.2019.121851

Fei, F., Yu, Y., Schmitt, A., Rojewski, M. T., Chen, B., Götz, M., et al. (2009). Dasatinib Inhibits the Proliferation and Function of CD4+CD25+ Regulatory T Cells. *Br. J. Haematol.* 144, 195–205. doi:10.1111/j.1365-2141.2008.07433.x

Furlong, M. T., Agrawal, S., Hawthorne, D., Lago, M., Unger, S., Krueger, L., et al. (2012). A Validated LC-MS/MS Assay for the Simultaneous Determination of the Anti-leukemic Agent Dasatinib and Two Pharmacologically Active Metabolites in Human Plasma: Application to a Clinical Pharmacokinetic Study. *J. Pharm. Biomed. Anal.* 58, 130–135. doi:10.1016/j.jpba.2011.09.008

Giannoudis, A., Davies, A., Lucas, C. M., Harris, R. J., Pirmohamed, M., and Clark, R. E. (2008). Effective Dasatinib Uptake May Occur without Human Organic Cation Transporter 1 (hOCT1): Implications for the Treatment of Imatinib-Resistant Chronic Myeloid Leukemia. *Blood* 112, 3348–3354. doi:10.1182/blood-2007-10-116236

Guilhot, F., Apperley, J., Kim, D. W., Bullorsky, E. O., Baccarani, M., Roboz, G. J., et al. (2007). Dasatinib Induces Significant Hematologic and Cytogenetic Responses in Patients with Imatinib-Resistant or -intolerant Chronic Myeloid Leukemia in Accelerated Phase. *Blood* 109, 4143–4150. doi:10.1182/blood-2006-09-046839

Haouala, A., Widmer, N., Guidi, M., Montemurro, M., Leyvraz, S., Buclin, T., et al. (2013). Prediction of Free Imatinib Concentrations Based on Total Plasma Concentrations in Patients with Gastrointestinal Stromal Tumours. *Br. J. Clin. Pharmacol.* 75, 1007–1018. doi:10.1111/j.1365-2125.2012.04422.x

Haouala, A., Zanolari, B., Rochat, B., Montemurro, M., Zaman, K., Duchosal, M. A., et al. (2009). Therapeutic Drug Monitoring of the New Targeted Anticancer Agents Imatinib, Nilotinib, Dasatinib, Sunitinib, Sorafenib and Lapatinib by LC Tandem Mass Spectrometry. *J. Chromatogr. B Analyt Technol. Biomed. Life Sci.* 877, 1982–1996. doi:10.1016/j.jchromb.2009.04.045

Hegedus, C., Ozvegy-Laczka, C., Apáti, A., Magócsi, M., Német, K., Orfi, L., et al. (2009). Interaction of Nilotinib, Dasatinib and Bosutinib with ABCB1 and ABCG2: Implications for Altered Anti-cancer Effects and Pharmacological Properties. *Br. J. Pharmacol.* 158, 1153–1164. doi:10.1111/j.1476-5381.2009.00383.x

Hirasawa, T., Kikuchi, M., Shigeta, K., Takasaki, S., Sato, Y., Sato, T., et al. (2021). High-throughput Liquid Chromatography/electrospray Ionization-Tandem Mass Spectrometry Method Using In-Source Collision-Induced Dissociation for Simultaneous Quantification of Imatinib, Dasatinib, Bosutinib, Nilotinib, and Ibrutinib in Human Plasma. *Biomed. Chromatogr.* 35, e5124. doi:10.1002/bmc.5124

Hiwase, D. K., Saunders, V., Hewett, D., Frede, A., Zrim, S., Dang, P., et al. (2008). Dasatinib Cellular Uptake and Efflux in Chronic Myeloid Leukemia Cells: Therapeutic Implications. *Clin. Cancer Res.* 14, 3881–3888. doi:10.1158/1078-0432.CCR-07-5095

Hiwase, D. K., White, D., Zrim, S., Saunders, V., Melo, J. V., and Hughes, T. P. (2010). Nilotinib-mediated Inhibition of ABCB1 Increases Intracellular Concentration of Dasatinib in CML Cells: Implications for Combination TKI Therapy. *Leukemia* 24, 658–660. doi:10.1038/leu.2009.242

Hochhaus, A., Kantarjian, H. M., Baccarani, M., Lipton, J. H., Apperley, J. F., Druker, B. J., et al. (2007). Dasatinib Induces Notable Hematologic and Cytogenetic Responses in Chronic-phase Chronic Myeloid Leukemia after Failure of Imatinib Therapy. *Blood* 109, 2303–2309. doi:10.1182/blood-2006-09-047266

Horinkova, J., Sima, M., and Slanar, O. (2019). Pharmacokinetics of Dasatinib. *Prague Med. Rep.* 120, 52–63. doi:10.14712/23362936.2019.10

Hughes, A., and Yong, A. S. M. (2017). Immune Effector Recovery in Chronic Myeloid Leukemia and Treatment-free Remission. *Front. Immunol.* 8, 469. doi:10.3389/fimmu.2017.00469

Huynh, H. H., Pressiat, C., Sauvageon, H., Madelaine, I., Maslanka, P., Lebbé, C., et al. (2017). Development and Validation of a Simultaneous Quantification Method of 14 Tyrosine Kinase Inhibitors in Human Plasma Using LC-MS/MS. *Ther. Drug Monit.* 39, 43–54. doi:10.1097/FTD.0000000000000357

Ishida, Y., Murai, K., Yamaguchi, K., Miyagishima, T., Shindo, M., Ogawa, K., et al. (2016). Pharmacokinetics and Pharmacodynamics of Dasatinib in the Chronic Phase of Newly Diagnosed Chronic Myeloid Leukemia. *Eur. J. Clin. Pharmacol.* 72, 185–193. doi:10.1007/s00228-015-1968-y

Iwamoto, T., Monma, F., Ohishi, K., Umino, A., Suzuki, K., Oka, K., et al. (2019). Evaluation of Medication Adherence and Pharmacokinetics of Dasatinib for Earlier Molecular Response in Japanese Patients with Newly Diagnosed Chronic Myeloid Leukemia: A Pilot Study. *Ther. Drug Monit.* 41, 575–581. doi:10.1097/FTD.0000000000000639

Kamath, A. V., Wang, J., Lee, F. Y., and Marathe, P. H. (2008a). Preclinical Pharmacokinetics and *In Vitro* Metabolism of Dasatinib (BMS-354825): a Potent Oral Multi-Targeted Kinase Inhibitor against SRC and BCR-ABL. *Cancer Chemother. Pharmacol.* 61, 365–376. doi:10.1007/s00280-007-0478-8

Kamath, A. V., Wang, J., Lee, F. Y., and Marathe, P. H. (2008b). Preclinical Pharmacokinetics and *In Vitro* Metabolism of Dasatinib (BMS-354825): a Potent Oral Multi-Targeted Kinase Inhibitor against SRC and BCR-ABL. *Cancer Chemother. Pharmacol.* 61, 365–376. doi:10.1007/s00280-007-0478-8

Kantarjian, H., Pasquini, R., Hamerschlak, N., Rousselot, P., Holowiecki, J., Jootar, S., et al. (2007). Dasatinib or High-Dose Imatinib for Chronic-phase Chronic Myeloid Leukemia after Failure of First-Line Imatinib: a Randomized Phase 2 Trial. *Blood* 109, 5143–5150. doi:10.1182/blood-2006-11-056028

Kantarjian, H., Shah, N. P., Hochhaus, A., Cortes, J., Shah, S., Ayala, M., et al. (2010). Dasatinib versus Imatinib in Newly Diagnosed Chronic-phase Chronic Myeloid Leukemia. *N. Engl. J. Med.* 362, 2260–2270. doi:10.1056/NEJMoa1002315

Khodayari, P., Jalilian, N., Ebrahimzadeh, H., and Amini, S. (2021). Trace-level Monitoring of Anti-cancer Drug Residues in Wastewater and Biological Samples by Thin-Film Solid-phase Micro-extraction Using Electrospun polyfam/Co-MOF-74 Composite Nanofibers Prior to Liquid Chromatography Analysis. *J. Chromatogr. A.* 1655, 462484. doi:10.1016/j.chroma.2021.462484

Knoebel, R. W., and Larson, R. A. (2018). Pepsi® or Coke®? Influence of Acid on Dasatinib Absorption. *J. Oncol. Pharm. Pract.* 24, 156–158. doi:10.1177/1078155217692152

Koller, D., Vaitsekhovich, V., Mba, C., Steegmann, J. L., Zubiaur, P., Abad-Santos, F., et al. (2020). Effective Quantification of 11 Tyrosine Kinase Inhibitors and Caffeine in Human Plasma by Validated LC-MS/MS Method with Potent Phospholipids Clean-Up Procedure. Application to Therapeutic Drug Monitoring. *Talanta* 208, 120450. doi:10.1016/j.talanta.2019.120450

Lagas, J. S., Van Waterschoot, R. A., Van Tilburg, V. A., Hillebrand, M. J., Lankheet, N., Rosing, H., et al. (2009). Brain Accumulation of Dasatinib Is Restricted by P-Glycoprotein (ABCB1) and Breast Cancer Resistance Protein (ABCG2) and Can Be Enhanced by Elacridar Treatment. *Clin. Cancer Res.* 15, 2344–2351. doi:10.1158/1078-0432.CCR-08-2253

Lai, Y. H., Huang, Q. Y., Liang, Y. J., Huang, X. W., Li, C. Y., and Tang, S. H. (2020). Influencing Factors of Serum Valparaiso Acid Concentration in Children with Epilepsy Based on Multivariate Linear Regression. *J. Pediatr. Pharm.* 26, 37–39.

Levêque, D., Becker, G., Bilger, K., and Natarajan-Amé, S. (2020). Clinical Pharmacokinetics and Pharmacodynamics of Dasatinib. *Clin. Pharmacokinet.* 59, 849–856. doi:10.1007/s40262-020-00872-4

Lindauer, M., and Hochhaus, A. (2018). *Dasatinib*. Berlin, Germany: Springer International Publishing, 29–68. doi:10.1007/978-3-319-91439-8_2

Llopis, B., Robidou, P., Tissot, N., Pinna, B., Gougis, P., Aubart, F. C., et al. (2021). Development and Clinical Validation of a Simple and Fast UPLC-ESI-MS/MS Method for Simultaneous Quantification of Nine Kinase Inhibitors and Two Antiandrogen Drugs in Human Plasma: Interest for Their Therapeutic Drug Monitoring. *J. Pharm. Biomed. Anal.* 197, 113968. doi:10.1016/j.jpba.2021.113968

Lombardo, L. J., Lee, F. Y., Chen, P., Norris, D., Barrish, J. C., Behnia, K., et al. (2004). Discovery of N-(2-chloro-6-methyl- Phenyl)-2-(6-(4-(2-Hydroxyethyl)- Piperazin-1-Yl)-2-Methylpyrimidin-4- Ylamino)thiazole-5-Carboxamide (BMS-354825), a Dual Src/Abl Kinase Inhibitor with Potent Antitumor Activity in Preclinical Assays. *J. Med. Chem.* 47, 6658–6661. doi:10.1021/jm049486a

Lubach, J. W., Chen, J. Z., Hau, J., Imperio, J., Coraggio, M., Liu, L., et al. (2013). Investigation of the Rat Model for Preclinical Evaluation of pH-dependent Oral Absorption in Humans. *Mol. Pharm.* 10, 3997–4004. doi:10.1021/mp400283j

Luo, F. R., Barrett, Y. C., Yang, Z., Camuso, A., Mcglinchey, K., Wen, M. L., et al. (2008). Identification and Validation of Phospho-SRC, a Novel and Potential Pharmacodynamic Biomarker for Dasatinib (SPRYCEL), a Multi-Targeted Kinase Inhibitor. *Cancer Chemother. Pharmacol.* 62, 1065–1074. doi:10.1007/s00280-008-0699-5

Luo, F. R., Yang, Z., Camuso, A., Smykla, R., Mcglinchey, K., Fager, K., et al. (2006a). Dasatinib (BMS-354825) Pharmacokinetics and Pharmacodynamic Biomarkers in Animal Models Predict Optimal Clinical Exposure. *Clin. Cancer Res.* 12, 7180–7186. doi:10.1158/1078-0432.CCR-06-1112

Luo, F. R., Yang, Z., Camuso, A., Smykla, R., Mcglinchey, K., Fager, K., et al. (2006b). Dasatinib (BMS-354825) Pharmacokinetics and Pharmacodynamic Biomarkers in Animal Models Predict Optimal Clinical Exposure. *Clin. Cancer Res.* 12, 7180–7186. doi:10.1158/1078-0432.CCR-06-1112

Maher, H. M., Alzoman, N. Z., Shehata, S. M., and Abanmy, N. O. (2018). Validated UPLC-MS/MS Method for the Quantification of Dasatinib in Plasma: Application to Pharmacokinetic Interaction Studies with Nutraceuticals in Wistar Rats. *PLoS One* 13, e0199208. doi:10.1371/journal.pone.0199208

Matsuoka, A., Takahashi, N., Miura, M., Niioka, T., Kawakami, K., Matsunaga, T., et al. (2012). H2-receptor Antagonist Influences Dasatinib Pharmacokinetics in a Patient with Philadelphia-positive Acute Lymphoblastic Leukemia. *Cancer Chemother. Pharmacol.* 70, 351–352. doi:10.1007/s00280-012-1900-4

Merienne, C., Rousset, M., Ducint, D., Castaing, N., Titier, K., Molimard, M., et al. (2018). High Throughput Routine Determination of 17 Tyrosine Kinase Inhibitors by LC-MS/MS. *J. Pharm. Biomed. Anal.* 150, 112–120. doi:10.1016/j.jpba.2017.11.060

Mikus, G., and Foerster, K. I. (2017). Role of CYP3A4 in Kinase Inhibitor Metabolism and Assessment of CYP3A4 Activity. *Transl. Cancer Res.* 6, S1592–S1599. doi:10.21037/tcr.2017.09.10

Miura, M., and Takahashi, N. (2019). Management Using the Plasma Concentration of Tyrosine Kinase Inhibitors for the Treatment of Chronic Myelogenous Leukemia: an Update. *Rinsho Ketsueki* 60, 1140–1147. doi:10.11406/rinketsu.60.1140

Miura, M., and Takahashi, N. (2016). Routine Therapeutic Drug Monitoring of Tyrosine Kinase Inhibitors by HPLC-UV or LC-MS/MS Methods. *Drug Metab. Pharmacokinet.* 31, 12–20. doi:10.1016/j.dmpk.2015.09.002

Mizuta, S., Sawa, M., Tsurumi, H., Matsumoto, K., Miyao, K., Hara, T., et al. (2018). Plasma Concentrations of Dasatinib Have a Clinical Impact on the Frequency of Dasatinib Dose Reduction and Interruption in Chronic Myeloid Leukemia: an Analysis of the DARIA 01 Study. *Int. J. Clin. Oncol.* 23, 980–988. doi:10.1007/s10147-018-1300-9

Mukai, Y., Yoshida, T., Kondo, T., Inotsume, N., and Toda, T. (2020). Novel High-Performance Liquid Chromatography-Tandem Mass Spectrometry Method for Simultaneous Quantification of BCR-ABL and Bruton's Tyrosine Kinase Inhibitors and Their Three Active Metabolites in Human Plasma. *J. Chromatogr. B Analyt Technol. Biomed. Life Sci.* 1137, 121928. doi:10.1016/j.jchromb.2019.121928

Mustjoki, S., Auvinen, K., Kreutzman, A., Rousselot, P., Hernesniemi, S., Melo, T., et al. (2013). Rapid Mobilization of Cytotoxic Lymphocytes Induced by Dasatinib Therapy. *Leukemia* 27, 914–924. doi:10.1038/leu.2012.348

O'hare, T., Eide, C. A., Agarwal, A., Adrian, L. T., Zabriskie, M. S., Mackenzie, R. J., et al. (2013). Threshold Levels of ABL Tyrosine Kinase Inhibitors Retained in Chronic Myeloid Leukemia Cells Determine Their Commitment to Apoptosis. *Cancer Res.* 73, 3356–3370. doi:10.1158/0008-5472.CAN-12-3904

Orr, J. M., Abbott, F. S., Farrell, K., Ferguson, S., Sheppard, I., and Godolphin, W. (1982). Interaction between Valproic Acid and Aspirin in Epileptic Children: Serum Protein Binding and Metabolic Effects. *Clin. Pharmacol. Ther.* 31, 642–649. doi:10.1038/clpt.1982.89

Pape, E., Michel, D., Scala-Bertola, J., Schiestel, T., Harlé, A., Bouchet, S., et al. (2016). Effect of Esomeprazole on the Oral Absorption of Dasatinib in a Patient with Philadelphia-positive Acute Lymphoblastic Leukemia. *Br. J. Clin. Pharmacol.* 81, 1195–1196. doi:10.1111/bcp.12895

Pauli-Magnus, C., Rekersbrink, S., Klotz, U., and Fromm, M. F. (2001). Interaction of Omeprazole, Lansoprazole and Pantoprazole with P-Glycoprotein. *Naunyn Schmiedebergs Arch. Pharmacol.* 364, 551–557. doi:10.1007/s00210-001-0489-7

Polli, J. W., Olson, K. L., Chism, J. P., John-Williams, L. S., Yeager, R. L., Woodard, S. M., et al. (2009). An Unexpected Synergist Role of P-Glycoprotein and Breast Cancer Resistance Protein on the central Nervous System Penetration of the Tyrosine Kinase Inhibitor Lapatinib (N-{3-chloro-4-[(3-fluorobenzyl)oxy]phenyl}-6-[5-({[2-(methylsulfonyl)ethyl]amino}methyl)-2-furyl]-4-quinazolinamine; GW572016). *Drug Metab. Dispos* 37, 439–442. doi:10.1124/dmd.108.024646

Porkka, K., Koskenvesa, P., Lundán, T., Rimpiläinen, J., Mustjoki, S., Smykla, R., et al. (2008). Dasatinib Crosses the Blood-Brain Barrier and Is an Efficient Therapy for central Nervous System Philadelphia Chromosome-Positive Leukemia. *Blood* 112, 1005–1012. doi:10.1182/blood-2008-02-140665

Rousselot, P., Mollica, L., Guilhot, J., Guerci, A., Nicolini, F. E., Etienne, G., et al. (2021). Dasatinib Dose Optimisation Based on Therapeutic Drug Monitoring Reduces Pleural Effusion Rates in Chronic Myeloid Leukaemia Patients. *Br. J. Haematol.* 194, 393–402. doi:10.1111/bjh.17654

Shah, N. P., Kantarjian, H. M., Kim, D. W., Réa, D., Dorlhiac-Llacer, P. E., Milone, J. H., et al. (2008a). Intermittent Target Inhibition with Dasatinib 100 Mg once

Daily Preserves Efficacy and Improves Tolerability in Imatinib-Resistant and -Intolerant Chronic-phase Chronic Myeloid Leukemia. *J. Clin. Oncol.* 26, 3204–3212. doi:10.1200/JCO.2007.14.9260

Shah, N. P., Kasap, C., Weier, C., Balbas, M., Nicoll, J. M., Bleickardt, E., et al. (2008b). Transient Potent BCR-ABL Inhibition Is Sufficient to Commit Chronic Myeloid Leukemia Cells Irreversibly to Apoptosis. *Cancer Cell* 14, 485–493. doi:10.1016/j.ccr.2008.11.001

Shah, N. P., Kim, D. W., Kantarjian, H., Rousselot, P., Llacer, P. E., Enrico, A., et al. (2010). Potent, Transient Inhibition of BCR-ABL with Dasatinib 100 Mg Daily Achieves Rapid and Durable Cytogenetic Responses and High Transformation-free Survival Rates in Chronic Phase Chronic Myeloid Leukemia Patients with Resistance, Suboptimal Response or Intolerance to Imatinib. *Haematologica* 95, 232–240. doi:10.3324/haematol.2009.011452

Shah, N. P., Rousselot, P., Schiffer, C., Rea, D., Cortes, J. E., Milone, J., et al. (2016). Dasatinib in Imatinib-Resistant or -intolerant Chronic-phase, Chronic Myeloid Leukemia Patients: 7-year Follow-Up of Study CA180-034. *Am. J. Hematol.* 91, 869–874. doi:10.1002/ajh.24423

Skoglund, K., Moreno, S. B., Baytar, M., Jönsson, J. I., and Gréen, H. (2013). ABCB1 Haplotypes Do Not Influence Transport or Efficacy of Tyrosine Kinase Inhibitors *In Vitro*. *Pharmgenomics Pers Med.* 6, 63–72. doi:10.2147/PGPM.S45522

Snead, J. L., O'hare, T., Adrian, L. T., Eide, C. A., Lange, T., Druker, B. J., et al. (2009). Acute Dasatinib Exposure Commits Bcr-abl-dependent Cells to Apoptosis. *Blood* 114, 3459–3463. doi:10.1182/blood-2007-10-113969

Sumimoto, T., Nakahara, R., Suzuki, Y., Tanaka, R., Yoshida, N., Ogata, M., et al. (2021). Development of a Sensitive and High-Throughput Assay for Simultaneous Quantification of Five Tyrosine Kinase Inhibitors and Two Active Metabolites in Human Plasma Using Ultra-high Performance Liquid Chromatography Coupled to Tandem Mass Spectrometry. *Ther. Drug Monit.* doi:10.1097/ftd.0000000000000922

Takahashi, N., Miura, M., Niioka, T., and Sawada, K. (2012a). Influence of H2-Receptor Antagonists and Proton Pump Inhibitors on Dasatinib Pharmacokinetics in Japanese Leukemia Patients. *Cancer Chemother. Pharmacol.* 69, 999–1004. doi:10.1007/s00280-011-1797-3

Takahashi, N., Miura, M., Scott, S. A., Niioka, T., and Sawada, K. (2012b). Pharmacokinetics of Dasatinib for Philadelphia-positive Acute Lymphocytic Leukemia with Acquired T315I Mutation. *J. Hematol. Oncol.* 5, 23. doi:10.1186/1756-8722-5-23

Talpaz, M., Shah, N. P., Kantarjian, H., Donato, N., Nicoll, J., Paquette, R., et al. (2006). Dasatinib in Imatinib-Resistant Philadelphia Chromosome-Positive Leukemias. *N. Engl. J. Med.* 354, 2531–2541. doi:10.1056/NEJMoa055229

Tsume, Y., Takeuchi, S., Matsui, K., Amidon, G. E., and Amidon, G. L. (2015). *In Vitro* dissolution Methodology, Mini-Gastrointestinal Simulator (mGIS), Predicts Better *In Vivo* Dissolution of a Weak Base Drug, Dasatinib. *Eur. J. Pharm. Sci.* 76, 203–212. doi:10.1016/j.ejps.2015.05.013

Uchiyama, T., Sato, N., Narita, M., Yamahira, A., Iwabuchi, M., Furukawa, T., et al. (2013). Direct Effect of Dasatinib on Proliferation and Cytotoxicity of Natural Killer Cells in *In Vitro* Study. *Hematol. Oncol.* 31, 156–163. doi:10.1002/hon.2034

Vainstein, V., Eide, C. A., O'Hare, T., Shukron, O., and Druker, B. J. (2013). Integrating *In Vitro* Sensitivity and Dose-Response Slope Is Predictive of Clinical Response to ABL Kinase Inhibitors in Chronic Myeloid Leukemia. *Blood* 122, 3331–3334. doi:10.1182/blood-2012-08-452409

Verheijen, R. B., Yu, H., Schellens, J. H. M., Beijnen, J. H., Steeghs, N., and Huitema, A. D. R. (2017). Practical Recommendations for Therapeutic Drug Monitoring of Kinase Inhibitors in Oncology. *Clin. Pharmacol. Ther.* 102, 765–776. doi:10.1002/cpt.787

Verougstraete, N., Stove, V., Verstraete, A. G., and Stove, C. (2021). Quantification of Eight Hematological Tyrosine Kinase Inhibitors in Both Plasma and Whole Blood by a Validated LC-MS/MS Method. *Talanta* 226, 122140. doi:10.1016/j.talanta.2021.122140

Wang, X., Roy, A., Hochhaus, A., Kantarjian, H. M., Chen, T. T., and Shah, N. P. (2013). Differential Effects of Dosing Regimen on the Safety and Efficacy of Dasatinib: Retrospective Exposure-Response Analysis of a Phase III Study. *Clin. Pharmacol.* 5, 85–97. doi:10.2147/CPAA.S42796

Wang, X., Hochhaus, A., Kantarjian, H. M., Agrawal, S., Roy, A., Pfister, M., et al. (2008). Dasatinib Pharmacokinetics and Exposure-Response (E-R): Relationship to Safety and Efficacy in Patients (Pts) with Chronic Myeloid Leukemia (CML). *J. Clin. Oncol.* 26, 3590. doi:10.1200/jco.2008.26.15_suppl.3590

Weersma, R. K., Zhernakova, A., and Fu, J. (2020). Interaction between Drugs and the Gut Microbiome. *Gut* 69, 1510–1519. doi:10.1136/gutjnl-2019-320204

Widmer, N., Bardin, C., Chatelut, E., Paci, A., Beijnen, J., Levêque, D., et al. (2014). Review of Therapeutic Drug Monitoring of Anticancer Drugs Part Two - Targeted Therapies. *Eur. J. Cancer* 50, 2020–2036. doi:10.1016/j.ejca.2014.04.015

Wojnicz, A., Colom-Fernández, B., Steegmann, J. L., Muñoz-Calleja, C., Abad-Santos, F., and Ruiz-Nuño, A. (2017). Simultaneous Determination of Imatinib, Dasatinib, and Nilotinib by Liquid Chromatography-Tandem Mass Spectrometry and its Application to Therapeutic Drug Monitoring. *Ther. Drug Monit.* 39, 252–262. doi:10.1097/FTD.0000000000000406

Yago, M. R., Frymoyer, A., Benet, L. Z., Smelick, G. S., Frassetto, L. A., Ding, X., et al. (2014). The Use of Betaine HCl to Enhance Dasatinib Absorption in Healthy Volunteers with Rabeprazole-Induced Hypochlorhydria. *Aaps j* 16, 1358–1365. doi:10.1208/s12248-014-9673-9

Yu, H., Steeghs, N., Nijenhuis, C. M., Schellens, J. H., Beijnen, J. H., and Huitema, A. D. (2014). Practical Guidelines for Therapeutic Drug Monitoring of Anticancer Tyrosine Kinase Inhibitors: Focus on the Pharmacokinetic Targets. *Clin. Pharmacokinet.* 53, 305–325. doi:10.1007/s40262-014-0137-2

Yu, M., Liu, M., Zhang, W., and Ming, Y. (2018). Pharmacokinetics, Pharmacodynamics and Pharmacogenetics of Tacrolimus in Kidney Transplantation. *Curr. Drug Metab.* 19, 513–522. doi:10.2174/1389200219666180129151948

Zeng, J., Cai, H. L., Jiang, Z. P., Wang, Q., Zhu, Y., Xu, P., et al. (2017). A Validated UPLC-MS/MS Method for Simultaneous Determination of Imatinib, Dasatinib and Nilotinib in Human Plasma. *J. Pharm. Anal.* 7, 374–380. doi:10.1016/j.jpha.2017.07.009

Zhang, W., Chang, Y. Z., Kan, Q. C., Zhang, L. R., Li, Z. S., Lu, H., et al. (2010). CYP3A4*1G Genetic Polymorphism Influences CYP3A Activity and Response to Fentanyl in Chinese Gynecologic Patients. *Eur. J. Clin. Pharmacol.* 66, 61–66. doi:10.1007/s00228-009-0726-4

Zhou, H. S., Dai, M., Wei, Y., Wang, Q., Xu, N., Yin, C., et al. (2013). Isolated central Nervous System Relapse in Patient with Blast-Crisis Chronic Myeloid Leukemia in Durable Complete Cytogenetic Remission on Dasatinib Treatment: Pharmacokinetics and ABL Mutation Analysis in Cerebrospinal Fluid. *Leuk. Lymphoma* 54, 1557–1559. doi:10.3109/10428194.2012.745933

Conflict of Interest: The authors declare that the research was conducted in the absence of any commercial or financial relationships that could be construed as a potential conflict of interest.

Publisher's Note: All claims expressed in this article are solely those of the authors and do not necessarily represent those of their affiliated organizations, or those of the publisher, the editors, and the reviewers. Any product that may be evaluated in this article, or claim that may be made by its manufacturer, is not guaranteed or endorsed by the publisher.

frontiers in Oncology

SYSTEMATIC REVIEW
published: 15 December 2021
doi: 10.3389/fonc.2021.781386

MTHFR Polymorphism Is Associated With Severe Methotrexate-Induced Toxicity in Osteosarcoma Treatment

Wenchao Zhang[1,2†], *Zhongyue Liu*[1,2†], *Zhimin Yang*[1,2], *Chengyao Feng*[1], *Xiaowen Zhou*[3], *Chao Tu*[1,2*] *and Zhihong Li*[1,2*]

[1] Department of Orthopaedics, The Second Xiangya Hospital, Central South University, Changsha, China, [2] Hunan Key Laboratory of Tumor Models and Individualized Medicine, The Second Xiangya Hospital, Central South University, Changsha, China, [3] Xiangya School of Medicine, Central South University, Changsha, China

Background: Previous studies have revealed the critical role of methylene tetrahydrofolate reductase (MTHFR) polymorphisms in response to high-dose methotrexate (MTX)-induced toxicity in osteosarcoma patients. However, the conclusions remain controversial. In this setting, we performed a meta-analysis to determine their association more precisely.

Method: Eligible studies were searched and screened in PubMed, Web of Science, Cochrane Library, Clinical-Trials.gov, Embase, and China National Knowledge Infrastructure (CNKI) following specific inclusion and exclusion criteria. The required information was retrieved and collected for subsequent meta-analysis. Association between MTHFR polymorphism and MTX toxicity was evaluated by odds ratios (ORs).

Results: Seven studies containing 585 patients were enrolled and analyzed in this meta-analysis. Overall, the MTX related grade 3-4 liver toxicity was significantly associated with MTHFR rs1801133 allele (T *vs.* C: OR=1.61, 95%CI=1.07-2.42, P=0.024), homozygote (TT *vs.* CC: OR=2.11, 95%CI=1.06-4.21, P=0.011), and dominant genetic model (TT/TC *vs.* CC: OR=3.15, 95%CI=1.30-7.60, P=0.035) in Asian population. Meanwhile, close associations between MTX mediated grade 3-4 mucositis and MTHFR rs1801133 polymorphism were identified in allele contrast (T *vs.* C: OR=2.28, 95%CI=1.49-3.50, P<0.001), homozygote comparison (TT *vs.* CC: OR=4.07, 95%CI=1.76-9.38, P=0.001), heterozygote comparison (TC *vs.* CC: OR=2.55, 95%CI=1.20-5.42, P=0.015), recessive genetic model (TT *vs.* TC/CC: OR=2.09, 95%CI=1.19-3.67, P=0.010), and dominant genetic model (TT/TC *vs.* CC: OR=2.97, 95%CI=1.48-5.96, P=0.002). Additionally, kidney toxicity was corelated with the heterozygote comparison (TC *vs.* CC: OR=2.63, 95%CI=1.31-5.29, P=0.007) of rs1801133 polymorphism.

Conclusion: The MTHFR rs1801133 polymorphism was significantly associated with severer liver toxicity induced by high-dose MTX treatment in the Asian population. In the meantime, patients with MTHFR rs1801133 polymorphism were predisposed to MTX-related mucositis.

Keywords: MTHFR, polymorphism, osteosarcoma, methotrexate, toxicity

OPEN ACCESS

Edited by:
Yao Liu,
Daping Hospital, China

Reviewed by:
Xiaoyang Li,
Chinese Academy of Medical Sciences and Peking Union Medical College, China
Bin Yuan,
Anhui Medical University, China

***Correspondence:**
Chao Tu
tuchao@csu.edu.cn
Zhihong Li
lizhihong@csu.edu.cn

[†]These authors have contributed equally to this work

Specialty section:
This article was submitted to Pharmacology of Anti-Cancer Drugs, a section of the journal Frontiers in Oncology

Received: *22 September 2021*
Accepted: *17 November 2021*
Published: *15 December 2021*

Citation:
Zhang W, Liu Z, Yang Z, Feng C, Zhou X, Tu C and Li Z (2021) MTHFR Polymorphism Is Associated With Severe Methotrexate-Induced Toxicity in Osteosarcoma Treatment. Front. Oncol. 11:781386. doi: 10.3389/fonc.2021.781386

INTRODUCTION

Primarily occurring in adolescents, osteosarcoma has been the second malignancy among young teenagers (1) and the most prevalent primary osseous tumor with an annual incidence of 1~3 cases per million worldwide (2). It is characterized by the production of osteoid tissue and immature bone mainly in the metaphysis of long bones (3). Though the prognosis of osteosarcoma has improved significantly over the past decades, outcomes for most patients remain variable, under the influence of multiple elements, for instance, the genetic and epigenetic background (4–7).

The existing treatment for osteosarcoma involves neoadjuvant chemotherapy, lesion resection, and chemotherapy. Adjuvant or neoadjuvant chemotherapy has substantially improved the long-term survival rate since the early 1970s (8). The common chemotherapy regimens comprise high-dose methotrexate (MTX), doxorubicin, ifosfamide, cisplatin, and vincristine. However, the chemotherapy-related toxicity and adverse effects remain intractable and unpredictable, which are the main obstacles that lead to dose decrease and even interruption or discontinuation of chemotherapy. MTX, an inhibitor of dihydrofolate reductase, plays a role in interrupting the DNA synthesis and normal cellular metabolism in both the cancerous and normal cells (9). Previous studies have reported a high incidence of medication toxicity during high-dose MTX treatment for osteosarcoma patients (10, 11). Adverse events induced by high-dose MTX (>1g/m^2) include renal insufficiency, hepatocellular damage, nausea/vomiting, skin/subcutaneous induration, anemia, mucositis, etc. (10). The presence of toxicity is influenced by multiple factors such as age, gender, ethnicity, and genetic background (9, 12). In this setting, patients may benefit from individualized chemotherapy that is tailored according to their disease characteristics and background.

Methylene tetrahydrofolate reductase (MTHFR) is a crucial enzyme in the folate metabolism and DNA synthesis regulatory network, which promotes the conversion of 5,10-methylenetetrahydrofolate to 5-methyltetrahydrofolate (13). Until now, two types of polymorphisms have been identified for MTHFR, containing rs1801133 and rs1801131. Rs1801133 polymorphism is characterized by the C to T substitution at nucleotide position 677, leading to amino acid change from alanine to valine, which decreases the enzymatic activity significantly by more than 30% (14). While nucleotide 1289 A is substituted with C in rs1801131. Studies have shed light on the relationship between different MTHFR variants and MTX treatment toxicity in various diseases. For instance, Lv et al. have shown more frequent MTX-related side effects in MTHFR-TT carriers compared with MTHFR-677CC in rheumatoid arthritis (RA) patients (15). The evidence also indicated that the MTHFR 677T mutation decreased the chemosensitivity of breast cancer cells to MTX (16). And the MTHFR C677T polymorphism was remarkably associated with relapse after MTX treatment in pediatric acute lymphoblastic leukemia (ALL) (17). Meanwhile, several studies have revealed the association between MTHFR variants and MTX toxicity in osteosarcoma (18–24). However, the current conclusions remain controversial. Therefore, we conducted this meta-analysis, with the aim to reach a more precise consensus.

MATERIALS AND METHODS

Search Strategy

This meta-analysis follows the instruction of Preferred Reporting Items for Systematic Reviews and Meta-Analyses (PRISMA) guidelines (25). Studies related to the meta-analysis topic were retrieved from PubMed, Web of Science, Cochrane Library, Clinical-Trials.gov, Embase, and China National Knowledge Infrastructure (CNKI) under the search terms "MTHFR and (polymorphism or variant or mutation) and osteosarcoma" updated on July 26, 2021. Two researchers (WCZ, ZYL) screened and selected the eligible studies independently in all the research hits by reviewing their title, abstract or full text.

Inclusion and Exclusion Criteria

All enrolled studies were sorted according to the specific inclusion and exclusion criteria. The inclusion criteria include: (1) the case control study, (2) assessment of the association between MTHFR polymorphism and MTX toxicity in the treatment of osteosarcoma, (3) containing available allele and genotype distribution information to calculate odds ratios (ORs) and 95% confidence interval (CI). Accordingly, the exclusion criteria were: (1) studies with duplicate data, (2) articles such as conference abstracts, letters, reviews, case reports, sequencing data, bioinformatic analyses, and meta-analyses, (3) studies without extractable toxicity response grouped by detailed genotyping.

Data extraction and Quality Evaluation

Two independent researchers (WCZ, ZYL) extracted all needed information from the included studies, comprising the first author's name, published year, country, ethnicity, genotyping methods, sample size, investigated SNPs, MTX dose, ORs, 95% CI for different genotype (allele contrast T vs. C, homozygote comparison TT vs. CC, heterozygote comparison TC vs. CC, recessive genetic model TT vs. TC/CC, and dominant genetic model TT/TC vs. CC), and MTX related toxicity (liver toxicity, kidney toxicity, mucositis, and anemia). The result was then checked and confirmed by another researcher (ZMY). The quality of each enrolled study was assessed using the Newcastle-Ottawa Scale (NOS) as previously described (26).

Statistical Analyses

The ORs and the corresponding 95% CI were calculated to assess the relationship between MTHFR polymorphisms and MTX toxicity. An OR>1 connoted a risk factor for the analyzed outcome, while an OR<1 indicated a protective factor. Four MTX-related adverse events were evaluated under different genotype contrasts. The ORs and 95% CI from all enrolled studies were pooled by using the Stata software (Version 12.0; StataCorp LP, College Station, TX, USA). The fixed model (Mantel-Haenszel method) was used if the heterogeneity was

not significant (I^2<50%, P>0.05), otherwise the random model (DerSimonian and Laird method) was adopted as previously described (27). For several analyses with great heterogeneity, we performed a subgroup analysis to determine the sources of heterogeneity including sample size, genotyping method, and ethnicity.

Meanwhile, the stability of the results was evaluated by sensitivity analysis, which determined the impact of every single study on the pooled results through recalculation after deleting each one. Egger's linear regression test and Begg's test were utilized to investigate the potential publication bias. An asymmetric plot indicated the possibility of publication bias. Statistical significance was defined as p<0.05 in all statistical analyses.

RESULTS

Enrolled Studies and Quality Assessment

Overall, 88 search results were identified in multiple databases according to the search strategy. After duplicates removal, there were 49 studies remaining, and 34 records of reviews, bibliometrics, or unrelated to the topic were further excluded. Subsequently, the full text of 15 studies were screened and 8 studies were obviated because of the lack of extractable clinical data. Finally, seven eligible studies remained for the next step analysis. PRISMA flowchart showed the detailed processes (**Figure 1**). The NOS scores of the included studies were all higher than 7, indicating the adequate quality of these researches.

Characteristics of Included Studies

Overall, this meta-analysis has included seven studies containing 585 patients through careful screening (**Figure 1**). Four studies focused on the rs1801133 and rs1801131 polymorphisms while three only mentioned the rs1801133. Since data for rs1801131 polymorphism were unextractable in three studies, we can only analyze the association between rs1801133 polymorphism and MTX toxicity. Of all studies, four principal adverse events were construed, comprising liver toxicity, kidney toxicity, mucositis, and anemia. As to the ethnicity, three studies investigated the Caucasian population and four studies focused on the Asian population. Genotyping methods included Microarray,

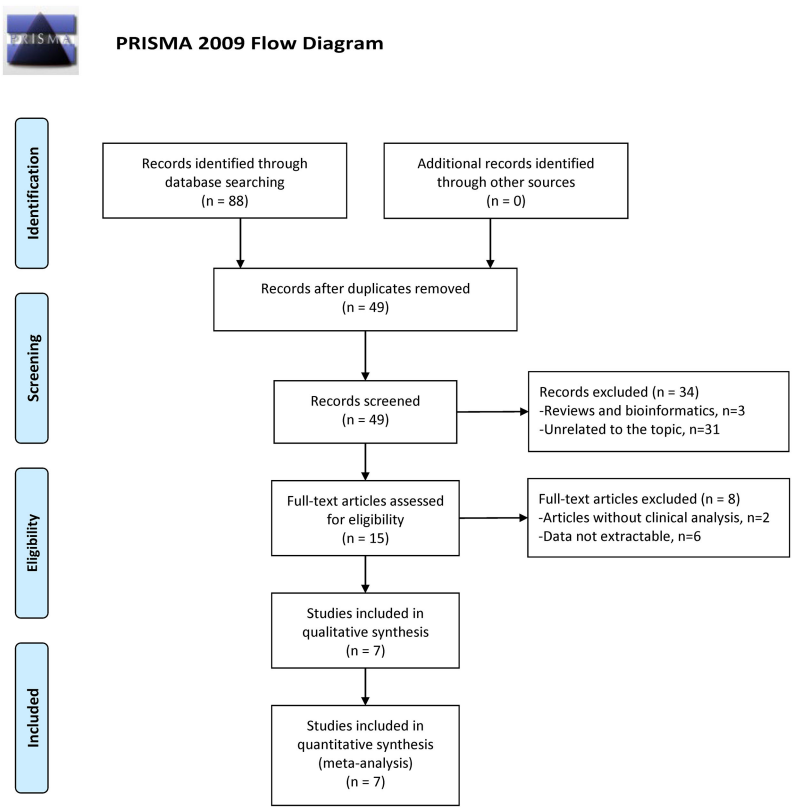

FIGURE 1 | Flow diagram for study identification with criteria in the meta-analysis (28).

MassARRAY, PCR, and TaqMan SNP Genotyping Assay. The sample size ranged from 37 to 210 with a mean size of 83.57. The MTX dosage was 12 g/m^2 in most cases while one study administered 200mg/kg of MTX. More specific characteristics of enrolled studies were listed in **Table 1**.

Quantitative Synthesis Revealing Toxicity Related Genotype

To demonstrate the association between MTX toxicity and various genotype, ORs and 95% CI from different studies were incorporated (data were shown in **Table 2**). Summarily, the

TABLE 1 | Characteristics of all enrolled studies.

Author	Year	Country	Ethnicity	Genotyping methods	Sample size	Investigated SNPs	Methotrexate dose	NOS score
Windsor (19)	2012	United Kingdom	Caucasian	Microarray	60	rs1801133, rs1801131	12 g/m^2	7
Jabeen (20)	2015	Norway	Caucasian	MassARRAY	62	rs1801133	12 g/m^2 (mean)	8
Park (21)	2016	Korea	Asian	MassARRAY	37	rs1801133, rs1801131	12 g/m^2	7
Lambrecht (22)	2017	Belgium	Caucasian	PCR	48	rs1801133	12 g/m^2	8
Xie (23)	2018	China	Asian	RT-PCR	59	rs1801133, rs1801131	10-12 g/m^2 week twice	8
Xu (24)	2018	China	Asian	TaqMan SNP Genotyping Assay	109	rs1801133, rs1801131	10 g/m^2/d	8
Ren (29)	2011	China	Asian	RT-PCR	210	rs1801133	200mg/kg	7

TABLE 2 | Meta-analysis of the MTHFR polymorphisms with MTX-related toxicity.

Comparison	Ethnicity	N	OR	Low 95%CI	High 95% CI	P	Mode	Heterogeneity			Sensitive analysis	Publication bias	
								χ^2	P	I^2		Begg's Test p-value	Egger's test p-value
Liver toxicity													
TT vs CC	Caucasian	1	0.81	0.38	1.71	NA	NA	NA	NA	NA	NA	1.000	0.697
	Asian	3	3.15	1.30	7.60	0.011	Fixed	0.61	0.739	0.0%	Good		
	Overall	4	2.04	0.94	4.41	0.218	Fixed	4.55	0.207	34.1%	Good		
TC vs CC	Caucasian	1	0.31	0.10	0.96	NA	NA	NA	NA	NA	NA	0.734	0.718
	Asian	3	1.87	0.90	3.89	0.095	Fixed	3.81	0.149	47.5%	Good		
	Overall	4	1.23	0.36	4.20	0.746	Random	10.64	0.014	71.8%	Good		
TT vs. TC/CC	Caucasian	2	1.03	0.40	2.65	0.945	Fixed	0.19	0.663	0.0%	Good	1.000	0.856
	Asian	3	1.58	0.39	6.45	0.521	Random	6.42	0.04	68.9%	Good		
	Overall	5	1.38	0.78	2.42	0.265	Fixed	7.16	0.128	44.2%	Good		
TT/TC vs. CC	Caucasian	1	0.35	0.13	0.97	NA	NA	NA	NA	NA	NA	0.734	0.836
	Asian	3	2.11	1.06	4.21	0.043	Fixed	1.04	0.595	0.0%	Good		
	Overall	4	1.26	0.43	3.67	0.035	Random	9.25	0.024	67.6%	Good		
T vs C	Caucasian	1	0.81	0.38	1.72	NA	NA	NA	NA	NA	NA	1.000	0.477
	Asian	3	1.61	1.07	2.42	0.024	Fixed	1.72	0.424	0.0%	Good		
	Overall	4	1.37	0.96	1.97	0.085	Fixed	4.17	0.244	28.0%	Good		
Kidney toxicity													
TT vs CC	Overall	4	3.82	0.57	25.78	0.168	Random	12.66	0.005	76.3%	Good	0.734	0.748
TC vs CC	Overall	4	2.63	1.31	5.29	0.007	Fixed	5.57	0.125	47.8%	Good	0.308	0.340
TT vs. TC/CC	Overall	3	1.48	0.20	11.18	0.704	Random	12.23	0.002	83.7%	Good	1.000	0.659
TT/TC vs. CC	Overall	4	3.43	0.93	12.66	0.064	Random	9.46	0.024	68.3%	Good	0.734	0.465
T vs C	Overall	3	1.93	0.43	8.67	0.392	Random	19.87	0.000	89.9%	Good	1.000	0.936
Mucositis													
TT vs CC	Overall	3	4.07	1.76	9.38	0.001	Fixed	0.60	0.739	0.0%	Good	0.296	0.063
TC vs CC	Overall	3	2.55	1.20	5.42	0.015	Fixed	0.11	0.947	0.0%	Good	1.000	0.603
TT vs. TC/CC	Overall	4	2.09	1.19	3.67	0.010	Fixed	3.33	0.344	9.8%	Good	1.000	0.134
TT/TC vs. CC	Overall	3	2.97	1.48	5.96	0.002	Fixed	0.10	0.953	0.0%	Good	1.000	0.385
T vs C	Overall	3	2.28	1.49	3.50	0.000	Fixed	1.67	0.434	0.0%	Good	1.000	0.173
Anemia													
TT vs CC	Overall	2	1.08	0.33	3.51	0.092	Fixed	0.94	0.322	0.0%	NA	NA	NA
TC vs CC	Overall	2	1.26	0.38	4.13	0.890	Random	2.94	0.087	66.0%	NA	NA	NA
TT vs. TC/CC	Overall	3	1.25	0.64	2.45	0.521	Fixed	0.21	0.901	0.0%	Good	1.000	0.441
TT/TC vs. CC	Overall	2	1.10	0.39	3.05	0.992	Random	2.48	0.115	59.7%	NA	NA	NA
T vs C	Overall	2	1.17	0.63	2.16	0.617	Fixed	1.16	0.282	13.5%	NA	NA	NA

NA, Not available.

MTX-related high-level liver toxicity (grade 3–4) was significantly associated with MTHFR rs1801133 polymorphism under allele contrast (T vs. C: OR=1.61, 95%CI=1.07-2.42, P=0.024), homozygote comparison (TT vs. CC: OR=2.11, 95%CI=1.06-4.21, P=0.011), and dominant genetic model (TT/TC vs. CC: OR=3.15, 95%CI=1.30-7.60, P=0.035) in the Asian population but not in the overall population (**Figure 2**). Meanwhile, close relations between MTX mediated high level mucositis (grade 3–4) and MTHFR rs1801133 polymorphism were identified in allele contrast (T vs. C: OR=2.28, 95%CI=1.49-3.50, P<0.001), homozygote comparison (TT vs. CC: OR=4.07, 95%CI=1.76-9.38, P=0.001), heterozygote comparison (TC vs. CC: OR=2.55, 95%CI=1.20-5.42, P=0.015), recessive genetic model (TT vs. TC/CC: OR=2.09, 95%CI=1.19-3.67, P=0.010), and dominant genetic model (TT/TC vs. CC: OR=2.97, 95%CI=1.48-5.96, P=0.002) (**Figure 3**). Additionally, the presence of the TC genotype indicated a high risk of kidney toxicity compared to the CC genotype (TC vs. CC: OR=2.63, 95%CI=1.31-5.29, P=0.007) (**Figure 4**). There was no correlation between rs1801133 polymorphism and MTX-related Anemia (**Figure 5**).

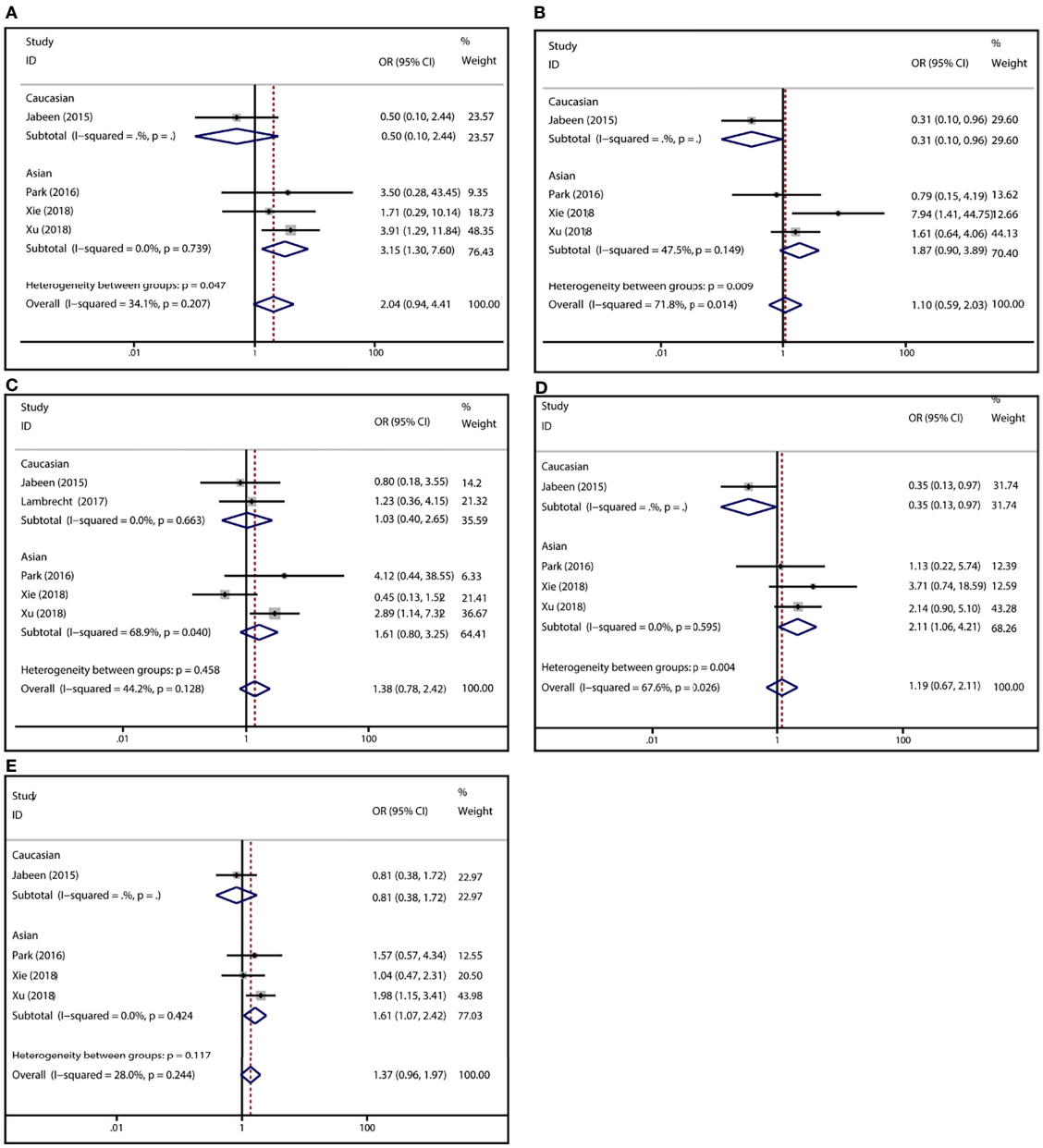

FIGURE 2 | Forest plots for the association between MTX-induced liver toxicity and MTHFR rs1801133 polymorphism. **(A)** homozygote comparison TT vs. CC; **(B)** heterozygote comparison TC vs. CC; **(C)** recessive genetic model TT vs. TC/CC; **(D)** dominant genetic model TT/TC vs. CC; **(E)** allele contrast T vs. C.

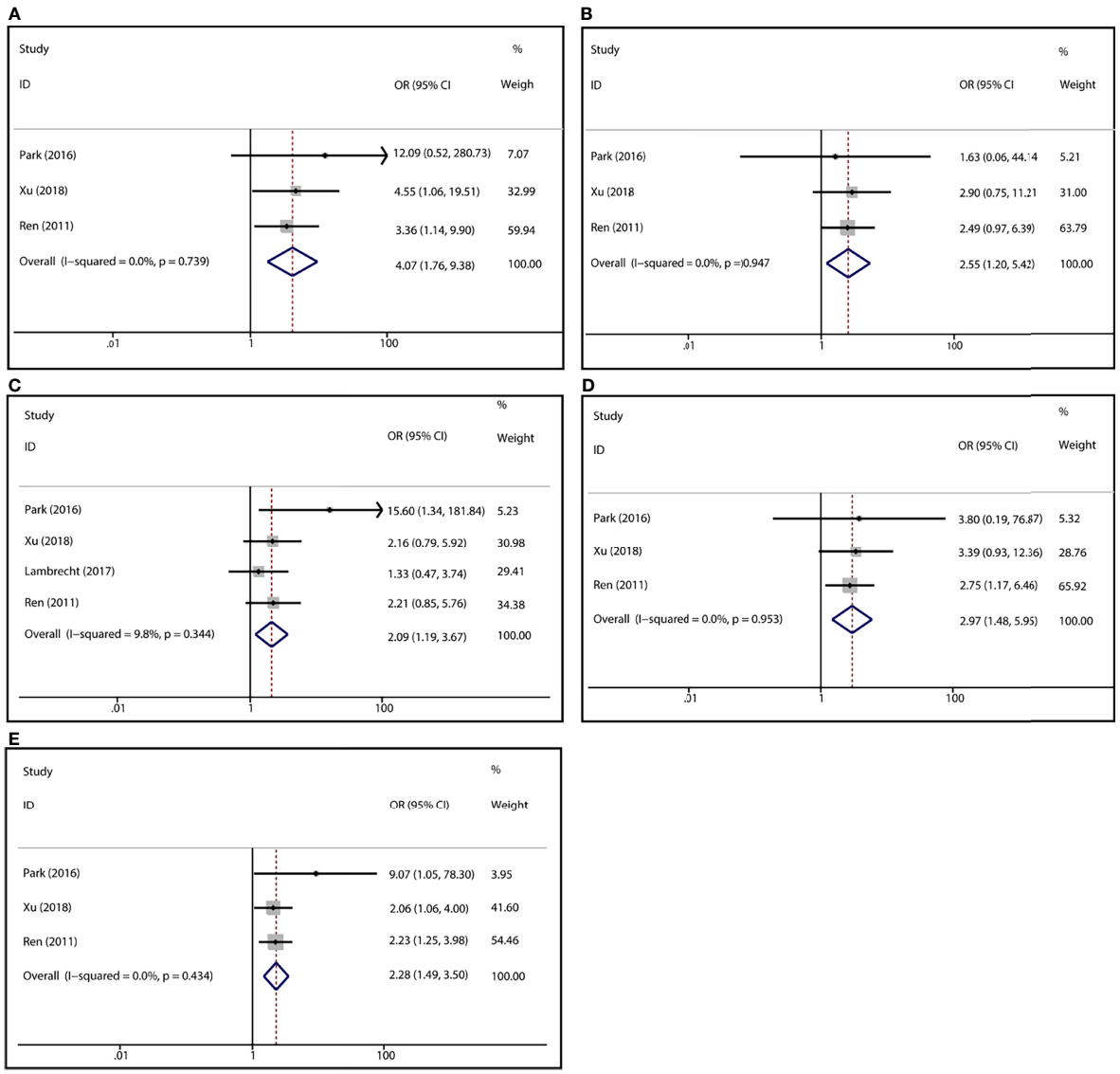

FIGURE 3 | Forest plots for the association between MTX-induced mucositis and MTHFR rs1801133 polymorphism. **(A)** homozygote comparison TT vs. CC; **(B)** heterozygote comparison TC vs. CC; **(C)** recessive genetic model TT vs. TC/CC; **(D)** dominant genetic model TT/TC vs. CC; **(E)** allele contrast T vs. C.

Heterogeneity Analysis

Significant heterogeneity has been identified in rs1801133 polymorphism and liver toxicity. Considering the potential sources of heterogeneity including ethnicity, genotyping method, and sample size, subgroup analysis uncovered that grouping by ethnicity obviously decreased the initial heterogeneity. Meanwhile, remarkable heterogeneity existed in rs1801133 polymorphism and kidney toxicity. Meta-regression was unable to identify the potential source of heterogeneity among various factors containing publication year, ethnicity, genotyping method, and sample size. However, the elimination of one study by Ren et al. could substantially reduce the heterogeneity.

Sensitive Analysis

Sensitive analysis was performed by recalculating the pooled ORs and 95% CI after dislodging each individual study. The removal of any single study did not affect the quantitative results significantly (**Table 2**, **Figure 6**), suggesting the reliability of this analysis.

Publication Bias

We used Egger's test and Begg's test to identify potential publication bias among studies. No evidence of publication bias was found (**Table 2**). And the Begg's test funnel plots did not show obvious asymmetry (**Figure 7**).

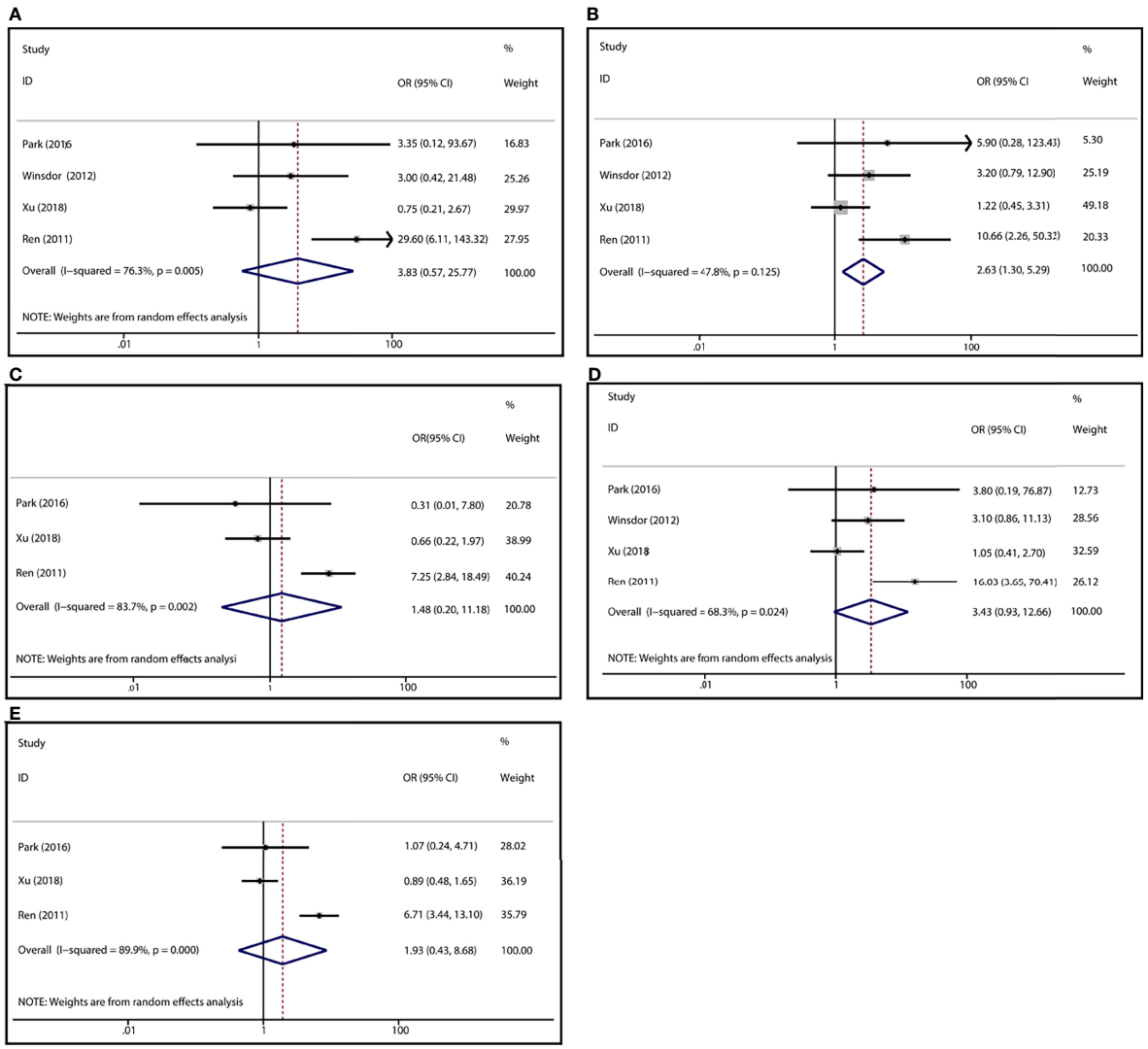

FIGURE 4 | Forest plots for the association between MTX-induced Kidney toxicity and MTHFR rs1801133 polymorphism. **(A)** homozygote comparison TT vs. CC; **(B)** heterozygote comparison TC vs. CC; **(C)** recessive genetic model TT vs. TC/CC; **(D)** dominant genetic model TT/TC vs. CC; **(E)** allele contrast T vs. C.

DISCUSSION

Treatment for osteosarcoma has made substantial progress since the adoption of several effective therapeutic strategies over the past decades, including but not limited to adjuvant or neoadjuvant chemotherapy (30). The backbone for treatment comprises the MTX, cisplatin, doxorubicin, and ifosfamide, which have shown great efficacy in osteosarcoma management (31). However, chemotherapy-related toxicities have contributed to a variety of adverse outcomes, varying highly among patients. In most cases, patients are stratified largely relying on their concrete characteristics such as the clinical manifestations, radiographic features, pathological biopsy, etc. And they are prescribed with a relatively fixed regimen schedule even in those with or without metastases at diagnosis (32), leading to unsatisfied outcome. Fortunately, the biological biomarkers especially genome feature may conduce to more precise stratification and therapeutic optimization. Of the current studies, impact of pharmacogenetics on drug toxicities in osteosarcoma have been largely focused on (33), which includes genes related to DNA repair (34), drug metabolism associated genes (35), and genes involved in drug transport (36).

Although MTX has achieved great clinical success, its unpredictable toxicities such as liver failure, kidney damage, mucositis, hematologic toxicity, anemia, cardiotoxicity, and ototoxicity remain challenging in clinical management, especially in high-dose usage (9, 33). As aforementioned, MTHFR participates in MTX metabolism and its single nucleotide polymorphisms (SNPs) including rs1801133 and rs1801131 may partially determine drug toxicity. Considering

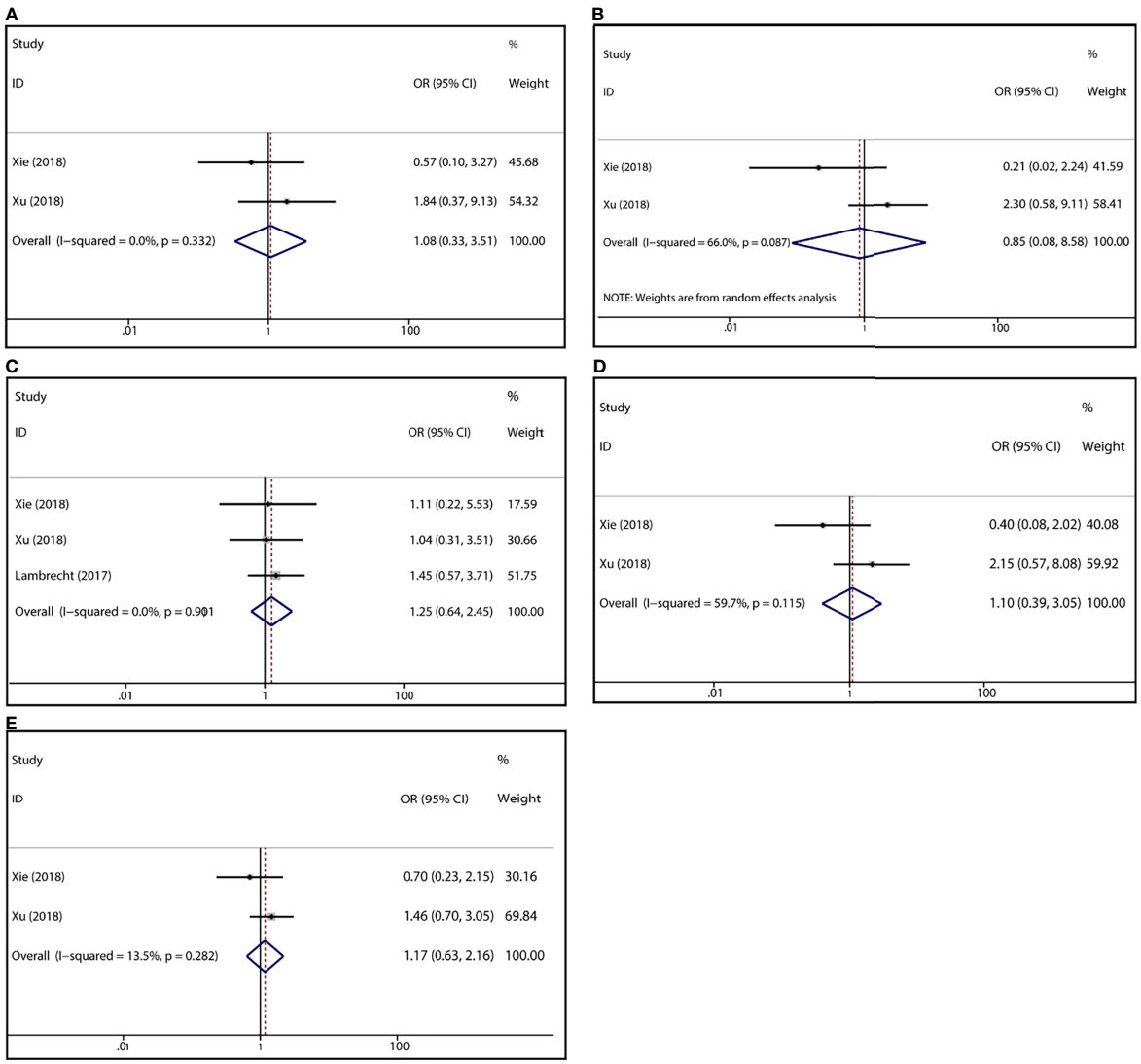

FIGURE 5 | Forest plots for the association between MTX-induced Anemia and MTHFR rs1801133 polymorphism. **(A)** homozygote comparison TT vs. CC; **(B)** heterozygote comparison TC vs. CC; **(C)** recessive genetic model TT vs. TC/CC; **(D)** dominant genetic model TT/TC vs. CC; **(E)** allele contrast T vs. C.

the contradictory results among different studies and the insufficient reliability of single study, we have reviewed the existing studies and conducted a meta-analysis to reduce random error.

In this meta-analysis, we have interrogated the relationship between MTHFR rs1801133 polymorphism and MTX-induced toxicities. The findings suggested that grade 3-4 liver toxicity was significantly associated with rs1801133 polymorphism under various contrasts in the Asian population but not in the overall population, indicating the influence of ethnicity on the toxicity-polymorphism association. Previous studies have shown the inconsistences of MTX-related toxicities in populations from different ethnicities (37). Meanwhile, a significant association was also noticed between grade 3-4 mucositis and MTHFR rs1801133 polymorphism. Patients with C to T variants are more vulnerable to MTX-related mucositis, which was similar to a previous study (38). Particularly, a retrospective cohort study in Chinese pediatric patients revealed the close relevance of MTHFR rs1801133 polymorphism to mucositis (39). In other conditions such as RA and hematological malignancies, a close relationship between MTHFR C677T polymorphism and risk of hepatic or gastrointestinal toxicities has also been demonstrated (38, 40, 41). Additionally, high-grade (grade 3-4) kidney toxicity was correlated with the heterozygote comparison (TC vs. CC) of rs1801133 polymorphism but not in other genotype contrasts. This result may be unreliable due to the high heterogeneity among studies. Further, no association was identified between rs1801133 polymorphism and anemia, which was consistent with the finding in hematological malignancies by Zhao et al. (40).

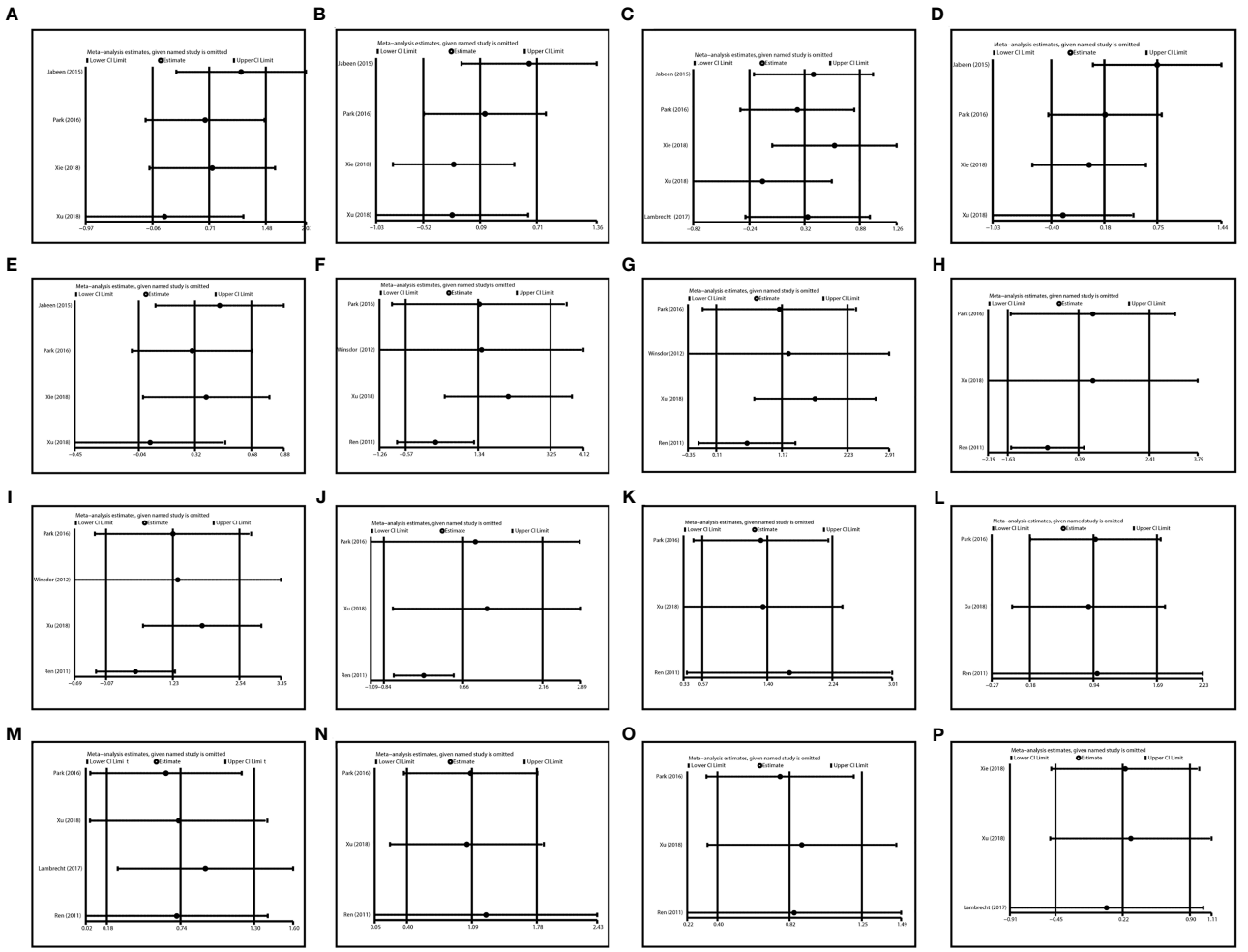

FIGURE 6 | Sensitivity analysis in various comparisons. **(A)** TT vs CC in liver toxicity; **(B)** TC vs CC in liver toxicity; **(C)** TT vs. TC/CC in liver toxicity; **(D)** TT/TC vs. CC in liver toxicity; **(E)** T vs C in liver toxicity; **(F)** TT vs CC in kidney toxicity; **(G)** TC vs CC in kidney toxicity; **(H)** TT vs. TC/CC in kidney toxicity; **(I)** TT/TC vs. CC in kidney toxicity; **(J)** T vs. C in kidney toxicity; **(K)** TT vs CC in Mucositis; **(L)** TC vs CC in Mucositis; **(M)** TT vs. TC/CC in Mucositis; **(N)** TT/TC vs. CC in Mucositis; **(O)** T vs. C in Mucositis; **(P)** TT vs. TC/CC in Anemia.

High-dose MTX (>1 g/m^2) is usually adopted for the treatment of osteosarcoma. An increase in efficacy is accompanied by a high risk of MTX-induced toxicity. Despite the usage of leucovorin rescue to mitigate adverse events, it remains challenging in overcoming severe toxicities in every individual. In this setting, upfront knowledge of drug toxicity based on the patients' genetic features may pave the way for individualized management and optimization. Herein, we have suggested the close association between MTHFR rs1801133 polymorphism and various MTX toxicities, providing a potential tool to prognosticate the patient's drug exposure and sensitivity to toxicities.

Although this meta-analysis has interrogated the significant relationship between MTHFR polymorphism and MTX-induced toxicities comprehensively, there are still some limitations. In the first place, the included studies in this meta-analysis investigated the Asian and Caucasian population, but lack the data for other ethnicities such as the African population. Populations from different ethnicities vary in lifestyle and genetic background. Thus, the conclusion may be not representative of all populations. Secondly, only seven studies were included in this meta-analysis, so the sample size is relatively small. Further studies on this topic are needed to enrich the current conclusions, for instance, analysis for another MTHFR polymorphism, rs1801131. Thirdly, heterogeneity in the analysis of kidney toxicity and MTHFR polymorphism was significant. However, the source of heterogeneity was untrackable because of the limited data. Fourthly, this meta-analysis was limited by the insufficient available data, thus factors regarding age, gender, surgery, radiation, etc. could not be analyzed to reach a more comprehensive conclusion.

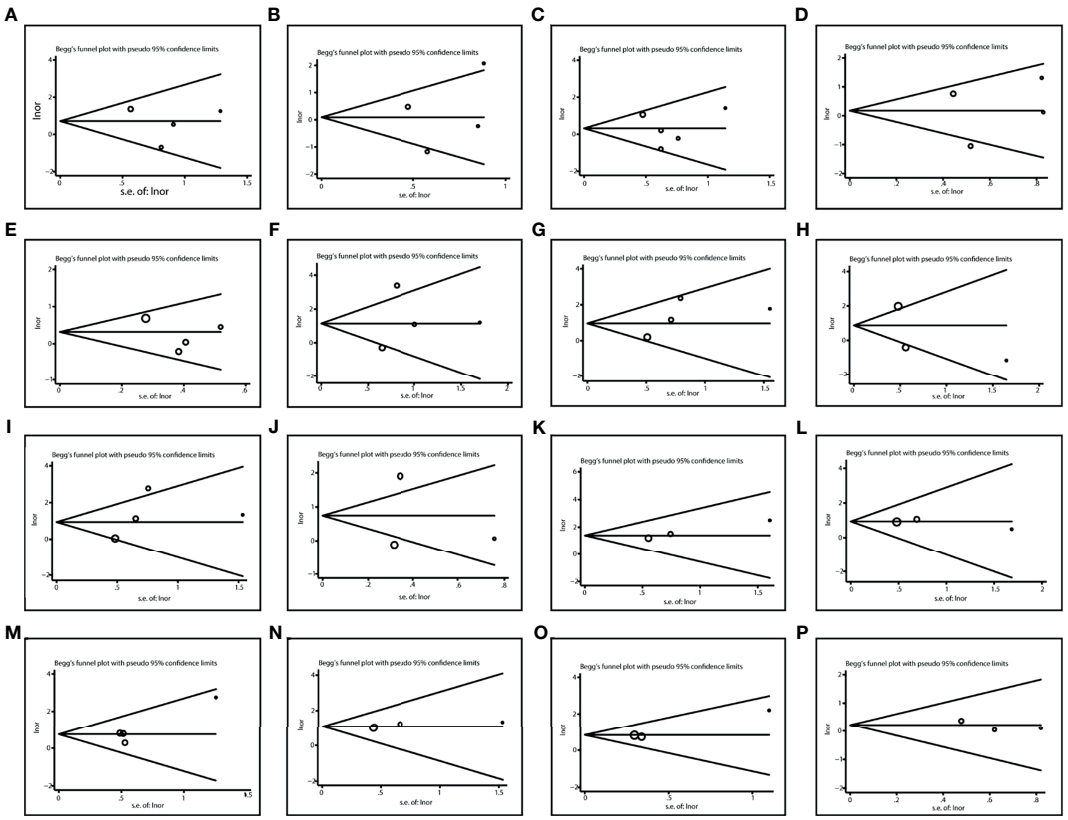

FIGURE 7 | Publication bias in various comparisons. **(A)** TT vs CC in liver toxicity; **(B)** TC vs CC in liver toxicity; **(C)** TT vs. TC/CC in liver toxicity; **(D)** TT/TC vs. CC in liver toxicity; **(E)** T vs C in liver toxicity; **(F)** TT vs CC in kidney toxicity; **(G)** TC vs CC in kidney toxicity; **(H)** TT vs. TC/CC in kidney toxicity; **(I)** TT/TC vs. CC in kidney toxicity; **(J)** T vs. C in kidney toxicity; **(K)** TT vs CC in Mucositis; **(L)** TC vs CC in Mucositis; **(M)** TT vs. TC/CC in Mucositis; **(N)** TT/TC vs. CC in Mucositis; **(O)** T vs. C in Mucositis; **(P)** TT vs. TC/CC in Anemia.

CONCLUSION

To date, this is the first meta-analysis in regard to the association between MTHFR polymorphism and MTX-induced toxicities. A significant relationship between the rs1801133 variant and MTX-related hepatic toxicity in the Asian population has been identified. Meanwhile, mucositis was closely correlated with the rs1801133 polymorphism under various comparisons. In clinical implementations, genotyping patients according to their MTHFR polymorphism for tailored treatment largely contributes to the enhancement of treatment outcomes in osteosarcoma.

DATA AVAILABILITY STATEMENT

The original contributions presented in the study are included in the article/supplementary material. Further inquiries can be directed to the corresponding authors.

AUTHOR CONTRIBUTIONS

WZ and ZYL conceived and designed the work. Material preparation, data collection and analysis were performed by WZ, ZY, and ZYL. The first draft of the manuscript was written by WZ. ZYL, CF, and XZ wrote sections of the manuscript. All authors commented on previous versions of the manuscript. CT revised the manuscript. ZHL contributed to article drafting, critical revision and final approval of the version to be published. All authors contributed to the article and approved the submitted version.

FUNDING

This work was funded by the National Natural Science Foundation of China (No. 81902745, No.82172500, No.82103228), Hunan Provincial Research and Development Program in Key Areas (2020DK2003), and China Postdoctoral Science Foundation (No. 2021M693557).

REFERENCES

1. Liao J, Han R, Wu Y, Qian Z. Review of a New Bone Tumor Therapy Strategy Based on Bifunctional Biomaterials. *Bone Res* (2021) 9(1):18. doi: 10.1038/s41413-021-00139-z
2. Kansara M, Teng MW, Smyth MJ, Thomas DM. Translational Biology of Osteosarcoma. *Nat Rev Cancer* (2014) 14(11):722–35. doi: 10.1038/nrc3838
3. Shijie L, Zhen P, Kang Q, Hua G, Qingcheng Y, Dongdong C. Deregulation of CLTC Interacts With TFG, Facilitating Osteosarcoma via the TGF-Beta and AKT/mTOR Signaling Pathways. *Clin Transl Med* (2021) 11(6):e377. doi: 10.1002/ctm2.377
4. Tu C, He J, Qi L, Ren X, Zhang C, Duan Z, et al. Emerging Landscape of Circular RNAs as Biomarkers and Pivotal Regulators in Osteosarcoma. *J Cell Physiol* (2020) 235(12):9037–58. doi: 10.1002/jcp.29754
5. Zhang W, He L, Liu Z, Ren X, Qi L, Wan L, et al. Multifaceted Functions and Novel Insight Into the Regulatory Role of RNA N(6)-Methyladenosine Modification in Musculoskeletal Disorders. *Front Cell Dev Biol* (2020) 8:870. doi: 10.3389/fcell.2020.00870
6. He J, Ling L, Liu Z, Ren X, Wan L, Tu C, et al. Functional Interplay Between Long Non-Coding RNAs and the Wnt Signaling Cascade in Osteosarcoma. *Cancer Cell Int* (2021) 21(1):313. doi: 10.1186/s12935-021-02013-8
7. Zhang C, He J, Qi L, Wan L, Wang W, Tu C, et al. Diagnostic and Prognostic Significance of Dysregulated Expression of Circular RNAs in Osteosarcoma. *Expert Rev Mol Diagn* (2021) 21(2):235–44. doi: 10.1080/14737159.2021.1874922
8. Anwar MA, El-Baba C, Elnaggar MH, Elkholy YO, Mottawea M, Johar D, et al. Novel Therapeutic Strategies for Spinal Osteosarcomas. *Semin Cancer Biol* (2020) 64:83–92. doi: 10.1016/j.semcancer.2019.05.018
9. Holmboe L, Andersen AM, Mørkrid L, Slørdal L, Hall KS. High Dose Methotrexate Chemotherapy: Pharmacokinetics, Folate and Toxicity in Osteosarcoma Patients. *Br J Clin Pharmacol* (2012) 73(1):106–14. doi: 10.1111/j.1365-2125.2011.04054.x
10. van Dalen EC, van As JW, de Camargo B. Methotrexate for High-Grade Osteosarcoma in Children and Young Adults. *Cochrane Database Syst Rev* (2011) 2011(5):Cd006325. doi: 10.1002/14651858.CD006325.pub3
11. Wippel B, Gundle KR, Dang T, Paxton J, Bubalo J, Stork L, et al. Safety and Efficacy of High-Dose Methotrexate for Osteosarcoma in Adolescents Compared With Young Adults. *Cancer Med* (2019) 8(1):111–6. doi: 10.1002/cam4.1898
12. Young EP, Cheng WS, Bernhardt MB, Wang LL, Rainusso N, Foster JH. Risk Factors Associated With Delayed Methotrexate Clearance and Increased Toxicity in Pediatric Patients With Osteosarcoma. *Pediatr Blood Cancer* (2020) 67(4):e28123. doi: 10.1002/pbc.28123
13. Ozger H, Kilicoglu O, Yilmaz H, Ergen HA, Yaylim I, Zeybek U, et al. Methylenetetrahydrofolate Reductase C677T Gene Polymorphism in Osteosarcoma and Chondrosarcoma Patients. *Folia Biol (Praha)* (2008) 54(2):53–7.
14. Frosst P, Blom HJ, Milos R, Goyette P, Sheppard CA, Matthews RG, et al. A Candidate Genetic Risk Factor for Vascular Disease: A Common Mutation in Methylenetetrahydrofolate Reductase. *Nat Genet* (1995) 10(1):111–3. doi: 10.1038/ng0595-111
15. Lv S, Fan H, Li J, Yang H, Huang J, Shu X, et al. Genetic Polymorphisms of TYMS, MTHFR, ATIC, MTR, and MTRR Are Related to the Outcome of Methotrexate Therapy for Rheumatoid Arthritis in a Chinese Population. *Front Pharmacol* (2018) 9:1390. doi: 10.3389/fphar.2018.01390
16. Sohn KJ, Croxford R, Yates Z, Lucock M, Kim YI. Effect of the Methylenetetrahydrofolate Reductase C677T Polymorphism on Chemosensitivity of Colon and Breast Cancer Cells to 5-Fluorouracil and Methotrexate. *J Natl Cancer Inst* (2004) 96(2):134–44. doi: 10.1093/jnci/djh015
17. Aplenc R, Thompson J, Han P, La M, Zhao H, Lange B, et al. Methylenetetrahydrofolate Reductase Polymorphisms and Therapy Response in Pediatric Acute Lymphoblastic Leukemia. *Cancer Res* (2005) 65(6):2482–7. doi: 10.1158/0008-5472.Can-04-2606
18. Huayi R, Xiao Z. Clinical Investigation on the Relationship Between MTHFR 677 Genotype and High Dose MTX Combined With Calcium Leucovorin Treatment for the Patients With Osteosarcoma. *Anti-Tumor Pharm* (2011) 2011(1):48–50.
19. Windsor RE, Strauss SJ, Kallis C, Wood NE, Whelan JS. Germline Genetic Polymorphisms may Influence Chemotherapy Response and Disease Outcome in Osteosarcoma: A Pilot Study. *Cancer* (2012) 118(7):1856–67. doi: 10.1002/cncr.26472
20. Jabeen S, Holmboe L, Alnæs GI, Andersen AM, Hall KS, Kristensen VN. Impact of Genetic Variants of RFC1, DHFR and MTHFR in Osteosarcoma Patients Treated With High-Dose Methotrexate. *Pharmacogenom J* (2015) 15(5):385–90. doi: 10.1038/tpj.2015.11
21. Park JA, Shin HY. Influence of Genetic Polymorphisms in the Folate Pathway on Toxicity After High-Dose Methotrexate Treatment in Pediatric Osteosarcoma. *Blood Res* (2016) 51(1):50–7. doi: 10.5045/br.2016.51.1.50
22. Lambrecht L, Sleurs C, Labarque V, Dhooge C, Laenen A, Sinnaeve F, et al. The Role of the MTHFR C677T Polymorphism in Methotrexate-Induced Toxicity in Pediatric Osteosarcoma Patients. *Pharmacogenomics* (2017) 18(8):787–95. doi: 10.2217/pgs-2017-0013
23. Xie L, Guo W, Yang Y, Ji T, Xu J. More Severe Toxicity of Genetic Polymorphisms on MTHFR Activity in Osteosarcoma Patients Treated With High-Dose Methotrexate. *Oncotarget* (2018) 9(14):11465–76. doi: 10.18632/oncotarget.23222
24. Xu L, Wang L, Xue B, Wang S. MTHFR Variant Is Associated With High-Dose Methotrexate-Induced Toxicity in the Chinese Osteosarcoma Patients. *J Bone Oncol* (2018) 13:143–7. doi: 10.1016/j.jbo.2018.10.002
25. Moher D, Liberati A, Tetzlaff J, Altman DG. Preferred Reporting Items for Systematic Reviews and Meta-Analyses: The PRISMA Statement. *Ann Intern Med* (2009) 151(4):264–9. doi: 10.7326/0003-4819-151-4-200908180-00135
26. Stang A. Critical Evaluation of the Newcastle-Ottawa Scale for the Assessment of the Quality of Nonrandomized Studies in Meta-Analyses. *Eur J Epidemiol* (2010) 25(9):603–5. doi: 10.1007/s10654-010-9491-z
27. Zhang W, Ren X, Qi L, Zhang C, Tu C, Li Z. The Value of lncRNAs as Prognostic Biomarkers on Clinical Outcomes in Osteosarcoma: A Meta-Analysis. *BMC Cancer* (2021) 21(1):202. doi: 10.1186/s12885-021-07882-w
28. Ren H, Zhou X. Clinical Investigation on the Relationship Between MTHFR 677 Genotype and High Dose MTX Combined With Calcium Leucovorin Treatment for the Patients With Osteosarcoma. *Anti-Tumor Pharm* (2011) 1(1):48–50. doi: 10.3969/j.issn.2095-1264.2011.01.011
29. Yuan G, Chen J, Wu D, Gao C. Neoadjuvant Chemotherapy Combined With Limb Salvage Surgery in Patients With Limb Osteosarcoma of Enneking Stage II: A Retrospective Study. *Onco Targets Ther* (2017) 10:2745–50. doi: 10.2147/ott.S136621
30. Anninga JK, Gelderblom H, Fiocco M, Kroep JR, Taminiau AH, Hogendoorn PC, et al. Chemotherapeutic Adjuvant Treatment for Osteosarcoma: Where Do We Stand? *Eur J Cancer* (2011) 47(16):2431–45. doi: 10.1016/j.ejca.2011.05.030
31. Vos HI, Coenen MJ, Guchelaar HJ, Te Loo DM. The Role of Pharmacogenetics in the Treatment of Osteosarcoma. *Drug Discov Today* (2016) 21(11):1775–86. doi: 10.1016/j.drudis.2016.06.022
32. Hattinger CM, Patrizio MP, Luppi S, Serra M. Pharmacogenomics and Pharmacogenetics in Osteosarcoma: Translational Studies and Clinical Impact. *Int J Mol Sci* (2020) 21(13):4569. doi: 10.3390/ijms21134659
33. Madhusudan S, Middleton MR. The Emerging Role of DNA Repair Proteins as Predictive, Prognostic and Therapeutic Targets in Cancer. *Cancer Treat Rev* (2005) 31(8):603–17. doi: 10.1016/j.ctrv.2005.09.006
34. Michael M, Doherty MM. Tumoral Drug Metabolism: Overview and its Implications for Cancer Therapy. *J Clin Oncol* (2005) 23(1):205–29. doi: 10.1200/jco.2005.02.120
35. Liu S, Yi Z, Ling M, Shi J, Qiu Y, Yang S. Predictive Potential of ABCB1, ABCC3, and GSTP1 Gene Polymorphisms on Osteosarcoma Survival After Chemotherapy. *Tumour Biol* (2014) 35(10):9897–904. doi: 10.1007/s13277-014-1917-x
36. Hughes LB, Beasley TM, Patel H, Tiwari HK, Morgan SL, Baggott JE, et al. Racial or Ethnic Differences in Allele Frequencies of Single-Nucleotide Polymorphisms in the Methylenetetrahydrofolate Reductase Gene and Their Influence on Response to Methotrexate in Rheumatoid Arthritis. *Ann Rheum Dis* (2006) 65(9):1213–8. doi: 10.1136/ard.2005.046797
37. Maagdenberg H, Oosterom N, Zanen J, Gemmati D, Windsor RE, Heil SG, et al. Genetic Variants Associated With Methotrexate-Induced Mucositis in Cancer Treatment: A Systematic Review and Meta-Analysis. *Crit Rev Oncol Hematol* (2021) 161:103312. doi: 10.1016/j.critrevonc.2021.103312

38. Gong Y, Luo L, Wang L, Chen J, Chen F, Ma Y, et al. Association of MTHFR and ABCB1 Polymorphisms With MTX-Induced Mucositis in Chinese Paediatric Patients With Acute Lymphoblastic Leukaemia, Lymphoma or Osteosarcoma-A Retrospective Cohort Study. *J Clin Pharm Ther* (2021) 46 (6):1557–63. doi: 10.1111/jcpt.13505
39. Zhao M, Liang L, Ji L, Chen D, Zhang Y, Zhu Y, et al. MTHFR Gene Polymorphisms and Methotrexate Toxicity in Adult Patients With Hematological Malignancies: A Meta-Analysis. *Pharmacogenomics* (2016) 17(9):1005–17. doi: 10.2217/pgs-2016-0004
40. Shao W, Yuan Y, Li Y. Association Between MTHFR C677T Polymorphism and Methotrexate Treatment Outcome in Rheumatoid Arthritis Patients: A Systematic Review and Meta-Analysis. *Genet Test Mol Biomarkers* (2017) 21 (5):275–85. doi: 10.1089/gtmb.2016.0326
41. Moher D, Liberati A, Tetzlaff J, Altman DG. Preferred Reporting Items for Systematic Reviews and Meta-Analyses: The PRISMA Statement. *PloS Med* (2009) 6(7):e1000097. doi: 10.1371/journal.pmed.1000097

Conflict of Interest: The authors declare that the research was conducted in the absence of any commercial or financial relationships that could be construed as a potential conflict of interest.

Publisher's Note: All claims expressed in this article are solely those of the authors and do not necessarily represent those of their affiliated organizations, or those of the publisher, the editors and the reviewers. Any product that may be evaluated in this article, or claim that may be made by its manufacturer, is not guaranteed or endorsed by the publisher.

frontiers in Oncology

ORIGINAL RESEARCH
published: 20 December 2021
doi: 10.3389/fonc.2021.807171

Suspected Adverse Drug Reactions in Pediatric Cancer Patients in China: An Analysis of Henan Province Spontaneous Reporting System Database

*Zhiming Jiao[1], Zhanchun Feng[1], Ziqi Yan[1], Jinwen Zhang[2], Gang Li[1], Ganyi Wang[3,4], Qianyu Wang[1] and Da Feng[5]**

[1] School of Medicine and Health Management, Tongji Medical College, Huazhong University of Science and Technology, Wuhan, China, [2] Department of Pharmacy, Tongji Hospital, Tongji Medical College, Huazhong University of Science and Technology, Wuhan, China, [3] Medical Products Administration and Center for Adverse Drug Reaction (ADR) Monitoring of Henan, Zhengzhou, China, [4] College of Public Administration, Huazhong University of Science and Technology, Wuhan, China, [5] School of Pharmacy, Tongji Medical College, Huazhong University of Science and Technology, Wuhan, China

OPEN ACCESS

Edited by:
Miao Yan,
Central South University, China

Reviewed by:
Igor Magalhães,
Federal University of Amazonas, Brazil
Yoshihiro Noguchi,
Gifu Pharmaceutical University, Japan
Hamdollah Sharifi,
Urmia University of Medical Sciences, Iran

***Correspondence:**
Da Feng
fengda@hust.edu.cn

Specialty section:
This article was submitted to Pharmacology of Anti-Cancer Drugs, a section of the journal Frontiers in Oncology

Received: *01 November 2021*
Accepted: *30 November 2021*
Published: *20 December 2021*

Citation:
Jiao Z, Feng Z, Yan Z, Zhang J, Li G, Wang G, Wang Q and Feng D (2021) Suspected Adverse Drug Reactions in Pediatric Cancer Patients in China: An Analysis of Henan Province Spontaneous Reporting System Database. Front. Oncol. 11:807171. doi: 10.3389/fonc.2021.807171

Introduction: Adverse drug reactions (ADRs) in pediatric cancer patients have not yet received due attention in the world. Antineoplastic drugs are frequently related to ADRs. Few studies focus on the ADR and the intervention measures in pediatric cancer patients.

Methods: ADR reports submitted to Henan Adverse Drug Reaction Monitoring Center from 2016 to 2020 for individuals aged from birth to 17 years (including 17 years) were included. Data were analyzed with respect to gender, age, disease types, past history of ADR, occurrence time of ADR, polypharmacy, route of administration, off-label drug use, name of suspected drugs per ADR report, and severity of ADR reports.

Results: A total of 431 ADR reports related to antineoplastic drugs in pediatric patients were collected, 31.55% were serious ADRs (SADRs). The median age of patients was six years (inter quartile range, IQR: 3-11), the age groups with higher reporting rates were concentrated in 1-3-year-olds (130). Past history of ADR, occurrence time of ADR and polypharmacy were statistically associated with SADR. Myelosuppression was the most frequent ADR (15.55%), cytarabine was the most frequent drug (26.22%). The signal mining method produced 14 signals, three signals were off-label ADRs.

Conclusions: This study described the characteristics of ADRs in pediatric cancer patients. By conducting signal mining method, three off-label ADRs need further study. We should pay more attention to these ADRs and develop relative management strategies. More researches are needed to achieve a better understanding of the characteristics of ADRs in pediatric cancer patients of China.

Keywords: pharmacovigilance, drug monitoring, adverse drug reaction reporting systems, pediatric, medical oncology

INTRODUCTION

As a leading cause of death, cancer is a growing public health problem worldwide (1). Approximately 18.1 million new cancer cases and 9.6 million cancer deaths were recorded in 2018 (2). Cancers rarely occur before the age of 20 (3). However, more than 1,000 children are diagnosed with cancer every day globally, and the disease remains the leading cause of death in children and adolescents (3). Approximately 84% of childhood cancers occur in low-income and middle-income countries (4).

As the developing country with the highest population in the world, China has a tough condition of cancer in childhood and adolescents (5). A growing body of literature has investigated childhood and adolescent cancer in China. The first national childhood cancer profile in China was reported in 2015 (6). It provided nationwide incidence, mortality, and temporal trends for childhood cancer from 2003 to 2005. A recent study assessed the childhood cancer incidence patterns from 2000 to 2015 and showed that cancer incidence has increased significantly in children and adolescents in China (5).

Childhood cancer incidence is on the rise worldwide. Pediatric patients have to face problems due to adverse drug reactions (ADR), which are harmful or unpleasant reactions resulting from an intervention related to the use of a medicinal products (7). A meta-analysis of the incidence of ADRs in hospitalized patients showed that the overall incidence of serious ADRs was 6.7%, and fatal ADRs was reported in 0.32% of hospitalized patients (8). A systematic review showed that the overall incidence of ADRs in hospitalized children was 9.53%, and severe reactions accounted for 12.29% of the total. Moreover, 39.3% of the ADRs that caused hospital admissions were fatal reactions (9). A previous research has suggested that some subgroups of children and adolescents are at greater risk of developing ADRs, particularly pediatric cancer patients (10).

However, few studies focused on the ADR in pediatric cancer patients. Mascolo (11) analyzed the safety profiles of antineoplastic drugs in Italy and described the off-label use in pediatric patients. Amaro-Hosey (12) assessed the incidence and characteristics of ADRs in a pediatric oncohematological population in Spain. Research on intervention measures in pediatric cancer patients still has gaps. Studies about ADRs in pediatric cancer patients are limited in China.

This study aimed to analyze serious and normal ADR reports and identify safety signals in children, which improves the safety profile of pediatric cancer patients in clinical practice.

METHODS

Study Design and Setting

We carried out a cross-sectional study of pediatric cancer patients with suspected ADRs based on the Henan Provincial Adverse Drug Reaction Monitoring Center, China. We designed to analyze different variables in the reports — mainly the difference between serious ADRs and normal ADRs.

Participants

The following inclusion criteria were used: 1) reported between 2016 and 2020; 2) reports of certain, probable, and possible relationships of drugs; 3) drugs suspectedly associated with ADR was antineoplastic drug; 4) age of 0–17.

The exclusion criteria were as follows: 1) reports before 2016 and after 2020; 2) duplicate records; 3) missing critical information, particularly drug name, and specific records of ADR; 4) unreasonable records, such as records older than 120 years, record that does not match the age, and negative number pertaining to the occurrence time of ADRs.

Variables

Gender, age, disease types, past history of ADR, occurrence time of ADR, polypharmacy, route of administration, off-label drug use, name of suspected drugs per ADR report, and severity of ADR reports (serious, normal) were collected. The ADRs and clinical manifestations were organized according to the Medical Dictionary for Regulatory Activities (MedDRA) (version 24.0). ADR reports with antineoplastic drug were identified from the 2nd level of the Anatomical Therapeutic Chemical (ATC) Classification System (L01-antineoplastic agents). The generic names of drugs were standardized and coded according to the catalog of generic names for common prescription drugs. The catalog was issued by the Ministry of Health of China in 2007. The most common definition for polypharmacy in children included the use of two or more medications (13). However, the use of multiple therapeutic classes of medications is likely warranted in "complex chronic conditions" such as childhood cancer (14). Thus, our study also adopted the more conservative definition of polypharmacy (five or more medications). Off-label drug use was classified into the following categories: defined as the administration of a prescription drug outside the age range for which the product was licensed; defined as the prescription of a drug for therapeutic indications that were not licensed. The severity of ADR was classified by the reporters and included in the database. Based on the Reporting and Monitoring Administration Measure on ADR issued by the Ministry of health of China (15), the "Serious ADRs" (SADRs) was defined as and the other cases were regarded as "Normal ADRs": 1. results in death; 2. is life-threatening; 3. carcinogenesis, teratogenesis and congenital disabilities; 4. results in persistent or significant disability/incapacity; 5. require inpatient hospitalization or prolongation of existing hospitalization; 6. leading to other important medical events, such as the situations listed above may occur without treatment.

Data Sources

We classified and analyzed the Henan Provincial Adverse Drug Reaction Monitoring Center data from 2016 to 2020. The center is subordinate to the National Center for ADR Monitoring, China. These data were reported by Henan medical institutions, enterprises, and the public. Because the data generated from the spontaneous report system (SRS), we cannot get ADR incidence rates as the true extent of drug use was unknown, so all the data in the study were frequency of reports.

Study Size

A total of 394,037 initial data were obtained. According to the inclusion and exclusion criteria, 431 records were retained. To prevent the repetitive analysis of some reports, we selected one of the main adverse reactions included.

Statistical Methods

The demographic characteristics, disease types, past history of ADRs, occurrence time of ADRs, polypharmacy, route of administration, and off-label drug use in the report were subjected to descriptive analysis, Fisher exact test and Chi-square test. All data analyses were performed using SPSS 24.0 (IBM Corp. Armonk, NY). A p-value of less than 0.05 was considered statistically significant.

The number of ADRs of each drug was sorted for ADR signal mining, which quantified the qualitative nature of the relationship between drugs and ADRs. In ADR signal mining, the reporting odds ratio (ROR), proportional reporting ratio (PRR), and comprehensive standard method (MHRA) were adopted as measures of disproportionality, which are generally used in detecting the imbalance of target events compared with other events in the database (16, 17). When the target drug event combination (DEC) frequency was significantly higher than the background frequency and reached the threshold, a signal was considered generated. The strength of the association between drugs and ADRs was expressed as the ROR and PRR with 95% confidence intervals (CIs). We listed the equations and criteria for the three algorithms in **Table 1**.

RESULTS

A total of 15,910 ADR reports related to antineoplastic drugs were collected in Henan Provincial Adverse Drug Reaction Monitoring Center from 2016 to 2020, of which 431 (2.71%) occurred in pediatric patients.

Sample Characteristics

Table 2 shows patient characteristics based on ADR severity. More ADRs were reported for boys than girls in every age group. No significant difference in the severity of ADRs was found between genders. The median age of patients was 6 years (inter quartile range, IQR: 3–11), and no report about patients younger than 1 was found. The gender differences in specific age groups were significant. The age groups with high reporting rates were concentrated in 1–3 years (130) and 4–6 years (103) (see **Figure 1**). **Figure 2** describes serious and normal reports in different age groups and the proportion of serious reports in each age group. Notably, the proportion of serious reports steadily increased with age, except in 15–17 year age group. Approximately 3.94% of patients suffered more than one disease before the ADRs occurred, and 10.44% had a history of ADR. Moreover, 29.7% of ADRs occurred 1–3 days after use. Approximately 79.8% of ADRs were reported within 1 week of medication, and only 1.62% of ADRs occurred after 1 month.

The Medication Characteristics

Table 3 shows the ADR characteristics according to the severity. Difference in the proportion of polypharmacy was found ($p < 0.001$). Most patients received injection therapy (94.20%). Off-label drug use was not common in pediatric patients (7.42%).

The ADR Characteristics

Table 4 shows drug characteristics according to the severity of ADR. The largest share of ADRs were reported for cytarabine (26.22% of the total reports), followed by asparaginase (12.76%). Doxorubicin, daunorubicin, and cytarabine had the most proportions of SADRs. A total of 431 events involved 18 system organ class (SOC) reports, mainly including gastrointestinal, blood and lymphatic system, and skin and subcutaneous tissue disorders. The majority of ADRs for each SOC were normal, except blood and lymphatic system disorders and cardiac disorders. According to the statistics, 69 ADRs were identified, which were concentrated in myelosuppression, rash, and vomiting.

Signal Mining

According to the calculation formulas and thresholds, DEC signals that did not meet the criteria were excluded. The three signal mining methods produced a total of 14 signals (see **Table 5**). The strength of the correlation between the drug and ADR increased with the ROR and PRR values.

TABLE 1 | Formulas and criteria for generating signals of ROR, PRR and MHRA.

Method	Formula	Criteria and threshold
ROR	$ROR = \frac{(a/c)}{(b/d)}$	a≥3 and lower limit of 95%CI >1
	$95\,\%\,CI = e^{\ln(ROR)\pm1.96\sqrt{\frac{1}{a}+\frac{1}{b}+\frac{1}{c}+\frac{1}{d}}}$	
PRR	$PRR = \frac{a/(a+b)}{c/(c+d)}$	a≥3, PRR≥2 and lower limit of 95%CI >1
	$95\,\%\,CI = e^{\ln(PRR)\pm1.96\sqrt{\frac{1}{a}+\frac{1}{b}+\frac{1}{c}+\frac{1}{d}}}$	
MHRA	$\chi^2 = \frac{n(\lvert ad-bc\rvert-\frac{n}{2})^2}{(a+b)(a+c)(b+c)(c+d)}$	a≥3 and $\chi 2 \geq 4$

a: number of reports containing both the suspect drug and the suspect ADR;
b: number of reports containing the suspect ADR with other medications (except the drug of a);
c: number of reports containing the suspect drug with other ADRs (except the event of a);
d: number of reports containing other medications and other ADRs.

TABLE 2 | The characteristics of patients aspect by severity of ADR.

Characteristic	Serious N = 136 (%)	Normal N = 295 (%)	*p* value[a]
Gender			
Male	88 (33.0)	179 (67.0)	0.423
Female	48 (29.3)	116 (70.7)	
Age group (years)			
1-3	31 (23.8)	99 (76.2)	0.060
4-6	30 (29.1)	73 (70.9)	
7-11	38 (37.6)	63 (62.4)	
12-14	26 (42.6)	35 (57.4)	
15-17	11 (30.6)	25 (69.4)	
Disease types			
Single	127 (31.3)	279 (68.7)	0.622
Multiple	9 (36.0)	16 (64.0)	
Past history of ADR			
Yes	22 (48.9)	23 (51.1)	0.008
No	114 (29.5)	272 (70.5)	
Occurrence time of ADR (days)			
On the day	30 (23.4)	98 (76.6)	<0.001[b]
1-3	31 (22.1)	109 (77.9)	
4-7	25 (32.9)	51 (67.1)	
8-14	42 (63.6)	24 (36.4)	
15-30	6 (42.9)	8 (57.1)	
Over a month	2 (28.6)	5 (71.4)	

[a]*Chi-squared test;* [b]*Fisher exact test.*

DISCUSSION

To the best of our knowledge, our study was the first to examine the safety profile of antineoplastic drugs in pediatric cancer patients in China on the basis of the data of Henan Provincial Adverse Drug Reaction Monitoring Center. Our study showed that approximately 2.71% (n = 431) of cancer patients' reports were related to pediatric cancer patients. This percentage was in accordance with the result of the study in the Campania, south of Italy, where 3% of all individual case safety reports were found (11). Moreover, cancer is a rare disease in children, representing only 2% of all cancer cases (18).

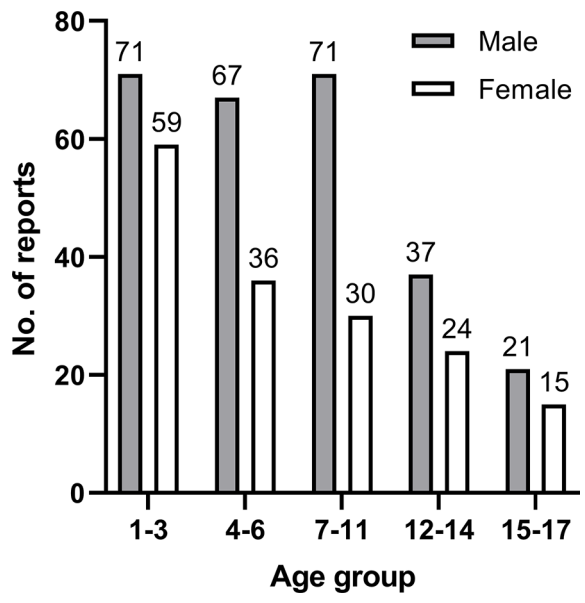

FIGURE 1 | Number of reports in each age group by gender.

SADRs seriously threaten the lives and health of patients and cause waste of medical resources. The China Adverse Drug Reaction Monitoring System has received 1.676 million ADR reports in 2020, and SADRs accounted for 10% of these reports (19). Our study found that the frequency of SADRs in children (31.55%) was higher than was generally reported in other pharmacovigilance studies. A retrospective analysis concerning children in Spanish Pharmacovigilance System observed 1419 ADRs, of which 4.4% were serious (20). Therefore, medical staff must carry out relevant health education to patients and their families to increase their knowledge about diseases, drugs, and ADRs.

Some pediatric studies found that a high proportion of reports about ADRs in males (21, 22). In our research, nearly three-fifths of the reports were related to males (n = 267). Due to the limitation of the database, the total number of patients using the drugs was unknown. According to the research of cancer incidence and mortality among children from 2010 to 2014 in Henan Province, China, the cancer incidence was predominant in boys, and the sex ratio was 1.19 (23). The difference in cancer incidence indicates that even if the number of reports differs between males and females, this does not mean that it is a gender difference. And no evidence of an association (p = 0.423) between gender and ADR severity was found. Further investigations are needed to explain this finding.

In our study, more than 50% of the ADRs were reported in children aged 1–6, and 30% of children are between 1 and 3.

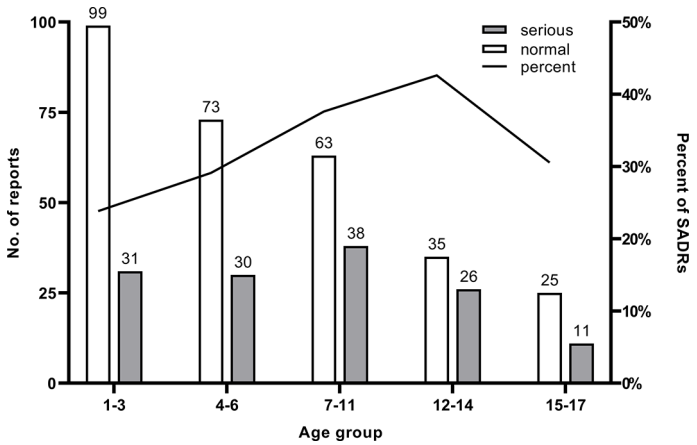

FIGURE 2 | Number of reports and the proportion of SADR reports in each age group.

Although the proportion of SADRs increased with age, the overall number of ADR reports decreased with the age, and the result was not statistically significant. Because the data is collected from the spontaneous reporting system, it captures only a small fraction of the ADR that actually takes place (24). Due to the lack of consideration for the overall ADR incidence rate in the general population, the result only inflected the status of pediatric cancer patients who have been suffered from ADR in the region, or even more limited. Similar findings were observed in other studies (22, 25). Some reasons might have contributed to the high reporting rates in young children. First, immature tubular function reduces metabolism and liver function in young children, increasing the possibility of ADRs. Second, physicians and parents monitored young children closely because children lack expression ability, and thus ADRs were immediately found and reported in time. Physicians have to consider children's sensitive physical conditions and the characteristics of chemotherapeutic agents when treating pediatric cancer patients.

The results showed that the proportion of pediatric patients with multiple disease was only 5.80%, identical to the expected result. Some studies in adults demonstrated that suffering from multiple diseases is a risk factor for SADRs (26), and might correlate with the decrease in drug metabolism or the damage to liver and kidney functions. Interaction among diseases might result in poor physical, emotional and social functions (27). However, in our study, children with multiple disease did not show significant differences in ADR severity.

The statistics showed that the severity of ADR in children who had ADR histories was significantly higher. Physicians should pay more attention to patients who have past histories of ADR and take caution when treating patients who are unsure about whether or not they have a history of drug allergies. This finding was also reflected in the reports. In 49.42% of these reports, physicians abandoned suspected drugs after ADRs occurred and did not continue using them.

In terms of the occurrence time of ADRs, 32.48% occurred 1–3 days after administration, and approximately 80% were

TABLE 3 | The characteristics of physicians aspect by severity of ADR.

Characteristic	Serious N = 136 (%)	Normal N = 295 (%)	*p* value[a]
Polypharmacy (≥2 medications)			
Polypharmacy	86 (40.4)	127 (59.6)	<0.001
Non-polypharmacy	50 (22.9)	168 (77.1)	
Polypharmacy (≥5 medications)			
Polypharmacy	19 (59.4)	13 (40.6)	<0.001
Non-polypharmacy	117 (29.3)	282 (70.7)	
Route of administration			
Parenteral	130 (32.0)	276 (68.0)	0.656[b]
Oral	3 (30.0)	7 (70.0)	
Others	3 (20.0)	12 (80.0)	
Off-label drug use			
Yes	8 (25.0)	24 (75.0)	0.407
No	128 (32.1)	271 (67.9)	

[a]*Chi-squared test;* [b]*Fisher exact test.*

TABLE 4 | The characteristics of ADRs aspect by the severity.

Characteristic	Serious N = 136 (%)	Normal N = 295 (%)
Drugs (top 10)		
Cytarabine	48 (42.5)	65 (57.5)
Asparaginase	11 (20.0)	44 (80.0)
Methotrexate	10 (20.4)	39 (79.6)
Pegaspargase	13 (35.1)	24 (64.9)
Cyclophosphamide	9 (30.0)	21 (70.0)
Etoposide	8 (36.4)	14 (63.6)
Vincristine sulfate	3 (17.6)	14 (82.4)
Cisplatin	4 (33.3)	8 (66.7)
Daunorubicin	5 (45.5)	6 (54.5)
Doxorubicin	6 (66.7)	3 (33.3)
System organ class (top 10)		
Gastrointestinal disorders	19 (14.6)	111 (85.4)
Blood and lymphatic system disorders	73 (70.9)	30 (29.1)
Skin and subcutaneous tissue disorders	15 (17.6)	70 (82.4)
General disorders and administration site conditions	10 (21.3)	37 (78.7)
Respiratory, thoracic, and mediastinal disorders	5 (41.7)	7 (58.3)
Nervous system disorders	1 (10.0)	9 (90.0)
Hepatobiliary disorders	4 (40.0)	6 (60.0)
Metabolism and nutrition disorders	0 (0)	7 (100)
Cardiac disorders	4 (57.1)	3 (42.9)
Immune system disorders	1 (20.0)	4 (80.0)
ADR (top 10)		
Myelosuppression	57 (85.1)	10 (14.9)
Rash	9 (15.0)	51 (85.0)
Vomiting	7 (13.7)	44 (86.3)
Fever	9 (24.3)	28 (75.7)
Nausea	3 (11.5)	23 (88.5)
Gastrointestinal reaction	2 (10.0)	18 (90.0)
Fibrinogen decreased	3 (25.0)	9 (75.0)
Leukocyte count decreased	6 (60.0)	4 (40.0)
Dyspnea	4 (44.4)	5 (55.6)
Hepatic failure	4 (44.4)	5 (55.6)

found within 1 week. Early observation played a crucial role in pediatric patients. Family members should be reminded to monitor patients closely and continue to observe them for a week in order that ADRs can be detected and treated in time. Our results suggest evidence of an association ($p<0.001$) between occurrence time and the severity of an ADR. SADR was more common in chronic ADR from one week to one month, which means that long-term monitoring and follow-up of patients were desirable.

Polypharmacy is increasingly common, and a constant flow of novel therapeutic agents and treatment indications for existing medications has been observed (28, 29). The number of reported ADRs is expected to increase (22). Many studies showed the risk

TABLE 5 | Signals of ADRs.

Drug	ADR	No.	ROR	95% CI Lower limit	PRR	95% CI Lower limit	χ^2
Vincristine	Alopecia	4	63.39	10.64	48.71	10.90	327253.85
Asparaginase	Cyanosis[a]	3	21.64	2.21	20.51	2.22	114461.47
Pegaspargase	Itch[a]	3	17.29	2.79	15.97	2.82	94729.67
Methotrexate	Mucositis oral	7	63.50	7.63	54.57	7.69	42646.14
Asparaginase	Dyspnea	6	15.22	3.69	13.67	3.73	11950.02
Methotrexate	Hepatic failure	4	6.70	1.74	6.24	1.75	11208.07
Pegaspargase	Fibrinogen decreased	4	5.85	1.67	5.32	1.69	8295.83
Asparaginase	Fibrinogen decreased	8	15.83	4.59	13.67	4.65	5071.55
Cyclophosphamide	Reaction gastrointestinal	7	9.08	3.31	7.20	3.41	2756.44
Fludarabine	Myelosuppression	3	17.02	1.74	5.00	3.74	1256.66
Cisplatin	Vomiting	6	8.31	2.57	4.66	3.00	686.61
Etoposide	Rash[a]	7	3.14	1.22	2.46	1.29	236.91
Pegaspargase	Rash	13	4.00	1.91	2.95	2.01	73.08
Asparaginase	Rash	18	3.87	2.02	2.93	2.12	25.59

[a]*Off-label ADR.*

of SADR increases with the increase of the number of drugs (30, 31). Our results demonstrated that under two different definitions, the analysis showed significant association between polypharmacy exposure and SADR ($p<0.001$). Although many combinations of drugs have been found effective in relevant studies, formulating reasonable drug treatment strategies are still needed to minimize the risk of ADRs in children. In order to minimize the risk of SADRs, physicians should pay particular attention to children who are prescribed two or more drugs and closely monitor drug administration and (32).

Nearly all ADRs related to antineoplastic drugs occurred after injection given that drugs enter directly into the bloodstream and elicit reactions from the immune system. The safety of pediatric injection has been a concern. According to the Annual Report for National ADR Monitoring (2020) released by the China National Center of ADR Monitoring, more than 70% of ADRs in children are related to injections. As a special group, children are more sensitive to drugs and less tolerable because their organ development is incomplete. Thus, their risk of injection medication needs to be thoroughly examined.

Many medicines are prescribed to pediatric patients on an unlicensed or 'off-label' basis. Owing to the lack of adequately tested or authorized drugs, the use of off-label drugs exposes a child to a high risk of SADRs (33). The availability of medicines specifically designed for pediatric patients is limited, and less than 15% of currently marketed drugs specifically intended for children are operated on the basis of clinical trials. This reality is currently faced by many pediatricians (34). In our study, we found a low number of ADRs classified as off-label (7.42%). The proportion of SADR reports related to off-label drug use was low, but the existing evidence can not prove the reliability of off-label drug use. Among the off-label reports, most reports explored the use of vindesine for lymphocytic leukemia. In the literature, data on the efficacy and safety of vindesine for acute lymphocytic leukemia in children dated back to the 1980s, and attention should be paid to its clinical drug resistance (35, 36). The majority of ADRs observed in off-label cases belonged to gastrointestinal disorders and were mainly about myelosuppression and gastrointestinal reactions. In China, no relevant regulations on off-label drug use have been established. The China Food and Drug Administration (now called the NMPA) issued The Regulations on Drug Insert and Label in 2006. However, the regulation does not require specific information on pediatric populations and has not been revised (37). Thus, strengthening early assessment and risk management is imperative and crucial to the improvement of drug response and reduction of ADRs.

Our study showed that doxorubicin, daunorubicin, and cytarabine are the specific drugs with the most percentage reported associated with SADR. The frequency of cytarabine use was the largest, and the principal ADR was myelosuppression. We found that main indications for cytarabine as a myelosuppressive agent were used to treat acute myeloid leukemia. Cutaneous reactions were reported in the literature, and such events were found in our study (38). As for doxorubicin and daunorubicin, myelosuppressive and vomiting were reported (39, 40). Prevention and self-management education for patients and their families should be considered when ADRs are explained to them. This approach enables them to become familiar with the specific drugs they use.

The distribution of ADRs by system organ class was similar to the records in Italy (41), but more ADRs affected the blood and lymphatic system disorders in our study. Among the gastrointestinal disorders with the highest number of reports, chemotherapy-induced vomiting, nausea, and gastrointestinal reactions were the most common ADRs. The possible reason was that almost all drug regimens increased the risk of gastrointestinal system disorders, particularly cytarabine (42), methotrexate (43), and pegaspargase (44). SADRs accounted for the highest proportions of blood and lymphatic system disorders. Myelosuppression is the most common ADR and presents the most SADR reports in the study probably because of the prevalence of patients diagnosed with hematological tumors was the highest. Thus, strategies for monitoring, early detecting, confirming diagnosis, and providing appropriate supportive care are needed for hematological tumor therapy (45).

In the context of antineoplastic drugs in pediatric cancer patients, some common ADRs do not generate signals in data mining. By contrast, the ADRs of some drugs generated signals. This finding indicated that the ADRs and drugs were related. Combined with drug instructions, three off-label ADRs were found, including asparaginase-cyanosis, pegaspargase-itch, and etoposide-rash.

Cyanosis seemed to be an uncommon ADR of asparaginase. Few cases were found in related studies. Norman found that 16 cases of asparaginase had two cases of cyanosis and choking episodes, and these side effects were generally mild (46). However, the specific mechanism is unclear.

No report of itch caused by pegaspargase was found, but a study reported a pruritus ADR. One analysis consisted of eight individuals who had drug-induced liver injuries caused by asparaginase or pegaspargase, and only one patient mentioned itch (47). This finding may be attributed to metabolic status rather than to pharmacologic metabolism.

Many reports of rash when etoposide was used were found, which supported the results of this study. Mansfield found 65 cases of rash in 394 cases that used atezolizumab and carboplatin combined with etoposide (48). In-depth research should be performed to uncover their mechanisms of damage to the skin.

LIMITATIONS

In China, ADR reports were reported by basic units (including drug manufacturers, pharmacies, and medical institutions) to provincial ADR monitoring centers. The reports are then evaluated by provincial and national ADR monitoring centers. The strict evaluation process ensures the accuracy of ADR reports but leads to a high rate of under-reporting. In our research, nearly all reports came from hospitals. A much higher number of ADRs may have occurred in real life. We encourage consumers and non-medical personnel to report ADRs to the system for the assessment of ADRs and reduction of bias.

Due to the limitation of the signal mining method and sample quantity, the results cannot represent the inevitable causal relationship between drugs and adverse reactions. The causal relationship, which includes the potential impact of false positives or negatives, needs further evaluation and verification. The methods we used — including ROR, PRR and MHRA — were frequentist statistical approaches, which means the limits of detecting false-positive signals and low specificity were unavoidable (49). When the number of reports is small, its stability will be greatly affected. Thus, signal mining aims to detect unknown ADR signals and provide more information and reference.

This study has several limitations. First, this study used the database of Henan Province, which does not necessarily represent the actual situation of the whole country. Second, because we selected one of the main adverse reactions from one report, the potential relationship between ADR and drugs may not be explored. More research is needed to confirm the possible potential relationship. Third, subject to the spontaneous reporting system and the database, our research has some limitations, such as underreporting, unstable reporting, not getting incidence rates, and difficulty determining causality. Further studies using larger databases are needed to evaluate ADRs in greater detail.

CONCLUSION

The incidence of ADRs in pediatric cancer patients during therapy was high, with different features involving various systems organs class. Most ADRs were normal in severity, while some were serious. These ADRs were mostly acute and occurred within one week of administration. Age, past history of ADR, occurrence time of ADR, and polypharmacy may be relative to the severity of ADRs. Signal mining produced 14 signals. Three of them were off-label ADR. Therefore, the characteristics of ADRs obtained in this study could accumulate experience for clinical staff to carry out ADRs management to ensure the safety of pediatric patients. More researches are needed to achieve a better understanding of the characteristics of ADRs in pediatric cancer patients of China.

DATA AVAILABILITY STATEMENT

The datasets for this article are not publicly available because the pharmacovigilance data in single, non-aggregated form are available only under a specific authorization released by the Medical Products Administration and Center for ADR Monitoring of Henan. Requests to access the datasets should be directed to the Medical Products Administration and Center for ADR Monitoring of Henan.

ETHICS STATEMENT

The studies involving human participants were reviewed and approved by the Ethics Committee of Tongji Medical College, Huazhong University of Science and Technology (2020S204). Written informed consent to participate in this study was provided by the participants' legal guardian/next of kin.

AUTHOR CONTRIBUTIONS

All authors were involved in the conception and design of the study, interpretation of data, and drafting or revising the manuscript critically for important intellectual content.

FUNDING

This work was supported by the National Youth Natural Science Foundation of China (No. 71804052), the National Natural Science Foundation of China (No. 72074088) and the Health Commission of Hubei Province Fund (Grant Number: WJ2021Q022).

REFERENCES

1. Bray F, Laversanne M, Weiderpass E, Soerjomataram I. The Ever-Increasing Importance of Cancer as a Leading Cause of Premature Death Worldwide. *Cancer Am Cancer Soc* (2021) 127(16):3029–30. doi: 10.1002/cncr.33587
2. Bray F, Ferlay J, Soerjomataram I, Siegel RL, Torre LA, Jemal A. Global Cancer Statistics 2018: GLOBOCAN Estimates of Incidence and Mortality Worldwide for 36 Cancers in 185 Countries. *CA Cancer J Clin* (2018) 68 (6):394–424. doi: 10.3322/caac.21492
3. Steliarova-Foucher E, Colombet M, Ries LAG, Moreno F, Dolya A, Bray F, et al. International Incidence of Childhood Cancer, 2001–10: A Population-Based Registry Study. *Lancet Oncol* (2017) 18(6):719–31. doi: 10.1016/S1470-2045(17)30186-9
4. Magrath I, Steliarova-Foucher E, Epelman S, Ribeiro RC, Harif M, Li C, et al. Paediatric Cancer in Low-Income and Middle-Income Countries. *Lancet Oncol* (2013) 14(3):e104–16. doi: 10.1016/S1470-2045(13)70008-1
5. Sun K, Zheng R, Zhang S, Zeng H, Wang S, Chen R, et al. Patterns and Trends of Cancer Incidence in Children and Adolescents in China, 2011–2015: A Population-Based Cancer Registry Study. *Cancer Med* (2021) 10(13):4575–86. doi: 10.1002/cam4.4014
6. Zheng R, Peng X, Zeng H, Zhang S, Chen T, Wang H, et al. Incidence, Mortality and Survival of Childhood Cancer in China During 2000–2010 Period: A Population-Based Study. *Cancer Lett* (2015) 363(2):176–80. doi: 10.1016/j.canlet.2015.04.021
7. Edwards IR, Aronson JK. Adverse Drug Reactions: Definitions, Diagnosis, and Management. *Lancet* (2000) 356(9237):1255–9. doi: 10.1016/S0140-6736(00)02799-9
8. Lazarou J, Pomeranz BH, Corey PN. Incidence of Adverse Drug Reactions in Hospitalized Patients. *JAMA* (1998) 279(15):1200. doi: 10.1001/jama.279.15.1200
9. Impicciatore P, Choonara I, Clarkson A, Provasi D, Pandolfini C, Bonati M. Incidence of Adverse Drug Reactions in Paediatric in/Out-Patients: A Systematic Review and Meta-Analysis of Prospective Studies. *Br J Clin Pharmacol* (2001) 52(1):77–83. doi: 10.1046/j.0306-5251.2001.01407.x
10. Posthumus AAG, Alingh CCW, Zwaan CCM, van Grootheest KK, Hanff LLM, Witjes BBCM, et al. Adverse Drug Reaction-Related Admissions in

Paediatrics, A Prospective Single-Centre Study. *BMJ Open* (2012) 2(4): e000934. doi: 10.1136/bmjopen-2012-000934
11. Mascolo A, Scavone C, Bertini M, Brusco S, Punzo F, Pota E, et al. Safety of Anticancer Agents Used in Children: A Focus on Their Off-Label Use Through Data From the Spontaneous Reporting System. *Front Pharmacol* (2020) 11:621. doi: 10.3389/fphar.2020.00621
12. Amaro-Hosey K, Danés I, Vendrell L, Alonso L, Renedo B, Gros L, et al. Adverse Reactions to Drugs of Special Interest in a Pediatric Oncohematology Service. *Front Pharmacol* (2021) 12:670945. doi: 10.3389/fphar.2021.670945
13. Bakaki PM, Horace A, Dawson N, Winterstein A, Waldron J, Staley J, et al. Defining Pediatric Polypharmacy: A Scoping Review. *PloS One* (2018) 13(11): e0208047. doi: 10.1371/journal.pone.0208047
14. Ewig CLY, Cheng YM, Li HS, Wong JCL, Cho AHY, Poon FMH, et al. Use of Chronic Prescription Medications and Prevalence of Polypharmacy in Survivors of Childhood Cancer. *Front Oncol* (2021) 11:642544. doi: 10.3389/fonc.2021.642544
15. Ministry of Health of The People's Republic of China. (2011). Available at: https://www.nmpa.gov.cn/xxgk/fgwj/bmgzh/20110504162501325.html (Accessed 11/26 2021).
16. van Puijenbroek ENP, Bate A, Leufkens HGM, Lindquist M, Orre R, Egberts ACG. A Comparison of Measures of Disproportionality for Signal Detection in Spontaneous Reporting Systems for Adverse Drug Reactions. *Pharmacoepidemiol Drug Saf* (2002) 11(1):3–10. doi: 10.1002/pds.668
17. Evans SJW, Waller PC, Davis S. Use of Proportional Reporting Ratios (PRRs) for Signal Generation From Spontaneous Adverse Drug Reaction Reports. *Pharmacoepidemiol Drug Saf* (2001) 10(6):483–6. doi: 10.1002/pds.677
18. Davidoff AM. Pediatric Oncology. *Semin Pediatr Surg* (2010) 19(3):225–33. doi: 10.1053/j.sempedsurg.2010.03.007
19. National Center for ADR Monitoring, China. (2021). Available at: https://www.cdr-adr.org.cn/tzgg_home/202103/t20210326_48414.html (Accessed 2021/10/15).
20. Morales-Olivas FJ, Martıínez-Mir I, Ferrer JM, Rubio E, Palop V. Adverse Drug Reactions in Children Reported by Means of the Yellow Card in Spain. *J Clin Epidemiol* (2000) 53(10):1076–80. doi: 10.1016/S0895-4356(00)00190-6
21. Workalemahu G, Abdela OA, Yenit MK. Chemotherapy-Related Adverse Drug Reaction and Associated Factors Among Hospitalized Paediatric Cancer Patients at Hospitals in North-West Ethiopia. *Drug Healthc Patient Saf* (2020) 12:195–205. doi: 10.2147/DHPS.S254644
22. Li H, Guo X, Ye X, Jiang H, Du W, Xu J, et al. Adverse Drug Reactions of Spontaneous Reports in Shanghai Pediatric Population. *PloS One* (2014) 9(2): e89829. doi: 10.1371/journal.pone.0089829
23. Chen Q, Guo Z, Liu S, Quan P, Cao X, Guo L, et al. The Cancer Incidence and Mortality Among Children and Adolescents During the Period of 2010-2014 in Henan Province, China. *Cancer Med* (2019) 8(2):814–23. doi: 10.1002/cam4.1952
24. Ahmad SR. Adverse Drug Event Monitoring at the Food and Drug Administration. *J Gen Intern Med* (2003) 18(1):57–60. doi: 10.1046/j.1525-1497.2003.20130.x
25. Vieira JMDL, de Matos GC, Da Silva FAB, Bracken LE, Peak M, Lima EDC. Serious Adverse Drug Reactions and Safety Signals in Children: A Nationwide Database Study. *Front Pharmacol* (2020) 11:964. doi: 10.3389/fphar.2020.00964
26. Yan Z, Feng Z, Jiao Z, Chen C, Wang G, Feng D. The Severity of Adverse Drug Reactions and Their Influencing Factors Based on the ADR Monitoring Center of Henan Province. *Sci Rep UK* (2021) 11(1):20402. doi: 10.1038/s41598-021-99908-3
27. Yamamoto K, Yano I. Genetic Polymorphisms Associated With Adverse Reactions of Molecular-Targeted Therapies in Renal Cell Carcinoma. *Med Oncol* (2018) 35(2):16. doi: 10.1007/s12032-017-1077-0
28. Rambhade S, Shrivastava A, Rambhade A, Chakarborty A, Patil U. A Survey on Polypharmacy and Use of Inappropriate Medications. *Toxicol Int* (2012) 19(1):68. doi: 10.4103/0971-6580.94506
29. Koh NY, Koo WH. Polypharmacy in Palliative Care: Can It be Reduced? *Singapore Med J* (2002) 43(6):279–83.
30. Zopf Y, Rabe C, Neubert A, Hahn EG, Dormann H. Risk Factors Associated With Adverse Drug Reactions Following Hospital Admission. *Drug Saf* (2008) 31(9):789–98. doi: 10.2165/00002018-200831090-00007
31. Rashed AN, Wong ICK, Cranswick N, Tomlin S, Rascher W, Neubert A. Risk Factors Associated With Adverse Drug Reactions in Hospitalised Children: International Multicentre Study. *Eur J Clin Pharmacol* (2012) 68(5):801–10. doi: 10.1007/s00228-011-1183-4
32. Du R, Wang X, Ma L, Larcher LM, Tang H, Zhou H, et al. Adverse Reactions of Targeted Therapy in Cancer Patients: A Retrospective Study of Hospital Medical Data in China. *BMC Cancer* (2021) 21(1):206. doi: 10.1186/s12885-021-07946-x
33. Aagaard L, Hansen EH. Prescribing of Medicines in the Danish Paediatric Population Outwith the Licensed Age Group: Characteristics of Adverse Drug Reactions. *Br J Clin Pharmacol* (2011) 71(5):751–7. doi: 10.1111/j.1365-2125.2011.03915.x
34. Napoleone E. Children and ADRs (Adverse Drug Reactions). *Ital J Pediatr* (2010) 36(1):4. doi: 10.1186/1824-7288-36-4
35. Vats TS, Mehta P, Trueworthy RC, Smith SD, Klopovich P. Vindesine and Prednisone for Remission Induction in Children With Acute Lymphocytic Leukemia. *Cancer Am Cancer Soc* (1981) 47(12):2789–92. doi: 10.1002/1097-0142(19810615)47:123.0.CO;2-X
36. Krivit W, Anderson J, Chilcote R, Pyesmany A, Chard R, Hammond D. A Study of the Cross-Resistance of Vincristine and Vindesine in Reinduction Therapy for Acute Lymphocytic Leukemia in Relapse. A Report for Children's Cancer Study Group. *Am J Pediatr Hematol Oncol* (1980) 2(3):217–21. doi: 10.1007/BF00257193
37. Zhang Y, Wagner A, Du H, Han T, Gupta S, Denburg AE, et al. Childhood Cancer Drugs in China: An Overview and Comparison of Regulatory Approvals in China and the United States. *Int J Cancer* (2021). doi: 10.1002/ijc.33818
38. Cetkovska P, Pizinger K, Cetkovsky P. High-Dose Cytosine Arabinoside-Induced Cutaneous Reactions. *J Eur Acad Dermatol* (2002) 16(5):481–5. doi: 10.1046/j.1468-3083.2002.00395.x
39. Hortobágyi GN. Anthrazykline in Der Krebstherapie. *Drugs* (1997) 54 (Supplement 4):1–7. doi: 10.2165/00003495-199700544-00003
40. Richly H, Henning BF, Kupsch P, Passarge K, Grubert M, Hilger RA, et al. Results of a Phase I Trial of Sorafenib (BAY 43-9006) in Combination With Doxorubicin in Patients With Refractory Solid Tumors. *Ann Oncol* (2006) 17 (5):866–73. doi: 10.1093/annonc/mdl017
41. Lombardi N, Crescioli G, Bettiol A, Marconi E, Vitiello A, Bonaiuti R, et al. Characterization of Serious Adverse Drug Reactions as Cause of Emergency Department Visit in Children: A 5-Years Active Pharmacovigilance Study. *BMC Pharmacol Toxicol* (2018) 19(1):16. doi: 10.1186/s40360-018-0207-4
42. Niktoreh N, Lerius B, Zimmermann M, Gruhn B, Escherich G, Bourquin J, et al. Gemtuzumab Ozogamicin in Children With Relapsed or Refractory Acute Myeloid Leukemia: A Report by Berlin-Frankfurt-Münster Study Group. *Haematologica* (2018) 104(1):120–7. doi: 10.3324/haematol.2018.191841
43. Lu L, Bao C, Dai M, Teng J, Fan W, Du F, et al. Multicenter, Randomized, Double-Blind, Controlled Trial of Treatment of Active Rheumatoid Arthritis With T-614 Compared With Methotrexate. *Arthritis Rheum* (2009) 61 (7):979–87. doi: 10.1002/art.24643
44. Zhao Q, Fan S, Chang Y, Liu X, Li W, Ma Q, et al. Clinical Efficacy of Cisplatin, Dexamethasone, Gemcitabine and Pegaspargase (DDGP) in the Initial Treatment of Advanced Stage (Stage III–IV) Extranodal NK/T-Cell Lymphoma, and Its Correlation With Epstein-Barr Virus. *Cancer Manag Res* (2019) 11:3555–64. doi: 10.2147/CMAR.S191929
45. Carey PJ. Drug-Induced Myelosuppression. *Drug Saf* (2003) 26(10):691–706. doi: 10.2165/00002018-200326100-00003
46. Jaffe N, Traggis D, Das L, Frauenberger G, Hann HW, Kim BS, et al. Favorable Remission Induction Rate With Twice Weekly Doses of L-Asparaginase. *Cancer Res* (1973) 33(1):1–4.
47. Kamal N, Koh C, Samala N, Fontana RJ, Stolz A, Durazo F, et al. Asparaginase-Induced Hepatotoxicity: Rapid Development of Cholestasis and Hepatic Steatosis. *Hepatol Int* (2019) 13(5):641–8. doi: 10.1007/s12072-019-09971-2
48. Mansfield AS, Każarnowicz A, Karaseva N, Sánchez A, De Boer R, Andric Z, et al. Safety and Patient-Reported Outcomes of Atezolizumab, Carboplatin, and Etoposide in Extensive-Stage Small-Cell Lung Cancer (IMpower133): A Randomized Phase I/III Trial. *Ann Oncol* (2020) 31(2):310–7. doi: 10.1016/j.annonc.2019.10.021

49. Noguchi Y, Tachi T, Teramachi H. Detection Algorithms and Attentive Points of Safety Signal Using Spontaneous Reporting Systems as a Clinical Data Source. *Brief Bioinform* (2021) 22(6):1–14. doi: 10.1093/bib/bbab347

Conflict of Interest: The authors declare that the research was conducted in the absence of any commercial or financial relationships that could be construed as a potential conflict of interest.

Publisher's Note: All claims expressed in this article are solely those of the authors and do not necessarily represent those of their affiliated organizations, or those of the publisher, the editors and the reviewers. Any product that may be evaluated in this article, or claim that may be made by its manufacturer, is not guaranteed or endorsed by the publisher.

frontiers in Oncology

PERSPECTIVE
published: 06 January 2022
doi: 10.3389/fonc.2021.815040

Perspectives and Expertise in Establishing a Therapeutic Drug Monitoring Programme for Challenging Childhood Cancer Patient Populations

Shelby Barnett[1], *Victoria Holden*[2], *Quentin Campbell-Hewson*[3] *and Gareth J. Veal*[1]*

[1] Newcastle University Centre for Cancer, Newcastle University, Newcastle upon Tyne, United Kingdom, [2] Leeds General Infirmary, Leeds, United Kingdom, [3] Great North Children's Hospital, Newcastle upon Tyne, United Kingdom

OPEN ACCESS

Edited by:
Miao Yan,
Central South University, China

Reviewed by:
Hua He,
China Pharmaceutical University, China
Dominique Leveque,
Hôpital d'Hautepierre, France
Neeltje Steeghs,
The Netherlands Cancer Institute (NKI), Netherlands

***Correspondence:**
Gareth J. Veal
G.J.Veal@ncl.ac.uk

Specialty section:
This article was submitted to Pharmacology of Anti-Cancer Drugs, a section of the journal Frontiers in Oncology

Received: 14 November 2021
Accepted: 09 December 2021
Published: 06 January 2022

Citation:
Barnett S, Holden V, Campbell-Hewson Q and Veal GJ (2022) Perspectives and Expertise in Establishing a Therapeutic Drug Monitoring Programme for Challenging Childhood Cancer Patient Populations. Front. Oncol. 11:815040. doi: 10.3389/fonc.2021.815040

The utility of Therapeutic Drug Monitoring (TDM) in the setting of childhood cancer is a largely underused tool, despite the common use of cytotoxic chemotherapeutics. While it is encouraging that modern advances in chemotherapy have transformed outcomes for children diagnosed with cancer, this has come at the cost of an elevated risk of life-changing long-term morbidity and late effects. This concern can limit the intensity at which these drugs are used. Widely used chemotherapeutics exhibit marked inter-patient variability in drug exposures following standard dosing, with fine margins between exposures resulting in toxicity and those resulting in potentially suboptimal efficacy, thereby fulfilling criteria widely accepted as fundamental for TDM approaches. Over the past decade in the UK, the paediatric oncology community has increasingly embraced the potential benefits of utilising TDM for particularly challenging patient groups, including infants, anephric patients and those receiving high dose chemotherapy. This has been driven by a desire from paediatric oncologists to have access to clinical pharmacology information to support dosing decisions being made. This provides the potential to modify doses between treatment cycles based on a comprehensive set of clinical information, with individual patient drug exposures being used alongside clinical response and tolerability data to inform dosing for subsequent cycles. The current article provides an overview of recent experiences of conducting TDM in a childhood cancer setting, from the perspectives of the clinicians, scientists and pharmacists implementing TDM-based dosing recommendations. The ongoing programme of work has facilitated investigations into the validity of current approaches to dosing for some of the most challenging childhood cancer patient groups, with TDM approaches now being expanded from well-established cytotoxic drugs through to newer targeted treatments.

Keywords: Therapeutic drug monitoring, children, cancer, chemotherapy, dosing adaptation

INTRODUCTION

Every year in the UK, there are approximately 1,800 children diagnosed with cancer, with incidence rates highest in children less than 5 years of age (1). Only a small proportion of the most common childhood cancers are curable with local therapy and prior to the widespread adoption of systemic cytotoxic chemotherapy, cure was rare. The use of increasingly complex chemotherapy regimes has been transformative for children and young people affected by malignancy, with 5 year survival rates for children with cancer in the UK rising from 44% between 1973-77 to 84% between 2011-15 (2). Increased survival has been strongly associated with increased intensity of cytotoxic therapy, an approach clearly demonstrated for cancers such as neuroblastoma (3) and Ewing sarcoma (4).

While it is encouraging that modern advances in cancer treatment now mean that over 70% of childhood cancer patients will survive for twenty years or more following diagnosis, this comes at the cost of an elevated risk of life-changing long-term morbidity and late effects (5, 6). With an estimated 40,000+ childhood cancer survivors now living in the UK, this is clearly a major issue, both in terms of the quality of life experienced by those affected, as well as the financial impact on both the individual and the NHS (7, 8). On the other hand, undertreatment to avoid toxicity risks compromising survival.

The vast majority of childhood cancer patients are treated with non-selective cytotoxic anticancer drugs, with significant potential to damage host tissue at doses used to achieve anti-tumour activity. Widely used drugs which are effective against a wide range of childhood cancers include carboplatin and cisplatin, cyclophosphamide, vincristine, doxorubicin and etoposide, and have been a mainstay of treatment for several decades. However, these drugs are associated with a plethora of toxicities and late effects including organ dysfunction, hearing loss, infertility, secondary malignancies and cognitive problems (9–13). As drug toxicity is dependent on immediate and cumulative dose for the majority of chemotherapeutic drugs, drug exposure is clearly an important factor.

The utility of therapeutic drug monitoring (TDM) is widely used across a range of disease specialties and drug classes, including antibiotics, antipsychotics, anticonvulsants and immunosuppressants (14). However, it has remained an underused tool in an oncology setting, despite a number of published studies highlighting its potential clinical benefit (15–18). More recently, studies supportive of TDM approaches for newer targeted anticancer drugs have been published (19–22). The understated use of TDM for well established cytotoxic drugs is particularly surprising, when we consider that these drugs commonly exhibit the characteristics widely accepted as fundamentals for utilising TDM approaches. These include marked inter-patient variability in drug exposures following standard dosing, the existence of a narrow therapeutic window, with fine margins between exposures resulting in toxicity and those resulting in potentially suboptimal efficacy, and evidence for relationships between drug exposure and clinical endpoints (23). A recent review on the use of TDM for the widely used anticancer drug carboplatin, provides a good level of detail on this how this drug meets the characteristics commonly associated with TDM (18).

While there are certainly challenges in implementing TDM in an oncology setting, including the use of traditional dosing regimens and common use of drug combinations, as highlighted in some excellent reviews on the subject (24–26), these hurdles are certainly not unsurmountable if the problem is approached in the right way. Indeed, TDM approaches have been shown to be beneficial and are commonly used for the anticancer drugs methotrexate and busulfan across a range of cancer types. Over the past decade in the UK, the paediatric oncology community has increasingly embraced the potential benefits of utilising TDM approaches for particularly challenging patient groups, including neonates and infants, anephric patients and those receiving high dose chemotherapy regimens. This has very much been led by a desire from paediatric oncologists to have access to clinical pharmacology information as an additional tool when making difficult dosing decisions. This approach means that a clinician can modify doses between cycles of treatment based on a more comprehensive set of clinical information, with individual patient drug exposure following the initial drug dose being used alongside clinical response and tolerability data to inform dosing for subsequent cycles. The current article looks at the recent experiences of conducting TDM in a childhood cancer setting from the perspectives of the clinicians requesting the use of TDM for their patients, the scientists carrying out sample clinical sample analysis, and the pharmacists implementing TDM-based dosing recommendations.

VIEW FROM THE PAEDIATRIC ONCOLOGIST

Delivery of the optimum dose of chemotherapy is crucial if we are to achieve the best survival outcome at the least toxic cost to our patients. Drug exposure is known to be closely related to a range of factors including body mass and composition and drug elimination and detoxification, usually by the renal or hepatic systems (27, 28). Standard dosing of treatment may be assumed for children who lie within the normal range of these parameters, but a meaningful proportion of children lie outside them (29, 30). For patient size, most concern has been with small or very young children and infants, who it has been feared might be overdosed with standard dosing regimens. However, larger children or those with disproportionate body fat may be as problematic, particularly where chemotherapy dosing is capped. Children with immature and developing liver and kidney function, as well as those with diminished function following disease, physical injury or drug toxicity, might be overexposed to drugs. For the large part, the availability of dosing guidelines that we can have confidence in has been unachievable in these patient groups, partly due to the relatively small numbers of cases that we are presented with.

Concerns about body size have led to reticence and anxiety surrounding the use of these highly effective chemotherapy drugs and also guidelines on "safe" dosing. These typically set a cut-off

weight and commonly adopt a weight-based dose calculation, as opposed to the standard surface area-based dosing approach usually employed. Weight-based dosing typically yields a lower drug exposure than dosing based on surface area, although the implication is that it is equivalent. In the previous European Paediatric Soft Tissue Sarcoma RMS 2005 Rhabdomyosarcoma study, a child of 10 kg would receive 30-40% less vincristine, ifosfamide, actinomycin and doxorubicin, when calculated by weight as opposed to surface area (31). Similarly, for the previous SIOPEN High Risk Neuroblastoma protocol, a child of 12kg similarly would receive 30-40% lower doses of carboplatin, vincristine, etoposide, cisplatin and cyclophosphamide (32). Unless these dose reductions are justified by a difference in the handling of these drugs in smaller children, then these patients may be receiving a substantial under-treatment, which may have fatal consequences. In this respect, a review looking at currently available evidence for dosing guidance of a wide range of anticancer drugs used in infants and neonates has recently been published and provides a valuable tool (33).

Altered drug elimination by temporary or permanent renal or liver dysfunction appears even more unpredictable than size. Most drugs are cleared by more than one mechanism, making it very challenging to establish reliable guidelines. In this scenario, current guidelines are even more crude than size guidance, with dosing being reduced by 50% or even involving the omission of drugs altogether (34). In children out-with the usual norms of size and excretion, the clinician faces the anxiety provoking choice of accepting the recommended dose reductions or administering doses with the potential to achieve maximum efficacy. In the latter case, this would be undertaken in the knowledge that severe toxicity would leave them open to the charge of negligently overdosing, with a lack of guideline or evidence support for the decisions taken.

In our experience, utilising a TDM approach in these challenging patient groups provides evidence to support the administration of chemotherapy dosing regimens most likely to achieve the best outcomes. In children who would have what amount to dose reductions due to their size, it has allowed us to tailor doses to the actual patient. This has almost always resulted in dosing regimens more equivalent to those used to dose older children, thus calling into question the widely used lower weight-based dosing guidelines. In most cases TDM enables us to give higher doses of treatment, with the expectation of better response rates and survival. The ability to therapeutically monitor repeated cycles of a wide range of drugs has repeatedly allowed us to adapt treatment for very young infants as they progress through organ maturation, without compromising treatment.

VIEW FROM THE SCIENTIST

A formal clinical trial to allow the collection and analysis of patient information alongside the quantification of drug levels in defined groups of childhood cancer patients was initiated in 2019 (ISRCTN 10139334). This study was established due to an increasing number of clinical requests to monitor hard-to-treat childhood cancer patients, where drug exposure may be altered relative to older children. This formal clinical study has allowed us to collect patient clinical information relating to toxicity/efficacy alongside pharmacokinetic data, in order to better assess dosing regimens and understand relationships between drug exposure and clinical outcome in these challenging groups. The study opened for recruitment in April 2019, since then over 150 patients (average 5 patients per month) have been recruited from 16 primary treatment centres across the UK. Focusing on the first 150 patients recruited between April 2019 and October 2021 (**Figure 1**), a range of tumour types, hard-to-treat groups and chemotherapy regimens have been enrolled onto the study. The highest recruiting tumour types are neuroblastoma and retinoblastoma (**Figure 1A**), likely due to the established practice of carboplatin TDM (**Figure 1B**) (18). Additional tumour types in the 'other' grouping in this figure include infantile myofibromatosis, ependymoma, kidney tumours, Inflammatory myofibroblastic tumour and metastatic yolk sac tumour. Carboplatin is the drug most commonly analysed, with TDM carried out for over 60% of patients recruited onto the study, followed by vincristine (35%) and etoposide (28%), as these three drugs are commonly given in combination. Neonates and infants represent the highest recruiting group of the study to date, accounting for nearly two thirds of patients (**Figure 1C**). The second highest recruiting group included patients where there were concerns regarding poor tolerability to initial dosing regimens (11%). For these 'toxicity' patients, TDM is used to determine if the standard dose is contributing to excessive exposure and subsequent toxicities. Alternatively, TDM can be used to determine if suitable exposures are being achieved in patients who have experienced excessive toxicity and are receiving dosage reductions. The remaining hard-to-treat groups (high dose chemotherapy, obesity, renal impairment and other) had an equal spread of numbers between them, accounting for 4-9% of the patients for each group (**Figure 1C**). Patients recruited under the 'other' category included patients with low body weight for age, rare genetic conditions and hepatic dysfunction. It is important to note that patients may fall within multiple hard-to-treat groups, but are represented here as their primary group.

As patients often receive multiple chemotherapeutic agents as part of their treatment, in many cases TDM was conducted for more than one drug per patient (**Figure 1E**). From a laboratory perspective co-ordination of patient sample analysis on such a large scale can be challenging (**Figure 2**). Of the 150 patients on the study 40% received TDM on more than one occasion (**Figure 1E**), with two patients being monitored on as many as eight TDM cycles. Whilst challenging however, this can provide valuable information on intra-patient variability for a particular drug, which can be a key factor influencing the likely success of the TDM approach to treatment. In addition, just under half (47%) of the patients on the study were monitored for more than one drug (**Figure 1D**). Carboplatin is the only drug where TDM is conducted in real time, i.e. samples are received, analysed and the results reported on day 2 of treatment in order to adjust the

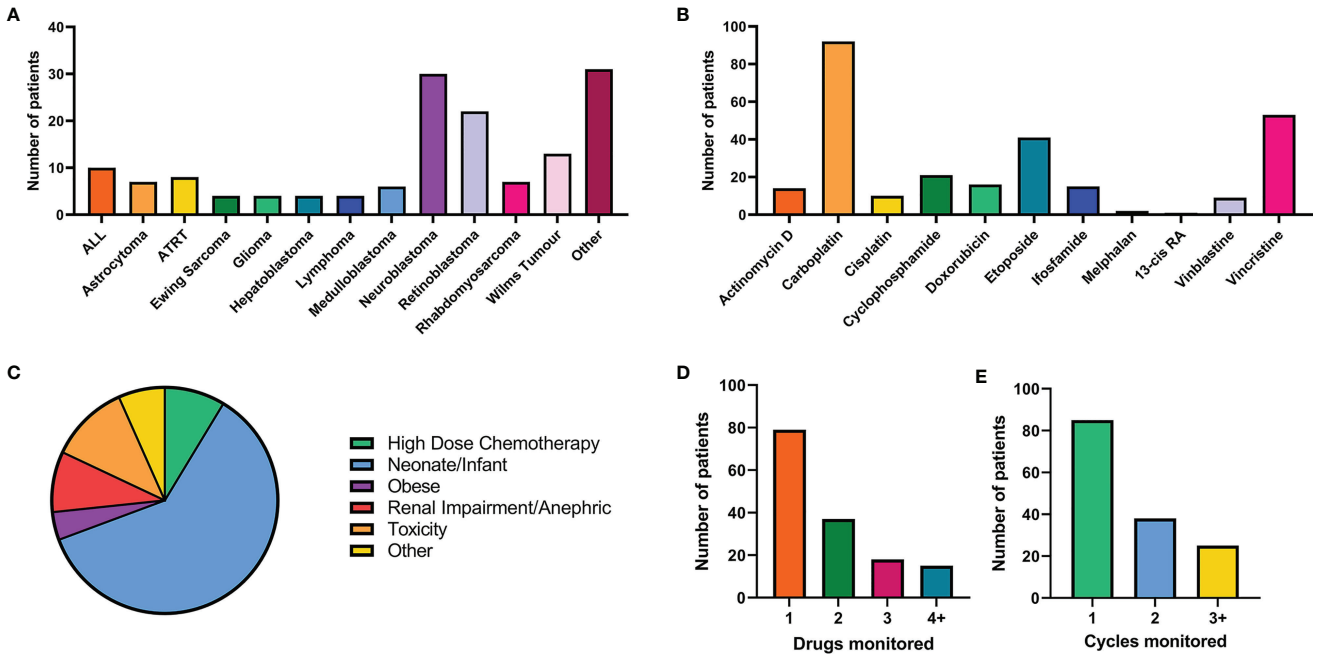

FIGURE 1 | Summary of patient recruitment for the first 150 patient recruited on to the NCCPG TDM 2018 study. **(A)** Breakdown of tumour types and number of patients (cut off level for each tumour type of 3 patients). **(B)** Number of patients receiving each chemotherapeutic agent of interest. **(C)** Patient recruitment by hard-to-treat group. **(D)** The number of drugs monitored for each patient. **(E)** Number of cycles of chemotherapy monitored using TDM for each patient.

dose on day 3 (18). For the remaining drugs (**Figure 1B**), the results are reported ahead of the next cycle of chemotherapy, in order to make informed dose adjustments as required. This is partly a result of the more complex sample extraction and analysis used for these drugs compared to platinum containing agents (**Figure 2**). Furthermore, if more than one chemotherapeutic agent is being monitored then a separate assay has to be conducted for each drug of interest. Consequently, it may take several days to complete the analysis for a single patient. This is something that ideally will be simplified in the future, with the development of validated multi-drug assays to quantifying levels of several anticancer drugs simultaneously. Co-ordination of patient sample shipment, analysis and results, has been an important aspect of this complex multi-centre TDM study, to ensure that results are reported in a timely manner for all patients. This can require batching patient samples to reduce the number of assays and prioritising experiments based on when patient results are needed for clinical care.

VIEW FROM THE PHARMACIST

A significant challenge for a children's cancer pharmacist when prescribing or verifying chemotherapy prescriptions, is the choice of chemotherapy doses in certain patient groups. These include infants, pre-term babies and children at extremes of body mass index (BMI) for age, as well as children with renal or hepatic impairment. In addition, the pharmacist is often asked for advice on chemotherapy dosing for children who have developed toxicity following previous courses of treatment.

The challenge of dosing in infants is compounded by a lack of consistent guidance in national and international treatment guidelines and clinical trials, with artificial cut-off points for mg/kg dosing in infants leading to sometimes large discrepancies in dose as compared to patients receiving mg/m^2 dosing. Similarly, despite recent ASCO guidance in adults advising that dosing in obesity should be based on actual body weight (35), there is no national position statement or standard advice for dosing chemotherapy in obesity in children. In a paediatric setting, decisions on dose capping are often decided on an individual patient basis considering the patient's BMI, renal and hepatic function, the drug's toxicity profile and most importantly the clinician and pharmacist's previous experiences with the drug in a similar patient group. Choice of dose in children with renal and liver impairment can be difficult due to varying or lack of advice in treatment guidelines, and minimal or cautious advice from the drug companies. There is also a lack of consistent dose modification guidance in protocols for patients who have experienced adverse effects on previous courses of treatment. The pharmacist is left juggling a delicate balance between desired therapeutic outcome and acceptable toxicity in such patients.

Carboplatin represents the drug most commonly administered using a TDM approach in childhood cancer in the UK, ensuring safe dosing in infants, children with renal impairment and patients receiving high dose chemotherapy

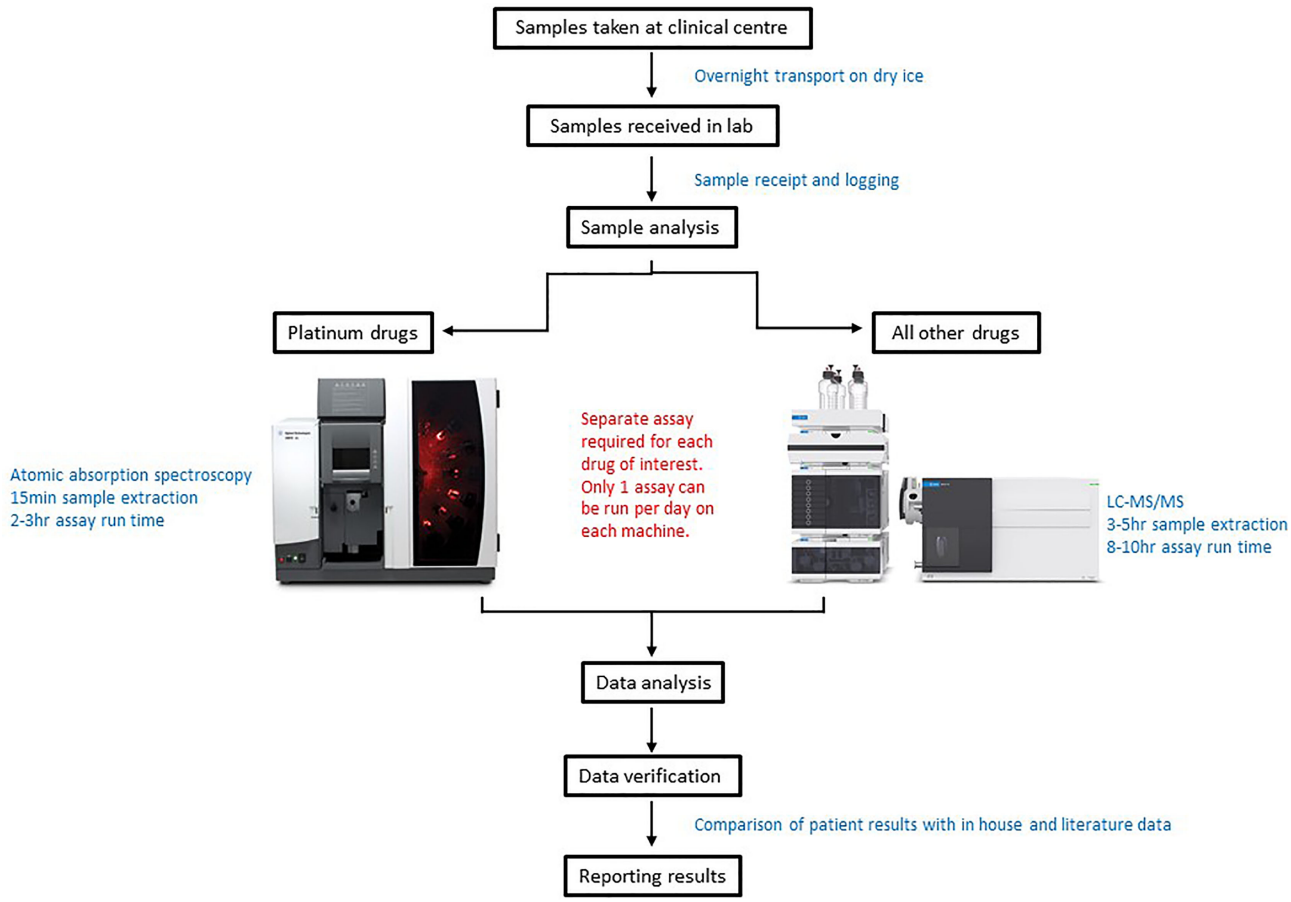

FIGURE 2 | Schematic diagram of the sample analysis processes for patients utilising a Therapeutic Drug monitoring (TDM) approach to treatment.

prior to stem cell rescue. This is based on evidence from studies showing clear relationships between carboplatin drug exposure (AUC) and clinical outcome (18). The carboplatin dose is usually fractionated over 3 days and the AUC from day one used to advice the dose on day 3 (18). Whilst this is invaluable in terms of delivering an accurate dose of carboplatin, it can provide practical challenges for the children's cancer pharmacist, as the carboplatin dose needs to be amended on the electronic prescribing system. Instead of prescribing the full carboplatin dose on day 1, the prescription is amended so that a third of the proposed dose is prescribed on each the first two days of treatment and then the third day left blank until the AUC results are known. The pharmacist liaises with both pharmacy aseptics and the research nurse team, to ensure the drug is available to start treatment early in the morning, and the research team have the staff resource to take the appropriately timed blood samples and to arrange transport of the samples for analysis. Once information on drug exposure is available, in terms of the observed AUC on day 1, the pharmacist and clinician review the data together, to agree a dose to prescribe for the third treatment day. The original prescription is then amended and a new dose prepared, often at short notice, by the aseptics unit. Whilst this is achievable for hospitals with an onsite aseptics unit, such an approach may not be possible for centres that outsource their chemotherapy. Experience has shown that communication and team working with other members of the multi-disciplinary team (MDT) is key to the successful delivery of real time TDM.

Based on positive experiences with carboplatin dosing, expansion of TDM approaches to a wide range of commonly used drugs now provides invaluable information to aid pharmacists with chemotherapy dosing decisions on a regular basis. It is reassuring to know that chemotherapy drug levels can be determined in individual patients, and the results provided can help guide dosing for subsequent courses of treatment. Suitable patients for TDM are identified by the pharmacists or clinicians at MDT meetings. After analysis of TDM samples, the pharmacist is provided with information that shows the drug level achieved, as compared to the usual therapeutic range. The results are used to determine if the dosage can remain the same or should be reduced or increased for the next chemotherapy cycle. As well as recommending TDM for the previously highlighted patient groups, the pharmacist may recommend TDM when a child has had significant adverse effects with a

drug. Establishing whether or not toxicity is potentially related to excessive drug levels can help guide future patient management. For example, if vincristine dose is reduced by 50% due to drug-induced neuropathy, it is important to know that a potentially efficacious drug exposure is still being achieved at the reduced dose level, allowing this dose to be maintained for the remainder of treatment to minimise further neurological toxicity.

DISCUSSION

The successful utility of TDM dosing for patients treated across UK paediatric oncology primary treatment centres requires a collective commitment and effective teamwork between the scientists, research nurses, clinicians and pharmacists involved. The ongoing programme of work has facilitated investigations into the validity of current approaches to dosing for some of the most challenging childhood cancer patient groups. As an example of the impact of the information being generated from this study, we recently reported on current approaches to vincristine dosing in infants and neonates relative to older children (36). The results showed the feasibility of utilising a TDM treatment approach in this patient group and importantly, highlighted that infants receiving vincristine doses <0.05mg/kg were achieving significantly lower exposures compared to those dosed at ≥0.05mg/kg, and older children dosed at 1.5 mg/m^2. Furthermore, infants with lower exposures tolerated dose increases well, suggesting that infants should not be initiating treatment with some of the lower mg/kg dosing regimens currently being used. It is hoped that similar analyses will be feasible for additional drugs being monitored on the study, leading to the generation of further data to support future dosing in these challenging patient populations. This approach to treatment is now being expanded from well established cytotoxic drugs through to newer targeted treatments, as they become increasingly utilised in a childhood cancer setting.

AUTHOR CONTRIBUTIONS

The manuscript was conceptualized by GV. All authors contributed to the writing of the article and approved the submitted version.

FUNDING

The TDM programme of work is currently supported by the Little Princess Trust (CCLGA 2021 08 Veal), Cancer Research UK (C9380/A25138) and the Experimental Cancer Medicine Centre Network (C9380/A25169), with previous funding from the National Institute for Health Research (NIHR) Research for Patient Benefit programme (PB-PG-1216-20032).

REFERENCES

1. Cancer Research UK. *Children's Cancer Statistics*. Available at: https://www.cancerresearchuk.org/health-professional/cancer-statistics/childrens-cancers.
2. *NCIN Website–Childhood Cancer Statistics, England Annual Report 2018* (H:/Downloads/Childhood_Cancer_Statistics_England_FINAL_updated.pdf).
3. Pearson AD, Pinkerton CR, Lewis IJ, Imeson J, Ellershaw C, Machin D, et al. High-Dose Rapid and Standard Induction Chemotherapy for Patients Aged Over 1 Year With Stage 4 Neuroblastoma: A Randomised Trial. *Lancet Oncol* (2008) 9:247–56. doi: 10.1016/S1470-2045(08)70069-X
4. Granowetter L, Womer R, Devidas M, Krailo M, Wang C, Bernstein M, et al. Dose-Intensified Compared With Standard Chemotherapy for Nonmetastatic Ewing Sarcoma Family of Tumors: A Children's Oncology Group Study. *J Clin Oncol* (2009) 20:27:2536–41. doi: 10.1200/JCO.2008.19.1478
5. Gibson TM, Mostoufi-Moab S, Stratton KL, Leisenring WM, Barnea D, Chow EJ, et al. Temporal Patterns in the Risk of Chronic Health Conditions in Survivors of Childhood Cancer Diagnosed 1970-99: A Report From the Childhood Cancer Survivor Study Cohort. *Lancet Oncol* (2018) 19 (12):1590–601. doi: 10.1016/S1470-2045(18)30537-0
6. Ruggiero A, Skinner R, Zekri WZK. Editorial: Adverse and Toxic Effects of Childhood Cancer Treatments. *Front Oncol* (2021) 11:795664. doi: 10.3389/fonc.2021.795664
7. Huang I-C, Bhakta N, Brinkman TM, Klosky JL, Krull KR, Srivastava D, et al. Determinants and Consequences of Financial Hardship Among Adult Survivors of Childhood Cancer: A Report From St. Jude Lifetime Cohort Study. *J Natl Cancer Inst* (2019) 1112:189–200. doi: 10.1093/jnci/djy120
8. Rebholz CE, Reulen RC, Toogood AA, Frobisher C, Lancashire ER, Winter DL, et al. Health Care Use of Long-Term Survivors of Childhood Cancer: The British Childhood Cancer Survivor Study. *J Clin Oncol* (2011) 29:4181–8. doi: 10.1200/JCO.2011.36.5619
9. Oeffinger KC, Mertens AC, Sklar CA, Kawashima T, Hudson MM, Meadows AT, et al. Childhood Cancer Survivor Study. Chronic Health Conditions in Adult Survivors of Childhood Cancer. *N Engl J Med* (2006) 355:1572–82. doi: 10.1056/NEJMsa060185
10. Camet ML, Spence A, Hayashi SS, Wu N, Henry J, Sauerburger K, et al. Cisplatin Ototoxicity: Examination of the Impact of Dosing, Infusion Times, and Schedules in Pediatric Cancer Patients. *Front Oncol* (2021) 11:673080. doi: 10.3389/fonc.2021.673080
11. Barton SE, Najita JS, Ginsburg ES, Leisenring WM, Stovall M, Weathers RE, et al. Infertility, Infertility Treatment, and Achievement of Pregnancy in Female Survivors of Childhood Cancer: A Report From the Childhood Cancer Survivor Study Cohort. *Lancet Oncol* (2013) 14:873–81. doi: 10.1016/S1470-2045(13)70251-1
12. Reulen RC, Frobisher C, Winter DL, Kelly J, Lancashire ER, Stiller CA, et al. Long-Term Risks of Subsequent Primary Neoplasms Among Survivors of Childhood Cancer. *JAMA* (2011) 305:2311–9. doi: 10.1001/jama.2011.747
13. Kadan-Lottick NS, Zeltzer LK, Liu Q, Yasui Y, Ellenberg L, Gioia G, et al. Neurocognitive Functioning in Adult Survivors of Childhood Noncentral Nervous System Cancers. *J Natl Cancer Inst* (2010) 102:881–93. doi: 10.1093/jnci/djq156
14. Ghiculescu RA. Therapeutic Drug Monitoring: Which Drugs, Why, When and How to Do It. *Aust Prescr* (2008) 31:42–4. doi: 10.18773/austprescr.2008.025
15. Gamelin E, Delva R, Jacob J, Merrouche Y, Raoul JL, Pezet D, et al. Individual Fluorouracil Dose Adjustment Based on Pharmacokinetic Follow-Up Compared With Conventional Dosage: Results of a Multicenter Randomized Trial in Patients With Metastatic Colorectal Cancer. *J Clin Oncol* (2008) 26:2009–105. doi: 10.1200/JCO.2007.13.3934
16. Evans WE, Relling MV, Rodman JH, Crom WR, Boyett JM, Pui CH. Conventional Compared With Individualized Chemotherapy for Childhood Acute Lymphoblastic Leukemia. *N Eng J Med* (1998) 338:499–505. doi: 10.1056/NEJM199802193380803

17. Hill BT, Rybicki LA, Urban TA, Lucena M, Jagadeesh D, Gerds AT, et al. Therapeutic Dose Monitoring of Busulfan Is Associated With Reduced Risk of Relapse in Non-Hodgkin Lymphoma Patients Undergoing Autologous Stem Cell Transplantation. *Biol Blood Marrow Transplant* (2020) 26(2):262–71. doi: 10.1016/j.bbmt.2019.09.033
18. Barnett S, Kong J, Makin G, Veal GJ. Over a Decade of Experience With Carboplatin Therapeutic Drug Monitoring in a Childhood Cancer Setting in the United Kingdom. *Br J Clin Pharmacol* (2021) 87:256–62. doi: 10.1111/bcp.14419
19. Gao B, Yeap S, Clements A, Balakrishnar B, Wong M, Gurney H, et al. Evidence for Therapeutic Drug Monitoring of Targeted Anticancer Therapies. *J Clin Oncol* (2012) 30(32):4017–25. doi: 10.1200/JCO.2012.43.5362
20. Mueller-Schoell A, Groenland SL, Scherf-Clavel O, van Dyk M, Huisinga W, Michelet R, et al. Therapeutic Drug Monitoring of Oral Targeted Antineoplastic Drugs. *Eur J Clin Pharmacol* (2021) 77:441–64. doi: 10.1007/s00228-020-03014-8
21. Lankheet NAG, Desar IME, Mulder SF, Burger DM, Kweekel DM, van Herpen CML, et al. Optimizing the Dose in Cancer Patients Treated With Imatinib, Sunitinib and Pazopanib. *Br J Clin Pharmacol* (2017) 83:2195–204. doi: 10.1111/bcp.13327
22. Demetri GD, Wang Y, Wehrle E, Racine A, Nikolova Z, Blanke CD, et al. Imatinib Plasma Levels Are Correlated With Clinical Benefit in Patients With Unresectable/Metastatic Gastrointestinal Stromal Tumors. *J Clin Oncol* (2009) 27:3141–7. doi: 10.1200/JCO.2008.20.4818
23. Le Guellec C, Simon N, Hulot JS, Billaud EM, Marquet P, et le groupe STP, et al. Evidence-Based Therapeutic Drug Monitoring: A Systematic Assessment. *La Lettre Pharmacologue* (2009) 23:29–34.
24. Kim HY, Martin JH, Mclachlan AJ, Boddy AV. Precision Dosing of Targeted Anticancer Drugs—Challenges in the Real World. *Transl Cancer Res* (2017) 6 (Suppl 10):S1500–11. doi: 10.21037/tcr.2017.10.30
25. Salman B, Al-Khabori M. Applications and Challenges in Therapeutic Drug Monitoring of Cancer Treatment: A Review. *J Oncol Pharm Pract* (2021) 27 (3):693–701. doi: 10.1177/1078155220979048
26. Bardin C, Veal G, Paci A, Chatelut E, Astier A, Levêque D, et al. Therapeutic Drug Monitoring in Cancer – Are We Missing a Trick? *Eur J Cancer* (2014) 50:2005–9. doi: 10.1016/j.ejca.2014.04.013
27. Estlin EJ, Veal GJ. Clinical and Cellular Pharmacology in Relation to Solid Tumours of Childhood. *Cancer Treat Rev* (2003) 29:253–73. doi: 10.1016/S0305-7372(02)00109-3
28. Felici A, Verweij J, Sparreboom A. Dosing Strategies for Anticancer Drugs: The Good, the Bad and Body-Surface Area. *Eur J Cancer* (2002) 38:1677–84. doi: 10.1016/S0959-8049(02)00151-X
29. Balis FM, Womer RB, Berg S, Winick N, Adamson PC, Fox E, et al. Dosing Anticancer Drugs in Infants: Current Approach and Recommendations From the Children Oncology Group's Chemotherapy Standardization Task Force. *Pediatr Blood Cancer* (2017) 64:e26636. doi: 10.1002/pbc.26636
30. Kendrick JG, Carr RR, Ensom MHH. Pharmacokinetics and Drug Dosing in Obese Children. *J Pediatr Pharmacol Ther* (2010) 15:94–109. doi: 10.5863/1551-6776-15.2.94
31. *RMS 2005–A Protocol for Non-Metastatic Rhabdomyosarcoma*. Available at: https://www.skion.nl/workspace/uploads/Protocol-EpSSG-RMS-2005-1-3-May-2012_1.pdf.
32. *High-Risk Neuroblastoma Study 2 of SIOP-Europa-Neuroblastoma (SIOPEN) (HR-NBL2)*. Available at: https://clinicaltrials.gov/ct2/show/NCT04221035.
33. Nijstad AL, Barnett S, Lalmohamed A, Bérénos IM, Parke E, Carruthers V, et al. Clinical Pharmacology of Cytotoxic Drugs in Neonates and Infants: Providing Evidence-Based Dosing Guidance. *Eur J Cancer* (2021). doi: 10.1016/j.ejca.2021.11.001
34. Hendrayana T, Wilmer A, Kurth V, Schmidt-Wolf IGH, Jaehde U. Anticancer Dose Adjustment for Patients With Renal and Hepatic Dysfunction: From Scientific Evidence to Clinical Application. *Sci Pharm* (2017) 85:8. doi: 10.3390/scipharm85010008
35. Griggs JJ, Bohlke K, Balaban EP, Dignam JJ, Hall ET, Harvey RD, et al. Appropriate Systemic Therapy Dosing for Obese Adult Patients With Cancer: ASCO Guideline Update. *J Clin Oncol* (2021) 39:2037–48. doi: 10.1200/JCO.21.00471
36. Barnett S, Hellmann F, Parke E, Makin G, Tweddle DA, Osborne C, et al. Vincristine Dosing, Drug Exposure and Therapeutic Drug Monitoring in Neonate and Infant Cancer Patients. *Eur J Cancer* (2021). doi: 10.1016/j.ejca.2021.09.014

Author Disclaimer: The views expressed are those of the authors and not necessarily those of the funders, the NIHR or the Department of Health and Social Care. None of the funding bodies played a role in the study design, the collection, analysis or interpretation of data, the writing of the report or the decision to submit the article for publication.

Conflict of Interest: The authors declare that the research was conducted in the absence of any commercial or financial relationships that could be construed as a potential conflict of interest.

Publisher's Note: All claims expressed in this article are solely those of the authors and do not necessarily represent those of their affiliated organizations, or those of the publisher, the editors and the reviewers. Any product that may be evaluated in this article, or claim that may be made by its manufacturer, is not guaranteed or endorsed by the publisher.

frontiers in Oncology

REVIEW
published: 10 January 2022
doi: 10.3389/fonc.2021.814699

Precision Cardio-Oncology: Use of Mechanistic Pharmacokinetic and Pharmacodynamic Modeling to Predict Cardiotoxicities of Anti-Cancer Drugs

Hai-ni Wen[1†], *Chen-yu Wang*[1†], *Jin-meng Li*[2] *and Zheng Jiao*[1*]

[1] Department of Pharmacy, Shanghai Chest Hospital, Shanghai Jiao Tong University, Shanghai, China, [2] Department of Pharmacy, Affiliated Hangzhou Chest Hospital, Zhejiang University School of Medicine, Hangzhou, China

The cardiotoxicity of anti-cancer drugs presents as a challenge to both clinicians and patients. Significant advances in cancer treatments have improved patient survival rates, but have also led to the chronic effects of anti-cancer therapies becoming more prominent. Additionally, it is difficult to clinically predict the occurrence of cardiovascular toxicities given that they can be transient or irreversible, with large between-subject variabilities. Further, cardiotoxicities present a range of different symptoms and pathophysiological mechanisms. These notwithstanding, mechanistic pharmacokinetic (PK) and pharmacodynamic (PD) modeling offers an important approach to predict cardiotoxicities and offering precise cardio-oncological care. Efforts have been made to integrate the structures of physiological and pharmacological networks into PK-PD modeling to the end of predicting cardiotoxicities based on clinical evaluation as well as individual variabilities, such as protein expression, and physiological changes under different disease states. Thus, this review aims to report recent progress in the use of PK-PD modeling to predict cardiovascular toxicities, as well as its application in anti-cancer therapies.

Keywords: cardiotoxicity, cardio-oncology, pharmacokinetic and pharmacodynamic modeling, mechanistic modeling, toxicity, anti-cancer drugs

OPEN ACCESS

Edited by:
Miao Yan,
Central South University, China

Reviewed by:
Andrea Camerini,
Azienda Usl Toscana nord ovest, Italy
Maria Laura Canale,
Azienda Usl Toscana nord ovest, Italy

****Correspondence:***
Zheng Jiao
jiaozhen@online.sh.cn

[†]These authors have contributed equally to this work and share first authorship

Specialty section:
This article was submitted to Pharmacology of Anti-Cancer Drugs, a section of the journal Frontiers in Oncology

Received: *14 November 2021*
Accepted: *15 December 2021*
Published: *10 January 2022*

Citation:
Wen H-n, Wang C-y, Li J-m and Jiao Z (2022) Precision Cardio-Oncology: Use of Mechanistic Pharmacokinetic and Pharmacodynamic Modeling to Predict Cardiotoxicities of Anti-Cancer Drugs. Front. Oncol. 11:814699. doi: 10.3389/fonc.2021.814699

INTRODUCTION

Advances in cancer treatment have dramatically improved patient survival rates. At the same time, however, the issue of preventing and managing treatment-associated chronic adverse events has become increasingly important. Cardiovascular complications have been identified as one of the leading causes of mortality in cancer survivors, regardless of the cancer type (1, 2). This has led to the development of a novel field, cardio-oncology, which focuses on reducing or managing the cardiotoxicity of anti-cancer agents, while maximizing therapeutic effects and managing patients with cancer having cardiovascular comorbidities. Further, cardio-oncology is increasingly becoming part of the standardized care for patients with cancer (3), and cardiovascular complications associated with cancer therapies, including

arrhythmia, hypertension, and heart failure, have been observed in clinical practice. Furthermore, the mechanisms behind these clinical symptoms can be categorized into: (1) drug-induced electrocardiograph changes; (2) drug-induced hemodynamic changes; and (3) drug-induced changes in molecular signaling pathways (4).

Pharmacokinetic and pharmacodynamic (PK-PD) modeling is an approach by which concentration-driven drug effects can be quantitatively predicted. Traditionally, in PK models, multiple compartments are applied to describe the kinetic behaviors of therapeutic drugs, with the different compartments representing various organs or tissue levels, within which the action of the relevant drugs is kinetically consistent. Additionally, in classical PD models, empirical mathematical models are used to describe drug effects. Therefore, by offering the possibility to gain a deeper understanding regarding basic pharmacology and with the development of computational capacities, mechanistic PK-PD modeling can be used for the integration of physiological and pharmacological mechanisms (5).

Further, mechanistic PK-PD modeling is an emerging field, the definition of which is constantly evolving (6). Specifically, basic mechanism-based PK-PD modeling often incorporates one or more critical drug action steps, such as receptor binding or cell turnover, to capture major rate-limiting steps in drug dispositions and explain between-subject variabilities (7). Furthermore, systems pharmacology modeling provides a comprehensive modeling approach that has as objective to integrate the structures of physiological and pharmacological networks through PK-PD modeling (8, 9). On the one hand, the physiological-based pharmacokinetic (PBPK) modeling framework enables the mechanistic description of drug absorption, distribution, metabolism, and excretion processes at the physiological level. Thus, these mechanistic descriptions can be extrapolated to different populations and disease states if the associated physiological changes can be elucidated (10). On the other hand, with the development of high-throughput analytical methods, bioinformatics, and system biology, quantitative systems pharmacology (QSP) aims to quantitatively describe the behaviors of biological systems, and explain between-subject variabilities at genetic, protein, cellular, and whole-body levels (9).

To date, mechanistic PK-PD modeling has been extensively applied to quantify the cardiovascular toxicities of therapeutic drugs and predict the toxicities of anti-cancer drugs. In a few studies, mechanistic models have been established to describe the cardiotoxicities of anti-cancer drugs. Therefore, in this work, our aim was to review the role of mechanistic PK-PD modeling with respect to cardiovascular safety and its application in cardio-oncology.

MODELING OF CHANGES IN ELECTROCARDIOGRAPH

Mechanisms of Drug-Induced Changes in Electrocardiographs

Several patients with cancer experience arrhythmias that are associated with anti-cancer therapies or cancers (11). Further, drug-induced arrhythmias can lead to life-threatening adverse events or sudden death, and clinically, this is frequently evidenced by changes in the electrocardiographs of patients (12). Among the various forms of arrhythmias, torsades de pointes (TdP) are the most dangerous. Specifically, TdP, meaning "twist of the points", is a polymorphic ventricular tachycardia (VT) that is potentially fatal, and given that its occurrence is associated with QT interval prolongation, QT intervals are widely recognized as a proxy for TdP, as well as an index of cardiovascular safety (13). Thus, the quantitative modeling of QT intervals is the most popular strategy by which the proarrhythmic properties of a given drug can be clarified.

Basic Mechanism-Based Modeling of Electrocardiograph Changes

The drug concentration-driven prolongation of QT intervals can be quantitatively predicted using PK-PD modeling. Additionally, the response of the QT interval to anti-cancer drugs has been successfully described empirically for several drugs, including dofetilide, azithromycin, and moxifloxacin, using (log-) linear models as well as simple and sigmoid E_{max} models (4). As the QT interval is strongly dependent on factors, such as heart rate and circadian rhythm, several attempts have been made to model it by correcting for these factors. For example, Chain et al. established a PD model to describe the corrected QT interval as a function of both physiological conditions and drug effects (14), as expressed below.

$$QT_C = QT_0 \times RR^{\alpha} + A \times \cos\left(\frac{2\pi}{24}(t-\phi)\right) + Slope \times C$$

where QT_0 represents the baseline for the QT-RR relationship, RR represents the interval between the R waves on the electrocardiogram, α represents an individual correction factor, the cosine function describes the circadian rhythm of the heart in different phases, and C represents drug concentration. In this case, the drug effect was modeled linearly.

Additionally, the QT interval is a sensitive but non-specific index of cardiac safety. In fact, several drugs share the same QT interval prolongation effect, but have different proarrhythmic properties (15). Thus, another biomarker of drug-induced arrhythmic risk, the human Ether-à-go-go-related Gene (hERG) channel block (16), has been identified. Arrhythmic risk is presumed to be dependent on the affinity of the drug in question to the different ion channels that control the action potential (AP) duration of the heart. Therefore, the half-maximal inhibitory concentration (hERG IC_{50}) value of a compound, which is defined as the concentration of a given drug that will decrease the current flow through the hERG channel by 50%, can be used to indicate the potency of a given drug to induce TdP. With the aid of mathematical cardiac electrophysiology models, drug-ion channel interactions have been mechanistically modeled to predict the effects of drugs on AP duration. For example, Mirams et al. (17) predicted the TdP risks associated with various drugs using their reported hERG IC_{50} values. Specifically, the conductance of a given channel, j (g_j), as a

function of the drug amount (D) and the IC_{50} value can be modeled as follows:

$$g_j = g_{control,j}\left(1 + \left(\frac{(D)}{(IC_{50})j}\right)^n\right)^{-1}$$

where $g_{control,\ j}$ represents the baseline maximal conductance of channel *j*. Additionally, the conductance of the channel can then be linked to channel currents and membrane voltages to predict changes in AP duration. In this regard, the application of cardiac electrophysiology models has enabled the classification of compounds as high-, intermediate-, and low-risk compounds with respect to the occurrence of TdP.

Systems Pharmacology Modeling of Electrocardiograph Changes

Recent studies have shown that cardiac electrophysiology models fail to capture the binding dynamics in drug-channel interactions. Thus, they cannot be used to distinguish between drugs with different binding rates to ion channels. In this regard, to further improve the prediction of drug-induced arrhythmic risks, Li et al. (18) proposed a novel hERG model that integrates cardiac electrophysiology and multi-ion channel pharmacology, as illustrated in **Figure 1**.

By applying a PD model with three drug-bound states, the model proposed by Li et al. can be used to distinguish the proarrhythmic risks associated with trapped compounds from those associated with their untrapped counterparts, as the former often have higher proarrhythmic risks for the same hERG IC_{50} value. The left-hand side of **Figure 1** shows the physiological part of the model, which describes the closing (C), inactivated closing (IC), and opening (O) states of ion channels. Conversely, the pharmacodynamic part (right-hand side) assumes three drug-bound states: open bound (O*), inactivated open bound (IO*), and closed bound (C*). This implies that the drug in question can be trapped in the C* state, implying that this proposed model can be used to successfully predict the TdP risk levels of all training compounds (n = 12).

Even though system pharmacology modeling can be used to describe the binding dynamics of drugs, parameters such as E_{max} and IC_{50} can only be estimated based on preclinical studies. Thus, the model needs measurable patient parameters patients such as the QT interval before its use can be extended to clinical practice.

MODELING OF HEMODYNAMIC CHANGES

Mechanisms of Drug-Induced Hemodynamic Changes

Blood pressure (BP) elevations and heart failure, which are common cardiovascular side effects of anti-cancer drugs, are often associated with hemodynamic changes. Specifically, hemodynamics is the study of blood flow dynamics, which are governed by BP and vascular resistance in different parts of the system, as well as by the contractability of the heart. Unlike TdP, BP elevations are not typically life-threatening, thus they have received less attention from pharmacometricians. Conversely, the occurrence of heart failure, which involves both hemodynamic and pathological changes, can be chronic and acute. Additionally, heart failure could also be the consequence of the direct cardiotoxicity of anticancer drugs, such as trastuzumab and anthracyclines (19, 20). Therefore, the modeling of heart failure is complicated and specific to a certain class of drugs.

Basic Mechanism-Based Modeling of Hemodynamic Changes

Empirical PD models are frequently used to describe drug-induced BP elevations. For example, a linear function with a cyclical diurnal variation of mean aortic BP (MBP) has been applied in a PD model of regorafenib (21).

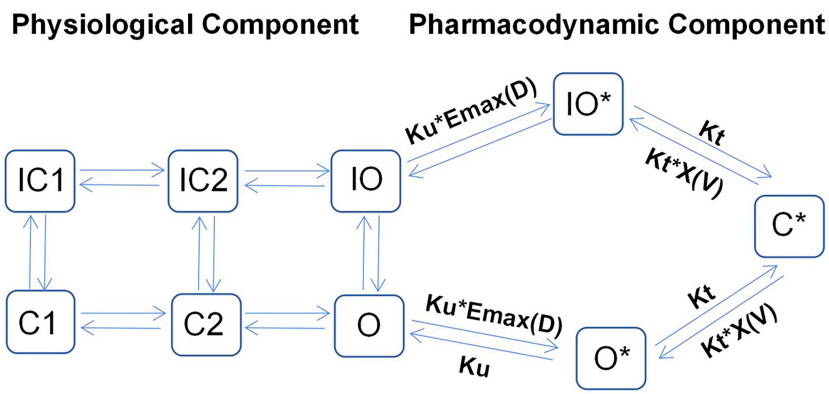

FIGURE 1 | Illustrative structure of a dynamic hERG-binding model. The left part corresponds to the physiological component of the model, where C1 and C2 represent the closed states of the channel and O represents the open state, with the corresponding inactivated states indicated as IC1, IC2, and IO, respectively. The right part represents the pharmacodynamic component, which assumes three drug-bound states: open bound (O*), inactivated open bound (IO*), and closed bound (C*). The drug can be trapped in the C* state.

$$BP = E_0 + slope \times C$$

$$E_0 = E_{BL} + \text{Amp} \times \cos\left(\frac{2\pi(t - Tshift)}{Freq}\right)$$

where E_0 represents baseline BP, which is influenced by the circadian rhythm. Further, C represents drug concentration, which is linked to response *via* a linear function.

Van Hasselt et al. (22) developed a population PK-PD model corresponding to the relationship between the left ventricular ejection fraction (LVEF) and trastuzumab exposure. They also identified the associated clinically relevant covariates (**Figure 2**), and observed that the LVEF values could be best described using an effect-compartment model. Additionally, the population's LVEF recovery half-life after trastuzumab treatment ($T_{1/2rec}$) was estimated to be 49.7 d, and the cumulative anthracycline dose was found to be a significant determinant of the half-maximal effect concentration (EC_{50}). Further, they also observed that anthracycline caused a 45.9% increase in sensitivity (i.e., a decrease in EC_{50}) at its maximum cumulative dose.

Systems Pharmacology Modeling of Hemodynamic Changes

Traditionally, hemodynamic parameters, such as BP or heart rate (HR), are often quantified independently, without considering the inter-relationships between them. Important variables for cardiovascular hemodynamics include: HR; mean arterial, diastolic, and systolic BP (MAP, DBP, and SBP, respectively); stroke volume (SV); cardiac output (CO); and total peripheral resistance (TPR), and the interrelationships between MAP, TPR, CO, HR, and SV are expressed as: (i) MAP = CO × TPR and (ii) CO = HR × SV (4). Further, the interrelationships between these variables are complex owing to the feedback mechanism of hemodynamics. Therefore, to compute these variables simultaneously, a systems approach that integrates cardiovascular physiology and the interactions between these variables is needed. In this regard, Snelder et al. (23) proposed a systems model with negative homeostatic feedback through MAP that can be used to describe changes in TPR, HR, and SV, as illustrated in **Figure 3**.

In the structure of this model, three turnover models that are regulated by homeostatic feedback through MAP (FB-MAP) are linked together to describe changes in HR, SV, and TPR. Additionally, in each equation, K_{in_i} represents the zero-order production rate of each parameter, while k_{out_i} represents the first-order elimination rate of each parameter.

$$\frac{dHR}{dt} = K_{in\_HR} \times (1 - FB \times MAP) - k_{out\_HR} \times HR$$

$$\frac{dSV^*}{dt} = K_{in\_SV} \times (1 - FB \times MAP) - k_{out\_SV} \times SV^*$$

$$\frac{dTPR}{dt} = K_{in\_TPR} \times (1 - FB \times MAP) - k_{out\_TPR} \times TPR$$

$$SV = SV^* \times (1 - HR\_SV \times LN(HR/BSL\_HR))$$

$$CO = HR \times SV$$

$$MAP = CO \times TPR$$

Considering the circadian rhythm as well as drug effects, these equations can be written as follows:

$$\frac{dHR}{dt} = K_{in\_HR} \times (1 + CR_{HR}) \times (1 - FB \times MAP) \times (1 + EFF + HD_{HR}) - k_{out\_HR} \times HR$$

$$\frac{dSV^T}{dt} = K_{in\_SV} \times (1 - FB \times MAP) \times (1 + EFF) - k_{out\_SV} \times SV^T$$

$$\frac{dTPR}{dT} = K_{in\_TPR} \times (1 + CR_{TPR}) \times (1 - FB \times MAP) \times (1 + EFF + HD_{TPR}) - k_{out\_TPR} \times TPR$$

where CR_i represents the circadian rhythm of each carrier and EFF represents drug effect, which for different drugs, is assessed based on linear, power, E_{max}, or Sigmoid E_{max} models.

The abovementioned model has enabled the prediction of drug-induced hemodynamic changes based on HR and MAP measurements. More recently, Sang et al. (24) utilized the model for predicting anthracycline-induced heart failure, and by quantifying the interactions between preload, afterload, and the myocardial contraction of the cardiovascular system in the QSP model, they were able to distinguish pre-existing diseases or disease progression from drug effects. Further, in this study by Sang et al., the QSP-PK-PD model of doxorubicin-induced cardiotoxicity showed desirable prediction in a population consisting of individuals with and without preexisting cardiovascular conditions.

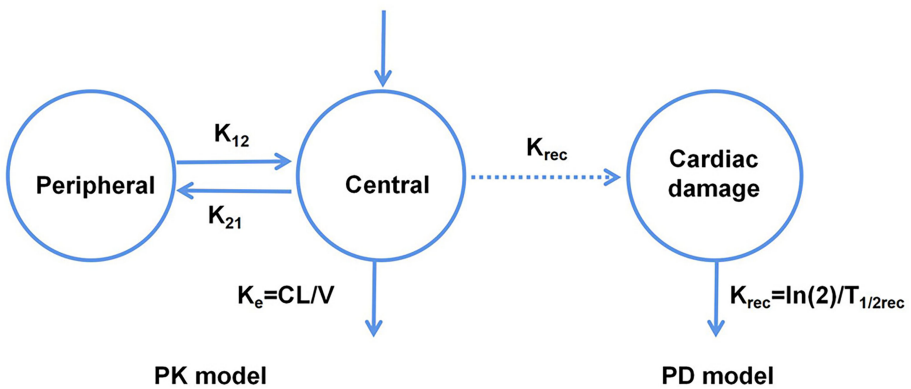

FIGURE 2 | Schematic representation of the PK-PD model corresponding to the relationship between the left ventricular ejection fraction and trastuzumab exposure.

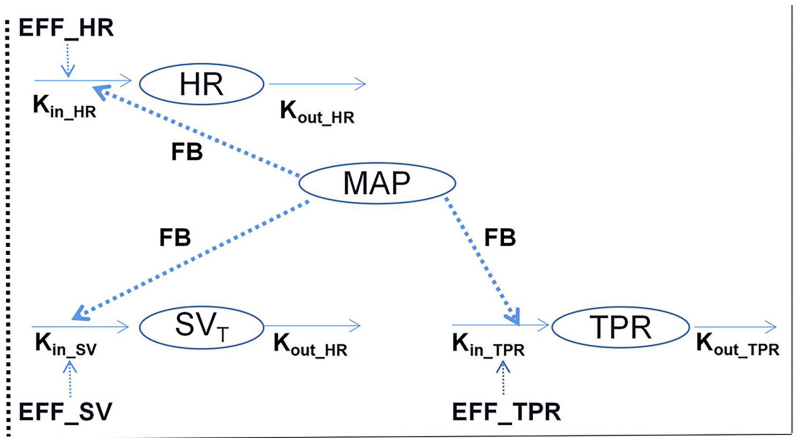

FIGURE 3 | Illustrative structure of the hemodynamic system pharmacology model developed by Snelder et al. (23). HR, heart rate; TPR, total peripheral resistance; MAP, mean arterial pressure; and SV, stroke volume. FB- represents the negative feedback mechanism through MAP. The effects on HR, SV, and TPR are described using turnover models. K_{in_HR}, K_{in_SV}, and K_{in_TPR} represent the zero-order production rate constants and k_{out_HR}, k_{out_SV}, and k_{out_TPR} represent the first-order elimination rate constants.

MODELING OF DRUG-INDUCED CHANGES IN MOLECULAR SIGNALING PATHWAYS

Drug-Induced Changes in Molecular Signaling Pathways

While the effects of cancer drugs on electrocardiographs and the hemodynamic functions of the cardiovascular systems are a shared mechanism of drug-induced cardiotoxicities, in recent studies, more interest has been given to revealing the drug-specific mechanisms that underlie cardiotoxicities, especially with respect to impact on molecular signaling pathways (25).

The cardiac side effects of chemotherapies were first reported following the introduction of daunorubicin. Additionally, the cardiotoxicity of anthracyclines has been widely investigated since their introduction (26). Specifically, anthracycline-induced cardiomyopathy can occur at both early and late onset cancers, and the well-accepted mechanism of such cardiotoxicity involves the iron-dependent generation of reactive oxygen species (ROS), which thereafter cause oxidative damage to cardiomyocytes (27). Further, recent studies have revealed that ROS production is dependent on topoisomerase-2β, which seemingly, is a key mediator of doxycycline (DOX)-related cardiomyopathy (28).

In the past, the cardiac side effects of targeted therapies were initially considered minimal, as kinases were not constitutively active in normal tissues. However, the long-term use of targeted therapies still result in cardiovascular side effects, such as heart failure, QT interval prolongation, and myocardial injury. Further, considering tyrosine kinase inhibitors (TKIs) as examples, these treatments target the proliferation pathways of cardiomyocytes as well as cancer cells. Thus, the inhibition of these pro-survival kinases in normal cardiomyocytes results in the cardiotoxicities of TKI.

Basic Mechanism-Based Modeling of Drug-Induced Changes in Molecular Signaling Pathways

It has been observed that anthracycline-induced cardiotoxicities are dose-dependent. Moreover, there seems to be a correlation between cardiotoxicity and drug peak plasma levels (29). Despite various proposed dosing strategies, such as the limiting of total dose and increasing infusion duration, the observed variability in individual responses to anthracyclines is still unclear. Therefore, PK-PD modeling provides a potential solution for anthracycline precision dosing.

He et al. (30) developed a multiscale PK model that involves the assessment of doxorubicin dispositions as well as interstitial tissues, cells, and cellular organelles (**Figure 4**). Additionally, in most previous studies, it has been observed that cardiotoxicity is associated with the average plasma concentrations of different drugs. However, the most relevant concentrations with respect to cytotoxicity are those in cells or nuclei. In this regard, the nucleus sub-compartment equation was defined as follows:

$$C_{e\_org} = 0.5 \times \left(\left(C_{et\_org} - CN_{org} - K_d \right) + \sqrt{\left(C_{et\_org} - CN_{org} - K_d \right)^2 + 4 \times K_d \times C_{et\_org}} \right)$$

$$C_{DNA\_bound} = C_{et\_org} - C_{e\_org}$$

where C_{et_org} represents total intracellular concentration, C_{e_org} represents free intracellular concentrations, CN_{org} represents DNA concentration, and C_{DNA_bound} represents DNA bound concentration.

The model predicted that prolonged infusion did not reduce doxorubicin-deoxyribonucleic acid (DNA) adducts at the tumor nucleus. This is consistent with clinical observations that prolonged infusion do not compromise the anti-tumor effect, indicating that DNA torsion is a primary anti-tumor mechanism (31).

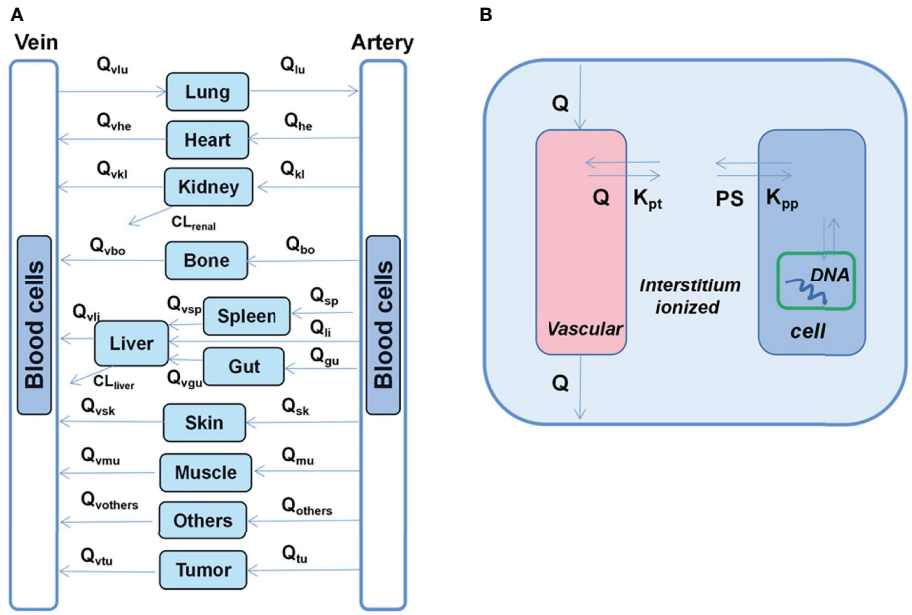

FIGURE 4 | Schematic diagram of the developed multiscale PB-PK model for doxorubicin. **(A)** Whole-body PB-PK model comprising seven tissues and two blood compartments. The blood compartments are further divided into plasma and blood cell sub-compartments. **(B)** Tissue model; each tissue is divided into the vascular, interstitial, intracellular, and nucleus DNA-bound sub-compartments.

Systems Pharmacology Modeling of Drug-Induced Changes in Molecular Signaling Pathways

TKI-induced cardiotoxicity can be attributed to the activity of one or more tyrosine kinases in cardiomyocytes. Further, critical processes, such as survival signaling, energy homeostasis, and excitation-contraction coupling are controlled by molecular signaling pathways. Thus, QSP approaches seem to be well suited for the study of TKI-induced cardiotoxicity given that tyrosine kinase signaling encompasses large as well as complex networks with numerous feedback loops.

Vaidya et al. (32) recently investigated two TKIs, dasatinib and sorafenib. Further, QSP models have been developed to capture various trends in protein signaling and cellular responses regarding parameter estimates. In this regard, the key signal transduction pathways are shown in **Figure 5**.

The proteins in the apoptotic pathway that involves pBAD, pBcl2, Caspase-9, and active Caspase-3 have been described in the QSP model. Additionally, the model can be used to predict the IC_{50} values corresponding to different drug concentrations; these simulation results have been verified using data based on *in vitro* studies.

Additionally, the QSP platform is useful for elucidating cardiotoxicity mechanisms, and simulations based thereon can facilitate the evaluation of drug dosing strategies to the end of alleviating cardiotoxicity. Therefore, it offers the possibility to overcome the problem of cardiotoxicity without compromising the cytotoxic activity of the different drugs that are used to treat specific malignancies.

DISCUSSION

As an emerging field of interest, cardio-oncology aims to identify patients with risk factors, prevent cardiovascular damage, and monitor or manage the progress of cardiovascular toxicities (33). Mechanistic PK-PD modeling offers a potential approach for the prevention and identification of cardiovascular toxicities by quantifying exposure-response relationships. Limitations of PK-PD modeling should also be noted. First, while examples of mechanistic PK-PD modeling in cardiovascular safety with respect to anti-cancer drugs exist, they have been limited to a few drugs. Second, such PK/PD models should be further evaluated by large prospective clinical investigations before applying to the real clinical settings. Third, PK-Pd models could be considered as an additional tool to predict cardiac toxicity but they do not substitute to clinical evaluation. Complementary to clinical evaluations, further investigations of predictive performances are essential to their clinical applications.

Based on published studies, drug-induced electrocardiograph and hemodynamic changes can be sufficiently modeled using various model structures. Additionally, modeling techniques for electrocardiograph and hemodynamic changes are flexible and versatile, and pharmacometricians can choose the appropriate ones based on the purpose of modeling as well as the characteristics of the data used. However, these models lack information on the drug-specific mechanisms associated with cardiovascular toxicity, and their applications in clinical scenarios are

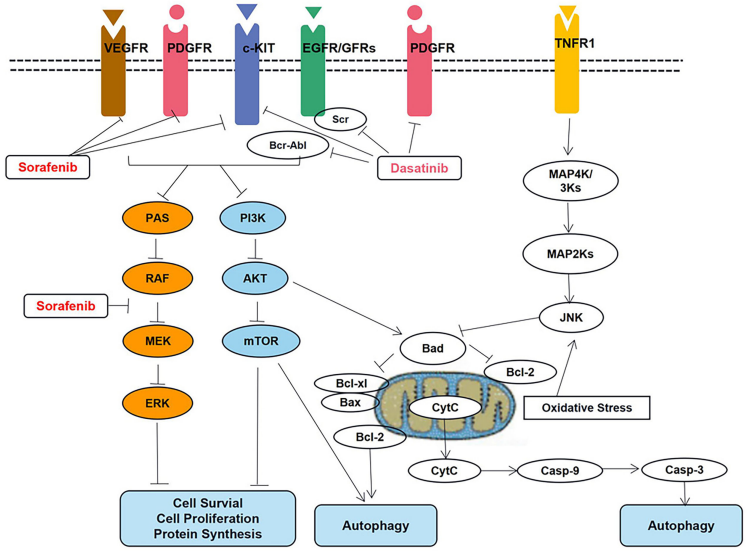

FIGURE 5 | Key signal transduction pathways involved in dasatinib- and sorafenib-induced toxicity in cardiomyocytes. AKT, AKT8 virus oncogene cellular homolog; BAD, Bcl2-associated death promoter; BAX, Bcl2-associated X protein; Bcl-2, B-cell lymphoma 2 protein; Bcl-xl, B-cell lymphoma extra-large protein; Bcr-Abl, fusion protein encoded by the Philadelphia chromosome; Casp-3, caspase-3; Casp-9, caspase-9; c-KIT, stem cell growth factor receptor; Cyt, C cytochrome c; EGFR, epidermal growth factor receptor; ERK, extracellular signal regulated kinase; JNK, Jun N-terminal kinase; MAPK, mitogen activated protein kinase; MEK, MAPK/ERK kinase; mTOR, mammalian target of rapamycin; PDGFR, platelet derived growth factor receptor; PI3K, phosphoinositide 3 kinase; RAF, rapidly accelerated fibrosarcoma kinase protein; RAS, prototypical member of the Ras superfamily of proteins (belonging to the small GTPase group of proteins); Src Rous, sarcoma oncogene cellular homolog tyrosine kinase protein; TNFR1, tumor necrosis factor receptor 1; VEGFR, vascular endothelial growth factor receptor.

limited. Therefore, in the future, drug-specific mechanisms can be incorporated into these models to enhance their performance with respect to predictabilities, and bridge the gaps between theoretical modeling and real clinical scenarios.

Additionally, the modeling of drug-induced changes in molecular signaling pathways tends to be comprehensive and drug-specific, and the prerequisite for successful modeling is an understanding of molecular pathways and dose-driven relationships. QSP provide the potential approaches given that they offer the possibility to construct biological interactions within systems. Moreover, QSP approaches can eventually be applied to distinguish disease populations from healthy ones, and also bridge the gap between application in ideal populations and real-world populations (34, 35). However, high-throughput experiments with system-level information, as well as computational techniques are required for the establishment of QSP networks. Thus, it is evident that QSP applications are still limited to preclinical research for some drugs of particular interest.

CONCLUSIONS

In conclusion, mechanistic PK-PD modeling has been extensively applied to quantify the cardiovascular toxicities of anti-cancer drugs. Further, drug-induced changes in physio-electricity and hemodynamics can be well modeled using quantitative systems biology. Therefore, in future, bridging the gap between mechanistic cardiovascular models and clinical realities would offer the possibility to quantify the cardiovascular toxicities of anti-cancer drugs. Such PK/PD models should be further evaluated by large prospective clinical investigations before applying to the real clinical settings.

AUTHOR CONTRIBUTIONS

H-NW: Funding acquisition, visualization, writing — original draft, review, and editing. C-YW: Conceptualization, validation, writing — original draft, review, and editing. J-ML: Visualization, source, writing — review & editing. ZJ: Methodology, supervision, writing — original draft, writing — review, and editing. All authors contributed to the article and approved the submitted version.

FUNDING

This study was supported by Shanghai "Rising Stars of Medical Talents" Youth Development Program-Youth Medical Talents: Clinical Pharmacist Program (SHWSRS(2021)_099), Bethune Charitable Foundation (B-19-H-20200622) and Wu Jieping Medical Foundation (320.6750.2020-10-103).

REFERENCES

1. Patnaik JL, Byers T, DiGuiseppi C, Dabelea D, Denberg TD. Cardiovascular Disease Competes With Breast Cancer as the Leading Cause of Death for Older Females Diagnosed With Breast Cancer: A Retrospective Cohort Study. *Breast Cancer Res* (2011) 13(3):1–9. doi: 10.1186/BCR2901
2. Sturgeon KM, Deng L, Bluethmann SM, Zhou S, Trifiletti DM, Jiang C, et al. A Population-Based Study of Cardiovascular Disease Mortality Risk in US Cancer Patients. *Eur Heart J* (2019) 40:3889–97. doi: 10.1093/EURHEARTJ/EHZ766
3. Lenneman CG, Sawyer DB. Cardio-Oncology: An Update on Cardiotoxicity of Cancer-Related Treatment. *Circ Res* (2016) 118:1008–20. doi: 10.1161/CIRCRESAHA.115.303633
4. Collins TA, Bergenholm L, Abdulla T, Yates JWT, Evans N, Chappell MJ, et al. Modeling and Simulation Approaches for Cardiovascular Function and Their Role in Safety Assessment. *CPT Pharmacometrics Syst Pharmacol* (2015) 4:175–88. doi: 10.1002/PSP4.18
5. Danhof M, de Lange ECM, Della Pasqua OE, Ploeger BA, Voskuyl RA. Mechanism-Based Pharmacokinetic-Pharmacodynamic (PK-PD) Modeling in Translational Drug Research. *Trends Pharmacol Sci* (2008) 29:186–91. doi: 10.1016/J.TIPS.2008.01.007
6. Jusko WJ. Moving From Basic Toward Systems Pharmacodynamic Models. *J Pharm Sci* (2013) 102:2930–40. doi: 10.1002/JPS.23590
7. Danhof M, De Jongh J, De Lange ECM, Della Pasqua O, Ploeger BA, Voskuyl RA. Mechanism-Based Pharmacokinetic-Pharmacodynamic Modeling: Biophase Distribution, Receptor Theory, and Dynamical Systems Analysis. *Annu Rev Pharmacol Toxicol* (2007) 47:357–400. doi: 10.1146/ANNUREV.PHARMTOX.47.120505.105154
8. Gadkar K, Kirouac D, Parrott N, Ramanujan S. Quantitative Systems Pharmacology: A Promising Approach for Translational Pharmacology. *Drug Discov Today Technol* (2016) 21–22:57–65. doi: 10.1016/J.DDTEC.2016.11.001
9. Azer K, Kaddi CD, Barrett JS, Bai JPF, McQuade ST, Merrill NJ, et al. History and Future Perspectives on the Discipline of Quantitative Systems Pharmacology Modeling and Its Applications. *Front Physiol* (2021) 12:637999. doi: 10.3389/FPHYS.2021.637999
10. Sager JE, Yu J, Ragueneau-Majlessi I, Isoherranen N. Physiologically Based Pharmacokinetic (PBPK) Modeling and Simulation Approaches: A Systematic Review of Published Models, Applications, and Model Verification. *Drug Metab Dispos* (2015) 43:1823–37. doi: 10.1124/dmd.115.065920
11. Alexandre J, Moslehi JJ, Bersell KR, Funck-Brentano C, Roden DM, Salem JE. Anticancer Drug-Induced Cardiac Rhythm Disorders: Current Knowledge and Basic Underlying Mechanisms. *Pharmacol Ther* (2018) 189:89–103. doi: 10.1016/J.PHARMTHERA.2018.04.009
12. Tisdale JE, Chung MK, Campbell KB, Hammadah M, Joglar JA, Leclerc J, et al. Drug-Induced Arrhythmias: A Scientific Statement From the American Heart Association. *Circulation* (2020) 142:E214–33. doi: 10.1161/CIR.0000000000000905
13. Passman R, Kadish A. Polymorphic Ventricular Tachycardia, Long Q-T Syndrome, and Torsades De Pointes. *Med Clin North Am* (2001) 85:321–41. doi: 10.1016/S0025-7125(05)70318-7
14. Chain ASY, Dubois VFS, Danhof M, Sturkenboom MCJM, Della Pasqua O. Identifying the Translational Gap in the Evaluation of Drug-Induced QTc Interval Prolongation. *Br J Clin Pharmacol* (2013) 76:708–24. doi: 10.1111/BCP.12082
15. Ahmad K, Dorian P. Drug-Induced QT Prolongation and Proarrhythmia: An Inevitable Link? *Europace* (2007) 9 Suppl 4:iv16–22. doi: 10.1093/EUROPACE/EUM167
16. Witchel HJ. Drug-Induced hERG Block and Long QT Syndrome. *Cardiovasc Ther* (2011) 29:251–9. doi: 10.1111/J.1755-5922.2010.00154.X
17. Mirams GR, Cui Y, Sher A, Fink M, Cooper J, Heath BM, et al. Simulation of Multiple Ion Channel Block Provides Improved Early Prediction of Compounds' Clinical Torsadogenic Risk. *Cardiovasc Res* (2011) 91:53–61. doi: 10.1093/CVR/CVR044
18. Li Z, Dutta S, Sheng J, Tran PN, Wu W, Chang K, et al. Improving the In Silico Assessment of Proarrhythmia Risk by Combining hERG (Human Ether-À-Go-Go-Related Gene) Channel-Drug Binding Kinetics and Multichannel Pharmacology. *Circ Arrhythm Electrophysiol* (2017) 10(2):e004628. doi: 10.1161/CIRCEP.116.004628
19. Nishi M, Wang P, Hwang PM. Cardiotoxicity of Cancer Treatments: Focus on Anthracycline Cardiomyopathy. *Arterioscler Thromb Vasc Biol* (2021) 41:2648–60. doi: 10.1161/ATVBAHA.121.316697
20. Wu Q, Bai B, Tian C, Li D, Yu H, Song B, et al. The Molecular Mechanisms of Cardiotoxicity Induced by HER2, VEGF, and Tyrosine Kinase Inhibitors: An Updated Review. *Cardiovasc Drugs Ther* (2021). doi: 10.1007/S10557-021-07181-3
21. Collins T, Gray K, Bista M, Skinner M, Hardy C, Wang H, et al. Quantifying the Relationship Between Inhibition of VEGF Receptor 2, Drug-Induced Blood Pressure Elevation and Hypertension. *Br J Pharmacol* (2018) 175:618–30. doi: 10.1111/BPH.14103
22. Van Hasselt JGC, Boekhout AH, Beijnen JH, Schellens JHM, Huitema ADR. Population Pharmacokinetic-Pharmacodynamic Analysis of Trastuzumab-Associated Cardiotoxicity. *Clin Pharmacol Ther* (2011) 90:126–32. doi: 10.1038/CLPT.2011.74
23. Snelder N, Ploeger BA, Luttringer O, Rigel DF, Fu F, Beil M, et al. Drug Effects on the CVS in Conscious Rats: Separating Cardiac Output Into Heart Rate and Stroke Volume Using PKPD Modelling. *Br J Pharmacol* (2014) 171:5076–92. doi: 10.1111/BPH.12824
24. Sang L, Yuan Y, Zhou Y, Zhou Z, Jiang M, Liu X, et al. A Quantitative Systems Pharmacology Approach to Predict the Safe-Equivalent Dose of Doxorubicin in Patients With Cardiovascular Comorbidity. *CPT Pharmacometrics Syst Pharmacol* (2021) 10:1512–24. doi: 10.1002/PSP4.12719
25. Ewer MS, Ewer SM. Cardiotoxicity of Anticancer Treatments. *Nat Rev Cardiol* (2015) 12:547–58. doi: 10.1038/NRCARDIO.2015.65
26. Tan C, Tasaka H, Yu K-P, Murphy ML, Karnofsky DA. Daunomycin, an Antitumor Antibiotic, in the Treatment of Neoplastic Disease. Clinical Evaluation With Special Reference to Childhood Leukemia. *Cancer* (1967) 20:333–53. doi: 10.1002/1097-0142(1967)20:3<333::aid-cncr2820200302>3.0.co;2-k
27. Link G, Tirosh R, Pinson A, Hershko C. Role of Iron in the Potentiation of Anthracycline Cardiotoxicity: Identification of Heart Cell Mitochondria as a Major Site of Iron-Anthracycline Interaction. *J Lab Clin Med* (1996) 127:272–8. doi: 10.1016/S0022-2143(96)90095-5
28. Zhang S, Liu X, Bawa-Khalfe T, Lu LS, Lyu YL, Liu LF, et al. Identification of the Molecular Basis of Doxorubicin-Induced Cardiotoxicity. *Nat Med* (2012) 18:1639–42. doi: 10.1038/NM.2919
29. Vejpongsa P, Yeh ETH. Prevention of Anthracycline-Induced Cardiotoxicity: Challenges and Opportunities. *J Am Coll Cardiol* (2014) 64:938–45. doi: 10.1016/J.JACC.2014.06.1167
30. He H, Liu C, Wu Y, Zhang X, Fan J, Cao Y. A Multiscale Physiologically-Based Pharmacokinetic Model for Doxorubicin to Explore its Mechanisms of Cytotoxicity and Cardiotoxicity in Human Physiological Contexts. *Pharm Res* (2018) 35:174. doi: 10.1007/S11095-018-2456-8
31. Shapira J, Gotfried M, Lishner M, Ravid M. Reduced Cardiotoxicity of Doxorubicin by a 6-Hour Infusion Regimen. A Prospective Randomized Evaluation. *Cancer* (1990) 65:870–3. doi: 10.1002/1097-0142(19900215)65:4<870::aid-cncr2820650407>3.0.co;2-d
32. Vaidya T, Kamta J, Chaar M, Ande A, Ait-Oudhia S. Systems Pharmacological Analysis of Mitochondrial Cardiotoxicity Induced by Selected Tyrosine Kinase Inhibitors. *J Pharmacokinet Pharmacodyn* (2018) 45:401–18. doi: 10.1007/S10928-018-9578-9
33. Barros-Gomes S, Herrmann J, Mulvagh SL, Lerman A, Lin G, Villarraga HR. Rationale for Setting Up a Cardio-Oncology Unit: Our Experience at Mayo Clinic. *Cardiooncology* (2016) 2(1):1–9. doi: 10.1186/S40959-016-0014-2
34. Stern AM, Schurdak ME, Bahar I, Berg JM, Taylor DL. A Perspective on Implementing a Quantitative Systems Pharmacology Platform for Drug Discovery and the Advancement of Personalized Medicine. *J Biomol Screen* (2016) 21:521–34. doi: 10.1177/1087057116635818
35. Bradshaw EL, Spilker ME, Zang R, Bansal L, He H, Jones RDO, et al. Applications of Quantitative Systems Pharmacology in Model-Informed Drug Discovery: Perspective on Impact and Opportunities. *CPT Pharmacometrics Syst Pharmacol* (2019) 8:777. doi: 10.1002/PSP4.12463

Conflict of Interest: The authors declare that the research was conducted in the absence of any commercial or financial relationships that could be construed as a potential conflict of interest.

frontiers in Oncology

PERSPECTIVE
published: 19 January 2022
doi: 10.3389/fonc.2021.801199

Cutaneous Toxicity Associated With Enfortumab Vedotin: A Real-Word Study Leveraging U.S. Food and Drug Administration Adverse Event Reporting System

Hui Yang, Xiaojia Yu and Zhuoling An *

Department of Pharmacy, Beijing Chao-Yang Hospital, Capital Medical University, Beijing, China

Introduction: Enfortumab vedotin (EV) has been demonstrated to have a significant response rate in early phase trials and is known for its tolerable side-effect profile. Emerging case reports have raised awareness of cutaneous toxicities, which may be a potentially fatal complication.

Objective: To assess the potential relevance between EV and cutaneous toxicities reports through data mining of the U.S. Food and Drug Administration (FDA) adverse event reporting system (FAERS).

Methods: Data from January 1, 2019, to November 4, 2021, in the FAERS database were retrieved. Information component (IC) and reporting odds ratio (ROR) were used to evaluate the association between EV and cutaneous toxicities events.

Results: EV was significantly associated with cutaneous toxicities in the database compared with both all other drugs (ROR 12.90 [10.62–15.66], IC 2.76 [2.52–3.01], middle signal) and platinum-based therapy (ROR 15.11 [12.43–18.37], IC 2.91 [2.66–3.15], middle signal) in the FAERS database. A significant association was detected between EV and all the cutaneous adverse effects (AEs) except erythema, palmar–plantar erythrodysesthesia syndrome, and dermatitis allergic. Both Stevens–Johnson syndrome and toxic epidermal necrolysis occurred 15 times as frequently for EV compared with all other drugs (ROR = 15.20; ROR = 15.52), while Stevens–Johnson syndrome occurred 18 times and toxic epidermal necrolysis occurred 7 times as frequently for EV compared with platinum-based therapy in the database (ROR = 18.74; ROR = 7.80). All groups that limited the gender and age showed a significant association between EV and cutaneous toxicities.

Conclusions: A significant signal was detected between EV use and cutaneous toxicities. It is worth noting that Stevens–Johnson syndrome and toxic epidermal necrolysis were significantly associated with EV use.

Keywords: cutaneous toxicity, EV, Food and Drug Administration Adverse Event Reporting System, disproportionality analysis, real-word study

OPEN ACCESS

Edited by:
Jennifer Martin,
The University of Newcastle, Australia

Reviewed by:
Tapas Ranjan Behera,
Cleveland Clinic, United States
Simone Scagnoli,
Sapienza University of Rome, Italy

***Correspondence:**
Zhuoling An
anzhuoling@163.com

Specialty section:
This article was submitted to Pharmacology of Anti-Cancer Drugs, a section of the journal Frontiers in Oncology

Received: *25 October 2021*
Accepted: *22 December 2021*
Published: *19 January 2022*

Citation:
Yang H, Yu X and An Z (2022) Cutaneous Toxicity Associated With Enfortumab Vedotin: A Real-Word Study Leveraging U.S. Food and Drug Administration Adverse Event Reporting System. Front. Oncol. 11:801199. doi: 10.3389/fonc.2021.801199

INTRODUCTION

Urothelial cancer (UC) is the ninth most common cancer worldwide (1). At presentation, about 70% of patients have non-muscle-invasive disease and 25% muscle-invasive disease, and 5% will be metastatic (2). Early stages of disease (non-muscle-invasive UC and muscle-invasive disease UC) are often treated with cisplatin-based chemotherapy with objective response rates of approximately 50% (3). And the immune checkpoint inhibitor (ICI) is considered the standard of care in patients who are either cisplatin-unfit or platinum-refractory (4). However, patients with metastatic UC (mUC) with disease progression on both platinum-based chemotherapy and an ICI had few treatment options available and often have a dismal prognosis (5).

Enfortumab vedotin (EV) is an antimitotic antibody–drug conjugate (ADC) that inhibits microtubule assembly, which received Food and Drug Administration (FDA)-accelerated approval for the treatment of adult patients with locally advanced or mUC who had failed in the previous treatment of ICIs and platinum-based chemotherapeutic agents in 2019 (6). The drug has been demonstrated to have a significant response rate in early phase trials and is known for its tolerable side-effect profile (7–11). Common toxicities that have been attributed to EV were fatigue, peripheral neuropathy, skin rashes, gastrointestinal issues, and hematological suppression (12). The first case of cutaneous toxicities induced by EV was found in 2019 (13). Recently, emerging case reports have raised awareness of cutaneous toxicities, which may be a potentially fatal complication (14–17). But the precise descriptions of cutaneous toxicities were limited. Perhaps because of inadequate understanding as a form of EV-related cutaneous toxicities, data are derived primarily from case reports and clinical trials that may not correctly represent the real world. Moreover, the characteristics, outcomes, and types of EV-related cutaneous toxicities are still unknown.

Considering the wide clinical use of EV and the potentially fatal consequences of EV-associated cutaneous toxicities, it is important to identify its clinical manifestations. Therefore, we aim to assess the potential relevance between EV and cutaneous toxicities through data mining of the U.S. FDA adverse event (AE) reporting system (FAERS).

MATERIALS AND METHODS

Data Sources and Study Variables

The data were obtained from the FAERS database, which is publicly available and contains spontaneous AE reports submitted to the U.S. FDA by healthcare professionals, consumers, drug manufacturers, and others. The FAERS database Quarterly Data Files (January 1, 2019, to November 4, 2021) were used. OpenVigil FDA, a validated pharmacovigilance tool, was adapted to access the FDA drug-event database with the additional openFDA drug mapping and duplicate detection functionality (18–20).

Abbreviations: UC, urothelial cancer; ICI, immune checkpoint inhibitor; mUC, metastatic UC; EV, enfortumab vedotin; ADC, antibody–drug conjugate; FDA, Food and Drug Administration; FAERS, FDA adverse event reporting system; AEs, adverse events; PTs, preferred terms; IC, information component; ROR, reporting odds ratio; MMAE, monomethyl auristatin E.

Pharmacovigilance Study Procedures

The reports in the FAERS database were coded using preferred terms (PTs) from the Medical Dictionary for Regulatory Activities. After literature review and summary of previous studies, we considered the following PTs as related to cutaneous toxicities: rash [10037844], rash pruritus [10037884], pruritus [10037087], rash erythematous [10037855], Stevens–Johnson syndrome [10042033], dry skin [10013786], toxic epidermal necrolysis [10044223], skin exfoliation [10040844], dermatitis bullous [10012441], rash maculopapular [10025423], skin discoloration [10040829], erythema [10015150], rash papular [10037876], skin reaction [10040914], skin toxicity [10059516], symmetrical drug-related intertriginous and flexural exanthema [10078325], dermatitis allergic [10012434], exfoliative rash [10064579], palmar–plantar erythrodysesthesia syndrome [10033553], and rash macular [10037867]. The clinical characteristics (gender, age, reporting time, etc.) of patients were collected.

Statistical Analysis

Standard descriptive statistics were used to summarize the study population characteristics. We conducted a disproportionality analysis using the Bayesian confidence propagation neural network of information component (IC) and reporting odds ratio (ROR) to calculate disproportionality (21). ROR and IC are recognized disproportionality methods to identify whether a given AE (in this case, cutaneous toxicities) is reported more frequently than expected with a given drug (in this case, EV), which allows testing the possible disproportionate association between a drug and an AE (18). For IC, a significant signal was defined as the lower bound of the 95% CI (IC_{025}) exceeded 0. If $0 < IC_{025} \leq 1.5$, then it is considered as weak signal; if $1.5 < IC_{025} \leq 3.0$, then it is considered as middle signal; if $IC_{025} > 3.0$, then it is considered as strong signal (22). Since IC-based signals were included in ROR-based ones (23), ROR was also calculated, and the significant signal was defined as the lower bound of the 95% CI (ROR_{025}) exceeded 1, with at least 3 cases (24–26). All the analyses were performed using R version 3.2.5. The IC and ROR with 95% CI can be calculated by the following:

$$IC = \log_2 \frac{(cxy + \gamma xy)(C + \alpha)(C + \beta)}{(C + \gamma)(cx+\alpha x)(cy + \beta y)} = \log_2 \frac{(cxy + \gamma xy)\gamma}{(C + \gamma)}$$

$$SD = \sqrt{\frac{\left\{\left(\frac{C-cxy+\gamma-\gamma xy}{(cxy+\gamma xy)(1+C+\gamma)}\right) + \left(\frac{C-cx+\alpha-\alpha x}{(cx+\alpha x)(1+C+\alpha)}\right) + \left(\frac{C-cy+\beta-\beta y}{(cy+\beta y)(1+C+\beta)}\right)\right\}}{(ln2)^2}}$$

$$IC_{95\,\%\,CI} = IC \pm 2SD$$

$$ROR = \frac{(a/c)}{(b/d)} = \frac{ad}{bc}\ ROR_{95\,\%\,CI}$$

$$= e\ln(ROR) \pm 1.96\sqrt{\left(\frac{1}{a} + \frac{1}{b} + \frac{1}{c} + \frac{1}{d}\right)}$$

a = number of target AE of EV alone
b = number of other AEs of EV alone

c = number of target AE of other drugs except for EV
d = number of other AEs of other drugs except for EV

$c_{xy} = a,\ c_x = a + b,\ c_y = a + c,\ C = a + b + c + d,\ \gamma_{xy} = 1,\ \alpha = 2,\ \beta = 2,\ \alpha_x = 1,\ \beta_y = 1$

$$\gamma = \gamma_{xy} \frac{(C + \alpha)(C + \beta)}{(cx + \alpha x)(cy + \beta y)}$$

RESULTS

Descriptive Analysis

Overall, 409 AE reports related to EV and 212 AE reports related to cutaneous toxicities were submitted to the FAERS between January 1, 2004, and November 4, 2021. We screened all reported EV-related cutaneous toxicities, and the clinical characteristics are summarized in **Table 1**. Rash was the most common cutaneous toxicities related to EV. All the cases were reported between 2020 and 2021. Most cases were male (76.42%). The median age of cases was 74.5 (6–92) years. Most cases were EV monotherapy (83.49%), while only a few patients accepted combination therapy (**Table 1**).

Signal Values Associated With Enfortumab Vedotin

EV was significantly associated with cutaneous toxicities compared with both all other drugs (ROR 12.90 [10.62–15.66], IC 2.76 [2.52–3.01], middle signal, **Table 2**) and platinum-based therapy (ROR 15.11 [12.43–18.37], IC 2.91 [2.66–3.15], middle signal, **Table 2**). And significant association was detected between EV and all the cutaneous AEs except erythema, palmar–plantar erythrodysesthesia syndrome, and dermatitis allergic (**Table 2**). Nine AEs were detected as middle signal including rash (IC_{025} = 2.85), rash erythematous (IC_{025} = 2.49), Stevens–Johnson syndrome (IC_{025} = 2.96), dry skin (IC_{025} = 2.15), rash maculopapular (IC_{025} = 1.51), toxic epidermal necrolysis (IC_{025} = 2.02), skin exfoliation (IC_{025} = 1.57), dermatitis bullous (IC_{025} = 1.91), and blister (IC_{025} = 1.97) compared with platinum-based therapy in the database, while rash pruritus was detected as strong signal (IC_{025} = 3.32).

Analysis of Life-Threatening Adverse Events Associated With Enfortumab Vedotin

Stevens–Johnson syndrome and toxic epidermal necrolysis were the life-threatening AEs induced by EV. Those two AEs were all detected as middle signal and significantly associated with EV use. Both Stevens–Johnson syndrome and toxic epidermal necrolysis occurred 15 times as frequently for EV compared with all other drugs in the database (ROR = 15.20 and ROR = 15.52), while Stevens–Johnson syndrome occurred 18 times and toxic epidermal necrolysis occurred 7 times as frequently for EV compared with platinum-based therapy in the database (ROR = 18.74; ROR = 7.80).

Thirty-five death cases from all causes related to EV were submitted to the FAERS, and three cases were reported to be related to cutaneous toxicities (8.57%). It is worth noting that three cases were all related to Stevens–Johnson syndrome. The mortality rate of Stevens–Johnson syndrome related to EV was 13.64% in the FAERS.

Signal Values Associated With Different Groups of Cases

We analyzed the association between EV and cutaneous toxicities in different groups that limited the gender and age. All groups showed significant association. Significant middle signals of cutaneous toxicities were shown in all groups (**Table 3**).

DISCUSSION

To our knowledge, this is the first comprehensive pharmacovigilance study on cutaneous toxicities associated with EV based on the FAERS database. Our study included the largest such collection of cases to date, and 212 AE reports related to cutaneous toxicities were analyzed.

Our study detected a significant signal between EV use and cutaneous toxicities. The most well-recognized AE of EV is rash. The rate of rash was noted in 48% of patients in the previous clinical trial (8). The median time to onset of skin reactions has been estimated to be 1 month. Of patients who experienced rash, nearly two-thirds experienced complete resolution, and approximately one-fifth experienced partial improvement (27). Besides rash, our study detected other cutaneous AEs induced by EV including pruritus and Stevens–Johnson syndrome. The mechanism for the AEs is unclear now. EV is an ADC with a monomethyl auristatin E (MMAE) payload targeting Nectin-4, a protein widely expressed on UC cells (28). Nectin-4 is important in the skin, which has a role in cell–cell adhesion, and a functional disturbance could lead to impaired cell–cell attachment (29, 30). Besides that, cutaneous toxicities also appeared to be a common AE in studies involving other ADC that incorporate MMAE (31–33). Therefore, dermatologic sequelae observed could be attributed solely to the MMAE payload. Alternatively, the proposed mechanism is targeting Nectin-4 by EV with the delivery of the MMAE payload to the skin resulting in the observed keratinocyte apoptosis (16).

Stevens–Johnson syndrome and toxic epidermal necrolysis were the life-threatening AEs. Those two AEs have always been not a recognized side effect of EV. The first case report of a 71-year-old male who suffered from EV-induced toxic epidermal necrolysis was published in 2020 (15). And Viscuse et al. highlighted a case of Stevens–Johnson syndrome/toxic epidermal necrolysis following enfortumab infusions in 2021 (16). Unfortunately, both of the patients in these cases were dead after treatment. Those cases aroused our attention on EV-induced life-threatening cutaneous toxicity. Our study found that those two AEs were significantly associated with EV use. This reminded doctors that patients must be monitored for cutaneous toxicities with early involvement of dermatology.

Our study found a significant signal of cutaneous toxicities in all groups that limited the gender and age. All the groups were detected as middle signal. Young people (≤60 years old) had

TABLE 1 | Characteristics of patients with enfortumab vedotin associated cutaneous toxicities sourced from the FAERS database.

Characteristics	N. of case	Gender			Age					
		Male n (%)	Female n (%)	Unknown or missing n (%)	Median (IQR)	≤60 n (%)	61–70 n (%)	71–80 n (%)	≧81 n (%)	Unknown or missing n (%)
Total	212	162 (76.42)	42 (19.81)	8 (3.77)	74.5 (6–92)	19 (8.96)	33 (15.57)	45 (21.23)	15 (7.08)	100 (47.17)
EV monotherapy	177	137 (77.40)	35 (19.77)	5 (2.83)	73 (6–92)	16 (9.04)	28 (15.82)	32 (18.08)	14 (7.91)	87 (49.15)
Combination therapy										
EV + pembrolizumab	22	19 (86.36)	1 (4.55)	2 (9.09)	72 (60–78)	2 (9.09)	5 (22.73)	12 (54.55)	0 (0.00)	3 (13.64)
EV + atezolizumab	2	1 (50.00)	1 (50.00)	0 (0.00)	—	0 (0.00)	0 (0.00)	1 (50.00)	0 (0.00)	1 (50.00)
EV + cisplatinum	3	1 (33.33)	2 (66.67)	0 (0.00)	—	0 (0.00)	0 (0.00)	0 (0.00)	0 (0.00)	3 (100.00)
EV + carboplatin	2	1 (50.00)	0 (0.00)	1 (50.00)	—	0 (0.00)	0 (0.00)	0 (0.00)	1 (50.00)	1 (50.00)
EV + pembrolizumab + erdafitinib	1	1 (100.00)	0 (0.00)	0 (0.00)	—	1 (100.00)	0 (0.00)	0 (0.00)	0 (0.00)	0 (0.00)
EV + pembrolizumab + erdafitinib	3	2 (66.67)	1 (33.33)	0 (0.00)	—	0 (0.00)	0 (0.00)	0 (0.00)	0 (0.00)	3 (100.00)
EV + pembrolizumab + cisplatinum	2	0 (0.00)	2 (100.00)	0 (0.00)	—	0 (0.00)	0 (0.00)	0 (0.00)	0 (0.00)	2 (100.00)
Adverse Effects (AEs)										
Rash	79	58 (73.42)	19 (24.05)	2 (2.53)	74 (6–90)	8 (10.13)	7 (8.86)	10 (12.66)	8 (10.13)	46 (58.23)
Rash pruritus	16	10 (62.50)	6 (37.50)	0 (0.00)	71.5 (8–92)	3 (18.75)	2 (12.50)	5 (31.25)	2 (12.50)	4 (25.00)
Pruritus	14	13 (92.85)	1 (7.14)	0 (0.00)	72 (65–88)	0 (0.00)	2 (14.29)	3 (21.43)	1 (7.14)	8 (57.14)
Rash erythematous	13	12 (92.31)	1 (7.69)	0 (0.00)	73 (7–81)	2 (15.38)	1 (7.69)	5 (38.46)	1 (7.69)	4 (30.77)
Stevens–Johnson syndrome	13	9 (69.23)	2 (15.38)	2 (15.38)	76 (67–78)	0 (0.00)	1 (7.69)	5 (38.46)	0 (0.00)	7 (53.85)
Dry skin	12	9 (75.00)	3 (25.00)	0 (0.00)	65.5 (40–83)	1 (8.33)	2 (16.67)	0 (0.00)	1 (8.33)	8 (66.67)
Rash maculopapular	10	8 (80.00)	2 (20.00)	0 (0.00)	70 (60–92)	1 (10.00)	4 (40.00)	2 (20.00)	1 (10.00)	2 (20.00)
Toxic epidermal necrolysis	9	5 (55.56)	1 (11.11)	3 (33.33)	72 (67–78)	0 (0.00)	1 (11.11)	3 (33.33)	0 (0.00)	5 (55.56)
Skin exfoliation	8	6 (75.00)	2 (25.00)	0 (0.00)	67 (40–85)	1 (12.50)	4 (50.00)	1 (14.29)	1 (12.50)	1 (12.50)
Dermatitis bullous	6	6 (100.00)	0 (0.00)	0 (0.00)	77 (65–78)	0 (0.00)	1 (16.67)	3 (50.00)	0 (0.00)	2 (33.33)
Skin discoloration	6	5 (83.33)	1 (16.67)	0 (0.00)	65 (60–66)	1 (16.67)	3 (50.00)	1 (16.67)	0 (0.00)	1 (16.67)
Blister	5	4 (80.00)	1 (20.00)	0 (0.00)	72 (67–77)	0 (0.00)	1 (20.00)	1 (20.00)	0 (0.00)	3 (60.00)
Erythema	4	3 (75.00)	1 (25.00)	0 (0.00)	60 (60–69)	2 (50.00)	1 (25.00)	0 (0.00)	0 (0.00)	1 (25.00)
Skin reaction	4	3 (75.00)	1 (25.00)	0 (0.00)	—	0 (0.00)	0 (0.00)	0 (0.00)	0 (0.00)	4 (100.00)
Exfoliative rash	3	3 (100.00)	0 (0.00)	0 (0.00)	75 (71–76)	0 (0.00)	0 (0.00)	3 (100.00)	0 (0.00)	0 (0.00)
Palmar–plantar erythrodysesthesia syndrome	3	2 (75.00)	1 (25.00)	0 (0.00)	—	0 (0.00)	0 (0.00)	1 (33.33)	0 (0.00)	2 (66.67)
Skin toxicity	3	2 (66.67)	0 (0.00)	1 (33.33)	—	0 (0.00)	1 (33.33)	0 (0.00)	0 (0.00)	2 (66.67)
Symmetrical drug-related intertriginous and flexural exanthema	3	3 (100.00)	0 (0.00)	0 (0.00)	70 (70–81)	0 (0.00)	2 (66.67)	1 (33.33)	0 (0.00)	0 (0.00)
Dermatitis allergic	1	1 (100.00)	0 (0.00)	0 (0.00)	—	0 (0.00)	0 (0.00)	1 (100.00)	0 (0.00)	0 (0.00)

N, number; EV, enfortumab vedotin; FAERS, Food and Drug Administration (FDA) adverse event reporting system; IQR, interquartile range.

TABLE 2 | Disproportionality analysis of enfortumab vedotin and cutaneous toxicities.

Category	N. of case	ROR (ROR_{025}–ROR_{975})		IC (IC_{025}–IC_{975}, signal strength)	
		Compared with all other drugs	Compared with platinum-based therapy	Compared with all other drugs	Compared with platinum-based therapy
Cutaneous toxicities	212	12.90 (10.62–15.66)	15.11 (12.43–18.37)	2.76 (2.52 to 3.01, middle)	2.91 (2.66 to 3.15, middle)
AEs					
Rash	79	11.64 (9.11–14.88)	12.29 (9.58–15.76)	3.18 (2.82 to 3.53, middle)	3.21 (2.85 to 3.56, middle)
Rash pruritus	16	15.91 (9.65–26.23)	41.21 (24.22–70.11)	3.74 (2.64 to 4.11, middle)	4.07 (3.32 to 4.82, Strong)
Pruritus	14	2.17 (1.27–3.69)	3.56 (2.09–6.09)	0.98 (0.20 to 1.77, weak)	1.62 (0.83 to 2.41, weak)
Rash erythematous	13	15.96 (9.19–27.74)	17.49 (9.91–30.86)	3.28 (2.47 to 4.09, middle)	3.31 (2.49 to 4.14, middle)
Stevens–Johnson syndrome	13	26.41 (15.20–45.90)	33.51 (18.74–59.94)	3.69 (2.88 to 4.50, middle)	3.79 (2.96 to 4.61, middle)
Dry skin	12	4.50 (2.81–8.88)	12.83 (7.14–23.05)	2.02 (1.18 to 2.86, weak)	3.00 (2.15 to 3.86, middle)
Rash maculopapular	10	8.74 (4.67–16.38)	7.74 (4.10–14.61)	2.58 (1.66 to 3.50, middle)	2.44 (1.51 to 3.37, middle)
Toxic epidermal necrolysis	9	30.05 (15.52–58.20)	15.34 (7.80–30.21)	3.48 (2.52 to 4.45, middle)	3.00 (2.02 to 3.98, middle)
Skin exfoliation	8	5.14 (2.55–10.34)	10.22 (5.02–20.81)	1.94 (0.92 to 2.97, weak)	2.6 (1.57 to 3.64, middle)
Dermatitis bullous	6	40.41 (18.04–90.53)	33.57 (14.35–78.53)	3.21 (2.02 to 4.39, middle)	3.10 (1.91 to 4.30, middle
Skin discoloration	6	6.34 (2.83–14.20)	14.00 (6.14–31.94)	2.04 (0.86 to 3.23, weak)	2.66 (1.47 to 3.85, middle)
Blister	5	4.72 (1.95–11.40)	—*	1.68 (0.38 to 2.97, weak)	3.28 (1.97 to 4.59, middle)
Erythema	4	0.93 (0.35–2.50)	0.70 (0.26–1.88)	–0.25 (–1.70 to 1.19, no)	–0.62 (–2.06 to 0.83, no)
Skin reaction	4	14.06 (5.25–37.66)	7.37 (2.72–19.97)	2.35 (0.91 to 3.79, weak)	1.92 (0.47 to 3.38, weak)
Skin toxicity	3	33.37 (10.71–103.94)	3.39 (1.08–10.62)	2.35 (0.69 to 4.01, weak)	1.11 (–0.56 to 2.78, no)
Symmetrical drug-related intertriginous and flexural exanthema	3	356.28 (113.77–1115.71)	—*	2.57 (0.91 to 4.23, weak)	2.56 (0.88 to 4.23, weak)
Exfoliative rash	3	55.28 (17.74–172.29)	27.60 (8.42–90.49)	2.44 (0.79 to 4.10, weak)	2.29 (0.61 to 3.96, weak)
Palmar–plantar erythrodysesthesia syndrome	3	6.53 (2.10–20.33)	1.44 (0.46–4.48)	1.65 (–0.014 to 3.31, no)	0.22 (–1.45 to 0.88, no)
Dermatitis allergic	1	—*	—*	–4.62 (–7.41 to –1.83, no)	0.63 (–2.17 to 3.42, no)

N, number; ROR, reporting odds ratio; ROR_{025}, the lower end of the 95% confidence interval of ROR; ROR_{975}, the upper end of the 95% confidence interval of ROR; IC, information component; IC_{025}, the lower end of the 95% confidence interval of IC; IC_{975}, the upper end of the 95% confidence interval of IC.
**ROR was not calculated for the reason that the cases were less than 3.*

TABLE 3 | Disproportionality analysis of enfortumab vedotin and cutaneous toxicities in different groups of cases.

Category	N. of case	ROR (ROR_{025}–ROR_{975})		IC (IC_{025}–IC_{975}, signal strength)	
		Compared with all other drugs	Compared with platinum-based therapy	Compared with all other drugs	Compared with platinum-based therapy
Total	212	12.90 (10.62–15.66)	15.11 (12.43–18.37)	2.76 (2.52–3.01, middle)	2.91 (2.66–3.15, middle)
Gender					
Male	162	13.12 (10.50–16.40)	15.11 (12.08–18.91)	2.73 (2.46–3.01, middle)	2.90 (2.62–3.18, middle)
Female	42	11.71 (7.65–17.91)	13.48 (8.81–20.64)	3.58 (2.05–3.12, middle)	2.75 (2.21–3.29, middle)
Age					
≤60	19	9.49 (5.20–17.32)	10.93 (5.98–10.96)	2.33 (1.55–3.11, middle)	2.49 (1.71–3.27, middle)
61–70	33	26.37 (14.32–48.55)	30.37 (16.49–55.94)	2.99 (2.35–3.63, middle)	3.15 (2.51–3.79, middle)
71–80	45	38.53 (21.15–70.19)	44.37 (24.35–80.87)	3.17 (2.60–3.72, middle)	3.33 (2.77–3.89, middle)
≥81	15	14.98 (7.01–32.01)	17.26 (8.07–36.88)	2.56 (1.66–3.46, middle)	2.71 (1.82–3.61, middle)

N, number; ROR, reporting odds ratio; ROR_{025}, the lower end of the 95% confidence interval of ROR; ROR_{975}, the upper end of the 95% confidence interval of ROR; IC, information component; IC_{025}, the lower end of the 95% confidence interval of IC; IC_{975}, the upper end of the 95% confidence interval of IC.

slightly lower reporting frequencies for cutaneous toxicities compared with old people.

Our study has limitations. First, the FAERS database was a spontaneous reporting system. Underreporting, selective reporting, and many missing data could bring reporting bias. Second, the limited data might not contribute to a better comprehensive evaluation of EV-induced cutaneous toxicities. Third, disproportionality analysis is a suitable tool to quantitate signals for the AE. But the causal relationship between drugs (EV) and the AE (cutaneous toxicities) cannot be verified without a clinically performed causality assessment, while confounders such as comorbidity and concomitant drugs cannot also be assessed properly.

CONCLUSION

Our study detected a significant signal between EV use and cutaneous toxicities. It is worth noting that Stevens–Johnson syndrome and toxic epidermal necrolysis were significantly associated with EV use. Patients must be monitored for cutaneous toxicities with early involvement of dermatology.

Further study is required with better data sources and research design to draw conclusions on the strength of the relationships.

DATA AVAILABILITY STATEMENT

The datasets presented in this study can be found in FAERs database. Further inquiries can be directed to the corresponding authors.

AUTHOR CONTRIBUTIONS

HY was responsible for the study conception and design, data acquisition, data analysis and interpretation, manuscript preparation, and manuscript editing. XY was responsible for the data acquisition. ZA was responsible for the data analysis and interpretation. All authors contributed to the article and approved the submitted version.

SUPPLEMENTARY MATERIAL

The Supplementary Material for this article can be found online at: https://www.frontiersin.org/articles/10.3389/fonc.2021.801199/full#supplementary-material

REFERENCES

1. Bray F, Ferlay J, Soerjomataram I, Siegel RL, Torre LA, Jemal A. Global Cancer Statistics 2018: GLOBOCAN Estimates of Incidence and Mortality Worldwide for 36 Cancers in 185 Countries. *CA Cancer J Clin* (2018) 68:394–424. doi: 10.3322/caac.21492
2. Alt M, Stecca C, Tobin S, Jiang DM, Sridhar SS. Enfortumab Vedotin in Urothelial Cancer. *Ther Adv Urol* (2020) 12:1756287220980192. doi: 10.1177/1756287220980192
3. von der Maase H, Hansen SW, Roberts JT, Dogliotti L, Oliver T, Moore MJ, et al. Gemcitabine and Cisplatin Versus Methotrexate, Vinblastine, Doxorubicin, and Cisplatin in Advanced or Metastatic Bladder Cancer: Results of a Large, Randomized, Multinational, Multicenter, Phase III Study. *J Clin Oncol* (2000) 18:3068–77. doi: 10.1200/JCO.2000.18.17.3068
4. Bellmunt J, de Wit R, Vaughn DJ, Fradet Y, Lee JL, Fong L, et al. Pembrolizumab as Second-Line Therapy for Advanced Urothelial Carcinoma. *N Engl J Med* (2017) 376:1015–26. doi: 10.1056/NEJMoa1613683
5. Sidaway P. Sacituzumab Govitecan is Safe and Effective. *Nat Rev Clin Oncol* (2021) 18(7):400. doi: 10.1038/s41571-021-00523-y
6. Hanna KS. Enfortumab Vedotin to Treat Urothelial Carcinoma. *Drugs Today (Barc)* (2020) 56(5):329–35. doi: 10.1358/dot.2020.56.5.3127027
7. Rosenberg J, Sridhar SS, Zhang J, Smith D, Ruether D, Flaig TW, et al. EV-101: A Phase I Study of Single-Agent Enfortumab Vedotin in Patients With Nectin-4–Positive Solid Tumors, Including Metastatic Urothelial Carcinoma. *J Clin Oncol* (2020) 38(10):1041–9. doi: 10.1200/JCO.19.02044
8. Rosenberg JE, O'Donnell PH, Balar AV, McGregor BA, Heath EI, Yu EY, et al. Pivotal Trial of Enfortumab Vedotin in Urothelial Carcinoma After Platinum and Anti-Programmed Death/Programmed Death Ligand 1 Therapy. *J Clin Oncol* (2019) 37(29):2592–600. doi: 10.1200/JCO.19.01140
9. Maas M, Stuhler V, Walz S, Stenzl A, Bedke J. Enfortumab Vedotin -Next Game- Changer in Urothelial Cancer. *Expert Opin Biol Ther* (2021) 21 (7):801–9. doi: 10.1080/14712598.2021.1865910
10. Hoimes CJ, Rosenberg JE, Srinivas S, Petrylak DP, Flaig T. EV-103: Initial Results of Enfortumab Vedotin Plus Pembrolizumab for Locally Advanced or Metastatic Urothelial Carcinoma. *Ann Oncol* (2019) 30(suppl_5):v356–402. doi: 10.1093/annonc/mdz249
11. van der Heijden MS, Gupta S, Galsky MD, Derleth C, Steinberg J, Kataria R, et al. 798tip Study EV-302: A 3-Arm, Open-Label, Randomized Phase III Study of Enfortumab Vedotin Plus Pembrolizumab and/or Chemotherapy, Versus Chemotherapy Alone, in Untreated Locally Advanced or Metastatic Urothelial Cancer. *Ann Oncol* (2020) 31(suppl_4):S550–0. doi: 10.1016/j.annonc.2020.08.2069
12. Keerty D, Graham L, Haynes E, Hembree TN. Flexural Exanthema From Enfortumab Vedotin. *Cureus* (2020) 12(5):e8102. doi: 10.7759/cureus.8102
13. Wu S, Adamson AS. Cutaneous Toxicity Associated With Enfortumab Vedotin Treatment of Metastatic Urothelial Carcinoma. *Dermatol Online J* (2019) 25(2):13030/qt4j44w7w6. doi: 10.5070/D3252042890
14. Sasaki R, Fujimura T, Lyu C, Aiba S. Severe Eczematoid and Lichenoid Eruption With Full-Thickness Epidermal Necrosis Developing From Metastatic Urothelial Cancer Treated With Enfortumab Vedotin. *J Dermatol* (2020) 47(12):1436–8. doi: 10.1111/1346-8138.15577
15. Francis A, Jimenez A, Sundaresan S, Kelly B. A Rare Presentation of Enfortumab Vedotin-Induced Toxic Epidermal Necrolysis. *JAAD Case Rep* (2020) 7:57–9. doi: 10.1016/j.jdcr.2020.10.020
16. Viscuse PV, Marques-Piubelli ML, Heberton MM, Parra ER, Shah AY, Siefker-Radtke A, et al. Case Report: Enfortumab Vedotin for Metastatic Urothelial Carcinoma: A Case Series on the Clinical and Histopathologic Spectrum of Adverse Cutaneous Reactions From Fatal Stevens-Johnson Syndrome/Toxic Epidermal Necrolysis to Dermal Hypersensitivity Reaction. *Front Oncol* (2021) 11:621591. doi: 10.3389/fonc.2021.621591
17. Dobry AS, Virgen CA, Hosking AM, Mar N, Doan L, Lee B, et al. Cutaneous Reactions With Enfortumab Vedotin: A Case Series and Review of the Literature. *JAAD Case Rep* (2021) 14:7–9. doi: 10.1016/j.jdcr.2021.05.020
18. Böhm R, von Hehn L, Herdegen T, Klein HJ, Bruhn O, Petri H, et al. OpenVigil FDA - Inspection of U.S. American Adverse Drug Events Pharmacovigilance Data and Novel Clinical Applications. *PLoS One* (2016) 11(6):e0157753. doi: 10.1371/journal.pone.0157753
19. Meng L, Yang B, Qiu F, Jia Y, Sun S, Yang J, et al. Lung Cancer Adverse Events Reports for Angiotensin-Converting Enzyme Inhibitors: Data Mining of the FDA Adverse Event Reporting System Database. *Front Med (Lausanne)* (2021) 8:594043. doi: 10.3389/fmed.2021.594043
20. Papazisis G, Spachos D, Siafis S, Pandria N, Deligianni E, Tsakiridis I, et al. Assessment of the Safety Signal for the Abuse Potential of Pregabalin and Gabapentin Using the FAERS Database and Big Data Search Analytics. *Front Psychiatry* (2021) 12:640264. doi: 10.3389/fpsyt.2021.640264
21. Andrews EB, Moore N. *Mann\"s Pharmacovigilance || History of Pharmacovigilance*. UK: John Wiley & Sons, Ltd (2014) p. 331–54.
22. Eudravigilance Expert Working Group (EV-EWG). *European Medicine Agency Guidelines*. London: Eudravigilance Expert Working Group (EV-EWG) (2006) p. 1–22.
23. Sakaeda T, Kadoyama K, Minami K, Okuno Y. Commonality of Drug-Associated Adverse Events Detected by 4 Commonly Used Data Mining Algorithms. *Int J Med Sci* (2014) 11(5):461–5. doi: 10.7150/ijms.7967
24. van Puijenbroek EP, Bate A, Leufkens HG, Lindquist M, Orre R, Egberts AC. A Comparison of Measures of Disproportionality for Signal Detection in Spontaneous Reporting Systems for Adverse Drug Reactions. *Pharmacoepidemiol Drug Saf* (2002) 11(1):3–10. doi: 10.1002/pds.668
25. Bate A, Evans SJ. Quantitative Signal Detection Using Spontaneous ADR Reporting. *Pharmacoepidemiol Drug Saf* (2009) 18(6):427–36. doi: 10.1002/pds.1742
26. Bate A. *The Use of Bayesian Confidence Propagation Neural Network in Pharmacovigilance [Internet] [PhD Dissertation]* (2003). Available at: http://urn.kb.se/resolve?urn=urn:nbn:se:umu:diva-83.
27. Yu EY, Petrylak DP, O'Donnell PH, Lee JL, van der Heijden MS, Loriot Y, et al. Enfortumab Vedotin After PD-1 or PD-L1 Inhibitors in Cisplatin-Ineligible Patients With Advanced Urothelial Carcinoma (EV–201): A Multicentre, Single-Arm, Phase 2 Trial. *Lancet Oncol* (2021) 22(6):872–82. doi: 10.1016/S1470-2045(21)00094-2
28. Hoffman-Censits J, Lombardo K, McConkey D, Hahn NM, Bashir B, Kelly WK, et al. New and Topics: Enfortumab Vedotin Mechanisms of Response

and Resistance in Urothelial Cancer - What do We Understand So Far? *Urol Oncol* (2021) 39(10):619–22. doi: 10.1016/j.urolonc.2021.05.013
29. Fortugno P, Josselin E, Tsiakas K, Agolini E, Cestra G, Teson M, et al. Nectin-4 Mutations Causing Ectodermal Dysplasia With Syndactyly Perturb the Rac1 Pathway and the Kinetics of Adherens Junction Formation. *J Invest Dermatol* (2014) 134(8):2146–53. doi: 10.1038/jid.2014.119
30. Rikitake Y, Mandai K, Takai Y. The Role of Nectins in Different Types of Cellecell Adhesion. *J Cell Sci* (2012) 125(16):3713–22. doi: 10.1242/jcs.099572
31. de Claro RA, McGinn K, Kwitkowski V, Bullock J, Khandelwal A, Habtemariam B, et al. U.S. Food and Drug Administration Approval Summary: Brentuximab Vedotin for the Treatment of Relapsed Hodgkin Lymphoma or Relapsed Systemic Anaplastic Large-Cell Lymphoma. *Clin Cancer Res* (2012) 18(21):5845–9. doi: 10.1158/1078-0432.CCR-12-1803
32. Yardley DA, Weaver R, Melisko ME, Saleh MN, Arena FP, Forero A, et al. EMERGE: A Randomized Phase II Study of the Antibody-Drug Conjugate Glembatumumab Vedotin in Advanced Glycoprotein NMB-Expressing Breast Cancer. *J Clin Oncol* (2015) 33(14):1609–19. doi: 10.1200/JCO.2014.56.2959
33. Palanca-Wessels MC, Czuczman M, Salles G, Assouline S, Sehn LH, Flinn I, et al. Safety and Activity of the Anti-CD79B Antibody–Drug Conjugate Polatuzumab Vedotin in Relapsed or Refractory B-Cell non-Hodgkin Lymphoma and Chronic Lymphocytic Leukaemia: A Phase 1 Study. *Lancet Oncol* (2015) 16(6):704–15. doi: 10.1016/S1470-2045(15)70128-2

Conflict of Interest: The authors declare that the research was conducted in the absence of any commercial or financial relationships that could be construed as a potential conflict of interest.

Publisher's Note: All claims expressed in this article are solely those of the authors and do not necessarily represent those of their affiliated organizations, or those of the publisher, the editors and the reviewers. Any product that may be evaluated in this article, or claim that may be made by its manufacturer, is not guaranteed or endorsed by the publisher.

frontiers in Pharmacology

CASE REPORT
published: 27 January 2022
doi: 10.3389/fphar.2021.795884

Case Report: Successful Avatrombopag Treatment for Two Cases of Anti-PD-1 Antibody-Induced Acquired Amegakaryocytic Thrombocytopenia

Xiaofang Tu, Ali Xue, Suye Wu, Mengmeng Jin, Pu Zhao and Hao Zhang**

Department of Hematology, The Third Affiliated Hospital of Wenzhou Medical University, Wenzhou, China

Background: Anti-PD-1/PD-L1 immunotherapy has achieved impressive responses in multiple types of malignancies in recent years. However, immune-related adverse events (irAEs) occur and limit their continuous clinical use. Among these irAEs, acquired amegakaryocytic thrombocytopenia (AAT) is rare but often clinically serious, life-threatening and refractory to multiple treatment approaches.

Case summary: We reported for the first time the successful treatment of avatrombopag in two cases of anti-PD1 antibody-induced AAT (in particular, one case had progressed to aplastic anemia), which was refractory or intolerant to glucocorticoids, ciclosporin, intravenous immunoglobulin (IVIG), recombinant human thrombopoietin (rh-TPO) and even TPO receptor agonist (TPO-RA) eltrombopag. To date, the two cases manifested as normal platelet counts and are independent of transfusion.

Conclusion: Anti-PD1 antibody-induced AAT occurs with low frequency but is often serious and difficult to manage, for which this study proposed vatrombopag as a potential curative and safe approach.

Keywords: immune-related adverse events, acquired amegakaryocytic thrombocytopenia, anti-PD-1 antibody, thrombopoietin receptor agonists, avatrombopag

OPEN ACCESS

Edited by:
Jennifer Martin,
The University of Newcastle, Australia

Reviewed by:
Anna Pegoraro,
University of Ferrara, Italy
Cristina Tecchio,
University of Verona, Italy

****Correspondence:***
Pu Zhao
zp9600@126.com
Hao Zhang
hellohaozi@126.com

Specialty section:
This article was submitted to Pharmacology of Anti-Cancer Drugs, a section of the journal Frontiers in Pharmacology

Received: *15 October 2021*
Accepted: *20 December 2021*
Published: *27 January 2022*

Citation:
Tu X, Xue A, Wu S, Jin M, Zhao P and Zhang H (2022) Case Report: Successful Avatrombopag Treatment for Two Cases of Anti-PD-1 Antibody-Induced Acquired Amegakaryocytic Thrombocytopenia. Front. Pharmacol. 12:795884. doi: 10.3389/fphar.2021.795884

INTRODUCTION

Programmed cell death protein 1 (PD-1) is a member of the immunoglobulin supergene family that is expressed upon lymphocyte activation in $CD4^+$ and $CD8^+$ T cells, which acts as a natural brake that modulates the T cell response. Blockade of the PD-1/programmed cell death ligand 1 (PD-L1) pathway by monoclonal antibodies has emerged as a highly effective approach to reinvigorate T cells in treating several types of malignancies such as melanoma, lung cancer, renal cell carcinoma, gastric cancer and certain types of lymphoma. However, immune-related adverse events (irAEs) frequently

Abbreviations: PD-1, programmed cell death protein 1; PD-L1, programmed cell death ligand 1; irAEs, immune-related adverse events; AAT, acquired amegakaryocytic thrombocytopenia; ITP, immune thrombocytopenia; rh-TPO, recombinant human thrombopoietin; TPO-RAs, thrombopoietin receptor agonists; IVIG, intravenous immunoglobulin; G-CSF, granulocyte colony-stimulating factors; HSCs, hematopoietic stem cells

occur and can potentially affect all organs, which limits the continued use of anti-PD1/PD-L1 antibodies (De Velasco et al., 2017).

Hematological irAEs induced by anti-PD-1/PD-L1 immunotherapy are much less frequent than those induced with conventional cytotoxic chemotherapy and account for approximately 3.6% of total irAEs with the most common type of neutropenia, autoimmune hemolytic anemia and immune thrombocytopenia each in 26%, followed by pancytopenia or aplastic anemia in 14% (Delanoy et al., 2019; Michot et al., 2019). In particular, a rare hematological disorder, which is called acquired amegakaryocytic thrombocytopenia (AAT), is characterized by severe thrombocytopenia and a complete or nearly complete absence of megakaryocytes in the bone marrow (Agarwal et al., 2006). AAT is distinguished from megakaryocyte maturation disorder in immune thrombocytopenia (ITP). AAT is often clinically serious and life-threatening due to the significantly increased risk of vital organ bleeding. To date, only sporadic cases of anti-PD-1/PD-L1 immunotherapy-induced AAT have been reported. The standard treatment of AAT has not been defined, and the management is often thorny because of their refractoriness to possible treatment choices, including immunosuppressive therapy, rituximab, interleukin-11, recombinant human thrombopoietin (rh-TPO) and even some thrombopoietin receptor agonists (TPO-RAs). As a newly FDA approved TPO-RA for immune ITP, avatrombopag promotes platelet production by stimulating TPO receptor (c-Mpl) with high efficacy and safety (Deng et al., 2021; Gilreath et al., 2021). However, little is known about its effects in the treatment of AAT, especially anti-PD-1/PD-L1 antibody-induced AAT. In this study, we report for the first time the successful treatment of avatrombopag in two patients with anti-PD-1 antibody-induced AAT.

CASE PRESENTATIONS

Patient 1

A 67-year-old male was diagnosed with ureter neoplasm with right hydronephrosis and retroperitoneal lymph node metastasis in May 2020. After three cycles of combined chemotherapy (gemcitabine and carboplatin), the patient was administered tislelizumab at a dose of 200 mg every 3 weeks. Three weeks after the second treatment with tislelizumab, routine blood examination indicated thrombocytopenia with a platelet count of 4.8×10^4/μL. Tislelizumab was discontinued, and rh-TPO was used at a dose of 15,000 U/day for 13 consecutive days, but repeated examination showed a further decreased platelet count of 2.1×10^4/μL. Considering anti-PD-1 antibody-related immune thrombocytopenia, the patient received methylprednisolone 80 mg daily for three consecutive weeks until skin hemorrhages and petechiae appeared on his extremities and abdomen, and the platelet count decreased to 0.5×10^4/μL. Bone marrow morphology showed an almost absence of megakaryocytes with no significant abnormal presentation of other cell linages. Excluding other possible secondary thrombocytopenia (other immune diseases, drugs, or infections induced thrombocytopenia), anti-PD-1 antibody-induced AAT was considered. Due to the risk of life-threatening bleeding, the patient received intravenous immunoglobulin (IVIG) 20 g/day for 5 days and irregular platelet infusion. Unfortunately, there was still no improvement in his platelet count. The following administration of cyclosporine 100 mg daily was discontinued 1 week later because severe pneumonia occurred.

As a potentially effective strategy, TPO-RAs were considered. Oral eltrombopag 50 mg daily was initiated and lasted for a total of 3 months, but it ended in limited responses. The patient was transitioned to avatrombopag at a dose of 40 mg daily. Surprisingly, the platelet count increased to 2.8×10^4/μL 2 weeks later and above 10×10^4/μL 2 months after the avatrombopag initiation. To date, the platelet count of the patient has remained normal (**Figure 1**), and no obvious adverse effects have been observed.

Patient 2

A 71-year-old female who was diagnosed with bladder cancer received surgical resection of the tumor and four cycles of chemotherapy (gemcitabine and cisplatin) in 2019. Due to the evaluation as a poor prognosis, she was started on treatment with triplezumab 200 mg every 3 weeks. After two courses of treatment, she developed thrombocytopenia with a platelet count of 2.6×10^4/μL. Rh-TPO was given at a dose of 15,000 U daily for 17 consecutive days, and the platelet count returned to 5×10^4/μL. Approximately 1 month later, repeated routine blood examination showed a decreased platelet count of 2.9×10^4/μL. Bone marrow examination demonstrated megakaryophthisis, and AAT was diagnosed in the absence of evidence that other causes induced thrombocytopenia. Five days of IVIG (20 g/day) and 2 weeks of rh-TPO (15,000 U/day) were administered, but no response was observed, and the platelet count continuously decreased to 1.5×10^4/μL. Then, she received eltrombopag 50 mg daily but discontinued because of economic considerations and limited responses within 2 weeks.

At 5 months later, the patient developed bleeding on her skin and gums with severe thrombocytopenia (platelet count 0.2×10^4/μL), anemia (hemoglobin 5.7 g/dl) and granulocytopenia (white blood cell count 1.9×10^3/μL). Repeated bone marrow examination suggested multilineage hypoplasia with a near absence of megakaryocytes, and immune-related aplastic anemia was diagnosed. The combination of methylprednisolone (40 mg/day), rh-TPO (15,000 U/day) and granulocyte colony-stimulating factors (G-CSF) (200 U/day) was administered for 2 weeks, and no response was observed. Considering the age and potential immunocompromise, the patient refused the use of cyclosporin.

After another 5 months, the patient agreed to the treatment of avatrombopag because of sustained pancytopenia and accompanying complications. Encouragingly, at a dose of 40 mg daily for 1 month, routine blood examination showed a significant improvement in blood cell count. Two months after the avatrombopag administration, a satisfactory blood cell count was achieved with a platelet count of 9.4×10^4/μL, a hemoglobin count of 10.6 g/dl and a white blood cell count of 3.2×10^3/μL

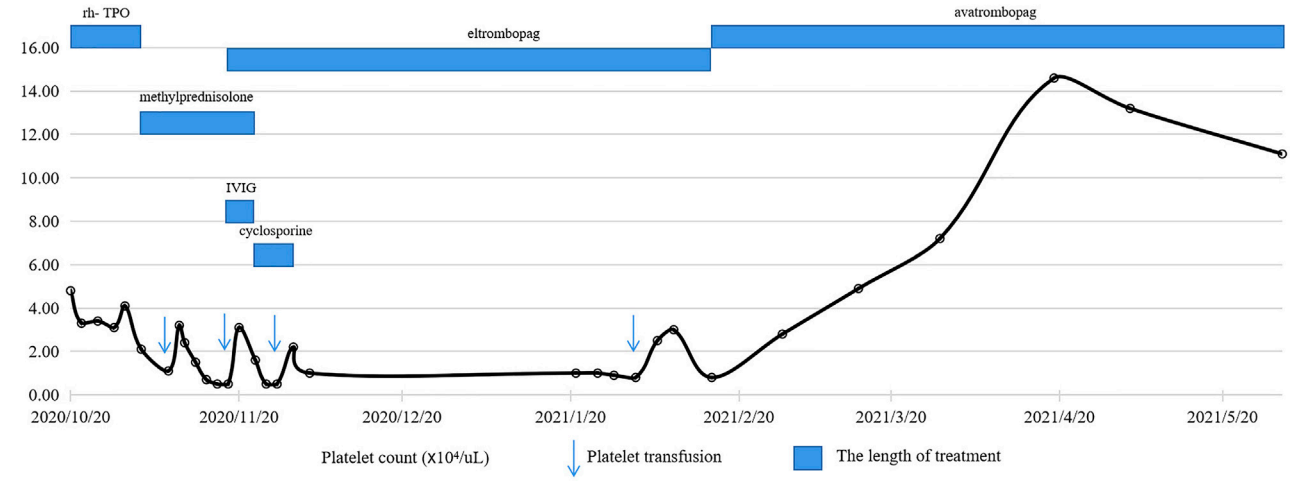

FIGURE 1 | Schedule of treatment and dynamics of platelet counts for patient 1. After two courses of tislelizumab treatment, the platelet count gradually decreased with the lowest level of 0.5×10^4/μL, which was refractory to glucocorticoids, IVIG, rh-TPO, cyclosporine and eltrombopag. With the administration of avatrombopag 40 mg daily, the platelet count rapidly increased and remained above 10×10^4/μL.

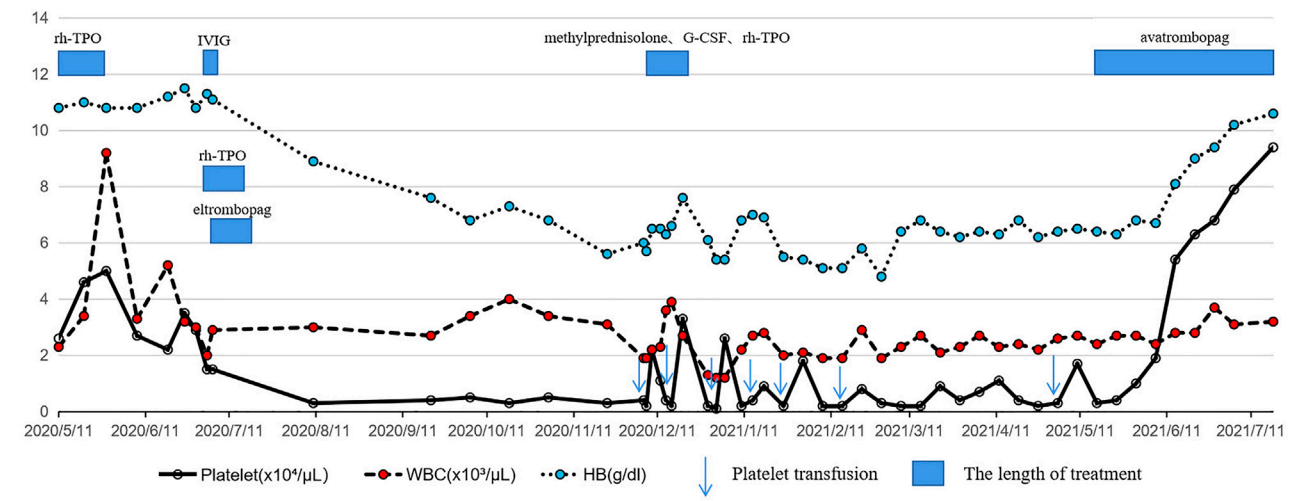

FIGURE 2 | Schedule of treatment and the dynamics of white blood cells, hemoglobin and platelets for patient 2. Two courses of triplezumab treatment induced a gradually decreased platelet count followed by pancytopenia with no response to glucocorticoids, IVIG, rh-TPO or eltrombopag. With the use of avatrombopag 40 mg daily, a rapid increase in platelet count, hemoglobin and white blood cell count was observed and maintained.

(**Figure 2**). During follow-up, no significant adverse events were observed with continued use of avatrombopag.

DISCUSSION

With the widespread application of anti-PD-1/PD-L1 antibodies in multiple malignancies, irAEs have been frequently observed in the clinic. Hematological irAEs, especially AAT, occur with a low frequency, but severe bleeding is often life-threatening. Although immune-related disorders are thought to be causative, the exact underlying pathogenesis remains unclear. The possible mechanisms associated with AAT involve activated T cells (T suppressor activated lymphocytes (Benedetti et al., 1994), T-cell large granular lymphocytes (Rajpurkar et al., 2019)), humoral immunity (anti-TPO antibody (Shiozaki et al., 2000), anti-c-Mpl antibody (Son et al., 2019)) or cytokine (Kimura et al., 1996)-mediated disorders of megakaryocyte generation. For anti-PD-1/PD-L1-induced AAT specifically, the underlying mechanism may be similar to those antitumor responses, which refer to the expansion of the T-cell repertoire. Iyama S et al. suggested that cell-mediated instead of humoral immunity possibly participated in anti-PD-1 antibody-induced AAT in studies where no significant difference was observed in growth effects

between patient and control plasma samples on BFU-E, CFU-GM and CFU-GEMM (Iyama et al., 2020). The role of affected B cell responses and induced autoantibody production, such as anti-TPO, anti-c-Mpl or platelet-associated IgG, in anti-PD-1/PD-L1-induced AAT is unclear due to the limited number of cases and the absence of related clinical and experimental data.

Published reports demonstrated preserved megakaryocytes in most cases of anti-PD-1/PD-L1-induced immune thrombocytopenia, some of which were successfully treated with glucocorticoids, cyclosporins (IVIGs), rituximab or TPO-RA (Suyama et al., 2021). However, based on the possible different pathogenesis in anti-PD-1/PD-L1-induced AAT, treatment responses greatly varied in limited individuals. Thus, effective or optimal therapeutic choices remain confusing and controversial. Nishino S et al. (Nishino et al., 2018) reported a case with anti-PD-1/PD-L1-induced AAT that responded dramatically to glucocorticoids, while the case provided by Suyama T et al. did not respond to glucocorticoids but was cured by TPO-RA eltrombopag (Suyama et al., 2021). Nevertheless, in the present two cases of this study, tislelizumab/triplezumab-induced AATs were refractory to glucocorticoids, IVIG, rh-TPO and even TPO-RA eltrombopag. In addition, due to the potential risk of infection or tumor progression caused by immunocompromise in patients with malignancies, the application of long-term or strong immunosuppressive therapy was restricted, such as cyclosporin and anti-thymocyte globulin.

Similar to eltrombopag, avatrombopag specifically binds to the TPO receptor (c-Mpl) and stimulates the proliferation and differentiation of megakaryocytes and even hematopoietic stem cells (HSCs), which results in resumed production of platelets. Due to its safety and effectiveness, avatrombopag was approved by the FDA to treat chronic ITP in adults (Provan et al., 2019) and thrombocytopenia in adult patients with chronic liver disease (Shirley, 2018). According to the manufacturer's instructions, a daily dose of 20–40 mg is recommended for patients with chronic ITP, and the standard length of treatment is not defined. TPO-RAs differ in their specific molecular structure, pharmacokinetic characteristics, binding site and the manner in which they stimulate the TPO receptor. Thus, patients who experience intolerance or lack of efficacy with one TPO-RA may benefit from switching to an alternate TPO-RA (Khellaf et al., 2013; Lakhwani et al., 2017). Surprisingly, by transitioning to avatrombopag, both patients in this study achieved satisfactory hematologic responses. The different responses induced by eltrombopag and avatrombopag in the present cases could also be dose-related, since it has been reported that daily 20 mg doses of avatrombopag produce 3–5 times higher peak platelet counts than daily 75 mg doses of eltrombopag (Al-Samkari and Kuter, 2018). Meanwhile, it is also worth considering whether the duration of treatment affects the outcome, since the length of eltrombopag administration was only 2 weeks, and avatrombopag lasted several months in patient 2. No obvious adverse reactions were observed with continued use of avatrombopag in the two cases, although pooled data from clinical trials in ITP indicated that some patients experienced headache, fatigue, epistaxis, infections, etc.

Of note, because anti-PD-1/PD-L1 antibody-induced immune attack can theoretically affect all types of cells, including HSCs and myeloid progenitors, some AATs may progress to aplastic anemia (Delanoy et al., 2019; Novotny et al., 2017). Based on TPO receptors expressed on HSCs, TPO-RA treatment was associated with multilineage clinical responses in some patients with aplastic anemia (Olnes et al., 2012; Scheinberg, 2018). To our knowledge, the application of avatrombopag in aplastic anemia, particularly anti-PD-1/PD-L1 antibody-induced aplastic anemia, has not been reported. The nearly complete response achieved by avatrombopag in patient 2 with AAT progression into aplastic anemia proposed a promising therapeutic approach for such diseases.

In conclusion, anti-PD-1/PD-L1 antibody-induced AAT is rare but often serious and refractory to multiple treatments. This study proposed avatrombopag as a potential curative and safe approach for such patients with limited efficacy or intolerance to immunosuppressive therapy or other recommended treatments.

DATA AVAILABILITY STATEMENT

The original contributions presented in the study are included in the article/supplementary material, further inquiries can be directed to the corresponding authors.

ETHICS STATEMENT

The studies involving human participants were reviewed and approved by the Ethical Committee of The Third Affiliated Hospital of Wenzhou Medical University. The patients/participants provided their written informed consent to participate in this study.

AUTHOR CONTRIBUTIONS

The original manuscript was written by HZ and XT and reviewed by PZ. AX, SW and MJ participated in the treatments for the patients. All authors read and approved the final manuscript.

ACKNOWLEDGMENTS

We thank the Department of Oncology, The Third Affiliated Hospital of Wenzhou Medical University for the support of tumor-related therapy.

REFERENCES

Agarwal, N., Spahr, J. E., Werner, T. L., Newton, D. L., and Rodgers, G. M. (2006). Acquired Amegakaryocytic Thrombocytopenic Purpura. *Am. J. Hematol.* 81, 132–135. doi:10.1002/ajh.20510

Al-Samkari, H., and Kuter, D. J. (2018). Relative Potency of the Thrombopoietin Receptor Agonists Eltrombopag, Avatrombopag and Romiplostim in a Patient with Chronic Immune Thrombocytopenia. *Br. J. Haematol.* 183, 168. doi:10.1111/bjh.15432

Benedetti, F., de Sabata, D., and Perona, G. (1994). T Suppressor Activated Lymphocytes (CD8+/DR+) Inhibit Megakaryocyte Progenitor Cell Differentiation in a Case of Acquired Amegakaryocytic Thrombocytopenic Purpura. *Stem cells* 12, 205–213. doi:10.1002/stem.5530120209

De Velasco, G., Je, Y., Bossé, D., Awad, M. M., Ott, P. A., Moreira, R. B., et al. (2017). Comprehensive Meta-Analysis of Key Immune-Related Adverse Events from CTLA-4 and PD-1/pd-L1 Inhibitors in Cancer Patients. *Cancer Immunol. Res.* 5, 312–318. doi:10.1158/2326-6066.CIR-16-0237

Delanoy, N., Michot, J. M., Comont, T., Kramkimel, N., Lazarovici, J., Dupont, R., et al. (2019). Haematological Immune-Related Adverse Events Induced by Anti-PD-1 or Anti-PD-L1 Immunotherapy: a Descriptive Observational Study. *Lancet Haematol.* 6, e48–e57. doi:10.1016/S2352-3026(18)30175-3

Deng, J., Hu, H., Huang, F., Huang, C., Huang, Q., Wang, L., et al. (2021). Comparative Efficacy and Safety of Thrombopoietin Receptor Agonists in Adults with Thrombocytopenia: A Systematic Review and Network Meta-Analysis of Randomized Controlled Trial. *Front. Pharmacol.* 12, 704093. doi:10.3389/fphar.2021.704093

Gilreath, J., Lo, M., and Bubalo, J. (2021). Thrombopoietin Receptor Agonists (TPO-RAs): Drug Class Considerations for Pharmacists. *Drugs* 81, 1285–1305. doi:10.1007/s40265-021-01553-7

Iyama, S., Takada, K., Yoshida, M., Takahashi, D., and Kobune, M. (2020). Acquired Amegakaryocytic Thrombocytopenic Purpura Possibly Induced by Anti-PD-1 Antibody. *Ann. Hematol.* 99, 1669–1670. doi:10.1007/s00277-020-04053-y

Khellaf, M., Viallard, J. F., Hamidou, M., Cheze, S., Roudot-Thoraval, F., Lefrere, F., et al. (2013). A Retrospective Pilot Evaluation of Switching Thrombopoietic Receptor-Agonists in Immune Thrombocytopenia. *Haematologica* 98, 881–887. doi:10.3324/haematol.2012.074633

Kimura, F., Nakamura, Y., Sato, K., Wakimoto, N., Kato, T., Tahara, T., et al. (1996). Cyclic Change of Cytokines in a Patient with Cyclic Thrombocytopenia. *Br. J. Haematol.* 94, 171–174. doi:10.1046/j.1365-2141.1996.d01-1783.x

Lakhwani, S., Perera, M., Fernández-Fuertes, F., Ríos de Paz, M. A., Torres, M., Raya, J. M., et al. (2017). Thrombopoietin Receptor Agonist Switch in Adult Primary Immune Thrombocytopenia Patients: A Retrospective Collaborative Survey Involving 4 Spanish Centres. *Eur. J. Haematol.* 99, 372–377. doi:10.1111/ejh.12932

Michot, J. M., Lazarovici, J., Tieu, A., Champiat, S., Voisin, A. L., Ebbo, M., et al. (2019). Haematological Immune-Related Adverse Events with Immune Checkpoint Inhibitors, How to Manage? *Eur. J. Cancer* 122, 72–90. doi:10.1016/j.ejca.2019.07.014

Nishino, S., Kodaka, T., Sawada, Y., Goka, T., Gotoh, Y., Tsunemine, H., et al. (2018). Marked Rebound Thrombocytosis in Response to Glucocorticoids in a Patient with Acquired Amegakaryocytic Thrombocytopenia. *J. Clin. Exp. Hematop* 58, 166–170. doi:10.3960/jslrt.18016

Novotný, J. P., Köhler, B., Max, R., and Egerer, G. (2017). Acquired Amegakaryocytic Thrombocytopenic Purpura Progressing into Aplastic Anemia. *Prague Med. Rep.* 118, 147–155. doi:10.14712/23362936.2017.16

Olnes, M. J., Scheinberg, P., Calvo, K. R., Desmond, R., Tang, Y., Dumitriu, B., et al. (2012). Eltrombopag and Improved Hematopoiesis in Refractory Aplastic Anemia. *N. Engl. J. Med.* 367, 11–19. doi:10.1056/NEJMoa1200931

Provan, D., Arnold, D. M., Bussel, J. B., Chong, B. H., Cooper, N., Gernsheimer, T., et al. (2019). Updated International Consensus Report on the Investigation and Management of Primary Immune Thrombocytopenia. *Blood Adv.* 3, 3780–3817. doi:10.1182/bloodadvances.2019000812

Rajpurkar, M., Buck, S., Lafferty, J., Wakeling, E., Ravindranath, Y., and Savaşan, S. (2019). Acquired Pure Red Cell Aplasia and Acquired Amegakaryocytic Thrombocytopenia Associated with Clonal Expansion of T-Cell Large Granular Lymphocytes in a Patient with Lipopolysaccharide-Responsive Beige-like Anchor (LRBA) Protein Deficiency. *J. Pediatr. Hematol. Oncol.* 41, e542–e545. doi:10.1097/MPH.0000000000001292

Scheinberg, P. (2018). Activity of Eltrombopag in Severe Aplastic Anemia. *Hematol. Am Soc Hematol Educ Program* 2018, 450–456. doi:10.1182/asheducation-2018.1.450

Shiozaki, H., Miyawaki, S., Kuwaki, T., Hagiwara, T., Kato, T., and Miyazaki, H. (2000). Autoantibodies Neutralizing Thrombopoietin in a Patient with Amegakaryocytic Thrombocytopenic Purpura. *Blood* 95, 2187–2188.

Shirley, M. (2018). Avatrombopag: First Global Approval. *Drugs* 78, 1163–1168. doi:10.1007/s40265-018-0949-8

Son, B., Park, H. S., Han, H. S., Kim, H. K., Baek, S. W., Yang, Y., et al. (2019). A Case of Acquired Amegakaryocytic Thrombocytopenia with Anti-c-mpl Autoantibody: Comparison with Idiopathic Thrombocytopenic Purpura. *Acta Haematol.* 142, 239–243. doi:10.1159/000499523

Suyama, T., Hagihara, M., Kubota, N., Osamura, Y., Shinka, Y., and Miyao, N. (2021). Acquired Amegakaryocytic Thrombocytopenia after Durvalumab Administration. *J. Clin. Exp. Hematop* 61, 53–57. doi:10.3960/jslrt.20047

Conflict of Interest: The authors declare that the research was conducted in the absence of any commercial or financial relationships that could be construed as a potential conflict of interest.

frontiers in Oncology

ORIGINAL RESEARCH
published: 28 January 2022
doi: 10.3389/fonc.2022.749954

An Insight on the Pathways Involved in Crizotinib and Sunitinib Induced Hepatotoxicity in HepG2 Cells and Animal Model

Lin Guo[1†], Tingli Tang[1†], Dongmei Fang[1,2], Hui Gong[1], Bikui Zhang[1], Yueyin Zhou[3], Leiyi Zhang[4] and Miao Yan[1*]*

[1] Department of Pharmacy, The Second Xiangya Hospital, Central South University, Changsha, China, [2] School of Pharmaceutical Sciences, Sun Yat-Sen University, Guangzhou, China, [3] Orthodontic Department of Xiangya Stomatology Hospital, Central South University, Changsha, China, [4] Department of General Surgery, The Second Xiangya Hospital, Central South University, Changsha, China

OPEN ACCESS

Edited by:
Nehad M. Ayoub,
Jordan University of Science and Technology, Jordan

Reviewed by:
Olfat Ali Hammam,
Theodor Bilharz Research Institute, Egypt
Seyithan Taysi,
University of Gaziantep, Turkey

***Correspondence:**
Leiyi Zhang
zhangleiyi@csu.edu.cn
Miao Yan
yanmiao@csu.edu.cn

[†]These authors have contributed equally to this work and share the first authorship

Specialty section:
This article was submitted to Pharmacology of Anti-Cancer Drugs, a section of the journal Frontiers in Oncology

Received: 30 July 2021
Accepted: 13 January 2022
Published: 28 January 2022

Citation:
Guo L, Tang T, Fang D, Gong H, Zhang B, Zhou Y, Zhang L and Yan M (2022) An Insight on the Pathways Involved in Crizotinib and Sunitinib Induced Hepatotoxicity in HepG2 Cells and Animal Model. Front. Oncol. 12:749954. doi: 10.3389/fonc.2022.749954

Both crizotinib and sunitinib, novel orally-active multikinase inhibitors, exhibit antitumor activity and extend the survival of patients with a malignant tumor. However, some patients may suffer liver injury that can further limit the clinical use of these drugs, however the mechanisms underlying hepatotoxicity are still to be elucidated. Thus, our study was designed to use HepG2 cells *in vitro* and the ICR mice model *in vivo* to investigate the mechanisms of hepatotoxicity induced by crizotinib and sunitinib. Male ICR mice were treated orally with crizotinib (70 mg/kg/day) or sunitinib (7.5 mg/kg/day) for four weeks. The results demonstrated that crizotinib and sunitinib caused cytotoxicity in HepG2 cells and chronic liver injury in mice, which were associated with oxidative stress, apoptosis and/or necrosis. Crizotinib- and sunitinib-induced oxidative stress was accompanied by increasing reactive oxygen species and malondialdehyde levels and decreasing the activity of superoxide dismutase and glutathione peroxidase. Notably, the activation of the Kelch-like ECH-associated protein-1/Nuclear factor erythroid-2 related factor 2 signaling pathway was involved in the process of oxidative stress, and partially protected against oxidative stress. Crizotinib and sunitinib induced apoptosis *via* the mitochondrial pathway, which was characterized by decreasing Bcl2/Bax ratio to dissipate the mitochondrial membrane potential, and increasing apoptotic markers levels. Moreover, the pan-caspase inhibitor Z-VAD-FMK improved the cell viability and alleviated liver damage, which further indicated the presence of apoptosis. Taken together, this study demonstrated that crizotinib- and sunitinib-caused oxidative stress and apoptosis finally impaired hepatic function, which was strongly supported by the histopathological lesions and markedly increased levels of serum alanine aminotransferase, alkaline phosphatase and lactate dehydrogenase.

Keywords: crizotinib, sunitinib, hepatotoxicity, Keap1/Nrf2, apoptosis, liver mitochondrial injury

INTRODUCTION

Crizotinib, an oral inhibitor of anaplastic lymphoma kinase, MET proto-oncogene, and c-ros oncogene 1 tyrosine kinases, was approved by the U.S. Food and Drug Administration (FDA) in 2011 for non-small cell lung cancer (1). Although crizotinib has been documented to improve survival in cancer patients, it can cause severe adverse effects, including pulmonary toxicity (2), acute and fulminant hepatitis (3). In clinical trials, the frequency of elevated serum transaminases in patients treated with crizotinib was 10-38% for all grades, 16% for grade 3 to grade 4 and nearly 0.1% for fatal hepatotoxicity (4). Recently, two clinical cases reported that patients treated with crizotinib presented with fatal liver failure despite the discontinuation of crizotinib and intensive supportive therapy (5, 6).

As another oral multitargeted inhibitor of platelet-derived growth factor receptors, vascular endothelial growth factor receptor and c-Kit tyrosine kinases, sunitinib was approved by FDA in 2006 for patients with metastatic renal-cell carcinoma, imatinib-resistant gastrointestinal stromal tumors and pancreatic neuroendocrine tumors (7). Nevertheless, sunitinib showed some potentially severe adverse reactions including cardiac dysfunction and potentially life-threatening hepatotoxicity (8, 9). Sunitinib-induced liver failure has been reported in many clinical cases (10). In clinical trials, 2-5% of patients treated with sunitinib developed grade 3 and grade 4 elevated aminotransferase (11) and hepatic failure happened in 0.3% of patients (12). The US FDA requested a black box warning of hepatotoxicity for the use of sunitinib pending warnings of fatal liver damage reports in 2010 (4). Hepatotoxicity has limited the clinical application of crizotinib and sunitinib. Therefore, there is an urgent need to further explore the molecular mechanisms and pathways associated with crizotinib- and sunitinib-induced hepatotoxicity for clinical medication guidance and hepatotoxicity avoidance. Recently, researchers have reported that crizotinib did not significantly affect mitochondrial function in isolated rat liver mitochondria (13) and HepG2 cells (14) at concentrations of 20- to 100-fold peak blood levels. However, some *in vitro* studies suggested that crizotinib induced ATP depletion, caspase activation in primary rat and human hepatocytes (15), and reactive oxygen species (ROS) generation in HL7702 cells (16). Similarly, Zhang and his colleagues reported that sunitinib showed no effects on intact mitochondria or submitochondrial particles even at the highest concentrations tested in isolated rat liver mitochondria (13). Nevertheless, recent research showed that sunitinib generated toxic metabolites causing mitochondrial toxicity in mice (17, 18), and apoptosis was induced in HepG2 cells and HepaRG cells (19). The results of the previous studies appear to be incompatible or contradictory in different cell lines and animal models. Thus, it is important to investigate whether oxidative damage and mitochondrial-related apoptosis are involved in crizotinib- and sunitinib-induced hepatotoxicity. Therefore, the present study was conducted using HepG2 cells as an *in vitro* model and ICR mice as an *in vivo* model to explore potential mechanisms associated with crizotinib- and sunitinib-induced hepatotoxicity. Our results confirmed that crizotinib and sunitinib treatment induced liver toxicity, which manifested in terms of elevated liver enzymes, elevated oxidative stress, and mitochondrial dysfunction, which subsequently lead to hepatocyte apoptosis. Importantly, we were the first to find that the Kelch-like ECH-associated protein-1 (Keap1)/Nuclear factor erythroid-2 related factor 2 (Nrf2) signaling pathway was involved in the process of crizotinib- and sunitinib induced oxidative stress. Our findings indicate that the activation of the Keap-Nrf2 pathway may participate in the elimination of ROS to alleviate oxidative injury.

MATERIALS AND METHODS

Drugs and Reagents

Crizotinib (purity≥98%) and sunitinib (purity≥99%) were obtained from Huateng pharmaceuticals-company (Hunan, China). DMEM medium and phosphate-buffered saline (PBS) were obtained from Gibco (Grand Island, NY, USA). Fetal bovine serum (FBS) was obtained from Biological Industries (Israel). Dimethyl sulfoxide (DMSO) and 3-(4, 5-dimethylthiazol-2-yl)-2, 5-diphenyltetrazolium bromide (MTT) were obtained from Sigma-Aldrich (St. Louis, MO, USA). Trypsin, penicillin, and streptomycin were obtained from Hyclone (Logan, USA). The primary antibodies used were anti-Nrf2 (sc-722, Santa Cruz), anti-Keap1 (af5266, Affinity), anti-cleaved caspase3 (af7022, Affinity), anti-Bcl2 (ab692, Abcam), anti-Bax (ab32503, Abcam), anti-Histone H3 (af0863, Affinity), and anti-β-actin (ac006, ABclonal).

HepG2 Cell Culture

HepG2 cells were cultured in DMEM medium supplemented with 10% FBS and 1% streptomycin and penicillin. The cells were maintained in a water-jacket CO_2 incubator at 37°C with 5% CO_2. In all experiments, the cells were inoculated with an appropriate density according to the experimental design and cultured for 24 h before the treatment.

Animal Treatment and Drug Administration

ICR male mice (body weight of 18-22 g) were purchased from Hunan Slack Jingda Experimental Animal Co., Ltd. (Hunan, China). The mice were acclimatized for one week and were maintained under a standard conditioned environment. Water and normal chow were given ad libitum. Animal care was following institutional guidelines. The study was approved by the Institutional Animal Care and Use Committee of Central South University (Hunan, China). The mice were randomly divided into vehicle-treated group (control, n=8), crizotinib-treated group (n=8, 35 mg/kg, twice daily) and sunitinib-treated group (n=8, 7.5 mg/kg/day, once daily). The mice received either 0.5% (w/v) carboxymethyl cellulose sodium once daily, crizotinib twice daily or sunitinib once daily *via* intragastric administration for 4 weeks consecutively. After 24 h of the last treatment, the animals were euthanized, blood samples were collected and livers were surgically excised and collected in 10% phosphate-buffered formalin for further determination.

Cytotoxicity Assay

HepG2 cells were seeded (5×10^3 cells/well) in 96-well plates, with 200 μL media per well. Cells were exposed to different

concentrations of crizotinib (0, 5, 10, 15, 20, 30, 40 μM) or sunitinib (0, 3.2, 6.6, 13.1, 19.6, 26.1, 39.2, 52.2 μM) for 12, 24, and 48 h. Cells were incubated with fresh MTT solution (100 μL/well; stock 5 mg/mL in PBS) for 3-4 h. After the crystal dissolved, the plates were read on an automated microplate spectrophotometer (Thermo Multiskan Spectrum, Thermo Electron Corporation, USA) and absorbance at 570 nm was measured.

Hepatotoxicity Assessments

After crizotinib and sunitinib treatment of HepG2 cells, the supernatant was collected and the biochemical parameters alanine aminotransferase (ALT), aspartic acid transferase (AST), alkaline phosphatase (ALP) and lactate dehydrogenase (LDH) were measured by the full-automatic clinical analyzer in the laboratory of the second Xiangya hospital (7600, HITACHI Ltd., Tokyo, Japan).

Liver samples of the mice were fixed in 10% phosphate-buffered formalin and embedded in paraffin. In brief, the liver tissue was embedded in paraffin, then deparaffinized with xylene, stained with hematoxylin and eosin, then dehydrated and sealed, and finally evaluated for damage under light microscopy.

Apoptosis Determined by Annexin V-FITC and TUNEL Assay

Apoptosis was detected through flow cytometry using FITC Annexin V Apoptosis Detection Kit (Bestbio, Shanghai, China). Drug-treated cells (culture in the incubator for 24 h) were digested by trypsin without EDTA, centrifuged, and resuspended with PBS for 3 times strictly. The fluorescence maker was added and cells were incubated in a dark place at 2-8°C for 15 min, followed by sample loading and detection through flow cytometry. All samples were analyzed within 1 h to ensure the effect.

Terminal deoxynucleotidyl transferase-mediated dUTP nick end labeling (TUNEL) assay was conducted with the TUNEL kit according to the manufacturer's instructions. In brief, the liver tissue was embedded in paraffin, then deparaffinized with xylene, stained with TUNEL reaction mixture, then stained by DAPI staining and anti-fluorescence quenching were performed. Finally, the obtained slices were observed and photographed at a suitable high magnification, with the apoptotic cells appearing green and the nuclei appearing in blue.

Accumulation of ROS

The level of ROS was determined using the fluorescent probe DCFH-DA (Beyotime Biotechnology, Shanghai, China). HepG2 cells (3.5×10^5 cells/well) were treated with different concentrations of crizotinib (0, 8, 15, 20 μM) or sunitinib (0, 5, 9, 14 μM) for 24 h. After DCFH-DA was added at a final concentration of 10.0 μM to the culture medium, the hepatocytes in 24-wells were incubated at 37°C for an additional 20-30 min, and then washed with PBS, and measured immediately by fluorescence microscope (Thermo Electron Corporation, USA). Increased green fluorescence intensity was used to quantify intracellular ROS production.

Measurement of Glutathione Peroxidase (GPx), Superoxide Dismutase (SOD) and Malondialdehyde (MDA)

The extent of oxidative stress was estimated in liver homogenates by measuring activities of GPx, SOD and MDA using commercial kits (Jiancheng Bioengineering Institute, Nanjing, China) according to the manufacturer's instructions. GPx is an important selenoprotein that reduces hydroperoxides as well as hydrogen peroxide (H_2O_2) while oxidizing glutathione, which can protect the structure and function of the cell membrane (20, 21). Briefly, GPx can promote the reaction of H_2O_2 with reduced glutathione (GSH) to produce H_2O and glutathione oxidized. The activity of GPx was measured by spectrophotometer assay at 412 nm from the oxidation of GSH in the presence of H_2O_2 used as substrate.

The activity of SOD was determined by the xanthine oxidase (hydroxylamine) method. This redox produced superoxide which oxidizes hydroxylamine to nitrite by reacting with the reagent producing a purple-red dye. The absorbance of the color which was inversely proportional to the SOD activity was determined by a spectrophotometer at 550 nm (22).

The production of MDA was assessed with the thiobarbituric acid reactive substances method (TBA). TBA was added to each sample tube and vortexed. The reaction mixture was incubated at 95°C for 60 min. After cooling, the pink pigment was read spectrophotometrically at 532 nm (22).

Mitochondrial Membrane Potential (MMP)

Mitochondrial membrane potential assay kit with JC-1 (Beyotime Biotechnology, Shanghai, China) is a fast and sensitive assay kit that uses JC-1 as a cationic dye to detect membrane potential changes in cells, tissues or purified mitochondria, which can be used for early detection of apoptosis. After the liver tissue was digested, cell precipitation was collected, then fluorescence probe was loaded and cells were incubated at 37°C for 20 min, mixed well every 3-5 min, and washed with dyeing buffer (1×) at 4°C and centrifuged three times, finally detected by flow cytometry.

Western Blotting

The HepG2 cell and animal liver protein samples were extracted with enhanced RIPA lysate (Boster, Hubei, China), the cytoplasmic and nuclear proteins were prepared with the subcellular structure cell nucleus and cytoplasmic protein extraction kit (Boster, Hubei, China) according to the manufacturer's instruction. The protein concentration of whole-cell lysates was determined using the BCA method (Boster, Hubei, China). Protein lysates (15-30 μg) were loaded on 8-12% SDS-PAGE gels, separated electrophoretically and transferred to the PVDF membrane. Subsequently, the membranes were incubated in a blocking solution at room temperature for 1 h. After blocking, membranes were separately incubated at 4°C on a rocker with primary antibodies specific to the protein of interest; these were rabbit anti-Keap1 antibody (1:1000), anti-cleaved caspase3 antibody (1:1000), anti-Bax antibody (1:5000), anti-Histone H3 antibody

(1:1000), anti-β-actin antibody (1:500-1:2000), mouse anti-Nrf2 antibody (1:800), and anti-Bcl2 antibody (1:500). Subsequently, the membranes were incubated with a suitable HRP-conjugated secondary antibody (Proteintech, USA) for 1h, and then signal detection was conducted with an ECL kit (Boster, Hubei, China) according to the manufacturer's protocol.

Statistical Analysis

The data were presented as the means ± standard derivation (SD). The significance of differences between groups was determined with the one-way analysis of variance (ANOVA) and SPSS 20.0 software (SPSS Inc., Chicago, IL, USA), and comparison between two groups was done with an independent sample t-test. Figures were drawn with GraphPad Prism 6 (GraphPad Software, La Jolla, CA, USA).

RESULTS

Crizotinib and Sunitinib Induced Hepatotoxicity

The results showed that HepG2 cell viability was reduced in a concentration- and time-dependence manner (**Figures 1A, B**). When cells were treated for 24 h, crizotinib 15 μM and sunitinib 9 μM were used in subsequent experiments. The levels of ALT, AST, and LDH are sensitive markers of hepatocyte damage. **Figure 1C** showed that ALT and AST levels increased significantly in the supernatant from treated HepG2 cells at a concentration of 15μM and 20 μM, but LDH levels were not significantly altered in the crizotinib treatment compared to vehicle. According to **Figure 1D**, sunitinib treatment significantly elevated the levels of ALT, AST, and LDH compared to vehicle.

Serum levels of the hepatic enzymes ALT and ALP were significantly elevated in crizotinib-treated group, while the levels of ALT and LDH were significantly elevated in animals treated with sunitinib compared to the control group (**Figure 2A**). Also, histopathological analysis of liver sections from the crizotinib group (**Figure 2B-b**) showed small pockets of inflammatory cells infiltrate around the hepatic lobules and the central veins, compared with those of the control group (**Figure 2B-a**). More hepatocyte edema, cytoplasm loose light dye, and a small amount of hepatocyte edema to balloon-like degeneration, cell swelling, cytoplasmic cavitation (**Figure 2B-c**), and a small amount of focal lymphocyte infiltration (**Figure 2B-d**) were seen in the sunitinib group, but not in the control group. These findings support drug-induced liver injury for animals treated with crizotinib and sunitinib *in vivo*.

Hepatotoxicity Induced by Crizotinib and Sunitinib Is Mediated by Cell Apoptosis and Necrosis

As shown in **Figure 3A**, an upward tendency pattern was apparent, when the HepG2 cells were treated with different

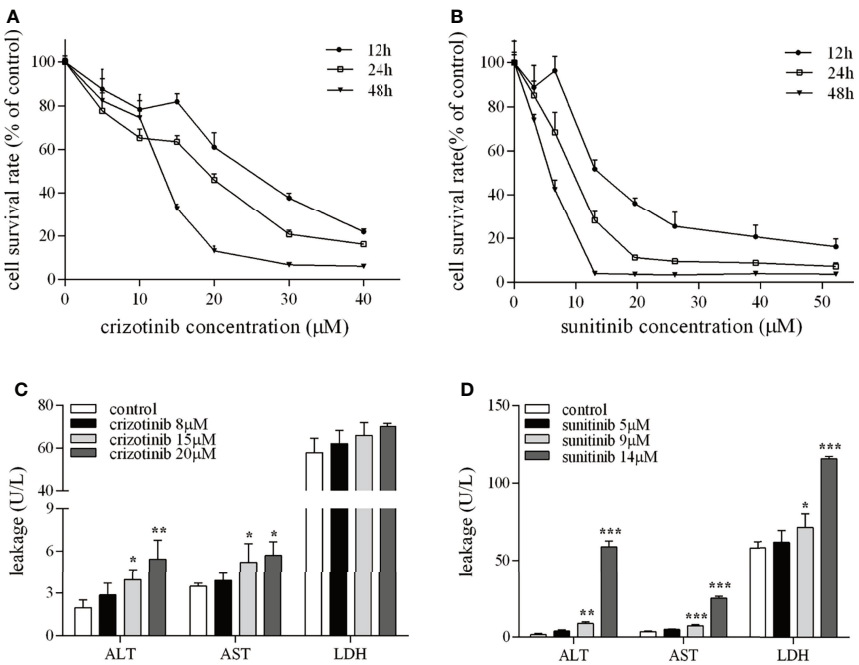

FIGURE 1 | The hepatotoxicity of crizotinib and sunitinib *in vitro*. **(A, B)** Cytotoxicity of crizotinib or sunitinib alone at the various concentration for 12, 24 and 48 h in HepG2 cells (n=5-6). **(C, D)** ALT, AST and LDH levels in the supernatant following HepG2 cell treatment with crizotinib or sunitinib at different concentrations for 24 h (n = 3). *P < 0.05, **P < 0.01 or ***P < 0.001 (the crizotinib or sunitinib alone vs. control). ALT, alanine aminotransferase; AST, aspartic acid transferase; LDH, lactate dehydrogenase.

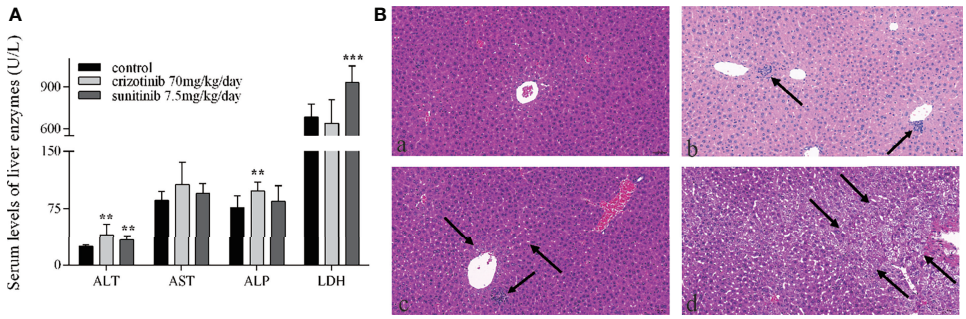

FIGURE 2 | The hepatotoxicity of crizotinib and sunitinib *in vivo*. **(A)** Blood levels of different liver enzymes in male ICR mice after the administration of crizotinib or sunitinib treatment (n = 8). **(B)** Histopathological analysis of liver micro-tissues from animals in the different experimental groups. Representative images from: (a) control group; (b) crizotinib-treated animals, 70 mg/kg/day; (c, d) sunitinib-treated animals, 7.5 mg/kg/day. Magnification of photomicrographs at 20x. **P < 0.01 or ***P < 0.001 (the crizotinib or sunitinib alone vs. control). ALT, alanine aminotransferase; AST, aspartic acid transferase; ALP, alkaline phosphatase; LDH, lactate dehydrogenase.

concentrations of crizotinib (0, 8, 15, 20, 25 μM) for 24 h, which supported the hypothesis that crizotinib induced hepatocyte apoptosis and/or necrotic. Subsequently, a time-dependent increase was observed, and HepG2 cells treated for 24 h and 48 h with crizotinib showed greater apoptosis and/or necrosis (**Figure 3C**). The percentage of cells undergoing apoptosis and/or necrosis in crizotinib-treated hepatocytes increased dramatically compared with non-treated cells (**Figures 3B, D**). Activation of caspase 3 is the most critical apoptotic executive event in apoptosis. Sunitinib was associated with a significant concentration-dependent increase in cleaved caspase 3 starting at 9 μM (**Figure 3E**). Moreover, Z-VAD-FMK, an irreversible pan-caspase inhibitor, was applied to block apoptosis. The results showed that Z-VAD-FMK increased cell viability and relieved drug-induced toxicity to HepG2 cells, as shown in **Figures 3F, G**.

As shown in **Figures 4A, B**, the number of TUNEL-positive cells in the liver tissue of ICR mice increased significantly after crizotinib and sunitinib treatment. When crizotinib and sunitinib were applied to mice, the expression of cleaved caspase 3 was increased significantly, which was consistent with the results of TUNEL assay (**Figures 4C, D**). These results further revealed that apoptosis and/or necrosis contributed to crizotinib- and sunitinib-induced hepatocyte death.

Crizotinib and Sunitinib Induced Oxidative Stress

As shown in **Figures 5A, B**, treatment with crizotinib or sunitinib (24 h) increased the production of ROS in a concentration-dependent manner compared with control cells. As shown in **Figure 6**, a significant reduction in the activity of GPx was found in both crizotinib- and sunitinib-treated animals compared to the control group. However, accumulation of MDA and a decrease of the activity of SOD were significantly observed in the sunitinib but not crizotinib treatment group. Accordingly, The function of the endogenous antioxidant defense system is impaired as demonstrated by a decrease of SOD activity and an increase of MDA which cannot remove ROS effectively leading to the accumulation of ROS in the liver tissues of mice. Subsequently, we investigated the changes in the Keap1/Nrf2 pathway which played an important role in oxidative stress. When HepG2 cells were exposed to crizotinib or sunitinib for 24 h, the protein expression of total Keap1 was down-regulated while nuclear Nrf2 was up-regulated (**Figures 7A, B**). Similar to *in vitro* findings, crizotinib- and sunitinib-treated animal groups showed down-regulation and up-regulation for the expression of Keap1and nuclear Nrf2, respectively (**Figures 7C, D**).

The Mitochondrial Dysfunction Was Involved in Crizotinib- and Sunitinib-Induced Hepatotoxicity

Mitochondria are a crucial component of the intrinsic pathway of apoptosis, a major mechanism of drug-induced cytotoxicity. MMP is an important indicator of mitochondrial function. In **Figure 8**, red fluorescence represents JC-1 aggregates in the normal mitochondria whereas green fluorescence represents JC-1 monomer indicating MMP dissipation. When the ratio of red-to-green fluorescence intensity decreases, it indicates a loss of MMP that is widely probed by JC-1 staining. *In vivo*, flow cytometry results showed that the ratio of JC-1 aggregates/JC-1-monomer was reduced in the crizotinib- and sunitinib-treated groups, indicating the impairments of MMP (**Figures 8A, B**). Also, crizotinib and sunitinib altered the balance between the anti-apoptotic protein Bcl2 and the pro-apoptotic protein Bax on the mitochondrial membrane (**Figures 9A, B**). *In vivo*, compared with the untreated group, crizotinib and sunitinib induced a concentration-dependent decrease in the Bcl2/Bax ratio (**Figures 9C, D**).

DISCUSSION

Small molecule kinase inhibitors, such as tyrosine kinases inhibitors (TKIs), which are designed to inhibit the action of

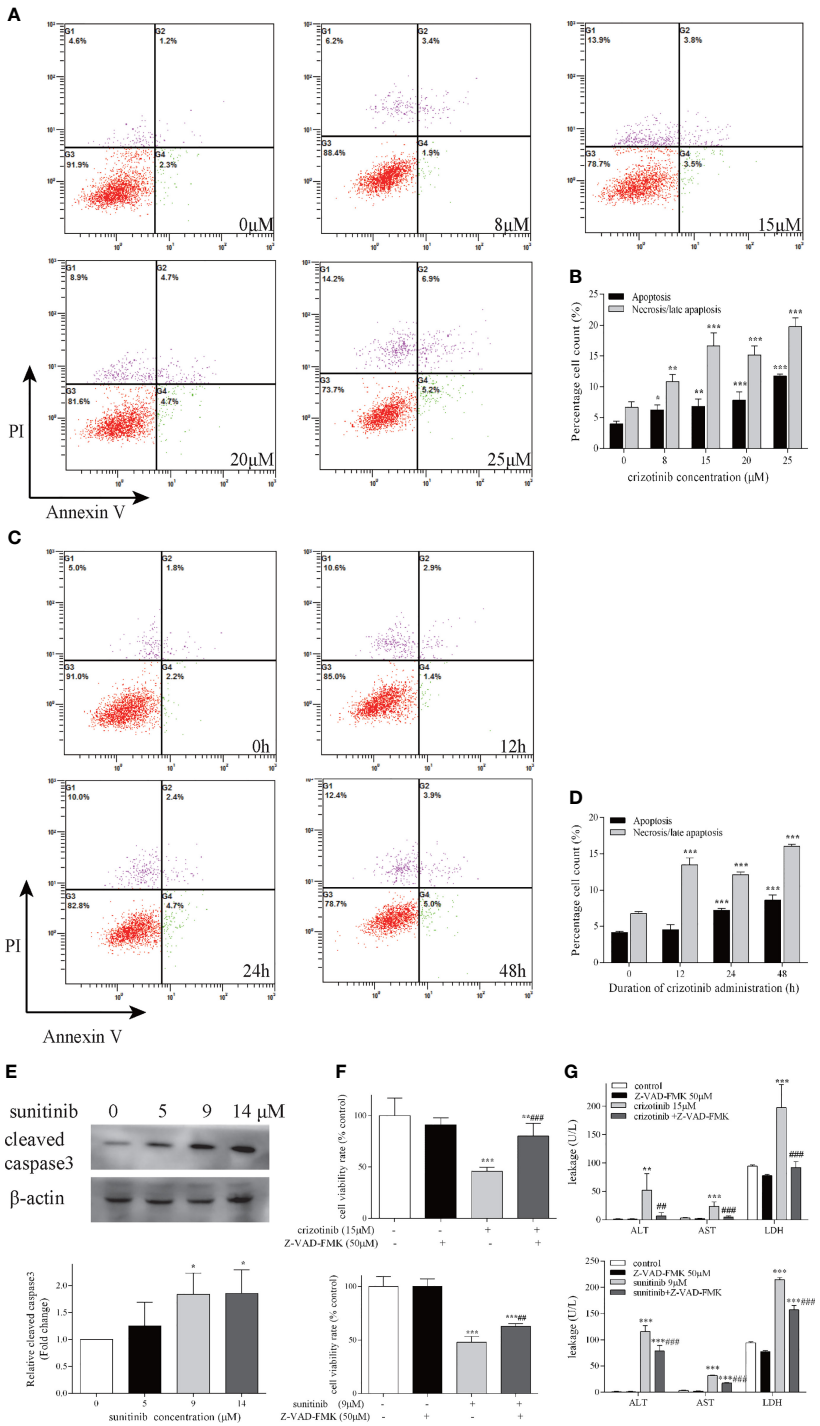

FIGURE 3 | Crizotinib and sunitinib induced apoptosis in HepG2 cells. Following treatment of cells with increasing doses of crizotinib for 24 h **(A)** and increasing administration time of crizotinib 15 μM **(C)**, cell apoptosis was measured by Annexin V–FITC/PI double staining assay. In the flow cytometry plot, live, early apoptotic, late apoptotic and necrotic cells were shown in the lower left, lower right, upper right and upper left quadrants, respectively. **(B)** Quantification of experiments shown in **(A)**. **(D)** Quantification of experiments shown in **(C)**. **(E)** Western blot analysis for the level of cleaved caspase 3 after sunitinib exposure for 24 h (n=3). **(F)** The cell survival rate for HepG2 cells after treatment with crizotinib or sunitinib with or without Z-VAD-FMK. Cell viability was measured by the MTT assay, and **(G)** The levels of ALT, AST, and LDH in the supernatant of HepG2 cells treated with crizotinib or sunitinib with or without Z-VAD-FMK (n=3). In these experiments, cells were pretreated with Z-VAD-FMK 50 μM for 24 h before crizotinib (15 μM) or sunitinib (9 μM) treatment. *P < 0.05, **P < 0.01 or ***P < 0.001 (the crizotinib or sunitinib alone vs. control). $^{\#\#}$P < 0.01 $^{\#\#\#}$P < 0.001 (the crizotinib or sunitinib alone vs. the crizotinib or sunitinib pretreated with Z-VAD-FMK). ALT, alanine aminotransferase; AST, aspartic acid transferase; LDH, lactate dehydrogenase.

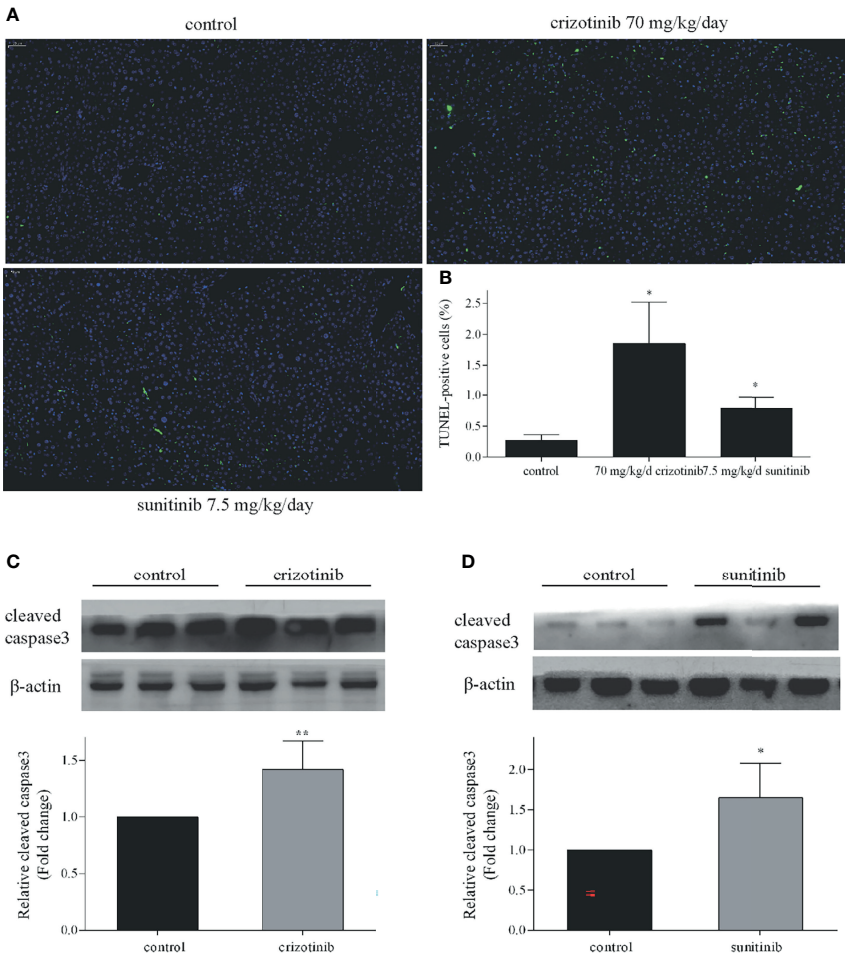

FIGURE 4 | Crizotinib and sunitinib induced apoptosis *in vivo*. **(A)** The ICR mice hepatocyte apoptosis in liver tissue (TUNEL, 20×). The blue fluorescence indicates nuclei, and the green fluorescence indicates apoptotic cells. **(B)** TUNEL-positive cells were quantified. **(C, D)** The protein expression of cleaved caspase 3 in ICR mice treated with vehicle, crizotinib, or sunitinib treatment (n = 6). *P < 0.05 or **P < 0.01 (the crizotinib or sunitinib alone vs. control).

mutated or over-expressed tyrosine kinases in cancer cells, have improved the management of cancers and significantly extended survival in cancer patients compared with traditional chemotherapy agents (23). However, unexpected toxic reaction of hepatotoxicity has been reported for several TKIs, including imatinib, gefitinib, sunitinib, crizotinib, lapatinib, pazopanib, ponatinib, and regorafenib (11, 24, 25). As of October 2019, the FDA has approved 53 small molecule kinase inhibitors, seven (sunitinib, lapatinib, pazopanib, regorafenib, ponatinib, idelalisib, pexidartinib) of which had a black box warning of liver toxicity, and twenty-nine of which had warnings and precautions for hepatotoxicity in their product labeling (26). Many case reports demonstrated that crizotinib and sunitinib induced hepatotoxicity, even acute liver failure (ALF) (27–29). However, dose adjustment or drug discontinuation are the common strategies to reduce or manage hepatotoxicity induced by crizotinib or sunitinib. Also, alternative agents such as alectinib though belongs to the same drug class, could be a choice in cases of crizotinib-induced liver toxicity, however more evidence is awaited (28). Thus, monitoring of liver function is recommended for patients using crizotinib or sunitinib, especially in patients with liver impairment or those using antisecretory drugs (30). Furthermore, applying the above-described measures may contribute to treatment failure and tumor progression in some cases. A limited number of systematic studies described the molecular mechanism(s) associated with crizotinib- and sunitinib-induced hepatotoxicity. Therefore, it is necessary to elucidate the molecular mechanisms and pathways associated with crizotinib- and sunitinib-induced liver toxicity.

In this study, we established an animal model that mimicked the clinical dose and duration of administration of crizotinib and sunitinib to investigate their hepatotoxicity. In addition, HepG2 cells are a well-characterized human cell system suitable for investigating mitochondrial drug toxicity (31, 32). Findings from our study demonstrated that crizotinib and sunitinib treatment

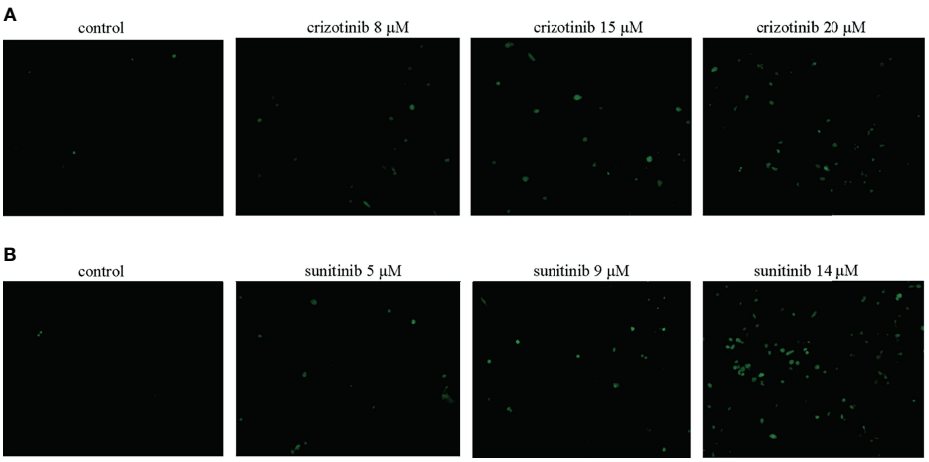

FIGURE 5 | **(A, B)** Crizotinib and sunitinib increased ROS levels in HepG2 cells (n = 3). The intracellular ROS levels were measured using DCFH-DA. The microscopic images of the intensity of DCH fluorescence of respective experimental group (magnification ×200).

reduced viability of HepG2 cells and induced liver toxicity in animal model. A study indicated that the pattern of liver injury in patients receiving TKIs is typically hepatocellular (29), so we investigated the main way of hepatocyte death caused by crizotinib and sunitinib. Apoptosis and necrosis are the two major forms of cell death, which are relevant to drug-induced liver injury (33, 34). In our study, the flow cytometry results demonstrated that the percentage of HepG2 cells undergoing apoptosis or necrosis is increased in crizotinib-treated cells when compared with the untreated hepatocytes, consistent with previously published reports (14, 15, 35). Although sunitinib cannot be treated with fluorescent dyes to investigate apoptosis because of autofluorescence, Western blotting demonstrated that the level of cleaved caspase 3 increased in HepG2 cells and liver tissue after both crizotinib and sunitinib treatment. Meanwhile, the results of crizotinib- and sunitinib-mediated apoptosis were also confirmed by TUNEL assay *in vivo*. In addition, Z-VAD-FMK, the caspase inhibitor, effectively protected from drug-induced liver cell death and reduced the release hepatic enzymes ALT, AST, and LDH caused by crizotinib and sunitinib.

Mitochondria play an important role in oxidative stress and the intrinsic apoptotic pathway (36). Bcl2 and Bax proteins are important regulators factors of MMP. Bcl2/Bax ratio can control the release of cytochrome C from mitochondria and the activation of downstream caspase 3 to promote cell survival or apoptosis (37, 38). Previous studies indicated that crizotinib dissipated MMP starting at high concentrations (starting at 50 μM) and inhibited glycolysis only weakly when applied to HepG2 cells (14), and MMP

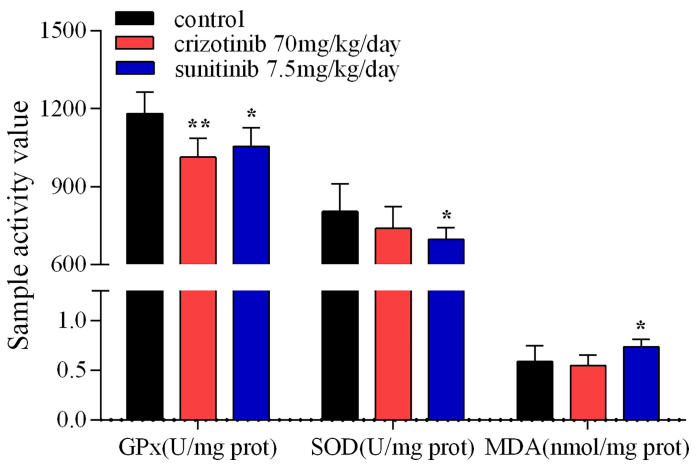

FIGURE 6 | The activity assay of hepatic GPx, SOD and MDA in mice treated with crizotinib or sunitinib (n = 6-8). *P < 0.05 and **P < 0.01 (the crizotinib or sunitinib alone vs. control). GPx, glutathione peroxidase; SOD, superoxide dismutase; MDA, malondialdehyde.

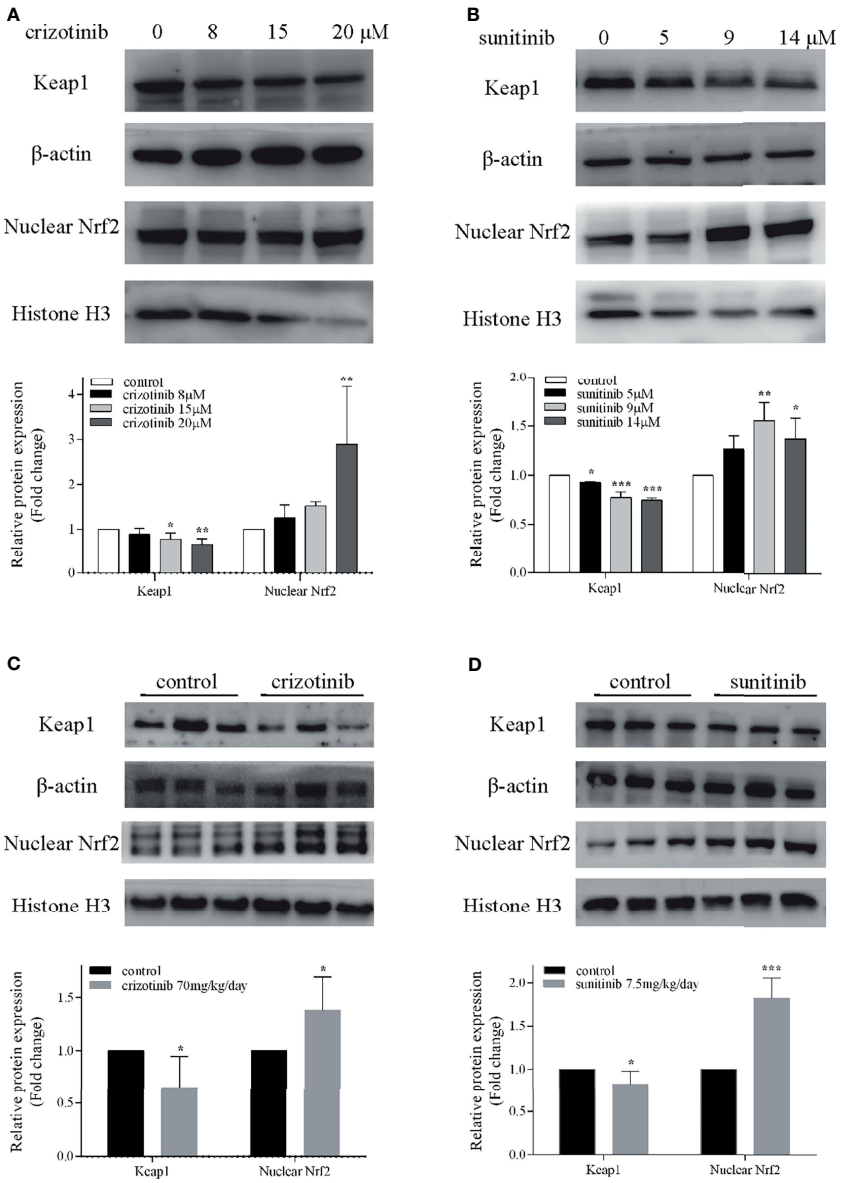

FIGURE 7 | Involvement of the Nrf2 pathway in crizotinib- or sunitinib-mediated hepatotoxicity *in vitro* and *in vivo*. **(A, B)** The protein expression of Keap1 and nuclear Nrf2 in HepG2 cells (n = 3). **(C, D)** The hepatic Keap1 and nuclear Nrf2 protein levels in mice treated with crizotinib or sunitinib alone (n = 6). β-actin: loading control of total protein; Histone H3: nuclear loading control. *P < 0.05, **P < 0.01 or ***P < 0.001 (the crizotinib or sunitinib alone vs. control). Keap1, Kelch-like ECH-associated protein-1; Nrf2, Nuclear factor erythroid-2 related factor 2.

was not affected in rat liver mitochondria (13). Notably, we found that crizotinib could dissipate the MMP by decreasing the expression of Bcl2/Bax in the liver tissue. In addition, an *in vitro* study reported that sunitinib has mitochondrial toxicity, which reduced the MMP starting at 1 μM in HepG2 cells and after exposure for 15 min at 10 μM in isolated mouse liver mitochondria (19). However, there were other reports that sunitinib did not disrupt the MMP of rat heart mitochondria (39), mouse liver mitochondria (40), and isolated rat liver mitochondria (13). In our study, after sunitinib treatment, the MMP of liver tissue dissipated significantly and the expression of Bcl2/Bax decreased significantly. The different findings can be explained by differences in the experimental models and settings applied according to Peach et al. (17). Taken together, our findings demonstrate regulatory roles for Bcl2 and Bax in altering MMP in crizotinib- and sunitinib-induced mitochondrial apoptotic pathway.

In a case report by Kreitman et al., treatment with N-acetylcysteine (NAC), a ROS scavenger, partially restored liver function tests to normal level and partially relieved ALF induced by crizotinib in a patient (27). In line with this, we previously

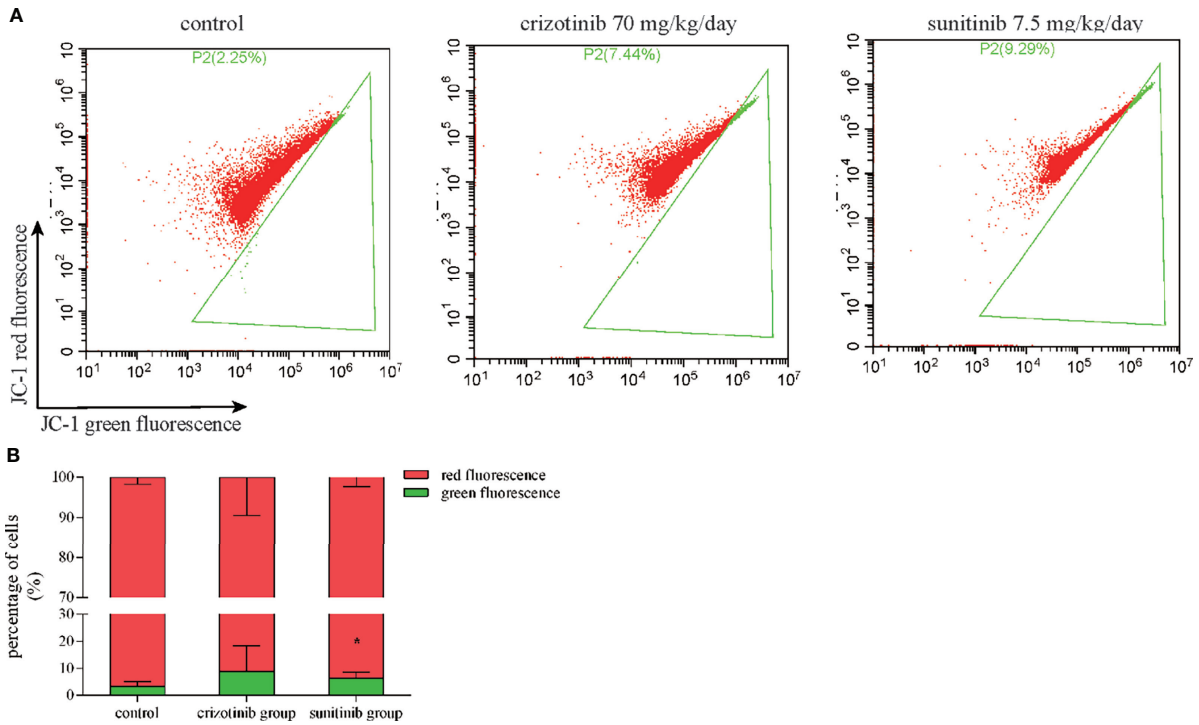

FIGURE 8 | Crizotinib and sunitinib disrupt MMP in liver tissue. **(A)** Treatment with crizotinib or sunitinib decreased MMP in animals treated for 4 weeks compared to the control group as measured by flow cytometry and JC-1 staining. Red fluorescence represents JC-1 aggregates in the normal mitochondria whereas green fluorescence represents JC-1 monomer indicating MMP dissipation. **(B)** Quantification of high- and low-MMP cells in liver tissue (n = 8). *P < 0.05 (the crizotinib or sunitinib alone vs. control). MMP, mitochondrial membrane potential.

indicated that NAC treatment decreased hepatocyte damage induced by crizotinib and sunitinib in HL7702 cells (35). Therefore, the results of these efforts indicated that the underlying mechanism might be related to oxidative stress. Oxidative stress results from an imbalance between ROS and antioxidants, which has long been recognized as a critical pathogenic factor in acute injury, including acute kidney injury and acute liver injury (41, 42). The overproduction of ROS can reduce the content of GPx and SOD which are two major antioxidant enzymes to reduce oxidative stress. Meanwhile, high levels of ROS can cause lipid peroxidation to damage cellular membranes, and MDA is a significant marker of lipid peroxidation (43). Our research revealed that crizotinib and sunitinib significantly increased the level of ROS in a concentration-dependent manner in HepG2 cells, and markedly reduced the content of GPx and SOD, and increased MDA in liver tissue. However, the change of ROS was not statistically significant in experimental animals. Possible reasons for the variability in results might include differences in animal models used, the drug dose used, and the experimental assays used to detect ROS in isolated liver mitochondria. These results demonstrate that the imbalance between ROS and antioxidative function leads to oxidative stress, which contributes to hepatocyte damage.

Currently, strategies for the prevention and treatment of hepatotoxicity induced by TKIs are very limited, and it is necessary to find the key targets in TKIs-induced liver injury. Nrf2, which is an imperative redox-sensitive transcription factor targeting of elimination of ROS, and its activation is widely thought to alleviate the liver diseases triggered by oxidatie stress (44, 45). Under stress conditions, Nrf2 dissociates from Keap1, translocates to the nucleus and binds to antioxidant response elements, which results in the expression of diverse antioxidant and metabolic genes to relieve oxidative stress (46, 47). Importantly, we first found that low doses of crizotinib and sunitinib activated the Keap1/Nrf2 signaling pathway *in vitro* and *in vivo* to alleviate self-induced hepatotoxicity, which is following previously published papers on drug-induced liver injury (42, 48, 49). Therefore, our findings indicated that the activation of the Keap1/Nrf2 signaling pathway could be a potential therapeutic target for TKIs in the treatment of liver injury.

CONCLUSIONS

The results show that crizotinib and sunitinib induce hepatic oxidative stress and apoptosis that lead to hepatotoxicity. The activation of the Keap1/Nrf2 signaling pathway was involved in crizotinib- and sunitinib-induced oxidative stress, which might partially protect against their induced oxidative damage. However, the specific mechanism underlying the relationship between crizotinib- and sunitinib-induced oxidative stress and

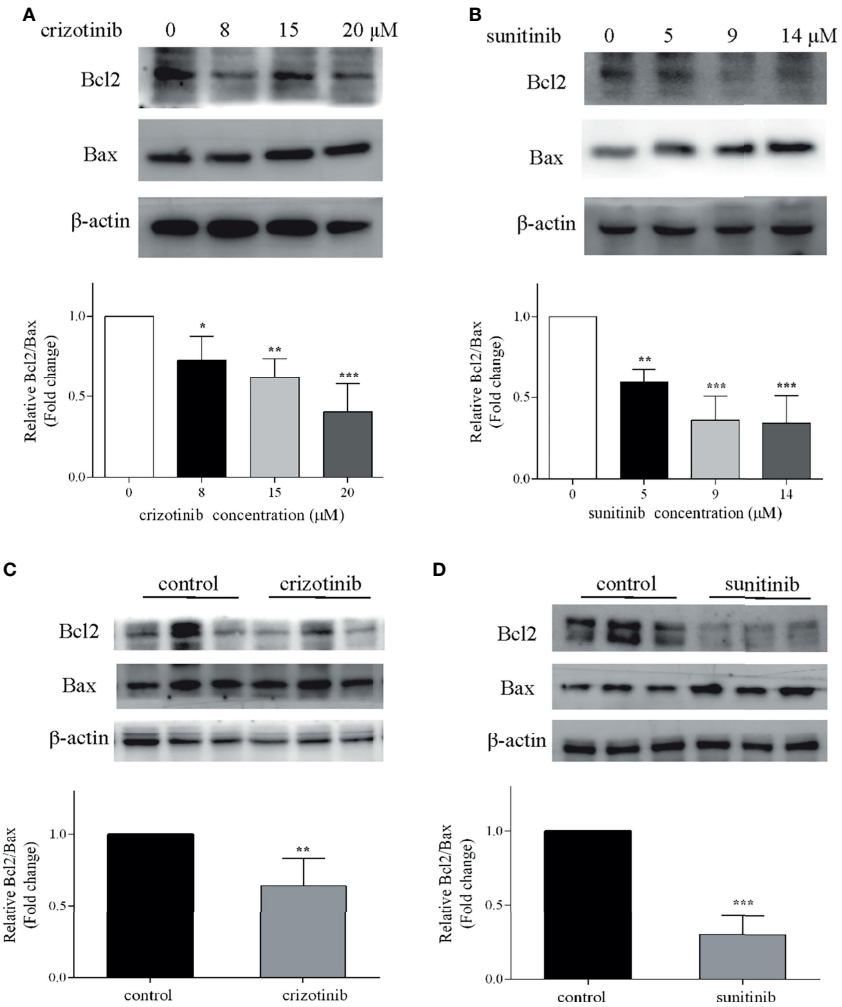

FIGURE 9 | Crizotinib or sunitinib treatment altered the levels of Bcl2 and Bax in HepG2 cells and in liver tissue. **(A, B)** Protein levels of Bcl2 and Bax in HepG2 cells treated with crizotinib or sunitinib for 24 h (n = 3). **(C, D)** Protein level of Bcl2 and Bax in liver tissue in mice treated with crizotinib or sunitinib for 4 weeks (n = 6). *P < 0.05, **P < 0.01 or ***P < 0.001 (the crizotinib or sunitinib alone vs. control).

mitochondrial apoptotic pathway requires further investigations. Therefore, we will continue to explore additional biomarkers for hepatotoxicity and other potential signaling pathways associated with crizotinib- and sunitinib-induced liver injury.

DATA AVAILABILITY STATEMENT

The original contributions presented in the study are included in the article/supplementary material. Further inquiries can be directed to the corresponding authors.

ETHICS STATEMENT

The animal study was reviewed and approved by the Institutional Animal Care and Use Committee of Central South University (Hunan, China).

AUTHOR CONTRIBUTIONS

LG contributed to conceiving and designing the experiments. TT and DF performed the data analyses and wrote the manuscript. LZ and MY contributed significantly to analysis and manuscript preparation. HG, BZ, and YZ helped perform the analysis with constructive discussions. All authors contributed to the article and approved the submitted version.

FUNDING

This research was funded by the National Natural Science Foundation of China, grant number 81974532 and No. 81803830, the Natural Science Foundation of Hunan

Province, China, grant number 2020JJ4130, and Science and Technology Department of Hunan Province, China, grant number 2017SK1030.

ACKNOWLEDGMENTS

We are very grateful to Yan-Lin Du and Sheng-Ke Zhou for their help.

REFERENCES

1. Girard N, Audigier-Valette C, Cortot AB, Mennecier B, Debieuvre D, Planchard D, et al. ALK-Rearranged Non-Small Cell Lung Cancers: How Best to Optimize the Safety of Crizotinib in Clinical Practice? *Expert Rev Anticancer Ther* (2015) 15:225–233. doi: 10.1586/14737140.2014.986103
2. Scagliotti G, Stahel RA, Rosell R, Thatcher N, Soria JC. ALK Translocation and Crizotinib in Non-Small Cell Lung Cancer: An Evolving Paradigm in Oncology Drug Development. *Eur J Cancer* (2012) 48:961–73. doi: 10.1016/j.ejca.2012.02.001
3. Gumusay O, Esendagli-Yilmaz G, Uner A, Cetin B, Buyukberber S, Benekli M, et al. Crizotinib-Induced Toxicity in an Experimental Rat Model. *Wien Klin Wochenschr* (2016) 128:435–41. doi: 10.1007/s00508-016-0984-y
4. *The DailyMed* . Washington (DC: National Institutes of Health, U.S.National Library of Medicine, Health & Human Services. Available at: https://dailymed.nlm.nih.gov/dailymed (Accessed July 01, 2021).
5. van Geel RM, Hendrikx JJ, Vahl JE, van Leerdam ME, van den Broek D, Huitema AD, et al. Crizotinib-Induced Fatal Fulminant Liver Failure. *Lung Cancer* (2016) 93:17–9. doi: 10.1016/j.lungcan.2015.12.010
6. Zhang Y, Xu YY, Chen Y, Li JN, Wang Y. Crizotinib-Induced Acute Fatal Liver Failure in an Asian ALK-Positive Lung Adenocarcinoma Patient With Liver Metastasis: A Case Report. *World J Clin cases* (2019) 7:1080–6. doi: 10.12998/wjcc.v7.i9.1080
7. Goodman VL, Rock EP, Dagher R, Ramchandani RP, Abraham S, Gobburu JV, et al. Approval Summary: Sunitinib for the Treatment of Imatinib Refractory or Intolerant Gastrointestinal Stromal Tumors and Advanced Renal Cell Carcinoma. *Clin Cancer Res* (2007) 13:1367–73. doi: 10.1158/1078-0432.CCR-06-2328
8. Mueller EW, Rockey ML, Rashkin MC. Sunitinib-Related Fulminant Hepatic Failure: Case Report and Review of the Literature. *Pharmacotherapy* (2008) 28:1066–70. doi: 10.1592/phco.28.8.1066
9. Demetri GD, van Oosterom AT, Garrett CR, Blackstein ME, Shah MH, Verweij J, et al. Efficacy and Safety of Sunitinib in Patients With Advanced Gastrointestinal Stromal Tumour After Failure of Imatinib: A Randomised Controlled Trial. *Lancet* (2006) 368:1329–38. doi: 10.1016/S0140-6736(06)69446-4
10. Guillen SS, Meijer M, de Jongh FE. Lethal Acute Liver Failure in a Patient Treated With Sunitinib. *BMJ Case Rep* (2016) 2016:bcr2015213624. doi: 10.1136/bcr-2015-213624
11. Shah RR, Morganroth J, Shah DR. Hepatotoxicity of Tyrosine Kinase Inhibitors: Clinical and Regulatory Perspectives. *Drug Saf* (2013) 36:491–503. doi: 10.1007/s40264-013-0048-4
12. Amaya GM, Durandis R, Bourgeois DS, Perkins JA, Abouda AA, Wines KJ, et al. Cytochromes P450 1A2 and 3A4 Catalyze the Metabolic Activation of Sunitinib. *Chem Res Toxicol* (2018) 31:570–84. doi: 10.1021/acs.chemrestox.8b00005
13. Zhang J, Salminen A, Yang X, Luo Y, Wu Q, White M, et al. Effects of 31 FDA Approved Small-Molecule Kinase Inhibitors on Isolated Rat Liver Mitochondria. *Arch Toxicol* (2017) 91:2921–38. doi: 10.1007/s00204-016-1918-1
14. Mingard C, Paech F, Bouitbir J, Krähenbühl S. Mechanisms of Toxicity Associated With Six Tyrosine Kinase Inhibitors in Human Hepatocyte Cell Lines. *J Appl Toxicol* (2018) 38:418–31. doi: 10.1002/jat.3551
15. Zhang J, Ren L, Yang X, White M, Greenhaw J, Harris T, et al. Cytotoxicity of 34 FDA Approved Small-Molecule Kinase Inhibitors in Primary Rat and Human Hepatocytes. *Toxicol Lett* (2018) 291:138–48. doi: 10.1016/j.toxlet.2018.04.010
16. Yan H, Du J, Chen X, Yang B, He Q, Yang X, et al. ROS-Dependent DNA Damage Contributes to Crizotinib-Induced Hepatotoxicity via the Apoptotic Pathway. *Toxicol Appl Pharmacol* (2019) 383:114768. doi: 10.1016/j.taap.2019.114768
17. Paech F, Abegg VF, Duthaler U, Terracciano L, Bouitbir J, Krähenbühl S. Sunitinib Induces Hepatocyte Mitochondrial Damage and Apoptosis in Mice. *Toxicology* (2018) 409:13–23. doi: 10.1016/j.tox.2018.07.009
18. Paludetto MN, Bijani C, Puisset F, Bernardes-Génisson V, Arellano C, Robert A. Metalloporphyrin-Catalyzed Oxidation of Sunitinib and Pazopanib, Two Anticancer Tyrosine Kinase Inhibitors: Evidence for New Potentially Toxic Metabolites. *J Med Chem* (2018) 61:7849–60. doi: 10.1021/acs.jmedchem.8b00812
19. Paech F, Bouitbir J, Krähenbühl S. Hepatocellular Toxicity Associated With Tyrosine Kinase Inhibitors: Mitochondrial Damage and Inhibition of Glycolysis. *Front Pharmacol* (2017) 8:367. doi: 10.3389/fphar.2017.00367
20. Gul M, Demircan B, Taysi S, Oztasan N, Gumustekin K, Siktar E, et al. Effects of Endurance Training and Acute Exhaustive Exercise on Antioxidant Defense Mechanisms in Rat Heart. *Comp Biochem Physiol A Mol Integr Physiol* (2006) 143:239–45. doi: 10.1016/j.cbpa.2005.12.001
21. Gumustekin K, Taysi S, Alp HH, Aktas O, Oztasan N, Akcay F, et al. Vitamin E and Hippophea Rhamnoides L. Extract Reduce Nicotine-Induced Oxidative Stress in Rat Heart. *Cell Biochem Funct* (2010) 28:329–33. doi: 10.1002/cbf.1663
22. Xue T, Luo P, Zhu H, Zhao Y, Wu H, Gai R, et al. Oxidative Stress is Involved in Dasatinib-Induced Apoptosis in Rat Primary Hepatocytes. *Toxicol Appl Pharmacol* (2012) 261:280–91. doi: 10.1016/j.taap.2012.04.010
23. Hartmann JT, Haap M, Kopp HG, Lipp HP. Tyrosine Kinase Inhibitors - a Review on Pharmacology, Metabolism and Side Effects. *Curr Drug Metab* (2009) 10:470–81. doi: 10.2174/138920009788897975
24. Weng Z, Luo Y, Yang X, Greenhaw JJ, Li H, Xie L, et al. Regorafenib Impairs Mitochondrial Functions, Activates AMP-Activated Protein Kinase, Induces Autophagy, and Causes Rat Hepatocyte Necrosis. *Toxicology* (2015) 327:10–21. doi: 10.1016/j.tox.2014.11.002
25. Josephs DH, Fisher DS, Spicer J, Flanagan RJ. Clinical Pharmacokinetics of Tyrosine Kinase Inhibitors: Implications for Therapeutic Drug Monitoring. *Ther Drug Monit* (2013) 35:562–87. doi: 10.1097/FTD.0b013e318292b931
26. Shi Q, Yang X, Ren L, Mattes WB. Recent Advances in Understanding the Hepatotoxicity Associated With Protein Kinase Inhibitors. *Expert Opin Drug Metab Toxicol* (2020) 16:217–26. doi: 10.1080/17425255.2020.1727886
27. Kreitman K, Nair SP, Kothadia JP. Successful Treatment of Crizotinib-Induced Fulminant Liver Failure: A Case Report and Review of Literature. *Case Rep Hepatol* (2020) 2020:8247960. doi: 10.1155/2020/8247960
28. Duarte FA, Rodrigues LB, Paes FR, Diniz PHC, Lima H. Successful Treatment With Alectinib After Crizotinib-Induced Hepatitis in ALK-Rearranged Advanced Lung Cancer Patient: A Case Report. *BMC Pulm Med* (2021) 21:43. doi: 10.1186/s12890-020-01390-6
29. Aqsa A, Droubi S, Amarnath S, Al-Moussawi H, Abergel J. Sunitinib-Induced Acute Liver Failure. *Case Rep Gastroenterol* (2021) 15:17–21. doi: 10.1159/000511249
30. Jung D, Han JM, Yee J, Kim JY, Gwak HS. Factors Affecting Crizotinib-Induced Hepatotoxicity in Non-Small Cell Lung Cancer Patients. *Med Oncol* (2018) 35:154. doi: 10.1007/s12032-018-1213-5
31. Kamalian L, Chadwick AE, Bayliss M, French NS, Monshouwer M, Snoeys J, et al. The Utility of HepG2 Cells to Identify Direct Mitochondrial Dysfunction in the Absence of Cell Death. *Toxicol In Vitro* (2015) 29:732–40. doi: 10.1016/j.tiv.2015.02.011
32. Brecht K, Riebel V, Couttet P, Paech F, Wolf A, Chibout SD, et al. Mechanistic Insights Into Selective Killing of OXPHOS-Dependent Cancer Cells by Arctigenin. *Toxicol In Vitro* (2017) 40:55–65. doi: 10.1016/j.tiv.2016.12.001
33. Rachek LI, Yuzefovych LV, Ledoux SP, Julie NL, Wilson GL. Troglitazone, But Not Rosiglitazone, Damages Mitochondrial DNA and Induces Mitochondrial Dysfunction and Cell Death in Human Hepatocytes. *Toxicol Appl Pharmacol* (2009) 240:348–54. doi: 10.1016/j.taap.2009.07.021
34. Yang X, Chao X, Wang ZT, Ding WX. The End of RIPK1-RIPK3-MLKL-Mediated Necroptosis in Acetaminophen-Induced Hepatotoxicity? *Hepatology* (2016) 64:311–2. doi: 10.1002/hep.28263
35. Guo L, Gong H, Tang TL, Zhang BK, Zhang LY, Yan M. Crizotinib and Sunitinib Induce Hepatotoxicity and Mitochondrial Apoptosis in L02 Cells *via* ROS and Nrf2 Signaling Pathway. *Front Pharmacol* (2021) 12:620934. doi: 10.3389/fphar.2021.620934

36. Krueger A, Baumann S, Krammer PH, Kirchhoff S. FLICE-Inhibitory Proteins: Regulators of Death Receptor-Mediated Apoptosis. *Mol Cell Biol* (2001) 21:8247–54. doi: 10.1128/MCB.21.24.8247-8254.2001
37. Walensky LD. BCL-2 in the Crosshairs: Tipping the Balance of Life and Death. *Cell Death Differ* (2006) 13:1339–50. doi: 10.1038/sj.cdd.4401992
38. Ho WP, Chan WP, Hsieh MS, Chen RM. Runx2-Mediated Bcl-2 Gene Expression Contributes to Nitric Oxide Protection Against Hydrogen Peroxide-Induced Osteoblast Apoptosis. *J Cell Biochem* (2009) 108:1084–93. doi: 10.1002/jcb.22338
39. Will Y, Dykens JA, Nadanaciva S, Hirakawa B, Jamieson J, Marroquin LD, et al. Effect of the Multitargeted Tyrosine Kinase Inhibitors Imatinib, Dasatinib, Sunitinib, and Sorafenib on Mitochondrial Function in Isolated Rat Heart Mitochondria and H9c2 Cells. *Toxicol Sci* (2008) 106:153–61. doi: 10.1093/toxsci/kfn157
40. Porceddu M, Buron N, Roussel C, Labbe G, Fromenty B, Borgne-Sanchez A. Prediction of Liver Injury Induced by Chemicals in Human With a Multiparametric Assay on Isolated Mouse Liver Mitochondria. *Toxicol Sci* (2012) 129:332–45. doi: 10.1093/toxsci/kfs197
41. Pavlakou P, Liakopoulos V, Eleftheriadis T, Mitsis M, Dounousi E. Oxidative Stress and Acute Kidney Injury in Critical Illness: Pathophysiologic Mechanisms-Biomarkers-Interventions, and Future Perspectives. *Oxid Med Cell Longev* (2017) 2017:6193694. doi: 10.1155/2017/6193694
42. Lv H, Zhu C, Wei W, Lv X, Yu Q, Deng X, et al. Enhanced Keap1-Nrf2/Trx-1 Axis by Daphnetin Protects Against Oxidative Stress-Driven Hepatotoxicity via Inhibiting ASK1/JNK and Txnip/NLRP3 Inflammasome Activation. *Phytomedicine* (2020) 71:153241. doi: 10.1016/j.phymed.2020.153241
43. Yang X, Wang J, Dai J, Shao J, Ma J, Chen C, et al. Autophagy Protects Against Dasatinib-Induced Hepatotoxicity *via* P38 Signaling. *Oncotarget* (2015) 6:6203–17. doi: 10.18632/oncotarget.3357
44. Lu MC, Ji JA, Jiang ZY, You QD. The Keap1-Nrf2-ARE Pathway As a Potential Preventive and Therapeutic Target: An Update. *Med Res Rev* (2016) 36:924–63. doi: 10.1002/med.21396
45. Chan K, Han XD, Kan YW. An Important Function of Nrf2 in Combating Oxidative Stress: Detoxification of Acetaminophen. *Proc Natl Acad Sci USA* (2001) 98:4611–6. doi: 10.1073/pnas.081082098
46. Keum YS, Choi BY. Molecular and Chemical Regulation of the Keap1-Nrf2 Signaling Pathway. *Molecules* (2014) 19:10074–89. doi: 10.3390/molecules190710074
47. Saw CL, Guo Y, Yang AY, Paredes-Gonzalez X, Ramirez C, Pung D, et al. The Berry Constituents Quercetin, Kaempferol, and Pterostilbene Synergistically Attenuate Reactive Oxygen Species: Involvement of the Nrf2-ARE Signaling Pathway. *Food Chem Toxicol* (2014) 72:303–11. doi: 10.1016/j.fct.2014.07.038
48. Lee BW, Jeon BS, Yoon BI. Exogenous Recombinant Human Thioredoxin-1 Prevents Acetaminophen-Induced Liver Injury by Scavenging Oxidative Stressors, Restoring the Thioredoxin-1 System and Inhibiting Receptor Interacting Protein-3 Overexpression. *J Appl Toxicol* (2018) 38:1008–17. doi: 10.1002/jat.3609
49. Li L, Huang W, Wang S, Sun K, Zhang W, Ding Y, et al. Astragaloside IV Attenuates Acetaminophen-Induced Liver Injuries in Mice by Activating the Nrf2 Signaling Pathway. *Molecules* (2018) 23(8):2032. doi: 10.3390/molecules23082032

Conflict of Interest: The authors declare that the research was conducted in the absence of any commercial or financial relationships that could be construed as a potential conflict of interest.

frontiers in Oncology

REVIEW
published: 10 February 2022
doi: 10.3389/fonc.2022.804212

Mechanism of Lethal Skin Toxicities Induced by Epidermal Growth Factor Receptor Inhibitors and Related Treatment Strategies

*Yanping Li†, Ruoqiu Fu†, Tingting Jiang, Dongyu Duan, Yuanlin Wu, Chen Li, Ziwei Li, Rui Ni, Li Li and Yao Liu**

Department of Pharmacy, Daping Hospital, Army Medical University, Chongqing, China

Epidermal growth factor receptor (EGFR) inhibitors are widely used to treat various types of cancers such as non-small cell lung cancer, head and neck cancer, breast cancer, pancreatic cancer. Adverse reactions such as skin toxicity, interstitial lung disease, hepatotoxicity, ocular toxicity, hypomagnesemia, stomatitis, and diarrhea may occur during treatment. Because the EGFR signaling pathway is important for maintaining normal physiological skin function. Adverse skin reactions occurred in up to 90% of cancer patients treated with EGFR inhibitors, including common skin toxicities (such as papulopustular exanthemas, paronychia, hair changes) and rare fatal skin toxicities (e.g., Stevens–Johnson syndrome, toxic epidermal necrolysis, acute generalized exanthematous pustulosis). This has led to the dose reduction or discontinuation of EGFR inhibitors in the treatment of cancer. Recently, progress has been made about research on the skin toxicity of EGFR inhibitors. Here, we summarize the mechanism of skin toxicity caused by EGFR inhibitors, measures to prevent severe fatal skin toxicity, and provide reference for medical staff how to give care and treatment after adverse skin reactions.

Keywords: EGFR inhibitors, lethal skin toxicities, drug induced disease, treatment strategies, preventive measures

OPEN ACCESS

Edited by:
Husain Yar Khan, Wayne State University, United States

Reviewed by:
Valentina Audrito, University of Turin, Italy
Marcelo Sobral-Leite, The Netherlands Cancer Institute (NKI), Netherlands

***Correspondence:**
Yao Liu
swhliuyao@163.com

†These authors have contributed equally to this work and share first authorship

Specialty section:
This article was submitted to Pharmacology of Anti-Cancer Drugs, a section of the journal Frontiers in Oncology

Received: *29 October 2021*
Accepted: *17 January 2022*
Published: *10 February 2022*

Citation:
Li Y, Fu R, Jiang T, Duan D, Wu Y, Li C, Li Z, Ni R, Li L and Liu Y (2022) Mechanism of Lethal Skin Toxicities Induced by Epidermal Growth Factor Receptor Inhibitors and Related Treatment Strategies. Front. Oncol. 12:804212. doi: 10.3389/fonc.2022.804212

INTRODUCTION

The epidermal growth factor receptor (EGFR, also named HER1) is a 170 kDa transmembrane glycoprotein receptor that is coded by the c-erbB1 proto-oncogene located on the human 7q22 chromosome (1). Asparagine-linked glycosylation is a post-translational modification necessary for its active function (2). EGFR is a member of the ErbB receptor family of tyrosine protein kinases, which also includes ErbB-2 (HER2), ErbB-3 (HER3), and ErbB-4 (HER4) (3). EGFR is highly expressed in lung cancer (4), breast cancer, human glioblastoma (5), gastric carcinoma (3), rectal cancer, and head and neck cancer (6) compared to healthy tissues. The EGFR signaling pathway is involved in normal biological processes of cells, and the destruction of the dynamic balance will lead to pathological changes in healthy tissues. Overexpression of EGFR promotes cell proliferation, adhesion, metastasis, and angiogenesis and inhibits apoptosis, all of which can induce tumorigenesis (7). Therefore, EGFR inhibitors have been utilized for cancer treatment.

EGFR inhibitors are divided into monoclonal antibodies (mAb) and small molecule intracellular tyrosine kinase inhibitors (TKIs). EGFR mAb competitively inhibit ligand binding to EGFR extracellular domain with higher affinity than ligand to reduce EGFR signaling pathway activity (8). The small molecule EGFR-TKIs are ATP analogs that competitively bind to the intracellular catalytic domain of EGFR, which blocks ATP-mediated phosphorylation (9). Although EGFR inhibitors have good efficacy for a variety of tumors, adverse reactions such as skin toxicity, interstitial lung disease, hepatotoxicity, ocular toxicity, hypomagnesemia, stomatitis, and diarrhea may occur during treatment (10). These adverse reactions lead to organ, tissue, and system damage, resulting in corresponding drug induced diseases. Finally reduce patient compliance and even lead to the withdrawal of antitumor drugs. Skin toxicities is one of the most common adverse reactions caused by EGFR inhibitors

These skin toxicities may result in fatal complications if they are ignored (11). Doctors, pharmacists, and nurses must consider how to avoid severe skin toxicity in their patients and determine which patients would be prone to fatal skin toxicity. Understanding the molecular and cellular mechanism of skin toxicity and the relationship between skin toxicity and drug efficacy is essential for safe, effective, and rational use of EGFR inhibitors. Here, we focus on the mechanism of skin toxicity and fatal skin toxicity caused by EGFR inhibitors and clinical countermeasures as a mean to alleviate adverse reactions and ultimately achieve the purpose of reducing adverse emotions of the patients during the treatment phase, improving medication compliance, and effectively treating related cancers.

ACTIVATION MECHANISM OF EGFR SIGNALING PATHWAY

The four members of the human ErbB family have similar structures that are divided into the extracellular domain, transmembrane domain, cytoplasmic domain, and C-terminal tail domain (3). Mature EGFR consists of 1186 amino acid residues and is divided into three parts from N-terminal to C-terminal: extracellular domain (621 amino acids), hydrophobic lipophilic short transmembrane domain (23 amino acids), and cytoplasmic domain (542 amino acids) (**Figure 1**).

The extracellular region of EGFR can be subdivided into four domains: I, II, III, and IV. Domains I (amino acids 1-133, exons 1-4) and III (amino acids 313-445, exons 8-12) are rich in leucine and are the main fragments involved in ligand binding in the extracellular domain (7). Domains II (amino acids 134-312, exons 5-7) and IV (amino acids 446-621, exons 13-16) contain 51 cysteine residues and are not involved in ligand binding. However, domain II is involved in the formation of homodimers and heterodimers with other members of the ErbB family (7, 12, 13).

The specific ligands of EGFR include epidermal growth factor (EGF), transforming growth factor-α, and amphiregulin, while non-specific ligands include epiregulin, betacellulin, heparin binding EGF-like growth factor, and epiregulin (14, 15). EGF, the ligand of EGFR, was first isolated from the mouse submandibular gland and is associated with epidermal proliferation and keratinization (16). Asparagine-linked glycosylation is a post-translational modification necessary for functional EGFR, and the extracellular domain of EGFR contains 12 sites for asparagine-linked glycosylation (2, 12). The transmembrane domain of EGFR (amino acids 622-644, exon 17) serves to link the two functional domains of the extracellular and cytoplasmic domains (13). The cytoplasmic domain of EGFR (amino acids 645-1186, exons 18-28) includes a tyrosine kinase domain (exons 18-24) and C-terminal tail (exons 25-28). The tyrosine kinase domain can be subdivided into the N-lobe and C-lobe. ATP binds to the gap formed by the two lobes. EGFR-TKIs inhibit the activation of tyrosine kinase and subsequent signaling pathways by competitively binding the ATP-binding site of the tyrosine kinase domain (17–19).

EGFR is activated in four phases (7, 20–22) (**Figure 2**): 1) The ligand binds to the extracellular domain of EGFR; 2) Homodimerization or heterodimerization with ErbB-2, ErbB-3, and ErbB-4 (also known as HER-2, HER-3, and HER-4, respectively) occurs. ErbB-2 is the most common

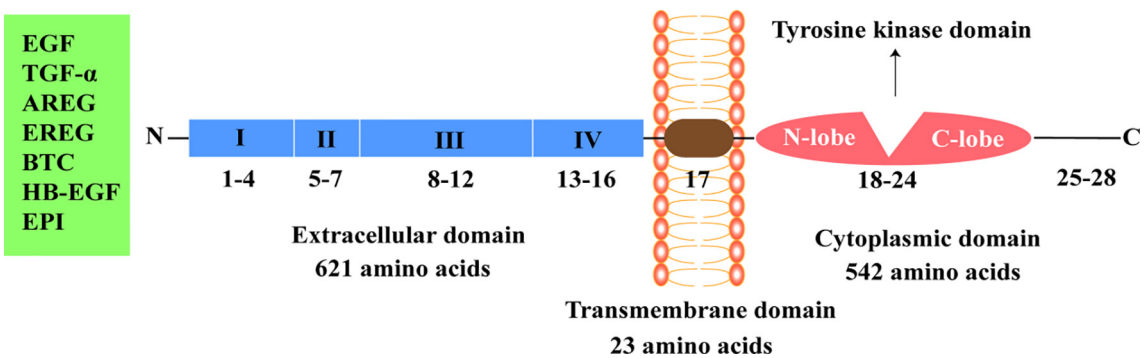

FIGURE 1 | Epidermal growth factor receptor structure. EGF, epidermal growth factor; TGF-α, transforming growth factor-α; AREG, amphiregulin; EREG, epiregulin; BTC, betacellulin; HB-EGF, heparin binding epidermal growth factor-like growth factor; EPI, epiregulin.

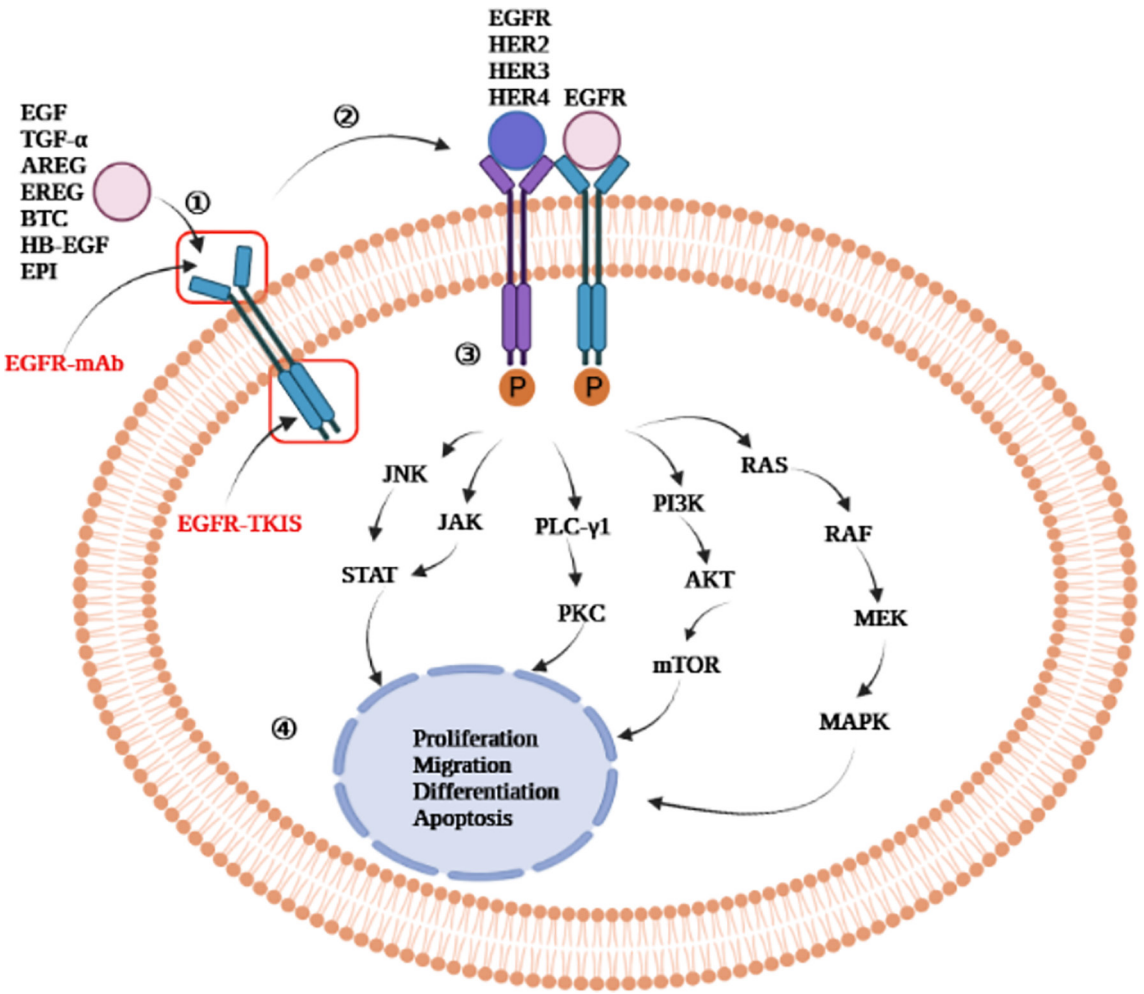

FIGURE 2 | Epidermal growth factor receptor activation mechanism. EGFR-mAb: Cetuximab, panitumumab, zalutumumab, nimotuzumab; EGFR-TKIs: gefitinib, erlotinib, lapatinib, icotinib, neratinib, dacomitinib, afatinib, olmutinib, osimertinib, furmonertinib mesylate, brigatinib; JNK, jun amino-terminal kinase; JAK, janus activated kinase; STAT, signal transducer and activator of transcription; PLC-γ1, phospholipase C-γ1; PKC, protein kinase C; MAPK, mitogen-activated protein kinase; PI3K, phosphatidylinositol-3- kinase; mTOR, mammalian target of rapamycin; AKT, protein kinase B; RAS, rat sarcoma virus gene homolog; RAF, rapidly accelerated fibrosarcoma serine/threonine kinase; MEK, mitogen-activated protein kinase kinase; ERK, extracellular signal-regulated kinase; EGF, epidermal growth factor; TGF-α, transforming growth factor-α; AREG, amphiregulin; EREG, epiregulin; BTC, betacellulin; HB-EGF, heparin binding epidermal growth factor-like growth factor; EPI, epiregulin; EGFR, epidermal growth factor receptor; HER, human epidermal growth factor receptor; mAb, monoclonal antibody; TKIs, tyrosine kinase inhibitors.

heterodimerization partners of EGFR; 3) Autophosphorylation of tyrosine residues in the cytoplasmic domain occurs; 4) The activation of the intracellular signaling pathway occurs, which regulates cell proliferation, migration, differentiation, and apoptosis.

EGFR INHIBITORS USED CLINICALLY

At present, there are four generations of EGFR-TKIs (**Table 1**) and multiple EGFR-mAbs (**Table 2**) that have been developed, such as cetuximab, panitumumab, zalutumumab, and nimotuzumab. The chemical formula of EGFR-TKIs for clinical use is shown in **Figure 3**.

The first-generation EGFR-TKIs includes gefitinib, erlotinib, lapatinib, and icotinib. Gefitinib was the first agent designed to receive approval from the United States Food and Drug Administration (FDA) for the treatment of lung cancer (62, 63). Gefitinib was considered to be safe and effective for adjuvant treatment of operable stage II-IIIA non-small cell lung cancer (NSCLC) in addition to the treatment of conventional mutated NSCLC (64, 65). Seong et al. (28) reported a rare case of necrolytic migratory erythema during the use of gefitinib. Gefitinib has also been reported to cause fatal skin toxicity such as toxic epidermal necrolysis (TEN) (26) and acute generalized exanthematous pustulosis (AGEP) (25). Although gefitinib shows excellent antitumor effects, it was eventually

TABLE 1 | Clinically used EGFR-TKIs.

Classification	Molecular mechanism	Drug name	Targets	Clinical application	Severe skin toxicity (reference)
First generation EGFR-TKIs	The first generation EGFR-TKIs can reversibly inhibit EGFR phosphorylation by competitive binding of tyrosine kinase catalytic structure with ATP through noncovalent bonds (23)	Gefitinib (ZD1839)	EGFR	NSCLC (24)	AGEP (25); TEN (26, 27); NME (28)
		Erlotinib (CP-358774)	EGFR; EGFR (del19); EGFR (L858R)	NSCLC; Pancreatic cancer (29)	SJS (30); TEN (31); AGEP (32)
		Lapatinib (GW572016)	EGFR; HER2	Breast cancer (33)	AGEP (34)
		Icotinib (BPI-2009)	EGFR (T790M); EGFR (L858R); EGFR (L861Q)	NSCLC (35)	DIHS (35)
Second generation EGFR-TKIs	The second generation of EGFR-TKIs irreversibly inhibits multiple ErbB receptors by competitively binding to the tyrosine kinase catalytic domain with ATP *via* a covalent bond (36)	Neratinib (HKI-272)	EGFR; HER2; HER4	Breast cancer (37)	
		Dacomitinib (PF-00299804)	EGFR; EGFR (del19); EGFR (L858R); HER2; HER4 (38);	NSCLC (24)	
		Afatinib (BIBW 2992)	EGFR; EGFR (L858R); HER2; HER4	NSCLC (39)	SJS (40); DIHS (41); SJS/TEN (42); SJS (39)
Third generation EGFR-TKIs	The third generation of EGFR-TKIs covalently binds to the ATP-binding site, CYS797, of the EGFR tyrosine kinase domain (43, 44)	Olmutinib (HM61713/ BI1482694)	EGFR; EGFR (del19); EGFR (L858R); EGFR (T790M)	NSCLC (45)	SJS/TEN (45)
		Osimertinib (AZD9291)	EGFR; EGFR (del19); EGFR (L858R); EGFR (T790M)	NSCLC (46)	SJS (47); TEN (48)
		Furmonertinib mesylate (AST2818)	EGFR (del19); EGFR (L858R); EGFR (T790M)	NSCLC (49)	
Fourth generation EGFR-TKIs	The fourth generation of EGFR-TKIs irreversibly binds to the ATP binding pocket of C797S/T790M/activating mutation (triple mutation) of EGFR (50)	Brigatinib (AP26113)	EGFR; ALK; ROS1; IGF-1R; FLT-3	ALK-positive NSCLC (51)	

Del19, exon 19 deletion; L858R, exon 21 mutations; T790M, mutation of the 790th amino acid threonine of EGFR to methionine; C797S, cysteine is replaced by serine at position 797; EGFR, epidermal growth factor receptor; TKIs, tyrosine kinase inhibitors; NSCLC, non-small cell lung cancer; AGEP, acute generalized exanthematous pustulosis; TEN, toxic epidermal necrolysis; NME, necrolytic migratory erythema; SJS, Stevens-Johnson syndrome; HER, human epidermal growth factor receptor; DIHS, drug-induced hypersensitivity syndrome; ALK, anaplastic lymphoma kinase; IGF-1R, insulin-like growth factor-1 receptor; FLT-3, fms-like tyrosine kinase 3; Ig, immunoglobulin; mCRC, metastatic colorectal cancer.

discontinued due to these severe skin toxicities. Erlotinib, a derivative of quinazoline was approved by the FDA on November 18, 2004 for use in NSCLC with exon 19 deletion (del19) or exon 21 point mutation (L858R) (66). Erlotinib often causes papulopustular exanthemas characterized by pruritus (67). Lapatinib (GW572016) is an ATP-competitive, reversible small-molecule inhibitor of ErbB-2 and EGFR tyrosine kinases that has been approved for the treatment of patients with metastatic breast cancer (68–71).

The mutation of amino acid 790 from threonine to methionine (T790M) increases the affinity of EGFR for ATP, which competitively reduces the efficacy of EGFR-TKIs. Therefore, EGFR (T790M) is one of the reasons for resistance to first-generation EGFR-TKIs (68, 72). In order to overcome

TABLE 2 | Clinically used EGFR-mAbs.

Classification	Molecular mechanism	Drug name	Targets	Clinical application	Severe skin toxicity (reference)
EGFR-mAb	Cetuximab is a chimeric IgG1 mAb that competes with endogenous ligands to bind to the extracellular domain of EGFR (52)	Cetuximab (IMC-C225)	EGFR	Head and neck cancer (52); mCRC (53)	SJS (25) TEN (54)
	Panitumumab is a fully human IgG2 mAb that competitively inhibits endogenous ligand binding to the extracellular domain of EGFR (55)	Panitumumab (ABX-EGF)	EGFR	mCRC (55)	SJS (56)
	Zalutumumab is a fully human IgG1 mAb that targets the ligand-binding extracellular domain III of EGFR (57)	Zalutumumab (HuMax-EGFr)	EGFR	HNSCC (58)	
	Nimotuzumab is a humanized IgG1 mAb that competitively binds to the extracellular domain III (amino acids 353-358) of EGFR with ligands (59, 60)	Nimotuzumab (h-R3)	EGFR	HNSCC (53) NPC (61)	

EGFR, epidermal growth factor receptor; mAb, monoclonal antibody; SJS, stevens-Johnson syndrome; TEN, toxic epidermal necrolysis; Ig, immunoglobulin; mCRC, metastatic colorectal cancer; HNSCC, head and neck squamous cell carcinoma; NPC, nasopharyngeal carcinoma.

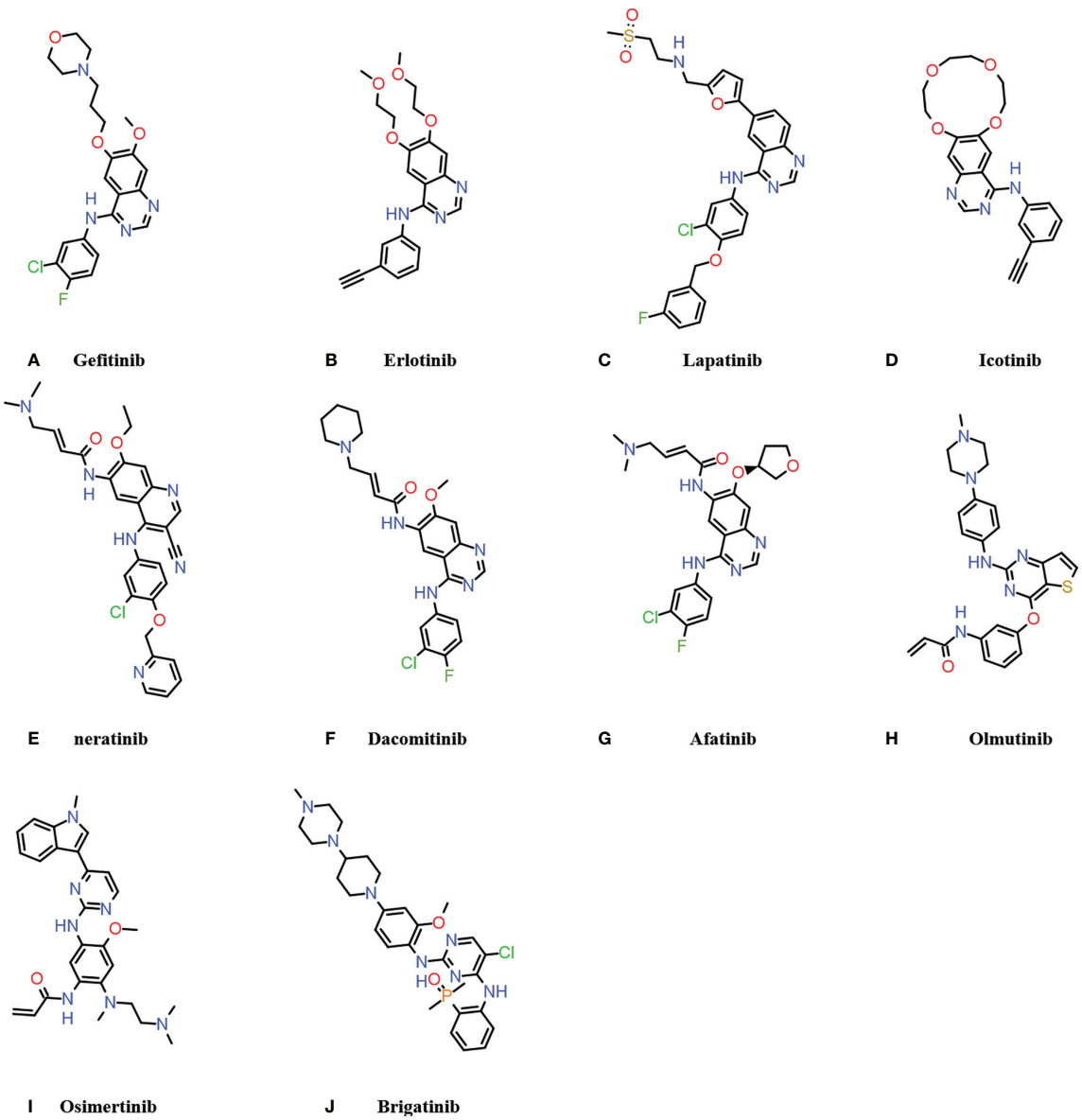

FIGURE 3 | Chemical formula of clinically used EGFR-TKIs. **(A–D)** are the first generation EGFR-TKIs; **(E–G)** are the second generation EGFR-TKIs; **(H, I)** are the third generation EGFR-TKIs; **(J)** is the fourth generation EGFR-TKIs.

drug resistance, the second-generation EGFR-TKIs, afatinib and dacomitinib, were developed (73). Dacomitinib was approved by the FDA on September 27, 2018 for the treatment of NSCLC patients with EGFR del19 or exon 21 L858R mutations (73). However, second-generation EGFR-TKIs were not able to be administered at full strength to inhibit T790M mutant lung cancer due to adverse side effects, such as rash caused by inhibition of normal cells (23). Ding et al. (74) concluded in a meta-analysis of clinical trials that afatinib resulted in a higher risk of rash than erlotinib or gefitinib.

In order to overcome the resistance of first and second-generation EGFR-TKIs, the third-generation EGFR-TKIs were developed. Osimertinib was approved by the FDA in 2015 to treat NSCLC patients with the EGFR T790M mutation (75, 76). In March 2021, furmonertinib mesylate was first approved in China for the treatment NSCLC patients with the EGFR T790M mutation (49). Osimertinib is no longer the only third generation EGFR-TKIs approved for the treatment of EGFR T790M mutant NSCLC. However, during the application of the third-generation EGFR-TKIs, a cysteine-to-serine mutation (C797S) occurred at C797 in the kinase binding site. The C797S mutation blocks the formation of a covalent bond at 797, which ultimately reduced the efficacy of the third-generation EGFR-TKIs (77, 78).

EGFR C797S is the most common tertiary mutation in patients with T790M-positive NSCLC treated with third-generation EGFR-TKI osimertinib. In order to overcome the EGFR C797S mutation, brigatinib was developed as a fourth-generation EGFR-TKI. It is effective against the EGFR C797S-T790M-del19 triple mutant (79). Brigatinib received approval for the treatment of anaplastic lymphoma kinase-positive metastatic NSCLC patients who had progressive disease while taking crizotinib or who were intolerant to crizotinib (80).

CELLULAR AND MOLECULAR MECHANISM OF SKIN TOXICITY CAUSED BY EGFR INHIBITORS

Skin is the first line of defense against the invasion of external pathogens. Skin structure from the outside to the inside is the epidermis, dermis, and subcutaneous tissue. The skin contains accessory organs such as nails, sebaceous glands, sweat glands, hair follicles, cutaneous nerves, and subcutaneous blood vessels. EGFR is widely expressed in skin keratinocytes, dendritic cells, connective tissue cells, and skin appendage organelles (e.g. sebaceous glands, sweat glands, and hair follicles) and associated with proliferation, apoptosis, migration, and differentiation of normal cells (81–84). Normal activation of EGFR signaling promotes wound healing, inhibits inflammation, and stimulates capillary constriction (85).

EGFR is widely distributed in the skin, and skin toxicity is one of the most common adverse reactions for EGFR inhibitor treatment. EGFR-mAbs generally produce more severe skin toxicity than EGFR-TKIs (14). Rare purpuric drug eruptions have been reported when using EGFR-TKIs such as gefitinib, erlotinib and afatinib. The main clinical manifestations are purpuric macules, papules, and confluent plaques on the lower extremities. These adverse side effects occur because blocking EGFR leads to endothelial inflammation, decreased vascular tone, and ultimately increased vascular permeability (86). Besides the common rash, rare severe lethal skin toxicities from EGFR inhibitors, such as Stevens-Johnson syndrome (SJS), TEN, and AGEP, are often important causes of drug discontinuation. SJS (10% mortality) and TEN (50% mortality) are two related skin and mucosal diseases caused by delayed drug hypersensitivity. They are characterized by extensive epidermal necrosis and skin detachment (the range of detached surface area:SJS < 10%, TEN > 30%, and SJS/TEN = 10%-30%) (87, 88). AGEP is characterized by the formation of sterile non-follicular pustules on the base of the erythema, often accompanied by neutrophilia and fever, which can involve multiple organs in severe cases and may be life-threatening in approximately 4% of patients (25, 89).

Because EGFR homodimers are typically associated with normal skin tissue and primary keratinocytes (90), it is speculated that EGFR inhibitors block activation of EGFR due to the inability of EGFR to homodimerize. Therefore, skin toxicity in normal cells occurs. However, the pathophysiology and mechanisms of skin toxicity caused by EGFR inhibitors have not been fully elucidated. We explain the causes of skin toxicity caused by EGFR inhibitors from the following four aspects: destruction of the physical barrier of the skin by damage to the epidermal layer, damage of hair follicles, destruction of skin homeostasis, inflammation, and host immune activation, and radiotherapy.

Destruction of the Physical Barrier of the Skin by Damage to the Epidermal Layer

Keratinocytes stratify into enucleated flattened surface squames to form a skin barrier that moisturizes and isolates pathogens. The barrier is maintained by the precise proliferation and differentiation of keratinocytes (91, 92). EGF promotes keratinocyte proliferation by increasing Ki67 and filaggrin expression through the rapidly accelerated fibrosarcoma serine/threonine kinase/mitogen-activated protein kinase kinase/extracellular signal-regulated kinase signaling pathway (93). In addition, EGFR regulates the terminal differentiation of keratinocytes through the phospholipase C-γ1-protein kinase C pathway to maintain and continuously regenerate the epidermal barrier (94). EGFR inhibitors can lead to destruction of physical and immune balance barriers in the epidermis, which results in skin toxicity such as dryness and rashes (93). Claudins, as essential components for the formation of tight junctions, are critical for maintaining the normal skin barrier (95). Fang et al. (96) found that gefitinib may damage the skin barrier by reducing claudin-1 and claudin-4 and increasing claudin-2 expression in keratinocytes, resulting in skin toxicity.

The epidermis is composed of five parts: basal layer, spinous layer, granular layer, stratum lucidum, and stratum corneum. EGFR is abundant in keratinocytes in the basal layer of the epidermis (97). Upon separation of proliferating basal keratinocytes from the basement membrane, they cross the spinous and granular layers and enter the stratum corneum where they stop proliferating and terminally differentiate. Then, keratinization occurs (98). EGFR inhibitors reduce the expression of the proliferation marker Ki67 suggesting keratinocyte growth arrest and premature differentiation, which ultimately results in abnormal formation and thinning of the stratum corneum (the outermost layer of the epidermis) (99, 100). Moreover, when the EGFR signaling pathway is inhibited, patients become susceptible to pathogenic bacteria, such as *Staphylococcus aureus*. The aggravation of inflammation further inhibits epidermal differentiation and exacerbates keratinocyte damage, leading to the occurrence of eczema-like skin reactions (86). An EGFR knockout model demonstrated that the skin of the mouse became dry and fragile (101). Therefore, EGFR inhibitors damage the natural moisturizing function of the skin and destroy skin homeostasis by damaging the physical barrier of the stratum corneum, leading to dry skin, itching, and rashes.

Damage of Hair Follicles

EGFR is also expressed abundantly in undifferentiated keratinocytes proliferating in the external root sheath of hair follicles (102). Treatment with EGFR inhibitors induces secretion of pro-

inflammatory factors and lymphocyte infiltration, which leads to folliculitis and hair follicle rupture as the disease progresses (85, 103). Folliculitis is also known as acneiform rash and papulopustular exanthema, and the primary lesions are inflammatory follicular papules and pustules. The histopathology of papulopustular exanthema demonstrates purulent folliculitis with ectatic follicular infundibula and rupture of the epithelial lining. Keratin plugs and microorganisms are seen in the dilated infundibulum (104, 105). EGFR plays an essential role during the hair growth cycle (106). In addition, *in vitro* studies have shown that the concentration of EGF regulates the conversion between hair follicle growth and inhibition (107). Some studies have also confirmed that EGFR inhibitors have different effects on hair on different parts of the body. Hair will become brittle, thin, curly, or even be lost, while eyelashes will grow and curl (105, 108, 109).

Destruction of Skin Homeostasis-Inflammation and Host Immune Activation

In human skin, keratinocytes differentiate to provide a physical barrier in the stratum corneum, but they will also secrete various cytokines, chemokines, and antimicrobial peptides to participate in the innate immune response to resist pathogen invasion (110). Park et al. (111) found that the expression of β-defensin, an antimicrobial peptide produced by human symbiotic bacteria, decreased after using EGFR inhibitors leading to bacterial susceptibility. This may be one of the reasons for skin toxicity.

EGFR inhibitors also activate nuclear factor-κB in both cancer and normal cells, leading to destruction of immune balance and an inflammatory microenvironment (21). When EGFR signaling was inhibited, CCL2, CCL5, and CXCL10 expression levels increased and CXCL8 expression level decreased, which increased leukocyte recruitment and inflammatory infiltration (112). Wan et al. (113) induced a skin rash in female Brown Norway rats with gefitinib and found that macrophages infiltrated to the skin and secreted large amounts of inflammatory cytokines such as TREM-1, CINC-2, and CINC-3.

Furthermore, when EGFR inhibitors are used, the expression level of proapoptotic genes (such as secreted frizzled related protein 1, the apoptosis inhibitor survivin, and BCL2 associated athanogene) are upregulated, and the expression level of antiapoptotic genes (such as death associated protein kinase-1 and apoptosis response zinc finger protein requiem) are downregulated (21). The combination of tumor-induced inflammation with iatrogenic apoptotic lysis may be an important factor of associated skin toxicity.

Severe disruption of skin homeostasis induced by microbial susceptibility, inflammatory activation, and increased apoptosis ultimately leads to the generation of cutaneous toxicity.

Radiotherapy

Radiation therapy is often combined with chemotherapy or targeted therapy during tumor therapy, and the duration, dose, and area of radiation have a significant impact on the severity of skin toxicity induced by EGFR inhibitors (114). EGFR inhibitors are associated with an increased risk of severe radiation dermatitis during the first few weeks of radiation therapy when radiation damages epidermal basal cells (115). Radiotherapy and chemotherapy cause the release of chemoradiation associated molecular patterns. They play an integral role in the generation of inflammation, which causes adverse skin reactions from EGFR inhibitors more severe and complex (116). In addition, skin xerosis caused by cetuximab may aggravate dermatitis caused by radiotherapy (117).

FACTORS LEADING TO FATAL SKIN TOXICITY

Severe and fatal skin toxicities occur in only a small number of patients treated with EGFR inhibitors, but the pathogenic mechanism remains unclear. Le-Rademacher et al. (118) found that androgens may mediate adverse skin reactions caused by EGFR inhibitors, and anti-androgen therapy may be a method to treat or alleviate skin toxicity. Another study showed that patients with high sebaceous gland activity and sebum secretion were more sensitive to EGFR inhibitors and developed acneiform rash more frequently (119). Takahashi et al. (120) also found that men and high-weight patients who used EGFR inhibitors were more susceptible to severe skin toxicity. High male hormones, high sebum secretion, and smoking (more prevalent in males than females) are risk factors causing male lung cancer patients to have more severe adverse skin reactions.

Other risk factors leading to skin toxicity after EGFR-TKI treatment require further investigation. For example, individuals with mutations in interleukin-36 receptor antagonist may be at an increased risk of AGEP development after drug treatment (89). Ethnicity may also be a risk factor. The frequency of EGFR-TKI-associated SJS/TEN is higher in Asian countries than in other regions (121). In addition, sulfonamides, anti-epileptic drugs (carbamazepine, phenytoin, phenobarbital, lamotrigine), nonsteroidal anti-inflammatory drugs of the oxicam type, and allopurinol have been shown to be high-risk drugs for inducing delayed type hypersensitivity SJS/TEN. Therefore, the possible risk of serious adverse effects should be considered when EGFR inhibitors are used in combination with these drugs (122). When more than one susceptibility factor for lethal skin toxicity exists, the treatment of related cancers with EGFR inhibitors should be evaluated early and continuously monitored. The treatment of skin toxicity should be started early to reduce the pain and death risk of patients.

THE RELATIONSHIP BETWEEN SKIN TOXICITY AND ANTICANCER EFFICACY

EGFR is essential for maintaining the development and normal physiological functions of the epidermis in the skin. The main cause of skin toxicity is the targeting effect of anti-tumor drugs on wild-type EGFR. It has been suggested that skin response can be used as a biomarker of EGFR efficacy (123). A review of 116 patients treated with cetuximab and panitumumab by Jaka et al. (124) also confirmed that more severe rashes were associated

with better outcomes. Because of the observed positive correlation of rash with efficacy, studies have suggested a new administration in which the dose is increased until the rash is most tolerable to the patient. The severity of EGFR inhibitor-induced skin toxicity is positively correlated with the therapeutic effect, making related skin toxicity a potential marker for predicting drug efficacy.

Determining how to predict whether a patient will have skin toxicity is an important area of investigation In 2004, Amador et al. (125) found that the number of single sequence repeats in EGFR intron 1 was related to the skin toxicity and anti-tumor activity of EGFR inhibitors. Kimura et al. (126) found that compared with patients who did not show any skin toxicity, the plasma macrophage inflammatory protein level was significantly decreased in patients with skin toxicity, suggesting that macrophage inflammatory protein levels in plasma might be a predictor of dermal toxicity in patients treated with gefitinib. In 2012, Moreno Garcia et al. (127) observed that elevated plasma creatine kinase was associated with EGFR-TKI-induced rash, and *in vitro* experiments showed that the expression level of cytosolic isoforms of creatine kinase-brain increased after EGFR-TKIs stimulated human keratinocytes. Steffens et al. (128) found that patients treated with higher erlotinib/O-demethyl-erlotinib (O-demethyl-erlotinib is the main active metabolite of erlotinib) had longer progression free survival and overall survival. They were also more prone to adverse skin reactions. The occurrence of rash was positively correlated with progression free survival and overall survival. The identification of biomarkers for severe skin toxicity can help doctors to take preventive measures to prevent severe or even fatal skin toxicity in patients. These blood biomarkers can predict drug efficacy or serious skin toxicity earlier than the occurrence of a skin rash, and it is more appropriate to predict the effect of EGFR inhibitors for patients who are not prone to skin toxicity.

Whether the efficacy of all EGFR inhibitors can be measured by skin toxicity is debatable. When applying the less targetable first-generation EGFR-TKIs (e.g., erlotinib, gefitinib, afatinib), the targeted toxicity of the skin may serve as a biomarker to measure anticancer efficacy. However, skin toxicity as an indicator of efficacy is not applicable to all EGFR-TKIs. Osimertinib (third-generation EGFR-TKIs) is typically used for treatment of NSCLC patients with the T790M resistance mutation. It has significantly greater activity against tumor EGFR with mutations del19, L858R, and T790M than wild-type EGFR (129, 130). The incidence of adverse skin reactions is lower with osimertinib than with erlotinib, but it is an effective treatment for NSCLC with T790M mutations. Further investigations are needed because the use of skin toxicity as an indicator of EGFR inhibitor efficacy is incomplete (131).

THERAPEUTIC STRATEGIES FOR SKIN TOXICITY

Up to 90% of cancer patients treated with EGFR inhibitors have skin adverse reactions. Of these, 76% of patients reported that they interrupted the EGFR inhibitor therapy, 32% of patients completely discontinued the EGFR inhibitor therapy, and 60% of patients reduced the dose of the EGFR inhibitor (132, 133). The most common skin toxicity caused by EGFR inhibitors is follicular papulopustular exanthemas, also known as follicular rash. It usually occurs on the head, back, and upper chest in the first few weeks of treatment. The lesions disappear without sequelae upon withdrawal of the EGFR inhibitor (134). Sebostasis, epidermal atrophy, itchy eczema, skin xerosis, paronychia, and changes in hair (such as hair and eyelashes) often occur after 1 to 2 months of treatment (132). In addition, skin toxicity caused by EGFR inhibitors is often accompanied by severe pain and extreme itching causing patients to endure physical pain and psychological stress. The clinical manifestations and basic grades of common skin toxicities (e.g., papulopustular exanthemas, pruritus, xerosis, paronychia, hair changes) caused by EGFR inhibitors are shown in **Table 3**.

Treatment strategies for skin toxicity caused by EGFR inhibitors currently include empirical treatment and expert consensus in countries such as the United Kingdom (141), Germany (142), Taiwan (136), France (143, 144), Italy (145), and Spain (146). These consensuses general principles of treatment about skin toxicities are consistent but differ slightly. They mainly describe treatment strategies for common skin toxicities caused by EGFR inhibitors, but not for fatal skin toxicities. Moreover, most treatments are focused on alleviating symptoms without effective etiological treatment. There is no recognized authoritative guide for the treatment of EGFR inhibitors related skin toxicity. This is an urgent clinical problem that needs to be solved.

Symptomatic Treatment

Papulopustular Exanthemas

When grade 1 rash occurs, the patient can continue to use EGFR inhibitors and to use non-alcoholic emollients (141). Reduction or discontinuation of EGFR inhibitors should be considered when grade 2 rash duration is unmanageable or the patient is unable to tolerate it. EGFR inhibitor therapy should be temporarily discontinued when ≥ grade 3 rash appears (141). Therapeutic measures are shown in more detail in **Table 4**.

Pruritus Due to Papulopustular Exanthemas and Xerosis

Grade 1-2 can be treated with topical steroids (0.05% clobetasol), and oral antihistamines (cetirizine, loratadine, etc.) can be used for grade 3 pruritus. In addition to the drugs mentioned above, gamma-aminobutyric acid agonists, neurokinin-1 receptor antagonists, antidepressants, corticosteroids, and other drugs can be added for treatment (150, 151). However, caution should be taken to avoid systemic steroids as they can have acneiform rash-like side effects (152). However, when a rash of grade ≥ 3 occurs, systemic dexamethasone or prednisolone is usually used for treatment (83).

Once bacterial infection occurs, systemic antibiotics can be selected for treatment based on a drug sensitivity test (153). If local use of metronidazole is not enough to control symptoms of

TABLE 3 | Clinical manifestations and classification of common skin toxicities of EGFR inhibitors.

Common skin toxicities	Clinical manifestations	Grades criteria (NCI-CTCAE v 5.0) (135)
Papulopustular exanthemas	Predominantly occurring on the face back and upper chest within two weeks from the start of EGFR inhibitor treatment; manifests as red papules and/or pustules without comedone (136, 137)	Grade 1: Papules and/or pustules covering <10% BSA, with or without pruritus or tenderness Grade 2: Papules and/or pustules covering 10-30% BSA, with or without symptoms of pruritus or tenderness; with psychosocial impact; limiting instrumental activities of daily living; papules and/or pustules covering >30% BSA but mild symptoms Grade 3: Papules and/or pustules covering >30% BSA, with moderate to severe symptoms; limiting self-care activities of daily living; associated with local superinfection with oral antibiotics indicated Grade 4: Papules and/or pustules covering any % BSA; with unlimited symptoms; associated with extensive superinfection with IV antibiotics indicated; life-threatening consequences Grade 5: Death
Pruritus	A disorder characterized by an intense itching sensation, accompanies the papulopustular exanthemas and xerosis at onset (138)	Grade 1:Mild or localized; topical intervention indicated Grade 2: Intense or widespread; intermittent; skin changes from scratching (e.g., edema, papulation, excoriations, lichenification, oozing/crusts); limiting instrumental activities of daily living Grade 3: Intense or widespread; constant; limiting self-care activities of daily living or sleep; oral corticosteroid or immunosuppressive therapy indicated
Skin Xerosis	Dry skin, often accompanied by pruritus, scaly, flaking skin appears over the extremities, the fingertips and toes may develop dry areas with cracks, or fissures (85, 139)	Grade 1:Covering <10% BSA and no associated erythema or pruritus Grade 2: Covering 10-30% BSA and associated with erythema or pruritus; limiting instrumental activities of daily living Grade 3: Covering >30% BSA and associated with pruritus; limiting self-care activities of daily living
Paronychia	Nail-fold edema or erythema, damaged skin around nail, disruption of the cuticle, nail-plate separation, granulation tissue formation (140)	Grade 1: Nail fold edema or erythema; disruption of the cuticle. Grade 2: Nail fold edema or erythema with pain; associated with discharge or nail plate separation; limits instrumental activities of daily living; topical or oral anti-infective therapy indicated Grade 3: Surgical intervention or intravenous antibiotic treatment indicated; limits self-care activities of daily living
Hair changes	Hair become brittle, thin, curly, or even be lost, eyelashes grow and curl (85, 109)	/

Grading of papulopustular exanthemas pruritus, xerosis, and paronychia according to the NCI-CTCAE version 5.0. CTCAE, Common Terminology Criteria for Adverse Events; NCI, National Cancer Institute; BSA, body surface area.

papulopustular lesions, then they can be treated by oral tetracycline (152, 154). For skin toxicity with pustules and a large amount of exudate (typically grade 3 or higher), the use of both tetracycline and saline compresses (15 minutes, 2 to 3 times a day) can effectively control inflammation (152, 155). Doxycycline is recommended for patients with renal insufficiency, and minocycline is recommended for patients living in areas with high ultraviolet exposure (156). At the

TABLE 4 | Treatments of papulopustular exanthemas caused by EGFR inhibitors.

Grade	Therapeutic measures
1	Continue EGFR inhibitors at the original dose; moisturizing and sunscreen (sun protection factor SPF ≥30); topical antibiotics (clindamycin 1-2% gel, erythromycin 1%, nadifloxacin 1%; fusidic acid 2% or preparations containing metronidazole 0.75%); topical calcineurin inhibitors (tacrolimus 0.1% ointment or pimecrolimus 1% cream bid); reassess after at least 2 weeks or any worsening of symptoms (136, 141, 142, 147)
2	Symptom deterioration or patient intolerance (reduction or discontinuation of EGFR inhibitors); moisturizing and sunscreen; topical corticosteroids (hydrocortisone 1-2.5%, prednicarbate 0.02% cream, mometasone furoate 0.1%, desoximetasone 0.25%); topical antibiotics (clindamycin 1-2% gel, erythromycin 1%, nadifloxacin 1%; fusidic acid 2% or preparations containing metronidazole 0.75%); topical calcineurin inhibitors (tacrolimus 0.1% ointment or pimecrolimus 1% cream bid.); Oral antibiotics [such as tetracycline (250-500 mg), doxycycline (100-200 mg, bid), oxytetracycline (500 mg, bid) or minocycline (100 mg, bid)]; antihistamines; reassess after at least 2 weeks or any worsening of symptom (133, 136, 141, 142, 147–149)
3	Temporary discontinuation of EGFR inhibitors; moisturizing and sunscreen; oral antibiotics [such as tetracycline (250-500 mg), doxycycline (100-200 mg, bid), oxytetracycline (500 mg, bid) or minocycline (100 mg, bid)] plus a short course of oral corticosteroid (prednisolone 0.5-1 mg/kg/day for 5–7 days); consider oral isotretinoin at low doses (20-30 mg/day); reassess after at least 2 weeks or any worsening of symptoms (133, 141, 142, 146, 147, 149)
4	Same as grade 3
5	Discontinuation of EGFR inhibitors

same time, attention should be paid to the intestinal microflora disorder caused by long-term systemic antibiotics in the treatment of rash (157).

In addition to the conventional treatment mentioned above, Bavetta et al. (158) found a significant improvement in skin symptoms after 4 weeks of treatment with a cream containing 1.5% polydatin (a natural precursor of resveratrol), suggesting that it may be used as an adjunctive agent for prophylactic treatment of papulopustular exanthemas and as an alternative to corticosteroids. Lacouture et al. (159) showed that although BRAF inhibitors can activate mitogen-activated protein kinase downstream of EGFR, topical use of BRAF inhibitor LUT014 can improve the skin toxicity induced by EGFR inhibitors cetuximab or panitumumab. Additionally, topical use of recombinant human EGF may ameliorate the rash produced by EGFR inhibitors by regulating the normal proliferation and differentiation of keratinocytes and reducing the expression of inflammatory factors (93).

Skin Xerosis

Patients with dry skin should use moisturizing emollients several times a day, avoid bathing with soap and hot water, and use emollients to moisturize the skin after cleansing (147). Water-based creams aggravate dry skin and very greasy emollients increase the risk of folliculitis. Therefore, ointment is recommended for the care of dry skin. Specific emollients and soap substitutes are recommended by the United Kingdom EGFR-TKI expert consensus on adverse event management published in 2015 (141). In addition, skin dryness with eczematous lesions is treated with topical steroids (160).

Paronychia

Paronychia can be extremely painful to the patient, leading to difficulty in walking and limited mobility by affecting the nails of the fingers and toes (148). A retrospective study by Osio et al. (103) found that patients using EGFR inhibitors for more than 6 months had a > 50% chance of developing paronychia. Patients with paronychia can be treated with silver nitrate, preservatives, topical corticosteroids, and antibiotics. For grade 1 and 2 paronychia, topical betamethasone valerate (2-3 times, qd) is recommended; for grade 3 paronychia, local use of clobetasol cream (2-3 times, qd) is recommended. Patients with periungual granulomas can be treated with nitrate first. If there is no response, then curettage and cauterization can be utilized (133, 148, 161). Therapeutic measures are shown in more detail in **Table 5**.

Hair Changes

Topical minoxidil is recommended for non-cicatricial alopecia of the head caused by EGFR inhibitors. Topical steroids are recommended for inflammatory and cicatricial alopecia (160). Curled hypertrophic long eyelashes can be trimmed, and facial hirsutism can be treated with laser hair removal (160).

Management of Lethal Severe Cutaneous Adverse Reactions

Rare but fatal adverse skin reactions such as AGEP, SJS, TEN, and SJS/TEN may be caused when EGFR inhibitors are used. Their clinical manifestations and related therapeutic measures are shown in the **Table 6**. The general treatment principle is to stop the relevant EGFR inhibitors, reduce fluid loss, replenish body fluids, control pain, and provide adequate nutrition (88). AGEP symptoms usually resolve rapidly after discontinuing EGFR inhibitors. Topical corticosteroids and systemic antihistamines are recommended for symptom control (168).

For more severe skin toxicities such as SJS, TEN, SJS/TEN, conservative treatment (e.g., applying emollients) recommends maintaining skin integrity and preventing fluid loss. Surgical debridement is recommended only when infection occurs. Aggressive treatment recommends removing exfoliated epidermis that may be infected (88). In subsequent treatment, emollients and steroid creams can be used alternately for moisturizing and anti-inflammation. Gauze soaked with betadine can be used for bandaging (169).

A meta-analysis of the literature suggested that cyclosporine was effective in reducing mortality from SJS/TEN, and the combination of cyclosporine and systemic steroids may be an effective treatment for SJS/TEN (170–172). Mucosal damage caused by TEN often affects the eyes, gastrointestinal tract, and respiratory tract. TEN often causes eye keratitis and corneal erosion. It is recommended to consult an ophthalmologist, use antibiotic eye drops to prevent bacterial infection, and use eye lubricant combined with topical corticosteroids for the treatment of eye complications. Attention should be paid to secondary glaucoma caused by steroid treatment (173, 174). Oral ulcers are the most common in TEN and can be treated with topical lidocaine gel or cocaine mouthwash. In addition, the mucous membrane of the respiratory tract may fall off and cause respiratory distress that requires management by a specialized physician (169).

Preventive Measures

Due to the important role of EGFR in the normal physiological function of the skin, the incidence of adverse skin reactions

TABLE 5 | Treatments of paronychia caused by EGFR inhibitors.

Grade	Therapeutic measures
1	Continue EGFR inhibitors at original dose; antiseptic hand bath (povidone iodine 1:10, potassium permanganate 1:10000, white vinegar in water 1:1); topical betamethasone valerate (2-3 times, qd); reassess after 2 weeks (133, 142)
2	Continue EGFR inhibitors at original dose; silver nitrate solution 20% weekly (administer cryotherapy or other chemical/electric cauterization if granulation); povidone-iodine 2% ointment; topical betamethasone valerate 0.1% ointment (2-3 times, qd); oral antibiotics are recommended; reassess after 2 weeks (133, 136, 142, 149)
3	Temporary discontinuation of EGFR inhibitors; topical clobetasol cream (2-3 times, qd); povidone-iodine 2% ointment; systemic antibiotics oral or intravenously following pathogenic culture; continue to apply topical antibiotics; reassess after 2 weeks (136, 142, 148, 149, 161)

TABLE 6 | Clinical manifestations and therapeutic measures of severely fatal skin toxicities.

Lethal Skin Toxicities	Clinical manifestations	Therapeutic measures
AGEP	Fever ≥38°C, sterile non-follicular pustules on the base of the erythema, leukocytosis, neutrophils ≥7000, mild eosinophilia, multiple organs involved (89, 162)	EGFR inhibitors withdrawal; topical corticosteroids, systemic antihistamines (162, 163)
TEN	Fever≥38°C, influenza-like syndrome, respiratory tract symptoms, Lymphopenia, transitory neutropenia, mild cytolysis, blisters, multiple organs involved, Nikolsky's sign, skin detachment ≥30% (162)	EGFR inhibitors withdrawal; corticosteroids, cyclosporine, intravenous immunoglobulins, TNF-α inhibitors; plasmapheresis (163, 164)
SJS	The clinical manifestations were similar to TEN, skin detachment <10% (162)	SJS treatment strategy is the same as TEN
NME	Annular-circinate, erythematous, scaly rash, superficial epidermal necrosis, plasma glucagon levels increased, diabetes mellitus or glucose intolerance (11, 165)	EGFR inhibitors withdrawal; oral prednisolone (0.5 mg/kg/d); octreotide and lanreotide; clobetasol propionate ointment 0.05% (28, 165, 166)
DIHS	Fever ≥38°C, extensive rash, atypical lymphocytosis, eosinophilia, lymphadenopathy, multiple organ dysfunction, reactivation of human herpes virus 6 and human herpes virus 7 (35, 41)	EGFR inhibitors withdrawal; oral prednisolone (0.5 mg/kg/day); cyclosporine (5 mg/kg/day) (41, 167)

caused by EGFR inhibitors is 60%-85%. These adverse reactions often lead to the reduction or even withdrawal of antitumor drugs (175). Therefore, preventing skin toxicity is increasingly gaining attention by investigators. Prophylactic use of emollients, sunscreen, mild body wash and facial cleansers, are ointment containing EGF are beneficial measures to prevent or reduce skin toxicity in patients treated with EGFR inhibitors (141, 142, 176).

A phase III clinical trial conducted in Canada in 2016 showed that the preventive use of minocycline (100 mg twice a day for 1 month) before erlotinib did not reduce the incidence of rashes but reduced the incidence of grade 3 skin toxicity while not affecting efficacy (177). Takahashi et al. (120) also showed that the grade of acneiform rash was lower after preventive use of minocycline. Meanwhile, Ichiki et al. (178) found that prophylactic use of minocycline (50 mg twice a day for 4 weeks) reduced rashes and paronychia induced by afatinib. In addition, preventive use of minocycline and topical corticosteroids may be effective for afatinib-induced paronychia, but elevated transaminase was found in patients during the use of minocycline. Therefore, long-term use of minocycline should be noted for possible liver damage (179).

Preventive use of doxycycline (100 mg twice a day for 4 weeks) can reduce the incidence of grade 2 or high adverse skin reactions caused by dacomitinib (180). In the treatment of refractory metastatic colorectal cancer with panitumumab, prophylactic doxycycline (100 mg twice a day for 6 weeks) and topical moisturizers, sunblock, and 1% hydrocortisone cream reduced the incidence of panitumumab-induced skin toxicity higher than grade 2 by 50% (181). Petrelli et al. (182) conducted a systematic review and meta-analysis of studies on the use of antibiotics to prevent skin rashes before 2016 and found that preventive use of minocycline or doxycycline reduced the absolute risk of all skin rashes (grade1-4) and severe skin rashes (grade 2-4) by 10% and 25%, respectively.

A randomized, open-label trial confirmed that tetracycline (250 mg twice a day for 4 weeks) was effective for afatinib-induced acneiform rash, and prophylactic use of tetracycline reduced the incidence and severity of rashes (183). However, Jatoi et al. (184) found that prophylactic use of tetracycline (500 mg orally twice a day for 28 days) did not reduce the incidence or severity of rashes induced by EGFR inhibitors. The different doses may be the reason for the inconsistent research results. Petrelli et al. (182) concluded that tetracycline could significantly reduce the incidence of severe rash induced by EGFR inhibitors after analyzing 13 clinical studies. Hofheinz et al. (185) recommended prophylactic use of antibiotics (such as tetracycline, doxycycline, and minocycline) on the first day of EGFR therapy to reduce the severity of adverse skin reactions and improve patient compliance. However, Italian experts do not recommend the preventive use of antibiotics as a treatment method to prevent serious skin toxicity of EGFR inhibitors (145). For skin toxicity caused by EGFR inhibitors, whether to use antibiotics prophylactically needs to be determined by comprehensively considering the situation of the patient.

In addition to the aforementioned studies on the preventive use of antibiotics, nonsteroidal anti-inflammatory drugs may also play a role in preventing EGFR inhibitor-related rashes (186). Local prophylactic use of 3% chloramphenicol + 0.5% prednisolone ointment significantly reduced the severity of facial papulopustular exanthemas induced by EGFR inhibitors (175). Although studies have shown that preventive use of vitamin K3 cream does not reduce the number of papulopustular exanthemas (187), preventive use of vitamin K1 cream can reduce the incidence of grade 2 or higher rashes (188). A randomized single-blind trial conducted by Chayahara et al. (189) showed that compared with the control group adapalene treatment did not prevent acneiform rash and may have harmful effects. Therefore, adapalene is not recommended to prevent acneiform rash caused by EGFR inhibitors.

CONCLUSION

To avoid the lethal skin toxicity caused by EGFR inhibitors, more targeted drugs need to be developed as well as conducting further investigations on efficacious preventive measures before cancer treatment and beneficial treatment measures after adverse skin reactions occur. In addition, there is no official or unified guidelines to deal with skin toxicities induced by EGFR inhibitors. Therefore, to create an authoritative guide would be beneficial to clinicians. The occurrence of adverse skin reactions and fatal skin toxicity are the most widespread reasons that limit anti-tumor treatments with EGFR inhibitors. Using the existing evidence for prevention and treatment should be an area of interest for medical staff and scientific researchers.

This paper summarized the cellular and molecular mechanisms of EGFR signaling and adverse skin reactions caused by EGFR inhibitors to provide ideas for the use of EGFR inhibitors and the prevention of related skin toxicity in cancer treatment. Effectively preventing and treating skin toxicity without damaging the anti-tumor efficacy of EGFR inhibitors is the ultimate goal we want to achieve. Treatment after the occurrence of skin toxicity is the key to effective anti-tumor treatment and a good prognosis of patients. This will require medical care providers to summarize and record more treatment details during their daily work, formulate a series of effective treatment schemes, and publish these results.

AUTHOR CONTRIBUTIONS

LY conceived and supervised the project. LYP summed up the literature and drafted the manuscript. FRQ collected and organized the inhibitors and revised the manuscript. All authors contributed to the article and approved the submitted version.

FUNDING

This study was funded by the Chongqing Clinical Pharmacy Key Specialties Construction Project.

REFERENCES

1. Sabbah DA, Hajjo R, Sweidan K. Review on Epidermal Growth Factor Receptor (EGFR) Structure, Signaling Pathways, Interactions, and Recent Updates of EGFR Inhibitors. *Curr Top Med Chem* (2020) 20(10):815–34. doi: 10.2174/1568026620666200303123102
2. Lopez Sambrooks C, Baro M, Quijano A, Narayan A, Cui W, Greninger P, et al. Oligosaccharyltransferase Inhibition Overcomes Therapeutic Resistance to EGFR Tyrosine Kinase Inhibitors. *Cancer Res* (2018) 78 (17):5094–106. doi: 10.1158/0008-5472.CAN-18-0505
3. Arienti C, Pignatta S, Tesei A. Epidermal Growth Factor Receptor Family and its Role in Gastric Cancer. *Front Oncol* (2019) 9:1308. doi: 10.3389/fonc.2019.01308
4. Paez JG, Janne PA, Lee JC, Tracy S, Greulich H, Gabriel S, et al. EGFR Mutations in Lung Cancer: Correlation With Clinical Response to Gefitinib Therapy. *Science* (2004) 304(5676):1497–500. doi: 10.1126/science.1099314
5. Sugawa N, Ekstrand AJ, James CD, Collins VP. Identical Splicing of Aberrant Epidermal Growth Factor Receptor Transcripts From Amplified Rearranged Genes in Human Glioblastomas. *Proc Natl Acad Sci USA* (1990) 87(21):8602–6. doi: 10.1073/pnas.87.21.8602
6. Arteaga CL, Engelman JA. ERBB Receptors: From Oncogene Discovery to Basic Science to Mechanism-Based Cancer Therapeutics. *Cancer Cell* (2014) 25(3):282–303. doi: 10.1016/j.ccr.2014.02.025
7. Wee P, Wang Z. Epidermal Growth Factor Receptor Cell Proliferation Signaling Pathways. *Cancers (Basel)* (2017) 9(5):52. doi: 10.3390/cancers9050052
8. Reddavid R, Dagatti S, Franco C, Puca L, Tomatis M, Corso S, et al. Molecularly Targeted Therapies for Gastric Cancer. *State Art Cancers (Basel)* (2021) 13(16):4094. doi: 10.3390/cancers13164094
9. Ciardiello F, Tortora G. EGFR Antagonists in Cancer Treatment. *N Engl J Med* (2008) 358(11):1160–74. doi: 10.1056/NEJMra0707704
10. Shah RR, Shah DR. Safety and Tolerability of Epidermal Growth Factor Receptor (EGFR) Tyrosine Kinase Inhibitors in Oncology. *Drug Saf* (2019) 42(2):181–98. doi: 10.1007/s40264-018-0772-x
11. Abdelli W, Alaoui F, Souissi A, Sassi W, Chelly I, Haouet S, et al. Case of Delayed Diagnosis of Necrolytic Migratory Erythema. *Clin Case Rep* (2021) 9(12):e05179. doi: 10.1002/ccr3.5179
12. Ullrich A, Coussens L, Hayflick JS, Dull TJ, Gray A, Tam AW, et al. Human Epidermal Growth Factor Receptor Cdna Sequence and Aberrant Expression of the Amplified Gene in A431 Epidermoid Carcinoma Cells. *Nature* (1984) 309(5967):418–25. doi: 10.1038/309418a0
13. Roskoski R Jr. The Erbb/HER Family of Protein-Tyrosine Kinases and Cancer. *Pharmacol Res* (2014) 79:34–74. doi: 10.1016/j.phrs.2013.11.002
14. Li T, Perez-Soler R. Skin Toxicities Associated With Epidermal Growth Factor Receptor Inhibitors. *Target Oncol* (2009) 4(2):107–19. doi: 10.1007/s11523-009-0114-0
15. Singh B, Carpenter G, Coffey RJ. EGF Receptor Ligands: Recent Advances. *F1000Res* (2016) 5:1–11. doi: 10.12688/f1000research.9025.1
16. Cohen S, Elliott GA. The Stimulation of Epidermal Keratinization by a Protein Isolated From the Submaxillary Gland of the Mouse. *J Invest Dermatol* (1963) 40:1–5. doi: 10.1038/jid.1963.1
17. Walton GM, Chen WS, Rosenfeld MG, Gill GN. Analysis of Deletions of the Carboxyl Terminus of the Epidermal Growth Factor Receptor Reveals Self-Phosphorylation at Tyrosine 992 and Enhanced *In Vivo* Tyrosine Phosphorylation of Cell Substrates. *J Biol Chem* (1990) 265(3):1750–4. doi: 10.1016/S0021-9258(19)40080-X
18. Stamos J, Sliwkowski MX, Eigenbrot C. Structure of the Epidermal Growth Factor Receptor Kinase Domain Alone and in Complex With a 4-Anilinoquinazoline Inhibitor. *J Biol Chem* (2002) 277(48):46265–72. doi: 10.1074/jbc.M207135200
19. Duggirala KB, Lee Y, Lee K. Chronicles of EGFR Tyrosine Kinase Inhibitors: Targeting EGFR C797S Containing Triple Mutations. *Biomol Ther (Seoul)* (2021) 30(1):19–27. doi: 10.4062/biomolther.2021.047
20. Graus-Porta D, Beerli RR, Daly JM, Hynes NE. Erbb-2, the Preferred Heterodimerization Partner of All Erbb Receptors, is a Mediator of Lateral Signaling. *EMBO J* (1997) 16(7):1647–55. doi: 10.1093/emboj/16.7.1647
21. Woodworth CD, Michael E, Marker D, Allen S, Smith L, Nees M. Inhibition of the Epidermal Growth Factor Receptor Increases Expression of Genes That Stimulate Inflammation, Apoptosis, and Cell Attachment. *Mol Cancer Ther* (2005) 4(4):650–8. doi: 10.1158/1535-7163.MCT-04-0238
22. Lee CS, Milone M, Seetharamu N. Osimertinib in EGFR-Mutated Lung Cancer: A Review of the Existing and Emerging Clinical Data. *Onco Targets Ther* (2021) 14:4579–97. doi: 10.2147/OTT.S227032
23. Papini F, Sundaresan J, Leonetti A, Tiseo M, Rolfo C, Peters GJ, et al. Hype or Hope - can Combination Therapies With Third-Generation EGFR-Tkis Help Overcome Acquired Resistance and Improve Outcomes in EGFR-Mutant Advanced/Metastatic NSCLC? *Crit Rev Oncol Hematol* (2021) 166:103454. doi: 10.1016/j.critrevonc.2021.103454
24. Wu YL, Cheng Y, Zhou X, Lee KH, Nakagawa K, Niho S, et al. Dacomitinib Versus Gefitinib as First-Line Treatment for Patients With EGFR-Mutation-Positive Non-Small-Cell Lung Cancer (ARCHER 1050): A Randomised, Open-Label, Phase 3 Trial. *Lancet Oncol* (2017) 18(11):1454–66. doi: 10.1016/S1470-2045(17)30608-3
25. Chen CB, Wu MY, Ng CY, Lu CW, Wu J, Kao PH, et al. Severe Cutaneous Adverse Reactions Induced by Targeted Anticancer Therapies and Immunotherapies. *Cancer Manag Res* (2018) 10:1259–73. doi: 10.2147/CMAR.S163391
26. Huang JJ, Ma SX, Hou X, Wang Z, Zeng YD, Qin T, et al. Toxic Epidermal Necrolysis Related to AP (Pemetrexed Plus Cisplatin) and Gefitinib Combination Therapy in a Patient With Metastatic Non-Small Cell Lung Cancer. *Chin J Cancer* (2015) 34(2):94–8. doi: 10.5732/cjc.014.10151
27. Jackman DM, Cioffredi LA, Jacobs L, Sharmeen F, Morse LK, Lucca J, et al. A Phase I Trial of High Dose Gefitinib for Patients With Leptomeningeal Metastases From Non-Small Cell Lung Cancer. *Oncotarget* (2015) 6 (6):4527–36. doi: 10.18632/oncotarget.2886
28. Seong JY, Kong SH, Choi YS, Suh HS. Necrolytic Migratory Erythema-Like Skin Lesion During Gefitinib Treatment: A Rare Cutaneous Adverse Reaction. *JAMA Dermatol* (2016) 152(8):947–8. doi: 10.1001/jamadermatol.2016.1098
29. Modjtahedi H, Essapen S. Epidermal Growth Factor Receptor Inhibitors in Cancer Treatment: Advances, Challenges and Opportunities. *Anticancer Drugs* (2009) 20(10):851–5. doi: 10.1097/CAD.0b013e3283330590

30. Wnorowski AM, de Souza A, Chachoua A, Cohen DE. The Management of EGFR Inhibitor Adverse Events: A Case Series and Treatment Paradigm. *Int J Dermatol* (2012) 51(2):223–32. doi: 10.1111/j.1365-4632.2011.05082.x
31. Li X, Kamenecka TM, Cameron MD. Cytochrome P450-Mediated Bioactivation of the Epidermal Growth Factor Receptor Inhibitor Erlotinib to a Reactive Electrophile. *Drug Metab Dispos* (2010) 38 (7):1238–45. doi: 10.1124/dmd.109.030361
32. Komiya N, Takahashi K, Kato G, Kubota M, Tashiro H, Nakashima C, et al. Acute Generalized Exanthematous Pustulosis Caused by Erlotinib in a Patient With Lung Cancer. *Case Rep Oncol* (2021) 14(1):599–603. doi: 10.1159/000514146
33. Ouyang DJ, Chen QT, Anwar M, Xie N, Ouyang QC, Fan PZ, et al. The Efficacy of Pyrotinib as a Third- or Higher-Line Treatment in HER2-Positive Metastatic Breast Cancer Patients Exposed to Lapatinib Compared to Lapatinib-Naive Patients: A Real-World Study. *Front Pharmacol* (2021) 12:682568. doi: 10.3389/fphar.2021.682568
34. Lakshmi C, Pillai S, Srinivas CR. Lapatinib-Induced Acute Generalized Exanthematous Pustulosis. *Indian Dermatol Online J* (2010) 1(1):14–7. doi: 10.4103/2229-5178.73251
35. Chen X, Wang S, Li L. A Case of Drug-Induced Hypersensitivity Syndrome Induced by Icotinib Managed by Intravenous Immunoglobulin and Systemic Corticosteroids. *Indian J Dermatol Venereol Leprol* (2018) 84(3):350–2. doi: 10.4103/ijdvl.IJDVL_490_17
36. Shah R, Lester JF. Tyrosine Kinase Inhibitors for the Treatment of EGFR Mutation-Positive Non-Small-Cell Lung Cancer: A Clash of the Generations. *Clin Lung Cancer* (2020) 21(3):e216–28. doi: 10.1016/j.cllc.2019.12.003
37. Le Du F, Dieras V, Curigliano G. The Role of Tyrosine Kinase Inhibitors in the Treatment of HER2+ Metastatic Breast Cancer. *Eur J Cancer* (2021) 154:175–89. doi: 10.1016/j.ejca.2021.06.026
38. Kris MG, Camidge DR, Giaccone G, Hida T, Li BT, O'Connell J, et al. Targeting HER2 Aberrations as Actionable Drivers in Lung Cancers: Phase II Trial of the Pan-HER Tyrosine Kinase Inhibitor Dacomitinib in Patients With HER2-Mutant or Amplified Tumors. *Ann Oncol* (2015) 26(7):1421–7. doi: 10.1093/annonc/mdv186
39. Doesch J, Debus D, Meyer C, Papadopoulos T, Schultz ES, Ficker JH, et al. Afatinib-Associated Stevens-Johnson Syndrome in an EGFR-Mutated Lung Cancer Patient. *Lung Cancer* (2016) 95:35–8. doi: 10.1016/j.lungcan.2016.02.015
40. Honda Y, Hattori Y, Katsura S, Terashima T, Manabe T, Otsuka A, et al. Stevens-Johnson Syndrome-Like Erosive Dermatitis Possibly Related to Afatinib. *Eur J Dermatol* (2016) 26(4):413–4. doi: 10.1684/ejd.2016.2807
41. Oyama B, Morikawa K, Sakaguchi T, Tsunoda A, Kida H, Inoue T, et al. Drug-Induced Hypersensitivity Syndrome by EGFR-TKI in a Patient With Lung Cancer. *Intern Med* (2021) 60(3):441–4. doi: 10.2169/internalmedicine.4237-19
42. Nuhnen VP, Schon MP, Mossner R. Stevens-Johnson Syndrome/Toxic Epidermal Necrolysis Overlap in a NSCLC Patient Treated With Afatinib. *J Dtsch Dermatol Ges* (2018) 16(2):199–201. doi: 10.1111/ddg.13412
43. Wu SG, Shih JY. Management of Acquired Resistance to EGFR TKI-Targeted Therapy in Advanced Non-Small Cell Lung Cancer. *Mol Cancer* (2018) 17(1):38. doi: 10.1186/s12943-018-0777-1
44. Zhou W, Ercan D, Chen L, Yun CH, Li D, Capelletti M, et al. Novel Mutant-Selective EGFR Kinase Inhibitors Against EGFR T790M. *Nature* (2009) 462 (7276):1070–4. doi: 10.1038/nature08622
45. Nagasaka M, Zhu VW, Lim SM, Greco M, Wu F, Ou SI. Beyond Osimertinib: The Development of Third-Generation EGFR Tyrosine Kinase Inhibitors for Advanced EGFR+ NSCLC. *J Thorac Oncol* (2021) 16 (5):740–63. doi: 10.1016/j.jtho.2020.11.028
46. Hirashima T, Satouchi M, Hida T, Nishio M, Kato T, Sakai H, et al. Osimertinib for Japanese Patients With T790M-Positive Advanced Non-Small-Cell Lung Cancer: A Pooled Subgroup Analysis. *Cancer Sci* (2019) 110 (9):2884–93. doi: 10.1111/cas.14120
47. Lin YT, Chu CY. Osimertinib-Induced Stevens-Johnson Syndrome in a Patient With EGFR T790M Mutation-Positive Non-Small Cell Lung Cancer. *Lung Cancer* (2019) 129:110–1. doi: 10.1016/j.lungcan.2018.12.030
48. Wang J, Cheng X, Lu Y, Zhou B. A Case Report of Toxic Epidermal Necrolysis Associated With AZD-9291. *Drug Des Devel Ther* (2018) 12:2163–7. doi: 10.2147/DDDT.S168248
49. Deeks ED. Furmonertinib: First Approval. *Drugs* (2021) 81(15):1775–80. doi: 10.1007/s40265-021-01662-3
50. Uchibori K, Inase N, Araki M, Kamada M, Sato S, Okuno Y, et al. Brigatinib Combined With Anti-EGFR Antibody Overcomes Osimertinib Resistance in EGFR-Mutated Non-Small-Cell Lung Cancer. *Nat Commun* (2017) 8:14768. doi: 10.1038/ncomms14768
51. Camidge DR, Kim HR, Ahn MJ, Yang JC, Han JY, Lee JS, et al. Brigatinib Versus Crizotinib in ALK-Positive Non-Small-Cell Lung Cancer. *N Engl J Med* (2018) 379(21):2027–39. doi: 10.1056/NEJMoa1810171
52. Espinosa ML, Abad C, Kurtzman Y, Abdulla FR. Dermatologic Toxicities of Targeted Therapy and Immunotherapy in Head and Neck Cancers. *Front Oncol* (2021) 11:605941. doi: 10.3389/fonc.2021.605941
53. Kozakiewicz P, Grzybowska-Szatkowska L. Application of Molecular Targeted Therapies in the Treatment of Head and Neck Squamous Cell Carcinoma. *Oncol Lett* (2018) 15(5):7497–505. doi: 10.3892/ol.2018.8300
54. Lin WL, Lin WC, Yang JY, Chang YC, Ho HC, Yang LC, et al. Fatal Toxic Epidermal Necrolysis Associated With Cetuximab in a Patient With Colon Cancer. *J Clin Oncol* (2008) 26(16):2779–80. doi: 10.1200/JCO.2007.15.7883
55. McGregor M, Price TJ. Panitumumab in the Treatment of Metastatic Colorectal Cancer, Including Wild-Type RAS, KRAS and NRAS Mcrc. *Future Oncol* (2018) 14(24):2437–59. doi: 10.2217/fon-2017-0711
56. Fukata T, Ito Y, Miyagaki H, Nishida H, Toyoda Y, Shingai T, et al. [a Case of Stevens-Johnson Syndrome Induced by Chemotherapy for Metastatic Colon Cancer]. *Gan To Kagaku Ryoho* (2019) 46(4):748–50.
57. Cohen RB. Current Challenges and Clinical Investigations of Epidermal Growth Factor Receptor (EGFR)- and Erbb Family-Targeted Agents in the Treatment of Head and Neck Squamous Cell Carcinoma (HNSCC). *Cancer Treat Rev* (2014) 40(4):567–77. doi: 10.1016/j.ctrv.2013.10.002
58. Tang L, Liu T, Chen J, Dang J, Li G. Immune-Checkpoint Inhibitors Versus Other Systemic Therapies in Advanced Head and Neck Cancer: A Network Meta-Analysis. *Immunotherapy* (2021) 13(6):541–55. doi: 10.2217/imt-2020-0070
59. Koramati SL, Sarathy V, Varayathu H, Thomas BE, Naik R. Addition of Nimotuzumab to Standard TPF Regimen in Locally Advanced Head and Neck Cancer: A Single Institutional Study. *J Oncol* (2021) 2021:6641963. doi: 10.1155/2021/6641963
60. Cai WQ, Zeng LS, Wang LF, Wang YY, Cheng JT, Zhang Y, et al. The Latest Battles Between EGFR Monoclonal Antibodies and Resistant Tumor Cells. *Front Oncol* (2020) 10:1249. doi: 10.3389/fonc.2020.01249
61. Liang R, Yang L, Zhu X. Nimotuzumab, an Anti-EGFR Monoclonal Antibody, in the Treatment of Nasopharyngeal Carcinoma. *Cancer Control* (2021) 28:1073274821989301. doi: 10.1177/1073274821989301
62. Lynch TJ, Bell DW, Sordella R, Gurubhagavatula S, Okimoto RA, Brannigan BW, et al. Activating Mutations in the Epidermal Growth Factor Receptor Underlying Responsiveness of Non-Small-Cell Lung Cancer to Gefitinib. *N Engl J Med* (2004) 350(21):2129–39. doi: 10.1056/NEJMoa040938
63. Sanford M, Scott LJ. Gefitinib: A Review of its Use in the Treatment of Locally Advanced/Metastatic Non-Small Cell Lung Cancer. *Drugs* (2009) 69 (16):2303–28. doi: 10.2165/10489100-000000000-00000
64. Zhang Y, Fu F, Hu H, Wang S, Li Y, Hu H, et al. Gefitinib as Neoadjuvant Therapy for Resectable Stage II-IIIA Non-Small Cell Lung Cancer: A Phase II Study. *J Thorac Cardiovasc Surg* (2021) 161(2):434–42 e2. doi: 10.1016/j.jtcvs.2020.02.131
65. Xie H, Wang H, Xu L, Li M, Peng Y, Cai X, et al. Gefitinib Versus Adjuvant Chemotherapy in Patients With Stage II-IIIA Non-Small-Cell Lung Cancer Harboring Positive EGFR Mutations: A Single-Center Retrospective Study. *Clin Lung Cancer* (2018) 19(6):484–92. doi: 10.1016/j.cllc.2018.05.007
66. Shalata W, Jacob BM, Agbarya A. Adjuvant Treatment With Tyrosine Kinase Inhibitors in Epidermal Growth Factor Receptor Mutated Non-Small-Cell Lung Carcinoma Patients, Past, Present and Future. *Cancers (Basel)* (2021) 13(16):4119–33. doi: 10.3390/cancers13164119
67. Melosky B, Hirsh V. Management of Common Toxicities in Metastatic NSCLC Related to Anti-Lung Cancer Therapies With EGFR-Tkis. *Front Oncol* (2014) 4:238. doi: 10.3389/fonc.2014.00238
68. Bello M. Binding Mechanism of Kinase Inhibitors to EGFR and T790M, L858R and L858R/T790M Mutants Through Structural and Energetic Analysis. *Int J Biol Macromol* (2018) 118(Pt B):1948–62. doi: 10.1016/j.ijbiomac.2018.07.042

69. Konecny GE, Pegram MD, Venkatesan N, Finn R, Yang G, Rahmeh M, et al. Activity of the Dual Kinase Inhibitor Lapatinib (GW572016) Against HER-2-Overexpressing and Trastuzumab-Treated Breast Cancer Cells. *Cancer Res* (2006) 66(3):1630–9. doi: 10.1158/0008-5472.CAN-05-1182
70. Rusnak DW, Lackey K, Affleck K, Wood ER, Alligood KJ, Rhodes N, et al. The Effects of the Novel, Reversible Epidermal Growth Factor Receptor/Erbb-2 Tyrosine Kinase Inhibitor, GW2016, on the Growth of Human Normal and Tumor-Derived Cell Lines *In Vitro* and *In Vivo*. *Mol Cancer Ther* (2001) 1(2):85–94. doi: 10.1097/00008390-200112000-00011
71. Wood ER, Truesdale AT, McDonald OB, Yuan D, Hassell A, Dickerson SH, et al. A Unique Structure for Epidermal Growth Factor Receptor Bound to GW572016 (Lapatinib): Relationships Among Protein Conformation, Inhibitor Off-Rate, and Receptor Activity in Tumor Cells. *Cancer Res* (2004) 64(18):6652–9. doi: 10.1158/0008-5472.CAN-04-1168
72. Kobayashi S, Boggon TJ, Dayaram T, Janne PA, Kocher O, Meyerson M, et al. EGFR Mutation and Resistance of Non-Small-Cell Lung Cancer to Gefitinib. *N Engl J Med* (2005) 352(8):786–92. doi: 10.1056/NEJMoa044238
73. Lavacchi D, Mazzoni F, Giaccone G. Clinical Evaluation of Dacomitinib for the Treatment of Metastatic Non-Small Cell Lung Cancer (NSCLC): Current Perspectives. *Drug Des Devel Ther* (2019) 13:3187–98. doi: 10.2147/DDDT.S194231
74. Ding PN, Lord SJ, Gebski V, Links M, Bray V, Gralla RJ, et al. Risk of Treatment-Related Toxicities From EGFR Tyrosine Kinase Inhibitors: A Meta-Analysis of Clinical Trials of Gefitinib, Erlotinib, and Afatinib in Advanced EGFR-Mutated Non-Small Cell Lung Cancer. *J Thorac Oncol* (2017) 12(4):633–43. doi: 10.1016/j.jtho.2016.11.2236
75. Zhang T, Qu R, Chan S, Lai M, Tong L, Feng F, et al. Discovery of a Novel Third-Generation EGFR Inhibitor and Identification of a Potential Combination Strategy to Overcome Resistance. *Mol Cancer* (2020) 19 (1):90. doi: 10.1186/s12943-020-01202-9
76. Choi G, Kim D, Oh J. AI-Based Drug Discovery of Tkis Targeting L858R/T790M/C797S-Mutant EGFR in Non-Small Cell Lung Cancer. *Front Pharmacol* (2021) 12:660313. doi: 10.3389/fphar.2021.660313
77. Yu HA, Tian SK, Drilon AE, Borsu L, Riely GJ, Arcila ME, et al. Acquired Resistance of EGFR-Mutant Lung Cancer to a T790M-Specific EGFR Inhibitor: Emergence of a Third Mutation (C797S) in the EGFR Tyrosine Kinase Domain. *JAMA Oncol* (2015) 1(7):982–4. doi: 10.1001/jamaoncol.2015.1066
78. Leonetti A, Sharma S, Minari R, Perego P, Giovannetti E, Tiseo M. Resistance Mechanisms to Osimertinib in EGFR-Mutated Non-Small Cell Lung Cancer. *Br J Cancer* (2019) 121(9):725–37. doi: 10.1038/s41416-019-0573-8
79. To C, Jang J, Chen T, Park E, Mushajiang M, De Clercq DJH, et al. Single and Dual Targeting of Mutant EGFR With an Allosteric Inhibitor. *Cancer Discov* (2019) 9(7):926–43. doi: 10.1158/2159-8290.CD-18-0903
80. Umbela S, Ghacha S, Matuknauth R, Gause S, Joshee S, Deshmukh RR. Brigatinib: New-Generation ALK Inhibitor for Nonsmall Cell Lung Cancer. *Curr Probl Cancer* (2019) 43(6):100477. doi: 10.1016/j.currproblcancer.2019.03.005
81. Joly-Tonetti N, Ondet T, Monshouwer M, Stamatas GN. EGFR Inhibitors Switch Keratinocytes From a Proliferative to a Differentiative Phenotype Affecting Epidermal Development and Barrier Function. *BMC Cancer* (2021) 21(1):5. doi: 10.1186/s12885-020-07685-5
82. Annunziata MC, De Stefano A, Fabbrocini G, Leo S, Marchetti P, Romano MC, et al. Current Recommendations and Novel Strategies for the Management of Skin Toxicities Related to Anti-EGFR Therapies in Patients With Metastatic Colorectal Cancer. *Clin Drug Investig* (2019) 39 (9):825–34. doi: 10.1007/s40261-019-00811-7
83. Kozuki T. Skin Problems and EGFR-Tyrosine Kinase Inhibitor. *Jpn J Clin Oncol* (2016) 46(4):291–8. doi: 10.1093/jjco/hyv207
84. Yano S, Kondo K, Yamaguchi M, Richmond G, Hutchison M, Wakeling A, et al. Distribution and Function of EGFR in Human Tissue and the Effect of EGFR Tyrosine Kinase Inhibition. *Anticancer Res* (2003) 23(5A):3639–50. doi: 10.1097/01.cad.0000089693.26177.3c
85. Mitchell EP, Perez-Soler R, Van Cutsem E, Lacouture ME. Clinical Presentation and Pathophysiology of EGFRI Dermatologic Toxicities. *Oncol (Williston Park)* (2007) 21(11 Suppl 5):4–9.
86. Cho YT, Chen KL, Sheen YS, Yang CW, Liau JY, Cheng YP, et al. Purpuric Drug Eruptions Caused by Epidermal Growth Factor Receptor Inhibitors for Non-Small Cell Lung Cancer: A Clinicopathologic Study of 32 Cases. *JAMA Dermatol* (2017) 153(9):906–10. doi: 10.1001/jamadermatol.2017.0903
87. Roujeau JC, Stern RS. Severe Adverse Cutaneous Reactions to Drugs. *N Engl J Med* (1994) 331(19):1272–85. doi: 10.1056/NEJM199411103311906
88. Mustafa SS, Ostrov D, Yerly D. Severe Cutaneous Adverse Drug Reactions: Presentation, Risk Factors, and Management. *Curr Allergy Asthma Rep* (2018) 18(4):26. doi: 10.1007/s11882-018-0778-6
89. Hadavand MA, Kaffenberger B, Cartron AM, Trinidad JC. Clinical Presentation and Management of Atypical and Recalcitrant Acute Generalized Exanthematous Pustulosis (AGEP). *J Am Acad Dermatol* (2020) S0190-9622(20):32609–17. doi: 10.1016/j.jaad.2020.09.024
90. Laux I, Jain A, Singh S, Agus DB. Epidermal Growth Factor Receptor Dimerization Status Determines Skin Toxicity to HER-Kinase Targeted Therapies. *Br J Cancer* (2006) 94(1):85–92. doi: 10.1038/sj.bjc.6602875
91. Quiroz FG, Fiore VF, Levorse J, Polak L, Wong E, Pasolli HA, et al. Liquid-Liquid Phase Separation Drives Skin Barrier Formation. *Science* (2020) 367 (6483):1–34. doi: 10.1126/science.aax9554
92. Madison KC. Barrier Function of the Skin: "La Raison D'etre" of the Epidermis. *J Invest Dermatol* (2003) 121(2):231–41. doi: 10.1046/j.1523-1747.2003.12359.x
93. Kim JM, Ji JH, Kim YS, Lee S, Oh SY, Huh SJ, et al. Rhegf Treatment Improves EGFR Inhibitor-Induced Skin Barrier and Immune Defects. *Cancers (Basel)* (2020) 12(11):3120–37. doi: 10.3390/cancers12113120
94. Wolf C, Qian Y, Brooke MA, Kelsell DP, Franzke CW. ADAM17/EGFR Axis Promotes Transglutaminase-Dependent Skin Barrier Formation Through Phospholipase C Gamma1 and Protein Kinase C Pathways. *Sci Rep* (2016) 6:39780. doi: 10.1038/srep39780
95. Lynn KS, Peterson RJ, Koval M. Ruffles and Spikes: Control of Tight Junction Morphology and Permeability by Claudins. *Biochim Biophys Acta Biomembr* (2020) 1862(9):183339. doi: 10.1016/j.bbamem.2020.183339
96. Fang H, Wang Y, Xu L, Zhou S, Bai J, Wu Y, et al. EGFR Inhibitor Gefitinib Regulates Barrier Function in Human Epidermal Keratinocytes *via* the Modulation of the Expression of Claudins. *Int J Mol Med* (2019) 43 (3):1522–30. doi: 10.3892/ijmm.2018.4046
97. Nanney LB, Magid M, Stoscheck CM, King LE Jr. Comparison of Epidermal Growth Factor Binding and Receptor Distribution in Normal Human Epidermis and Epidermal Appendages. *J Invest Dermatol* (1984) 83 (5):385–93. doi: 10.1111/1523-1747.ep12264708
98. Denning MF. Epidermal Keratinocytes: Regulation of Multiple Cell Phenotypes by Multiple Protein Kinase C Isoforms. *Int J Biochem Cell Biol* (2004) 36(7):1141–6. doi: 10.1016/j.biocel.2003.12.004
99. Baselga J, Rischin D, Ranson M, Calvert H, Raymond E, Kieback DG, et al. Phase I Safety, Pharmacokinetic, and Pharmacodynamic Trial of ZD1839, a Selective Oral Epidermal Growth Factor Receptor Tyrosine Kinase Inhibitor, in Patients With Five Selected Solid Tumor Types. *J Clin Oncol* (2002) 20 (21):4292–302. doi: 10.1200/JCO.2002.03.100
100. Tan AR, Yang X, Hewitt SM, Berman A, Lepper ER, Sparreboom A, et al. Evaluation of Biologic End Points and Pharmacokinetics in Patients With Metastatic Breast Cancer After Treatment With Erlotinib, an Epidermal Growth Factor Receptor Tyrosine Kinase Inhibitor. *J Clin Oncol* (2004) 22 (15):3080–90. doi: 10.1200/JCO.2004.08.189
101. Threadgill DW, Dlugosz AA, Hansen LA, Tennenbaum T, Lichti U, Yee D, et al. Targeted Disruption of Mouse EGF Receptor: Effect of Genetic Background on Mutant Phenotype. *Science* (1995) 269(5221):230–4. doi: 10.1126/science.7618084
102. Eames T, Kroth J, Flaig MJ, Ruzicka T, Wollenberg A. Perifollicular Xanthomas Associated With Epidermal Growth Factor Receptor Inhibitor Therapy. *Acta Derm Venereol* (2010) 90(2):202–3. doi: 10.2340/00015555-0792
103. Osio A, Mateus C, Soria JC, Massard C, Malka D, Boige V, et al. Cutaneous Side-Effects in Patients on Long-Term Treatment With Epidermal Growth Factor Receptor Inhibitors. *Br J Dermatol* (2009) 161(3):515–21. doi: 10.1111/j.1365-2133.2009.09214.x
104. Brodell LA, Hepper D, Lind A, Gru AA, Anadkat MJ. Histopathology of Acneiform Eruptions in Patients Treated With Epidermal Growth Factor Receptor Inhibitors. *J Cutan Pathol* (2013) 40(10):865–70. doi: 10.1111/cup.12202
105. Robert C, Soria JC, Spatz A, Le Cesne A, Malka D, Pautier P, et al. Cutaneous Side-Effects of Kinase Inhibitors and Blocking Antibodies. *Lancet Oncol* (2005) 6(7):491–500. doi: 10.1016/S1470-2045(05)70243-6
106. Mak KK, Chan SY. Epidermal Growth Factor as a Biologic Switch in Hair Growth Cycle. *J Biol Chem* (2003) 278(28):26120–6. doi: 10.1074/jbc.M212082200

107. Zhang H, Nan W, Wang S, Zhang T, Si H, Wang D, et al. Epidermal Growth Factor Promotes Proliferation of Dermal Papilla Cells *via* Notch Signaling Pathway. *Biochimie* (2016) 127:10–8. doi: 10.1016/j.biochi.2016.04.015
108. Celik T, Kosker M. Ocular Side Effects and Trichomegaly of Eyelashes Induced by Erlotinib: A Case Report and Review of the Literature. *Cont Lens Anterior Eye* (2015) 38(1):59–60. doi: 10.1016/j.clae.2014.08.005
109. Koksal UI, Pilanci KN, Ordu C, Okutur K, Saglam S, Demir G. Trichomegaly Induced by Cetuximab: Case Series and Review the Literature. *Am J Ther* (2016) 23(5):e1226–9. doi: 10.1097/MJT.0000000000000189
110. Chieosilapatham P, Kiatsurayanon C, Umehara Y, Trujillo-Paez JV, Peng G, Yue H, et al. Keratinocytes: Innate Immune Cells in Atopic Dermatitis. *Clin Exp Immunol* (2021) 204(3):296–309. doi: 10.1111/cei.13575
111. Park K, Ommori R, Imoto K, Asada H. Epidermal Growth Factor Receptor Inhibitors Selectively Inhibit the Expressions of Human Beta-Defensins Induced by Staphylococcus Epidermidis. *J Dermatol Sci* (2014) 75(2):94–9. doi: 10.1016/j.jdermsci.2014.04.011
112. Mascia F, Mariani V, Girolomoni G, Pastore S. Blockade of the EGF Receptor Induces a Deranged Chemokine Expression in Keratinocytes Leading to Enhanced Skin Inflammation. *Am J Pathol* (2003) 163(1):303–12. doi: 10.1016/S0002-9440(10)63654-1
113. Wan L, Wang Y, Tang Y, Tan Y, He F, Zhang Y, et al. Gefitinib-Induced Cutaneous Toxicities in Brown Norway Rats are Associated With Macrophage Infiltration. *Inflammation* (2020) 43(6):2137–46. doi: 10.1007/s10753-020-01281-2
114. Russi EG, Moretto F, Rampino M, Benasso M, Bacigalupo A, De Sanctis V, et al. Acute Skin Toxicity Management in Head and Neck Cancer Patients Treated With Radiotherapy and Chemotherapy or EGFR Inhibitors: Literature Review and Consensus. *Crit Rev Oncol Hematol* (2015) 96 (1):167–82. doi: 10.1016/j.critrevonc.2015.06.001
115. Lacouture ME, Anadkat MJ, Bensadoun RJ, Bryce J, Chan A, Epstein JB, et al. Clinical Practice Guidelines for the Prevention and Treatment of EGFR Inhibitor-Associated Dermatologic Toxicities. *Support Care Cancer* (2011) 19(8):1079–95. doi: 10.1007/s00520-011-1197-6
116. Russi EG, Raber-Durlacher JE, Sonis ST. Local and Systemic Pathogenesis and Consequences of Regimen-Induced Inflammatory Responses in Patients With Head and Neck Cancer Receiving Chemoradiation. *Mediators Inflammation* (2014) 2014:518261. doi: 10.1155/2014/518261
117. Russi EG, Numico G, Merlano MC, Pinto C. Cetuximab-Related Radiation Dermatitis in Head-and-Neck Cancer Patients: In Regard to Studer Et al. (Int J Radiat Oncol Biol Phys in Press). *Int J Radiat Oncol Biol Phys* (2011) 79 (4):1278. author reply -9. doi: 10.1016/j.ijrobp.2010.10.047
118. Le-Rademacher JG, Rowland K, Atherton PJ, Dakhil C, Sun Z, Tan A, et al. Androgen Mediation-and Antiandrogens Mitigation-of the Epidermal Growth Factor Receptor (EGFR) Inhibitor-Induced Rash: Results From a Pilot Randomized Trial and Small Translational Case Series. *Am J Hosp Palliat Care* (2019) 36(6):519–25. doi: 10.1177/1049909118819820
119. Nakahara T, Moroi Y, Takayama K, Itoh E, Kido-Nakahara M, Nakanishi Y, et al. Changes in Sebum Levels and the Development of Acneiform Rash in Patients With Non-Small Cell Lung Cancer After Treatment With EGFR Inhibitors. *Oncol Targets Ther* (2015) 8:259–63. doi: 10.2147/OTT.S76860
120. Takahashi H, Asaka J, Tairabune T, Ujiie H, Matsuura Y, Nihei S, et al. Analysis of Risk Factors for Skin Disorders Caused by Anti-Epidermal Growth Factor Receptor Antibody Drugs and Examination of Methods for Their Avoidance. *J Clin Pharm Ther* (2021) 46(5):1404–11. doi: 10.1111/jcpt.13475
121. Sato I, Mizuno H, Kataoka N, Kunimatsu Y, Tachibana Y, Sugimoto T, et al. Osimertinib-Associated Toxic Epidermal Necrolysis in a Lung Cancer Patient Harboring an EGFR Mutation-a Case Report and a Review of the Literature. *Medicina (Kaunas)* (2020) 56(8):403–9. doi: 10.3390/medicina56080403
122. Lerch M, Mainetti C, Terziroli Beretta-Piccoli B, Harr T. Current Perspectives on Stevens-Johnson Syndrome and Toxic Epidermal Necrolysis. *Clin Rev Allergy Immunol* (2018) 54(1):147–76. doi: 10.1007/s12016-017-8654-z
123. Shah DR, Shah RR, Morganroth J. Tyrosine Kinase Inhibitors: Their on-Target Toxicities as Potential Indicators of Efficacy. *Drug Saf* (2013) 36 (6):413–26. doi: 10.1007/s40264-013-0050-x
124. Jaka A, Gutierrez-Rivera A, Lopez-Pestana A, del Alcazar E, Zubizarreta J, Vildosola S, et al. Predictors of Tumor Response to Cetuximab and Panitumumab in 116 Patients and a Review of Approaches to Managing Skin Toxicity. *Actas Dermosifiliogr* (2015) 106(6):483–92. doi: 10.1016/j.ad.2015.01.006
125. Amador ML, Oppenheimer D, Perea S, Maitra A, Cusatis G, Iacobuzio-Donahue C, et al. An Epidermal Growth Factor Receptor Intron 1 Polymorphism Mediates Response to Epidermal Growth Factor Receptor Inhibitors. *Cancer Res* (2004) 64 (24):9139–43. doi: 10.1158/0008-5472.CAN-04-1036
126. Kimura H, Kasahara K, Sekijima M, Tamura T, Nishio K. Plasma MIP-1beta Levels and Skin Toxicity in Japanese Non-Small Cell Lung Cancer Patients Treated With the EGFR-Targeted Tyrosine Kinase Inhibitor, Gefitinib. *Lung Cancer* (2005) 50(3):393–9. doi: 10.1016/j.lungcan.2005.07.012
127. Moreno Garcia V, Thavasu P, Blanco Codesido M, Molife LR, Vitfell Pedersen J, Puglisi M, et al. Association of Creatine Kinase and Skin Toxicity in Phase I Trials of Anticancer Agents. *Br J Cancer* (2012) 107 (11):1797–800. doi: 10.1038/bjc.2012.482
128. Steffens M, Paul T, Hichert V, Scholl C, von Mallek D, Stelzer C, et al. Dosing to Rash?–the Role of Erlotinib Metabolic Ratio From Patient Serum in the Search of Predictive Biomarkers for EGFR Inhibitor-Mediated Skin Rash. *Eur J Cancer* (2016) 55:131–9. doi: 10.1016/j.ejca.2015.11.022
129. Chen P, Chen F, Lei J, Zhou B. Curative Effectiveness and Safety of Osimertinib in the Treatment for Non-Small-Cell Lung Cancer: A Meta-Analysis of the Experimental Evidence. *Onco Targets Ther* (2018) 11:9033–47. doi: 10.2147/OTT.S182077
130. Bollinger MK, Agnew AS, Mascara GP. Osimertinib: A Third-Generation Tyrosine Kinase Inhibitor for Treatment of Epidermal Growth Factor Receptor-Mutated Non-Small Cell Lung Cancer With the Acquired Thr790Met Mutation. *J Oncol Pharm Pract* (2018) 24(5):379–88. doi: 10.1177/1078155217712401
131. Liao BC, Lin CC, Lee JH, Yang JC. Update on Recent Preclinical and Clinical Studies of T790M Mutant-Specific Irreversible Epidermal Growth Factor Receptor Tyrosine Kinase Inhibitors. *J BioMed Sci* (2016) 23(1):86. doi: 10.1186/s12929-016-0305-9
132. Gutzmer R, Wollenberg A, Ugurel S, Homey B, Ganser A, Kapp A. Cutaneous Side Effects of New Antitumor Drugs: Clinical Features and Management. *Dtsch Arztebl Int* (2012) 109(8):133–40. doi: 10.3238/arztebl.2012.0133
133. Aw DC, Tan EH, Chin TM, Lim HL, Lee HY, Soo RA. Management of Epidermal Growth Factor Receptor Tyrosine Kinase Inhibitor-Related Cutaneous and Gastrointestinal Toxicities. *Asia Pac J Clin Oncol* (2018) 14 (1):23–31. doi: 10.1111/ajco.12687
134. Gutzmer R, Becker JC, Enk A, Garbe C, Hauschild A, Leverkus M, et al. Management of Cutaneous Side Effects of EGFR Inhibitors: Recommendations From a German Expert Panel for the Primary Treating Physician. *J Dtsch Dermatol Ges* (2011) 9(3):195–203. doi: 10.1111/j.1610-0387.2010.07561.x
135. National Cancer Institute. *Common Terminology Criteria for Adverse Events (CTCAE) Version 5.0*. Washington: U.S. Department of Health and Human Services (2017).
136. Chu CY, Chen KY, Wen-Cheng Chang J, Wei YF, Lee CH, Wang WM. Taiwanese Dermatological Association Consensus for the Prevention and Management of Epidermal Growth Factor Receptor Tyrosine Kinase Inhibitor-Related Skin Toxicities. *J Formos Med Assoc* (2017) 116(6):413–23. doi: 10.1016/j.jfma.2017.03.001
137. Tohyama M, Hamada M, Harada D, Kozuki T, Nogami N, Monden N, et al. Clinical Features and Treatment of Epidermal Growth Factor Inhibitor-Related Late-Phase Papulopustular Rash. *J Dermatol* (2020) 47(2):121–7. doi: 10.1111/1346-8138.15170
138. Fischer A, Rosen AC, Ensslin CJ, Wu S, Lacouture ME. Pruritus to Anticancer Agents Targeting the EGFR, BRAF, and CTLA-4. *Dermatol Ther* (2013) 26(2):135–48. doi: 10.1111/dth.12027
139. Clabbers JMK, Boers-Doets CB, Gelderblom H, Stijnen T, Lacouture ME, van der Hoeven KJM, et al. Xerosis and Pruritus as Major EGFRI-Associated Adverse Events. *Support Care Cancer* (2016) 24(2):513–21. doi: 10.1007/s00520-015-2781-y
140. Beech J, Germetaki T, Judge M, Paton N, Collins J, Garbutt A, et al. Management and Grading of EGFR Inhibitor-Induced Cutaneous Toxicity. *Future Oncol* (2018) 14(24):2531–41. doi: 10.2217/fon-2018-0187
141. Califano R, Tariq N, Compton S, Fitzgerald DA, Harwood CA, Lal R, et al. Expert Consensus on the Management of Adverse Events From EGFR Tyrosine Kinase Inhibitors in the UK. *Drugs* (2015) 75(12):1335–48. doi: 10.1007/s40265-015-0434-6
142. Potthoff K, Hofheinz R, Hassel JC, Volkenandt M, Lordick F, Hartmann JT, et al. Interdisciplinary Management of EGFR-Inhibitor-Induced Skin Reactions: A German Expert Opinion. *Ann Oncol* (2011) 22(3):524–35. doi: 10.1093/annonc/mdq387

143. Bachmeyer C, Reguiai Z, Peuvrel L, Bachet JB, Bensadoun RJ, Ychou M, et al. [Cutaneous Adverse Reactions of EGFR (Epidermal Growth Factor Receptor)-Inhibitors: Therapeutic Algorithm of the French PROCUR Group]. *Bull Cancer* (2013) 100(5):417–26. doi: 10.1684/bdc.2013.1735
144. Peuvrel L, Bachmeyer C, Reguiai Z, Bachet JB, Andre T, Bensadoun RJ, et al. Survey on the Management of Skin Toxicity Associated With EGFR Inhibitors Amongst French Physicians. *J Eur Acad Dermatol Venereol* (2013) 27(4):419–29. doi: 10.1111/j.1468-3083.2011.04421.x
145. Pinto C, Barone CA, Girolomoni G, Russi EG, Merlano MC, Ferrari D, et al. Management of Skin Reactions During Cetuximab Treatment in Association With Chemotherapy or Radiotherapy: Update of the Italian Expert Recommendations. *Am J Clin Oncol* (2016) 39(4):407–15. doi: 10.1097/COC.0000000000000291
146. Gravalos C, Sanmartin O, Gurpide A, Espana A, Majem M, Suh Oh HJ, et al. Clinical Management of Cutaneous Adverse Events in Patients on Targeted Anticancer Therapies and Immunotherapies: A National Consensus Statement by the Spanish Academy of Dermatology and Venereology and the Spanish Society of Medical Oncology. *Clin Transl Oncol* (2019) 21 (5):556–71. doi: 10.1007/s12094-018-1953-x
147. Hofheinz RD, Segaert S, Safont MJ, Demonty G, Prenen H. Management of Adverse Events During Treatment of Gastrointestinal Cancers With Epidermal Growth Factor Inhibitors. *Crit Rev Oncol Hematol* (2017) 114:102–13. doi: 10.1016/j.critrevonc.2017.03.032
148. Melosky B, Leighl NB, Rothenstein J, Sangha R, Stewart D, Papp K. Management of Egfr Tki-Induced Dermatologic Adverse Events. *Curr Oncol* (2015) 22(2):123–32. doi: 10.3747/co.22.2430
149. Lacouture ME, Sibaud V, Gerber PA, van den Hurk C, Fernandez-Penas P, Santini D, et al. Prevention and Management of Dermatological Toxicities Related to Anticancer Agents: ESMO Clinical Practice Guidelines(). *Ann Oncol* (2021) 32(2):157–70. doi: 10.1016/j.annonc.2020.11.005
150. Wu J, Lacouture ME. Pruritus Associated With Targeted Anticancer Therapies and Their Management. *Dermatol Clin* (2018) 36(3):315–24. doi: 10.1016/j.det.2018.02.010
151. Macdonald JB, Macdonald B, Golitz LE, LoRusso P, Sekulic A. Cutaneous Adverse Effects of Targeted Therapies: Part I: Inhibitors of the Cellular Membrane. *J Am Acad Dermatol* (2015) 72(2):203–18. quiz 19-20. doi: 10.1016/j.jaad.2014.07.032
152. Segaert S, Van Cutsem E. Clinical Signs, Pathophysiology and Management of Skin Toxicity During Therapy With Epidermal Growth Factor Receptor Inhibitors. *Ann Oncol* (2005) 16(9):1425–33. doi: 10.1093/annonc/mdi279
153. Farahnik B, Kwong B, Murase J. General Management Strategy for Epidermal Growth Factor Receptor Inhibitor-Associated Papulopustular Eruption. *J Am Acad Dermatol* (2016) 75(5):e191. doi: 10.1016/j.jaad.2016.07.036
154. Segaert S, Van Cutsem E. Clinical Management of EGFRI Dermatologic Toxicities: The European Perspective. *Oncol (Williston Park)* (2007) 21(11 Suppl 5):22–6.
155. Higgins PJ, Draper M, Nelson M. Anti-Inflammatory Activity of Tetracyclines: Applications to Human Disease. *Antiinflamm Antiallergy Agents Med Chem* (2011) 10(2):132–52. doi: 10.2174/1871523011109020132
156. Stulhofer Buzina D, Martinac I, Ledic Drvar D, Ceovic R, Bilic I, Marinovic B. The Most Common Cutaneous Side Effects of Epidermal Growth Factor Receptor Inhibitors and Their Management. *Acta Dermatovenerol Croat* (2015) 23(4):282–8.
157. Mihai MM, Ion A, Giurcaneanu C, Nitipir C, Popa AM, Chifiriuc MC, et al. The Impact of Long-Term Antibiotic Therapy of Cutaneous Adverse Reactions to EGFR Inhibitors in Colorectal Cancer Patients. *J Clin Med* (2021) 10(15):3219–38. doi: 10.3390/jcm10153219
158. Bavetta M, Silvaggio D, Campione E, Sollena P, Formica V, Coletta D, et al. The Effects of Association of Topical Polydatin Improves the Preemptive Systemic Treatment on EGFR Inhibitors Cutaneous Adverse Reactions. *J Clin Med* (2021) 10(3):466–74. doi: 10.3390/jcm10030466
159. Lacouture ME, Wainberg ZA, Patel AB, Anadkat MJ, Stemmer SM, Shacham-Shmueli E, et al. Reducing Skin Toxicities From EGFR Inhibitors With Topical BRAF Inhibitor Therapy. *Cancer Discov* (2021) 11 (9):2158–67. doi: 10.1158/2159-8290.CD-20-1847
160. Cury-Martins J, Eris APM, Abdalla CMZ, Silva GB, Moura VPT, Sanches JA. Management of Dermatologic Adverse Events From Cancer Therapies: Recommendations of an Expert Panel. *Bras Dermatol* (2020) 95(2):221–37. doi: 10.1016/j.abd.2020.01.001
161. Gisondi P, Geat D, Mattiucci A, Lombardo F, Santo A, Girolomoni G. Incidence of Adverse Cutaneous Reactions to Epidermal Growth Factor Receptor Inhibitors in Patients With Non-Small-Cell Lung Cancer. *Dermatology* (2021) 237(6):929–33. doi: 10.1159/000513233
162. Duong TA, Valeyrie-Allanore L, Wolkenstein P, Chosidow O. Severe Cutaneous Adverse Reactions to Drugs. *Lancet* (2017) 390(10106):1996–2011. doi: 10.1016/S0140-6736(16)30378-6
163. Chen CB, Abe R, Pan RY, Wang CW, Hung SI, Tsai YG, et al. An Updated Review of the Molecular Mechanisms in Drug Hypersensitivity. *J Immunol Res* (2018) 2018:6431694. doi: 10.1155/2018/6431694
164. Hasegawa A, Abe R. Recent Advances in Managing and Understanding Stevens-Johnson Syndrome and Toxic Epidermal Necrolysis. *F1000Res* (2020) 9:1–12. doi: 10.12688/f1000research.24748.1
165. Tolliver S, Graham J, Kaffenberger BH. A Review of Cutaneous Manifestations Within Glucagonoma Syndrome: Necrolytic Migratory Erythema. *Int J Dermatol* (2018) 57(6):642–5. doi: 10.1111/ijd.13947
166. Foss MG, Ferrer-Bruker SJ. *Necrolytic Migratory Erythema*. Treasure Island (FL: StatPearls (2021).
167. Kuschel SL, Reedy MS. Cyclosporine Treatment of Drug Reaction With Eosinophilia and Systemic Symptoms (DRESS) Syndrome: A Case Report and Brief Review of the Literature. *Pract Dermatol* (2018) 2018:41–3.
168. Ingen-Housz-Oro S, Hotz C, Valeyrie-Allanore L, Sbidian E, Hemery F, Chosidow O, et al. Acute Generalized Exanthematous Pustulosis: A Retrospective Audit of Practice Between 1994 and 2011 at a Single Centre. *Br J Dermatol* (2015) 172(5):1455–7. doi: 10.1111/bjd.13540
169. Abela C, Hartmann CE, De Leo A, de Sica Chapman A, Shah H, Jawad M, et al. Toxic Epidermal Necrolysis (TEN): The Chelsea and Westminster Hospital Wound Management Algorithm. *J Plast Reconstr Aesthet Surg* (2014) 67(8):1026–32. doi: 10.1016/j.bjps.2014.04.003
170. Gonzalez-Herrada C, Rodriguez-Martin S, Cachafeiro L, Lerma V, Gonzalez O, Lorente JA, et al. Cyclosporine Use in Epidermal Necrolysis is Associated With an Important Mortality Reduction: Evidence From Three Different Approaches. *J Invest Dermatol* (2017) 137(10):2092–100. doi: 10.1016/j.jid.2017.05.022
171. Zimmermann S, Sekula P, Venhoff M, Motschall E, Knaus J, Schumacher M, et al. Systemic Immunomodulating Therapies for Stevens-Johnson Syndrome and Toxic Epidermal Necrolysis: A Systematic Review and Meta-Analysis. *JAMA Dermatol* (2017) 153(6):514–22. doi: 10.1001/jamadermatol.2016.5668
172. Roujeau JC, Mockenhaupt M, Guillaume JC, Revuz J. New Evidence Supporting Cyclosporine Efficacy in Epidermal Necrolysis. *J Invest Dermatol* (2017) 137(10):2047–9. doi: 10.1016/j.jid.2017.07.828
173. Ueta M. Stevens-Johnson Syndrome/Toxic Epidermal Necrolysis With Severe Ocular Complications. *Expert Rev Clin Immunol* (2020) 16(3):285–91. doi: 10.1080/1744666X.2020.1729128
174. Sotozono C, Ueta M, Koizumi N, Inatomi T, Shirakata Y, Ikezawa Z, et al. Diagnosis and Treatment of Stevens-Johnson Syndrome and Toxic Epidermal Necrolysis With Ocular Complications. *Ophthalmology* (2009) 116(4):685–90. doi: 10.1016/j.ophtha.2008.12.048
175. Amitay-Laish I, Prag-Naveh H, Ollech A, Davidovici B, Leshem YA, Snast I, et al. Prophylactic Topical Treatment for EGFR Inhibitor-Induced Papulopustular Rash: A Randomized Clinical Trial. *Dermatology* (2020) 237 (6):988–94. doi: 10.1159/000511869
176. Papoui E, Papastavrou E, Merkouris A, Charalambous A. The Extent to Which the Last Decade has Yielded Additional Treatment Options for EGFR-Associated Rash Besides Classic Treatment With Antibiotics and Corticosteroids - a Systematic Review. *Eur J Oncol Nurs* (2021) 50:101896. doi: 10.1016/j.ejon.2021.101896
177. Melosky B, Anderson H, Burkes RL, Chu Q, Hao D, Ho V, et al. Pan Canadian Rash Trial: A Randomized Phase III Trial Evaluating the Impact of a Prophylactic Skin Treatment Regimen on Epidermal Growth Factor Receptor-Tyrosine Kinase Inhibitor-Induced Skin Toxicities in Patients With Metastatic Lung Cancer. *J Clin Oncol* (2016) 34(8):810–5. doi: 10.1200/JCO.2015.62.3918
178. Ichiki M, Wataya H, Yamada K, Tsuruta N, Takeoka H, Okayama Y, et al. Preventive Effect of Kampo Medicine (Hangeshashin-to, TJ-14) Plus Minocycline Against Afatinib-Induced Diarrhea and Skin Rash in Patients With Non-Small Cell Lung Cancer. *Onco Targets Ther* (2017) 10:5107–13. doi: 10.2147/OTT.S145613
179. Okajima M, Miura S, Watanabe S, Tanaka H, Ito K, Ishida T, et al. A Prospective Phase II Study of Multimodal Prophylactic Treatment for

Afatinib-Induced Adverse Events in Advanced Non-Small Cell Lung Cancer (Niigata Lung Cancer Treatment Group 1401). *Transl Lung Cancer Res* (2021) 10(1):252–60. doi: 10.21037/tlcr-20-649

180. Lacouture ME, Keefe DM, Sonis S, Jatoi A, Gernhardt D, Wang T, et al. A Phase II Study (ARCHER 1042) to Evaluate Prophylactic Treatment of Dacomitinib-Induced Dermatologic and Gastrointestinal Adverse Events in Advanced Non-Small-Cell Lung Cancer. *Ann Oncol* (2016) 27(9):1712–8. doi: 10.1093/annonc/mdw227
181. Lacouture ME, Mitchell EP, Piperdi B, Pillai MV, Shearer H, Iannotti N, et al. Skin Toxicity Evaluation Protocol With Panitumumab (STEPP), a Phase II, Open-Label, Randomized Trial Evaluating the Impact of a Pre-Emptive Skin Treatment Regimen on Skin Toxicities and Quality of Life in Patients With Metastatic Colorectal Cancer. *J Clin Oncol* (2010) 28(8):1351–7. doi: 10.1200/JCO.2008.21.7828
182. Petrelli F, Borgonovo K, Barni S. Preventing or Treating Anti-EGFR Related Skin Rash With Antibiotics? *Ann Transl Med* (2016) 4(16):312. doi: 10.21037/atm.2016.07.01
183. Arrieta O, Vega-Gonzalez MT, Lopez-Macias D, Martinez-Hernandez JN, Bacon-Fonseca L, Macedo-Perez EO, et al. Randomized, Open-Label Trial Evaluating the Preventive Effect of Tetracycline on Afatinib Induced-Skin Toxicities in Non-Small Cell Lung Cancer Patients. *Lung Cancer* (2015) 88 (3):282–8. doi: 10.1016/j.lungcan.2015.03.019
184. Jatoi A, Dakhil SR, Sloan JA, Kugler JW, Rowland KM Jr, Schaefer PL, et al. Prophylactic Tetracycline Does Not Diminish the Severity of Epidermal Growth Factor Receptor (EGFR) Inhibitor-Induced Rash: Results From the North Central Cancer Treatment Group (Supplementary N03CB). *Support Care Cancer* (2011) 19(10):1601–7. doi: 10.1007/s00520-010-0988-5
185. Hofheinz RD, Deplanque G, Komatsu Y, Kobayashi Y, Ocvirk J, Racca P, et al. Recommendations for the Prophylactic Management of Skin Reactions Induced by Epidermal Growth Factor Receptor Inhibitors in Patients With Solid Tumors. *Oncologist* (2016) 21(12):1483–91. doi: 10.1634/theoncologist.2016-0051
186. Iimura Y, Shimomura H, Yasu T, Imanaka K, Ogawa R, Ito A, et al. Nsaids may Prevent EGFR-TKI-Related Skin Rash in Non-Small Cell Lung Cancer Patients. *Int J Clin Pharmacol Ther* (2018) 56(11):551–4. doi: 10.5414/CP203323
187. Eriksen JG, Kaalund I, Clemmensen O, Overgaard J, Pfeiffer P. Placebo-Controlled Phase II Study of Vitamin K3 Cream for the Treatment of Cetuximab-Induced Rash. *Support Care Cancer* (2017) 25(7):2179–85. doi: 10.1007/s00520-017-3623-x
188. Hofheinz RD, Lorenzen S, Trojan J, Ocvirk J, Ettrich TJ, Al-Batran SE, et al. EVITA-a Double-Blind, Vehicle-Controlled, Randomized Phase II Trial of Vitamin K1 Cream as Prophylaxis for Cetuximab-Induced Skin Toxicity. *Ann Oncol* (2018) 29(4):1010–5. doi: 10.1093/annonc/mdy015
189. Chayahara N, Mukohara T, Tachihara M, Fujishima Y, Fukunaga A, Washio K, et al. Adapalene Gel 0.1% Versus Placebo as Prophylaxis for Anti-Epidermal Growth Factor Receptor-Induced Acne-Like Rash: A Randomized Left-Right Comparative Evaluation (APPEARANCE). *Oncologist* (2019) 24(7):885–e413. doi: 10.1634/theoncologist.2019-0156

Conflict of Interest: The authors declare that the research was conducted in the absence of any commercial or financial relationships that could be construed as a potential conflict of interest.

Publisher's Note: All claims expressed in this article are solely those of the authors and do not necessarily represent those of their affiliated organizations, or those of the publisher, the editors and the reviewers. Any product that may be evaluated in this article, or claim that may be made by its manufacturer, is not guaranteed or endorsed by the publisher.

frontiers in Oncology

ORIGINAL RESEARCH
published: 08 March 2022
doi: 10.3389/fonc.2022.790343

A Risk Scoring System Utilizing Machine Learning Methods for Hepatotoxicity Prediction One Year After the Initiation of Tyrosine Kinase Inhibitors

*Ji Min Han[1], Jeong Yee[2], Soyeon Cho[2,3], Min Kyoung Kim[4,5], Jin Young Moon[2,6], Dasom Jung[3,4], Jung Sun Kim[2,5] and Hye Sun Gwak[2]**

[1] College of Pharmacy, Chungbuk National University, Cheongju-si, South Korea, [2] College of Pharmacy and Graduate School of Pharmaceutical Sciences, Ewha Womans University, Seoul, South Korea, [3] Department of Pharmacy, Asan Medical Center, Seoul, South Korea, [4] Graduate School of Converging Clinical and Public Health, Ewha Womans University, Seoul, South Korea, [5] Department of Pharmacy, Seoul National University Hospital, Seoul, South Korea, [6] Department of Pharmacy, National Cancer Center, Goyang-si, South Korea

OPEN ACCESS

Edited by:
Jennifer Martin,
The University of Newcastle, Australia

Reviewed by:
Shawn D. Spencer,
Philadelphia College of Osteopathic Medicine (PCOM), United States
Yves Horsmans,
Cliniques Universitaires Saint-Luc, Belgium

***Correspondence:**
Hye Sun Gwak
hsgwak@ewha.ac.kr
orcid.org/0000-0003-0278-2563

Specialty section:
This article was submitted to Pharmacology of Anti-Cancer Drugs, a section of the journal Frontiers in Oncology

Received: 06 October 2021
Accepted: 14 February 2022
Published: 08 March 2022

Citation:
Han JM, Yee J, Cho S, Kim MK, Moon JY, Jung D, Kim JS and Gwak HS (2022) A Risk Scoring System Utilizing Machine Learning Methods for Hepatotoxicity Prediction One Year After the Initiation of Tyrosine Kinase Inhibitors. Front. Oncol. 12:790343. doi: 10.3389/fonc.2022.790343

Background: There is currently no method to predict tyrosine kinase inhibitor (TKI) -induced hepatotoxicity. The purpose of this study was to propose a risk scoring system for hepatotoxicity induced within one year of TKI administration using machine learning methods.

Methods: This retrospective, multi-center study analyzed individual data of patients administered different types of TKIs (crizotinib, erlotinib, gefitinib, imatinib, and lapatinib) selected in five previous studies. The odds ratio and adjusted odds ratio from univariate and multivariate analyses were calculated using a chi-squared test and logistic regression model. Machine learning methods, including five-fold cross-validated multivariate logistic regression, elastic net, and random forest were utilized to predict risk factors for the occurrence of hepatotoxicity. A risk scoring system was developed from the multivariate and machine learning analyses.

Results: Data from 703 patients with grade II or higher hepatotoxicity within one year of TKI administration were evaluated. In a multivariable analysis, male and liver metastasis increased the risk of hepatotoxicity by 1.4-fold and 2.1-fold, respectively. The use of anticancer drugs increased the risk of hepatotoxicity by 6.0-fold. Patients administered H2 blockers or PPIs had a 1.5-fold increased risk of hepatotoxicity. The area under the receiver-operating curve (AUROC) values of machine learning methods ranged between 0.73-0.75. Based on multivariate and machine learning analyses, male (1 point), use of H2 blocker or PPI (1 point), presence of liver metastasis (2 points), and use of anticancer drugs (4 points) were integrated into the risk scoring system. From a training set, patients with 0, 1, 2-3, 4-7 point showed approximately 9.8%, 16.6%, 29.0% and 61.5% of risk of hepatotoxicity, respectively. The AUROC of the scoring system was 0.755 (95% CI, 0.706-0.804).

Conclusion: Our scoring system may be helpful for patient assessment and clinical decisions when administering TKIs included in this study.

Keywords: tyrosine kinase inhibitor, hepatotoxicity, prediction, machine learning, risk scoring system

INTRODUCTION

Tyrosine kinase inhibitor (TKI) is a prominent cancer treatment. Tyrosine kinase is a major enzyme involved in cell signaling, growth, and division during cell signal transduction (1). TKI inhibits tyrosine kinase, which is involved in cancer (2). Since the U.S. Food and Drug Administration (FDA) approved imatinib for the treatment of chronic myeloid leukemia in 2001, over 30 TKIs have been developed (3, 4).

Hepatotoxicity is a major safety concern when using tyrosine kinase inhibitors (5). The FDA requires five TKIs (lapatinib, pazopanib, ponatinib, regorafenib, and sunitinib) to have black box warnings for liver damage (4, 6). Several studies have investigated TKI-induced hepatotoxicity, mostly in patients experiencing grade I-IV hepatotoxicity (7). However, it is difficult to find clinically significant grade I cases as these include mild and asymptomatic patients.

Since there are no reliable markers for the detection of drug-induced hepatotoxicity, it is important to exclude other possible causes (8, 9). The follow-up period should be limited, as longer observation periods make it difficult to detect drug-induced hepatotoxicity because other factors may come into play (7, 10, 11). The period from TKI initiation to hepatotoxicity onset varies widely, with the latency to the onset of hepatotoxicity reported within two months for crizotinib and several days to several months for lapatinib (12). A proper observation period for hepatotoxicity has not been established, but one year (365 days) may be appropriate.

Machine learning establishes computational modeling for automatic learning based on existing data (13). Since the machine learning approach can devise learning algorithms to deduce clinical action and decision making, it has been applied in various ways in the field of health science, including risk prediction (14, 15). Utilizing various methods of machine learning may build models with higher risk predictability that can explain risk factors.

Risk scoring systems, such as the GerontoNet ADR risk score for elderly patients and TIMI risk score for cardiovascular disease, allow a rapid assessment of patients for medical decision-making and patient management (16). They reveal the relationship between patient risk factors and the incidence of an adverse event and a disease (17). Although it may help clinicians predict hepatotoxicity after TKI administration, a risk scoring system has not yet been investigated.

Although TKI-induced hepatotoxicity is a significant clinical concern, there is currently no tool to predict its development. The purpose of this study is to identify risk factors for TKI-induced hepatotoxicity of grade II or higher that occur within one year of TKI initiation using machine learning methods and to propose a risk scoring system of TKI-induced hepatotoxicity.

MATERIALS AND METHODS

Dataset

The dataset was constructed from five previous studies that demonstrated factors affecting the hepatotoxicity of selected TKIs (gefitinib, erlotinib, crizotinib, imatinib, and lapatinib). The detailed methodology was reported in five published studies. In a gefitinib study, patients with non-small cell lung cancer (NSCLC) were orally administered 250 mg of gefitinib per day (18). Patients with NSCLC or pancreatic cancer were administered 150 mg or 100 mg of erlotinib, respectively (19). Patients with NSCLC containing an anaplastic lymphoma kinase (ALK) rearrangement or c-ros oncogene 1 (ROS1) rearrangement were orally administered 250 mg of crizotinib twice per day (20). Patients with Philadelphia chromosome-positive acute lymphoblastic leukemia (ALL), chronic myeloid leukemia (CML), gastrointestinal stromal tumors (GIST), or other malignancies were orally administered imatinib (100-800 mg/day) (21). Patients with metastatic breast cancer were orally administered lapatinib (750-1250 mg/day) (22). In all five studies, aspartate aminotransferase (AST) and alanine aminotransferase (ALT) levels were measured before initiation of TKI therapy and then every two to three months thereafter. Eligible patients were those who were followed up in a year.

The following baseline data were obtained: sex, age, body weight, height, body surface area (BSA), alcohol history, underlying disease, liver metastasis, HBsAg, and concomitant medications. Concomitant drugs included cytochrome P450 (CYP) 3A4 inducers, CYP3A4 inhibitors, anticancer drugs, H2 blockers, and proton pump inhibitors (PPIs). CYP3A4 inducers included bosentan, carbamazepine, dexamethasone, efavirenz, ethosuximide, etravirine, fosphenytoin, modafinil, nafcillin, oxcarbazepine, phenobarbital, phenytoin, prednisolone, primidone, rifabutin, and rifampicin (rifampin). CYP3A4 inhibitors were amiodarone, aprepitant, atazanavir, cimetidine, ciprofloxacin, clarithromycin, cyclosporine, danazol, diltiazem, erythromycin, fluconazole, fluoxetine, fluvoxamine, grapefruit juice, itraconazole, ketoconazole, nicardipine, nifedipine, posaconazole, ritonavir, tamoxifen, verapamil, and voriconazole. Anticancer drugs included capecitabine, cisplatin, cyclophosphamide, cytarabine, docetaxel, trastuzumab, vincristine, and vinorelbine. H2 blockers were cimetidine, famotidine, lafutidine, nizatidine, and ranitidine. PPIs included (es)omeprazole, (dex)lansoprazole, pantoprazole, and rabeprazole.

Assessment of Hepatotoxicity

Serum AST and ALT values were assessed according to the severity of hepatotoxicity. The hepatotoxicity grade was determined using Common Terminology Criteria for Adverse Events (CTCAE) version 4.0. The CTCAE defines grade I, grade II, grade III, and grade IV toxicity levels of AST and ALT as 1-3

times, 3-5 times, 5-20 times, and more than 20 times the upper limit of normal, respectively. In this study, hepatotoxicity was defined as grade II or higher.

Statistical Analysis

The chi-squared or Fisher's exact test was performed to compare categorical variables between patients with and without hepatotoxicity. Multivariate logistic regression analysis was performed to identify independent risk factors for hepatotoxicity. Factors having a P-value < 0.05 from the univariate analysis with strong confounding factors (age, BSA, and sex) were included in the multivariate analysis. The odds ratio (OR) and adjusted OR were calculated by univariate and multivariate analyses, respectively.

Machine learning models were developed to predict the risk factors for hepatotoxicity. Classification methods, such as five-fold cross-validated multivariable logistic regression, elastic net, and random forest (RF) were utilized with an R package caret. For cross-validation, the dataset was randomly split into five equal folds. After portioning one data sample into five subsets, four subsets were used to construct machine learning models and the other subset was used for model validation. Each cross-validation iteration was repeated 100 times. The area under the receiver-operating curve (AUROC) was developed to predict hepatotoxicity.

A risk scoring system was developed from the multivariate and machine learning analyses. We randomly divided the data by a ratio of 7:3. Among a total of 703 samples included in this study, data from 503 patients were used to construct a risk scoring system, and the other 200 data were used to validate it. For the risk score, each coefficient from the logistic regression model was divided by the smallest one and rounded to the nearest integer.

P-values less than 0.05 were considered statistically significant. Univariate and multivariate analyses were performed with the Statistical Package for Social Sciences (SPSS) version 20.0 for Windows (SPSS Inc., Chicago, Illinois, USA). Machine learning models were developed using R software version 3.6.0 (RFoundation for Statistical Computing, Vienna, Austria).

RESULTS

Among the 999 patients eligible in this study, patients were excluded if they did not have AST/ALT value results before TKI administration (n = 72), if they had elevated AST/ALT before TKI administration (n = 123), and if they already had underlying liver disease (n = 101). We analyzed data from 703 patients. For the excluded patients, the mean age, proportion of patients ≥ 60 years, and proportion of males were 60.6 ± 13.1 years, 56.3%, and 47.8%, respectively. There were no significant differences in the mean age or proportion of sex between the included and excluded patients.

As shown in **Table 1**, 191 patients experienced the hepatotoxicity induced by the selected TKIs during the study period. Around half (50.2%) of the patients were older than 60 years of age. Drugs concomitantly administered with TKI included CYP3A4 inhibitors (n = 26), CYP3A4 inducers (n = 33), H2 blockers (n = 202), PPIs (n = 114), and anticancer drugs (n = 161). In the univariate analysis, liver metastasis, CYP3A4 inhibitors, CYP3A4 inducers, anticancer drugs, H2 blockers, PPIs, and H2 blockers or PPIs were significant factors for hepatotoxicity.

Multivariate analysis demonstrated that male patients and patients with liver metastasis had increased risk for TKI-induced hepatotoxicity by 1.4-fold and 2.1-fold, respectively. The use of anticancer drugs increased the risk of hepatotoxicity by 6.0-fold. Patients using H2 blockers or PPIs had a 1.5-fold increased risk of hepatotoxicity (**Table 2**).

Machine learning methods were utilized to construct a prediction model for TKI-associated hepatotoxicity. The AUROC values (mean, 95% CI) across 100 random iterations using five-fold cross-validated multivariate logistic regression, elastic net, and RF models were 0.75, 0.75, and 0.73, respectively (**Table 3**). The ROC for five-fold cross-validated multivariate logistic regression, elastic net, and RF are shown in **Figure 1**. The hyperparameters and R code that we used are shown in **Table 4** and **Supplementary File 1**, respectively.

For the construction of risk scoring system, male (1 point), use of H2 blockers or PPIs (1 point), presence of liver metastasis (2 points), and use of anticancer drugs (4 points) were integrated into the analysis. From a training set, patients with 0, 1, 2-3, and 4-7 points showed approximately 9.8%, 16.6%, 29.0%, and 61.5% risk of hepatotoxicity, respectively. The respective value of the validation set was 10.2, 19.3, 30.8, and 57.1%. Although there were only two patients who scored 8 points (100% risk), they were all included in the training set. The logistic regression curve by mapping the scores to risk scores is presented in **Figure 2**, and the risk probability according to scores using logistic regression is shown in **Table 5**. The AUROC of the scoring system was 0.755 (95% CI 0.706-0.804).

DISCUSSION

This study demonstrated that the use of H2 blockers or PPIs and anticancer drugs increased the risk of the hepatotoxicity induced by the TKIs selected in this study (crizotinib, erlotinib, gefitinib, imatinib, and lapatinib) by 1.5-fold and 6.0-fold, respectively. Patients with liver metastasis and male patients had an increased risk of TKI-induced hepatotoxicity by 2.1-fold and by 1.4-fold, respectively. Machine learning analyses indicated good performance (higher than 0.7) of the constructed model.

In our study, the presence of liver metastasis was a significant factor with the two-fold increase in hepatotoxicity by TKIs included in this study. Because patients with elevated AST and ALT were excluded, all patients had normal AST/ALT values at the start of the study. The relationship between liver metastasis and drug-induced hepatotoxicity has been rarely reported. However, a retrospective observational study of pembrolizumab-induced liver injury showed that patients with pre-existing liver

TABLE 1 | Hepatotoxicity of TKI administration.

Characteristics		No. (%) (n=703)	Hepatotoxicity, No (%)		*P*-value
			Absence (n=512)	Presence (n=191)	
Sex					0.980
	Female	408 (58.0)	297 (58.0)	111 (58.1)	
	Male	295 (42.0)	215 (42.0)	80 (41.9)	
Age, years					0.064
	<60	350 (49.8)	244 (47.7)	106 (55.5)	
	≥60	353 (50.2)	268 (52.3)	85 (44.5)	
BW, kg[a]					0.253
	<60	379 (54.6)	268 (53.3)	111 (58.1)	
	≥60	315 (45.4)	235 (46.7)	80 (41.9)	
Height, cm[b]					0.540
	<160	336 (48.5)	247 (49.2)	89 (46.6)	
	≥160	357 (51.5)	255 (50.8)	102 (53.4)	
BSA, m^{2}[c]					0.346
	<1.6	321 (46.3)	227 (45.2)	94 (49.2)	
	≥1.6	372 (53.7)	275 (54.8)	97 (50.8)	
Alcohol history[d]					0.257
	Yes	86 (27.7)	67 (29.4)	19 (22.9)	
	No	225 (72.3)	161 (70.6)	64 (77.1)	
CVD or DM					0.289
	Yes	254 (36.1)	191 (37.3)	63 (33.0)	
	No	449 (63.9)	321 (62.7)	128 (67.0)	
Liver metastasis					<0. 001
	Yes	76 (10.8)	34 (6.6)	42 (22.0)	
	No	627 (89.2)	478 (93.4)	149 (78.0)	
HBsAg[e]					0.556
	Yes	18 (2.6)	12 (2.4)	6 (3.2)	
	No	665 (97.4)	485 (97.6)	180 (96.8)	
CYP3A4 inhibitors					<0. 001
	Yes	26 (3.7)	11 (2.1)	15 (7.9)	
	No	677 (96.3)	501 (97.9)	176 (92.1)	
CYP3A4 inducers					<0. 001
	Yes	33 (4.7)	14 (2.7)	19 (9.9)	
	No	670 (95.3)	498 (97.3)	172 (90.1)	
H2 blockers					0.005
	Yes	202 (28.7)	132 (25.8)	70 (36.6)	
	No	501 (71.3)	380 (74.2)	121 (63.4)	
PPIs					0.021
	Yes	114 (16.2)	73 (14.3)	41 (21.5)	
	No	589 (83.8)	439 (85.7)	150 (78.5)	
H2 blockers/PPIs					<0. 001
	Yes	281 (40.0)	183 (35.7)	98 (51.3)	
	No	422 (60.0)	329 (64.3)	93 (48.7)	
Anticancer drugs					<0. 001
	Yes	161 (22.9)	63 (12.3)	98 (51.3)	
	No	542 (77.1)	449 (87.7)	93 (48.7)	

BW, body weight; BSA, body surface area; CVD, cardiovascular diseases; CYP3A4, cytochrome P450 3A4; DM, diabetes mellitus; PPI, proton pump inhibitor.

[a]*Body weight data for 9 patients were missing.*

[b]*Height data for 10 patients were missing.*

[c]*Body surface area data for 10 patients were missing.*

[d]*Alcohol history data for 392 patients were missing.*

[e]*HBsAg data for 20 patients were missing.*

metastasis were at a 3.6-fold higher risk of developing hepatotoxicity compared to patients with no liver metastasis (23). As the main metabolic site for most TKIs is the liver, the presence of liver metastasis may lead to asymptomatic liver damage before TKI use and may amplify the effects of TKI-induced hepatotoxicity.

TKIs are often used in combination with other anticancer drugs. Previous studies have reported hepatotoxicity by many anticancer drugs, including methotrexate, cisplatin, gemcitabine, and paclitaxel (24). Thus, anticancer drugs used in combination with TKIs not only affect hepatotoxicity by themselves but may further aggravate the severity of hepatotoxicity caused by TKIs.

TABLE 2 | Univariate and multivariate analyses to identify predictors for hepatotoxicity related to TKI administration.

Characteristics	Unadjusted OR (95% CI)	Adjusted OR (95% CI)
Male	0.996 (0.711-1.394)	1.418 (0.962-2.090)
Age ≥ 60 years	0.730 (0.523-1.020)	
BSA ≥ 1.6	0.852 (0.610-1.189)	
Liver metastasis	3.963 (2.432-6.457)**	2.146 (1.224-3.762)**
CYP3A4 inhibitors	3.882 (1.750-8.611)**	
CYP3A4 inducers	3.929 (1.928-8.007)**	
Anticancer drugs	7.510 (5.098-11.063)**	6.002 (3.956-9.107)**
H2 blockers	1.665 (1.168-2.375)**	
PPIs	1.644 (1.075-2.514)*	
H2 blockers/PPIs	1.894 (1.353-2.652)**	1.461 (0.987-2.163)

BSA, body surface area; CYP3A4, cytochrome P450 3A4; OR, odds ratio; PPI, proton pump inhibitor.
**P < 0.05, **P < 0.01.*

For the construction of the risk scoring system, we included all factors that remained in the final multivariate analysis model, regardless of statistical significance. In addition to liver metastasis and anticancer drugs, male and the use of H2 blockers/PPIs were included in the risk scoring system. Contrary to our expectations, male sex increased the risk of TKI-induced hepatotoxicity in our study. Several studies have demonstrated that female patients generally had a higher risk of adverse drug reactions compared to male patients, and these results were similar for drug-induced hepatotoxicity (25, 26). Physiological or biological differences which can affect drug toxicity may contribute to these gender differences (27). Our unexpected result is probably due to the effect of alcohol history. Male patients accounted for the majority (70%) of patients with a history of alcohol use, and 70% of these individuals had hepatotoxicity. Considering that female patients accounted for more than half of our study population, alcohol history may be an influencing factor in the higher incidence of hepatotoxicity in male patients.

Concomitant use of PPIs or H2 blockers increased the risk of hepatotoxicity compared to non-users. ATP-binding cassette superfamily G member 2 (ABCG2) and ATP-binding cassette subfamily B member 1 (ABCB1) are drug efflux transporters situated in the liver (28). Since PPIs are known as an ABCG2 inhibitors, concomitant use of ABCG2 substrates and PPIs can increase the blood concentration of drugs that are ABCG2 substrates (18, 19). Among the five drugs included in our study, gefitinib and erlotinib are substrates of ABCG2. Since half of the total study population was patients administered these drugs, this may have affected the analysis of PPIs as a hepatotoxicity factor.

Both H2 blockers and TKIs are ABCB1 substrates. Co-administration of both ABCB1 substrates can cause competitive efflux transport, meaning other ABCB1 substrates such as TKIs remain in the liver instead of H2 blockers exiting. This increases the risk of TKI-induced hepatotoxicity.

TKIs as a class with different mechanisms were included in this study. Like differences between epidermal growth factor receptor (EGFR) TKIs and non-receptor TKIs, differences in mechanisms may affect the occurrence of TKI-induced toxicity (29). However, this was not found in this study, probably because many TKIs have multiple targets, as imatinib mainly targets bcr-abl but also affects a receptor tyrosine kinase, platelet-derived growth factor receptor (PDGFR).

TKIs included in this study were used as a single daily dose (gefitinib 250 mg, crizotinib 250 mg, and lapatinib 1250 mg) except for imatinib and erlotinib, and the effects of drug doses on hepatotoxicity were not found in both drugs. In the case of imatinib, the dose range was 100 to 800 mg daily; it was not a significant factor for imatinib-induced hepatotoxicity in the multivariate analysis. For erlotinib, the daily dose was either 100 mg or 150 mg, and the statistical significance was not found. Since the three drugs among five TKIs in this study were used as a single dose, the effect of drug doses on clinical efficacy and safety should be further investigated.

The AUROC values of machine learning methods ranged between 0.73-0.75. The machine learning methods that showed the best AUROC values were the five-fold multivariable logistic regression model and the elastic net model, a penalized linear regression model that combined the penalties of the lasso and ridge methods (30). The constructed risk scoring system showed good performance with the AUROC value of 0.75.

TABLE 3 | Machine learning models' performance.

Model	AUROC (95% CI)	Sensitivity	Specificity
Multivariate logistic regression	0.75 (0.701 - 0.804)	0.601	0.836
Elastic net	0.75 (0.703 - 0.805)	0.601	0.838
Random forest	0.73 (0.681 - 0.775)	0.601	0.838

AUROC, area under the receiver-operating curve; CI, confidence interval.

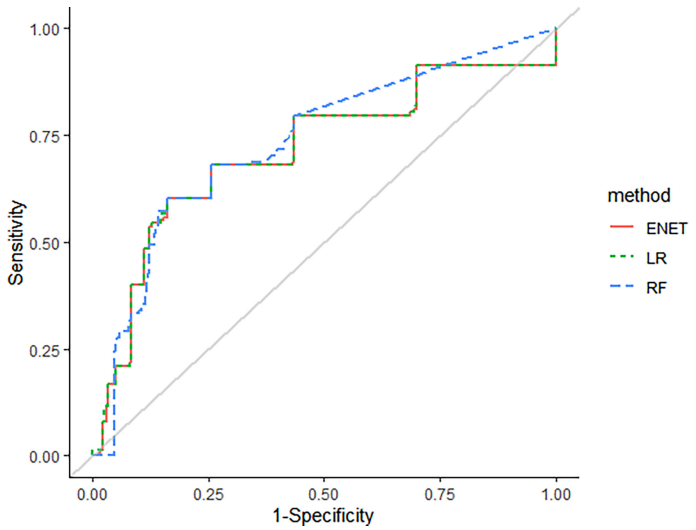

FIGURE 1 | The receiver-operating curves (ROC) for five-fold cross-validated multivariate logistic regression, elastic net, and random forest (RF).

TABLE 4 | Machine learning model specifics.

Method	Hyperparameter	
	Model specification and search grids	**Selected values**
Elastic net	λ: 100 equally spaced values in logarithmic scale between 10^{-4} and 0 α: 0, 0.2, 0.4, 0.6, 0.8, 1	λ: 0.03511192 α: 0
Random forests	mtry: 1-4	mtry: 1

SVM, Support vector machine.

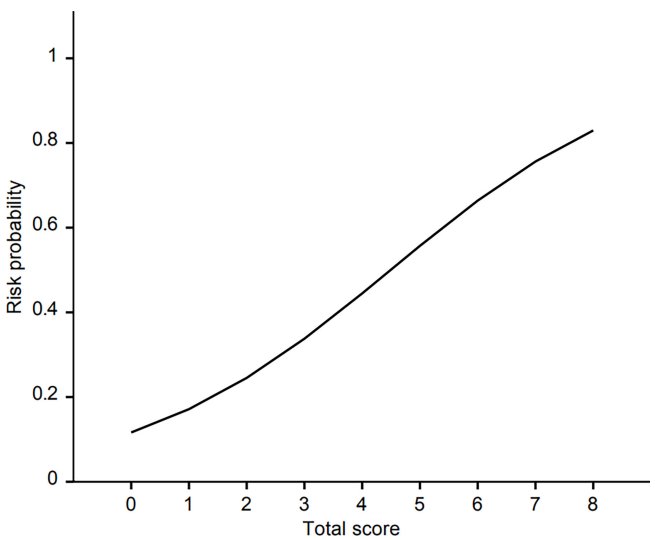

FIGURE 2 | The logistic regression curve of the probability of hepatotoxicity versus the proposed scoring scale.

TABLE 5 | Risk of hepatotoxicity according to scores using logistic regression.

Score	0	1	2	3	4	5	6	7	8
Risk probability	0.116	0.172	0.245	0.338	0.445	0.557	0.664	0.756	0.830

There are several limitations to this study. The main limitation is the retrospective design of our study. It was impossible to obtain the patient's drug concentration to assess the relationship with the onset of hepatotoxicity or the patient's tissue to analyze the pattern of hepatotoxicity. In addition, not all TKIs were included in this study; especially, only one TKI among five TKIs with black box warning for hepatotoxicity was analyzed, Therefore, it needs to be cautious to apply this result to other TKIs. Since a relatively large number of patients were excluded according to the exclusion criteria, it is possible that real-world data could be different. However, the characteristics between included patients and excluded patients were not significantly different. Despite several shortcomings, our study is significant because it is the first to develop a risk scoring system for the hepatotoxicity caused by the selected TKIs in cancer patients. Furthermore, machine learning models were used to predict the increased risk of hepatotoxicity.

In conclusion, our study demonstrated that the presence of liver metastasis and the concurrent use of PPIs or H2 blockers were related to TKI-induced hepatotoxicity. Male patients and patients administered anticancer drugs experienced an increased risk of hepatotoxicity. Before applying these results to clinical settings, it is necessary to consider other factors that may affect the efficacy and safety of the TKIs, such as daily dose, drug interaction, and genetic factors. Considering our retrospective study design and only five selected TKIs were included in this study, further prospective studies are needed to validate our findings.

DATA AVAILABILITY STATEMENT

The raw data supporting the conclusions of this article will be made available by the authors, without undue reservation.

ETHICS STATEMENT

All procedures performed in five studies involving human participants were in accordance with the ethical standards of the relevant ethics committees, which approved the studies. The Ethics committees were as follow; the Clinical Research Ethics Committee of the Seoul National University Hospitals, The Asan Medical Center Clinical Research Ethics Committee, the Institutional Review Board of National Cancer Center, Korea. Written informed consent for participation was not required for this study due to the retrospective nature of this study.

AUTHOR CONTRIBUTIONS

All the authors have made substantial contributions to the conception of the study. All the authors contributed to designing the study. JH, SC, MK, JM, DJ, and JK contributed to material preparation and data collection. JH, JY, and HG performed data analysis and interpretation. JH contributed to drafting of the manuscript. HG contributed to critical revision of the manuscript. All authors approved the final manuscript.

SUPPLEMENTARY MATERIAL

The Supplementary Material for this article can be found online at: https://www.frontiersin.org/articles/10.3389/fonc.2022.790343/full#supplementary-material

REFERENCES

1. Wang Z, Cole PA. Catalytic Mechanisms and Regulation of Protein Kinases. *Methods Enzymol* (2014) 548:1–21. doi: 10.1016/B978-0-12-397918-6.00001-X
2. Drake JM, Lee JK, Witte ON. Clinical Targeting of Mutated and Wild-Type Protein Tyrosine Kinases in Cancer. *Mol Cell Biol* (2014) 34(10):1722–32. doi: 10.1128/MCB.01592-13
3. Wu P, Nielsen TE, Clausen MH. FDA-Approved Small-Molecule Kinase Inhibitors. *Trends Pharmacol Sci* (2015) 36(7):422–39. doi: 10.1016/j.tips.2015.04.005
4. Paludetto MN, Puisset F, Chatelut E, Arellano C. Identifying the Reactive Metabolites of Tyrosine Kinase Inhibitors in a Comprehensive Approach: Implications for Drug-Drug Interactions and Hepatotoxicity. *Med Res Rev* (2019) 39(6):2105–52. doi: 10.1002/med.21577
5. Wu Z, Chen S, Du X, Wu Y, Xie X. Hepatotoxicity With Epidermal Growth Factor Receptor Tyrosine Kinase Inhibitors in Non-Small-Cell Lung Cancer Patients: A Network Meta-Analysis. *J Clin Pharm Ther* (2021) 46(2):310–8. doi: 10.1111/jcpt.13281
6. Zhang J, Ren L, Yang X, White M, Greenhaw J, Harris T, et al. Cytotoxicity of 34 FDA Approved Small-Molecule Kinase Inhibitors in Primary Rat and Human Hepatocytes. *Toxicol Lett* (2018) 291:138–48. doi: 10.1016/j.toxlet.2018.04.010
7. Qian J, Zhang X, Zhang B, Yan B, Wang L, Gu P, et al. Tyrosine Kinase Inhibitor-Related Hepatotoxicity in Patients With Advanced Lung Adenocarcinoma: A Real-World Retrospective Study. *Cancer Manag Res* (2020) 12:3293–9. doi: 10.2147/CMAR.S237968
8. Abboud G, Kaplowitz N. Drug-Induced Liver Injury. *Drug Saf* (2012) 20:277–94. doi: 10.2165/00002018-200730040-00001
9. Andrade R, Robles M, Fernandez-Gastaner A, Lopez-Ortega S, Lopez-Vega M, Lucena M. Assessment of Drug-Induced Hepatotoxicity in Clinical Practice: A Challenge for Gastroenterologists. *World J Gastroenterol* (2007) 13(3):329–40. doi: 10.3748/wjg.v13.i3.329
10. Grothey A, Cutsem E, Sobrero A, Siena S, Falcone A, Ychou M, et al. Regorafenib Monotherapy for Previously Treated Metastatic Colorectal Cancer (CORRECT): An International, Multicentre, Randomised, Placebo-Controlled, Phase 3 Trial. *Lancet* (2013) 381:303–12. doi: 10.1016/S0140-6736(12)61900-X
11. Argilés G, Saunders MP, Rivera F, Sobrero A, Benson A, Guillén Ponce C, et al. Regorafenib Plus Modified FOLFOX6 as First-Line Treatment of Metastatic Colorectal Cancer: A Phase II Trial. *Eur J Cancer* (2015) 51(8):942–9. doi: 10.1016/j.ejca.2015.02.013
12. Shah RR, Morganroth J, Shah DR. Hepatotoxicity of Tyrosine Kinase Inhibitors: Clinical and Regulatory Perspectives. *Drug Saf* (2013) 36(7):491–503. doi: 10.1007/s40264-013-0048-4

13. Shung DL, Au B, Taylor RA, Tay J, Laursen S, Stanley A, et al. Validation of a Machine Learning Model That Outperforms Clinical Risk Scoring Systems for Upper Gastrointestinal Bleeding. *Gastroenterology* (2020) 158(1):160–7. doi: 10.1053/j.gastro.2019.09.009
14. Kourou K, Exarchos TP, Exarchos KP, Karamouzis M, Fotiadis D. Machine Learning Applications in Cancer Prognosis and Prediction. *Comput Struct Biotechnol* (2015) 13:8–17. doi: 10.1016/j.csbj.2014.11.005
15. Weng SF, Reps J, Kai J, Garibaldi J, Qureshi N. Can Machine-Learning Improve Cardiovascular Risk Prediction Using Routine Clinical Data? *PloS One* (2017) 12(4):0174944. doi: 10.1371/journal.pone.0174944
16. Onder G, Petrovic M, Tangiisuran B, Meinardi T, Markito-Notenboom W, Somers A, et al. Development and Validation of a Score to Assess Risk of Adverse Drug Reactions Among in-Hospital Patients 65 Years or Older: The GerontoNet ADR Risk Score. *Arch Intern Med* (2010) 170(13):1142–8. doi: 10.1001/archinternmed.2010.153
17. Austin P, Lee D, D'Agostino R, Fine J. Developing Points-Based Risk-Scoring Systems in the Presence of Competing Risks. *Stat Med* (2016) 35(22):4056–72. doi: 10.1002/sim.6994
18. Cho S, Yee J, Kim JY, Rhie SJ, Gwak HS. Effects of Concomitant Medication Use on Gefitinib-Induced Hepatotoxicity. *J Clin Pharmacol* (2018) 58(2):263–8. doi: 10.1002/jcph.1010
19. Kim MK, Yee J, Cho YS, Jang HW, Han JM, Gwak HS. Risk Factors for Erlotinib-Induced Hepatotoxicity: A Retrospective Follow-Up Study. *BMC Cancer* (2018) 18(1):1–7. doi: 10.1186/s12885-018-4891-7
20. Jung D, Han JM, Yee J, Kim JY, Gwak HS. Factors Affecting Crizotinib-Induced Hepatotoxicity in Non-Small Cell Lung Cancer Patients. *Med Oncol* (2018) 35(12):1–7. doi: 10.1007/s12032-018-1213-5
21. Han JM, Yee J, Cho YS, Gwak HS. Factors Influencing Imatinib-Induced Hepatotoxicity. *Cancer Res Treat* (2020) 52(1):181–8. doi: 10.4143/crt.2019.131
22. Moon JY, Han JM, Seo I, Gwak HS. Risk Factors Associated With the Incidence and Time to Onset of Lapatinib-Induced Hepatotoxicity. *Breast Cancer Res Treat* (2019) 178(1):239–44. doi: 10.1007/s10549-019-05382-x
23. Tsung I, Dolan R, Lao C, Fecher L, Riggenbach K, Yeboah-Kprang A, et al. Liver Injury Is Most Commonly Due to Hepatic Metastases Rather Than Drug Hepatotoxicity During Pembrolizumab Immunotherapy. *Aliment Pharmacol Ther* (2019) 50(7):800–8. doi: 10.1111/apt.15413
24. Deleve L. Hepatotoxicity by Anticancer Therapy. In: DW Kufe, editor. *Holland-Frei Cancer Medicine*. Hamilton (ON: BC Decker (2003). p. 254–61.
25. Zopf Y, Rabe C, Neubert A, Gassmann K, Rascher W, Hahn E, et al. Women Encounter ADRs More Often Than do Men. *Eur J Clin Pharmacol* (2008) 64 (10):999–1004. doi: 10.1007/s00228-008-0494-6
26. Rademaker M. Do Women Have More Adverse Drug Reactions? *Am J Clin Dermatol* (2001) 2(6):349–51. doi: 10.2165/00128071-200102060-00001
27. Amacher D. Female Gender as a Susceptibility Factor for Drug-Induced Liver Injury. *Hum Exp Toxicol* (2014) 33(9):928–39. doi: 10.1177/0960327113512860
28. Sharom FJ. ABC Multidrug Transporters: Structure, Function and Role in Chemoresistance. *Pharmacogenomics* (2008) 9:105–27. doi: 10.2217/14622416.9.1.105
29. Sivven KS, Prabhu KS, Achkar IW, Kuttikrishnan S, Shyam S, Khan AQ, et al. Role of Non Receptor Tyrosine Kinases in Hematological Malignances and Its Targeting by Natural Products. *Mol Cancer* (2018) 17(1):31. doi: 10.1186/s12943-018-0788-y
30. Zou H, Hastie T. Regularization and Variable Selection *via* the Elastic Net. *J R Stat Soc Ser B Stat Methodol* (2005) 67:301–20. doi: 10.1111/j.1467-9868.2005.00503.x

Conflict of Interest: The authors declare that the research was conducted in the absence of any commercial or financial relationships that could be construed as a potential conflict of interest.

Publisher's Note: All claims expressed in this article are solely those of the authors and do not necessarily represent those of their affiliated organizations, or those of the publisher, the editors and the reviewers. Any product that may be evaluated in this article, or claim that may be made by its manufacturer, is not guaranteed or endorsed by the publisher.

frontiers in Pharmacology

REVIEW
published: 18 March 2022
doi: 10.3389/fphar.2022.854967

PD-1/PD-L1 Inhibitors in Patients With Preexisting Autoimmune Diseases

Ke Zhang[1†], Xiangyi Kong[1†], Yuan Li[1], Zhongzhao Wang[1], Lin Zhang[2,3,4]* and Lixue Xuan[1]**

[1]Department of Breast Surgical Oncology, National Cancer Center/National Clinical Research Center for Cancer/Cancer Hospital, Chinese Academy of Medical Sciences and Peking Union Medical College, Beijing, China, [2]School of Population Medicine and Public Health, Chinese Academy of Medical Sciences and Peking Union Medical College, Beijing, China, [3]Melbourne School of Population and Global Health, the University of Melbourne, Melbourne, VIC, Australia, [4]Centre of Cancer Research, Victorian Comprehensive Cancer Centre, Melbourne, VIC, Australia*

Autoimmune diseases and malignant tumors are the two hotspots and difficulties that are currently being studied and concerned by the medical field. The use of PD-1/PD-L1 inhibitors improves the prognosis of advanced tumors, but excessive immune responses can also induce immune-related adverse events (irAEs). Due to this concern, many clinical trials exclude cancer patients with preexisting autoimmune disease (AID). This review outlines the possible mechanisms of irAE, discusses the safety and efficacy of PD-1/PD-L1 inhibitors in cancer patients with preexisting AID, and emphasizes the importance of early recognition, continuous monitoring, and multidisciplinary cooperation in the prevention and management of cancer patients with preexisting AID.

Keywords: PD-1/PD-L1 inhibitors, autoimmune diseases, cancer, immune-related adverse events, immunotherapy

OPEN ACCESS

Edited by:
Miao Yan,
Central South University, China

Reviewed by:
Shiyu Xiao,
Peking University Third Hospital, China
Hong Huang,
Peking University First Hospital, China

****Correspondence:***
Zhongzhao Wang
wangzhongzhao206@sina.com
Lin Zhang
tony1982110@gmail.com
Lixue Xuan
xuanlx@hotmail.com

†These authors have contributed equally to this work

Specialty section:
This article was submitted to Pharmacology of Anti-Cancer Drugs, a section of the journal Frontiers in Pharmacology

Received: *14 January 2022*
Accepted: *17 February 2022*
Published: *18 March 2022*

Citation:
Zhang K, Kong X, Li Y, Wang Z, Zhang L and Xuan L (2022) PD-1/PD-L1 Inhibitors in Patients With Preexisting Autoimmune Diseases. Front. Pharmacol. 13:854967. doi: 10.3389/fphar.2022.854967

INTRODUCTION

Programmed cell death protein 1 receptor (PD-1), also known as CD279, is a type I transmembrane protein receptor containing 288 amino acids. It was first described in the early 1990s and is expressed during apoptosis induction in T cell hybridomas (Gong et al., 2018). Subsequent reports found that PD-1-deficient mice exhibited autoimmune disease-like features (lupus-like arthritis, glomerulonephritis, and splenomegaly), demonstrating that PD-1 is a negative regulator of immune response (Nishimura et al., 1999). PD-1 is expressed on activated T cells, B cells, macrophages, regulatory T cells (Tregs), and natural killer (NK) cells. Binding to programmed death ligand 1 (PD-L1 or B7-H1) or PD-L2 (B7-DC) negatively regulates T cell-mediated immune responses in peripheral tissues to limit the effector T cell responses and protect the tissues from immune-mediated tissue damage (Keir et al., 2008). The interaction of PD-1/PD-L1 in the tumor microenvironment can promote T cell dysfunction, failure, apoptosis, neutralization, and the formation of IL-10, thus enhancing the proliferation and survival of tumor cells to promote the development and progression of cancer (Akinleye and Rasool, 2019). Studies have shown that tumors are highly infiltrated by Treg cells, and the co-inhibitory receptors expressed on Tregs (such as PD1) and a series of co-inhibitory ligands (such as PD-L1/PD-L2) can significantly promote tumor escape (Nishimura et al., 1999). In this context, PD-1/PD-L1 signal transduction represents a viable target for novel anticancer therapy. PD-1/PD-L1 inhibitors came into being and gradually became the focus of attention **Figure 1**.

Although PD-1/PD-L1 inhibitors have been shown to be more effective and less toxic than chemotherapy, immune-related adverse events (irAEs) that may be related to their mechanism have been observed (Okwundu et al., 2021). Common sites of irAE include the thyroid, gastrointestinal tract, skin, and liver, but any organ system can be affected (Okwundu et al., 2021). Although most

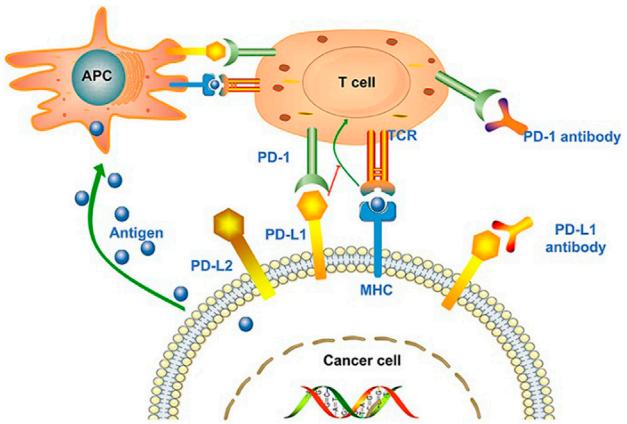

FIGURE 1 | Tumor cell-mediated immune escape and the treatability of PD-1/PD-L1 inhibitors. Antigen-presenting cells (APCs) recognize the antigens released by tumor cells and present them to T cells to promote the activation of T cell. However, the ligand PD-L1 expressed on tumor cells binds to PD-1 on T cells, promoting T cell dysfunction and inhibiting immune response. In the context of MHC, tumor cell antigens can also be presented directly to activate T cells. PD-1/PD-L1 inhibitors can block the binding of T cells to tumor cells and inhibit immune evasion. Reprinted from Su et al. (2020). Copyright © 2020 Su, Wang, Liu, Guo, Zhang, Li, Zhou, Yan, Zhou, and Zhang.

irAEs are usually reversible or easily controllable, they may be associated with irreversible organ damage or death in rare cases (Wang et al., 2018).

Autoimmune diseases are generally considered relatively uncommon [the overall prevalence is about 3–5% (Wang et al., 2015) in the general population], but their impact on mortality and morbidity is significant. Under the influence of certain factors, the body's tissue components or the immune system itself has some abnormalities, causing the immune system to mistakenly treat its own components as foreign objects to attack, that is, the destruction of immune tolerance, which is the basis of autoimmune diseases. IrAEs caused by PD-1/PD-L1 inhibitors usually have similar phenotypes and physiological characteristics to autoimmune diseases. For patients with preexisting AID, the use of immunotherapy seems to exacerbate the underlying autoimmune diseases (Kennedy et al., 2019). Therefore, cancer patients with autoimmune diseases have traditionally been excluded from most clinical trials. At present, the efficacy and safety of PD-1/PD-L1 inhibitors in cancer patients with AID remain unknown. There are also concerns about whether the frequent baseline use of immunosuppressants such as corticosteroids at the beginning of PD-1/PD-L1 inhibitors in AID patients may reduce efficacy in these patients; whether the status and types of autoimmune diseases will alter the risk of adverse events; and whether patients with underlying autoimmune diseases may benefit more from immunotherapy. These questions are still unknown yet. In this review, we summarized the relevant retrospective studies and several similar reviews from basic to clinical to discuss the mechanism of irAE and the safety and effectiveness of PD-1/PD-L1 inhibitors in AID patients and finally gave an overall overview of the prevention and management of adverse events, introduced some novel therapeutic methods, and looked forward to the future.

Relationship Between Autoimmune Diseases and Cancer

Cancer and autoimmune diseases are two different pathological conditions, especially in terms of immunity, showing opposite patterns, that is, cancer can evade the immune system or weaken the host's immune response, while autoimmune diseases are the host's immune response to self-antigens. However, there is plenty of evidence to suggest that the association between cancer and autoimmune diseases is bidirectional (Giat et al., 2017). On the one hand, the antitumor immune response may cross-react with the autologous tissue, leading to the development of autoimmunity (Masetti et al., 2021). On the other hand, **Figure 2** suggests that an increased risk of malignancy was observed in different autoimmune diseases. This may be associated with chronic inflammation and tissue damage caused by autoimmunity, inability to clear carcinogenic viral infections, and long-term immunosuppressive therapy. In theory, chronic immunosuppression can promote the development and progression of malignant tumors, while enhanced immune function may reduce the incidence, progression, and aggressiveness of cancer. Therefore, clinicians may think that autoimmune diseases have a negative impact on tumor development, but this is precisely not true. The interaction between autoimmune and cancer is a complex multistep process.

Patients with AID have an increased risk of cancer, which is mainly related to hematological malignancies (Niccolai et al., 2020). Approximately 14%–25% (Khan et al., 2016; Haanen et al., 2020b) of patients diagnosed with lung cancer suffer from autoimmune diseases, including but not limited to rheumatoid arthritis (RA), psoriasis (PSO), polymyalgia rheumatica (PMR), systemic lupus erythematosus (SLE), inflammatory bowel disease (IBD), and Sjogren's syndrome (SS). Next, we will review the cancer risk of some autoimmune diseases. RA: In the meta-analysis of Simon and colleagues (Simon et al., 2015), the standardized incidence rate (SIR) of lymphoma was 2.46 (95% CI, 2.05–2.96), malignant lymphoma was 3.21 (95% CI, 2.42–4.27), and non-Hodgkin lymphoma was 2.26 (95% CI, 1.82–2.81). The risk of lung cancer (SIR, 1.64; 95% CI, 1.51–1.79) and melanoma (SIR, 1.23; 95% CI, 1.01–1.49) has also increased. It is speculated that RA itself may cause a continuous inflammatory state, and cancer may have common risk factors with RA, which lead to increased cancer risk (Pundole and Suarez-Almazor, 2020). PSO: In a systematic review and meta-analysis of 112 studies including more than 2 million patients (Geller et al., 2018; Vaengebjerg et al., 2020), the overall prevalence of cancer in patients with psoriasis was 4.78% (95% CI, 4.02%–5.59%). The overall cancer risk increased slightly, with a risk ratio (RR) of 1.21 (95% CI, 1.11–1.33). The risk of several cancers is increased, including keratinocyte carcinoma (RR, 2.28; 95% CI, 1.73–3.01), lymphoma (RR, 1.56; 95% CI, 1.37–1.78), lung cancer (RR, 1.26; 95% CI, 1.13–1.40), and bladder cancer (RR, 1.12; 95% CI, 1.04–1.19).

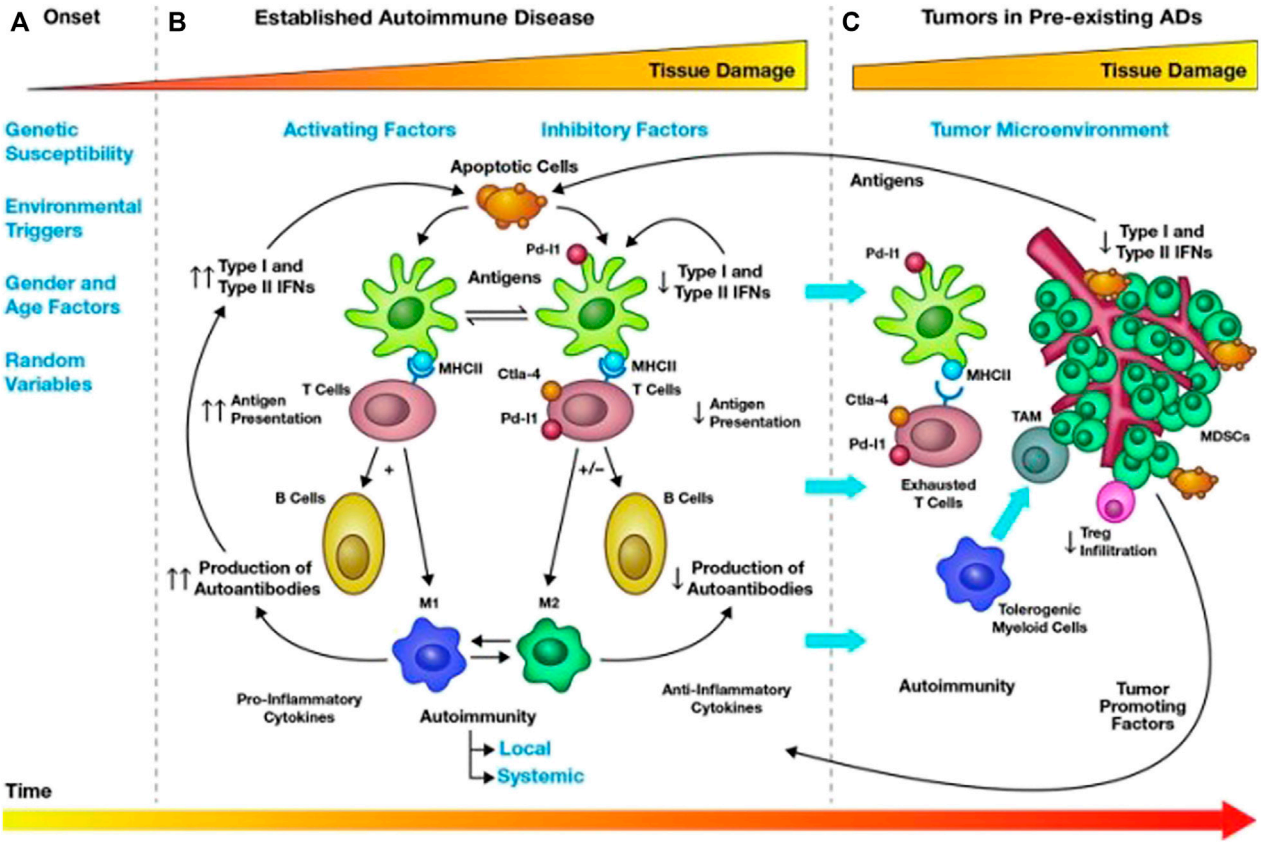

FIGURE 2 | Mechanisms of cancer occurrence and regulation in autoimmune diseases. Tumorigenesis in AID can be divided into three stages **(A–C)**. In the first stage [**(A)** Onset], genetic predisposition, environment, gender, age, and random factors can contribute to the development of autoimmunity in a healthy individual, which lasts about three or 4 years. In the second stage [**(B)** Established autoimmune disease], as time goes on, a runaway mix of pro-inflammatory and anti-inflammatory events, maintaining the balance between co-activators (type I and II interferon) and co-suppressors (PD-1/PD-L1 and CTLA4) through responsive feedback pathways activated by T cells, B cells, dendritic cells, and macrophages, which is the characteristic of AID, can cause the damage of organs and tissues. At the same time, chronic inflammation may lead to a loss of antiproliferative signals and abnormal differentiation of normal cells, eventually leading to the development of cancer. In the third stage [**(C)** Tumor in preexisting AIDs], tumors regulate the internal environment of autoimmunity, evade immune surveillance through tumor-promoting factors, and break the balance of chronic inflammation by causing T cells depletion and immune tolerance through co-inhibitory molecules. Therefore, we need to use immunotherapy to curb tumor progression. CTLA-4, cytotoxic T lymphocyte-associated proteins 4; IFN, interferon; MDSCs, myeloid-derived suppressor cells; MHC, major histocompatibility complex; PD-L1, programmed cell death-1 ligand; TAM, tumor-associated macrophages. Reprinted from Valencia et al. (2019). Copyright © 2019, Mary Ann Liebert, Inc., publishers.

SLE: In 2015, Cao et al. (2015) included 16 studies involving 59,662 SLE patients and found that the overall RR of cancer was 1.28 (95% CI, 1.17–1.41). In 2018, Song et al. (2018) included 24 studies, and the results showed that SLE was associated with an increased overall cancer risk (SIR, 1.28; 95% CI, 1.16–1.42). The underlying mechanism may explain the development of cancer in SLE patients. On the one hand, patients have a basic deficiency in their immune function, leading to immune disorders, which may prevent abnormal cells from being removed and ultimately lead to an increased risk of cancer. On the other hand, drugs used for immunosuppressive therapy may also exacerbate immune disorders and further increase the risk of cancer. IBD: The risk of cancer in IBD patients is related to time. It increases by 2% in 10 years, 8% in 20 years, and 18% in 30 years (Eaden et al., 2001; Nadeem et al., 2020). In IBD patients, chronic intestinal inflammation is the main risk factor for gastrointestinal malignancies. Cancers caused by chronic intestinal inflammation include colorectal cancer (SIR, 5.7; 95% CI, 4.6–7.0), small intestinal adenocarcinoma (SIR, 27.1; 95% CI, 14.9–49.2), intestinal lymphoma (SIR, 17.51; 95% CI, 6.43–38.11), anal cancer, and cholangiocarcinoma (Axelrad et al., 2016). SS: In a systematic review (Cappelli and Shah, 2020), the overall cancer risk of Sjogren's syndrome is higher than that of the general population, with a risk ratio of 1.53. The most common cancer is lymphoma. Patients with primary Sjogren's syndrome (pSS) are 10–44 times more likely to develop lymphoma than healthy individuals (Igoe et al., 2020). In order to lay the foundation of risk stratification and targeted cancer screening, larger longitudinal cohort studies that provide a more detailed framework of the links between cancer and autoimmunity are urgently needed. In view of the increased risk of cancer in patients with autoimmune diseases, for clinicians, it is important to be aware of the cancer risk of a patient with autoimmune disease. At the same time, when

TABLE 1 | Patients with autoimmune diseases may have an increased risk of developing cancer.

Autoimmune disease	Associated cancer	Risk metric (95%CI where available)	Reference
Rheumatoid arthritis	Multiple	SIR: 1.09 (1.06–1.13)	Simon et al. (2015)
Psoriasis	Multiple	RR: 1.21 (1.11–1.33)	Geller et al. (2018) Vaengebjerg et al. (2020)
Systemic lupus erythematosus	Multiple	RR: 1.28 (1.16–1.42)	Cao et al. (2015) Song et al. (2018)
Inflammatory bowel disease	Colorectal cancer	SIR: 1.7 (1.2–2.2)	Lutgens et al. (2013)
Sjogren's syndrome	Multiple	RR: 1.53 (1.17–1.88)	Liang et al. (2014)
Autoimmune gastritis	Gastric adenocarcinoma	OR: 2.18 (1.94–2.45)	Massironi et al. (2019)
Dermatomyositis	Multiple	OR: 14.5 (2.35–89.3)	Lau et al. (2021)

TABLE 2 | FDA-approved PD-1/PD-L1 inhibitors (Constantinidou et al., 2019).

Target	Molecular	Antibody type	Approved in	Company	Commercial name
PD-1	Nivolumab	Human IgG4	Unresectable or metastasized melanoma; squamous non-small cell lung cancer (NSCLC); advanced renal cell carcinoma (RCC); urothelial carcinoma; colorectal cancer; hepatocellular carcinoma (HCC); head and neck cancer (HNSCC)	Bristol-Myers Squibb	Opdivo
PD-1	Pembrolizumab	Humanized IgG4	Advanced or unresectable malignant melanoma; NSCLC; HNSCC; advanced gastric cancer; Hodgkin's lymphoma; urothelial carcinoma; bladder cancer; colorectal cancer; HCC; RCC	Merck	Keytruda
PD-1	Cemiplimab	Human IgG4	Cutaneous squamous cell carcinoma (CSCC); basal cell carcinoma; NSCLC	Sanofi, Regeneron	Libtayo
PD-L1	Atezolizumab	Humanized IgG1k	Urothelial carcinoma; NSCLC; small cell lung cancer (SCLC); breast cancer; HCC; unresectable or metastasized melanoma	Roche, Genentech	Tecentriq
PD-L1	Durvalumab	Human IgG1k	NSCLC; extensive stage-small cell lung cancer (ES-SCLC); urothelial carcinoma; bladder cancer	AstraZeneca	Imfinzi
PD-L1	Avelumab	Human IgG1	Merkel cell carcinoma (MCC); urothelial carcinoma; RCC	Merck Serono, Pfizer	Bavencio

receiving a cancer patient, it is necessary to distinguish whether the patient has previously had autoimmune diseases before making the next correct decision **Table 1**.

PD-1/PD-L1 Inhibitors and IrAE

There are currently six FDA-approved PD-1/PD-L1 inhibitors: nivolumab, pembrolizumab, cemiplimab, atezolizumab, durvalumab, and avelumab **Table 2**.

PD-1/PD-L1 inhibitors have changed the therapeutic prospects for patients with advanced malignancies. In carcinogen-induced cancers or virus-driven cancers such as Hodgkin's lymphoma, virus-driven skin Merkel cell carcinoma, and microsatellite instability cancer, the response rate is 50–90% (Ribas and Wolchok, 2018). The second high response rate is cancers with high immunogenicity such as melanoma, NSCLC, RCC, and HCC, and the objective response rate is between 20% and 40% (Wu et al., 2019). However, while bringing hope to patients, we also need to be alert to the unique toxicity caused by immune overactivation, that is, the emergence of immune-related adverse events (irAEs).

IrAE is very common, which can be occurred in 70% of patients treated with PD-1/PD-L1 inhibitors, and most of irAE occurs 3–6 months after the start of treatment (Michot et al., 2016). Recently, a meta-analysis (Nishijima et al., 2017) showed that PD1/PD-L1 inhibitors are associated with a lower risk of treatment-related symptoms (fatigue, anorexia, nausea, diarrhea, constipation, and sensory neuropathy) and hematological toxicity. However, in patients treated with PD1/PD-L1 inhibitors, the risk of irAE is increased. The most commonly reported irAEs are endocrine diseases (thyroid diseases such as hypothyroidism and hyperthyroidism, followed by pituitary and adrenal dysfunction), gastrointestinal tract symptoms (diarrhea, colitis, and nausea), lung disease (pneumonia), skin symptoms (rash, itch, and leukoplakia), and musculoskeletal symptoms (arthralgia and myalgia) (Khoja et al., 2017). Compared with CTLA-4 inhibitors, PD-1/PD-L1 inhibitors are more prone to pneumonia (OR 6.4; 95% CI, 3.2–12.7), hypothyroidism (OR, 4.3; 95% CI, 2.9–6.3), arthralgia (OR, 3.5; 95% CI, 2.6–4.8) and vitiligo (OR, 3.5; 95% CI, 2.2–5.3) (Igoe et al., 2020). Although irAEs are usually mild and can be controlled by clinicians, some can be fatal, such as pneumonia, cardiopulmonary arrest, heart failure, myocardial infarction, and stroke. There is evidence (Okwundu et al., 2021) that the incidence of fatal adverse events caused by immunosuppressive therapy is estimated to be 0.3%–1.3%, which is lower than the risk associated with traditional treatment, the platinum-containing dual-drug chemotherapy is about 0.9%, while the allogeneic hematopoietic stem cell transplantation is about 15%. The severity of irAE does not seem to be related to the dose of PD-1/PD-L1 inhibitors because the incidence of irAEs is very similar between 3 and 10 mg/kg nivolumab (Topalian et al.,

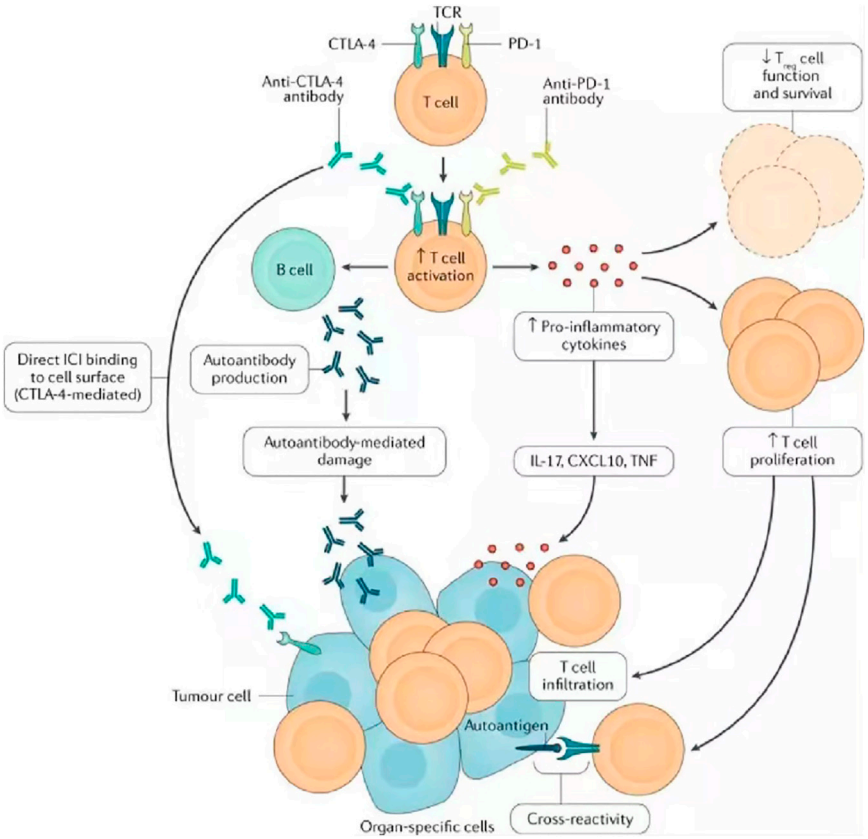

FIGURE 3 | Possible mechanisms of irAE, including cross-reactions between antitumor T cells and similar antigens on healthy cells, downregulation of the function of regulatory T cells, emergence of autoantibodies, and increase of pro-inflammatory cytokines. Research on the mechanism of irAE is not only helpful in establishing treatment strategies for irAE, managing irAE and improving the prognosis and quality of life of cancer patients but also important in understanding the underlying immunology of spontaneous autoimmune diseases. TCR, T cell receptor; TNF, tumor necrosis factor. Reprinted from Ramos-Casals et al. (2020). Copyright © 2020, Springer Nature Limited.

2014). In a cohort study (Robert et al., 2014), there was no significant difference in the incidence of irAE between 2 and 10 mg/kg pembrolizumab.

Diagnosing irAE is challenging due to their high variability and nonspecific clinical manifestations (Hommes et al., 2020). This makes it complicated to distinguish irAE from other diagnoses, such as infection or tumor progression, and often leads to a delay in diagnosis, so we need to identify the specific mechanisms of irAE and biomarkers that can predict or signal irAE at an early stage. The specific mechanism of irAE is still under study. At present, its mechanism is considered to be mainly mediated by T cells, but other immune cell types have also been proposed (Sanchez et al., 2019) **Figure 3**.

Cytotoxic T Cells Attack Normal Tissues

PD-1/PD-L1 inhibitors may cause the activation of cytotoxic T cells against antigens shared by tumors and normal tissues. It has been suggested that irAE may be related to epitope spreading (Lee et al., 2021). Because immunotherapy is not tumor-specific, both tumor cells and normal "bystander cells" are damaged, and neoantigens and autoantigens on tumor cells are released into the blood. Antigen-presenting cells (APCs) recognize and cross-present these antigens, triggering a secondary immune response (June et al., 2017). Epitope spreading allows T cells not only to attack more targets on the tumors but also to attack normal tissues, leading to irAE.

Loss of Homeostasis of Regulatory T Cells

Tregs (mainly $CD25^+Foxp3^+$ Tregs) can promote immune escape of tumor cells by inhibiting antitumor immunity. PD-L1 can induce Foxp3 expression and Tregs differentiation in the periphery (Kumar et al., 2020). A current study (Wang et al., 2009) has shown that decreased intracellular Foxp3 expression was observed in the peripheral blood mononuclear cell (PBMC) of patients treated with PD-1 inhibitors for melanoma, resulting in weakened Tregs function and loss of self-tolerance, thus leading to irAE.

B Cells and Antibody-Mediated Toxicity

A study (Das et al., 2018) has shown that immunotherapy can lead to a decrease in circulating B cells and an increase in $CD21^{lo}$ $PD1^+$ memory B cells and plasma cells. Single-cell RNA sequencing of $CD21^{lo}$ $PD1^+$ B cells showed that gene transcription related to cell activation and inflammatory cytokines increased after treatment. In

addition, $CD21^{lo}$ B cells expressed lower levels of lymphoid tissue-homing chemokine receptors CXCR4 and CXCR5 compared with $CD21^{hi}$ B cells, suggesting that $CD21^{lo}$ B cells may have a greater ability to transport to nonlymphoid tissues and contribute to the inflammatory process that may mediate autoimmunity (Liudahl and Coussens, 2018). Clinically, patients with early B cell changes experienced a higher incidence of irAE 6 months after treatment (Das et al., 2018). In another study (Osorio et al., 2017), when pembrolizumab was used to treat NSCLC, 21% of patients had thyroid dysfunction. Among these patients, 80% of patients developed antithyroid antibodies, and the appearance of antibodies was related to the use of PD-1/PD-L1 inhibitors. This indicates that PD-1/PD-L1 may regulate its own immune balance, leading to the rapid activation of memory B cells, recruiting classical complement and pro-inflammatory cells to signal damage. When studying the underlying mechanisms of irAE, B cell is also one of the roles that cannot be ignored.

Cytokines

The cascade of immune responses requires effective cell-to-cell communication. Cytokines have multiple regulatory effects to maintain immune balance. However, a strong cytokine storm after immunotherapy may lead to overactivation of T cells that target self-organizations. In a prospective study (Kurimoto et al., 2020), the higher levels of serum IL-1β, IL-2, and GM-CSF as well as IL-8, G-CSF, and MCP-1 that were reduced in the early treatment period, were significantly associated with the occurrence of thyroid irAE ($p < 0.05$). In another longitudinal analysis (Lim et al., 2019), the increased expression of 11 cytokines (G-CSF, GM-CSF, fractalkine, FGF-2, IFNα2, IL12p70, IL1a, IL1B, IL1RA, IL2, and IL13) is closely related to severe irAEs which require high-dose immunomodulator intervention. Overall, in these studies, low baseline levels and after treatment significantly elevated levels of key cytokines prove that cytokines appear to be associated with irAE.

Innate Immune Cells

In a retrospective analysis (Pavan et al., 2019), the low neutrophil-to-lymphocyte ratio (NLR) and low platelet-to-lymphocyte ratio (PLR) at baseline were significantly correlated with the occurrence of irAEs (OR, 2.2, $p = 0.018$; OR, 2.8, $p = 0.003$). In another retrospective analysis of 146 patients (Krishnan et al., 2020), patients with eosinophilia were more likely to have irAEs ($p = 0.042$). In addition, NK cells themselves may express PD-1, and the PD-1/PD-L1 axis inhibits NK cell responses *in vivo*. Therefore, treatment with PD-1/PD-L1 inhibitors may lead to the activation of NK cells, leading to potential irAEs (Hsu et al., 2018). At present, everyone is gradually beginning to focus on the specific mechanisms by which innate immune cells cause irAEs.

Environmental Factors

More and more evidences show that individual intestinal flora can change immune homeostasis and tolerance (Young et al., 2018). The impact of antibiotic use was explored in a group of patients receiving PD-1/PD-L1 inhibitors. Compared with the nonantibiotic group, patients who received antibiotic treatment before, during, or shortly after PD-1/PD-L1 inhibitors treatment had significantly lower

TABLE 3 | Frequencies associated with PD-1/PD-L1 inhibitors.

Study	PD-1/PD-L1 inhibitor	Disease	Dose (n)	Any-grade adverse event (grade ≥3 adverse events)								Ref
				Diarrhea	Colitis	Pneumonia	Hepatitis	Nephritis	Endocrine	Rash	Nervous system	
Checkmate 067	Nivolumab	Stage III + Stage IV melanoma	3 mg/kg every 2 weeks (313)	22% (3%)	3% (1%)	2% (0.3%)	8% (3%)	2% (1%)	17% (2%)	24% (0.3%)	—	Hodi et al. (2018)
Checkmate 017 + 057	Nivolumab	NSCLC	3 mg/kg every 2 weeks (418)	8.9% (1%)	—	5% (1%)	6% (1%)	3% (0.2%)	9% (0)	8.1% (0.5%)	0.4% (0)	Horn et al. (2017) Borghaei et al. (2021)
Keynote 024	Pembrolizumab	NSCLC	200 mg every 3 weeks (154)	16.2% (3.9%)	3.9% (1.9%)	7.8% (2.6%)	0.6% (0.6%)	0.6% (0.6%)	13% (0.6%)	10.4% (1.3%)	—	Reck et al. (2019)
Keynote 158	Pembrolizumab	Non-colorectal MSI-H/dMMR cancer	200 mg every 3 weeks (233)	12% (0)	3.9% (0.9%)	3.9% (1.3%)	1.7% (0.9%)	0.9% (0)	15% (0.8%)	5.2% (0)	—	Marabelle et al. (2020)
Empower-Lung 1	Cemiplimab	NSCLC	350 mg every 3 weeks	4.2% (0.3%)	0.3% (0.3%)	0.3% (0.3%)	0.6% (0.6%)	0.3% (0.3%)	—	5% (1%)	1% (0.3%)	Sezer et al. (2021)
Oak	Atezolizumab	NSCLC	1,200 mg every 3 weeks (609)	15.4% (0.7%)	0.3% (0)	1% (0.7%)	0.3% (0.3%)	—	—	—	—	Rittmeyer et al. (2017)
Mystic	Durvalumab	NSCLC	20 mg/kg every 4 weeks (369)	1.9% (0.3%)	0.5% (0.3%)	2.2% (1.1%)	0.3% (0.3%)	0 (0)	0.8% (0.3%)	1.4% (1.1%)	—	Rizvi et al. (2020)
Javelin Merkel 200	Avelumab	Metastatic Merkel cell carcinoma	10 mg/kg every 2 weeks (88)	2.3% (0)	1.1% (0)	—	2.2% (1.1%)	1.1% (0)	6.8% (1.1%)	5.7% (0)	—	D'Angelo et al. (2020)

TABLE 4 | Retrospective studies of PD-1/PD-L1 inhibitors in patients with preexisting AID.

Author	Patient	Tumor	AID exacerbation	*De novo* irAE	ORR
Menzies Menzies et al. (2017)	N = 52, rheumatoid arthritis (13), other rheumatic diseases (14), psoriasis (6)	Melanoma	20 (38%)	15 (29%)	17 (33%)
Alice Tison Tison et al. (2019)	N = 112 (PD-1/PD-L1 inhibitors n = 95), psoriasis (31), rheumatoid arthritis (20), and inflammatory bowel disease (14)	Melanoma (66), NSCLC (40), urinary cancer (4), MCC (2)	43 (45%)	34 (36%)	48 (52%)
Leonardi Leonardi et al. (2018)	N = 56, rheumatism (25), psoriasis (14), and endocrine diseases (9)	NSCLC	13 (23%)	21 (38%)	11 (22%)
Hoa Hoa et al. (2021)	N = 27, rheumatoid arthritis (8), psoriatic arthritis (8), and inflammatory bowel disease (4)	NSCLC (15), melanoma (8), other cancers (4)	14 (52%)	14 (52%)	14 (52%)
Monique van der Kooij et al. (2021)	N = 187, rheumatism (89), endocrine diseases (73), and IBD (31)	Melanoma	—	Grade 3 or 4 irAE, 31 (17%)	71 (40%)
Gutzmer Gutzmer et al. (2017)	N = 19, rheumatism (9), thyroiditis (5), and psoriasis (2)	Melanoma	8 (42%)	3 (16%)	6 (32%)
Loriot Loriot et al. (2020)	N = 35, psoriasis (15), thyroid disease (6), and rheumatoid arthritis (4)	Urinary system cancers	4 (11%)	—	4 (11%)
Fountzilas Fountzilas et al. (2022)	N = 123 (PD-1 inhibitors *n* = 102), rheumatism (54) and endocrine diseases (26)	NSCLC (84), melanoma (18), head and neck cancer (6)	31 (25.2%)	43 (35%)	57 (56.4%)
Richter Richter et al. (2018)	N = 16 (PD-1 inhibitors *n* = 12), rheumatism (16)	Melanoma (10), pulmonary (4), hematologic (2)	1 (6.3%)	6 (38.5%)	—

progression-free survival (PFS) and overall survival (OS) (Matson et al., 2018). Possible mechanisms linking microbes and immunotherapy include the stimulation of T cells by specific bacterial antigens, which then trigger cross-reactions against tumor neoantigens. Meanwhile, bacterial toxins can also stimulate the recruitment of T cells, thereby releasing inflammatory cytokines such as IL-17, and combat immune tolerance (Chau and Zhang, 2021). IrAEs may be related to bacterial metabolites, which have pro-inflammatory properties. In the case of ecological disorders, it may cause abnormal activation of the immune system **Table 3**. For example, short-chain fatty acids (SCFAs), the main end metabolite produced by the gut microbiota (Schirmer et al., 2016), can increase the level of IL-17, which is a pro-inflammatory cytokine that plays a key role in irAEs. It is also important to clarify the impact of non-GI tract microbiota and whether PD-1/PD-L1 inhibitors-driven irAEs is affected by other environmental factors. We still have a long way to go. It is worth mentioning that unlike PD-1 inhibitors, PD-L1 inhibitors only block the interaction between PD-1 and PD-L1 and retain the interaction between PD-1 and PD-L2. Although the overall toxicity characteristics of PD-1 inhibitors and PD-L1 inhibitors are similar, it has been suggested that targeted PD-L1 therapy reduces the frequency of irAEs to a certain extent and maintains self-tolerability (Buchbinder and Desai, 2016).

Safety and Effectiveness of PD-1/PD-L1 Inhibitors in Patients With Preexisting Autoimmune Diseases

PD-1/PD-L1 inhibitors are easy to cause irAEs, and the impaired function of PD-1/PD-L1 plays an important role in a variety of autoimmune diseases (Zamani et al., 2016). Many patients with autoimmune diseases are excluded from clinical trials of PD-1/PD-L1 inhibitors because of concerns about the activation of underlying autoimmune diseases, the flare of preexisting autoimmune diseases, and the potential susceptibility to severe irAEs. However, as PD-1/PD-L1 inhibitors are used in a wider range of cancers, the need to evaluate the risk-benefit ratio of immunosuppressants used in cancer patients with preexisting autoimmune diseases will gradually increase. Recent studies (Abdel-Wahab et al., 2018; Danlos et al., 2018; Cortellini et al., 2019; Tison et al., 2019; Xie et al., 2020) have shown that the risk of the flare of autoimmune diseases or *de novo* irAEs after receiving immunotherapy is statistically higher in patients with preexisting autoimmune diseases, but they are usually mild and can be controlled without stopping the drugs. With close monitoring of patients' symptoms and multidisciplinary cooperation, PD-1/PD-L1 inhibitors are relatively safe (Menzies et al., 2017; Pantuck et al., 2019). Next, we will summarize the data from several of these studies **Table 4**.

In a systematic review (Abdel-Wahab et al., 2018) of 123 cancer patients with preexisting autoimmune diseases, after treatment with PD-1/PD-L1 inhibitors, 92 (75%) patients had exacerbations of preexisting autoimmune diseases (41%), *de novo* irAEs (25%), or both (9%). In patients with active and inactive autoimmune diseases, no difference in adverse events was observed. It is interesting to note that CTLA-4 inhibitors are more likely to cause *de novo* irAEs, while PD-1/PD-L1 inhibitors are relatively more likely to cause the exacerbation of autoimmune diseases. In another article (Xie et al., 2020) that covers 619 AID patients receiving immunotherapy, 60% of patients had different degrees of exacerbation of the original autoimmune disease (27%), *de novo* irAEs (25%), or both (8%).

Most *de novo* irAEs are mild, occurring most commonly in colitis, thyroiditis, and hypophysitis. Interestingly, compared with other autoimmune diseases, patients with rheumatoid arthritis seem to tend to aggravate the onset of the disease (RR = 1.25–1.88). This suggests that the type of AID may have heterogeneity in the safety of patients.

In a prospective study (Danlos et al., 2018), 45 cancer patients with 53 AIDs were evaluated and compared with 352 non-AID patients included in the same period. The study found that 20 patients (44.4%) had at least one irAE, while 102 (29%) of non-AID patients had irAE. More than half of AID patients did not have a disease attack, and only 25% of irAE patients were in the need to stop PD-1 inhibitors. There was no significant difference between the AID group and the non-AID group in terms of overall survival time and objective response rate (p = 0.38 and 0.098), indicating that PD-1/PD-L1 inhibitors seem to be safe and effective in patients with AID as in patients without AID.

In a "real world" retrospective multicenter observational study (Cortellini et al., 2019), 56 (65.9%) and 8 (9.4%) patients experienced any grade of irAEs and grade 3/4 of irAEs, respectively. In contrast, among 666 non-AID patients, 266 (39.9%) and 59 (8.8%) patients had experienced any grade of irAEs and grade 3/4 of irAEs, respectively. This indicates that patients with preexisting AID have a significantly higher risk of irAEs ($p < 0.0001$), but they do not seem to be exposed to the risk of serious adverse events (p = 0.8863).

In summary, although the risk of irAEs is increased, most irAEs are mild and controllable. For most patients with AID, clinicians should consider the potential severity of AID in patients before administering treatment, properly inform patients of the risks and benefits of treatment, and these patients should be closely monitored during and after treatment. Under multidisciplinary cooperation and close monitoring, the use of PD-1/PD-L1 inhibitors may be not only safe but also effective (Rakshit and Molina, 2020). However, most of the evidences for the use of PD-1/PD-L1 inhibitors in preexisting AID patients are limited to retrospective analysis with associated risk of bias, such as selection bias. They also had a relatively small sample size, which could limit the validity of the results. Larger retrospective and prospective analyses will help further to characterize the risk of immunotherapy for patients with specific autoimmune diseases.

AID Types and Patients Safety

Tison et al. (2019) found that autoimmune diseases flare in patients receiving PD-1/PD-L1 inhibitors after treatment varies depending on the type of preexisting autoimmune disease. It is more common in patients with psoriatic/psoriatic arthritis or RA than in patients with lupus. The onset of inflammatory bowel disease is the most serious, and three patients require biological DMARD, so we must be careful with these patients. Fountzilas et al. (2022) found that patients with flare had more commonly underlying dermatologic diseases (n = 12, 38, 7%), with the vast majority (n = 10) having been diagnosed with psoriasis. Gutzmer et al. (2017) pointed out that the flare of AID seems to be more common in patients with rheumatism and psoriasis. Menzies et al. (2017) found that 14/27 (52%) patients with rheumatism, 3/8 (37.5%) patients with psoriasis, 1/4 (25%) patients with Graves' disease, and 2/2 (100%) patients with immune thrombocytopenic purpura developed autoimmune diseases flare, and in contrast, patients with gastrointestinal (n = 6), nervous system (n = 5), and respiratory (n = 2) diseases did not experience flare after treatment. Leonardi et al. (2018) reported that the flare of rheumatism was significantly higher than that of non-rheumatism AID patients (40% vs. 10%; p = 0.01). Xie et al. (2020) found that compared with Pso/PsA (RR, 1.25; 95% CI, 0.85–1.82), AIT (RR, 1.88; 95% CI, 0.92–3.85), or IBD (RR, 1.50; 95% CI, 0.86–2.63), the risk of flare of RA is numerically higher, but it does not reach statistical significance. At the same time, the study puts forward the trend of more flares in patients with rheumatism. In terms of mechanism, studies (Zamani et al., 2016) have shown that the single nucleotide polymorphism of the PD-1 encoding gene *PDCD1* may be related to the flare of autoimmune diseases. The polymorphism of intron 4 (PD1.3) interferes with the binding of runt-related transcription factor 1 (RUNX1) and affects the production of PD-1. There is a statistically significant association between the SNP at the RUNX1 binding site and the susceptibility to RA and psoriasis (Lee et al., 2009), which easily leads to the appearance of RA and psoriasis, while many other AIDs do not involve or rely heavily on the PD-1 signal path. This suggests that doctors should also consider AID types (Pantuck et al., 2019) when deciding whether to use PD-1/PD-L1 inhibitors. Compared with other autoimmune diseases, for patients with rheumatism or psoriasis, we should be more alert to the flare of original autoimmune diseases after treatment and should carefully weigh the benefits and risks of treatment. Due to the complexity and diversity of possible AID flares and irAEs, multiple sub-specialist physicians need to cooperate to care for these patients.

AID Status and Patients Safety

The intensity of the autoimmune response is often closely related to the condition. When the condition is active, the autoantibody titers increase, and when the condition is inactive, the autoantibody titers decrease. Therefore, we speculate that the state of autoimmune diseases can affect the immune system, and there seems to be a correlation with the incidence of adverse events in the immunotherapy of cancer patients. In a retrospective study of 751 stage IV cancer patients by Cortellini et al. (2019), in inactive AID, the incidence of any grade of irAEs and G3/G4 irAEs was 64.3% and 8.6%, respectively. In active AID, the incidence of any grade of irAEs and G3/G4 irAEs was 73.3% and 13.3%, respectively. The ORR of patients with preexisting inactive and active AID was 38.1% (95% CI, 24.4–56.6) and 50% (95% CI, 23.0–76.9), and the median PFS was 14.4 months (95% CI, 5.3–17.1) and 6.8 months (95% CI, 5.1–9.4), and the median OS was 15.7 months (95% CI, 10.3–24.3) and 9.8 months (95% CI, 5.8–24.6), respectively. Compared with inactive AID, patients with active AID have relatively higher irAEs and higher ORR but lower PFS and OS, which may be related to the increased morbidity and mortality of AID itself. Menzies et al. (2017) reported that symptomatic patients (9/15, 60%) had more

frequent disease flares and exacerbations than clinically inactive AID patients (11/37, 30%) (p = 0.039). Leonardi et al. (2018) retrospectively analyzed 56 AID patients with advanced NSCLC and found that the exacerbations of the original AID in symptomatic patients (n = 5, 50%) were significantly higher than those in asymptomatic AID patients (n = 8, 18%; p = 0.04). This indicates that the risk of irAEs for active AID is relatively higher. For safety reasons, it may be necessary to correctly treat and control severe active AID before immunotherapy starts. We are still unable to determine the best strategy for providing PD-1/PD-L1 inhibitors in patients with active or symptomatic AD, which presents a huge unmet medical need for the medical oncology community. Currently, there are no consensus guidelines for treatment for this particular patient population, nor is there a way to determine the risk-benefit ratio for individual patients. We strongly recommend that patients be aware of possible complications and corresponding comorbidities associated with treatment. Treatment can only be carried out after patient education and doctor–patient communication. Static AID patients can be regarded as non-AID patients (Danlos et al., 2018), but we still need a multidisciplinary team to closely monitor these patients to identify some predictable adverse events and provide consultation to patients.

Relationship Between IrAE and Treatment Efficacy

More and more literatures (Grangeon et al., 2019; Hussaini et al., 2021) indicate that there is a potential correlation between the onset of irAE and the efficacy of PD-1/PD-L1 inhibitors. Among patients with NSCLC, Hussaini et al. (2021) summarized 19 retrospective studies and found that ORR ($irAE^+$ $irAE^-$) was 41.49% (95% CI, 36.5–46.5) and 18.01% (95% CI, 13.5–22.6), the weighted average PFS was 8.97 months (95% CI, 7.14–10.8) and 3.06 months (95% CI, 2.4–3.72), OS ($irAE^+$ $irAE^-$) was 19.07 months (95% CI, 14.3–23.8) and 7.45 months (95% CI, 5.34–9.56), respectively. In another observational study (Grangeon et al., 2019) of 270 patients who had received PD-1/PD-L1 inhibitors, 44% of patients experienced any grade of irAEs. Compared with patients who did not experience irAEs, patients who experienced irAEs had a higher PFS (5.2 vs. 1.97 months, $p < 0.001$), ORR (22.9% vs. 5.7%, $p < 0.0001$), and disease control rate (DCR) (76% vs. 58%, $p < 0.001$). In patients with metastatic melanoma, multiple studies (Sanlorenzo et al., 2015; Hua et al., 2016) have shown that leukoplakia, a clinically visible irAE, may be related to the clinical benefit of PD-1/PD-L1 inhibitors. For example, in a prospective study (Hua et al., 2016) of melanoma patients receiving pembrolizumab, the remission rate of patients with vitiligo was 71%, while the remission rate of patients without vitiligo was 28%. In another retrospective analysis (Weber et al., 2017) of 576 patients with advanced melanoma treated with nivolumab monotherapy, the ORR of patients who experienced irAEs of any grade was significantly better than that of patients who did not experience them (48.6% vs. 17.8%, $p < 0.001$). A retrospective analysis (Verzoni et al., 2019) of 389 patients receiving nivolumab for advanced or metastatic RCC showed that patients with irAEs had a more significant survival benefit than patients without irAEs (median OS, not reach and 16.8 months, p = 0.002; 1-year OS, 75.4% and 59.8%; 2-year OS, 66.9% and 36.8%).

In summary, it is not difficult to find that in patients receiving PD-1/PD-L1 inhibitors, the occurrence of irAEs is positively correlated with the efficacy. Of course, one of the possible deviations is the duration of treatment. Its increase will lead to prolonged drug exposure, which leads to a higher probability of adverse events and better treatment results. In order to minimize the deviation of drug treatment time, Verzoni et al. (2019) conducted a landmark analysis of OS at the median time (6 weeks) of the appearance of irAEs and found that irAEs were still statistically significantly associated with improvement in OS (p = 0.006). In another study (Schadendorf et al., 2017), the authors evaluated the efficacy during the induction phase between patients who discontinued due to irAEs (n = 96) and patients who did not discontinue with irAEs (n = 233) (median duration of treatment was 1.4 and 9.4 months, respectively). The ORR of patients who discontinued the drug due to irAEs was 58.3%, the median PFS was 8.4 months, and the OS rate at 18 months was 67%, while the ORR of patients who did not discontinue the drug was 50.2%, and the median PFS was 10.8 months, and the OS rate at 18 months was 62%. The PFS, OS, and ORR between the two groups seem to be similar, indicating that the duration of the drug treatment is not the cause of the relationship between irAEs and drug efficacy.

Interestingly, different literatures have different results regarding the relationship between the severity of irAEs and the efficacy. IrAE is thought to be mainly mediated by T cells. Antigen-sharing or cross-reactivity leads to T cell-mediated responses not only against tumor cells but also against healthy cells. In terms of mechanism, it seems that the more severe the irAEs, the higher the activity of T cells, and therefore the better the efficacy of the drug. In a retrospective study (Fujii et al., 2018), 98 of 290 patients (34%) experienced any grade of irAEs, and 15 (5.2%) experienced grade 3 or higher irAEs. Compared with patients with irAEs below grade 3, patients with grade 3 irAEs had high ORR (25% vs. 6%; p = 0.039) and long median progression time (30 vs. 10 weeks; p = 0.0040). However, through multivariate analysis, Judd et al. (2017) found that low-grade irAEs have a higher ORR (p = 0.017), which may be related to the lower incidence of high-grade irAEs and the inability to detect its association through a small sample. In a retrospective analysis of 576 patients with advanced melanoma, Weber et al. (2017) found that patients with ≥grade 3 irAEs had no significant difference in ORR compared with other patients. The different conclusions may be related to the high-grade irAEs may lead to death, which confuses the difference in survival. In addition, severe toxicity is usually associated with more aggressive immunosuppression, which may also affect the efficacy (Das and Johnson, 2019). Future studies with larger sample sizes are needed to investigate the relationship between irAE severity and efficacy.

Efficacy and Safety of Baseline Immunosuppressive Therapy

Since the age of immunotherapy, corticosteroid therapy has been considered an antidote to irAE (Rossi et al., 2019). For patients with active autoimmune diseases, corticosteroid drugs also seem

to be necessary. Mechanistically, the use of PD-1/PD-L1 inhibitors, combined with baseline immunosuppressive drugs, appears to improve AID symptoms and irAEs, but on the other hand, whether it will reduce the efficacy of patients is still discussed. Menzies et al. (2017) found that the response rate of immunosuppressive drugs (3/20, 15%) at the beginning of treatment was lower than that of unused immunosuppressive drugs (14/32, 44%) (p = 0.033). After adjusting for prognostic factors (AJCC stage, brain metastases, ECOG PS, and LDH), it was still significant (p = 0.029). However, there were more AID flares after baseline immunosuppressive therapy at using PD-1 inhibitors (10/20, 50%) than without immunosuppressive therapy (10/32, 31%). Xie et al. (2020) indicated that the ORR of patients receiving immunosuppressive therapy is lower than that of patients not receiving immunosuppressive therapy, but this is not statistically significant (RR, 0.58; 95% CI, 0.26–1.33). In a national multicenter cohort study (Tison et al., 2019), Tison found that patients who received immunosuppressive therapy at the beginning of immunotherapy had a shorter median PFS (3.8 vs. 12 months; p = 0.006), but there was no significant difference in OS. Similarly, Fountzilas et al. (2022) observed an association between corticosteroid-treated AID patients at initiation of immune checkpoint inhibitors and shorter PFS (HR = 2.08, 95% CI, 1.18–3.68, Wald's p = 0.012). However, he found that the initiation of immunotherapy with immunomodulators (excluding corticosteroids) was not associated with PFS (p = 0.22). However, in the smaller case series reported by Leonardi et al. (2018), Gutzmer et al. (2017), no negative effects on tumor response were found. In a case review (Lipson et al., 2016), PD-1 inhibitors were administered to solid organ transplant recipients with metastatic squamous cell carcinoma of the skin (standard long-term immunosuppressive therapy). The patient has a strong antitumor response and rejection of allogeneic transplantation, indicating that PD-1 inhibitors can be very effective against cancer in the context of chronic immunosuppression. A recently published retrospective study by Ricciuti et al. (2019) showed that the worse ORR, PFS, and OS observed in patients receiving ≥10 mg prednisone appeared to be related to the indications for corticosteroid use. When corticosteroids are used in cancer-related palliative care, the prognosis is worse. However, when corticosteroids are used in the treatment of indications unrelated to cancer, such as autoimmune diseases, compared with patients receiving 0–10 mg prednisone, there were no significant differences in mPFS or mOS among patients receiving ≥10 mg prednisone for cancer-unrelated indications. In summary, the existing research may mainly support that it is not necessary to stop immunosuppressants such as corticosteroids before initiation of immunotherapy in AID patients with cancer because immunosuppressants can inhibit AID and irAEs and may have little effect on immune efficacy. In view of the small sample size of existing studies and the heterogeneity between patients, more prospective studies are needed in the future to clarify conflicting data regarding the use of PD-1/PD-L1 inhibitors in patients with preexisting AID. We hoped to have more data to study the efficacy of PD-1/PD-L1 inhibitors in patients with active AID not on therapy, AID controlled on therapy, and AID off therapy at time of initiation of immunotherapy (Dietz et al., 2021). We raised the issue that corticosteroids differ in efficacy from other immunomodulators, and that immunotherapy in patients treated with corticosteroids needs to be treated with caution.

Efficacy and Safety of Gender

Men and women have different immune responses to foreign and self-antigens and show differences in innate and adaptive immune responses (Klein and Flanagan, 2016). These gender-based immunological differences lead to changes in the incidence of autoimmune diseases, the response rate of immunotherapy, and relevant adverse events. Most autoimmune diseases are more common in women (Ngo et al., 2014). However, whether gender affects the efficacy and safety of immunotherapy remains controversial. Cortellini et al. (2019) found that in cancer patients with AID, women had a significant increase in irAEs after immunotherapy. Compared with men, the risk of irAEs was 1.4 times high. They speculated that the higher incidence of irAEs in women may be related to longer OS. However, in a recent meta-analysis of 1096 female patients and 1886 male patients, Jing et al. (2021) found that there was no statistically significant difference in irAEs between the sexes (OR = 1.19, 95% CI, 0.91–1.54, p = 0.21). When (Shah et al., 2020) performed univariate or multivariate analysis of 455 melanoma patients receiving PD-1/PD-L1 inhibitors, they found that gender was not related to the incidence of any irAEs, severe irAEs, or hospitalization. In terms of efficacy, Conforti et al. (2018) reported that immune checkpoint inhibitors can significantly improve the OS of patients, but compared with women, these drugs have a great therapeutic effect on men. For example, the reduction in the risk of death is twice as large in men as in women. They believe that the reason for the difference may be that women have stronger immunity than men (Klein and Flanagan, 2016). This means that female-developed tumors must escape more effective immune surveillance mechanisms, which can make advanced female tumors less immunogenicity and stronger ability to escape immunity than similar tumors in men, so they may be more resistant to immunotherapy. In contrast, Wallis et al. (2019) conducted a systematic review of 18 randomized clinical trials of PD-1 inhibitors for advanced solid cancers, including 7,198 men and 3,495 women. They found no statistically significant differences between genders (I^2 = 44%; p = 0.94). Botticelli (Botticelli et al., 2017) also reported that for OS (male and female, HR, 0.72; 95% CI, 0.64–0.83 and HR, 0.81; 95% CI, 0.70–0.94, p = 0.285) and PFS (male and female, HR, 0.66; 95% CI, 0.52–0.82 and HR, 0.85; 95% CI, 0.66–1.09, p = 0.158), although the HR of men is lower than that of women, it is not statistically significant. Ye et al. (2020) believed that the aforementioned meta-analyses are simply a collection of different clinical trials, which may not provide clear results. They found that male patients with colorectal cancer (p = 0.041) or glioblastoma multiforme (p = 0.011) showed better OS with PD-1/PD-L1 inhibitors treatment. Female patients with esophageal gastric cancer or NSCLC tend to have better OS. It was further observed that compared with male patients with NSCLC (6/24, 25%), female patients (16/32, 50%) had a high response rate, indicating that the immune characteristics of

different cancer types are closely related to gender (such as male bias in melanoma and female bias in lung squamous cell carcinoma). In summary, how gender affects cancer immunotherapy is still a key gap for us because it is related to precision medicine (Zhu and Boutros, 2021). Current retrospective studies related to gender are mixed with a large number of confounding factors, such as cancer types, race, and age. Instead of focusing only on the two variables of gender and efficacy, future research should control for variables such as cancer types, race, and age. How gender affects the cancer genome and molecular data related to immunotherapy should be something we need to pay attention to in the future.

Prevention and Management of IrAEs in AID Patients

The current consensus is that the best management of irAEs mainly depends on early identification to reduce the possibility of discontinuation of treatment, ensure the quality of life, and avoid or minimize the risk of rare fatal results (Martins et al., 2019). However, there is still a lack of biomarkers that can individually assess the risk of irAEs. In terms of internal factors, Hoefsmit et al. (2019) believed that the similarity of irAEs and autoimmune diseases supports the hypothesis that irAEs may be related to the susceptibility gene loci of various autoimmune diseases. It is also written previously that the use of PD-1/PD-L1 inhibitors in AID patients has an increased risk of irAEs, especially in patients with previous rheumatism and psoriasis as well as active AID diseases. Gender seems to also affect the onset of irAEs. In terms of external factors, the combination of PD-1/PD-L1 inhibitors and CTLA-4 inhibitors has a higher overall incidence of irAEs than monotherapy (Larkin et al., 2015). In addition, a literature (Kang et al., 2021) suggests that changes in cytokine concentration before and during immunotherapy may help early to predict the risk of irAEs in cancer patients. Nishino et al. (2016) found that the incidence of PD-1 inhibitors-related pneumonia in patients with NSCLC, RCC, and during combined treatment was higher, which was significantly higher than that of melanoma. This suggests that there seems to be a certain connection between the types of cancer and irAEs. The risk of specific irAE is increased. Meantime, clinicians began to pay attention to the relationship between the early increase of autoantibodies and irAE. Yoon et al. (2021) found that baseline anti-TPO antibody positivity and new development of anti-Tg antibody positivity during the therapy were significantly associated with the progression to hypothyroidism. In a cohort study (Toi et al., 2019) of 137 patients with advanced NSCLC treated with nivolumab or pembrolizumab, patients with classic autoreactive antibodies (such as ANA, rheumatoid factor, and antithyroid antibodies) had a higher incidence of irAEs (OR, 3.25, 95% CI, 1.59–6.65, p = 0.001), but they had higher PFS (6.5 months, 95% CI, 4.4–12.9 vs. 3.5 months, 95% CI, 2.4–4.1). Gowen et al. (2018) analyzed autoantibodies in patients with metastatic melanoma using high-throughput protein arrays, and their data showed that measuring patients' serum autoantibodies could predict the development and severity of irAEs. The likely mechanism is that PD-1/PD-L1 blockade or deletion of PD-1 can lead to an augmented B cell proliferative and antibody response to T cell-independent antigens as well as enhanced IgG isotype switching and longevity (Boland et al., 2020). These studies suggest a mechanism by which PD-1 blockade could lead to autoantibody expansion and subsequent irAE development. The assessment of relevant risk factors will help to identify patients that clinicians need to be highly vigilant or even unsuitable for immunotherapy, and help clinicians determine the risk-benefit ratio of individual patients to maximize the benefits of treatment while minimizing severe toxicity. It is worth mentioning that although AID patients are at high risk for irAEs, they are not contraindications to PD-1/PD-L1 inhibitors. The use of immunotherapy with caution may be acceptable, but the recurrence of underlying autoimmune diseases should be closely monitored at the same time (Brahmer et al., 2018).

The American Society of Clinical Oncology (ASCO) (Brahmer et al., 2018), the Society for Immunotherapy of Cancer (SITC) (Puzanov et al., 2017), the National Comprehensive Cancer Network (NCCN) (Thompson et al., 2020), and the European Society for Medical Oncology (ESMO) (Haanen et al., 2017) have issued management recommendations for irAE. These recommendations may be applicable to patients with preexisting autoimmunity disease (Tison et al., 2019). The recommended treatment usually includes topical or systemic steroids as first-line treatment. In certain cases, other drugs such as infliximab, mycophenolate mofetil, or cyclophosphamide may be recommended (Ramos-Casals et al., 2020). For example, (Brahmer et al., 2018), for grade 1 irAE, ASCO recommends continuing immunotherapy and monitoring closely. For grade 2 irAE, ASCO recommends temporarily stopping treatment, using moderate systemic steroids (0.5–1 mg/kg/d prednisone), and restarting immunotherapy when the toxicity drops to grade 1 or the symptoms disappear. For grade 3 irAE, ASCO recommends using high-dose steroids (1–2 mg/kg/d prednisone), gradually reducing the dose within 4–6 weeks, and adding immunosuppressive agents in some refractory cases. For grade 4 irAE, ASCO recommends permanent discontinuation of PD-1/PD-L1 inhibitors. With proper management, most irAEs will be resolved (Friedman et al., 2016). For AID patients, it has been discussed previously that although their risk of irAEs is increased, their toxicity is usually controllable. In the study of Danlos (Danlos et al., 2018), 20 subjects with preexisting autoimmune diseases developed irAEs, and only 25% needed to stop treatment. In another study (Gutzmer et al., 2017), adverse events were successfully controlled by immunosuppression and symptom management, and none of the patients required discontinuation of PD-1/PD-L1 inhibitors. The efficacy of PD-1/PD-L1 inhibitors with baseline corticosteroids remains controversial. In AID patients, long-term use of corticosteroids is likely to cause some drug-related adverse events (Puzanov et al., 2017), such as opportunistic infections, sleep disorders, gastritis, and even diabetes and osteoporosis. For active AID, proper control and treatment are required before immunotherapy starts. In this regard, Haanen et al. (2020b) proposed a two-step strategy. First, in order to reduce the risk of impairing the

efficacy before the start of immunotherapy, non-selective immunosuppressants (corticosteroids, mycophenolate mofetil, cyclophosphamide, and MTX) can be replaced by specific selective immunosuppressive drugs [RTX (anti-CD20), VDZ (anti-α4β7 integrin), and TCZ (anti-IL-6), anti-IL-12/23]. After 2–4 weeks, the combination of PD-1/PD-L1 inhibitors and selective immunosuppressants can prevent the deterioration of AID. Several documents seem to support the feasibility of this strategy. Dimitriou et al. (2021) believed that anti-IL6 therapy is effective in treating irAEs or preventing the flare of autoimmune diseases. Among 22 patients (20 patients received irAE treatment and 2 patients received the prophylactic treatment), 21 patients achieved clinical improvement and were well tolerated, and 11 (50%) patients experienced self-limiting and transient toxicity. Frohne et al. (2019) introduced a case of melanoma with IBD. The patient was treated with vedolizumab (anti-α4β7), and his IBD continued to remission. At the same time, pembrolizumab was used to successfully treat metastatic melanoma. With appropriately targeted immunotherapy, patients with preexisting autoimmune diseases can continue to receive immunosuppressive therapy and also receive immune checkpoint inhibitors therapy. Another case report (Uemura et al., 2016) also showed that PD-1/PD-L1 inhibitors combined with selective immunosuppressive drugs can bring clinical benefits. It may delay the deterioration of autoimmunity in patients with advanced melanoma and Crohn's disease, while the antitumor effect is not affected. UC (ulcerative colitis) patients with breast cancer can also be well controlled by anti-TNF therapy without tumor progression (Ben Musa et al., 2014). According to the literature (Yasunaga, 2020), IL-7R signaling plays an important role in the development and progression of lymphoid malignancies and autoimmune diseases, and the abnormal homing activity and steroid resistance caused by IL-7R signaling may worsen the prognosis. Therefore, anti-IL-7R-targeted antibody therapy may be beneficial in the treatment of these two diseases. These indicate that in patients with preexisting active AID, it seems that selective immunosuppressive agents can also be used with caution, but this conclusion still needs more prospective studies to verify. In addition, the combination of tumor-targeted delivery with the continuous expression and release of checkpoint molecules allows these inhibitors to be targeted to desired cells, thus improving efficacy and avoiding toxicity and off-target effects. Research interest in nanomedicine is shifting rapidly toward the adaptation of delivery platforms for improving the percentage of patients who derive clinical benefit from PD-1/PD-L1 inhibitors (Martin et al., 2020). Nanomedicine can reduce, but not eliminate, the risk of certain life-threatening toxicities. In a Phase III trial (NCT02425891), atezolizumab combined with nab-paclitaxel extended progression-free survival in patients with metastatic triple-negative breast cancer (Schmid et al., 2018), suggesting that nab-paclitaxel can enhance the anticancer activity of atezolizumab. The use of lipid-based nanodrugs to deliver vaccines to promote antitumor immunity is the focus of preclinical and clinical research (for example, NCT02410733). In addition to nanomaterials, different tumor-targeted delivery vehicles are under development, which include, but are not limited to, viral vectors, platelets or hematopoietic stem cells, DNA-encoded monoclonal antibodies, bacteria, injectable hydrogels, and matrix-binding checkpoint inhibitor conjugates (Lamichhane et al., 2019). We can use nanodrug delivery platforms with specific targeting properties for each component of the tumor microenvironment. The tumor microenvironment of targeted nanomedicine can reshape the immunosuppressive tumor microenvironment into a state of immune stimulation and enhance the immune response at the tumor site and improve the anticancer effect through immune checkpoint blocking combination therapy (Kim et al., 2021). Yasunaga (2020) had a vision for the future. He believed that next-generation antibody therapies, such as antibody–drug conjugates and bispecific antibodies (bsAbs), would have a promising application prospect in cancer patients with preexisting AID.

In addition, in the context of the increased probability of irAEs in AID patients, it is inevitable that many patients will stop using immunologic drugs due to serious adverse events during PD-1/PD-L1 inhibitors treatment. When the relevant irAEs are relieved, whether to continue to use PD-1/PD-L1 inhibitors and how to balance the clinical benefits and related toxicity of each patient become more and more challenging (Haanen et al., 2020a). In a retrospective analysis (Santini et al., 2018), among 482 NSCLC patients who received PD-L1 inhibitors, 68 (14%) had serious irAEs that required interruption of treatment. Among them, 38 (56%) patients were retreated, and 30 (44%) patients stopped treatment. In the retreatment cohort, 18 (48%) patients had no follow-up irAEs, 10 (26%) patients had initial irAEs recurrence, and 10 (26%) patients had *de novo* irAEs. Most recurrences/*de novo* irAEs were mild (58% were grade 1–2) and controllable (84% resolved or reduced to grade 1). In patients with no improvement in symptoms before the occurrence of irAEs, PFS and OS in the retreatment cohort were longer. In contrast, for those patients who had an objective response before irAEs, PFS, and OS in the retreatment and discontinuation cohorts were similar. Similarly, another retrospective analysis (Schadendorf et al., 2017) showed that many patients continued to benefit from previous immunotherapy even after the drugs were discontinued due to irAEs. ASCO believes that for patients who have not responded yet or have insufficient response, it is reasonable to consider resuming treatment after the toxicity is resolved. However, if the patient has achieved an objective response when the irAEs appear, the response is likely to be long-lasting, and it is not recommended to resume treatment because it comes with a risk of recurrence of toxicity.

CONCLUSION

Although there is a lack of prospective studies on the efficacy and safety of PD-1/PD-L1 inhibitors in cancer patients with preexisting AID, most retrospective analyses show that the efficacy of PD-1/PD-L1 inhibitors in AID patients is similar to that in the general population, and most of the irAEs were mild and controllable. The clinical manifestations of irAEs in AID patients are complex and

diverse, which requires clinical oncologists to increase their awareness of such patients, encourage multidisciplinary cooperation and interaction, and monitor patients individually according to the types of AID, the state of AID, cancer types, treatment drugs, and even gender. In addition, we also need to pay attention to basic research work to figure out the mechanism of irAEs and its relationship with autoimmune diseases. Only by understanding these, can many problems be solved, such as the biomarkers that are helpful for identifying irAEs and targeted therapy drugs in AID patients. The ultimate goal is to maximize the benefits of antitumor response for cancer patients with preexisting AID while minimizing the risk of irAEs.

AUTHOR CONTRIBUTIONS

KZ: investigation, data curation, visualization, methodology, and writing—original draft. XK: investigation, data curation, visualization, writing—original draft, and funding acquisition. YL: methodology, writing-original draft, and writing-review and editing. ZW: conceptualization, supervision, validation, and project administration. LX: conceptualization, resources, supervision, and funding acquisition. LZ: validation, supervision, and writing—review and editing.

FUNDING

This work was supported by the Chinese Academy of Medical Sciences Clinical and Translational Medicine Research Fund Project (No. 2019XK320067), the Natural Science Foundation of China (No. 82103047), the Beijing Municipal Natural Science Foundation (No. 7204293), the Beijing Hope Run Special Fund of Cancer Foundation of China (No. LC 2019B03), the Golden Bridge Project Seed Fund of Beijing Association for Science and Technology (No. ZZ20004), the 2021 Chaoyang District Social Development Science and Technology Plan Project (Medical and Health Field) (No. CYSF2115), the Chinese Young Breast Experts Research Project (No. CYBER-2021-005), the XianSheng Clinical Research Special Fund of China International Medical Foundation (No. Z-2014-06-2103), and the Beijing Xisike Clinical Oncology Research Foundation (No. Y-Young2021-0017).

REFERENCES

Abdel-Wahab, N., Shah, M., Lopez-Olivo, M. A., and Suarez-Almazor, M. E. (2018). Use of Immune Checkpoint Inhibitors in the Treatment of Patients with Cancer and Preexisting Autoimmune Disease: A Systematic Review. *Ann. Intern. Med.* 168 (2), 121–130. doi:10.7326/M17-2073

Akinleye, A., and Rasool, Z. (2019). Immune Checkpoint Inhibitors of PD-L1 as Cancer Therapeutics. *J. Hematol. Oncol.* 12 (1), 92. doi:10.1186/s13045-019-0779-5

Axelrad, J. E., Lichtiger, S., and Yajnik, V. (2016). Inflammatory Bowel Disease and Cancer: The Role of Inflammation, Immunosuppression, and Cancer Treatment. *World J. Gastroenterol.* 22 (20), 4794–4801. doi:10.3748/wjg.v22.i20.4794

Ben Musa, R., Usha, L., Hibbeln, J., and Mutlu, E. A. (2014). TNF Inhibitors to Treat Ulcerative Colitis in a Metastatic Breast Cancer Patient: a Case Report and Literature Review. *World J. Gastroenterol.* 20 (19), 5912–5917. doi:10.3748/wjg.v20.i19.5912

Boland, P., Pavlick, A. C., Weber, J., and Sandigursky, S. (2020). Immunotherapy to Treat Malignancy in Patients with Pre-existing Autoimmunity. *J. Immunother. Cancer* 8 (1). doi:10.1136/jitc-2019-000356

Borghaei, H., Gettinger, S., Vokes, E. E., Chow, L. Q. M., Burgio, M. A., de Castro Carpeno, J., et al. (2021). Five-Year Outcomes from the Randomized, Phase III Trials CheckMate 017 and 057: Nivolumab versus Docetaxel in Previously Treated Non-small-cell Lung Cancer. *J. Clin. Oncol.* 39 (7), 723–733. doi:10.1200/JCO.20.01605

Botticelli, A., Onesti, C. E., Zizzari, I., Cerbelli, B., Sciattella, P., Occhipinti, M., et al. (2017). The Sexist Behaviour of Immune Checkpoint Inhibitors in Cancer Therapy? *Oncotarget* 8 (59), 99336–99346. doi:10.18632/oncotarget.22242

Brahmer, J. R., Lacchetti, C., Schneider, B. J., Atkins, M. B., Brassil, K. J., Caterino, J. M., et al. (2018). Management of Immune-Related Adverse Events in Patients Treated with Immune Checkpoint Inhibitor Therapy: American Society of Clinical Oncology Clinical Practice Guideline. *J. Clin. Oncol.* 36 (17), 1714–1768. doi:10.1200/JCO.2017.77.6385

Buchbinder, E. I., and Desai, A. (2016). CTLA-4 and PD-1 Pathways: Similarities, Differences, and Implications of Their Inhibition. *Am. J. Clin. Oncol.* 39 (1), 98–106. doi:10.1097/COC.0000000000000239

Cao, L., Tong, H., Xu, G., Liu, P., Meng, H., Wang, J., et al. (2015). Systemic Lupus Erythematous and Malignancy Risk: a Meta-Analysis. *PLoS One* 10 (4), e0122964. doi:10.1371/journal.pone.0122964

Cappelli, L. C., and Shah, A. A. (2020). The Relationships between Cancer and Autoimmune Rheumatic Diseases. *Best Pract. Res. Clin. Rheumatol.* 34 (1), 101472. doi:10.1016/j.berh.2019.101472

Chau, J., and Zhang, J. (2021). Tying Small Changes to Large Outcomes: The Cautious Promise in Incorporating the Microbiome into Immunotherapy. *Int. J. Mol. Sci.* 22 (15). doi:10.3390/ijms22157900

Conforti, F., Pala, L., Bagnardi, V., De Pas, T., Martinetti, M., Viale, G., et al. (2018). Cancer Immunotherapy Efficacy and Patients' Sex: a Systematic Review and Meta-Analysis. *Lancet Oncol.* 19 (6), 737–746. doi:10.1016/S1470-2045(18)30261-4

Constantinidou, A., Alifieris, C., and Trafalis, D. T. (2019). Targeting Programmed Cell Death -1 (PD-1) and Ligand (PD-L1): A new era in Cancer Active Immunotherapy. *Pharmacol. Ther.* 194, 84–106. doi:10.1016/j.pharmthera.2018.09.008

Cortellini, A., Buti, S., Santini, D., Perrone, F., Giusti, R., Tiseo, M., et al. (2019). Clinical Outcomes of Patients with Advanced Cancer and Pre-existing Autoimmune Diseases Treated with Anti-programmed Death-1 Immunotherapy: A Real-World Transverse Study. *Oncologist* 24 (6), e327–e337. doi:10.1634/theoncologist.2018-0618

D'Angelo, S. P., Bhatia, S., Brohl, A. S., Hamid, O., Mehnert, J. M., Terheyden, P., et al. (2020). Avelumab in Patients with Previously Treated Metastatic Merkel Cell Carcinoma: Long-Term Data and Biomarker Analyses from the Single-Arm Phase 2 JAVELIN Merkel 200 Trial. *J. Immunother. Cancer* 8 (1). doi:10.1136/jitc-2020-000674

Danlos, F. X., Voisin, A. L., Dyevre, V., Michot, J. M., Routier, E., Taillade, L., et al. (2018). Safety and Efficacy of Anti-programmed Death 1 Antibodies in Patients with Cancer and Pre-existing Autoimmune or Inflammatory Disease. *Eur. J. Cancer* 91, 21–29. doi:10.1016/j.ejca.2017.12.008

Das, R., Bar, N., Ferreira, M., Newman, A. M., Zhang, L., Bailur, J. K., et al. (2018). Early B Cell Changes Predict Autoimmunity Following Combination Immune Checkpoint Blockade. *J. Clin. Invest.* 128 (2), 715–720. doi:10.1172/JCI96798

Das, S., and Johnson, D. B. (2019). Immune-related Adverse Events and Anti-tumor Efficacy of Immune Checkpoint Inhibitors. *J. Immunother. Cancer* 7 (1), 306. doi:10.1186/s40425-019-0805-8

Dietz, H., Weinmann, S. C., and Salama, A. K. (2021). Checkpoint Inhibitors in Melanoma Patients with Underlying Autoimmune Disease. *Cancer Manag. Res.* 13, 8199–8208. doi:10.2147/CMAR.S283217

Dimitriou, F., Hogan, S., Menzies, A. M., Dummer, R., and Long, G. V. (2021). Interleukin-6 Blockade for Prophylaxis and Management of Immune-Related

Adverse Events in Cancer Immunotherapy. *Eur. J. Cancer* 157, 214–224. doi:10.1016/j.ejca.2021.08.031

Eaden, J. A., Abrams, K. R., and Mayberry, J. F. (2001). The Risk of Colorectal Cancer in Ulcerative Colitis: a Meta-Analysis. *Gut* 48 (4), 526–535. doi:10.1136/gut.48.4.526

Fountzilas, E., Lampaki, S., Koliou, G. A., Koumarianou, A., Levva, S., Vagionas, A., et al. (2022). Real-world Safety and Efficacy Data of Immunotherapy in Patients with Cancer and Autoimmune Disease: the Experience of the Hellenic Cooperative Oncology Group. *Cancer Immunol. Immunother.* 71 (2), 327–337. doi:10.1007/s00262-021-02985-6

Friedman, C. F., Proverbs-Singh, T. A., and Postow, M. A. (2016). Treatment of the Immune-Related Adverse Effects of Immune Checkpoint Inhibitors: A Review. *JAMA Oncol.* 2 (10), 1346–1353. doi:10.1001/jamaoncol.2016.1051

Frohne, C. C., Llano, E. M., Perkovic, A., Cohen, R. D., and Luke, J. J. (2019). Complete Response of Metastatic Melanoma in a Patient with Crohn's Disease Simultaneously Receiving Anti-α4β7 and Anti-PD1 Antibodies. *J. Immunother. Cancer* 7 (1), 1. doi:10.1186/s40425-018-0484-x

Fujii, T., Colen, R. R., Bilen, M. A., Hess, K. R., Hajjar, J., Suarez-Almazor, M. E., et al. (2018). Incidence of Immune-Related Adverse Events and its Association with Treatment Outcomes: the MD Anderson Cancer Center Experience. *Invest. New Drugs* 36 (4), 638–646. doi:10.1007/s10637-017-0534-0

Geller, S., Xu, H., Lebwohl, M., Nardone, B., Lacouture, M. E., and Kheterpal, M. (2018). Malignancy Risk and Recurrence with Psoriasis and its Treatments: A Concise Update. *Am. J. Clin. Dermatol.* 19 (3), 363–375. doi:10.1007/s40257-017-0337-2

Giat, E., Ehrenfeld, M., and Shoenfeld, Y. (2017). Cancer and Autoimmune Diseases. *Autoimmun. Rev.* 16 (10), 1049–1057. doi:10.1016/j.autrev.2017.07.022

Gong, J., Chehrazi-Raffle, A., Reddi, S., and Salgia, R. (2018). Development of PD-1 and PD-L1 Inhibitors as a Form of Cancer Immunotherapy: a Comprehensive Review of Registration Trials and Future Considerations. *J. Immunother. Cancer* 6 (1), 8. doi:10.1186/s40425-018-0316-z

Gowen, M. F., Giles, K. M., Simpson, D., Tchack, J., Zhou, H., Moran, U., et al. (2018). Baseline Antibody Profiles Predict Toxicity in Melanoma Patients Treated with Immune Checkpoint Inhibitors. *J. Transl Med.* 16 (1), 82. doi:10.1186/s12967-018-1452-4

Grangeon, M., Tomasini, P., Chaleat, S., Jeanson, A., Souquet-Bressand, M., Khobta, N., et al. (2019). Association between Immune-Related Adverse Events and Efficacy of Immune Checkpoint Inhibitors in Non-small-cell Lung Cancer. *Clin. Lung Cancer* 20 (3), 201–207. doi:10.1016/j.cllc.2018.10.002

Gutzmer, R., Koop, A., Meier, F., Hassel, J. C., Terheyden, P., Zimmer, L., et al. (2017). Programmed Cell Death Protein-1 (PD-1) Inhibitor Therapy in Patients with Advanced Melanoma and Preexisting Autoimmunity or Ipilimumab-Triggered Autoimmunity. *Eur. J. Cancer* 75, 24–32. doi:10.1016/j.ejca.2016.12.038

Haanen, J., Ernstoff, M. S., Wang, Y., Menzies, A. M., Puzanov, I., Grivas, P., et al. (2020b). Autoimmune Diseases and Immune-Checkpoint Inhibitors for Cancer Therapy: Review of the Literature and Personalized Risk-Based Prevention Strategy. *Ann. Oncol.* 31 (6), 724–744. doi:10.1016/j.annonc.2020.03.285

Haanen, J., Carbonnel, F., Robert, C., Kerr, K. M., Peters, S., Larkin, J., et al. (2017). Management of Toxicities from Immunotherapy: ESMO Clinical Practice Guidelines for Diagnosis, Treatment and Follow-Up. *Ann. Oncol.* 28 (Suppl. l_4), iv119–iv142. doi:10.1093/annonc/mdx225

Haanen, J., Ernstoff, M., Wang, Y., Menzies, A., Puzanov, I., Grivas, P., et al. (2020a). Rechallenge Patients with Immune Checkpoint Inhibitors Following Severe Immune-Related Adverse Events: Review of the Literature and Suggested Prophylactic Strategy. *J. Immunother. Cancer* 8 (1). doi:10.1136/jitc-2020-000604

Hoa, S., Laaouad, L., Roberts, J., Ennis, D., Ye, C., Al Jumaily, K., et al. (2021). Preexisting Autoimmune Disease and Immune-Related Adverse Events Associated with Anti-PD-1 Cancer Immunotherapy: a National Case Series from the Canadian Research Group of Rheumatology in Immuno-Oncology. *Cancer Immunol. Immunother.* 70 (8), 2197–2207. doi:10.1007/s00262-021-02851-5

Hodi, F. S., Chiarion-Sileni, V., Gonzalez, R., Grob, J. J., Rutkowski, P., Cowey, C. L., et al. (2018). Nivolumab Plus Ipilimumab or Nivolumab Alone versus Ipilimumab Alone in Advanced Melanoma (CheckMate 067): 4-year Outcomes of a Multicentre, Randomised, Phase 3 Trial. *Lancet Oncol.* 19 (11), 1480–1492. doi:10.1016/S1470-2045(18)30700-9

Hoefsmit, E. P., Rozeman, E. A., Haanen, J., and Blank, C. U. (2019). Susceptible Loci Associated with Autoimmune Disease as Potential Biomarkers for Checkpoint Inhibitor-Induced Immune-Related Adverse Events. *ESMO Open* 4 (4), e000472. doi:10.1136/esmoopen-2018-000472

Hommes, J. W., Verheijden, R. J., Suijkerbuijk, K. P. M., and Hamann, D. (2020). Biomarkers of Checkpoint Inhibitor Induced Immune-Related Adverse Events-A Comprehensive Review. *Front. Oncol.* 10, 585311. doi:10.3389/fonc.2020.585311

Horn, L., Spigel, D. R., Vokes, E. E., Holgado, E., Ready, N., Steins, M., et al. (2017). Nivolumab versus Docetaxel in Previously Treated Patients with Advanced Non-small-cell Lung Cancer: Two-Year Outcomes from Two Randomized, Open-Label, Phase III Trials (CheckMate 017 and CheckMate 057). *J. Clin. Oncol.* 35 (35), 3924–3933. doi:10.1200/JCO.2017.74.3062

Hsu, J., Hodgins, J. J., Marathe, M., Nicolai, C. J., Bourgeois-Daigneault, M. C., Trevino, T. N., et al. (2018). Contribution of NK Cells to Immunotherapy Mediated by PD-1/pd-L1 Blockade. *J. Clin. Invest.* 128 (10), 4654–4668. doi:10.1172/JCI99317

Hua, C., Boussemart, L., Mateus, C., Routier, E., Boutros, C., Cazenave, H., et al. (2016). Association of Vitiligo with Tumor Response in Patients with Metastatic Melanoma Treated with Pembrolizumab. *JAMA Dermatol.* 152 (1), 45–51. doi:10.1001/jamadermatol.2015.2707

Hussaini, S., Chehade, R., Boldt, R. G., Raphael, J., Blanchette, P., Maleki Vareki, S., et al. (2021). Association between Immune-Related Side Effects and Efficacy and Benefit of Immune Checkpoint Inhibitors - A Systematic Review and Meta-Analysis. *Cancer Treat. Rev.* 92, 102134. doi:10.1016/j.ctrv.2020.102134

Igoe, A., Merjanah, S., and Scofield, R. H. (2020). Sjögren Syndrome and Cancer. *Rheum. Dis. Clin. North. Am.* 46 (3), 513–532. doi:10.1016/j.rdc.2020.05.004

Jing, Y., Zhang, Y., Wang, J., Li, K., Chen, X., Heng, J., et al. (2021). Association between Sex and Immune-Related Adverse Events during Immune Checkpoint Inhibitor Therapy. *J. Natl. Cancer Inst.* 113 (10), 1396–1404. doi:10.1093/jnci/djab035

Judd, J., Zibelman, M., Handorf, E., O'Neill, J., Ramamurthy, C., Bentota, S., et al. (2017). Immune-Related Adverse Events as a Biomarker in Non-melanoma Patients Treated with Programmed Cell Death 1 Inhibitors. *Oncologist* 22 (10), 1232–1237. doi:10.1634/theoncologist.2017-0133

June, C. H., Warshauer, J. T., and Bluestone, J. A. (2017). Corrigendum: Is Autoimmunity the Achilles' Heel of Cancer Immunotherapy? *Nat. Med.* 23 (5), 1004–1547. doi:10.1038/nm0817-1004b

Kang, J. H., Bluestone, J. A., and Young, A. (2021). Predicting and Preventing Immune Checkpoint Inhibitor Toxicity: Targeting Cytokines. *Trends Immunol.* 42 (4), 293–311. doi:10.1016/j.it.2021.02.006

Keir, M. E., Butte, M. J., Freeman, G. J., and Sharpe, A. H. (2008). PD-1 and its Ligands in Tolerance and Immunity. *Annu. Rev. Immunol.* 26, 677–704. doi:10.1146/annurev.immunol.26.021607.090331

Kennedy, L. C., Bhatia, S., Thompson, J. A., and Grivas, P. (2019). Preexisting Autoimmune Disease: Implications for Immune Checkpoint Inhibitor Therapy in Solid Tumors. *J. Natl. Compr. Canc Netw.* 17 (6), 750–757. doi:10.6004/jnccn.2019.7310

Khan, S. A., Pruitt, S. L., Xuan, L., and Gerber, D. E. (2016). Prevalence of Autoimmune Disease Among Patients with Lung Cancer: Implications for Immunotherapy Treatment Options. *JAMA Oncol.* 2 (11), 1507–1508. doi:10.1001/jamaoncol.2016.2238

Khoja, L., Day, D., Wei-Wu Chen, T., Siu, L. L., and Hansen, A. R. (2017). Tumour- and Class-specific Patterns of Immune-Related Adverse Events of Immune Checkpoint Inhibitors: a Systematic Review. *Ann. Oncol.* 28 (10), 2377–2385. doi:10.1093/annonc/mdx286

Kim, J., Hong, J., Lee, J., Fakhraei Lahiji, S., and Kim, Y. H. (2021). Recent Advances in Tumor Microenvironment-Targeted Nanomedicine Delivery Approaches to Overcome Limitations of Immune Checkpoint Blockade-Based Immunotherapy. *J. Control. Release* 332, 109–126. doi:10.1016/j.jconrel.2021.02.002

Klein, S. L., and Flanagan, K. L. (2016). Sex Differences in Immune Responses. *Nat. Rev. Immunol.* 16 (10), 626–638. doi:10.1038/nri.2016.90

Krishnan, T., Tomita, Y., and Roberts-Thomson, R. (2020). A Retrospective Analysis of Eosinophilia as a Predictive Marker of Response and Toxicity to

Cancer Immunotherapy. *Future Sci. OA* 6 (10), FSO608. doi:10.2144/fsoa-2020-0070

Kumar, P., Saini, S., and Prabhakar, B. S. (2020). Cancer Immunotherapy with Check point Inhibitor Can Cause Autoimmune Adverse Events Due to Loss of Treg Homeostasis. *Semin. Cancer Biol.* 64, 29–35. doi:10.1016/j.semcancer.2019.01.006

Kurimoto, C., Inaba, H., Ariyasu, H., Iwakura, H., Ueda, Y., Uraki, S., et al. (2020). Predictive and Sensitive Biomarkers for Thyroid Dysfunctions during Treatment with Immune-Checkpoint Inhibitors. *Cancer Sci.* 111 (5), 1468–1477. doi:10.1111/cas.14363

Lamichhane, P., Deshmukh, R., Brown, J. A., Jakubski, S., Parajuli, P., Nolan, T., et al. (2019). Novel Delivery Systems for Checkpoint Inhibitors. *Medicines (Basel)* 6 (3), 6030074. doi:10.3390/medicines6030074

Larkin, J., Chiarion-Sileni, V., Gonzalez, R., Grob, J. J., Cowey, C. L., Lao, C. D., et al. (2015). Combined Nivolumab and Ipilimumab or Monotherapy in Untreated Melanoma. *N. Engl. J. Med.* 373 (1), 23–34. doi:10.1056/NEJMoa1504030

Lau, L., Huang, L., Fu, E., Tan, T. C., Kong, K. O., and Lim, M. Y. (2021). Nasopharyngeal Carcinoma in Dermatomyositis. *Clin. Otolaryngol.* 46 (5), 1082–1088. doi:10.1111/coa.13764

Lee, D. J., Lee, H. J., Jr., Farmer, J. R., and Reynolds, K. L. (2021). Mechanisms Driving Immune-Related Adverse Events in Cancer Patients Treated with Immune Checkpoint Inhibitors. *Curr. Cardiol. Rep.* 23 (8), 98. doi:10.1007/s11886-021-01530-2

Lee, Y. H., Woo, J. H., Choi, S. J., Ji, J. D., and Song, G. G. (2009). Association of Programmed Cell Death 1 Polymorphisms and Systemic Lupus Erythematosus: a Meta-Analysis. *Lupus* 18 (1), 9–15. doi:10.1177/0961203308093923

Leonardi, G. C., Gainor, J. F., Altan, M., Kravets, S., Dahlberg, S. E., Gedmintas, L., et al. (2018). Safety of Programmed Death-1 Pathway Inhibitors Among Patients with Non-small-cell Lung Cancer and Preexisting Autoimmune Disorders. *J. Clin. Oncol.* 36 (19), 1905–1912. doi:10.1200/JCO.2017.77.0305

Liang, Y., Yang, Z., Qin, B., and Zhong, R. (2014). Primary Sjogren's Syndrome and Malignancy Risk: a Systematic Review and Meta-Analysis. *Ann. Rheum. Dis.* 73 (6), 1151–1156. doi:10.1136/annrheumdis-2013-203305

Lim, S. Y., Lee, J. H., Gide, T. N., Menzies, A. M., Guminski, A., Carlino, M. S., et al. (2019). Circulating Cytokines Predict Immune-Related Toxicity in Melanoma Patients Receiving Anti-PD-1-based Immunotherapy. *Clin. Cancer Res.* 25 (5), 1557–1563. doi:10.1158/1078-0432.CCR-18-2795

Lipson, E. J., Bagnasco, S. M., Moore, J., Jr., Jang, S., Patel, M. J., Zachary, A. A., et al. (2016). Tumor Regression and Allograft Rejection after Administration of Anti-PD-1. *N. Engl. J. Med.* 374 (9), 896–898. doi:10.1056/NEJMc1509268

Liudahl, S. M., and Coussens, L. M. (2018). B Cells as Biomarkers: Predicting Immune Checkpoint Therapy Adverse Events. *J. Clin. Invest.* 128 (2), 577–579. doi:10.1172/JCI99036

Loriot, Y., Sternberg, C. N., Castellano, D., Oosting, S. F., Dumez, H., Huddart, R., et al. (2020). Safety and Efficacy of Atezolizumab in Patients with Autoimmune Disease: Subgroup Analysis of the SAUL Study in Locally Advanced/metastatic Urinary Tract Carcinoma. *Eur. J. Cancer* 138, 202–211. doi:10.1016/j.ejca.2020.07.023

Lutgens, M. W., van Oijen, M. G., van der Heijden, G. J., Vleggaar, F. P., Siersema, P. D., and Oldenburg, B. (2013). Declining Risk of Colorectal Cancer in Inflammatory Bowel Disease: an Updated Meta-Analysis of Population-Based Cohort Studies. *Inflamm. Bowel Dis.* 19 (4), 789–799. doi:10.1097/MIB.0b013e31828029c0

Marabelle, A., Le, D. T., Ascierto, P. A., Di Giacomo, A. M., De Jesus-Acosta, A., Delord, J. P., et al. (2020). Efficacy of Pembrolizumab in Patients with Noncolorectal High Microsatellite Instability/Mismatch Repair-Deficient Cancer: Results from the Phase II KEYNOTE-158 Study. *J. Clin. Oncol.* 38 (1), 1–10. doi:10.1200/JCO.19.02105

Martin, J. D., Cabral, H., Stylianopoulos, T., and Jain, R. K. (2020). Improving Cancer Immunotherapy Using Nanomedicines: Progress, Opportunities and Challenges. *Nat. Rev. Clin. Oncol.* 17 (4), 251–266. doi:10.1038/s41571-019-0308-z

Martins, F., Sofiya, L., Sykiotis, G. P., Lamine, F., Maillard, M., Fraga, M., et al. (2019). Adverse Effects of Immune-Checkpoint Inhibitors: Epidemiology, Management and Surveillance. *Nat. Rev. Clin. Oncol.* 16 (9), 563–580. doi:10.1038/s41571-019-0218-0

Masetti, R., Tiri, A., Tignanelli, A., Turrini, E., Argentiero, A., Pession, A., et al. (2021). Autoimmunity and Cancer. *Autoimmun. Rev.* 20 (9), 102882. doi:10.1016/j.autrev.2021.102882

Massironi, S., Zilli, A., Elvevi, A., and Invernizzi, P. (2019). The Changing Face of Chronic Autoimmune Atrophic Gastritis: an Updated Comprehensive Perspective. *Autoimmun. Rev.* 18 (3), 215–222. doi:10.1016/j.autrev.2018.08.011

Matson, V., Fessler, J., Bao, R., Chongsuwat, T., Zha, Y., Alegre, M. L., et al. (2018). The Commensal Microbiome Is Associated with Anti-PD-1 Efficacy in Metastatic Melanoma Patients. *Science* 359 (6371), 104–108. doi:10.1126/science.aao3290

Menzies, A. M., Johnson, D. B., Ramanujam, S., Atkinson, V. G., Wong, A. N. M., Park, J. J., et al. (2017). Anti-PD-1 Therapy in Patients with Advanced Melanoma and Preexisting Autoimmune Disorders or Major Toxicity with Ipilimumab. *Ann. Oncol.* 28 (2), 368–376. doi:10.1093/annonc/mdw443

Michot, J. M., Bigenwald, C., Champiat, S., Collins, M., Carbonnel, F., Postel-Vinay, S., et al. (2016). Immune-related Adverse Events with Immune Checkpoint Blockade: a Comprehensive Review. *Eur. J. Cancer* 54, 139–148. doi:10.1016/j.ejca.2015.11.016

Nadeem, M. S., Kumar, V., Al-Abbasi, F. A., Kamal, M. A., and Anwar, F. (2020). Risk of Colorectal Cancer in Inflammatory Bowel Diseases. *Semin. Cancer Biol.* 64, 51–60. doi:10.1016/j.semcancer.2019.05.001

Ngo, S. T., Steyn, F. J., and McCombe, P. A. (2014). Gender Differences in Autoimmune Disease. *Front. Neuroendocrinol* 35 (3), 347–369. doi:10.1016/j.yfrne.2014.04.004

Niccolai, E., Boem, F., Emmi, G., and Amedei, A. (2020). The Link "Cancer and Autoimmune Diseases" in the Light of Microbiota: Evidence of a Potential Culprit. *Immunol. Lett.* 222, 12–28. doi:10.1016/j.imlet.2020.03.001

Nishijima, T. F., Shachar, S. S., Nyrop, K. A., and Muss, H. B. (2017). Safety and Tolerability of PD-1/pd-L1 Inhibitors Compared with Chemotherapy in Patients with Advanced Cancer: A Meta-Analysis. *Oncologist* 22 (4), 470–479. doi:10.1634/theoncologist.2016-0419

Nishimura, H., Nose, M., Hiai, H., Minato, N., and Honjo, T. (1999). Development of Lupus-like Autoimmune Diseases by Disruption of the PD-1 Gene Encoding an ITIM Motif-Carrying Immunoreceptor. *Immunity* 11 (2), 141–151. doi:10.1016/s1074-7613(00)80089-8

Nishino, M., Giobbie-Hurder, A., Hatabu, H., Ramaiya, N. H., and Hodi, F. S. (2016). Incidence of Programmed Cell Death 1 Inhibitor-Related Pneumonitis in Patients with Advanced Cancer: A Systematic Review and Meta-Analysis. *JAMA Oncol.* 2 (12), 1607–1616. doi:10.1001/jamaoncol.2016.2453

Okwundu, N., Grossman, D., Hu-Lieskovan, S., Grossmann, K. F., and Swami, U. (2021). The Dark Side of Immunotherapy. *Ann. Transl Med.* 9 (12), 1041. doi:10.21037/atm-20-4750

Osorio, J. C., Ni, A., Chaft, J. E., Pollina, R., Kasler, M. K., Stephens, D., et al. (2017). Antibody-mediated Thyroid Dysfunction during T-Cell Checkpoint Blockade in Patients with Non-small-cell Lung Cancer. *Ann. Oncol.* 28 (3), 583–589. doi:10.1093/annonc/mdw640

Pantuck, M., McDermott, D., and Drakaki, A. (2019). To Treat or Not to Treat: Patient Exclusion in Immune Oncology Clinical Trials Due to Preexisting Autoimmune Disease. *Cancer* 125 (20), 3506–3513. doi:10.1002/cncr.32326

Pavan, A., Calvetti, L., Dal Maso, A., Attili, I., Del Bianco, P., Pasello, G., et al. (2019). Peripheral Blood Markers Identify Risk of Immune-Related Toxicity in Advanced Non-small Cell Lung Cancer Treated with Immune-Checkpoint Inhibitors. *Oncologist* 24 (8), 1128–1136. doi:10.1634/theoncologist.2018-0563

Pundole, X., and Suarez-Almazor, M. E. (2020). Cancer and Rheumatoid Arthritis. *Rheum. Dis. Clin. North. Am.* 46 (3), 445–462. doi:10.1016/j.rdc.2020.05.003

Puzanov, I., Diab, A., Abdallah, K., Bingham, C. O., 3rd, Brogdon, C., Dadu, R., et al. (2017). Managing Toxicities Associated with Immune Checkpoint Inhibitors: Consensus Recommendations from the Society for Immunotherapy of Cancer (SITC) Toxicity Management Working Group. *J. Immunother. Cancer* 5 (1), 95. doi:10.1186/s40425-017-0300-z

Rakshit, S., and Molina, J. R. (2020). Immunotherapy in Patients with Autoimmune Disease. *J. Thorac. Dis.* 12 (11), 7032–7038. doi:10.21037/jtd-2019-cptn-10

Ramos-Casals, M., Brahmer, J. R., Callahan, M. K., Flores-Chávez, A., Keegan, N., Khamashta, M. A., et al. (2020). Immune-related Adverse Events of Checkpoint Inhibitors. *Nat. Rev. Dis. Primers* 6 (1), 38. doi:10.1038/s41572-020-0160-6

Reck, M., Rodríguez-Abreu, D., Robinson, A. G., Hui, R., Csőszi, T., Fülöp, A., et al. (2019). Updated Analysis of KEYNOTE-024: Pembrolizumab versus Platinum-Based Chemotherapy for Advanced Non-small-cell Lung Cancer with PD-L1 Tumor Proportion Score of 50% or Greater. *J. Clin. Oncol.* 37 (7), 537–546. doi:10.1200/JCO.18.00149

Ribas, A., and Wolchok, J. D. (2018). Cancer Immunotherapy Using Checkpoint Blockade. *Science* 359 (6382), 1350–1355. doi:10.1126/science.aar4060

Ricciuti, B., Dahlberg, S. E., Adeni, A., Sholl, L. M., Nishino, M., and Awad, M. M. (2019). Immune Checkpoint Inhibitor Outcomes for Patients with Non-small-cell Lung Cancer Receiving Baseline Corticosteroids for Palliative versus Nonpalliative Indications. *J. Clin. Oncol.* 37 (22), 1927–1934. doi:10.1200/JCO.19.00189

Richter, M. D., Pinkston, O., Kottschade, L. A., Finnes, H. D., Markovic, S. N., and Thanarajasingam, U. (2018). Brief Report: Cancer Immunotherapy in Patients with Preexisting Rheumatic Disease: The Mayo Clinic Experience. *Arthritis Rheumatol.* 70 (3), 356–360. doi:10.1002/art.40397

Rittmeyer, A., Barlesi, F., Waterkamp, D., Park, K., Ciardiello, F., von Pawel, J., et al. (2017). Atezolizumab versus Docetaxel in Patients with Previously Treated Non-small-cell Lung Cancer (OAK): a Phase 3, Open-Label, Multicentre Randomised Controlled Trial. *Lancet* 389 (10066), 255–265. doi:10.1016/S0140-6736(16)32517-X

Rizvi, N. A., Cho, B. C., Reinmuth, N., Lee, K. H., Luft, A., Ahn, M. J., et al. (2020). Durvalumab with or without Tremelimumab vs Standard Chemotherapy in First-Line Treatment of Metastatic Non-small Cell Lung Cancer: The MYSTIC Phase 3 Randomized Clinical Trial. *JAMA Oncol.* 6 (5), 661–674. doi:10.1001/jamaoncol.2020.0237

Robert, C., Ribas, A., Wolchok, J. D., Hodi, F. S., Hamid, O., Kefford, R., et al. (2014). Anti-programmed-death-receptor-1 Treatment with Pembrolizumab in Ipilimumab-Refractory Advanced Melanoma: a Randomised Dose-Comparison Cohort of a Phase 1 Trial. *Lancet* 384 (9948), 1109–1117. doi:10.1016/S0140-6736(14)60958-2

Rossi, G., Pezzuto, A., Sini, C., Tuzi, A., Citarella, F., McCusker, M. G., et al. (2019). Concomitant Medications during Immune Checkpoint Blockage in Cancer Patients: Novel Insights in This Emerging Clinical Scenario. *Crit. Rev. Oncol. Hematol.* 142, 26–34. doi:10.1016/j.critrevonc.2019.07.005

Sanchez, K., Page, D. B., and Urba, W. (2019). Immunotherapy Toxicities. *Surg. Oncol. Clin. N. Am.* 28 (3), 387–401. doi:10.1016/j.soc.2019.02.009

Sanlorenzo, M., Vujic, I., Daud, A., Algazi, A., Gubens, M., Luna, S. A., et al. (2015). Pembrolizumab Cutaneous Adverse Events and Their Association with Disease Progression. *JAMA Dermatol.* 151 (11), 1206–1212. doi:10.1001/jamadermatol.2015.1916

Santini, F. C., Rizvi, H., Plodkowski, A. J., Ni, A., Lacouture, M. E., Gambarin-Gelwan, M., et al. (2018). Safety and Efficacy of Re-treating with Immunotherapy after Immune-Related Adverse Events in Patients with NSCLC. *Cancer Immunol. Res.* 6 (9), 1093–1099. doi:10.1158/2326-6066.CIR-17-0755

Schadendorf, D., Wolchok, J. D., Hodi, F. S., Chiarion-Sileni, V., Gonzalez, R., Rutkowski, P., et al. (2017). Efficacy and Safety Outcomes in Patients with Advanced Melanoma Who Discontinued Treatment with Nivolumab and Ipilimumab Because of Adverse Events: A Pooled Analysis of Randomized Phase II and III Trials. *J. Clin. Oncol.* 35 (34), 3807–3814. doi:10.1200/JCO.2017.73.2289

Schirmer, M., Smeekens, S. P., Vlamakis, H., Jaeger, M., Oosting, M., Franzosa, E. A., et al. (2016). Linking the Human Gut Microbiome to Inflammatory Cytokine Production Capacity. *Cell* 167 (4), 1897–1136. doi:10.1016/j.cell.2016.11.046

Schmid, P., Adams, S., Rugo, H. S., Schneeweiss, A., Barrios, C. H., Iwata, H., et al. (2018). Atezolizumab and Nab-Paclitaxel in Advanced Triple-Negative Breast Cancer. *N. Engl. J. Med.* 379 (22), 2108–2121. doi:10.1056/NEJMoa1809615

Sezer, A., Kilickap, S., Gümüş, M., Bondarenko, I., Özgüroğlu, M., Gogishvili, M., et al. (2021). Cemiplimab Monotherapy for First-Line Treatment of Advanced Non-small-cell Lung Cancer with PD-L1 of at Least 50%: a Multicentre, Open-Label, Global, Phase 3, Randomised, Controlled Trial. *Lancet* 397 (10274), 592–604. doi:10.1016/S0140-6736(21)00228-2

Shah, K. P., Song, H., Ye, F., Moslehi, J. J., Balko, J. M., Salem, J. E., et al. (2020). Demographic Factors Associated with Toxicity in Patients Treated with Anti-programmed Cell Death-1 Therapy. *Cancer Immunol. Res.* 8 (7), 851–855. doi:10.1158/2326-6066.CIR-19-0986

Simon, T. A., Thompson, A., Gandhi, K. K., Hochberg, M. C., and Suissa, S. (2015). Incidence of Malignancy in Adult Patients with Rheumatoid Arthritis: a Meta-Analysis. *Arthritis Res. Ther.* 17, 212. doi:10.1186/s13075-015-0728-9

Song, L., Wang, Y., Zhang, J., Song, N., Xu, X., and Lu, Y. (2018). The Risks of Cancer Development in Systemic Lupus Erythematosus (SLE) Patients: a Systematic Review and Meta-Analysis. *Arthritis Res. Ther.* 20 (1), 270. doi:10.1186/s13075-018-1760-3

Su, C., Wang, H., Liu, Y., Guo, Q., Zhang, L., Li, J., et al. (2020). Adverse Effects of Anti-PD-1/pd-L1 Therapy in Non-small Cell Lung Cancer. *Front. Oncol.* 10, 554313. doi:10.3389/fonc.2020.554313

Thompson, J. A., Schneider, B. J., Brahmer, J., Andrews, S., Armand, P., Bhatia, S., et al. (2020). NCCN Guidelines Insights: Management of Immunotherapy-Related Toxicities, Version 1.2020. *J. Natl. Compr. Canc Netw.* 18 (3), 230–241. doi:10.6004/jnccn.2020.0012

Tison, A., Quéré, G., Misery, L., Funck-Brentano, E., Danlos, F. X., Routier, E., et al. (2019). Safety and Efficacy of Immune Checkpoint Inhibitors in Patients with Cancer and Preexisting Autoimmune Disease: A Nationwide, Multicenter Cohort Study. *Arthritis Rheumatol.* 71 (12), 2100–2111. doi:10.1002/art.41068

Toi, Y., Sugawara, S., Sugisaka, J., Ono, H., Kawashima, Y., Aiba, T., et al. (2019). Profiling Preexisting Antibodies in Patients Treated with Anti-PD-1 Therapy for Advanced Non-small Cell Lung Cancer. *JAMA Oncol.* 5 (3), 376–383. doi:10.1001/jamaoncol.2018.5860

Topalian, S. L., Sznol, M., McDermott, D. F., Kluger, H. M., Carvajal, R. D., Sharfman, W. H., et al. (2014). Survival, Durable Tumor Remission, and Long-Term Safety in Patients with Advanced Melanoma Receiving Nivolumab. *J. Clin. Oncol.* 32 (10), 1020–1030. doi:10.1200/JCO.2013.53.0105

Uemura, M., Trinh, V. A., Haymaker, C., Jackson, N., Kim, D. W., Allison, J. P., et al. (2016). Selective Inhibition of Autoimmune Exacerbation while Preserving the Anti-tumor Clinical Benefit Using IL-6 Blockade in a Patient with Advanced Melanoma and Crohn's Disease: a Case Report. *J. Hematol. Oncol.* 9 (1), 81. doi:10.1186/s13045-016-0309-7

Vaengebjerg, S., Skov, L., Egeberg, A., and Loft, N. D. (2020). Prevalence, Incidence, and Risk of Cancer in Patients with Psoriasis and Psoriatic Arthritis: A Systematic Review and Meta-Analysis. *JAMA Dermatol.* 156 (4), 421–429. doi:10.1001/jamadermatol.2020.0024

Valencia, J. C., Egbukichi, N., and Erwin-Cohen, R. A. (2019). Autoimmunity and Cancer, the Paradox Comorbidities Challenging Therapy in the Context of Preexisting Autoimmunity. *J. Interferon Cytokine Res.* 39 (1), 72–84. doi:10.1089/jir.2018.0060

van der Kooij, M. K., Suijkerbuijk, K. P. M., Aarts, M. J. B., van den Berkmortel, F. W. P. J., Blank, C. U., Boers-Sonderen, M. J., et al. (2021). Safety and Efficacy of Checkpoint Inhibition in Patients with Melanoma and Preexisting Autoimmune Disease : A Cohort Study. *Ann. Intern. Med.* 174 (5), 641–648. doi:10.7326/M20-3419

Verzoni, E., Cartenì, G., Cortesi, E., Giannarelli, D., De Giglio, A., Sabbatini, R., et al. (2019). Real-world Efficacy and Safety of Nivolumab in Previously-Treated Metastatic Renal Cell Carcinoma, and Association between Immune-Related Adverse Events and Survival: the Italian Expanded Access Program. *J. Immunother. Cancer* 7 (1), 99. doi:10.1186/s40425-019-0579-z

Wallis, C. J. D., Butaney, M., Satkunasivam, R., Freedland, S. J., Patel, S. P., Hamid, O., et al. (2019). Association of Patient Sex with Efficacy of Immune Checkpoint Inhibitors and Overall Survival in Advanced Cancers: A Systematic Review and Meta-Analysis. *JAMA Oncol.* 5 (4), 529–536. doi:10.1001/jamaoncol.2018.5904

Wang, D. Y., Salem, J. E., Cohen, J. V., Chandra, S., Menzer, C., Ye, F., et al. (2018). Fatal Toxic Effects Associated with Immune Checkpoint Inhibitors: A Systematic Review and Meta-Analysis. *JAMA Oncol.* 4 (12), 1721–1728. doi:10.1001/jamaoncol.2018.3923

Wang, L., Wang, F. S., and Gershwin, M. E. (2015). Human Autoimmune Diseases: a Comprehensive Update. *J. Intern. Med.* 278 (4), 369–395. doi:10.1111/joim.12395

Wang, W., Lau, R., Yu, D., Zhu, W., Korman, A., and Weber, J. (2009). PD1 Blockade Reverses the Suppression of Melanoma Antigen-specific CTL by CD4+ CD25(Hi) Regulatory T Cells. *Int. Immunol.* 21 (9), 1065–1077. doi:10.1093/intimm/dxp072

Weber, J. S., Hodi, F. S., Wolchok, J. D., Topalian, S. L., Schadendorf, D., Larkin, J., et al. (2017). Safety Profile of Nivolumab Monotherapy: A Pooled Analysis of

Patients with Advanced Melanoma. *J. Clin. Oncol.* 35 (7), 785–792. doi:10.1200/JCO.2015.66.1389

Wu, X., Gu, Z., Chen, Y., Chen, B., Chen, W., Weng, L., et al. (2019). Application of PD-1 Blockade in Cancer Immunotherapy. *Comput. Struct. Biotechnol. J.* 17, 661–674. doi:10.1016/j.csbj.2019.03.006

Xie, W., Huang, H., Xiao, S., Fan, Y., Deng, X., and Zhang, Z. (2020). Immune Checkpoint Inhibitors Therapies in Patients with Cancer and Preexisting Autoimmune Diseases: A Meta-Analysis of Observational Studies. *Autoimmun. Rev.* 19 (12), 102687. doi:10.1016/j.autrev.2020.102687

Yasunaga, M. (2020). Antibody Therapeutics and Immunoregulation in Cancer and Autoimmune Disease. *Semin. Cancer Biol.* 64, 1–12. doi:10.1016/j.semcancer.2019.06.001

Ye, Y., Jing, Y., Li, L., Mills, G. B., Diao, L., Liu, H., et al. (2020). Sex-associated Molecular Differences for Cancer Immunotherapy. *Nat. Commun.* 11 (1), 1779. doi:10.1038/s41467-020-15679-x

Yoon, J. H., Hong, A. R., Kim, H. K., and Kang, H. C. (2021). Characteristics of Immune-Related Thyroid Adverse Events in Patients Treated with PD-1/pd-L1 Inhibitors. *Endocrinol. Metab. (Seoul)* 36 (2), 413–423. doi:10.3803/EnM.2020.906

Young, A., Quandt, Z., and Bluestone, J. A. (2018). The Balancing Act between Cancer Immunity and Autoimmunity in Response to Immunotherapy. *Cancer Immunol. Res.* 6 (12), 1445–1452. doi:10.1158/2326-6066.CIR-18-0487

Zamani, M. R., Aslani, S., Salmaninejad, A., Javan, M. R., and Rezaei, N. (2016). PD-1/PD-L and Autoimmunity: A Growing Relationship. *Cell Immunol* 310, 27–41. doi:10.1016/j.cellimm.2016.09.009

Zhu, C., and Boutros, P. C. (2021). Sex Differences in Cancer Genomes: Much Learned, More Unknown. *Endocrinology* 162 (11), bqab170. doi:10.1210/endocr/bqab170

Conflict of Interest: The authors declare that the research was conducted in the absence of any commercial or financial relationships that could be construed as a potential conflict of interest.

Publisher's Note: All claims expressed in this article are solely those of the authors and do not necessarily represent those of their affiliated organizations, or those of the publisher, the editors, and the reviewers. Any product that may be evaluated in this article, or claim that may be made by its manufacturer, is not guaranteed or endorsed by the publisher.

frontiers in Pharmacology

ORIGINAL RESEARCH
published: 21 March 2022
doi: 10.3389/fphar.2022.836812

LC–MS/MS Method for Measurement of Thiopurine Nucleotides (TN) in Erythrocytes and Association of TN Concentrations With TPMT Enzyme Activity

Amol O. Bajaj[1], Mark M. Kushnir[1,2], Erik Kish-Trier[1], Rachel N. Law[1], Lauren M. Zuromski[1], Alejandro R. Molinelli[3], Gwendolyn A. McMillin[1,2] and Kamisha L. Johnson-Davis[1,2]**

[1]ARUP Institute for Clinical and Experimental Pathology, Salt Lake City, UT, United States, [2]University of Utah Health Sciences Center, Department of Pathology, Salt Lake City, UT, United States, [3]Department of Pharmaceutical Sciences, St. Jude Children's Research Hospital, Memphis, TN, United States

Monitoring concentrations of thiopurine metabolites is used clinically to prevent adverse effects in patients on thiopurine drug therapy. We developed a LC–MS/MS method for the quantification of 6-thioguanine (6-TG) and 6-methylmercaptopurine (6-MMP) in red blood cells (RBCs). This method utilizes an automated cell washer for RBC separation from whole blood samples and washing of the separated RBCs. The lower limit of quantification of the method was 0.2 µmol/L for 6-TG (~50 pmol/8 × 10^8 RBC) and 4 µmol/L for 6-MMP (~1,000 pmol/8 × 10^8 RBC). The total imprecision of the assay was <3.0%. The upper limit of linearity for 6-TG and 6-MMP was 7.5 µmol/L and 150 µmol/L, respectively. The stability of the thiopurine metabolites under pre- and post-analytically relevant conditions was also evaluated. A good agreement was observed between this method and validated LC–MS/MS methods from three laboratories, except for ~40% low bias for 6-MMP observed in one of the methods. The assessment of the association between 6-TG and 6-MMP concentrations with thiopurine S-methyltransferase (TPMT) phenotype and genotype demonstrated a statistically significant difference in the thiopurine metabolite concentrations between the TPMT groups with normal and intermediate activity of 6-MMP ($p < 0.0001$), while the difference in 6-TG concentrations was statistically not significant ($p = 0.096$). Among the samples with normal TPMT activity, higher concentrations of 6-MMP ($p = 0.015$) were observed in pediatric samples than in the samples of adults. No statistically significant differences were observed in the distributions of 6-TG and 6-MMP concentrations among the evaluated genotypes.

Keywords: 6-thioguanine, 6-methylmercaptopurine, mass spectromerty, thiopurine methyl transferase, clinical evaluation

OPEN ACCESS

Edited by:
Miao Yan,
Central South University, China

Reviewed by:
Gabriele Stocco,
University of Trieste, Italy
Evelyne Jacqz-Aigrain,
Institut National de la Santé et de la Recherche Médicale (INSERM), France
Eric Schafer,
Baylor College of Medicine, United States

***Correspondence:**
Kamisha L. Johnson-Davis
kamisha.johnson-davis@aruplab.com
Amol O. Bajaj
amol.bajaj@aruplab.com

Specialty section:
This article was submitted to Pharmacology of Anti-Cancer Drugs, a section of the journal Frontiers in Pharmacology

Received: *15 December 2021*
Accepted: *14 February 2022*
Published: *21 March 2022*

Citation:
Bajaj AO, Kushnir MM, Kish-Trier E, Law RN, Zuromski LM, Molinelli AR, McMillin GA and Johnson-Davis KL (2022) LC–MS/MS Method for Measurement of Thiopurine Nucleotides (TN) in Erythrocytes and Association of TN Concentrations With TPMT Enzyme Activity. Front. Pharmacol. 13:836812. doi: 10.3389/fphar.2022.836812

INTRODUCTION

The thiopurine drugs azathioprine (AZA) and 6-mercaptopurine (6-MP) are anticancer and immunosuppressive drugs, which are used to treat patients with acute lymphoblastic leukemia and several autoimmune diseases, including the inflammatory bowel disease (Karran and Attard, 2008; Sandborn, 2009). AZA is a prodrug that is converted to 6-MP, which may then enter several pathways. Hypoxanthine guanine phosphoribosyl transferase (HPRT) and several other purine salvage pathway enzymes participate in the conversion of 6-MP into the active cytotoxic metabolites, 6-thioguanine nucleotides (6-TGN) (**Supplementary Figure S1**). Two pharmacologically inactive metabolites, 6-thiouric acid and 6-methylmercaptopurine (6-MMP), are produced through the action of the enzymes thiopurine S-methyltransferase (TPMT) and xanthine oxidase (XO), respectively (Swann et al., 1996; Gearry and Barclay, 2005). 6-MMP and related 6-methylmercaptopurine nucleotides (6-MMPN) are potentially hepatotoxic. In patients with very low TPMT activity, there is an increased risk of developing myelosuppression, caused by the increased levels of cytotoxic 6-TGNs (Evans et al., 2001; Schwab et al., 2002). Enzyme NUDT15 is involved in the dephosphorylation of 6-TGNs to inactive metabolites; individuals with reduced or absent NUDT15 activity may experience myelosuppression (Moriyama et al., 2016). Due to concerns regarding the efficacy and risk of toxicity, genotypes of TPMT and NUDT15 (Relling et al., 2019), and/or enzymatic functionality of TPMT, are often considered prior to initiating therapy (Kaskas et al., 2003; Relling et al., 2011). Variation in therapeutic efficacy and toxicity of thiopurine drugs is largely affected by the activity of TPMT (Lennard, 2014) and NUDT15. Yang et al. reported that of all reported cases of thiopurine drug toxicity in children with acute lymphoblastic leukemia (ALL), ~20% can be explained by the TPMT activity and ~22% by NUDT15 (Yang et al., 2015), while toxicity varies among ethnicities (e.g., NUDT15 polymorphism occurring more often in individuals of Asian descent).

Monitoring concentrations of the thiopurine nucleotides 6-TGN and 6-MMPN in patient samples is useful in optimizing the dose of thiopurine drugs and, therefore, balances the efficacy of thiopurine drug therapy while minimizing adverse effects. Complicating factors for therapeutic monitoring of patients on thiopurine drug therapy include a narrow therapeutic range for 6-TGN and a large interpatient variability in thiopurine drug metabolism (Gearry and Barclay, 2005). Thiopurine drugs and thiopurine nucleotides are metabolized and act intracellularly; therefore, an appropriate sample type for the measurement of thiopurine nucleotide concentrations is washed red blood cells (RBCs). RBC concentrations of thiopurine nucleotides serve as a surrogate marker of thiopurine nucleotide intracellular concentrations in nucleated cells (Balis et al., 1998; Dervieux and Boulieu, 1998; Vikingsson et al., 2013). Elevated 6-TGN concentrations may cause leukopenia and myelotoxicity, while elevated 6-MMPN may be hepatotoxic. Because of this, treatment with thiopurine drugs requires routine monitoring (Cuffari et al., 2004; Nygaard et al., 2004; Dervieux et al., 2005).

Methods for the measurement of thiopurine nucleotides in RBCs involve hydrolysis to release the purine bases (6-TG and 6-MMP) and analysis using liquid chromatography-tandem mass spectrometry (LC–MS/MS) (Shipkova et al., 2003; Dervieux et al., 2005; Neurath et al., 2005; Cangemi et al., 2012). The poor storage stability of thiopurine nucleotides in whole blood (WB) samples has been reported (de Graaf et al., 2008; Yoo et al., 2018), emphasizing the importance of pre-analytical aspects and conditions used during the sample preparation.

The goals of this study were to develop, validate, and evaluate performance of a mass spectrometry method for quantification of 6-TG and 6-MMP in RBCs. The stability of thiopurine nucleotides under various conditions was evaluated to determine the appropriate pre- and post-analytical conditions and limitations. Using historic data on the analysis of routine patient samples, we assessed the association among concentrations of thiopurine nucleotides, TPMT phenotypes, and genotypes.

MATERIALS AND METHODS

Chemicals and Materials

The standards of 6-TG and 6-MMP, 2-amino-6-mercaptopurine-9-D-riboside hydrate (6-TGRib), 6-methylmercaptopurine riboside (6-MMPRib) and stable isotope-labeled analogs, 6-TG-$^{13}C_2{}^{15}N$ and 6-MMP-d_3, were purchased from Toronto Research Chemicals, Ontario, Canada. The stock standards were prepared in dimethyl sulfoxide (DMSO) at 10 mg/ml (1 mg/ml) for the unlabeled (stable isotope-labeled) analogs. Perchloric acid (70%), dithiothreitol (DTT), and ammonium acetate were purchased from Millipore-Sigma (St. Louis, MO, United States). LC–MS grade methanol (MeOH), acetonitrile, and formic acid (FA) were purchased from Thermo Fisher Scientific (Fair Lawn, NJ, United States). Working solutions were prepared by diluting the stock solutions in an aqueous solution of 0.02 M sodium hydroxide, 7.5 mM DTT, and 20% MeOH. Working calibration standards were prepared at concentrations of 20, 50, 100, 250, 500, and 750 pmol/μL for 6-TG; and 400, 1,000, 2000, 5,000, 10,000, and 15,000 pmol/μL for 6-MMP. Quality control (QC) samples were prepared at 75, 150, and 300 pmol/μL for 6-TGRib; 1,500, 3,000, and 6,000 pmol/μL for 6-MMPRib. The working standards and the QC were prepared in pooled thiopurine nucleotide-negative RBC pools. All analyzed batches of samples contained a set of six calibration standards and three QC samples.

Sample Preparation

Tubes with EDTA-anticoagulated WB patient samples were rocked using a rocking mixer for 15 min at room temperature (RT). One milliliter aliquots of WB samples were transferred into disposable glass tubes; RBC separation and washing were performed using the automated cell washer method as follows (Bajaj et al., 2021): Tubes with WB samples were placed in the rotor of a UltraCW® II instrument (Helmer Scientific, Noblesville, IN, United States) and centrifuged at 1,440 relative centrifugal force (RCF) for 4 min; during this step, RBCs were separated

from plasma by centrifugal packing, followed by decantation of the plasma supernatant. The decanting step was followed by resuspension, achieved by the addition of saline into the tubes and agitation of the tubes to disperse and distribute the RBCs in the saline. Resuspension was followed by the two cycles of addition of saline, agitation, pelleting RBC, and decanting the supernatant. At the end of the last wash cycle, the tubes contained washed RBCs in a small volume of saline. The packed RBCs were diluted with 400 µL of saline, and RBCs were counted using a hematological cell counter (Ac.T Diff, Beckman Coulter, Pasadena, CA, United States). The isolated RBCs were transferred into microcentrifuge tubes.

One hundred microliter aliquots of the washed/diluted RBCs were transferred into 1.5 ml microcentrifuge tubes (Eppendorf, Enfield, CT, United States), 20 µL of internal standard was added, and the samples were vortexed and held at RT for 15 min. Then, 150 µL of 4 mM DTT and 40 µL of 70% perchloric acid were added to the samples. The tubes were vortexed for 1 min at 1,000 rpm and then centrifuged at 16,000 RCF for 5 min at RT; 100 µL of the supernatant was transferred into glass vials; the vials were capped and incubated at 100°C for 2 h (for hydrolysis) with mixing at 500 rpm using a thermo mixer (Eppendorf). During the hydrolysis, 6-MMP is chemically converted to 6-MMP-imidazole (6-MMP*) {Oliveira et al., 2004 #1465; Dervieux and Boulieu, 1998 #1469}. After cooling to RT, 140 µL of 1M ammonium acetate was added to the tubes to neutralize the acidic solution, and then 15 µL of this solution was transferred into wells of a 96-well polypropylene plate (Agilent Technologies, Santa Clara, CA, United States), and diluted with 285 µL of 0.1% formic acid in water for instrumental analysis.

LC–MS/MS Analysis

An Agilent 6470 triple quadrupole mass spectrometer (Agilent Technologies) equipped with an electrospray (ESI) ion source was coupled to an Agilent 1260 Infinity II series HPLC system consisting of multisampler, binary pump, and column thermostat. Nitrogen was used as the drying gas, nebulizer gas, sheath gas, and collision gas; the acquisition was performed in a positive ion mode. The ion source parameters are listed in **Supplementary Table S1**; mass transitions with their respective fragmentor voltages and collision energies are listed in **Supplementary Table S2**. Chromatographic separation was performed using a XSelect Peptide HSS T3 LC column (2.5 µm, 100 Å, 2.1 × 100 mm; Waters Corporation, Milford, MA, United States). Mobile phase A was 0.1% formic acid in nanopure water (18.2 megohm ionic purity) and mobile phase B was 0.1% formic acid in acetonitrile. The flow rate was 0.4 ml/min and the column temperature was 40°C. After an initial hold at 2% B for 0.2 min, the following were performed: a gradient to 12.5% B at 3 min, column conditioning using 95% B between 3.1 and 5 min, and re-equilibration using 2% B between 5.1 and 7 min. The injection volume was 10 µL, and the total run time per sample was 7 min. The retention time of 6-TG was ~1.6 min and that of 6-MMP was ~2.7 min. The ratio of the peak area of the analyte to its corresponding IS was used for quantification using the MassHunter Workstation (Agilent Technologies). Calibration curves were fitted using linear regression with 1/x-weighting for 6-TG and $1/x^2$-weighting for 6-MMP*. The acceptability criterion for the ratio of mass transitions was set to ±30% (Kushnir et al., 2005).

Method Validation

Method validation included the evaluation of precision, sensitivity, linearity, accuracy, specificity, dilution integrity, carryover, robustness, method comparison, and assessment of matrix effect. Details of the experiments on the method performance evaluated are included in the **Supplementary Data**. The use of residual patient samples was approved by IRB protocols (University of Utah, United States).

Stability

The stability of thiopurine nucleotides in ETDA WB was evaluated using 15 neat patient sample pools (prepared from WB samples of patients on thiopurine drug therapy; 5–10 individual WB samples per pool); the samples were stored at 4°C for 5 h, and 4, 7, and 15 days; the observed concentrations were compared to the concentrations of 6-TG and 6-MMP in the aliquots of RBC separated from the pools at time zero, which were stored at −70°C. The stability of the thiopurine nucleotides in separated/washed RBC samples (N = 12) stored at −70 C was evaluated by preparing and analyzing the samples on 4 occasions over 5 months of storage and comparing the observed concentration with thiopurine nucleotide concentrations observed in the samples tested prior to the storage. The stability of the final extract (N = 15) was evaluated by the comparison of 6-TG and 6-MMP concentrations in fresh extracts *versus* those in extracts stored at −20°C for 2 weeks. For autosampler stability, a set of extracts (N = 33) was stored in a 96-well plate in an autosampler compartment at 4°C and analyzed for six consecutive days. The freeze/thaw stability of 6-TG and 6-MMP in separated/washed RBCs was evaluated in a set of patient samples (N = 10).

Historical Data Analysis

Two archived datasets were retrieved retrospectively (IRB protocols approved by the University of Utah Institutional Review Board). Data in Set 1 included results from 611 specimens, submitted for routine testing for the TPMT activity (phenotype) and thiopurine nucleotide quantification (both tests ordered for same patient); and data in Set 2 included results from 64 specimens with determined TPMT genotype; thiopurine nucleotides were also measured in these patients by referral laboratory. WB samples submitted for thiopurine nucleotide testing were shipped and stored refrigerated prior to testing within 1–3 days of the collection. Both, phenotype and genotype assays were validated for the clinical use in ARUP Laboratories. Data in Set 1 consisted of 4 patient samples with low TPMT activity, 93 patients with intermediate TPMT activity, and 514 patients with normal TPMT activity. Data in Set 2 consisted of one patient with *3A/*3A, two patients with *3A/*1, three patients with *3C/*1 variant alleles, and 58 patients with no variant alleles.

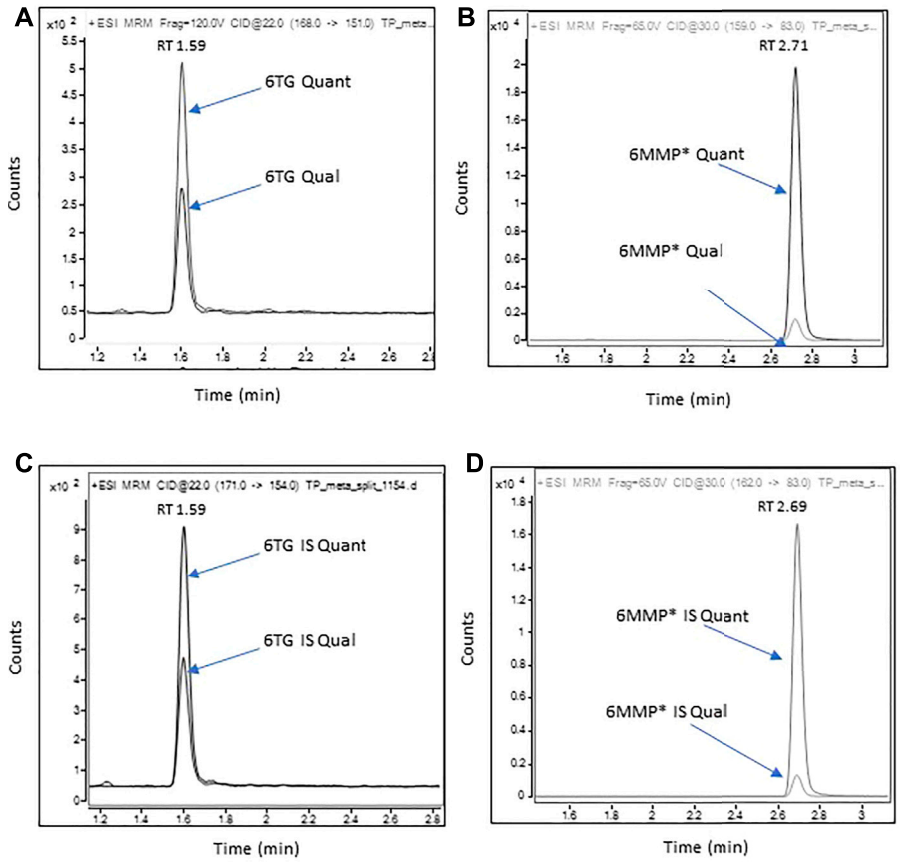

FIGURE 1 | Representative chromatograms of 6-TG and 6-MMP* in a patient sample containing 107 pmol/8*10^8 RBC of 6-TG and 6,400 pmol/8*10^8 RBC of 6-MMP.

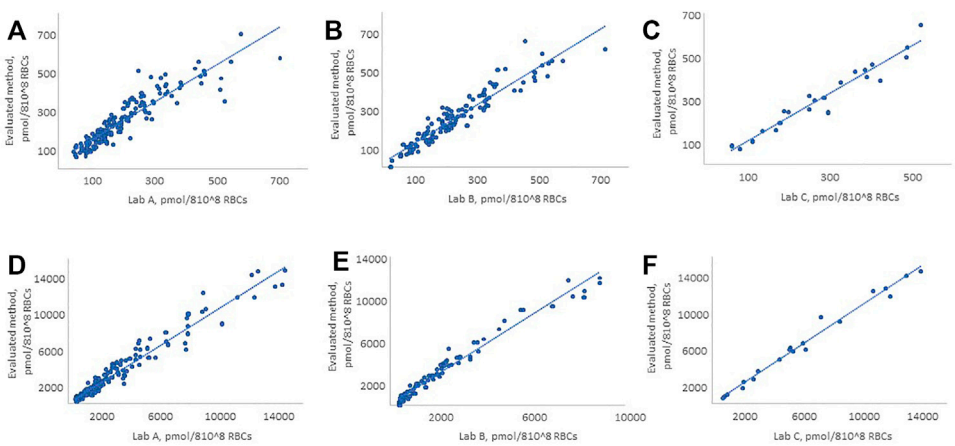

FIGURE 2 | Comparison of the evaluated method with LC–MS/MS methods of Lab A, Lab B, and Lab C for 6-TG and 6-MMP. **(A, D)** 6-TG and 6-MMP comparison with Lab A, **(B, E)** 6-TG and 6-MMP comparison with Lab B, and **(C, F)** 6-TG and 6-MMP comparison with Lab C. The figure shows only the patient samples where the observed concentrations were within the analytical measurement range of the method.

RESULTS

Sample Preparation, Chromatographic Separation, and LC–MS/MS Analysis

Representative chromatograms of 6-TG and 6-MMP* along with their corresponding IS are shown in **Figure 1**. The MRM transitions and the optimized instrument settings are summarized in **Supplementary Table S2**.

RBC separation from WB samples was performed using an automated method (Bajaj et al., 2021): the details of the method are summarized in **Supplementary Figure S2**. Data on the quantitative measurement of three example biomarkers (6-TGN, 6-MMPN, and Mg) with sample preparation performed using the automated vs. manual method for RBC separation and washing process demonstrate adequate performance of the automated method (**Supplementary Figures S3, S4**).

While developing this method, we evaluated numerous HPLC columns. Inadequate separation of the 6-TG peak from the solvent front was observed on all evaluated columns. The LC column used in the method provided the best chromatographic retention (separation from the solvent front) as compared to the other evaluated columns (**Supplementary Figure S5**). We found that the initial mobile phase composition had the greatest impact on the retention time of 6-TG and 6-MMP*, the 6-MMP* peak width, and the signal-to-noise ratio for the 6-TG peak, while the end-of-gradient mobile phase composition had a significant effect on the retention time of the 6-MMP* peak.

Assay Validation

Summary data for the evaluation of the method's imprecision are included in **Supplementary Table S5**; imprecision at all evaluated concentrations for 6-TG and 6-MMP was ≤3%. The limit of quantitation (LOQ) for 6-TG and 6-MMP was 20 and 400 pmol per 100 µL (0.2 and 4 µmol/L), respectively, of RBC lysate; data on imprecision and accuracy at the LOQ are summarized in **Supplementary Table S6**; the signal-to-noise ratio at the LOQ for the transitions of both analytes was ≥10. Data on method linearity are summarized in **Supplementary Figure S6**. Linear regression equations and coefficients of determination for correlation between the expected and the observed concentrations were $y = 1.01x + 3.28$, $R^2 = 0.996$ and $y = 0.97x + 316$, $R^2 = 0.998$, for 6-TG and 6-MMP, respectively.

The method's accuracy was evaluated by analysis of individual thiopurine nucleotide-negative patient RBC lysates spiked at six different concentrations with 6-TGRib and 6-MMPRib conjugates. The samples were prepared and analyzed in triplicate, and the expected and observed concentrations agreed within 1 and 15%, for 6-TG and 6-MMP, respectively, with imprecision among the replicates of <5% (**Supplementary Figure S7**).

Potential for interference was evaluated in the WB samples of individuals not on thiopurine drugs therapy ($n = 110$), and in lysed RBC pools spiked with common drugs and drug metabolites (**Supplementary Table S7**), there were no peaks in the mass transitions within the acquisition time of the assay.

Dilution integrity was evaluated by the analysis of five individual neat patient RBC lysate samples containing an elevated concentration of 6-TGN and 6-MMPN using 5-fold and 10-fold dilution, respectively, with a lysed thiopurine nucleotide-negative RBC pool. After normalizing the observed concentrations for the dilution factor, the agreement for both 6-TG and 6-MMP was within 17% (**Supplementary Table S8**).

No carryover to the following sample was observed after injection of samples containing 5,000 pmol/100 µL of 6-TG and 100,000 pmol/100 µL of 6-MMP.

The method comparison was performed using residual de-identified WB samples from patients receiving thiopurine drug therapy. The evaluated method was compared to LC–MS/MS methods of three commercial laboratories, which perform the test routinely (WB samples were split and sent refrigerated to the external laboratories). For comparison purposes, these laboratories are referred to as Lab A, Lab B, and Lab C. The developed method showed good agreement with Lab A and C, for both 6-TG and 6-MMP, and with Lab B for 6-TG, while concentrations of 6-MMP were underestimated using the method of Lab B (**Figure 2**). The number of patient samples tested, Deming regression equation slopes, intercepts, correlation coefficients (R), and percent bias are summarized in **Table 1**.

Samples' Stability

We assessed WB samples' stability by evaluating the measured 6-TG and 6-MMP concentrations in WB sample pools ($n = 15$) stored refrigerated (4°C) for 5 h, and 4, 7, and 14 days. After 7 (14) days of storage at 4°C, the measured concentrations of 6-TG (6-MMP) decreased by 0.5 (11)% and 3 (13)%, respectively (**Supplementary Figure S8**).

We also evaluated the analyte stability in washed RBC lysates stored at −70°C for up to 150 days. After 150 days of storage, the observed 6-TG and 6-MMP concentrations decreased by <10%, as compared to the Day 1 (**Supplementary Figure S9**).

In an experiment, on evaluation of 6-TGN and 6-MMPN stability in individual prepared samples stored at −20°C ($n = 15$) for 15 days, we observed <10% reduction in concentrations of 6-TG and 6-MMP (**Supplementary Figure S10**). The evaluation of 6-TG and 6-MMP stability in the samples prepared for analysis, stored at 4°C for up to 120 h, demonstrated no change in the measured 6-TG and 6-MMP concentrations (**Supplementary Figure S11**). The evaluation of the freeze-thaw stability (3 cycles) of 6-TGN and 6-MMPN in RBCs demonstrated ~8% (~6%) reduction in the concentration of 6-TG (6-MMP) (**Supplementary Figure S12**).

TPMT Phenotype/Activity and Thiopurine Metabolite Concentrations

Retrospective data analysis was performed to assess the correlation between the results of TPMT activity testing and thiopurine metabolite concentrations for the first occurrence of therapeutic drug monitoring. Of note, the dataset does not include serial patient monitoring. The dataset contained results corresponding to patient samples that were tested for both TPMT phenotype and thiopurine nucleotides (during the thiopurine

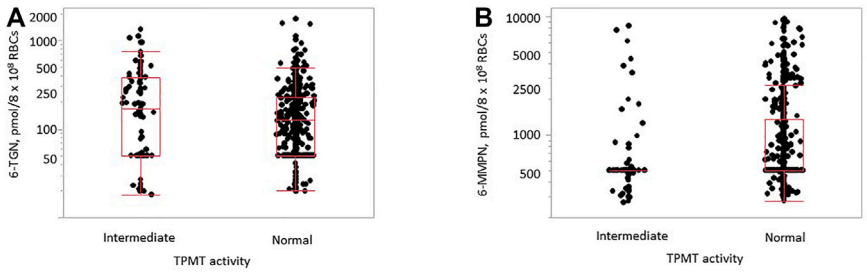

FIGURE 3 | Distribution of 6-TG [**(A)**, $p = 0.096$] and 6-MMP [**(B)**, $p < 0.0001$] concentrations in samples with normal ($n = 514$) and intermediate ($n = 93$) TPMT activity in samples of children and adults.

TABLE 1 | Summary of the results of method comparison.

Specifics	Lab A		Lab B		Lab C	
	6-TG	6-MMP	6-TG	6-MMP	6-TG	6-MMP
Number of samples	173	154	123	83	22	21
Slope	1.06	1.04	1.02	1.40	1.14	1.06
Intercept	26.6	6.7	9.9	112	–20.5	–55.4
(R)	0.914	0.975	0.950	0.985	0.971	0.992
% Bias	19.2	4.5	6.6	45.8	7.4	5.2

drug therapy, $n = 611$). Out of the entire dataset, 514 patients had shown the TPMT enzyme activity within the therapeutic range (24–44.0 U/mL), 93 had a reduced activity (17.0–23.9 U/mL) and 4 had a low TPMT activity (<17.0 U/mL). There were no patients in the dataset who had a high TPMT activity (>44.0 U/mL).

Out of the 514 patients with normal TPMT activity, 90 patients (17.5%) had 6-TG concentrations within the therapeutic range (235–450 pmol/8 × 10^8 RBCs), 396 patients (77.0%) had subtherapeutic 6-TG concentrations (<235 pmol/8 × 10^8 RBCs), and 28 patients (5.4%) had supratherapeutic 6-TG concentrations (>450 pmol/8 × 10^8 RBCs). Among the patients with intermediate TPMT activity, 23.7% had 6-TG concentrations within the therapeutic range, 60.2% were subtherapeutic, and 16.1% had 6-TG concentrations >450 pmol/8 × 10^8 RBCs. Among the four patients with low TPMT activity, two had 6-TG concentrations within the therapeutic range and two had subtherapeutic concentrations.

The distribution of 6-MMP concentrations demonstrated that among 514 patients with normal TPMT activity, 4.1% had concentrations >5,700 pmol/8 × 10^8 RBCs. Among 93 patients with intermediate TPMT activity, 3.2% had 6-MMP concentration >5,700 pmol/8 × 10^8 RBCs. All four patients with low TPMT activity had 6-MMP concentrations <5,700 pmol/8 × 10^8 RBCs.

The median (interquartile range) for the distribution of 6-TG and 6-MMP concentrations was 126 (50–238) pmol/8 × 10^8 RBCs and 500 (500–1,160) pmol/8 × 10^8 RBCs, respectively. The difference in the observed 6-TG concentrations between TPMT groups with normal and intermediate activity was not statistically significant ($p = 0.096$), while it was statistically significant for 6-MMP ($p < 0.0001$, **Figure 3**). There was no significant difference in the TPMT activity between males and females ($p = 0.824$ for 6-TG and $p = 0.734$ for 6-MMP). A statistically significant difference in 6-MMP concentrations was observed between samples of children and adults with normal TPMT activity ($p = 0.015$, **Supplementary Figure S13**), with higher concentrations observed in pediatric samples; no statistically significant difference was observed in 6-TG concentrations ($p = 0.147$).

In the evaluated dataset, there were 64 patients on thiopurine drug therapy who had thiopurine metabolite measurements performed along with the test for the TPMT genotype. Out of 58 patient samples of this set, who were classified as TPMT *1/*1 (wildtype), five patient samples (8.6%) had 6-TG concentrations within the therapeutic range (235–450 pmol/8 × 10^8 RBCs). Forty-four patients (75.9%) had subtherapeutic 6-TG concentrations (<235 pmol/8 × 10^8 RBCs) and nine patients (15.5%) had 6-TG concentrations >450 pmol/8 × 10^8 RBCs. When evaluating 6-MMP concentration, 45 patients (77.6%) had 6-MMP concentration <5,700 pmol/8 × 10^8 RBCs and 13 patients (22.4%) had >5,700 pmol/8 × 10^8 RBCs. Out of the patients included in this dataset, 91.1% had 6-TG concentrations outside of the therapeutic range; the median (interquartile range) for 6-TG and 6-MMP concentrations were 72 (50–253) pmol/8 × 10^8 RBCs, and 500 (500–3,218) pmol/8 × 10^8 RBCs, respectively.

DISCUSSION

Therapeutic drug monitoring for thiopurine metabolites is important to guide therapy to manage myelosuppression and to minimize the risk of hepatotoxicity {Relling et al., 2019 #8}. The novel aspects of this study include the following: 1) development of a LC–MS/MS method for the measurement of thiopurine nucleotides that use an automated method for separation and washing of RBCs from WB samples; 2) optimization of chromatographic separation, which enhanced the analytical sensitivity and reduced the potential for ion suppression; 3) optimization of the conditions for thiopurine metabolite conjugate hydrolysis and 6-MMPN conversion to 6-MMP*; 4) assessment of 6-TGN and 6-MMPN stability in WB samples, washed RBCs, and in the samples prepared for the

analysis; and 5) assessment of association between the TPMT phenotype and genotype and thiopurine nucleotide concentrations in routine patient samples.

The developed method utilizes automated RBC separation and washing from WB samples {Bajaj et al., 2021 #22}. Processing time for 24 WB samples is ~15 min, as compared to 2–2.5 h, required for manual sample processing (O'Connell et al., 1965; Thompson et al., 1984; Bosch et al., 1992; Connor et al., 1994). Our data suggest that this automated RBC separation and washing method holds a great promise for reducing the labor required for the sample processing in methods using RBC separation and washing.

We observed that performing RBC washes during the RBC separation was important for the adequate quantitative performance of the assay, as plasma may contain thiopurine metabolites, which could cause falsely elevated thiopurine nucleotide concentrations. In our method, there was no significant difference in the thiopurine nucleotide concentration between RBCs separated from samples that were washed two and three times; therefore, the method uses two washes.

In samples from patients on thiopurine drug therapy, 6-MMP concentrations in RBC samples were 10–20 times greater than 6-TG, which makes the simultaneous analysis of 6-TG and 6-MMP challenging. To address this issue, we evaluated 6-MMP mass transitions based on the first isotope (M+1) of 6-MMP* instead of mass transitions based on monoisotopic ions, which are typically used in MS/MS methods for quantitative analysis. The observed M+1 peak abundances were ~10 times lower than those from monoisotopic ions, resulting in comparable peak intensities of 6-TG and 6-MMP* in the calibrators, QC, and patient samples.

Our data demonstrated that the adequate recovery of 6-TG and 6-MMP from the respective conjugated forms of the thiopurine nucleotides present in RBC, and quantitative 6-MMPN conversion to 6-MMP*, requires hydrolysis at 100°C for 2 h, while hydrolysis at lower temperatures or shorter times resulted in incomplete hydrolysis, incomplete conversion to 6-MMP*, and underestimation of 6-TG and 6-MMP concentrations.

Numerous methods for the analysis of thiopurine metabolites in RBCs have been published (Erdmann et al., 1990; Lavi and Holcenberg, 1985; Lennard and Singleton, 1992; Moon et al., 2019; Thomas et al., 2018). Dervieux et al. developed the first LC–MS/MS method for the analysis of thiopurine nucleotides in RBCs and demonstrated its clinical utility (Dervieux et al., 2005). Kirchherr et al. (2013) changed the sample type from washed RBCs to WB with subsequent normalization to account for the WB sample variation in the RBC content. In our experience, measurement of thiopurine nucleotides in WB leads to overestimation of the concentrations in some samples. Hofmann et al. (2012) developed an LC–MS/MS method for simultaneous quantification of eleven thiopurine drug metabolites, including monophosphate, diphosphate, and triphosphate nucleotides of 6-TG and 6-MMP, and evaluated their clinical significance. Additional studies are needed to assess the clinical utility of measuring the individual phosphorylated nucleotide conjugates. Methods for the measurement of thiopurine metabolites in plasma have been developed (Tsutsumi et al., 1982; Sorouraddin et al., 2011; Al-Ghobashy et al., 2016), while very few plasma patient samples were analyzed as part of these studies, and clinical utility of these measurements was not demonstrated.

As reported by Simsek et al., poor agreement among methods of different laboratories may be attributed to the sample stability, standardization, or poor control of the hydrolysis of 6-TGN and 6-MMPN conjugates (Simsek et al., 2017). We observed systematic bias in 6-MMP concentrations in the method compared with one of the external laboratories. Due to insufficient method information, we cannot comment on the specific cause of this disagreement. Based on our data, despite a lack of certified reference materials and proficiency testing programs, the among-laboratory agreement in 6-TG and 6-MMP concentrations was strong.

The poor stability of thiopurine nucleotides in WB samples was reported in several publications (Pike et al., 2001; Hofmann et al., 2012; Yoo et al., 2018). Pike et al. (2001) reported a decrease in 6-TGN concentration by 2–4% per day in WB stored at ambient temperature, and Yoo et al. (2018) recommended that RBCs should be separated within four days of the blood draw, if WB samples are stored refrigerated. Our data are in agreement with those of Yoo et al., suggesting the adequate sample stability with storage at 4 C for up to 4 days after receipt by the laboratory.

Pike et al. (2001) reported that 6-TGN concentration decreased by about 12% after six months of storage at −80°C and that 6-MMPN concentration did not change after six months. Yoo et al. reported a decrease in 6-TGN (6-MMPN) concentrations by 5 (10)% after storage at −70°C for 180 days (Yoo et al., 2018). Our results on the stability of thiopurine nucleotides in separated/washed RBC samples are in agreement with the data from previous publications.

Because thiopurine drug therapy may cause life-threatening myelosuppression and hepatotoxicity, the assessment of TPMT enzyme activity prior to the initiation of therapy is recommended to identify patients at risk. Patients with low TPMT activity are expected to be at risk of bone marrow toxicity and are recommended to avoid the use of thiopurine drug therapy or to significantly reduce the dose. Patients with intermediate TPMT activity could also be at risk of bone marrow toxicity and are recommended to reduce the dose and have frequent thiopurine metabolites monitoring. Patients with high TPMT activity are not considered to be at a risk of bone marrow toxicity and standard dosing, and periodic thiopurine metabolite monitoring is recommended (Lee et al., 2021; Franca et al., 2021).

Data from our retrospective analysis demonstrated that TPMT activity better explained the concentrations of 6-MMP than concentrations of 6-TG. In agreement with earlier publications, there was not a significant difference in the TPMT activity between males and females (Wiwattanakul et al., 2017; Wu et al., 2019). No statistically significant difference in 6-TG concentrations was observed between children and adults in samples with normal or intermediate TPMT activity; however, statistically significantly higher 6-MMP concentrations were observed in pediatric samples than in samples of adults. Due to limited patient information in our laboratory information system, we cannot determine the exact

reason for this observation. This observation could be related to the difference in the dosage and treatment regimens in children with ALL, as compared to conditions for which thiopurine drug therapy is used in adults.

In addition to the TPMT phenotype, TPMT and NUDT15 genotypes have been used to identify patients at risk for adverse effects before initiation of thiopurine drug therapy (Wiwattanakul et al., 2017). Dervieux et al. observed association between the TPMT genotype and metabolite concentrations, illustrating the utility of pharmacogenetics in the management of patients for whom thiopurine drug treatment was recommended (Dervieux et al., 2005). We did not observe statistically significant differences in 6-TG and 6-MMP concentrations among the groups with different genotypes, which is likely explained by the relatively small size of our dataset.

Surprisingly, 6-TG concentration in 81.3% of the tested samples was outside of the therapeutic range, which highlights the clinical need for routine monitoring of thiopurine metabolites to help optimize therapy and to achieve the adequate clinical outcomes. Alternatively, the large percentage of samples with 6-TG concentration below the therapeutic range could be related to 6-TGN degradation during the time between the blood draw and analysis of the samples at a clinical laboratory. Future studies are needed, using samples from patients on thiopurine drug therapy, for whom clinical information is available, to determine the cause of the high frequency of observed 6-TGN concentrations below the therapeutic range.

Our study had some limitations. Due to the unavailability of large volumes of neat WB samples from patients on thiopurine drug therapy, evaluation of the method accuracy, precision, sensitivity, and linearity was performed using thiopurine nucleotide-negative RBC lysate samples spiked with 6-TG and 6-MMP ribose conjugates. The use of ribose conjugates allowed us to assess the effect of hydrolysis on the method's performance in all validation experiments.

In the data on retrospective data analysis, we did not have access to the clinical information of the participants [disease, dosing, dosing frequency, treatment compliance, and recent red blood cell transfusion (since blood cell transfusions can reflect the TPMT activity of the donor instead of the recipient)]. Moreover, it is unknown whether these patients were taking other medications or underwent treatments, which could alter the TPMT activity (Lewis et al., 1997; Lennard et al., 2001; Brouwer et al., 2005).

CONCLUSION

We developed and validated a LC–MS/MS method for quantification of 6-TG and 6-MMP in RBCs. As part of this method, we developed an automated procedure for RBC separation from WB samples and washing of the separated RBCs. Our data suggest that this automated method for RBC separation and washing has an adequate performance, and significantly reduces labor and time as compared to the manual methods. We observed reasonable inter-laboratory agreement in the measured concentrations of 6-TG and 6-MMP, while the among-laboratory agreement could likely be improved through standardization and harmonization. Some of the contributing factors impacting the accurate quantification of thiopurine nucleotides are a lack of certified reference materials and proficiency testing programs, poor stability of WB patient samples and the analyte standards, and among-laboratory differences in the methodologies. A review of the retrospective data revealed higher 6-MMP concentrations in samples of children than in samples of adults, and a high frequency of samples with 6-TG concentrations below the therapeutic range; future studies are needed to determine the cause of the aforementioned observations.

DATA AVAILABILITY STATEMENT

The original contributions presented in the study are included in the article/**Supplementary Material**; further inquiries can be directed to the corresponding authors.

AUTHOR CONTRIBUTIONS

AOB drafted the manuscript; AOB, MK, EK-T, GM, and KJ-D designed research; AOB performed the experimental work, data acquisition, analysis, and validation; AOB and MK conducted review and editing; AOB, MK, and EK-T performed interpretation of data; RL performed the pre-analytical work; LZ performed statistical analysis for patient data; AM provided patient samples; and GM and KJ-D provided project administration and resources for the project. All the authors critically reviewed the manuscript.

FUNDING

We thank the ARUP Institute for supporting this project and Clinical and Experimental Pathology for providing open access publication fees.

SUPPLEMENTARY MATERIAL

The Supplementary Material for this article can be found online at: https://www.frontiersin.org/articles/10.3389/fphar.2022.836812/full#supplementary-material

REFERENCES

Al-Ghobashy, M. A., Hassan, S. A., Abdelaziz, D. H., Elhosseiny, N. M., Sabry, N. A., Attia, A. S., et al. (2016). Development and Validation of LC-MS/MS Assay for the Simultaneous Determination of Methotrexate, 6-mercaptopurine and its Active Metabolite 6-thioguanine in Plasma of Children with Acute Lymphoblastic Leukemia: Correlation with Genetic Polymorphism. *J. Chromatogr. B Analyt Technol. Biomed. Life Sci.* 1038, 88–94. doi:10.1016/j.jchromb.2016.10.035

Bajaj, A. O., Kushnir, M. M., Kish-Trier, E., McMillin, G. A., and Johnson-Davis, K. L. (2021). "Automated Separation and Washing of Red Blood Cells (RBCs) from Whole blood.". The IP.com. Available at: https://priorart.ip.com/IPCOM/000264613 (Accessed October 25, 2021).

Balis, F. M., Holcenberg, J. S., Poplack, D. G., Ge, J., Sather, H. N., Murphy, R. F., et al. (1998). Pharmacokinetics and Pharmacodynamics of Oral Methotrexate and Mercaptopurine in Children with Lower Risk Acute Lymphoblastic Leukemia: a Joint Children's Cancer Group and Pediatric Oncology branch Study. *Blood* 92 (10), 3569–3577. doi:10.1182/blood.v92.10.3569

Bosch, F. H., Werre, J. M., Roerdinkholder-Stoelwinder, B., Huls, T. H., Willekens, F. L., and Halie, M. R. (1992). Characteristics of Red Blood Cell Populations Fractionated with a Combination of Counterflow Centrifugation and Percoll Separation. *Blood* 79 (1), 254–260. doi:10.1182/blood.v79.1.254.bloodjournal791254

Brouwer, C., De Abreu, R. A., Keizer-Garritsen, J. J., Lambooy, L. H. J., Ament, K. P., ter Riet, P. G. J. H., et al. (2005). Thiopurine Methyltransferase in Acute Lymphoblastic Leukaemia: Biochemical and Molecular Biological aspects. *Eur. J. Cancer* 41 (4), 613–623. doi:10.1016/j.ejca.2004.10.027

Cangemi, G., Barabino, A., Barco, S., Parodi, A., Arrigo, S., and Melioli, G. (2012). A Validated HPLC Method for the Monitoring of Thiopurine Metabolites in Whole Blood in Paediatric Patients with Inflammatory Bowel Disease. *Int. J. Immunopathol Pharmacol.* 25 (2), 435–444. doi:10.1177/039463201202500213

Connor, J., Pak, C. C., and Schroit, A. J. (1994). Exposure of Phosphatidylserine in the Outer Leaflet of Human Red Blood Cells. Relationship to Cell Density, Cell Age, and Clearance by Mononuclear Cells. *J. Biol. Chem.* 269 (4), 2399–2404. doi:10.1016/s0021-9258(17)41959-4

Cuffari, C., Dassopoulos, T., Turnbough, L., Thompson, R. E., and Bayless, T. M. (2004). Thiopurine Methyltransferase Activity Influences Clinical Response to Azathioprine in Inflammatory Bowel Disease. *Clin. Gastroenterol. Hepatol.* 2 (5), 410–417. doi:10.1016/s1542-3565(04)00127-2

de Graaf, P., de Boer, N. K., Jharap, B., Mulder, C. J., van Bodegraven, A. A., and Veldkamp, A. I. (2008). Stability of Thiopurine Metabolites: a Potential Analytical Bias. *Clin. Chem.* 54 (1), 216–218. doi:10.1373/clinchem.2007.092676

Dervieux, T., and Boulieu, R. (1998). Simultaneous Determination of 6-thioguanine and Methyl 6-mercaptopurine Nucleotides of Azathioprine in Red Blood Cells by HPLC. *Clin. Chem.* 44 (3), 551–555. doi:10.1093/clinchem/44.3.551

Dervieux, T., Meyer, G., Barham, R., Matsutani, M., Barry, M., Boulieu, R., et al. (2005). Liquid Chromatography-Tandem Mass Spectrometry Analysis of Erythrocyte Thiopurine Nucleotides and Effect of Thiopurine Methyltransferase Gene Variants on These Metabolites in Patients Receiving Azathioprine/6-Mercaptopurine Therapy. *Clin. Chem.* 51 (11), 2074–2084. doi:10.1373/clinchem.2005.050831

Erdmann, G. R., France, L. A., Bostrom, B. C., and Canafax, D. M. (1990). A Reversed Phase High Performance Liquid Chromatography Approach in Determining Total Red Blood Cell Concentrations of 6-thioguanine, 6-mercaptopurine, Methylthioguanine, and Methylmercaptopurine in a Patient Receiving Thiopurine Therapy. *Biomed. Chromatogr.* 4 (2), 47–51. doi:10.1002/bmc.1130040202

Evans, W. E., Hon, Y. Y., Bomgaars, L., Coutre, S., Holdsworth, M., Janco, R., et al. (2001). Preponderance of Thiopurine S-Methyltransferase Deficiency and Heterozygosity Among Patients Intolerant to Mercaptopurine or Azathioprine. *J. Clin. Oncol.* 19 (8), 2293–2301. doi:10.1200/jco.2001.19.8.2293

Franca, R., Braidotti, S., Stocco, G., and Decorti, G. (2021). Understanding Thiopurine Methyltransferase Polymorphisms for the Targeted Treatment of Hematologic Malignancies. *Expert Opin Drug Metab Toxicol.* 17 (10), 1187–1198. doi:10.1080/17425255.2021.1974398

Gearry, R. B., and Barclay, M. L. (2005). Azathioprine and 6-mercaptopurine Pharmacogenetics and Metabolite Monitoring in Inflammatory Bowel Disease. *J. Gastroenterol. Hepatol.* 20 (8), 1149–1157. doi:10.1111/j.1440-1746.2005.03832.x

Hofmann, U., Heinkele, G., Angelberger, S., Schaeffeler, E., Lichtenberger, C., Jaeger, S., et al. (2012). Simultaneous Quantification of Eleven Thiopurine Nucleotides by Liquid Chromatography-Tandem Mass Spectrometry. *Anal. Chem.* 84 (3), 1294–1301. doi:10.1021/ac2031699

Karran, P., and Attard, N. (2008). Thiopurines in Current Medical Practice: Molecular Mechanisms and Contributions to Therapy-Related Cancer. *Nat. Rev. Cancer* 8 (1), 24–36. doi:10.1038/nrc2292

Kaskas, B. A., Louis, E., Hindorf, U., Schaeffeler, E., Deflandre, J., Graepler, F., et al. (2003). Safe Treatment of Thiopurine S-Methyltransferase Deficient Crohn's Disease Patients with Azathioprine. *Gut* 52 (1), 140–142. doi:10.1136/gut.52.1.140

Kirchherr, H., Shipkova, M., and von Ahsen, N. (2013). Improved Method for Therapeutic Drug Monitoring of 6-thioguanine Nucleotides and 6-methylmercaptopurine in Whole-Blood by LC/MSMS Using Isotope-Labeled Internal Standards. *Ther. Drug Monit.* 35 (3), 313–321. doi:10.1097/FTD.0b013e318283ed5d

Kushnir, M. M., Rockwood, A. L., Nelson, G. J., Yue, B., and Urry, F. M. (2005). Assessing Analytical Specificity in Quantitative Analysis Using Tandem Mass Spectrometry. *Clin. Biochem.* 38 (4), 319–327. doi:10.1016/j.clinbiochem.2004.12.003

Lavi, L. E., and Holcenberg, J. S. (1985). A Rapid and Sensitive High-Performance Liquid Chromatographic Assay for 6-mercaptopurine Metabolites in Red Blood Cells. *Anal. Biochem.* 144 (2), 514–521. doi:10.1016/0003-2697(85)90148-4

Lee, S. D., Shivashankar, R., Quirk, D., Zhang, H., Telliez, J. B., Andrews, J., et al. (2021). Therapeutic Drug Monitoring for Current and Investigational Inflammatory Bowel Disease Treatments. *J. Clin. Gastroenterol.* 55 (3), 195–206. doi:10.1097/mcg.0000000000001396

Lennard, L., Chew, T. S., and Lilleyman, J. S. (2001). Human Thiopurine Methyltransferase Activity Varies with Red Blood Cell Age. *Br. J. Clin. Pharmacol.* 52 (5), 539–546. doi:10.1046/j.0306-5251.2001.01497.x

Lennard, L., and Singleton, H. J. (1992). High-performance Liquid Chromatographic Assay of the Methyl and Nucleotide Metabolites of 6-mercaptopurine: Quantitation of Red Blood Cell 6-thioguanine Nucleotide, 6-thioinosinic Acid and 6-methylmercaptopurine Metabolites in a Single Sample. *J. Chromatogr.* 583 (1), 83–90. doi:10.1016/0378-4347(92)80347-s

Lennard, L. (2014). Implementation of TPMT Testing. *Br. J. Clin. Pharmacol.* 77 (4), 704–714. doi:10.1111/bcp.12226

Lewis, L. D., Benin, A., Szumlanski, C. L., Otterness, D. M., Lennard, L., Weinshilboum, R. M., et al. (1997). Olsalazine and 6-Mercaptopurine-Related Bone Marrow Suppression: a Possible Drug-Drug Interaction. *Clin. Pharmacol. Ther.* 62 (4), 464–475. doi:10.1016/s0009-9236(97)90125-9

Moon, S. Y., Lim, J. H., Kim, E. H., Nam, Y., Yu, K. S., Hong, K. T., et al. (2019). Quantification of Thiopurine Nucleotides in Erythrocytes and Clinical Application to Pediatric Acute Lymphoblastic Leukemia. *Ther. Drug Monit.* 41 (1), 75–85. doi:10.1097/ftd.0000000000000575

Moriyama, T., Nishii, R., Perez-Andreu, V., Yang, W., Klussmann, F. A., Zhao, X., et al. (2016). NUDT15 Polymorphisms Alter Thiopurine Metabolism and Hematopoietic Toxicity. *Nat. Genet.* 48 (4), 367–373. doi:10.1038/ng.3508

Neurath, M. F., Kiesslich, R., Teichgräber, U., Fischer, C., Hofmann, U., Eichelbaum, M., et al. (2005). 6-thioguanosine Diphosphate and Triphosphate Levels in Red Blood Cells and Response to Azathioprine Therapy in Crohn's Disease. *Clin. Gastroenterol. Hepatol.* 3 (10), 1007–1014. doi:10.1016/s1542-3565(05)00697-x

Nygaard, U., Toft, N., and Schmiegelow, K. (2004). Methylated Metabolites of 6-mercaptopurine Are Associated with Hepatotoxicity. *Clin. Pharmacol. Ther.* 75 (4), 274–281. doi:10.1016/j.clpt.2003.12.001

O'Connell, D. J., Caruso, C. J., and Sass, M. D. (1965). Separation of Erythrocytes of Different Ages. *Clin. Chem.* 11, 771–781. doi:10.1093/clinchem/11.8.771

Oliveira, B. M., Romanha, A. J., Alves, T. M., Viana, M. B., and Zani, C. L. (2004). An Improved HPLC Method for the Quantitation of 6-mercaptopurine and its Metabolites in Red Blood Cells. *Braz. J. Med. Biol. Res.* 37 (5), 649–658. doi:10.1590/s0100-879x2004000500004

Pike, M. G., Franklin, C. L., Mays, D. C., Lipsky, J. J., Lowry, P. W., and Sandborn, W. J. (2001). Improved Methods for Determining the Concentration of 6-thioguanine Nucleotides and 6-methylmercaptopurine Nucleotides in Blood. *J. Chromatogr. B Biomed. Sci. Appl.* 757 (1), 1–9. doi:10.1016/s0378-4347(00)00513-2

Relling, M. V., Gardner, E. E., Sandborn, W. J., Schmiegelow, K., Pui, C. H., Yee, S. W., et al. (2011). Clinical Pharmacogenetics Implementation Consortium Guidelines for Thiopurine Methyltransferase Genotype and Thiopurine Dosing. *Clin. Pharmacol. Ther.* 89 (3), 387–391. doi:10.1038/clpt.2010.320

Relling, M. V., Schwab, M., Whirl-Carrillo, M., Suarez-Kurtz, G., Pui, C. H., Stein, C. M., et al. (2019). Clinical Pharmacogenetics Implementation Consortium Guideline for Thiopurine Dosing Based on TPMT and NUDT15 Genotypes: 2018 Update. *Clin. Pharmacol. Ther.* 105 (5), 1095–1105. doi:10.1002/cpt.1304

Sandborn, W. J. (2009). The Future of Inflammatory Bowel Disease Care. *Rev. Gastroenterol. Disord.* 9 (3), E69–E77.

Schwab, M., Schäffeler, E., Marx, C., Fischer, C., Lang, T., Behrens, C., et al. (2002). Azathioprine Therapy and Adverse Drug Reactions in Patients with Inflammatory Bowel Disease: Impact of Thiopurine S-Methyltransferase Polymorphism. *Pharmacogenetics* 12 (6), 429–436. doi:10.1097/00008571-200208000-00003

Shipkova, M., Armstrong, V. W., Wieland, E., and Oellerich, M. (2003). Differences in Nucleotide Hydrolysis Contribute to the Differences between Erythrocyte 6-thioguanine Nucleotide Concentrations Determined by Two Widely Used Methods. *Clin. Chem.* 49 (2), 260–268. doi:10.1373/49.2.260

Simsek, M., Meijer, B., Mulder, C. J. J., van Bodegraven, A. A., and de Boer, N. K. H. (2017). Analytical Pitfalls of Therapeutic Drug Monitoring of Thiopurines in Patients with Inflammatory Bowel Disease. *Ther. Drug Monit.* 39 (6), 584–588. doi:10.1097/ftd.0000000000000455

Sorouraddin, M. H., Khani, M. Y., Amini, K., Naseri, A., Asgari, D., and Rashidi, M. R. (2011). Simultaneous Determination of 6-Mercaptopurine and its Oxidative Metabolites in Synthetic Solutions and Human Plasma Using Spectrophotometric Multivariate Calibration Methods. *Bioimpacts* 1 (1), 53–62. doi:10.5681/bi.2011.008

Swann, P. F., Waters, T. R., Moulton, D. C., Xu, Y. Z., Zheng, Q., Edwards, M., et al. (1996). Role of Postreplicative DNA Mismatch Repair in the Cytotoxic Action of Thioguanine. *Science* 273 (5278), 1109–1111. doi:10.1126/science.273.5278.1109

Thomas, S. N., Li, L., Molinelli, A. R., and Clarke, W. (2018). ""Measurement of Thiopurine Metabolites in Erythrocytes to Optimize Thiopurine Therapy."," in Poster B-219 presented at 70th AACC Annual Scientific Meeting S203, McCormick Place, Chicago, Illinois, USA, July 29–August 02, 2018. Available at: https://meeting.aacc.org/abstracts/annual-meeting-abstract-archive.

Thompson, C. B., Galli, R. L., Melaragno, A. J., and Valeri, C. R. (1984). A Method for the Separation of Erythrocytes on the Basis of Size Using Counterflow Centrifugation. *Am. J. Hematol.* 17 (2), 177–183. doi:10.1002/ajh.2830170209

Tsutsumi, K., Otsuki, Y., and Kinoshita, T. (1982). Simultaneous Determination of Azathioprine and 6-mercaptopurine in Serum by Reversed-phase High-Performance Liquid Chromatography. *J. Chromatogr.* 231 (2), 393–399. doi:10.1016/s0378-4347(00)81863-0

Vikingsson, S., Almer, S., Peterson, C., Carlsson, B., and Josefsson, M. (2013). Monitoring of Thiopurine Metabolites - a High-Performance Liquid Chromatography Method for Clinical Use. *J. Pharm. Biomed. Anal.* 75, 145–152. doi:10.1016/j.jpba.2012.11.027

Wiwattanakul, S., Prommas, S., Jenjirattithigarn, N., Santon, S., Puangpetch, A., Pakakasama, S., et al. (2017). Development and Validation of a Reliable Method for Thiopurine Methyltransferase (TPMT) Enzyme Activity in Human Whole Blood by LC-MS/MS: An Application for Phenotypic and Genotypic Correlations. *J. Pharm. Biomed. Anal.* 145, 758–764. doi:10.1016/j.jpba.2017.07.039

Wu, F., Melis, R., McMillin, G. A., and Johnson-Davis, K. L. (2019). Retrospective Data Analysis of the Influence of Age and Sex on TPMT Activity and its Phenotype-Genotype Correlation. *J. Appl. Lab. Med.* 3 (5), 827–838. doi:10.1373/jalm.2018.027276

Yang, J. J., Landier, W., Yang, W., Liu, C., Hageman, L., Cheng, C., et al. (2015). Inherited NUDT15 Variant Is a Genetic Determinant of Mercaptopurine Intolerance in Children with Acute Lymphoblastic Leukemia. *J. Clin. Oncol.* 33 (11), 1235–1242. doi:10.1200/jco.2014.59.4671

Yoo, I. Y., Lee, K., Ji, O. J., Woo, H. I., and Lee, S. Y. (2018). Evaluation of Stability of Thiopurine Metabolites Using a Validated LC-MS/MS Method. *Ann. Lab. Med.* 38 (3), 255–260. doi:10.3343/alm.2018.38.3.255

Conflict of Interest: The authors declare that the research was conducted in the absence of any commercial or financial relationships that could be construed as a potential conflict of interest.

Publisher's Note: All claims expressed in this article are solely those of the authors and do not necessarily represent those of their affiliated organizations, or those of the publisher, the editors, and the reviewers. Any product that may be evaluated in this article, or claim that may be made by its manufacturer, is not guaranteed or endorsed by the publisher.

frontiers in Oncology

REVIEW
published: 22 March 2022
doi: 10.3389/fonc.2022.821807

Therapeutic Drug Monitoring of Tyrosine Kinase Inhibitors Using Dried Blood Microsamples

Nick Verougstraete[1,2], *Veronique Stove*[2,3], *Alain G. Verstraete*[2,3] *and Christophe P. Stove*[1]*

[1] Laboratory of Toxicology, Department of Bioanalysis, Faculty of Pharmaceutical Sciences, Ghent University, Ghent, Belgium, [2] Department of Laboratory Medicine, Ghent University Hospital, Ghent, Belgium, [3] Department of Diagnostic Sciences, Faculty of Medicine and Health Sciences, Ghent University, Ghent, Belgium

Therapeutic drug monitoring (TDM) of tyrosine kinase inhibitors (TKIs) is not yet performed routinely in the standard care of oncology patients, although it offers a high potential to improve treatment outcome and minimize toxicity. TKIs are perfect candidates for TDM as they show a relatively small therapeutic window, a wide inter-patient variability in pharmacokinetics and a correlation between drug concentration and effect. Moreover, most of the available TKIs are susceptible to various drug-drug interactions and medication adherence can be checked by performing TDM. Plasma, obtained *via* traditional venous blood sampling, is the standard matrix for TDM of TKIs. However, the use of plasma poses some challenges related to sampling and stability. The use of dried blood microsamples can overcome these limitations. Collection of samples *via* finger-prick is minimally invasive and considered convenient and simple, enabling sampling by the patients themselves in their home-setting. The collection of small sample volumes is especially relevant for use in pediatric populations or in pharmacokinetic studies. Additionally, working with dried matrices improves compound stability, resulting in convenient and cost-effective transport and storage of the samples. In this review we focus on the different dried blood microsample-based methods that were used for the quantification of TKIs. Despite the many advantages associated with dried blood microsampling, quantitative analyses are also associated with some specific difficulties. Different methodological aspects of microsampling-based methods are discussed and applied to TDM of TKIs. We focus on sample preparation, analytics, internal standards, dilution of samples, external quality controls, dried blood spot specific validation parameters, stability and blood-to-plasma conversion methods. The various impacts of deviating hematocrit values on quantitative results are discussed in a separate section as this is a key issue and undoubtedly the most widely discussed issue in the analysis of dried blood microsamples. Lastly, the applicability and feasibility of performing TDM using microsamples in a real-life home-sampling context is discussed.

Keywords: tyrosine kinase inhibitors, therapeutic drug monitoring, microsampling, dried blood microsamples, oncology drugs

OPEN ACCESS

Edited by:
Jennifer Martin,
The University of Newcastle, Australia

Reviewed by:
Gareth J. Veal,
Newcastle University, United Kingdom
Tommaso Lomonaco,
University of Pisa, Italy

***Correspondence:**
Christophe P. Stove
christophe.stove@ugent.be

Specialty section:
This article was submitted to Pharmacology of Anti-Cancer Drugs, a section of the journal Frontiers in Oncology

Received: *24 November 2021*
Accepted: *01 March 2022*
Published: *22 March 2022*

Citation:
Verougstraete N, Stove V, Verstraete AG and Stove CP (2022) Therapeutic Drug Monitoring of Tyrosine Kinase Inhibitors Using Dried Blood Microsamples. Front. Oncol. 12:821807. doi: 10.3389/fonc.2022.821807

INTRODUCTION: TDM OF TKIs

Therapeutic drug monitoring (TDM) refers to the determination of therapeutic drug concentrations in biological fluids, mostly serum, plasma or blood, with the aim of improving individual treatment by dose adjustment. In clinical practice, TDM is already routinely performed for several classes of therapeutic compounds, such as immunosuppressants, antibiotics and anti-epileptic drugs. Although evidence is accumulating that there also lies significant potential in the field of cancer treatment, TDM is not yet routinely performed for oncology drugs (1, 2).

Constitutive over-activation of tyrosine kinases (e.g. *via* mutations or *via* constitutive ligand-mediated activation) is known to underlie uncontrolled cell growth and proliferation, resistance to apoptosis and lack of differentiation. Tyrosine kinase inhibitors (TKIs) are a relatively new class of targeted cancer therapy specifically inhibiting tyrosine kinases responsible for deregulation of intracellular signaling pathways in tumor cells (3). A wide array of TKIs has become available that is increasingly being used for the treatment of various malignant diseases, including chronic myeloid leukemia (CML), gastrointestinal stromal tumor (GIST), non-small-cell lung carcinoma (NSCLC), renal cell carcinoma (RCC) and melanoma. In contrast to most classical cytotoxic agents, TKIs are administered orally enabling outpatient treatment. Besides, TKIs are usually given in non-individualized fixed doses (4).

TKIs have a relatively small therapeutic window and show high inter-individual pharmacokinetic variability after oral administration, caused by variation in absorption, distribution, metabolism and excretion (2, 4, 5). Following a given dose, a wide range of plasma concentrations among different patients are to be expected, which can possibly affect therapeutic responses and adverse effects (6). Bioavailability of TKIs depends on drug formulation, gastrointestinal absorption, concomitant food intake (e.g. increased bioavailability of nilotinib and pazopanib when administered under fed conditions (7)) and first-pass metabolism by the liver (8). As the majority of TKIs are primarily metabolized *via* the cytochrome P450 3A4 isoenzyme, this makes them prone to drug-drug interactions. The latter is highly relevant for TKIs as polypharmacy is common in cancer patients: for example, in acute myeloid leukemia (AML) treatment clinically relevant pharmacokinetic interactions have been described between the FLT3 inhibitors (midostaurin and gilteritinib) and azole antifungals (9, 10). Genetic polymorphisms, age, lifestyle factors (e.g. influence of smoking on erlotinib metabolic clearance (11)) and comorbidities also have an influence on the CYP enzymes' activity (2, 4, 12). Moreover, some of the TKIs are substrates for drug transporters, e.g. erlotinib is a P-glycoprotein substrate (12).

In the context of chronic conditions with a need for long-term oral treatment, medication adherence is very important and a major determinant in the therapeutic success of TKIs. Again, this can be assessed by monitoring trough TKI levels (6, 13, 14). Patients' adherence to oral anticancer drugs is highly variable, with reported rates varying from 100 down to 20% (15). In CML, poor adherence is the main reason for the lack of obtaining a molecular response (16). For most of the available TKIs, studies have already defined exposure-response relationships. On the one hand, underexposure may result in reduced efficacy with therapy failure and/or more rapid development of TKI resistance. On the other hand, if the exposure is too high, the risk of treatment-related toxicity, with occurrence of adverse effects is increased (6). This, in turn, may negatively impact adherence. Given the (once or twice) daily chronic administration of most TKIs, single steady-state trough levels (i.e. just before the next dose) allow estimating TKI exposure (2). Steady-state levels are achieved after 4-5 times the elimination half-life of the drug (4). For newer TKIs, exposure-response relationships and suitable pharmacokinetic thresholds associated with favorable outcome still need to be defined (5, 17–19). Furthermore, feasible dose-adaptation strategies should exist (4).

For the above-mentioned reasons, TKIs have been suggested as perfect candidates for routinely performing TDM. Based on evidence level, TDM is currently recommended for axitinib, gefitinib, imatinib, pazopanib, sunitinib and trametinib (5). Recently, the International Association of Therapeutic Drug Monitoring and Clinical Toxicology (IATDMCT) has published a consensus guideline for TDM of imatinib (20). The evidence level for TDM for the TKIs alectinib, crizotinib, erlotinib, gilteritinib, nilotinib and vemurafenib is categorized as "potentially useful" because exposure-response relationships and target concentrations have been established but TDM feasibility studies have not yet been performed. For a wide range of additional TKIs, including among others bosutinib, dasatinib, ibrutinib, midostaurin and ponatinib evidence is still in the exploratory phase. TDM of cobimetinib, entrectinib, lapatinib and larotrectinib is not recommended (5).

Lastly, considering the high costs of these drugs and the high consequences of subtherapeutic concentrations, efforts to ensure their therapeutic potential should be made. Related to this, a shift from a TKI fixed dosing paradigm to individual dosing based on TDM results is recommended. In the context of personalized cancer treatment, TDM is a relatively new strategy that could be valuable to optimize TKI dosage, resulting in better patient outcome.

TKI therapeutic ranges are typically expressed as plasma concentrations, hence plasma, obtained *via* conventional venous blood sampling, is the standard matrix for TDM of TKIs. However, the use of plasma as a matrix poses some challenges related to sampling and stability. Venous blood is acquired *via* an invasive venous blood sampling procedure, performed by qualified medical personnel. For cancer patients,

Abbreviations: AML, acute myeloid leukemia; CML, chronic myeloid leukemia; DBS, dried blood spot; DPS, dried plasma spot; EDTA, ethylenediaminetetraaectic acid; EQC, external quality control; GIST, gastrointestinal stromal tumor; Hct, hematocrit; IATDMCT, International Association of Therapeutic Drug Monitoring and Clinical Toxicology; IS, internal standard; LC-MS/MS, liquid chromatography tandem mass spectrometry; LLOQ, lower limit of quantitation; ME, matrix effect; MRM, multiple reaction monitoring; NIR, near infrared; NSCLC, non-small-cell lung carcinoma; QC, quality control; RCC, renal cell carcinoma; SIL, stable isotopically labeled; SKML, stichting kwaliteitsbewaking medische laboratoriumdiagnostiek; TDM, therapeutic drug monitoring; TKI, tyrosine kinase inhibitor; ULOQ, upper limit of quantification; VAMS, volumetric absorptive microsampling.

this conventional venous sampling may be challenging because of difficulties to access peripheral blood vessels due to the frequent blood sample collection, combined with the chemotherapy administration. Moreover, the preparation of plasma requires a centrifugation step of whole blood and for most TKIs refrigerated storage and transport of the sample (blood or plasma) is needed (21). The latter is relevant as TDM for TKIs is typically only performed at specialized centers, requiring transportation from the sampling site to a dedicated clinical lab. Stability can also be a key factor. Instability is for instance relevant for ibrutinib, which is subject to rapid degradation in plasma at room temperature and at 4°C (22, 23). Moreover, diminished stability in plasma samples stored at room temperature has also been reported for lapatinib and axitinib (<24 hours) (24) and sunitinib (<48 hours) (25).

The above-mentioned issues can be overcome using alternative sampling strategies, in which traditional matrices are collected *via* an alternative approach. Dried blood microsampling appears to be the most promising option for application of TDM of TKIs (1). It refers to the collection of a small amount of blood (typically <50 µL), most often following a finger-prick using an automatic (single-use) lancet. Dried blood microsamples are generally dried for 2-3 hours at ambient temperature. Given the minimal invasiveness and the low volume of sample collected, dried blood microsampling is considered more patient-friendly than conventional venous blood sampling. This is particularly relevant for use in pediatric populations. Moreover, given the convenient and simple sampling method, (micro)samples can be collected by the patients themselves outside the healthcare environment. This is advantageous for outpatients as they are not required to go to a medical center for a blood draw. Furthermore, sampling at predefined times (e.g. trough levels for most TDM applications) is also more convenient in a home-setting and will not lead to a delay in drug intake. Hence, it can be concluded that, overall, microsampling complies with a patient-centric view when it relates to sample collection. In addition, microsampling is also a valuable tool to investigate the pharmacokinetics of TKIs (12, 26), especially for the pharmacokinetic assessment of new investigational TKIs during clinical trials (27, 28). **Table 1** provides a summary of the advantages and challenges associated with dried blood microsampling for TDM of TKIs.

The most widespread and well-known microsampling technique is dried blood spot (DBS) sampling. DBS are generated by collecting a drop of capillary blood, derived from a finger- or heel-prick, on special filter paper. In a typical DBS workflow, a 3-6 mm diameter disc is punched from the DBS, followed by extraction of this subpunch. While there is a plethora of papers concerning TDM *via* DBS (29–33), relatively few of these deal with oral anticancer drugs or TKIs (34), although recently there is an increased interest. Apart from conventional DBS, other microsampling devices are also being explored for TKI monitoring. E.g., we recently reported on the determination of a TKI panel in samples collected *via* volumetric absorptive microsampling (VAMS) (35). Briefly, VAMS is a sampling technique in which a fixed volume of blood is wicked up by an absorbent tip attached to a plastic handler, used as an alternative to classical DBS sampling. **Table 2** gives an overview of published methods to determine TKIs in different dried blood microsamples. In what follows we will discuss these methods, along with the benefits and challenges, as outlined in **Table 1**.

METHODOLOGICAL ASPECTS OF DRIED BLOOD MICROSAMPLE METHODS FOR TKI TDM

Despite the many advantages associated with dried blood microsampling, quantitative analyses on these matrices requires tackling a few hurdles, which will be discussed in this section. The hematocrit (Hct)-effect will be discussed in a separate paragraph as this is a key issue and undoubtedly the most widely discussed issue in the analysis of dried blood microsamples (47–49). To guide successful incorporation of TDM methods in routine, the IATDMCT published an extensive guideline covering the development and validation of DBS-based methods, including both classical validation parameters and dried blood specific parameters. Furthermore, this guideline provides guidance on how to deal with specific dried blood associated issues and pitfalls during method development (50). In essence, it shouldn't matter whether a TKI is determined in liquid or dried blood, implying that concentrations measured in a dried blood microsample should

TABLE 1 | Advantages and challenges associated with TKI (dried) microsampling.

Advantages	Challenges
Minimally invasive sampling	Correlation with (venous) plasma concentrations
Small sample volume	Hematocrit effects: differential spreading of blood samples (DBS), impact on recovery and blood-to-plasma ratio
Convenient and cost-effective transport and storage	Influence of spotted volume & spot homogeneity (DBS)
No need for centrifugation step	Sensitive analytical techniques required
Compound stability	Dilution of samples >ULOQ
Home sampling	Lack of proficiency testing programs
Less biohazardous	Risk of inadequate sampling
	Extra validation steps needed
	Sampling material is more expensive than blood tubes
	Not compatible with track systems in clinical labs
	Need for drying for 2 hours

DBS, dried blood spots; ULOQ, upper limit of quantification.

TABLE 2 | Overview of published microsample TKI-based methods in alphabetical order of the first author.

Reference	Micro-sampling technique	Included TKIs	Assay range	Complete DBS vs DBS punch	Sample preparation	Internal standard	Application	Mean Hct (+ range) of study population
Antunes et al. (36)	DBS	Imatinib	50-4000 ng/mL	Punch: 6 mm d	Direct extraction with MeOH	SIL	Comparison between DBS and plasma samples from 50 CML patients	0.36 (0.29-0.43)
Boons et al. (37)	DBS	Nilotinib	17-4100 ng/mL	Punch: 8 mm d	Direct extraction with MeOH	SIL	Comparison between 40 DBS and plasma samples from 20 CML patients	0.41
de Wit et al. (38)	DBS	Pazopanib	0.1-50 µg/mL	Punch: 4 mm d	Direct extraction with FA and MeOH	SIL	Comparison between DBS and plasma samples from 12 mRCC patients	0.45 (0.40-0.49)
Iacuzzi et al. (39)	DBS	Imatinib	50-7500 ng/mL	Punch: 3 mm d	Direct extraction with 0.1% FA in MeOH	SIL	Comparison between 55 DBS (both from venous blood and from finger prick) and plasma samples from 26 GIST patients	0.38 (0.26-0.44)
		Norimatinib	10-1500 ng/mL					
Irie et al. (40)	DBS	Gefitinib	37.5-2400 ng/mL	Punch: 3 mm d	Direct extraction with MeOH	Erlotinib	Comparison between DBS and plasma samples from 10 NSCLC patients	0.39 (0.32-0.42)
Kralj et al. (41)	DBS	Imatinib	50-5000 ng/mL	Complete: 10 µL	Direct extraction with 0.1% FA in MeOH	SIL	Comparison between 24 DBS and plasma samples from CML patients	*
		Nilotinib	50-5000 ng/mL					
		Dasatinib	2.5-250 ng/mL					
Lee et al. (42)	DBS	Radotinib	5-2000 ng/mL	Punch: 6 mm d	Direct extraction with "extracting solvent"	*	Comparison between DBS and plasma samples from 45 CML patients	0.41
Martin et al. (28)	DBS	R406 (active metabolite of fostamatinib)	2.5-2500 ng/mL	*	*	SIL	Comparison between plasma, venous whole blood, finger prick-drawn DBS and pipette-drawn DBS samples from 24 patients in a phase I clinical dose study	*
Mukai et al. (43)	DPS	Dasatinib	1-200 ng/mL	Complete: 40 µL	Extraction with MeOH/ACN (50/50, v/v) followed by SPE and evaporation to dryness	SIL	Comparison between 96 (venous) DPS and plasma samples	NA
		Ponatinib	1-200 ng/mL					
		Ibrutinib	2-400 ng/mL					
		Bosutinib	5-1000 ng/mL					
		Imatinib	20-4000 ng/mL					
		Nilotinib						

(Continued)

TABLE 2 | Continued

Reference	Micro-sampling technique	Included TKIs	Assay range	Complete DBS vs DBS punch	Sample preparation	Internal standard	Application	Mean Hct (+ range) of study population
			20-4000 ng/mL					
Nijenhuis et al. (26, 44)	DBS	Vemurafenib	1-100 µg/mL	Punch: 3 mm d	Direct extraction with MeOH/ACN (50/50, v/v)	SIL	Comparison between 43 DBS and plasma samples from 8 melanoma patients (26)	0.40 (0.27-0.49) (26)
Parra-Guillen et al. (12)	DBS	Erlotinib	10-10000 ng/mL	Punch: 3 mm d	Direct extraction with MeOH/water (50/50, v/v)	SIL	Comparison between DBS and plasma samples from 36 patients with advanced NSCLC	*
		Metabolite OSI-420	2.5-2500 ng/mL					
Verheijen et al. (45)	DBS	Pazopanib	1-50 µg/mL	Punch: 3 mm d	Direct extraction with FA and subsequent MeOH	SIL	Comparison between 329 DBS and plasma samples from 30 patients with advanced solid tumors	0.40 (0.36-0.48)
Verougstraete and Stove (35)	VAMS	Bosutinib	5-675 ng/mL	NA	Pre-wetting VAMS tips with water followed by sonication, LLE with methyl-t-butyl ether and evaporation to dryness	SIL	Comparison between 27 (venous) DBS and liquid whole blood samples from oncology patients	0.39 (0.20-0.49)
		Dasatinib	0.5-450 ng/mL					
		Gilteritinib	25-675 ng/mL					
		Ibrutinib	5-675 ng/mL					
		Imatinib	10-2250 ng/mL					
		Midostaurin	30-2250 ng/mL					
		Nilotinib	10-2250 ng/mL					
		Ponatinib	1-450 ng/mL					
Xu et al. (27)	DBS	MK-1775 (adavosertib)	2-1000 ng/mL	Punch: 3 mm d	Direct extraction with 85% ACN – 10mM ammonium formate	SIL	Comparison between DBS and plasma samples from 12 solid tumor patients	(0.32-0.48)
Zimmermann et al. (46)	VAMS	Afatinib	2-500 ng/mL	NA	Rehydration of VAMS tips with water followed by addition of ACN as extraction solution and evaporation of the supernatant	SIL	24 VAMS samples from 5 patients with various malignancies	0.38 (0.31-0.41)
		Axitinib	2-500 ng/mL					
		Bosutinib	2-500 ng/mL					
		Cabozatinib	6-1500 ng/mL					

(Continued)

TABLE 2 | Continued

Reference	Micro-sampling technique	Included TKIs	Assay range	Complete DBS vs DBS punch	Sample preparation	Internal standard	Application	Mean Hct (+ range) of study population
		Dabrafenib	6-1500 ng/mL					
		Lenvatinib	2-500 ng/mL					
		Nilotinib	6-1500 ng/mL					
		Osimeritinib	6-1500 ng/mL					
		Ruxolitinib	2-500 ng/mL					
		Trametinib	2-500 ng/mL					

ACN, acetonitrile; CML, chronic myeloid leukemia; d, diameter; DBS, dried blood spot; DPS, dried plasma spot; FA, formic acid; GIST, gastro-intestinal stromal tumor; LLE, liquid-liquid extraction; MeOH, methanol; NA, not applicable; mRCC, metastatic renal cell carcinoma; NA, not applicable; NSCLC, non-small cell lung cancer; SIL, stable isotopically labeled; TKI, tyrosine kinase inhibitor; VAMS, volumetric absorptive microsampling.
**Information not described in the paper.*

mimic those obtained from liquid blood. If not, this points at a methodological issue associated with the dried blood-based method, which should be addressed.

a. Sample Preparation

For plasma-based methods for TKI TDM, simple protein precipitation with organic solvents is the most commonly used sample pretreatment approach (51). In dried blood microsample bioanalysis, sample preparation plays a pivotal role, as extractability issues (e.g. differences in recovery between aged *versus* fresh samples, or between samples with a different Hct) may be detrimental for a method's usefulness in clinical practice. Several sample preparation approaches have been described for TKI determination in dried blood microsamples. The easiest extraction method includes a single-step extraction by addition of an organic solvent or a mixture of solvents to the microsample. After subsequent shaking and centrifugation, the supernatant can be injected on the analytical column (12, 27, 36–42, 44, 45). This is the most preferred approach as the sample handling is simple and fast. However, the high amount of organic solvent in these extracts may influence the chromatographic run. If sensitivity allows, the extracts can be diluted with water prior to injection to eliminate this solvent-effect on chromatography (38, 44, 45). The concurrent determination of several TKIs may require a more sophisticated sample preparation strategy. For example, the sample preparation of dried plasma spots (DPS) for the measurement of bosutinib, dasatinib, ibrutinib, imatinib, nilotinib and ponatinib consisted of a liquid extraction step followed by solid-phase extraction and subsequent drying (43). In two VAMS-based methods, VAMS samples were pre-wetted with an aqueous solution prior to the addition of an organic solvent for extraction (35, 46). Overall, a robust extraction procedure is key to the reliability of a method using dried blood microsamples.

b. Analytics

All reported microsample-based TKI methods used in-house developed liquid chromatography coupled to tandem mass spectrometry (LC-MS/MS) as analytical technique. Concentration ranges in dried blood microsamples are similar to the ones observed in plasma matrices. A high sensitivity is required to attain adequate lower limits of quantitation (LLOQs) – ideally not higher than 50% of the lower end of the therapeutic range. Although current new-generation MS detectors offer a high sensitivity, this may still be a challenge when aiming at detecting TKIs with trough levels in the low-ng/mL range in dried blood microsamples corresponding to merely 3 to 10 µL blood (49, 51). Examples include dasatinib and talazoparib, with median reported trough levels of 2.61 ng/mL and 3.54 ng/mL, respectively (5). Published dried blood microsample-based methods for dasatinib had LLOQs of 2.5 ng/mL in 10-µL DBS (whole spot analysis) (41), 1 ng/mL in 40-µL DPS (43) and 0.5 ng/mL in 10-µL VAMS (35). Specificity is achieved by separation of the compounds on LC columns and detection in multiple reaction monitoring (MRM) mode. Several multi-TKI LC-MS/MS methods have been developed (35, 41, 43, 46), offering the advantage that one dedicated method can be applied for a variety of analytes (and,

hence patient samples), which is especially relevant in routine clinical settings. Known disadvantages of LC-MS/MS are the high investment and maintenance cost, the high technical expertise that is required and the need for time-consuming sample preparation, which is typically more laborious for dried microsamples, when compared with plasma samples. However, LC-MS/MS analyses of dried blood microsamples can be fully automated using robotics, thereby allowing a higher throughput, decreasing the workload and improving turn-around time in the clinical laboratory (30). For example, the CAMAG DBS autosampler (Camag, Muttenz, Switzerland) allows 500 DBS cards to be stacked, which can subsequently be subjected to fully automated extraction and LC-MS/MS analysis: from card to result with no hands-on (52, 53). There are currently no published methods for TKI TDM using automated sample preparation. Automation of VAMS sample processing is also feasible, although at this point only rarely being employed, with no published reports available on routine implementation.

c. Internal Standards

Stable isotopically labeled (SIL) internal standards (ISs) are regarded as the best choice to compensate for variations during sample preparation and LC-MS/MS analysis. The importance of using SIL-ISs was also observed in several dried blood microsample-based TKI methods: Antunes et al. found significant ion enhancement for imatinib in DBS, which was completely compensated using imatinib-D_8 as IS (36). In our own work, we observed substantial ion suppression for most compounds measured in VAMS samples, which was also adequately compensated for by using SIL-ISs. Moreover, the ISs also compensated for losses during sampling preparation (35). A non-SIL IS was used in only one method: in the DBS method of Irie et al., erlotinib was used as IS for quantification of gefitinib, both being EGFR-TKIs with similar structures (40).

d. Dilution of Dried Blood Microsamples

Patient samples with a TKI concentration above the measuring range should be diluted in order to obtain a correct quantitative result if clinically relevant. Whilst this is straightforward for plasma, this is less evident for dried microsamples, which cannot be directly diluted. Indeed, most published dried microsampling methods for TKI monitoring did not integrate dilution of samples as part of the validation. Nijenhuis et al. diluted DBS extracts with vemurafenib concentrations higher than the upper limit of quantification (ULOQ) (100 µg/mL) seven-fold with blank extracts (44). A similar approach was described for pazopanib: DBS extracts were diluted tenfold with a processed controlled matrix (45). Xu et al. described two different approaches to dilute DBS samples with MK-1775 concentrations above the assay ULOQ (1000 ng/mL). In the first method, blank DBS extract containing the IS was added to the DBS sample extract. The second approach involved mixing one subpunch from the DBS sample with five subpunches obtained from blank DBS. Both dilution methods provided accurate and reproducible results (27). If dilution of samples is to be performed in routine practice, dilution integrity should be an integral part of the method validation in order to report quantitative results above the highest point of the calibration line. Alternatively, clinically relevant ULOQs could be chosen for each TKI during method development. As a guidance, an ULOQ twice the upper limit of the therapeutic range can be considered adequate, with a reporting of ">ULOQ" when a signal above the ULOQ is encountered.

e. External Quality Controls

When implementing TDM analyses in routine care, laboratories should participate in proficiency testing programs. To the best of our knowledge, there are currently no proficiency testing programs for TDM of TKIs in microsamples, while such a program readily exists for TDM of immunosuppressant drugs in microsamples, set up by the Dutch organization SKML (54). As an alternative, independent dried blood quality control (QC) samples can be generated using plasma-based (e.g. Asqualab) external QC samples (EQC) by replacing part of the plasma of a blank whole blood sample by the external QC material (31, 55, 56). The resulting blood sample can then be used to generate DBS. As the amount of plasma being replaced by EQC material is known, it is even possible to convert the obtained DBS concentration to a plasma concentration post-analysis, which can be formally reported to the proficiency test organizer.

f. DBS Specific Validation Parameters

The use of DBS subpunches necessitates the evaluation of additional parameters during method validation. One aspect to be evaluated is whether the spotted volume of blood on the filter paper has an impact on the method accuracy. Nijenhuis et al. reported that for vemurafenib the volume of a blood drop affected the reproducibility of the method and volumes >20 µL increased the inaccuracy of the assay. However, the latter was considered clinically irrelevant as the authors stated that DBS samples collected *via* finger-prick typically correspond to blood volumes of approximately 10-20 µL (44). In other studies, for imatinib and norimatinib (39), pazopanib (45) or MK-1775 (27) no influence of spot sizes between 10 to 40 µL, 10 to 30 µL or 30 to 50 µL, respectively, were observed. Another aspect to be evaluated is the site of punching (central *versus* peripheral), as non-homogeneous distribution of drugs on filter paper has been described, commonly known as the "volcano effect" (48) (accumulation of red blood cells occurs at the very outer edge of a DBS). Several articles investigated this aspect by comparing results obtained from punches taken from the edge with those from punches taken at the center of a DBS. For imatinib and norimatinib (39), pazopanib (45) and MK-1775 (27) central and peripheral measurements gave equivalent results. Preferably, the volume and volcano effect should also be evaluated at different Hct and concentration levels (50).

g. Stability

Theoretically, working with dried matrices improves the stability of most compounds. This allows a more cost-effective transport and storage: in many instances dried microsamples can be transported *via* regular mail (under ambient conditions) and stored for prolonged periods at room temperature (21). The advantage of improved stability was nicely exemplified for

ibrutinib, which is only stable in plasma for a few hours, whereas in VAMS samples and DPS it was reported to be stable at room temperature for 2 (35) and 12 weeks (43), respectively. **Table 3** summarizes the reported stabilities of various TKIs in different types of microsamples. It should be noted that for TDM of TKIs long periods of sample storage are less relevant, as analyses typically need to be performed as quickly as possible, within 1 week (or less) after sampling. For TDM purposes it is mainly important that stability during the transport of the dried microsamples is guaranteed. Several authors investigated the stability of TKIs in dried microsamples stored at higher temperatures, to simulate extreme temperature conditions that could be encountered during transportation to the laboratory *via* regular mail (e.g. in a postbox fully exposed to the sun during summer): gefitinib was stable for 24h at 40°C (40), imatinib and nilotinib were stable for at least three days at 40°C (this was not the case for dasatinib) (41), imatinib for 36 days at 43°C (36) and most TKIs of two different TKI panels in VAMS for at least 2 days at 60°C (35, 46). It should be noted that not in all instances where instability was reported, the authors verified whether extractability wasn't affected, hence resulting in *apparent* instability (57). For protection from humidity, dried microsamples are advised to be transported and stored in closed plastic bags with a desiccant. Drying also inactivates pathogens present in the blood, which reduces the biohazard risk (58).

h. Hematocrit Effects

For a variety of reasons, deviating Hct values may impact dried blood microsample-based quantitative results. The best-known effect of the Hct of a blood sample is related to the spreading of blood on filter paper, when working with conventional DBS collected *via* direct application of a drop of blood. This is related to the viscosity of the blood: blood with a higher Hct will spread less than blood with a lower Hct and will result in more concentrated spots. Hence, when a fixed-diameter punch is taken from DBS with a higher Hct, the volume of blood and

TABLE 3 | Reported stability of TKIs in different microsamples in alphabetical order of the first author.

Reference	TKI	Microsample	Storage condition
Antunes et al. (36)	Imatinib	DBS	36 days at -20, 25 and 43°C
Boons et al. (37)	Nilotinib	DBS	7 months in refrigerator (2-8°C)
de Wit et al. (38)	Pazopanib	DBS	75 days at ambient temperature
Iacuzzi et al. (39)	Imatinib Norimatinib	DBS	16 months at RT
Irie et al. (40)	Gefitinib	DBS	5 months at RT 5 months at -20°C 24 hours at 40°C
Kralj et al. (41)	Imatinib Nilotinib Dasatinib	DBS	30 days at RT or -20°C 3 days at 40°C (except dasatinib)
Mukai et al. (43)	Bosutinib Dasatinib Ibrutinib Imatinib Nilotinib Ponatinib	DPS	72 hours at 40°C/90% RH 12 weeks at RT
Nijenhuis et al. (26)	Vemurafenib	DBS	827 days at ambient temperature
Verheijen et al. (45)	Pazopanib	DBS	398 days at ambient temperature
Verougstraete & Stove (35)	Bosutinib Dasatinib Ibrutinib Imatinib Gilteritinib Midostaurin Nilotinib Ponatinib	VAMS	1 month at -20°C, 4°C and RT (except ibrutinib 2 weeks at RT) 2 days at 60°C (except ibrutinib 1 day)
Xu et al. (27)	MK-1775 (adavosertib)	DBS	6 months at -20°C 14 months at ambient temperature 8 days at 40°C/75% RH
Zimmermann et al. (46)	Afatinib Axitinib Bosutinib Cabozatinib Dabrafenib Lenvatinib Nilotinib Osimeritinib Ruxolitinib Trametinib	VAMS	6 weeks at RT (19% RH) 2 days at 60°C (10% RH) (except afatinib and osimeritinib)

DBS, dried blood spot; DPS, dried plasma spot; RH, relative humidity; RT, room temperature; TKI, tyrosine kinase inhibitor; VAMS, volumetric absorptive microsampling.

thus the amount of analyte contained within this subpunch will be higher than in punches from DBS with a lower Hct. Spreading of the blood also depends on the type of filter paper used (47–49). For each DBS-based method, a Hct interval in which the impact of this 'area bias' is still acceptable should be established during method validation. This Hct effect is of particular importance in oncology patients, as the Hct may vary widely in this population: whereas the reported mean Hct of the different oncology study populations was quite constant, the ranges of these Hcts were wide (see **Table 2**). Furthermore, Hct values may also vary widely within the individual oncology patient due to concomitant chemotherapy, disease progression or overall clinical status.

Several approaches have been proposed that may allow to cope with the differential spreading of blood samples with varying Hct. A first approach implies the use of volumetrically applied DBS, followed by whole spot analysis. Kralj et al. followed this approach, after pipetting 10 μL EDTA whole blood onto filter paper (41). However, such accurate volumetric application of blood onto a filter paper is hard to envisage when aiming at home-sampling by the patients themselves. Another strategy is to determine or estimate the Hct of the blood used for DBS preparation, to correct for the Hct bias. For instance, Hct levels can be predicted by measuring the potassium concentration in DBS. Potassium concentrations correlate with the Hct because potassium is predominantly located intracellularly and erythrocytes are the prime cellular constituent of blood (59). Hct levels can also be predicted *via* determination of its total hemoglobin content, using non-contact single-wavelength reflectance spectroscopy (60, 61) or near infrared (NIR) spectroscopy (62–64). If the Hct level of the DBS (subpunch) is known, correction factors to alleviate the Hct bias can be used (61, 65) or plasma concentrations can be derived from the measured DBS concentrations (see further).

New devices, allowing an accurate volumetric collection of capillary dried blood microsamples, are continuously being developed. These maintain the benefits associated with DBS, while avoiding the above-described Hct-based area bias (66). One of the first strategies to achieve this is VAMS, which has evolved over the course of years into a valuable alternative to classical DBS sampling. VAMS devices (marketed as Mitra® and introduced in 2014 by Neoteryx, Torrance, CA) consist of a porous absorbent polymeric tip, connected to a plastic handle. Upon touching a drop of blood for a few seconds, the tips absorb a fixed volume of blood (10, 20 or 30 μL) by capillary action, irrespective of the sample's Hct (67, 68). Furthermore, compared to DBS, collection of VAMS samples has been scored as more simple and straightforward (69, 70). A current limitation of VAMS, when compared to DBS, is that there are hardly any reports on fully automated extraction and analysis – there is only one report describing the measurement of ten peptides in VAMS samples *via* an automated platform for protein extraction and digestion (71). As devices are being designed to enable easy, automated sample preparation by robotic liquid handling platforms (21), it is expected that VAMS samples will catch up with DBS in terms of automation for TDM analyses. For example, a Tecan® (Männedorf, Switzerland) platform has already been used for automatic preparation of blood-dipped VAMS tips which can be used as calibrators or QCs. This only results in automation and time saving for the preparation of the VAMS samples themselves, with extraction and chromatographic analysis still requiring manual processes (72). To date, two groups have investigated the measurement of TKIs using VAMS, establishing multi-analyte methods for the simultaneous quantification of eight (35) or ten TKIs (46). Other volumetric microsampling devices avoiding the Hct and inhomogeneity bias include the HemaPEN (Trajan, Melbourne, Australia), Capitainer qDBS (Capitainer, Solna, Sweden) and HemaXis DB 10 (HemaXis, Gland, Switzerland) device (66). To the best of our knowledge, none of these devices has been used for the determination of TKIs yet. A drawback associated with these alternative sampling devices is the higher cost and, for some, the more complex sampling and processing technique compared to conventional DBS. These aspects, together with the recency of these developments, may explain the hitherto limited implementation of these devices in clinical routine (66).

Another approach to minimize the Hct bias effect is to prepare calibration standards in blood with a Hct level close to the expected Hct of the target population (30). For this approach the Hct among the target population and within the individual patients should be quite constant, which is not the case for the heterogeneous population of cancer patients treated with TKIs (see above). Moreover, one should know whether the Hct level of the sample lies within the covered Hct range – the above-mentioned Hct prediction strategies allow to derive this information. In the different published TKI methods the standards were prepared in blank blood with a Hct of 0.40 (35), 0.42 (41), 0.35 (36), 0.44 (45), 0.40 (37), 0.38 (39) or 0.45 (46).

In most of the published TKI microsample methods the influence of the Hct on the accuracy of the method has been evaluated by preparing QC samples at different Hct levels and comparing the obtained results to those obtained from QC samples with the Hct value of the calibrators. No significant impact for the following Hct ranges on the accuracy was observed for imatinib [0.25-0.50] (36), imatinib combined with its active metabolite norimatinib [0.29-0.59] (39), imatinib included in a multi-TKI method together with dasatinib and nilotinib [0.30-0.60] (41), MK-1775 [0.16-0.85] (27), nilotinib [0.25-0.50] (37), pazopanib [0.20-0.65] (38) and [0.35-0.50] (45), vemurafenib [0.24-0.45] (44) and for a multi-analyte method containing eight [0.18-0.55] (35) and ten [0.30-0.55] (46) TKIs.

The second effect of the Hct on dried blood microsampling is its potential impact on the recovery of the analyte from the dried blood microsample. This is the case for both conventional DBS and for the newer microsampling devices: Hct-dependent recoveries have been described for DBS (73) and can even be more profound for VAMS samples (74, 75). Most often, high Hct levels have a negative effect on the analyte recovery, resulting in an underestimation of the analyte concentration (76). The latter has been explained for VAMS samples by the larger amounts of erythrocytes present at higher Hct levels, which may trap the analytes in the pores of the VAMS tip, resulting in a lower

recovery (75). Similarly, the recovery may be impacted upon ageing of the dried samples. Therefore, thorough optimization of the extraction procedure during method development is critical to ensure the robustness of a dried blood microsample-based method. Besides the use of different extraction solvents and elevated temperatures to obtain a more robust Hct-independent extraction (55, 56), Mano et al. concluded that the inclusion of a sonication step helps to improve the extraction of the compounds from the porous VAMS material (77). Importantly, as IS are typically added together with the extraction solvent, these will only compensate for post-extraction biases and will not compensate for recovery issues. The latter can potentially be solved for DBS analyses by spraying the IS onto the filter paper before sample extraction (78). However, in all the published TKI DBS methods, the ISs were added to the extraction solvent or directly added to the sample before extraction (12, 27, 36–41, 43–45). In a multi-analyte TKI method on VAMS samples clear Hct-dependent recovery issues were observed over a Hct range from 0.20 to 0.60 at different storage conditions (i.e. -80°C, room temperature and 60°C) during pre-validation stress testing. The issues were eventually resolved by developing a rigorous extraction protocol including pre-wetting of the VAMS tips, sonication and liquid-liquid extraction followed by an evaporation step. The robustness to the impact of Hct was formally demonstrated during method validation, where IS-compensated recoveries from VAMS samples, derived from blood with Hct ranging from 0.18 to 0.55, ranged from 83 to 125%, with all CVs being less than 11.6% (35). Next to its effect on recovery, samples with different Hct levels can also be considered as different matrices, with the potential to give rise to Hct-dependent matrix effects (MEs). It is therefore recommended that during method validation, next to the blank matrices obtained from six different individuals, blood samples covering a broad Hct range should also be included for the evaluation of MEs (50). When evaluating MEs and recovery of the assay, it is important that these are consistent, rather than being minimal (for ME) or maximal (for recovery). We demonstrated in our published TKI VAMS method that MEs and recoveries were Hct-independent over a broad Hct range (0.18-0.55) (35).

Lastly, the Hct of a sample may also influence the blood-to-plasma concentration ratio and thus the blood to plasma concentration conversion (79). The different approaches for converting an obtained dried blood result to a plasma concentration will be discussed thoroughly in the following section.

i. (Dried) Blood to Plasma Conversion

TKI target ranges are typically plasma-based, implying that for clinical interpretation dried blood matrix results should be converted to plasma concentrations. During (clinical) method validation a correlation study between DBS (blood) and plasma concentrations should be established using authentic patient samples. Most publications comparing TKI concentrations derived from DBS with those from corresponding plasma reported deviating (but correlating) concentrations. For those TKIs, the DBS concentrations should be converted to plasma concentrations. Equivalent concentrations were reported for gefitinib only for finger-prick DBS and venous plasma measurements, so for that analyte plasma results can be directly replaced by DBS concentrations without applying a conversion method (40). This means that gefitinib is probably slightly more partitioned in blood cells than in plasma, as upon equal partitioning a blood concentration is typically slightly lower than a plasma concentration.

In literature, dried blood TKI concentrations were converted to plasma concentrations based upon approaches that take into account a Hct correction, with or without considering the influence of blood-to-plasma partitioning of the TKI, or directly *via* empirically obtained regression equations or correction factors. When applying such experimentally determined correction factor or regression, it is essential that this is validated on an independent dataset which was not used for deriving that factor (80). Nilotinib plasma concentrations derived from capillary DBS concentrations were calculated, taking into account the Hct and the blood-to-plasma ratio using the formula described by Wilhelm et al. (30). Additionally, the plasma nilotinib concentrations were predicted based on an empirically obtained Deming regression equation. Both methods showed similar predictive performance and both could be used to predict plasma concentrations from DBS nilotinib concentrations (37). Vemurafenib plasma concentrations were predicted *via* a comparable Hct-based conversion method, taking into account the blood cell to plasma partition coefficient. The plasma concentrations were also appropriately predicted *via* an experimentally obtained regression equation (26). Alternatively, Antunes et al. took into account the fraction of the drug in plasma (f_p) for estimating imatinib plasma concentrations (C_p): $C_p = [C_{DBS}/(1\text{-Hct})] \times f_p$. The f_p imatinib value was determined as the value which resulted in a mean ratio between measured and estimated imatinib plasma concentration of 1. In line with the other studies, this group also set up a conversion using a correction factor to directly convert DBS concentrations to plasma concentrations without considering the Hct value nor other variables: both conversion methods resulted in a high agreement between calculated and measured imatinib plasma concentrations (36). Pazopanib (38), imatinib and norimatinib (39) and imatinib, nilotinib and dasatinib (41) plasma concentrations were calculated from DBS concentrations *via* a Hct correction using the formula: $C_p = C_{DBS}/(1\text{-Hct})$, which neglects the possible distribution of TKIs into the blood cells. This formula can be used for TKIs which are only present in the plasma compartment or for TKIs with a high protein binding (for example pazopanib >99.9%), since only the unbound fraction of TKIs can partition into blood cells and the unbound fraction can be considered to be negligible (38). Iacuzzi et al. compared the simple Hct-conversion method with a conversion *via* an experimentally determined correction factor and found that the latter yielded a slightly better agreement with the measured plasma concentrations (39). Verheijen et al. applied an empirical Deming regression equation to convert pazopanib DBS to plasma concentrations. Correction for individual Hct

did not improve the correlation between calculated and measured plasma concentrations (45). For radotinib, an approach was proposed in which plasma concentrations were calculated by using the measured Hct value in a second-degree polynomial function (42). When a Hct-based correction method is used, specific measured or predicted Hct levels or a fixed Hct applicable for the whole intended study population can be used (37, 38). The latter approach has the advantage that the individual Hct level of a microsample should not be measured or estimated, however this requires a population with rather homogenous Hct values. We previously determined the mean ratio between actual plasma and whole blood concentrations for TKIs used for treatment of hematological malignancies (i.e. bosutinib, dasatinib, gilteritinib, ibrutinib, imatinib, midostaurin, nilotinib and ponatinib) and found substantial differences, both for different TKIs, as well as (for certain TKIs) between different individuals, although larger patient sets are required to substantiate these findings (23). Similarly, Zimmermann and colleagues determined VAMS whole blood to plasma conversion factors for a panel of ten TKIs (i.e. afatinib, axitinib, bosutinib, cabozantinib, dabrafenib, lenvatinib, nilotinib, osimertinib, ruxolitinib and trametinib), noting that for cabozantinib, dabrafenib, lenvatinib, nilotinib, osimertinib and ruxolitinib the Hct impacted the VAMS whole blood to plasma concentration conversion. However, it should be noted that the latter experiments were performed *in vitro* on spiked blood samples and not on authentic patient samples (46). The obtained blood-plasma ratios are still to be evaluated clinically in elaborate dried blood microsample *versus* plasma comparison studies.

Using plasma instead of whole blood for the generation of dried matrix spots, resulting in DPS, allows to overcome the Hct effects and, in addition, overcomes the need to calculate a plasma concentration from a (dried) blood concentration. The availability of DPS should allow smooth application, without any need for conversion. Mukai et al. developed and validated an analytical method for the simultaneous quantification of bosutinib, dasatinib, ibrutinib, imatinib, nilotinib and ponatinib in DPS. DPS were generated by pipetting 20 μL of plasma onto a filter paper. Despite expecting to be equivalent matrices, significant systematic errors were observed between plasma and DPS concentrations for bosutinib, nilotinib and ponatinib, suggesting a methodological issue (43). Since the plasma was prepared by centrifugation of whole blood, this approach is not feasible for home-sampling. It only retains the benefits of more convenient sample transport and storage. Plasma separator devices which can generate volumetric DPS from a non-volumetrically applied drop of blood onto multilayered filter membranes are currently commercially available. While these devices have the advantage that the need for a centrifugation step is eliminated, only few applications have been published (81, 82). A disadvantage of DPS, compared to dried blood microsamples, is that for the generation of DPS higher sample volumes are required.

Last, for several TKIs with a high protein binding, the monitoring of the free TKI fractions can be theoretically more relevant as only this fraction is likely to penetrate into the tumor cells and induce pharmacologic effects. The high protein bound TKIs are predominantly bound to albumin and α-acid glycoprotein, which means that fluctuating levels of these proteins influence total TKI concentrations (6, 18). This poses an additional limitation for dried blood microsamples as -per definition- these can only be used for measuring total TKI concentrations. However, there is to date still a lack of consensus regarding the utility of unbound TKI measurements.

TOWARDS HOME-SAMPLING

Given the simple sample collection and stabilizing effect on the analyte, microsamples can be collected at home and can be sent to the laboratory *via* regular postal services under ambient conditions, prior to consultation. This allows the actual TKI level of the patient to be available at the time of consultation, allowing insight into the most recent data. As described earlier, TKI targets are generally based on trough concentrations. Obtaining trough levels is definitely not always easy when a patient has to come to the hospital or needs to visit a doctor for a blood draw. Home-based sampling is superior in this respect: within the comfort of the home-setting, the patient can self-collect a sample at the right time point. This will also prevent the risk of delay in drug intake when the patient should be sampled at a medical center. However, home-sampling is only feasible if the patients are clearly instructed and received adequate training about sample collection and, importantly, are aware of the importance of a correct sample collection (69, 70, 83, 84).

Most TKI studies artificially prepared dried microsamples in the lab by pipetting venous blood on filter paper (27, 35, 41, 43) or had DBS samples collected by trained personnel in a hospital environment (26, 28, 36–39, 42, 44, 45). In the study of Irie et al. the skin punctures were performed by the patients themselves, although it was not specified whether this was supervised or not and in which environment (40). Based on a questionnaire taken by Antunes and colleagues, patients preferred DBS collection over venous sampling as sampling method for performing TDM of imatinib (36). Boons et al. examined the feasibility of nilotinib DBS self-sampling for CML patients in a real home-sampling context. They concluded that DBS self-sampling is feasible in clinical practice after giving adequate sampling instructions. Moreover, the patients believed in the reliability of DBS self-sampling and considered the sampling easy and not painful. It should be noted that these authors only reported on the feasibility of applying such a sampling strategy in a home-sampling context, actual results from nilotinib concentrations or a correlation with clinical parameters were not reported (83). In a very recent study performed by Zimmermann et al., capillary VAMS samples were successfully collected by either healthcare professionals or patients at home for the determination of afatinib, cabozantinib, dabrafenib, trametinib, nilotinib and ruxolitinib, readily providing a first indication of real-life applicability (46).

Despite the above-mentioned blood *versus* plasma interpretation issues, dried blood microsamples are typically

taken by finger-prick in the home-environment. This means that capillary blood is used instead of venous blood, which may give rise to different concentrations (58). Differences between capillary and venous blood concentrations can be expected shortly after administration, during the (absorption and) distribution phase of the drug (79). Several publications report a good agreement between concentrations from finger-prick DBS samples and DBS samples generated by pipetting venous blood on the card, as exemplified for imatinib (and norimatinib) (39), pazopanib (38) and R406 (metabolite fostamatinib) (28). This suggests equivalence between capillary and venous blood concentrations for these components. However, for most TKIs such equivalence still needs to be examined.

We are not aware of any method using dried blood microsamples for TKI quantitation that has been implemented in routine clinical practice. An important factor that may hamper such implementation is the additional cost (for the lab) that may be associated with analyzing dried blood microsamples instead of conventional liquid blood or plasma samples. Examples of costs associated with dried blood microsample analysis include: a more extensive method development and validation, the set-up of comprehensive sample preparation protocols, shipping costs for the samples, as well as the cost of the microsampling device itself and lancets to perform a finger-prick. In this context, an intrinsic hurdle is often posed by the fact that the analyzing lab itself may not profit from the advantages (e.g. home-based sampling overcoming the need to come to a hospital) and cost savings (e.g. no specialized staff required for sampling) associated with dried blood microsampling, while being responsible for providing collection devices (with microsampling devices being more expensive than regular blood tubes). Furthermore, despite the above-mentioned methodological aspects inherent to dried blood microsamples, some other factors could be optimized to allow smoother implementation in clinical routine. E.g., the availability of fully automated methods/analyzers that are compatible with the workflow of clinical labs could help to decrease hands-on time and increase throughput of dried blood microsamples. Another example is the set-up of EQC programs enabling accreditation of lab-developed methods in clinical labs (85).

CONCLUSIONS/FUTURE PERSPECTIVES

Despite the growing evidence of the relevance for performing TDM of TKIs in oncology patients, it is still not integrated in the standards of care. Microsampling can be a useful tool to promote and further elaborate on studies of TDM of TKIs. Several papers have already been published in which TKI microsample-based methods are described, with most of these focusing on DBS. Despite the many benefits that are associated with the use of dried blood microsamples, a few issues should be tackled during method development and validation. Therefore, thorough optimization and evaluation of microsample-based analytical methods is essential. In the future, studies should be set up to confirm exposure-response relationships and to define therapeutic ranges for all TKIs. Subsequently, the use of TDM of TKIs in clinical oncology practice must be evaluated. For implementation of TDM in a home-sampling context, real-life home-sampling studies must be set up to evaluate the feasibility in specific oncology patient groups. To date there is no dried blood microsample-based TKI method used for TDM in routine yet. While we are on the right track to implement TDM of TKIs in standard care of oncology patients, we are not there yet, and using dried blood microsamples can be a useful tool to help to reach this goal.

AUTHOR CONTRIBUTIONS

NV wrote the manuscript. VS edited the manuscript. AV edited the manuscript. CS, supervisor, wrote the manuscript. All authors contributed to the article and approved the submitted version.

FUNDING

This work was supported by the Research Foundation-Flanders (FWO) (grant number 1703320N) to NV.

REFERENCES

1. Menz BD, Stocker SL, Verougstraete N, Kocic D, Galettis P, Stove CP, et al. Barriers and Opportunities for the Clinical Implementation of Therapeutic Drug Monitoring in Oncology. *Br J Clin Pharmacol* (2021) 87:227–36. doi: 10.1111/bcp.14372
2. Gao B, Yeap S, Clements A, Balakrishnar B, Wong M, Gurney H. Evidence for Therapeutic Drug Monitoring of Targeted Anticancer Therapies. *J Clin Oncol* (2012) 30:4017–25. doi: 10.1200/JCO.2012.43.5362
3. Arora A, Scholar EM. Role of Tyrosine Kinase Inhibitors in Cancer Therapy. *J Pharamcol Exp Ther* (2005) 315:971–9. doi: 10.1124/jpet.105.084145
4. Groenland SL, Mathijssen RHJ, Beijnen JH, Huitema ADR, Steeghs N. Individualized Dosing of Oral Targeted Therapies in Oncology is Crucial in the Era of Precision Medicine. *Eur J Clin Pharmacol* (2019) 75:1309–18. doi: 10.1007/s00228-019-02704-2
5. Mueller-Schoell A, Groenland SL, Scherf-Clavel O, van Dyk M, Huisinga W, Michelet R, et al. Therapeutic Drug Monitoring of Oral Targeted Antineoplastic Drugs. *Eur J Clin Pharmacol* (2021) 77:441–64. doi: 10.1007/s00228-020-03014-8
6. Cardoso E, Guidi M, Blanchet B, Schneider MP, Decosterd LA, Buclin T, et al. Therapeutic Drug Monitoring of Targeted Anticancer Protein Kinase Inhibitors in Routine Clinical Use: A Critical Review. *Ther Drug Monit* (2020) 42:33–44. doi: 10.1097/FTD.0000000000000699
7. Di Gion P, Kanefendt F, Lindauer A, Scheffler M, Doroshyenko O, Fuhr U, et al. Clinical Pharmacokinetics of Tyrosine Kinase Inhibitors: Focus on Pyrimidines, Pyridines and Pyrroles. *Clin Pharmacokinet* (2011) 50:551–603. doi: 10.2165/11593320-000000000-00000
8. Herbrink M, Nuijen B, Schellens JHM, Beijnen JH. Variability in Bioavailability of Small Molecular Tyrosine Kinase Inhibitors. *Cancer Treat Rev* (2015) 41:412–22. doi: 10.1016/j.ctrv.2015.03.005
9. Stemler J, Koehler P, Maurer C, Müller C, Cornely OA. Antifungal Prophylaxis and Novel Drugs in Acute Myeloid Leukemia: The Midostaurin and Posaconazole Dilemma. *Ann Hematol* (2020) 99:1429–40. doi: 10.1007/s00277-020-04107-1
10. James AJ, Smith CC, Litzow M, Perl AE, Altman JK, Shepard D, et al. Pharmacokinetic Profile of Gilteritinib: A Novel FLT-3 Tyrosine Kinase Inhibitor. *Clin Pharmacokinet* (2020) 59:1273–90. doi: 10.1007/s40262-020-00888-w

11. Hamilton M, Wolf JL, Rusk J, Beard SE, Clark GM, Witt K, et al. Effects of Smoking on the Pharmacokinetics of Erlotinib. *Clin Cancer Res* (2006) 27:2166–71. doi: 10.1158/1078-0432.CCR-05-2235
12. Parra-Guillen ZP, Berger PB, Haschke M, Donzelli M, Winogradova D, Pfister B, et al. Role of Cytochrome P450 3A4 and 1A2 Phenotyping in Patients With Advanced Non-Small-Cell Lung Cancer Receiving Erlotinib Treatment. *Basic Clin Pharmacol Toxicol* (2017) 121:309–15. doi: 10.1111/bcpt.12801
13. Cardoso E, Csajka C, Schneider MP, Widmer N. Effect of Adherence on Pharmacokinetic/ Pharmacodynamic Relationships of Oral Targeted Anticancer Drugs. *Clin Pharmacokinet* (2018) 57:1–6. doi: 10.1007/s40262-017-0571-z
14. Smy L, Sadler AJ, McMillin GA. Evaluation of Imatinib Concentrations in Samples Submitted for BCR-ABL1 or Imatinib Testing – Evidence to Support Therapeutic Drug Monitoring for Dose Optimization? *Ther Drug Monit* (2020) 42:559–64. doi: 10.1097/FTD.0000000000000771
15. Partridge AH, Avorn J, Wang PS, Winer EP. Adherence to Therapy With Oral Antineoplastic Agents. *J Natl Cancer Inst* (2002) 94:652–61. doi: 10.1093/jnci/94.9.652
16. Marin D, Bazeos A, Mahon FX, Eliasson L, Milojkovic D, Bua M, et al. Adherence Is the Critical Factor for Achieving Molecular Responses in Patients With Chronic Myeloid Leukemia Who Achieve Complete Cytogenetic Responses on Imatinib. *J Clin Oncol* (2010) 28:2381–8. doi: 10.1200/JCO.2009.26.3087
17. Widmer N, Bardin C, Chatelut E, Paci A, Beijnen J, Levêque D, et al. Review of Therapeutic Drug Monitoring of Anticancer Drugs Part Two – Targeted Therapies. *Eur J Cancer* (2014) 50:2020–36. doi: 10.1016/j.ejca.2014.04.015
18. Herviou P, Thivat E, Ricard D, Roche L, Dohou J, Pouget M, et al. Therapeutic Drug Monitoring and Tyrosine Kinase Inhibitors. *Oncol Lett* (2016) 12:1223–32. doi: 10.3892/ol.2016.4780
19. Verheijen RB, Yu H, Schellens JHM, Beijnen JH, Steeghs N, Huitema ADR. Practical Recommendations for Therapeutic Drug Monitoring of Kinase Inhibitors in Oncology. *Clin Pharmacol Ther* (2017) 102:765–76. doi: 10.1002/cpt.787
20. Clarke WA, Chatelut E, Fotoohi AK, Larson RA, Martin JH, Mathijssen RHJ, et al. Therapeutic Drug Monitoring in Oncology: International Association of Therapeutic Drug Monitoring and Clinical Toxicology Consensus Guidelines for Imatinib Therapy. *Eur J Cancer* (2021) 157:428–40. doi: 10.1016/j.ejca.2021.08.033
21. Londhe V, Rajadhyaksha M. Opportunities and Obstacles for Microsampling Techniques in Bioanalysis: Special Focus on DBS and VAMS. *J Pharm BioMed Anal* (2020) 182:113102. doi: 10.1016/j.jpba.2020.113102
22. Rood JJM, van Hoppe S, Schinkel AH, Schellens JHM, Beijnen JH, Sparidans RW. Liquid Chromatography – Tandem Mass Spectrometric Assay for the Simultaneous Determination of the Irreversible BTK Inhibitor Ibrutinib and its Dihydrodiol-Metabolite in Plasma and its Application in Mouse Pharmacokinetic Studies. *J Pharm BioMed Anal* (2016) 118:123–31. doi: 10.1016/j.jpba.2015.10.033
23. Verougstraete N, Stove V, Verstraete AG, Stove C. Quantification of Eight Hematological Tyrosine Kinase Inhibitors in Both Plasma and Whole Blood by a Validated LC-MS/MS Method. *Talanta* (2021) 226:122140. doi: 10.1016/j.talanta.2021.122140
24. Bouchet S, Chauzit E, Ducint D, Castaing N, Canal-Raffin M, Moore N, et al. Simultaneous Determination of Nine Tyrosine Kinase Inhibitors by 96-Well Solid-Phase Extraction and Ultra Performance LC-MS/MS. *Clin Chim Acta* (2011) 412:1060–7. doi: 10.1016/j.cca.2011.02.023
25. Haouala A, Zanolari B, Rochat B, Montemurro M, Zaman K, Duchosal MA, et al. Therapeutic Drug Monitoring of the New Targeted Anticancer Agents Imatinib, Nilotinib, Dasatinib, Sunitinib, Sorafenib and Lapatinib by LC Tandem Mass Spectrometry. *J Chromatogr B Analyt Technol BioMed Life Sci* (2009) 877:1982–96. doi: 10.1016/j.jchromb.2009.04.045
26. Nijenhuis CM, Huitema ADR, Marchetti S, Blank C, Haanen JBAG, van Thienen JV, et al. The Use of Dried Blood Spots for Pharmacokinetic Monitoring of Vemurafenib Treatment in Melanoma Patients. *J Clin Pharmacol* (2016) 56:1307–12. doi: 10.1002/jcph.728
27. Xu Y, Fang W, Zeng W, Leijen S, Woolf EJ. Evaluation of Dried Blood Spot (DBS) Technology Versus Plasma Analysis for the Determination of MK-1775 by HILIC-MS/MS in Support of Clinical Studies. *Anal Bioanal Chem* (2012) 404:3037–48. doi: 10.1007/s00216-012-6440-6
28. Martin P, Cheung SYA, Yen M, Han D, Gillen M. Characterization of the Disposition of Fostamatinib in Japanese Subjects Including Pharmacokinetic Assessment in Dry Blood Spots: Results From Two Phase I Clinical Studies. *Eur J Clin Pharmacol* (2016) 72:61–71. doi: 10.1007/s00228-015-1961-5
29. Edelbroek PM, van der Heijden J, Stolk LML. Dried Blood Spot Methods in Therapeutic Drug Monitoring: Methods, Assays, and Pitfalls. *Ther Drug Monit* (2009) 31:327–36. doi: 10.1097/FTD.0b013e31819e91ce
30. Wilhelm AJ, den Burger JCG, Swart EL. Therapeutic Drug Monitoring by Dried Blood Spot: Progress to Date and Future Directions. *Clin Pharmacokinet* (2014) 53:961–73. doi: 10.1007/s40262-014-0177-7
31. Velghe S, Capiau S, Stove CP. Opening the Toolbox of Alternative Sampling Strategies in Clinical Routine: A Key-Role for (LC-)MS/MS. *TrAC* (2016) 84:61–73. doi: 10.1016/j.trac.2016.01.030
32. Capiau S, Alffenaar JW, Stove CP. "Alternative Sampling Strategies for Therapeutic Drug Monitoring". In: W Clarke, A Dasgupta, editors. *Clinical Challenges in Therapeutic Drug Monitoring*. Amsterdam: Elsevier (2016). p. 279–336.
33. Tey HY, See HH. A Review of Recent Advances in Microsampling Techniques of Biological Fluids for Therapeutic Drug Monitoring. *J Chromatogr A* (2021) 1635:461731. doi: 10.1016/j.chroma.2020.461731
34. Sulochana SP, Daram P, Srinivas NR, Mullangi R. Review of DBS Methods as a Quantitative Tool for Anticancer Drugs. *BioMed Chromatogr* (2019) 33: e4445. doi: 10.1002/bmc.4445
35. Verougstraete N, Stove CP. Volumetric Absorptive Microsampling as a Suitable Tool to Monitor Tyrosine Kinase Inhibitors. *J Pharm BioMed Anal* (2021) 207:114418. doi: 10.1016/j.jpba.2021.114418
36. Antunes MV, Raymundo S, Wagner SC, Mattevi VS, Vieira N, Leite R, et al. DBS Sampling in Imatinib Therapeutic Drug Monitoring: From Method Development to Clinical Application. *Bioanalysis* (2015) 7:2105–17. doi: 10.4155/bio.15.101
37. Boons CCLM, Chahbouni A, Schimmel AM, Wilhelm AJ, den Hartog YM, Janssen JJWM, et al. Dried Blood Spot Sampling of Nilotinib in Patients With Chronic Myeloid Leukaemia: A Comparison With Venous Blood Sampling. *J Pharm Pharmacol* (2017) 69:1265–74. doi: 10.1111/jphp.12757
38. de Wit D, den Hartigh J, Gelderblom H, Qian Y, den Hollander M, Verheul H, et al. Dried Blood Spot Analysis for Therapeutic Drug Monitoring of Pazopanib. *J Clin Pharmacol* (2015) 55:1344–50. doi: 10.1002/jcph.558
39. Iacuzzi V, Posocco B, Zanchetta M, Montico M, Marangon E, Poetto AS, et al. Development and Validation of LC-MS/MS Method for Imatinib and Norimatinib Monitoring by Finger-Prick DBS in Gastrointestinal Stromal Tumor Patients. *PloS One* (2019) 14:e0225225. doi: 10.1371/journal.pone.0225225
40. Irie K, Shobu S, Hiratsuji S, Yamasaki Y, Nanjo S, Kokan C, et al. Development and Validation of a Method for Gefitinib Quantification in Dried Blood Spots Using Liquid Chromatography-Tandem Mass Spectrometry: Application to Finger-Prick Clinical Blood Samples of Patients With Non-Small Cell Lung Cancer. *J Chromatogr B Analyt Technol BioMed Life Sci* (2018) 1087–1088:81–5. doi: 10.1016/j.jchromb.2018.04.027
41. Kralj E, Trontelj J, Pajic T, Kristl A. Simultaneous Measurement of Imatinib, Nilotinib and Dasatinib in Dried Blood Spot by Ultra High Performance Liquid Chromatography Tandem Mass Spectrometry. *J Chromatogr B Analyt Technol BioMed Life Sci* (2012) 903:150–6. doi: 10.1016/j.jchromb.2012.07.011
42. Lee J, Jung SY, Choi MY, Park JS, Park SK, Lim SA, et al. Development of a Dried Blood Spot Sampling Method Towards Therapeutic Monitoring of Radotinib in the Treatment of Chronic Myeloid Leukaemia. *J Clin Pharm Ther* (2020) 45:1006–13. doi: 10.1111/jcpt.13124
43. Mukai Y, Yoshida Y, Yoshida T, Kondo T, Inotsume N, Toda T. Simultaneous Quantification of BCR-ABL and Bruton Tyrosine Kinase Inhibitors in Dried Plasma Spots and its Application to Clinical Sample Analysis. *Ther Drug Monit* (2021) 43:386–93. doi: 10.1097/FTD.0000000000000825
44. Nijenhuis CM, Rosing H, Schellens JHM, Beijnen JH. Quantifying Vemurafenib in Dried Blood Spots Using High-Performance LC-MS/MS. *Bioanalysis* (2014) 6:3215–24. doi: 10.4155/bio.14.171
45. Verheijen RB, Bins S, Thijssen B, Rosing H, Nan L, Schellens JHM, et al. Development and Clinical Validation of an LC-MS/MS Method for the Quantification of Pazopanib in DBS. *Bioanalysis* (2016) 8:123–34. doi: 10.4155/bio.15.235

46. Zimmermann S, Aghai F, Schilling B, Kraus S, Grigoleit GU, Kalogirou C, et al. Volumetric Absorptive Microsampling (VAMS) for the Quantification of Ten Kinase Inhibitors and Determination of Their *In Vitro* VAMS-To-Plasma Ratio. *J Pharm BioMed Anal* (2022) 211:114623. doi: 10.1016/j.jpba.2022.114623
47. De Kesel PMM, Sadones N, Capiau S, Lambert WE, Stove CP. Hemato-Critical Issues in Quantitative Analysis of Dried Blood Spots: Challenges and Solutions. *Bioanalysis* (2013) 5:2023–41. doi: 10.4155/bio.13.156
48. Velghe S, Delahaye L, Stove CP. Is the Hematocrit Still an Issue in Quantitative Dried Blood Spot Analysis? *J Pharm BioMed Anal* (2019) 163:188–96. doi: 10.1016/j.jpba.2018.10.010
49. de Kleijne V, Kohler I, Heijboer AC, Ackermans MT. Solutions for Hematocrit Bias in Dried Blood Spot Hormone Analysis. *Bioanalysis* (2021). doi: 10.4155/bio-2021-0119
50. Capiau S, Veenhof H, Koster RA, Bergqvist Y, Boettcher M, Halmingh O, et al. Official International Association for Therapeutic Drug Monitoring and Clinical Toxicology Guideline: Development and Validation of Dried Blood Spot-Based Methods for Therapeutic Drug Monitoring. *Ther Drug Monit* (2019) 41:409–30. doi: 10.1097/FTD.0000000000000643
51. Rood JJM, Schellens JHM, Beijnen JH, Sparidans RW. Recent Developments in the Chromatographic Bioanalysis of Approved Kinase Inhibitor Drugs in Oncology. *J Pharm BioMed Anal* (2016) 130:244–63. doi: 10.1016/j.jpba.2016.06.037
52. Velghe S, Deprez S, Stove CP. Fully Automated Therapeutic Drug Monitoring of Anti-Epileptic Drugs Making Use of Dried Blood Spots. *J Chromatogr A* (2019) 1601:95–103. doi: 10.1016/j.chroma.2019.06.022
53. Deprez S, Stove CP. Fully Automated Dried Blood Spot Extraction Coupled to Liquid Chromatography-Tandem Mass Spectrometry for Therapeutic Drug Monitoring of Immunosuppressants. *J Chromatogr A* (2021) 1653:462430. doi: 10.1016/j.chroma.2021.462430
54. Dutch Foundation for Quality Assessment in Medical Laboratories (SKML). *Immunosuppressant Microsampling* (2021). Available at: https://www.skml.nl/en/rondzendingen/overzicht/rondzending?id=251 (Accessed November 8, 2021).
55. Velghe S, Stove CP. Volumetric Absorptive Microsampling as an Alternative Tool for Therapeutic Drug Monitoring of First-Generation Anti-Epileptic Drugs. *Anal Bioanal Chem* (2018) 410:2331–41. doi: 10.1007/s00216-018-0866-4
56. Delahaye L, Dhont E, De Cock P, De Paepe P, Stove CP. Volumetric Absorptive Microsampling as an Alternative Sampling Strategy for the Determination of Paracetamol in Blood and Cerebrospinal Fluid. *Anal Bioanal Chem* (2019) 411:181–91. doi: 10.1007/s00216-018-1427-6
57. Xie I, Xu Y, Anderson M, Wang M, Xue L, Breidinger S, et al. Extractability-Mediated Stability Bias and Hematocrit Impact: High Extraction Recovery is Critical to Feasibility of Volumetric Adsorptive Microsampling (VAMS) in Regulated Bioanalysis. *J Pharm BioMed Anal* (2018) 156:58–66. doi: 10.1016/j.jpba.2018.04.001
58. Sharma A, Jaiswal S, Shukla M, Lal J. Dried Blood Spots: Concepts, Present Status, and Future Perspectives in Bioanalysis. *Drug Test Anal* (2014) 6:399–414. doi: 10.1002/dta.1646
59. Capiau S, Stove VV, Lambert WE, Stove CP. Prediction of the Hematocrit of Dried Blood Spots *via* Potassium Measurement on a Routine Clinical Chemistry Analyzer. *Anal Chem* (2013) 85:404–10. doi: 10.1021/ac303014b
60. Capiau S, Wilk LS, Aalders MCG, Stove CP. A Novel, Nondestructive, Dried Blood Spot-Based Hematocrit Prediction Method Using Noncontact Diffuse Reflectance Spectroscopy. *Anal Chem* (2016) 88:6538–46. doi: 10.1021/acs.analchem.6b01321
61. Capiau S, Wilk LS, De Kesel PMM, Aalders MCG, Stove CP. Correction for the Hematocrit Bias in Dried Blood Spot Analysis Using a Nondestructive, Single-Wavelength Reflectance-Based Hematocrit Prediction Method. *Anal Chem* (2018) 90:1795–804. doi: 10.1021/acs.analchem.7b03784
62. Oostendorp M, El Amrani M, Diemel EC, Hekman D, van Maarseveen EM. Measurement of Hematocrit in Dried Blood Spots Using Near-Infrared Spectroscopy: Robust, Fast, and Nondestructive. *Clin Chem* (2016) 62:1534–36. doi: 10.1373/clinchem.2016.263053
63. van de Velde D, van der Graaf JL, Boussaidi M, Huisman R, Hesselink D, Russcher H, et al. Development and Validation of Hematocrit Level Measurement in Dried Blood Spots Using Near-Infrared Spectroscopy. *Ther Drug Monit* (2021) 43:351–7. doi: 10.1097/FTD.0000000000000834
64. Delahaye L, Heughebaert L, Lühr C, Lambrecht S, Stove CP. Near-Infrared-Based Hematocrit Prediction of Dried Blood Spots: An in-Depth Evaluation. *Clin Chim Acta* (2021) 523:239–46. doi: 10.1016/j.cca.2021.10.002
65. De Kesel PMM, Capiau S, Stove VV, Lambert WE, Stove CP. Potassium-Based Algorithm Allows Correction for the Hematocrit Bias in Quantitative Analysis of Caffeine and its Major Metabolite in Dried Blood Spots. *Anal Bioanal Chem* (2014) 406:6749–55. doi: 10.1007/s00216-014-8114-z
66. Delahaye L, Veenhof H, Koch BCP, Alffenaar JWC, Linden R, Stove C. Alternative Sampling Devices to Collect Dried Blood Microsamples: State-of-the-Art. *Ther Drug Monit* (2021) 43:310–21. doi: 10.1097/FTD.0000000000000864
67. Denniff P, Spooner N. Volumetric Absorptive Microsampling: A Dried Sample Collection Technique for Quantitative Bioanalysis. *Anal Chem* (2014) 86:8489–95. doi: 10.1021/ac5022562
68. De Kesel PMM, Lambert WE, Stove CP. Does Volumetric Absorptive Microsampling Eliminate the Hematocrit Bias for Caffeine and Paraxanthine in Dried Blood Samples? A Comparative Study. *Anal Chim Acta* (2015) 881:65–73. doi: 10.1016/j.aca.2015.04.056
69. Verougstraete N, Lapauw B, Van Aken S, Delanghe J, Stove C, Stove V. Volumetric Absorptive Microsampling at Home as an Alternative Tool for the Monitoring of HbA1c in Diabetes Patients. *Clin Chem Lab Med* (2017) 55:462–9. doi: 10.1515/cclm-2016-0411
70. Verougstraete N, Stove V, Stove C. Wet Absorptive Microsampling at Home for HbA1c Monitoring in Diabetic Children. *Clin Chem Lab Med* (2018) 56:291–94. doi: 10.1515/cclm-2018-0207
71. van den Broek I, Fu Q, Kushon S, Kowalski MP, Millis K, Percy A, et al. Application of Volumetric Absorptive Microsampling for Robust, High-Throughput Mass Spectrometric Quantification of Circulating Protein Biomarkers. *Clin Mass Spectrom* (2017) 4–5:25–33. doi: 10.1016/j.clinms.2017.08.004
72. Yeung L, Ichetovkin M, Yang J, Dellatore S. *Implementation of Tecan® Automation With Neoteryx Mitra® Volumetric Absorptive Microsampling for Reagent Preparation for an Anti-Drug Antibody Assay [Conference Poster Presentation]. SLAS 2019.* Washington DC, United States (2019).
73. de Vries R, Barfield M, van de Merbel N, Schmid B, Siethoff C, Ortiz J, et al. The Effect of Hematocrit on Bioanalysis of DBS: Results From the EBF DBS-Microsampling Consortium. *Bioanalysis* (2013) 5:2147–60. doi: 10.4155/bio.13.170
74. Ye Z, Gao H. Evaluation of Sample Extraction Methods for Minimizing Hematocrit Effect on Whole Blood Analysis With Volumetric Absorptive Microsampling. *Bioanalysis* (2017) 9:349–57. doi: 10.4155/bio-2015-0028
75. Kok MGM, Fillet M. Volumetric Absorptive Microsampling: Current Advances and Applications. *J Pharm BioMed Anal* (2018) 147:288–96. doi: 10.1016/j.jpba.2017.07.029
76. Fang K, Bowen CL, Kellie JF, Karlinsey MZ, Evans CA. Drug Monitoring by Volumetric Absorptive Microsampling: Method Development Considerations to Mitigate Hematocrit Effects. *Bioanalysis* (2018) 10:241–55. doi: 10.4155/bio-2017-0221
77. Mano Y, Kita K, Kusano K. Hematocrit-Independent Recovery is a Key for Bioanalysis Using Volumetric Absorptive Microsampling Devices, Mitra™. *Bioanalysis* (2015) 7:1821–9. doi: 10.4155/bio.15.111
78. Abu-Rabie P, Denniff P, Spooner N, Chowdhry BZ, Pullen FS. Investigation of Different Approaches to Incorporating Internal Standards in DBS Quantitative Bioanalytical Workflows and Their Effect on Nullifying Hematocrit-Based Assay Bias. *Anal Chem* (2015) 87:4996–5003. doi: 10.1021/acs.analchem.5b00908
79. Emmons G, Rowland M. Pharmacokinetic Considerations as to When to Use Dried Blood Spot Sampling. *Bioanalysis* (2010) 2:1791–6. doi: 10.4155/bio.10.159
80. Iacuzzi V, Posocco B, Zanchetta M, Gagno S, Poetto AS, Guardascione M, et al. Dried Blood Spot Technique Applied in Therapeutic Drug Monitoring of Anticancer Drugs: A Review on Conversion Methods to Correlate Plasma and Dried Blood Spot Concentrations. *Pharm Res* (2021) 38:759–78. doi: 10.1007/s11095-021-03036-6
81. Kim JH, Woenker T, Adamec J, Regnier FE. Simple, Miniaturized Blood Plasma Extraction Method. *Anal Chem* (2013) 85:11501–8. doi: 10.1021/ac402735y
82. Sturm R, Henion J, Abbott R, Wang P. Novel Membrane Devices and Their Potential Utility in Blood Sample Collection Prior to Analysis of Dried Plasma Spots. *Bioanalysis* (2015) 7:1987–2002. doi: 10.4155/bio.15.98
83. Boons CCLM, Timmers L, Janssen JJWM, Swart EL, Hugtenburg JG, Hendrikse NH. Feasibility of and Patients' Perspective on Nilotinib Dried Blood Spot Self-Sampling. *Eur J Clin Pharmacol* (2019) 75:825–9. doi: 10.1007/s00228-019-02640-1

84. Van Uytfanghe K, Heughebaert L, Stove CP. Self-Sampling at Home Using Volumetric Absorptive Microsampling: Coupling Analytical Evaluation to Volunteers' Perception in the Context of a Large Scale Study. *Clin Chem Lab Med* (2020) 59:185–7. doi: 10.1515/cclm-2020-1180
85. Deprez S, Heughebaert L, Verougstraete N, Stove V, Verstraete AG, Stove CP. "Automation in Microsampling: At Your Fingertips?". In: *Patient Centric Blood Sampling and Quantitative Bioanalysis*.

Conflict of Interest: The authors declare that the research was conducted in the absence of any commercial or financial relationships that could be construed as a potential conflict of interest.

Publisher's Note: All claims expressed in this article are solely those of the authors and do not necessarily represent those of their affiliated organizations, or those of the publisher, the editors and the reviewers. Any product that may be evaluated in this article, or claim that may be made by its manufacturer, is not guaranteed or endorsed by the publisher.

frontiers | Frontiers in Oncology

ORIGINAL RESEARCH
published: 29 April 2022
doi: 10.3389/fonc.2022.874852

Inhibition of (Pro)renin Receptor-Mediated Oxidative Stress Alleviates Doxorubicin-Induced Heart Failure

Xiao-yi Du[1,2†], *Dao-chun Xiang*[3†], *Ping Gao*[4], *Hua Peng*[1*] *and Ya-li Liu*[1*]

[1] Department of Pediatrics, Union Hospital, Tongji Medical College, Huazhong University of Science and Technology, Wuhan, China, [2] Department of Pediatrics, Maternal and Child Hospital of Hubei Province, Tongji Medical College, Huazhong University of Science and Technology, Wuhan, China, [3] Department of Pharmacy, The Central Hospital of Wuhan, Tongji Medical College, Huazhong University of Science and Technology, Wuhan, China, [4] Department of Clinical Pharmacy, Wuhan Children's Hospital, Tongji Medical College, Huazhong University of Science and Technology, Wuhan, China

OPEN ACCESS

Edited by:
Miao Yan,
Central South University, China

Reviewed by:
Anchit Bhagat,
University of Texas MD Anderson Cancer Center, United States
Vgm Naidu,
National Institute of Pharmaceutical Education and Research, India

***Correspondence:**
Hua Peng
pe20200229@126.com
Ya-li Liu
whlyl2022@163.com

[†]These authors share first authorship

Specialty section:
This article was submitted to Pharmacology of Anti-Cancer Drugs, a section of the journal Frontiers in Oncology

Received: 13 February 2022
Accepted: 31 March 2022
Published: 29 April 2022

Citation:
Du X-Y, Xiang D-c, Gao P, Peng H and Liu Y-l (2022) Inhibition of (Pro) renin Receptor-Mediated Oxidative Stress Alleviates Doxorubicin-Induced Heart Failure. Front. Oncol. 12:874852. doi: 10.3389/fonc.2022.874852

Aim: Clinical utility of doxorubicin (DOX) is limited by its cardiotoxic side effect, and the underlying mechanism still needs to be fully elucidated. This research aimed to examine the role of (pro)renin receptor (PRR) in DOX-induced heart failure (HF) and its underlying mechanism.

Main Methods: Sprague Dawley (SD) rats were injected with an accumulative dosage of DOX (15 mg/kg) to induce HF. Cardiac functions were detected by transthoracic echocardiography examination. The levels of lactate dehydrogenase (LDH) and creatine kinase (CK) in serum were detected, and oxidative stress related injuries were evaluated. Furthermore, the mRNA expression of *PRR* gene and its related genes were detected by real-time PCR (RT-PCR), and protein levels of PRR, RAC1, NOX4 and NOX2 were determined by Western blot. Reactive oxygen species (ROS) were determined in DOX-treated rats or cells. Additionally, PRR and RAC1 were silenced with their respective siRNAs to validate the *in vitro* impacts of PRR/RAC1 on DOX-induced cardiotoxicity. Moreover, inhibitors of PRR and RAC1 were used to validate their effects *in vivo*.

Key Findings: *PRR* and *RAC1* expressions increased in DOX-induced HF. The levels of CK and LDH as well as oxidative stress indicators increased significantly after DOX treatment. Oxidative injury and apoptosis of cardiomyocytes were attenuated both *in vivo* and *in vitro* upon suppression of PRR or RAC1. Furthermore, the inhibition of PRR could significantly down-regulate the expressions of RAC1 and NOX4 but not that of NOX2, while the inhibition of RAC1 did not affect PRR.

Significance: Our findings showed that PRR inhibition could weaken RAC1-NOX4 pathway and alleviate DOX-induced HF *via* decreasing ROS production, thereby suggesting a promising target for the treatment of DOX-induced HF.

Keywords: doxorubicin, cardiotoxicity, heart failure, (Pro) renin receptor, RAC1

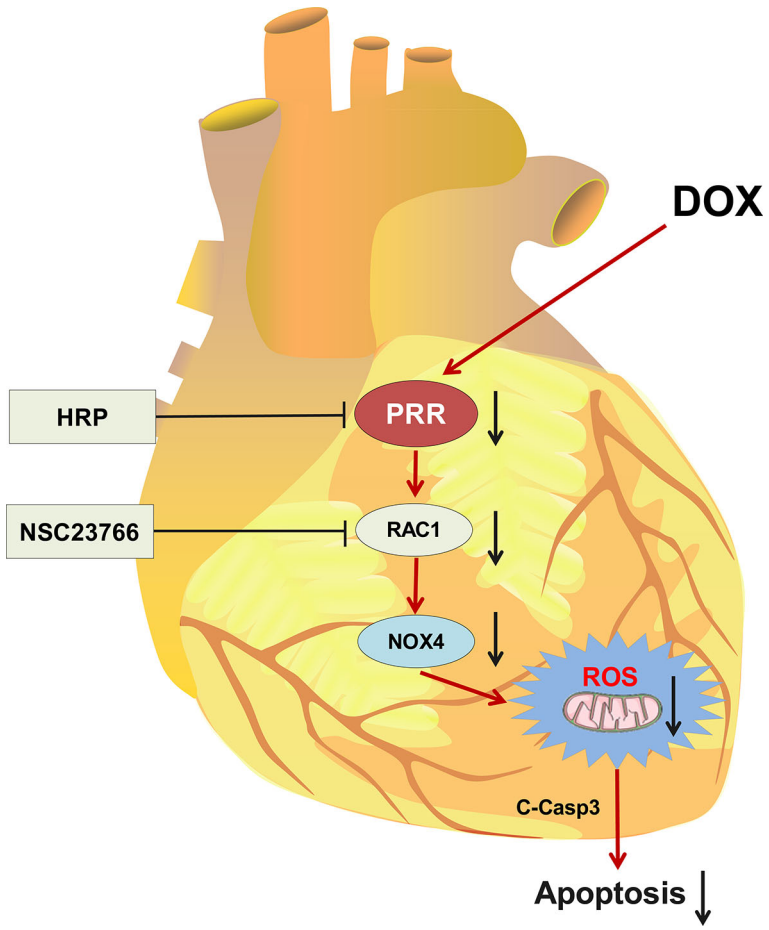

GRAPHICAL ABSTRACT |

INTRODUCTION

Doxorubicin (DOX) is a classical anthracyclines chemotherapeutic drug with wide clinical utility for acute leukemia, breast cancer, lymphoma, and ovarian cancer (1, 2). However, most patients receiving DOX chemotherapy are prone to develop acute, subacute, early or late cardiotoxicity (3, 4). DOX-induced serious cardiovascular complications mainly include hypotension, tachycardia, arrhythmia, ventricular dysfunction, and heart failure (HF) (4–7). Among them, HF is the most serious side effect which lead to a 3.5-fold increased mortality risk comparing to another idiopathic cardiomyopathy. The HF caused by DOX is dose-dependent, and its incidence increased to 48% as the lifetime accumulation dose of DOX increases to 700 mg/m^2 (8, 9). This toxicology may lead to premature morbidity and even death among those cancer survivors (9). But the treatment to DOX-induced HF is still limited at present and the mechanism still need to be fully elucidated.

Several studies suggest that DOX-induced myocardial damage involved in numerous alterations, such as mitochondrial injury, DNA damage, lipid peroxidation, mitochondrial injury, autophagy, oxidative stress, and apoptosis (2, 10). It is widely accepted that oxidative stress is a critical process in the development of DOX-induced HF (2, 11). DOX intake produces massive amounts of reactive oxygen species (ROS), thereby resulting in the impairment of mitochondrial function and damage to cells (12, 13). As a consequence, inhibiting oxidative stress might serve as a promising preventive measure against DOX-induced HF; however, the underlying mechanism of DOX-triggered oxidative injury remains unknown.

The (pro)renin receptor (PRR), also called APT6AP2, is a crucial modulators of ROS production (14, 15). By binding to pro-renin and renin, PRR has been shown to activate the rennin-angiotensin pathway and the binding process triggers the receptor itself, which is involved in a variety of intracellular physiological processes (11, 14, 16). Recently, PRR is thought to play a crucial role in heart diseases. Mahmud et al. reported overexpression of PRR in myocardial infarction animal models or the biopsy samples obtained from patients with dilated cardiomyopathy (17). And a previous study showed that overexpression of PRR in mice heart leads to atrial fibrillation

(18). Besides, PRR-activated Ras-related C3 botulinum toxin substrate 1(RAC1) in smooth muscle cells may participate in the pathogenesis of various diseases (19), and the activation of Rac1 contributes to oxidative stress-related injury in the myocardium (20). However, it is unclear whether PRR play a role in the DOX-induced cardiotoxicity. Therefore, the purpose of the present study was to examine the effects of PRR in DOX-induced HF and investigate its underlying mechanism.

MATERIALS AND METHODS

Reagents

An antibody directed against PRR (#A6531) was purchased from ABclonal (Cambridge, MA, USA). Anti-Rac1 antibody (#AF4200) and NADPH oxidase 4 (NOX4) (#DF6924) were obtained from Affinity Biosciences (OH, USA). Cleaved-caspase 3 (#9664) was procured from Cell Signaling Technology (MA, USA). Anti-GAPDH antibody (Abs132004a) was obtained from Absin BioscienceInc (Shanghai, China). An *in-situ* cell death detection kit (11684817910) (Roche, Penzberg, Germany) was used to perform the terminal deoxynucleotidyl transferase-mediated dUTP-biotin nick end labeling assay (TUNEL) assay. Rabbit polyclonal antibodies against CD31 were purchased from Abcam (Cambridge, UK). Dihydroethidium (DHE, D11347) was purchased from Molecular Probes Invitrogen (Carlsbad, CA, USA). 2,7-Dichlorodi-hydrofluorescein diacetate (DCFH-DA, S0033S) was purchased from Beyotime Institute of Biotechnology (Shanghai, China). The PRR inhibitor, handle region peptide (HRP), was obtained from Chinapeptides Co. Ltd. (Shanghai, China). The bicinchoninic acid (BCA) protein assay kit was obtained from Wuhan Kerui Technology Co. Ltd. (Wuhan, China). Cell counting kit 8 (CCK-8) was purchased from Dojindo Molecular Technologies, Inc. (MD, USA). The detection kits for lactate dehydrogenase (LDH, A020-1-1), creatine kinase (CK, A032-1-1), and oxidative stress-related enzymes, such as malondialdehyde (MDA, A003-1-2), superoxide dismutase (SOD, A001-3-2), glutathione (GSH, A006-2-1) and glutathione peroxidase (GSH-Px, A005-1-2) were purchased from the Nanjing Jiancheng Institute of Biotechnology (Nanjing, China).

Animals and Experimental Protocols

Male Sprague Dawley (SD) rats (SPF Biotechnology Co., Ltd., Beijing, China) were reared in specific pathogen-free (SPF) environment at the Experimental Animal Center of Tongji Medical College, Huazhong University of Science and Technology (Wuhan, China). Approval of all the experimental designs involving animals was granted by the Animal Ethics Committee of Tongji Medical College, Huazhong University of Science and Technology (Wuhan, China). After a week of adaptive feeding, animals in the DOX group were administered intraperitoneally with DOX at the dose of 2.5 mg/kg over a period of 2 weeks for an accumulative dosage of 15 mg/kg (21), whereas control rats were inoculated with an equivalent amount of 0.9% saline. Then eight days later, an osmotic minipump (2ML4, Alzet, CA, USA) was implanted subcutaneously for the infusion of the vehicle and HRP (0.1mg/kg/d for 7 successive days) under isoflurane anesthesia. NSC23766 (2.5 mg/kg/d) was administered *via* an intraperitoneal injection for the same duration (seven consecutive days) (n=8) (22). Finally, echocardiography was performed before the rats were sacrificed. Serum samples were collected, and heart tissues were immediately excised for further experiments.

Echocardiography

Rats received isoflurane anesthesia and then fixed on a plat board. Next, trans-thoracic and M-mode echocardiographic studies were performed using the 25.0 MHz Intelligent color Doppler echocardiography (EPIQ 7C) platform with L12-3 probes (Philips, Eindhoven, the Netherlands) at the end of the posttreatment period. Left ventricular functions, including fractional shortening (FS), left ventricular end-diastolic diameter (LVEDD), left ventricular ejection fraction (LVEF), and left ventricular end-systolic diameter (LVESD) was computed as described previously (23). For all measurements, an average of 3 successive cardiac cycles was evaluated. The LVEF was calculated using the following equation: LVEF (%) = (LVEDV - LVESV)/LVEDV×100%.

Histological Analysis

After sacrificing the rats, their left ventricles were collected and immediately fixed in 4% buffered paraformaldehyde. After embedding the heart tissue in paraffin and cutting it into 5 μm-thick slices, hematoxylin and eosin (H&E) staining was performed to examine the heart pathology. From each section, images of the heart tissues were captured using an optical microscope (Olympus, Tokyo, Japan; magnification 200×). Histopathological analysis was performed for randomly selected cortical fields and images were examined by a pathologist who was blinded to the treatment groups.

Detection of $CD31^+$ Cells

The immunohistochemical study was performed as Ammar, H. I. et al. described (24). After fixed by 10% formalin, cardiac samples were cut into 5 μm thick sections and air-dried overnight. After dewaxed in xylene, and rehydrated, the samples were for 15 minutes in antigen retrieval solution. Then the CD31 staining was performed by using primary antibody and secondary antibody. Then the sections were incubated with DAB at room temperature for 10 min. Finally, images were abstained for each sample using the microscope (Olympus, Japan) (magnification 400×).

Cell Culture and Treatment

The rat cardiomyoblasts cell line, H9C2, was kindly donated by Dr. Yang Sun of the Tongji Hospital Affiliated with Tongji Medical College, Huazhong University of Science and Technology, (Wuhan, China). In a humid chamber containing 5 percent CO_2 and 95 percent oxygen at a temperature of 37°C, the cells were maintained in Dulbecco's Modified Eagle's Medium (DMEM) (Hyclone, UT, USA) that contained 10 percent fetal bovine serum (FBS, Zhejiang Tianhang Biotechnology Co., Ltd., Hangzhou, China). H9C2 cells were

subsequently plated at a density of 6×10^3 cells/well and incubated for 24 hours. Next, DOX at varying concentrations (0-10 μM) was introduced to incubate the cells for 24h, and the optimal dose of DOX for subsequent analyses was identified.

Cell Viability and Apoptosis Assays

CCK-8 assay kit was employed to measure the viability of the cells. The H9C2 cells were placed into 96-well plates at a density of 1×10^4 cells/well and incubated for 24 hours. Following treatment, the medium from every well was replenished with 100 μL of DMEM comprising 10 percent CCK-8 reagent. Subsequently, the cells were subjected to incubation at 37°C for 2 hours. The absorbance of each sample was detected at 450 nm (Thermo Multiskan MK3 Microplate Reader, Thermo Fisher Scientific, MA, USA).

Cellular apoptosis assay was performed following a previously reported procedure (25). Briefly, after washed by PBS for three times, H9C2 cells were suspended and incubated in buffer with annexin V in the dark for 10 min. Following that, the H9C2 cells were incubated once again for 15 minutes using annexin V-FITC/propidium iodide. Finally, the H9C2 cells were analyzed utilizing flow cytometry (BD FACSCalibur, CA, USA) and the apoptosis was determined using FlowJo 10. All assays were performed in triplicates.

Small Interfering RNA (siRNA) Transfection

H9C2 cells were seeded into 6-well plates for 24h, followed by incubation overnight at a temperature of 37°C and a CO_2 concentration of 5%. Cells were transfected with siRNAs at 50-70% confluency. For silencing the PRR or RAC1 proteins, H9C2 cells were transfected with siRNAs constructs targeting PRR (RiboBio; Guangzhou, China) or RAC1 (Sigma-Aldrich, St Louis, USA.) for 24h before harvest according to the guidelines provided by the manufacturer. Scrambled siRNA (RiboBio; Guangzhou, China) was used as the control, and the sequence of negative control primers used in this study was as follows: 5'→3': UUCUCCGAACGUGUCACGUTT (100 nM final); 3'→5': ACGUGACACGUUCGGAGAATT (100 nM final). Furthermore, the transfection efficiency was analyzed as a measure of the knockdown.

Real-Time PCR

Quantitative real-time reverse transcription polymerase chain reaction (RT–PCR) was conducted to verify the changes in mRNA expressions. Extraction of the total RNA from cardiac tissues was performed utilizing the TRIzol (Invitrogen, MO, USA) reagent. Total RNA (1 mg) from each sample was denatured at 65°C for 10 min. Subsequently, the cDNA was synthesized at 37°C for 1 h using a cDNA synthesis kit (GeneCopoeia, Rockville, MD, USA). The 2-△△CT technique was applied to assess relative levels of gene expressions. Below is a list of the primer sequences used in the present study: rat PRR (forward 5′-TCTGTTCTCAA CTCGCTCC C-3 and reverse 5′-TCTCCATAACGCTTCCC AAG-3′); RAC1 (forward: 5′- CCTGCTCATCAGTTACACG ACCA-3′, reverse: 5′-GTCCCAGAGGCCCAGATTCA-3′), Wnt3A (forward: 5′-ACCATGTTCGGGACCTATTCCA-3′, reverse: 5′-GCCTGTAGCATCTCGCTTCCA-3′); Wnt8A (forward: 5′-GGAGGCCAGGAGAGATG-3, reverse: 5′-ACGG AGACCACAAAAGGA-3′), NOX2 (forward: CTGCCAGT GTGTCGGAATCT

-3′, reverse: 5′-TGTGAATGGCCGTGTGAAGT-3′), NOX4 (forward: 5′- ATGTTGGGCCTAGGATTGTGT -3′, reverse: 5′-TCCTGCTAGGGACCTTCTGT -3′) and GAPDH (forward 5′-AAGTTCAACGGCACAGTCAA-3′ and reverse 5′- TCTCGCT CCTGGAAGATGG -3).

Western Blotting Analysis

The total proteins from the cardiac tissues were homogenized in RIPA lysis solution that contained the phosphatase inhibitors and protease. The protein content was detected by performing BCA protein quantitation assay. Next, SDS-PAGE was used to isolate the protein samples (40 μg/lane), which were then loaded onto a PVDF membrane. Following the blocking of the membrane using 5% non-fatty milk for 1h, it was subjected to incubation with the corresponding primary antibodies overnight at 4°C, as follows: GAPDH (1:1000), PRR (1:1,000), RAC1 (1:1,000), NOX2 (1:1,000), NOX4 (1:1,000), Cleaved-caspase 3 (1:1000), and thioredoxin 2 (1:1000). After incubation with secondary antibodies for 1h, the proteins were visualized on an ECL detection system (Syngene, UK). GAPDH was utilized to normalize the band intensity values.

Detection of Serum Biochemical Indexes

In order to measure CK and LDH levels in serum, commercial kits were utilized in accordance with the manufacturer's specifications. Additionally, the GSH-Px, MDA, GSH, and SOD levels in heart tissues were evaluated in accordance with the protocols described by the manufacturers.

Measurement of Oxidant Species by DHE in Tissues or DCFH-DA in Cells

Oxidative stress levels in myocardial tissues, both *in vivo* and *in vitro* were measured as described previously (26). ROS production was determined by DHE or DCFH-DA staining. Briefly, after washing with phosphate-buffered saline (PBS), fresh myocardial tissues were frozen. Subsequently, the myocardial tissues were dissected into sections (5 μm) and incubated with DHE or DCFH-DA solution for 30 minutes at a temperature of 37°C. Sections were then rinsed with PBS and incubated with an anti-fluorescence quenching agent. The fluorescence intensities of cells and tissue sections were then visualized (excitation 590nm and emission 520 nm) using a fluorescence microscope (Zeiss AXIO Imager A1m). The fluorescence intensity of samples was quantified using Image J software (NIH, MD, USA). All tests were carried out three times.

Evaluating Apoptosis by TUNEL Assay

Apoptosis in cardiac myocytes was evaluated using the TUNEL assay as the manufacturer's protocol. After staining with the TUNEL reagents, the frozen rat heart sections were fixed, washed, and incubated with proteinase K for 30 minutes. Then, the sections were subjected to incubation with TdT/dUTP (1:9) enzyme reaction solution at a temperature of 37°C

for 1 hour in darkness, and subsequently, exposed to DAB solution at room temperature for 10 min. Finally, images were abstained for each sample using the microscope (Olympus, Japan; magnification 400×).

Statistical Analysis

All the results from the analyses are expressed as the mean ± standard error (SEM). All the statistical analyses were conducted utilizing the Graph Pad Prism 7.0 software (San Diego, CA, USA). The statistical significance of multiple comparisons was calculated by two-way ANOVA; the unpaired Student's t-test was employed to compare two groups. $P < 0.05$ or $p < 0.01$ was considered to have significance.

RESULTS

Effects of DOX on Rat Heart Tissues

During the experiment, we found that the rats in the DOX treated group showed inappetence, and less movement, and the DOX treatment reduced body weight gain in the animals (**Figure 1A**). tachypnea as compared to the control. Transthoracic echocardiography (**Figures 1B**) showed that cardiac dilatation was accompanied by cardiac dysfunction in DOX-treated rats. All the echocardiographic values of the DOX-treated rats reflected a decline in cardiac functions. LVEF and FS values decreased markedly, while those of LVESD and LVEDD increased remarkably after DOX treatment, as indicated by the M-mode echocardiograms (**Figure 1B**). Eight days after DOX injection, their hearts were excised, and H&E staining was performed. Histological examination suggested that the myocardial cells of the control rats were carefully organized and showed no abnormalities, while DOX-treated rats showed clusters of degenerating cardiomyocytes having extensive vacuolation and inflammatory infiltration (**Figure 1C**). As a marker of angiogenesis, CD31 was widely used in the research to investigate the microvessel (24) and was reduced significantly in the DOX treated group (**Figure 1D**). The cross-sectional areas (CSA) of cardiomyocytes in the LV increased after DOX treatment, which suggested the presence of cardiac hypertrophy in the DOX treated group (**Figure 1E**). Both CK and LDH levels increased significantly in the DOX group (**Figures 1F, G**). In addition, the levels of MDA in heart tissues increased remarkably in the DOX-treated rats, while those of GSH-Px, GSH, and SOD decreased significantly (**Figure 1H**). These results indicated that DOX could induce the HF in rats, and this process may be closely related to the oxidative damage.

The Protein of PRR and RAC1 Was Upregulated in DOX-Treated Rats

PRR and its related protein Wnt, RAC1 and NOX are involved in the cardiac dysfunction (11, 15). In this study, we detected the mRNA expression of these proteins in the DOX treated rats and found that DOX significantly affected the PRR mRNA levels, accompanied by significant upregulation in the expressions of RAC1, NOX2, and NOX4 (**Figure 2A**, $p < 0.05$), but Wnt3A and Wnt8A were not significantly affected ($p > 0.05$, **Figure 2A**). Furthermore, western blotting showed that the protein levels of PRR and RAC1 increased significantly by DOX treatment (**Figure 2B**), indicating that DOX induced HF was related to PRR and RAC1 expression.

PRR Inhibition Reduces Oxidative Stress and Apoptosis in H9C2 Cells Treated With DOX

H9C2 cells were employed to examine the impacts of PRR and RAC1 on DOX-induced myocardial cell injury. CCK-8 assay showed that cell viability reduced significantly in a dosage-dependent way following the DOX treatment (**Figure 3A**). Based on the results of optimization, we used 5 μM DOX to induce myocardial cell injury in the subsequent experiments. To further investigate the role of PRR-RAC1 pathway, the PRR-siRNA was used to silence the expression of the PRR (**Figure 3B**). Subsequently, ROS production and cell apoptosis were tested. As shown in **Figure 3C**, DOX treatment increased the ROS levels, and this impact was substantially attenuated by PRR-siRNA. In addition, flow cytometry suggested that cellular apoptosis decreased upon PRR-siRNA transfection in DOX-treated H9C2 cells (**Figure 3D**). These results demonstrated that PRR expression was significantly correlated with oxidative stress damage and cell apoptosis induced by DOX.

Next, we determined the expression of key proteins related to PRR in H9C2 cells to elucidate their underlying mechanisms. As shown in **Figure 3E**, DOX treatment significantly enhanced the expressions of RAC1, NOX4, NOX2, and cleaved caspase3 in H9C2 cells in contrast with the control ($p < 0.05$). These phenomena were reversed upon PRR silencing (**Figure 3E**). Moreover, as compared to the control group, PRR-siRNA down-regulated the expressions of RAC1 and NOX4 but not NOX2 in H9C2 cells (**Figure 3C**) ($p < 0.05$). Therefore, these data suggested that PRR could regulate RAC1 expression, thereby mediating DOX-induced myocardial oxidative stress injury.

RAC1 Was the Downstream of PRR

RAC1 is required for the activation of the majority of the myocardial superoxide production complexes for their subsequent role in the activation of nicotinamide adenine dinucleotide phosphate oxidase (NADPH oxidase, NOX) (27). In cardiac hypertrophy (28, 29), hyperglycemia (30), and failing human myocardium (31), RAC1 plays an important role in regulating the myocardial superoxide production. Previous studies also suggest that the activation of RAC1 is involved in PRR-related myocardium injury (19). To further study the potential mechanism underlying the regulation of PRR on RAC1 pathway and the effect of RAC1 on DOX-induced myocardial cell injury, we silenced the RAC1 expression to evaluate the expression of relative proteins and oxidative stress levels in DOX-treated H9C2 cells.

RAC1-siRNA knockdown was used to silence the expression of RAC1 in H9C2cells. RAC1-siRNA may substantially reduce

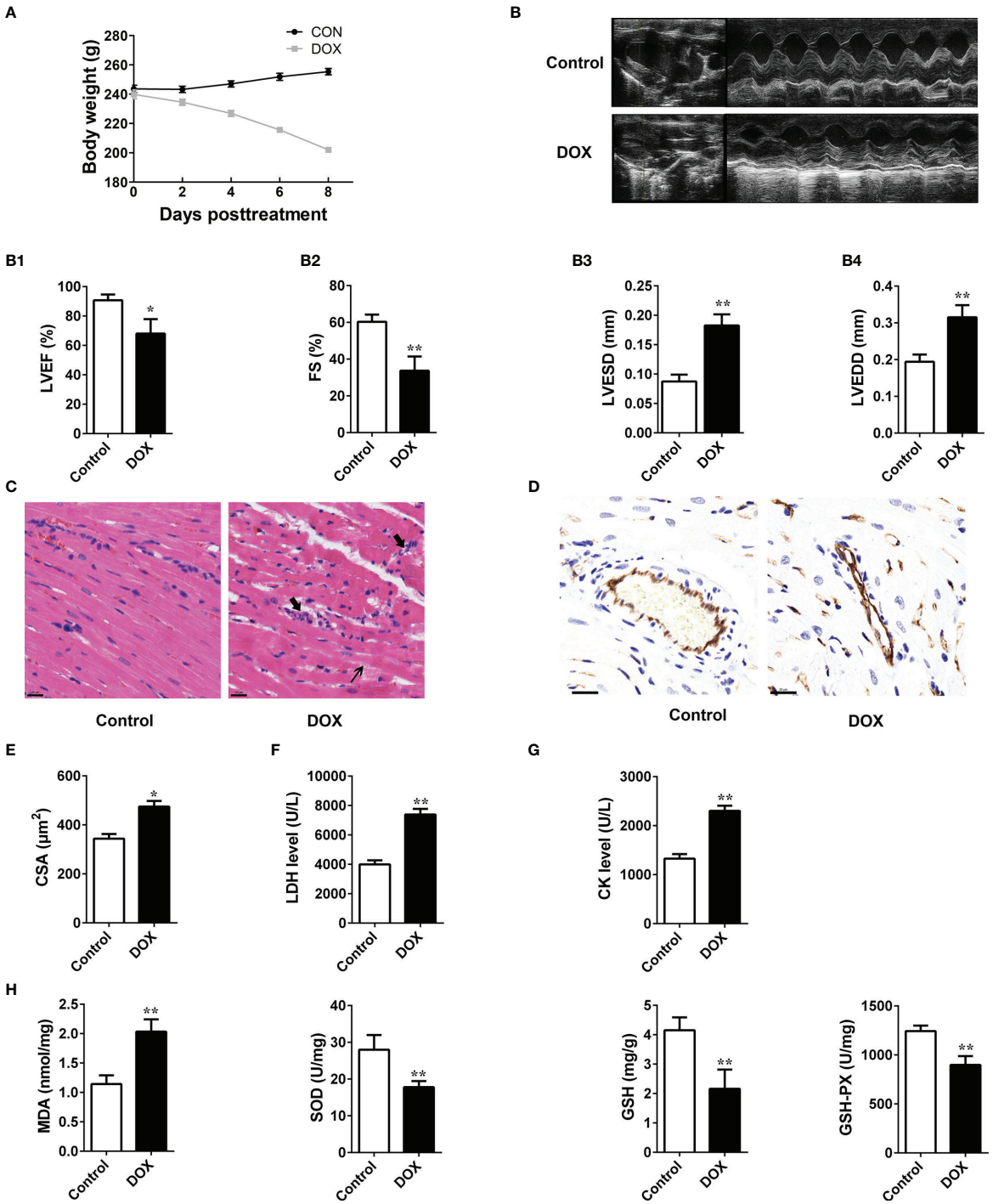

FIGURE 1 | The impacts of DOX on the rat heart. **(A)** Daily body weight changes. **(B)** Representation of M-mode left ventricular (LV) echocardiogram. (B1) Left ventricular ejection fraction (LVEF), (B2) FS: fractional shortening, (B3) left ventricular end-systolic diameter (LVESD) and (B4), left ventricular end-diastolic diameter (LVEDD). **(C)** Representative images of HE-staining of rat heart tissues treated with or without doxorubicin (DOX) for 8 days. The structure of dysregulated myocytes is marked as thin arrowhead, inflammatory cell infiltration marked as thick arrowhead. Scale bars: 20 μm (center and right panels). **(D)** Representative photos of CD31 immunohistochemical staining in each group. Scale bars: 20 μm. **(E)** Cross-sectional areas (CSA) of cardiomyocytes in the LV. **(F, G)** Serum levels of LDH and CK in rats. **(H)** Determination of MDA, SOD, GSH and GSH-Px in the tissues. Data are presented as the mean ± SEM. $^{*}p < 0.05$ and $^{**}p < 0.01$ *vs* control.

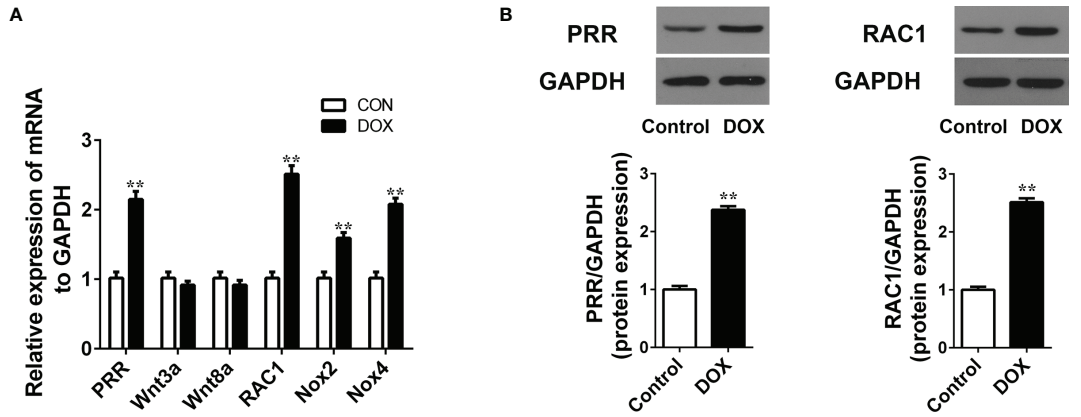

FIGURE 2 | Doxorubicin treatment increases the mRNA/protein expression of PRR and RAC1. **(A)** RT-qPCR assay to evaluate the mRNA levels of PRR, Wnt3A, Wnt8a, RAC1, NOX2 and NOX4 in heart tissues (n = 3). **(B)** Western blotting and statistical analysis of the (pro)renin receptor (PRR) protein expression(n = 3). Data are presented as the mean ± SEM. $^{**}p < 0.01$ *vs* control.

the protein expression level of RAC1(**Figure 4A**). As opposed to the DOX treatment group, NOX4 expressions were also downregulated after RAC1-siRNA knockdown, however, the protein level expression of PRR in H9C2 cells was not affected after RAC1-siRNA transfection (**Figure 4A**). Combined the above results (**Figure 3**), we reasonably concluded that PRR was upstream of RAC1. As shown in **Figure 4B**, ROS production increased after DOX treatment, which was subsequently reversed by RAC1-siRNA transfection.

Pharmacological Inhibition of PRR/RAC1 Ameliorates DOX-Induced Cardiac Hypertrophy and Cardiac Dysfunction

To further verify the effect PRR/RAC1 in DOX-induced HF, rats were treated using the PRR inhibitor HRP, and the RAC1 inhibitor NSC23766, after the DOX challenge. Cardiac dysfunction induced by DOX was ameliorated significantly upon treatment with HRP and NSC23766 (**Figure 5**). Next, transthoracic echocardiography showed that inhibition of PRR or RAC1 reversed the abnormal levels of LVEF, FS, LVESD, and LVEDD after DOX treatment in rats, thereby suggesting that inhibition of PRR or RAC1 further ameliorated cardiac dysfunction challenged by DOX in rats (**Figure 5A**). As illustrated in **Figure 5B**, DOX treatment caused substantial inflammatory, cell infiltration, and pyknosis, which was improved significantly upon HRP or NSC23766 treatment. To further investigate the effect of PRR/RAC1 inhibition on vascular structures, the immunohistochemistry of CD31 was detected. As shown in **Figures 5C**, staining for CD31 showed a significant increase in the number of capillaries after PRR or RAC1 inhibition in comparison to DOX treated rats. Moreover, CSA of cardiomyocytes in the LV region decreased by DOX treatment and could be partly reversed by treatment with HRP or NSC23766 (**Figure 5D**). Both the increased CK and LDH levels were downregulated by PRR or RAC1 inhibition (**Figures 5E, F**). Taken together, these findings suggested that abnormal expression of PRR/RAC1 was related to the pathogenesis of cardiac hypertrophy and cardiac dysfunction in DOX induced HF.

Pharmacological Inhibition of PRR/RAC1 Ameliorates ROS Production and Apoptosis in Rats With DOX-Induced HF

Next, we assessed the impact of PRR/RAC1 inhibition on oxidative stress levels and apoptosis in DOX-induced HF rats. In addition to alleviating the pathology reconstruction, HRP or NSC237666 could reduce the production of superoxide radicals induced by DOX (**Figures 6A, B**). Thus, these results indicated that PRR or RAC1 inhibition could significantly alleviate DOX-induced oxidative damage *in vivo*. To reliably evaluate cardiac cell damage and recovery in DOX-related HF, TUNEL staining was used to test the cytotoxicity and visually evaluate the effects of HRP and NSC23766. As illustrated in **Figure 6C**, the proportion of TUNEL positive cells increased markedly after DOX treatment, thereby indicating the occurrence of cell apoptosis of myocardial cytotoxicity. In contrast, both HRP and NSC23766 could alleviate cardiomyocytes from apoptosis to some extent. Taken together, these results indicated that inhibition of PRR or RAC1 could significantly protect the heart tissues from HF. Western blotting also showed that treatment with HRP or NSC23766 inhibited the DOX-related activation of PRR or RAC1, respectively (**Figure 6D**). Moreover, PRR remained unaffected in NSC23766-treated rats. In addition, the increased expression of cleaved caspase3 was reversed upon inhibition of PRR or RAC1.

DISCUSSION

Since the late 1960s, DOX has been widely used in acute leukemia, breast cancer, lymphoma, ovarian cancer treatment (32). Unfortunately, the cardiotoxicity of DOX can lead to

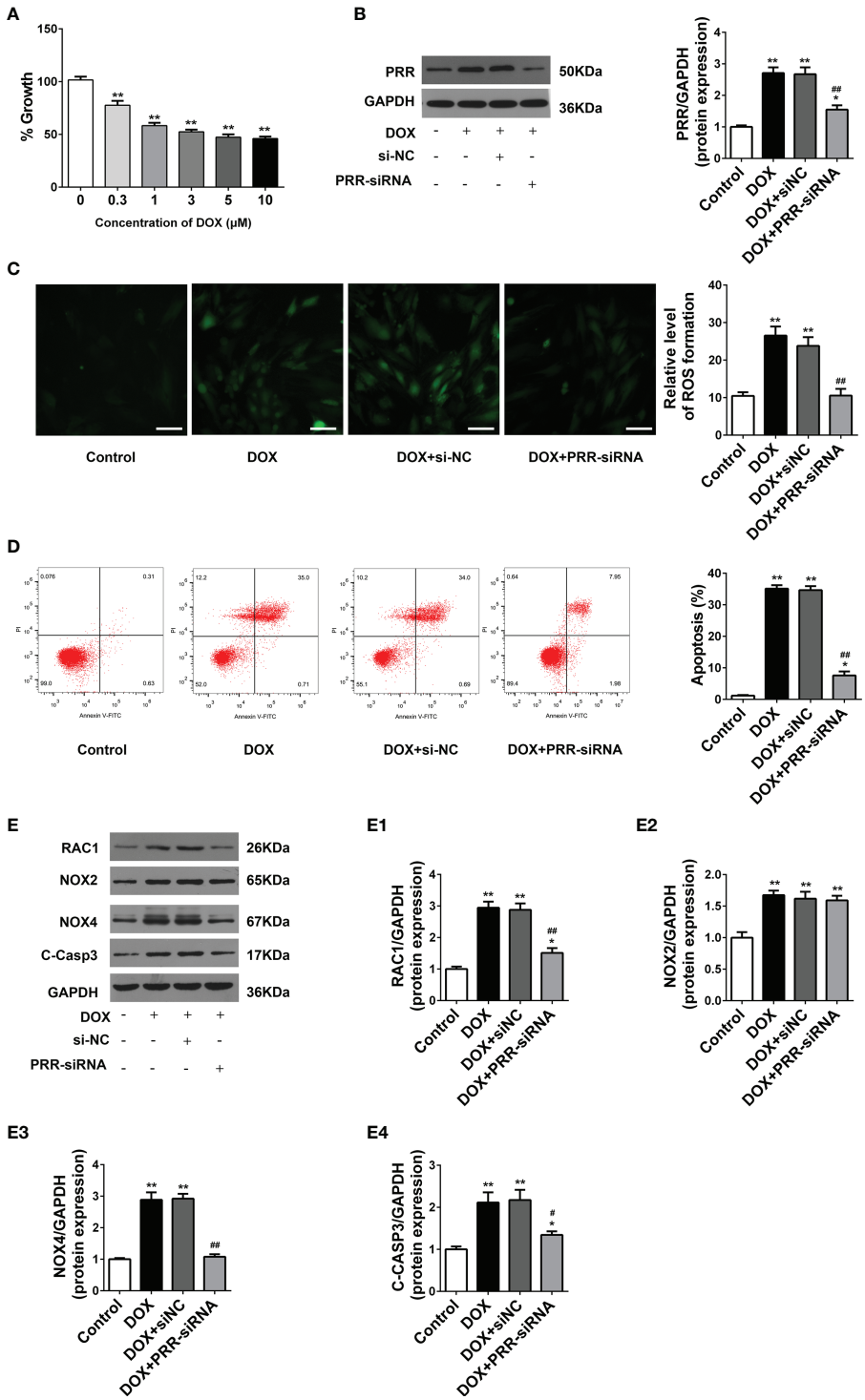

FIGURE 3 | PRR inhibition downregulated the overexpression of oxidant species and apoptosis in H9C2 cells treated with doxorubicin. **(A)** Cell viability of H9C2 cells treated with Doxorubicin (DOX) treated at different concentrations (0–10 μM). **(B)** The protein expression of PRR downregulated by PRR-siRNA in H9C2 cells. (B1) Quantification of PRR/GAPDH protein expression levels relative to changing PRR expression. **(C)** Representative oxidative stress based on DHE relative fluorescence intensity of H9C2 cells. **(D)** Flow cytometry shows that PRR expression is directly related to cell apoptosis in doxorubicin (DOX)-treated H9C2 cells. **(E)** The protein expression of RAC1, NOX2, NOX4, and cleaved caspase3 was regulated by PRR inhibition in H9C2 cells. (E1)-(E4) Quantification of RAC1/GAPDH, NOX2/GAPDH, NOX4/GAPDH, and cleaved caspase3/GAPDH protein expression levels relative to changing PRR expression. (*$p < 0.05$, **$p < 0.01$ *vs* the control group. $^{\#}p < 0.05$, $^{\#\#}p < 0.01$*vs* DOX group).

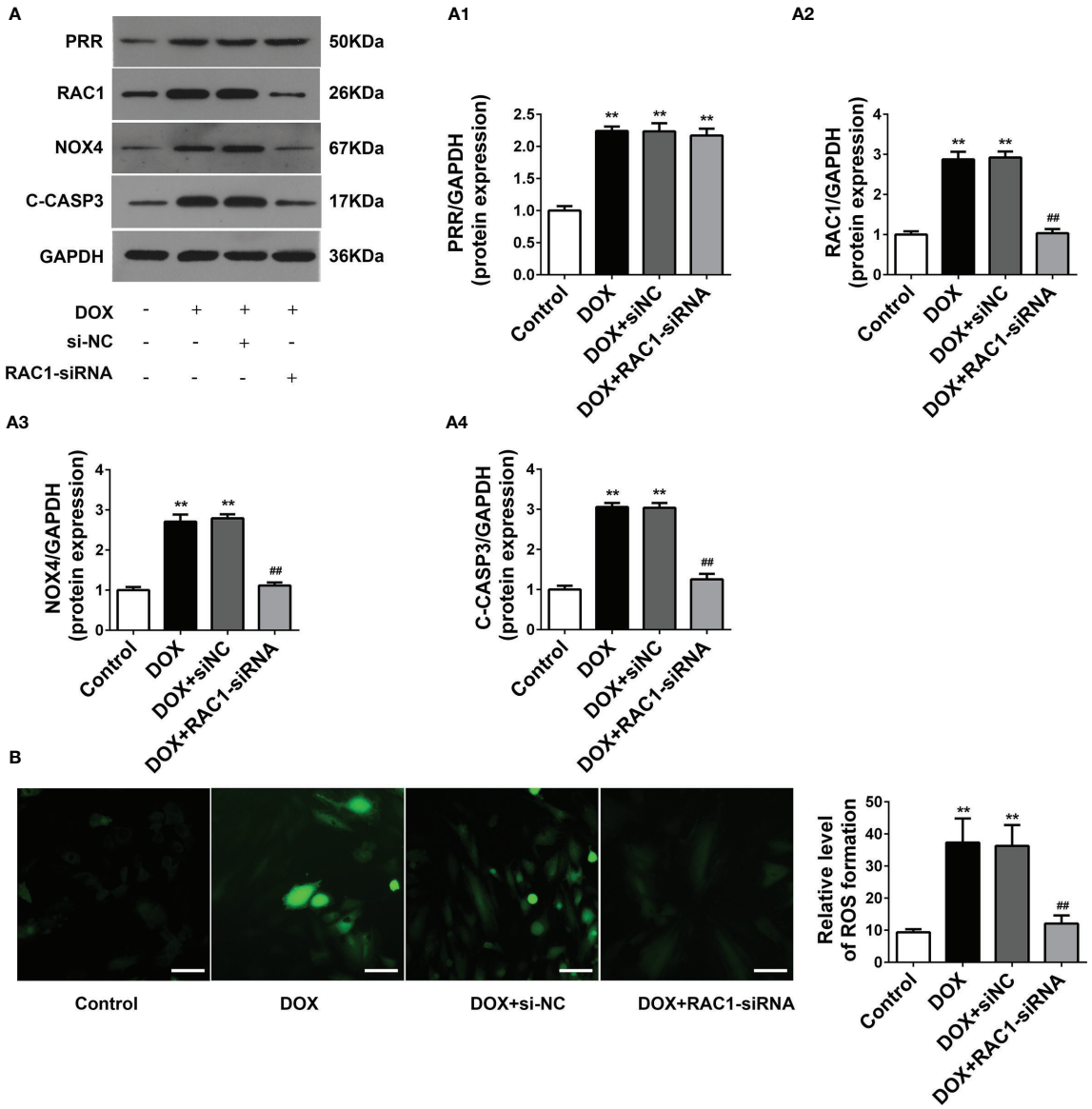

FIGURE 4 | The effect of RAC1 inhibition on the regulation of ROS-related protein levels in doxorubicin (DOX)-treated H9C2 cells. **(A)** Protein expressions of PRR, RAC1, NOX4 and cleaved Caspase3 after RAC1 inhibition in H9C2 cells. (A1)-(A4) Quantification of PRR/GAPDH, RAC1/GAPDH, and NOX4/GAPDH levels with a change in RAC1 expression. **(B)** Representative oxidative stress levels as determined by the DCFH-DA assay. ($^{**}p < 0.01$ *vs* the control group. $^{\#\#}p < 0.01$ *vs* DOX group).

structural and functional changes of heart and even HF (26, 33). Several studies suggest that the underlying mechanism of DOX-induced heart injury is correlated with the level of oxidative stress (34–36), however, the potential specific mechanisms underlying DOX-triggered oxidative injury remain unknown.

PRR is a receptor that consists of 350 amino acids residues and performs multiple functions (11). Recent studies showed that PRR plays an important role in a variety of myocardial diseases. In an earlier research report, PRR was suggested to be related to myocardial remodeling after *in situ* injection of the PRR gene into the heart (37). In the hearts of rats with diabetes, both PRR mRNA and protein level expressions showed a marked increase, thereby aggravating myocyte hypertrophy and deterioration of cardiac function (38). In post-myocardial infarction heart, PRR exacerbates myocardial fibrosis and deteriorates the cardiac function independent of Ang II (39). But the role of PRR in the DOX induced HF is still unknown. In the current study, we found that DOX stimulated severe myocardial dysfunction and oxidative injury along with PRR overexpression in rats. Our *in vivo* experiments also suggested that silencing of PRR could alleviate DOX-related endothelial injury and then heart injury *via* reducing oxidative stress (**Figure 5**). Therefore, these evidence suggested that PRR played a critical role in DOX-induced HF.

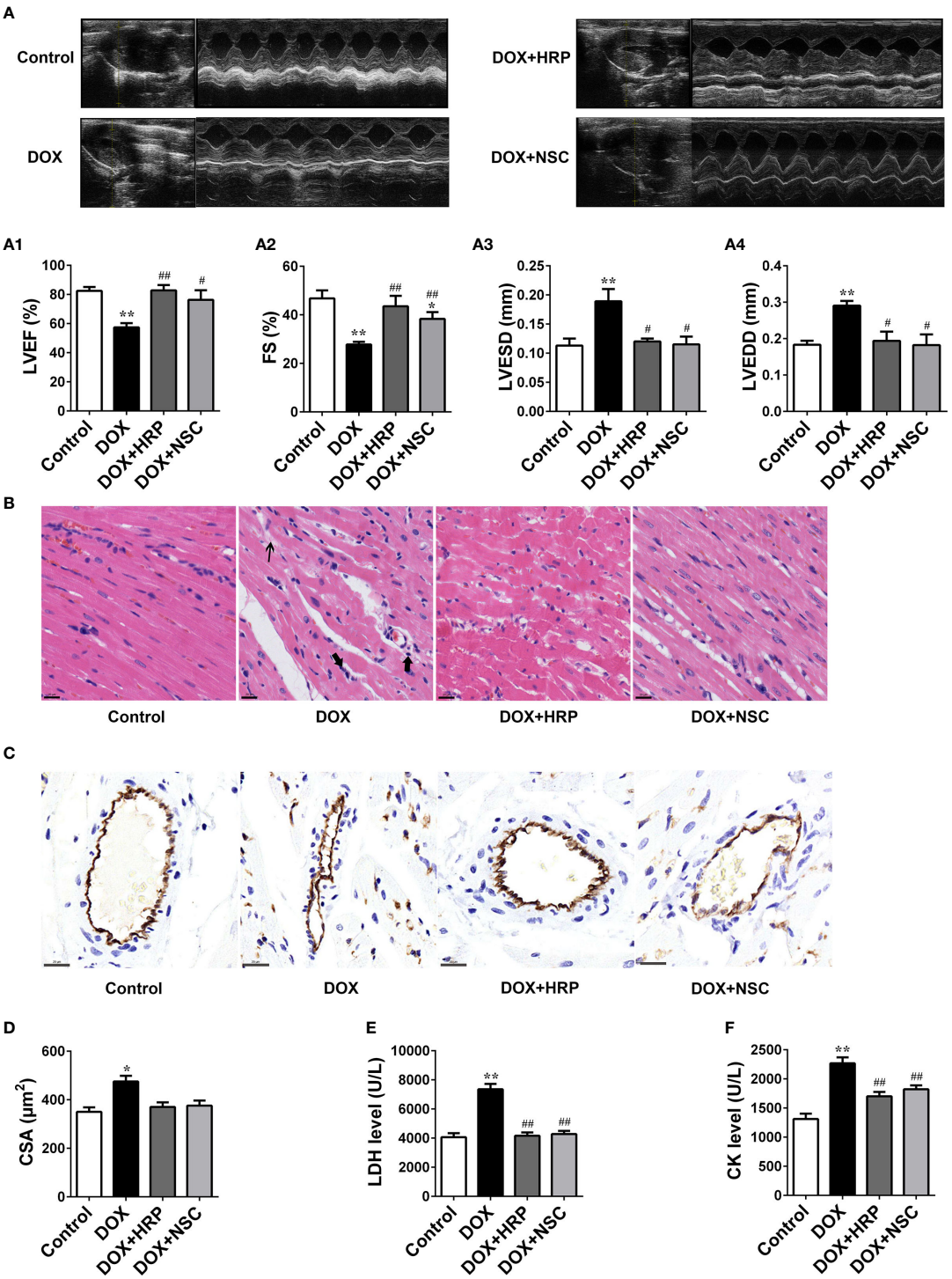

FIGURE 5 | Therapeutic effect of PRR/RAC1 inhibition on doxorubicin-induced HF in rats. Protective effects of pharmacological (pro)renin receptor (PRR) inhibition on doxorubicin (DOX)-induced cardiac hypertrophy and dysfunction. **(A)** Representative M-mode left ventricle (LV) echocardiogram. (A1) Left ventricular ejection fraction (LVEF). (A2) Fractional shortening (FS); (A3) left ventricular end-systolic diameter (LVESD). (A4) left ventricular end-diastolic diameter (LVEDD). **(B)** Representative photomicrographs of hematoxylin-eosin stained left ventricle (LV) sections. The structure of dysregulated myocytes is marked as thin arrowhead, inflammatory cell infiltration marked as thick arrowhead. **(C)** Representative photos of CD31 immunohistochemical staining in each group. Scale bars: 20 μm. **(D)** Cross-sectional areas (CSA) of cardiomyocytes in the LV. **(E, F)** Serum levels of LDH and CK in rats. Data are presented as the mean ± SEM. $^{*}p < 0.05$ and $^{**}p < 0.01$ *vs* control; $^{\#}p < 0.05$, $^{\#\#}p < 0.01$ *vs* the DOX group.

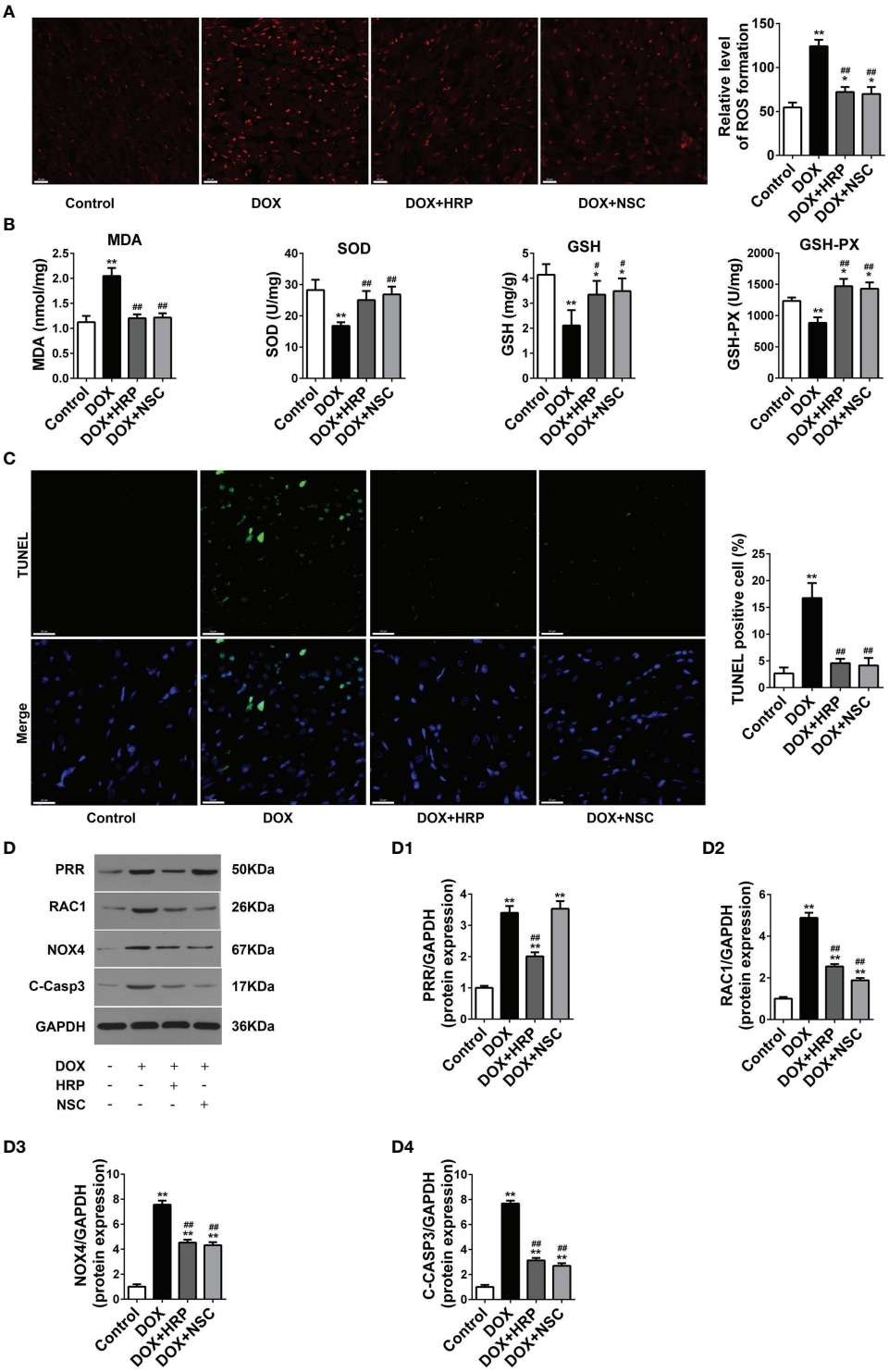

FIGURE 6 | Effects of handle region peptide (HRP) and RAC1 inhibitor, NSC23766 (NSC) on ROS production and cardiotoxicity in doxorubicin (DOX)-induced HF rats. **(A)** Representative photomicrographs of DHE stained of the LV. **(B)** Determination of MDA, SOD, GSH, and GSH-PX in heart tissues. **(C)** Representative photomicrographs of TUNEL stained LV sections, where blue fluorescence denotes the position of the nucleus and green fluorescence denotes apoptotic cells; Scale bars, 50 μm. **(D)** The protein expressions of PRR, RAC1, NOX4 and cleaved caspase3 in the hearts of doxorubicin (DOX)-treated rats. (D1)-(D4) Statistical analysis of the protein expressions of PRR, RAC1, NOX4 and cleaved caspase3 (C-Casp3); GAPDH was used as the loading control. The bar graph shows the results of densitometric analysis (n = 3 per group). Data are presented as the mean ± SEM, $^{*}p < 0.05$ and $^{**}p < 0.01$ *vs* control; $^{\#}p < 0.05$ vs the DOX group, $^{\#\#}p < 0.01$ *vs* the DOX group.

PRR can function as an accessory subunit linking the vacuolar proton pump, V-ATPase, and the low-density lipoprotein receptor-related protein 6 (LRP6), a coreceptor of Wnt receptor (40, 41). Recent studies found that PRR is involved in the transduction of various signals through the classic Wnt signaling pathway and exacerbates kidney damage by amplifying the Wnt signaling cascade (40, 41). However, the mRNA expressions of Wnt3A and Wnt8A did not increase in the DOX-induced HF in our study. Therefore, PRR may play roles *via* other mechanisms underlying DOX-induced HF.

As a critical functional constituent of the local tissue RAS, the pathophysiological roles of PRR have been widely studied. Previous study showed that prorenin induced cytoskeleton reorganization by activating the intracellular RAC1 (19). RAC1 inhibition is found to be relevant to the cardioprotective effects of lovastatin in mice (42). Our research also showed that the RAC1 expression was increased accompanied with PRR overexpression. Both *in vitro* and *in vivo* findings showed that the RAC1 inhibition was effective in alleviating oxidative stress in cardiac cells, thereby resulting in an attenuation of cardiac hypertrophy and dysfunction. Moreover, the inhibition of PRR downregulated the expression of RAC1, however, the inhibition of RAC1 did not significantly affect the expression of PRR (**Figures 4**, **6**), thereby suggesting a pathological role of PRR-mediated RAC1 activation in DOX-induced HF.

By binding to guanosine triphosphate (GTP) and migrating to the membrane with a core cytosolic complex, RAC1 is required for the activation of NOX, the leading source of superoxide production complex in the myocardium (27, 43). NOX–derived ROS plays a crucial role in several cardiovascular diseases (11, 44–46). With respect to all the isoforms of NOX, NOX4 and NOX2 are the major isoforms in the myocardium and play different roles in cardiac injury: NOX2 is primarily localized on the plasma membrane, whereas NOX4 is found primarily on intracellular membranes, mitochondria, the endoplasmic reticulum or the nucleus (47–49). A previous study indicates that NOX4 is the leading source of ROS production in a failing heart (50). In our study, both NOX2 and NOX4 expressions were upregulated in DOX-treated rats, thereby suggesting their role in the pathological processes. These findings were consistent with the previously published results (32). Whereas the suppression of PRR downregulated NOX4 but not NOX2 expression (**Figure 3C**), we thus reasonably suggest the presence of another pathway apart from PRR-RAC1 in NOX2 regulation which needs further study. In a study by PAN L L et al., knockdown of NOX4 was shown to attenuate myocardial fibrotic responses and intercellular ROS generation in cardiac fibroblasts (51). We found PRR or RAC1 inhibition reduced NOX4 expression both *in vitro* and *in vivo*, which suggested a critical function of NOX4 in the PRR-RAC1 pathway in DOX-related HF. These data suggested that the elevated PRR in DOX-induced HF rats might activate NOX4 *via* the RAC1 pathway, and subsequently aggregate oxidative injury.

CONCLUSION

In conclusion, we found that PRR plays an important role in DOX-induced HF, and cardiac function significantly improved upon the inhibition of PRR or its downstream RAC1, as indicated by the improvement in the levels of oxidative stress and histopathological changes. Thus, our findings suggested a candidate treatment approach for attenuating oxidative stress, thereby mitigating myocardial damage during DOX treatment.

DATA AVAILABILITY STATEMENT

The original contributions presented in the study are included in the article. Further inquiries can be directed to the corresponding authors.

ETHICS STATEMENT

The animal study was reviewed and approved by Animal Ethics Committee of Tongji Medical College, Huazhong University of Science and Technology (Wuhan, China).

AUTHOR CONTRIBUTIONS

X-yD and D-cX designated the study, performed the experiments, analyzed the data and wrote the manuscript. PG contributed to data collection and partly analyzed the data too. Y-lL and HP supervised the study. All authors contributed to the article and approved the submitted version.

ACKNOWLEDGMENTS

Thank Dr. Zhe Huang, an ultrasound expert for her technical support for this experiment.

REFERENCES

1. Gergely S, Hegedűs C, Lakatos P, Kovács K, Gáspár R, Csont T, et al. High Throughput Screening Identifies a Novel Compound Protecting Cardiomyocytes From Doxorubicin-Induced Damage. *Oxid Med Cell Longev* (2015) 2015:178513. doi: 10.1155/2015/178513
2. Zhao L, Tao X, Qi Y, Xu L, Yin L, Peng J. Protective Effect of Dioscin Against Doxorubicin-Induced Cardiotoxicity via Adjusting microRNA-140-5p-Mediated Myocardial Oxidative Stress. *Redox Biol* (2018) 16:189–98. doi: 10.1016/j.redox.2018.02.026
3. Bloom MW, Hamo CE, Cardinale D, Ky B, Nohria A, Baer L, et al. Cancer Therapy-Related Cardiac Dysfunction and Heart Failure: Part 1: Definitions, Pathophysiology, Risk Factors, and Imaging. *Circ Heart Fail* (2016) 9(1): e002661. doi: 10.1161/circheartfailure.115.002661
4. Hamo CE, Bloom MW, Cardinale D, Ky B, Nohria A, Baer L, et al. Cancer Therapy-Related Cardiac Dysfunction and Heart Failure: Part 2: Prevention,

Treatment, Guidelines, and Future Directions. *Circ Heart Fail* (2016) 9(2): e002843. doi: 10.1161/circheartfailure.115.002843
5. Christiansen S, Autschbach R. Doxorubicin in Experimental and Clinical Heart Failure. *Eur J Cardiothorac Surg* (2006) 30(4):611–6. doi: 10.1016/j.ejcts.2006.06.024
6. Lipshultz SE, Rifai N, Dalton VM, Levy DE, Silverman LB, Lipsitz SR, et al. The Effect of Dexrazoxane on Myocardial Injury in Doxorubicin-Treated Children With Acute Lymphoblastic Leukemia. *N Engl J Med* (2004) 351 (2):145–53. doi: 10.1056/NEJMoa035153
7. Wen SY, Tsai CY, Pai PY, Chen YW, Yang YC, Aneja R, et al. Diallyl Trisulfide Suppresses Doxorubicin-Induced Cardiomyocyte Apoptosis by Inhibiting MAPK/NF-κb Signaling Through Attenuation of ROS Generation. *Environ Toxicol* (2018) 33(1):93–103. doi: 10.1002/tox.22500
8. Li DL, Hill JA. Cardiomyocyte Autophagy and Cancer Chemotherapy. *J Mol Cell Cardiol* (2014) 71:54–61. doi: 10.1016/j.yjmcc.2013.11.007
9. Zamorano JL, Lancellotti P, Rodriguez Muñoz D, Aboyans V, Asteggiano R, Galderisi M, et al. 2016 ESC Position Paper on Cancer Treatments and Cardiovascular Toxicity Developed Under the Auspices of the ESC Committee for Practice Guidelines: The Task Force for Cancer Treatments and Cardiovascular Toxicity of the European Society of Cardiology (ESC). *Eur Heart J* (2016) 37(36):2768–801. doi: 10.1093/eurheartj/ehw211
10. Chen RC, Xu XD, Zhi Liu X, Sun GB, Zhu YD, Dong X, et al. Total Flavonoids From Clinopodium Chinense (Benth.) O. Ktze Protect Against Doxorubicin-Induced Cardiotoxicity *In Vitro* and *In Vivo*. *Evid Based Complement Alternat Med* (2015) 2015:472565. doi: 10.1155/2015/472565
11. Cao X, Yu S, Wang Y, Yang M, Xiong J, Yuan H, et al. Effects of the (Pro)renin Receptor on Cardiac Remodeling and Function in a Rat Alcoholic Cardiomyopathy Model *via* the PRR-ERK1/2-NOX4 Pathway. *Oxid Med Cell Longev* (2019) 2019:4546975. doi: 10.1155/2019/4546975
12. Damiani RM, Moura DJ, Viau CM, Caceres RA, Henriques JAP, Saffi J. Pathways of Cardiac Toxicity: Comparison Between Chemotherapeutic Drugs Doxorubicin and Mitoxantrone. *Arch Toxicol* (2016) 90(9):2063–76. doi: 10.3109/13880209.2015.1029052
13. Rochette L, Guenancia C, Gudjoncik A, Hachet O, Zeller M, Cottin Y, et al. Anthracyclines/trastuzumab: New Aspects of Cardiotoxicity and Molecular Mechanisms. *Trends Pharmacol Sci* (2015) 36(6):326–48. doi: 10.1016/j.tips.2015.03.005
14. Nguyen G, Delarue F, Burcklé C, Bouzhir L, Giller T, Sraer JD. Pivotal Role of the Renin/Prorenin Receptor in Angiotensin II Production and Cellular Responses to Renin. *J Clin Invest* (2002) 109(11):1417–27. doi: 10.1172/jci14276
15. Xu Q, Jensen DD, Peng H, Feng Y. The Critical Role of the Central Nervous System (Pro)Renin Receptor in Regulating Systemic Blood Pressure. *Pharmacol Ther* (2016) 164:126–34. doi: 10.1016/j.pharmthera.2016.04.006
16. Nguyen G, Muller DN. The Biology of the (Pro)Renin Receptor. *J Am Soc Nephrol* (2010) 21(1):18–23. doi: 10.1681/asn.2009030300
17. Mahmud H, Silljé HH, Cannon MV, van Gilst WH, de Boer RA. Regulation of the (Pro)Renin-Renin Receptor in Cardiac Remodelling. *J Cell Mol Med* (2012) 16(4):722–9. doi: 10.1111/j.1582-4934.2011.01377.x
18. Lian H, Wang X, Wang J, Liu N, Zhang L, Lu Y, et al. Heart-Specific Overexpression of (Pro)Renin Receptor Induces Atrial Fibrillation in Mice. *Int J Cardiol* (2015) 184:28–35. doi: 10.1016/j.ijcard.2015.01.088
19. Greco CM, Camera M, Facchinetti L, Brambilla M, Pellegrino S, Gelmi ML, et al. Chemotactic Effect of Prorenin on Human Aortic Smooth Muscle Cells: A Novel Function of the (Pro)Renin Receptor. *Cardiovasc Res* (2012) 95 (3):366–74. doi: 10.1093/cvr/cvs204
20. Cho KI, Koo SH, Cha TJ, Heo JH, Kim HS, Jo GB, et al. Simvastatin Attenuates the Oxidative Stress, Endothelial Thrombogenicity and the Inducibility of Atrial Fibrillation in a Rat Model of Ischemic Heart Failure. *Int J Mol Sci* (2014) 15(8):14803–18. doi: 10.3390/ijms150814803
21. Suzuki K, Murtuza B, Suzuki N, Smolenski RT, Yacoub MH. Intracoronary Infusion of Skeletal Myoblasts Improves Cardiac Function in Doxorubicin-Induced Heart Failure. *Circulation* (2001) 104(12 Suppl 1):I213–217. doi: 10.1161/hc37t1.094929
22. Ma J, Wang Y, Zheng D, Wei M, Xu H, Peng T. Rac1 Signalling Mediates Doxorubicin-Induced Cardiotoxicity Through Both Reactive Oxygen Species-Dependent and -Independent Pathways. *Cardiovasc Res* (2013) 97(1):77–87. doi: 10.1093/cvr/cvs309
23. Zhao Y, Jiang Y, Chen Y, Zhang F, Zhang X, Zhu L, et al. Dissection of Mechanisms of Chinese Medicinal Formula Si-Miao-Yong-An Decoction Protects Against Cardiac Hypertrophy and Fibrosis in Isoprenaline-Induced Heart Failure. *J Ethnopharmacol* (2020) 248:112050. doi: 10.1016/j.jep.2019.111880
24. Ammar HI, Sequiera GL, Nashed MB, Ammar RI, Gabr HM, Elsayed HE, et al. Comparison of Adipose Tissue- and Bone Marrow- Derived Mesenchymal Stem Cells for Alleviating Doxorubicin-Induced Cardiac Dysfunction in Diabetic Rats. *Stem Cell Res Ther* (2015) 6(1):148. doi: 10.1186/s13287-015-0142-x
25. Li H, Liu X, Xu Y, Wang X, Zhu H. Structure and Antitumor Activity of the Extracellular Polysaccharides From Aspergillus Aculeatus via Apoptosis and Cell Cycle Arrest. *Glycoconj J* (2016) 33(6):975–84. doi: 10.1007/s10719-016-9717-8
26. Zhu J, Wang Q, Li C, Lu Y, Hu H, Qin B, et al. Inhibiting Inflammation and Modulating Oxidative Stress in Oxalate-Induced Nephrolithiasis With the Nrf2 Activator Dimethyl Fumarate. *Free Radic Biol Med* (2019) 134:9–22. doi: 10.1016/j.freeradbiomed.2018.12.033
27. Satoh M, Ogita H, Takeshita K, Mukai Y, Kwiatkowski DJ, Liao JK. Requirement of Rac1 in the Development of Cardiac Hypertrophy. *Proc Natl Acad Sci USA* (2006) 103(19):7432–7. doi: 10.1073/pnas.0510444103
28. Laufs U, Kilter H, Konkol C, Wassmann S, Böhm M, Nickenig G. Impact of HMG CoA Reductase Inhibition on Small GTPases in the Heart. *Cardiovasc Res* (2002) 53(4):911–20. doi: 10.1016/s0008-6363(01)00540-5
29. Takemoto M, Node K, Nakagami H, Liao Y, Grimm M, Takemoto Y, et al. Statins as Antioxidant Therapy for Preventing Cardiac Myocyte Hypertrophy. *J Clin Invest* (2001) 108(10):1429–37. doi: 10.1172/jci13350
30. Shen E, Li Y, Li Y, Shan L, Zhu H, Feng Q, et al. Rac1 Is Required for Cardiomyocyte Apoptosis During Hyperglycemia. *Diabetes* (2009) 58 (10):2386–95. doi: 10.2337/db08-0617
31. Maack C, Kartes T, Kilter H, Schäfers HJ, Nickenig G, Böhm M, et al. Oxygen Free Radical Release in Human Failing Myocardium is Associated With Increased Activity of Rac1-GTPase and Represents a Target for Statin Treatment. *Circulation* (2003) 108(13):1567–74. doi: 10.1161/01.cir.0000091084.46500.bb
32. Brandt M, Garlapati V, Oelze M, Sotiriou E, Knorr M, Kröller-Schön S, et al. NOX2 Amplifies Acetaldehyde-Mediated Cardiomyocyte Mitochondrial Dysfunction in Alcoholic Cardiomyopathy. *Sci Rep* (2016) 6:32554. doi: 10.1038/srep32554
33. Zhang H, Tian Y, Liang D, Fu Q, Jia L, Wu D, et al. The Effects of Inhibition of MicroRNA-375 in a Mouse Model of Doxorubicin-Induced Cardiac Toxicity. *Med Sci Monit* (2020) 26:e920557. doi: 10.1186/s40959-016-0013-3
34. Hu C, Zhang X, Zhang N, Wei WY, Li LL, Ma ZG, et al. Osteocrin Attenuates Inflammation, Oxidative Stress, Apoptosis, and Cardiac Dysfunction in Doxorubicin-Induced Cardiotoxicity. *Clin Transl Med* (2020) 10(3):1–19. doi: 10.1055/s-0039-1697921
35. Lin MC, Yin MC. Preventive Effects of Ellagic Acid Against Doxorubicin-Induced Cardio-Toxicity in Mice. *Cardiovasc Toxicol* (2013) 13(3):185–93. doi: 10.1007/s12012-013-9197-z
36. Zhao D, Xue C, Li J, Feng K, Zeng P, Chen Y, et al. Adiponectin Agonist ADP355 Ameliorates Doxorubicin-Induced Cardiotoxicity by Decreasing Cardiomyocyte Apoptosis and Oxidative Stress. *Eur J Drug Metab Pharmacokinet* (2020) 533(3):304–12. doi: 10.1007/s13318-019-00592-6
37. Moilanen AM, Rysä J, Serpi R, Mustonen E, Szabò Z, Aro J, et al. (Pro)renin Receptor Triggers Distinct Angiotensin II-Independent Extracellular Matrix Remodeling and Deterioration of Cardiac Function. *PloS One* (2012) 7(7): e41404. doi: 10.1371/journal.pone.0041404
38. Connelly KA, Advani A, Kim S, Advani SL, Zhang M, White KE, et al. The Cardiac (Pro)Renin Receptor Is Primarily Expressed in Myocyte Transverse Tubules and is Increased in Experimental Diabetic Cardiomyopathy. *J Hypertens* (2011) 29(6):1175–84. doi: 10.1097/HJH.0b013e3283462674
39. Sharma V, Dogra N, Saikia UN, Khullar M. Transcriptional Regulation of Endothelial-to-Mesenchymal Transition in Cardiac Fibrosis: Role of Myocardin-Related Transcription Factor A and Activating Transcription Factor 3. *Can J Physiol Pharmacol* (2017) 95(10):1263–70. doi: 10.1139/cjpp-2016-0634
40. Cruciat CM, Ohkawara B, Acebron SP, Karaulanov E, Reinhard C, Ingelfinger D, et al. Requirement of Prorenin Receptor and Vacuolar H+-ATPase-Mediated Acidification for Wnt Signaling. *Science* (2010) 327(5964):459–63. doi: 10.1126/science.1179802
41. Li Z, Zhou L, Wang Y, Miao J, Hong X, Hou FF, et al. (Pro)renin Receptor Is an Amplifier of Wnt/β-Catenin Signaling in Kidney Injury and Fibrosis. *J Am Soc Nephrol* (2017) 28(8):2393–408. doi: 10.1681/asn.2016070811

42. Ohlig J, Henninger C, Zander S, Merx M, Kelm M, Fritz G. Rac1-Mediated Cardiac Damage Causes Diastolic Dysfunction in a Mouse Model of Subacute Doxorubicin-Induced Cardiotoxicity. *Arch Toxicol* (2018) 92(1):441–53. doi: 10.1016/j.yjmcc.2019.08.009
43. Hansen SS, Aasum E, Hafstad AD. The Role of NADPH Oxidases in Diabetic Cardiomyopathy. *Biochim Biophys Acta Mol Basis Dis* (2018) 1864(5 Pt B):1908–13. doi: 10.1016/j.bbadis.2017.07.025
44. Cai X, Yang C, Shao L, Zhu H, Wang Y, Huang X, et al. Targeting NOX 4 by Petunidin Improves Anoxia/Reoxygenation-Induced Myocardium Injury. *Eur J Pharmacol* (2020) 888:173414. doi: 10.1016/j.ejphar.2020.173414
45. Chen WJ, Chang SH, Chan YH, Lee JL, Lai YJ, Chang GJ, et al. Tachycardia-Induced CD44/NOX4 Signaling Is Involved in the Development of Atrial Remodeling. *J Mol Cell Cardiol* (2019) 135:67–78. doi: 10.1016/j.yjmcc.2019.08.006
46. Ren Y, Chen X, Li P, Zhang H, Su C, Zeng Z, et al. Si-Miao-Yong-An Decoction Ameliorates Cardiac Function Through Restoring the Equilibrium of SOD and NOX2 in Heart Failure Mice. *Pharmacol Res* (2019) 146:104318. doi: 10.1016/j.phrs.2019.104318
47. Ago T, Kuroda J, Pain J, Fu C, Li H, Sadoshima J. Upregulation of Nox4 by Hypertrophic Stimuli Promotes Apoptosis and Mitochondrial Dysfunction in Cardiac Myocytes. *Circ Res* (2010) 106(7):1253–64. doi: 10.1161/circresaha.109.213116
48. Bendall JK, Cave AC, Heymes C, Gall N, Shah AM. Pivotal Role of a Gp91 (Phox)-Containing NADPH Oxidase in Angiotensin II-Induced Cardiac Hypertrophy in Mice. *Circulation* (2002) 105(3):293–6. doi: 10.1161/hc0302.103712
49. Zhang M, Perino A, Ghigo A, Hirsch E, Shah AM. NADPH Oxidases in Heart Failure: Poachers or Gamekeepers? *Antioxid Redox Signal* (2013) 18(9):1024–41. doi: 10.1089/ars.2012.4550
50. Kuroda J, Ago T, Matsushima S, Zhai P, Schneider MD, Sadoshima J. NADPH Oxidase 4 (Nox4) Is a Major Source of Oxidative Stress in the Failing Heart. *Proc Natl Acad Sci USA* (2010) 107(35):15565–70. doi: 10.1073/pnas.1002178107
51. Pan LL, Liu XH, Shen YQ, Wang NZ, Xu J, Wu D, et al. Inhibition of NADPH Oxidase 4-Related Signaling by Sodium Hydrosulfide Attenuates Myocardial Fibrotic Response. *Int J Cardiol* (2013) 168(4):3770–8. doi: 10.1016/j.ijcard.2013.06.007

Conflict of Interest: The authors declare that the research was conducted in the absence of any commercial or financial relationships that could be construed as a potential conflict of interest.

Publisher's Note: All claims expressed in this article are solely those of the authors and do not necessarily represent those of their affiliated organizations, or those of the publisher, the editors and the reviewers. Any product that may be evaluated in this article, or claim that may be made by its manufacturer, is not guaranteed or endorsed by the publisher.

frontiers | Frontiers in Oncology

ORIGINAL RESEARCH
published: 12 May 2022
doi: 10.3389/fonc.2022.887026

Arsenic Trioxide Therapy During Pregnancy: ATO and Its Metabolites in Maternal Blood and Amniotic Fluid of Acute Promyelocytic Leukemia Patients

Meihua Guo[1†‡], Jian Lv[1‡], Xiaotong Chen[2‡], Mengliang Wu[3], Qilei Zhao[1] and Xin Hai[1†]*

[1] Department of Pharmacy, First Affiliated Hospital of Harbin Medical University, Harbin, China, [2] Department of Hematology, First Affiliated Hospital of Harbin Medical University, Harbin, China, [3] Department of Pharmacy, Heilongjiang University of Chinese Medicine, Harbin, China

OPEN ACCESS

Edited by:
Miao Yan,
Central South University, China

Reviewed by:
Yasen Maimaitiyiming,
Zhejiang University, China
Ratnakar Tiwari,
Northwestern University,
United States
Harry Iland,
Royal Prince Alfred Hospital, Australia

***Correspondence:**
Xin Hai
hai_xin@163.com

†ORCID:
Meihua Guo
orcid.org/0000-0002-8476-6702
Xin Hai
orcid.org/0000-0002-0360-8973

‡These authors have contributed equally to this work

Specialty section:
This article was submitted to Pharmacology of Anti-Cancer Drugs, a section of the journal Frontiers in Oncology

Received: 01 March 2022
Accepted: 13 April 2022
Published: 12 May 2022

Citation:
Guo M, Lv J, Chen X, Wu M, Zhao Q and Hai X (2022) Arsenic Trioxide Therapy During Pregnancy: ATO and Its Metabolites in Maternal Blood and Amniotic Fluid of Acute Promyelocytic Leukemia Patients. Front. Oncol. 12:887026. doi: 10.3389/fonc.2022.887026

Acute promyelocytic leukemia (APL) is extremely fatal if treatment is delayed. Management of APL in pregnancy is a challenging situation. Arsenic trioxide (ATO) is successfully applied to treat APL. ATO can be transformed into different arsenic species [arsenite (As^{III}), monomethylated arsenic (MMA, consists of MMA^{III} and MMA^{V}), dimethylated arsenic (DMA, consists of DMA^{III} and DMA^{V}), and arsenate (As^{V})], which produce different toxic effects. Investigating the maternal and fetal exposure to arsenic species is critical in terms of assessing maternal and fetal outcomes, choice of optimal treatment, and making decisions for attempting to preserve the obstetrical and fetal wellbeing. In this study, maternal blood and amniotic fluid (AF) from APL patients treated with ATO in pregnancy and blood samples of non-pregnant patients were collected. Concentrations of inorganic arsenic (iAs, iAs = As^{III}+As^{V}), MMA, and DMA were analyzed by high-performance liquid chromatography–hydride generation–atomic fluorescence spectrometry (HPLC–HG–AFS). The difference in arsenic species of plasma between pregnant patients and non-pregnant patients, distribution of arsenic compounds in AF and maternal plasma, and arsenic penetration into AF were explored. The outcomes of pregnant women treated with ATO and their fetus were analyzed. No significant differences in arsenic concentration, percentage, and methylation index [PMI: primary methylation index (MMA/iAs); SMI: secondary methylation index (DMA/MMA)] between pregnant women and non-pregnant women ($p > 0.05$) were observed. The mean ratios of AF to maternal plasma were as follows: iAs, 2.09; DMA, 1.04; MMA, 0.49; and tAs, 0.98. Abortion rate is higher with the diagnosis at an earlier gestational age, with 0%, 67%, and 100% of pregnancies ending in abortion during the third, second, and first trimester, respectively. The age of the pregnant women, the dose of ATO, and the duration of fetal exposure *in utero* had no influence on fetal outcomes. All APL women achieved complete remission (CR). Collectively, ATO and its metabolites can easily cross the placenta. Levels and distribution of arsenic species in maternal plasma and AF gave evidence that arsenic species had a different ability to penetrate the placenta into AF (iAs > DMA > MMA) and

indicated a relatively high fetal exposure to ATO and its metabolites *in utero*. Gestational age at diagnosis was more likely to be closely related to fetal outcomes, but had no effects on mother outcomes.

Keywords: acute promyelocytic leukemia, pregnancy, arsenic trioxide, arsenic species, amniotic fluid, arsenical penetration, fetal arsenic exposure

INTRODUCTION

Acute promyelocytic leukemia (APL) is a special subtype of acute myeloid leukemia. APL is characterized by life-threatening bleeding complications, which is extremely fatal if treatment is delayed. Arsenic trioxide [ATO, arsenite (As^{III}) in solution] has been shown to be highly effective for APL by PML/RARα targeting therapy (1, 2). ATO is recommended in the treatment of both relapsed and newly diagnosed patients (3, 4). APL in pregnancy presents extreme challenges to clinicians with currently limited evidence-based information available. Arsenic is known to be toxic. Understanding the link between maternal and fetal exposure to ATO is critical in terms of choice of optimal treatment and making decision for attempting to preserve the obstetrical and fetal wellbeing.

Published data on the reproductive toxicity of arsenic are limited, which are often restricted to animal studies or environmental exposure. Studies in pregnant animals have shown that exposure to arsenic can result in spontaneous abortion, fetal malformations, and birth defects, which are dose- and time-dependent (4–6). With regard to humans, a few studies were conducted in populations exposed to arsenic from environmental contaminants. Chronic exposure to environmental arsenic has been associated with spontaneous abortion, stillbirth, preterm birth, and neonatal death (7, 8). The mechanisms are poorly understood. Several reports have shown that exposure to arsenic during pregnancy can lead to oxidative stress and inflammation in the placenta and anomalous placental vasculogenesis, which affect pregnancy outcomes like preterm delivery (6, 9).

Arsenic can be metabolized from inorganic arsenic [iAs, arsenite (As^{III}) and arsenate (As^{V})] to monomethylated arsenic (MMA, consists of MMA^{III} and MMA^{V}) and dimethylated arsenic (DMA, consists of DMA^{III} and DMA^{V}) by a sequence of reductions and oxidative methylations (10–12). As^{III} and As^{V} undergo interconversion through natural oxidation and reduction by arsenate reductase (10, 11). The toxicities of different arsenic compounds vary and depend on their valency and concentration (10, 13). The gestation period is one of the most vulnerable periods of human development. Therefore, the evaluation of concentrations and the distribution of arsenic species in APL patients treated with ATO in pregnancy are critical to assess maternal and fetal outcomes in particularly challenging situations. However, no report on arsenic species measurement during pregnancy in APL patients is available. Placenta is important to fetus health, which serves as a protective shield between the fetus and harmful substances in maternal body. Although rarely investigated, some studies have demonstrated that arsenic can pass through the human placenta (14, 15), yet *in utero* fetus exposure to arsenic species during pregnancy in APL patients has not been studied.

Amniotic fluid (AF) plays a central role in quantifying the extent of transplacental passage and evaluating the accumulation of a drug in AF, which ultimately provides insight into the *in utero* drug exposition of the fetus. In this study, high-performance liquid chromatography–hydride generation–atomic fluorescence spectrometry (HPLC–HG–AFS) was used to determine the concentrations of iAs (As^{III} and As^{V}), MMA (MMA^{III} and MMA^{V}), and DMA (DMA^{III} and DMA^{V}) in AF and maternal plasma of pregnant APL patients treated with ATO. The distribution of ATO and its metabolites in AF, arsenic species penetration into AF, and the difference in arsenic species of plasma between pregnant patients and non-pregnant patients were explored for the first time. In addition, the safety of ATO in pregnant patients with APL was assessed based on data of this study and previous reports.

PATIENTS AND METHODS

Patients

This single-center, open-label study was approved by the First Affiliated Hospital of Harbin Medical University Ethics Committee. All patients with APL who were treated with ATO monotherapy in pregnancy were included. For comparison, non-pregnant women with APL who were treated with ATO monotherapy were also taken into this study. The subjects were tested only after written informed consent was obtained. Patients with liver or kidney failure were excluded. The follow-up was performed for the pregnant women who agreed.

Sample Collection and Determination

Blood samples from pregnant and non-pregnant women patients at the time of trough concentration (C_{trough}) were collected just before (within 30 min) the start of daily administration when ATO was continuously administered for >7 days. Maternal venous blood samples were also obtained immediately after delivery. As soon as the sample was collected, blood plasma was separated immediately by centrifugation at 4,000 rpm for 5 min at 4°C. If the collection did not interfere with the clinical management, AF samples were collected using a sterile 30-cc needleless syringe after rupture of membranes. All samples were immediately frozen at −80°C until analysis. The analysis of arsenic species in AF and plasma was performed by HPLC–HG–AFS (LC-AFS 6500, Beijing Haiguang Instruments Co., Ltd., China) (11, 16). The concentrations of arsenic compounds were expressed as the concentrations of the arsenic element (As).

Sample Preparation

AF or plasma sample (240 µl) was mixed with 120 µl of 30% H_2O_2, which was thoroughly vortex-mixed and kept at room temperature overnight. The 360-µl sample was prepared with 40 µl of $HClO_4$ (20%) for deproteinization, followed by vortex for 60 s. The mixture was then centrifuged at 15,000 rpm for 15 min at 4°C. The supernatant (100 µl) was injected into the HPLC–HG–AFS system for determination.

Case Review

To better understand how to manage APL with ATO treatment in pregnancy, we searched the PubMed, Web of Science, CNKI (China), and Wanfang Data (China) database (2009–2022) for articles about maternal and fetal outcomes resulting from APL patients with ATO treatment during pregnancy. Information on patient age, APL risk score, gestational age at diagnosis, treatment program, dose of ATO, duration of fetal exposure *in utero* to ATO, therapy outcome of APL, gestational age at delivery/abortion, delivery method, and fetal outcome was reviewed and investigated.

Statistical Analysis

Data analysis was performed with GraphPad Prism, version 5.0. A p-value <0.05 was considered statistically significant.

RESULTS

Patients

Eight plasma samples from 3 pregnant patients (P1–P3) and 5 non-pregnant patients (P4–P8) treated with ATO monotherapy were collected on day 8 after ATO administration. At the time of delivery, maternal plasma and AF samples were obtained from 2 pregnant patients (P1 and P2), but not from patient P3. In this study, 3 pregnant patients and 5 non-pregnant patients, aged from 26 to 38 (32 ± 4) years, were given ATO at a dose of 0.16–0.17 mg/kg once daily. ATO infusion was administered at a continuous slow rate (16, 17). The patients were also given transfusions of platelets, fibrinogen, and erythrocyte. No patients discontinued the treatment of ATO during the therapy. After the treatment, all the patients were negative for PML-*RARa;* fusion transcripts and achieved molecular and hematologic complete remission (CR). Clinical characteristics of these patients are presented in **Table 1**. Fetal outcomes of 3 pregnant women are presented in **Table 4**. Patient P1 and P2 did not accept follow-up. Patient P3 had completed her treatment. The treatment since 2016 has been induction with ATO monotherapy followed by 20 consolidation and maintenance cycles with ATO monotherapy (0.16–0.17 mg/day for 28 days). During the whole treatment phase, the patient showed no complication. The baby's growth and development were normal.

Separation of Arsenic Species

Figure 1 shows the representative HPLC–HG–AFS chromatograms of blank plasma, plasma spiked with standard arsenic compounds, plasma sample from a patient with APL, and AF sample from a patient with APL. The DMA, MMA, and iAs in samples and the spiked arsenic standards have the same chromatographic behavior. The interfering peaks from endogenous matrix components were not observed at the retention time.

Arsenic Species in Plasma of Pregnant and Non-Pregnant Women

Arsenic concentrations of plasma were determined in 8 APL patients treated with ATO. The C_{trough}, percentage, and

TABLE 1 | Baseline characteristics and therapy outcome of patients in this study.

	Pregnant patients			Non-pregnant patients				
	P1	**P2**	**P3**	**P4**	**P5**	**P6**	**P7**	**P8**
Age (years)	29	31	34	26	37	34	38	29
WBC count (×10^9/L)	6.48	9.58	6.32	15.33	1.14	2.60	2.05	0.62
Hemoglobin (g/L)	32.00	97.60	102.60	52.00	53.00	70.20	80.28	95.01
Platelet count (×10^9/L)	30.00	66.70	18.07	14.00	44.00	79.00	59.09	130.80
PT (s)	13.3	12.90	15.10	13.80	12.70	20.70	12.60	12.10
APTT (s)	26.8	28.50	23.30	25.60	28.30	29.50	24.20	25.50
FIB (g/L)	0.76	1.56	0.90	1.34	2.73	0.48	0.94	1.89
TT (s)	19.7	14.80	16.30	14.80	15.20	21.80	18.60	15.20
DD (mg/L)	5.29	9.05	6.69	7.16	8.24	19.87	5.40	8.32
ALT (U/L)	20.10	31.00	28.00	58.00	13.00	20.10	62.00	6.60
AST (U/L)	19.90	22.00	17.00	45.00	8.00	22.90	41.00	11.70
GGT (U/L)	7.40	75.00	43.00	17.00	21.00	18.50	25.00	12.40
TBIL (µmol/L)	8.10	9.87	9.06	13.12	13.10	18.30	17.46	10.20
BUN (mmol/L)	3.39	4.22	1.87	3.38	3.04	5.32	4.08	3.41
Creatinine (µmol/L)	38.2	69.70	50.30	49.60	55.80	69.60	57.10	58.20
Magnesium (mmol/L)	0.74	0.90	0.85	0.87	0.82	0.80	0.74	0.78
Potassium (mmol/L)	3.53	4.08	3.57	3.72	3.57	4.04	3.79	3.66
PML-RARA	Positive	Positive	Positive	Positive	Positive	Positive	Positive	Positive
Therapy outcome	CR	CR	CR	CR	CR	CR	CR	CR

PT, prothrombin time; APTT, activated partial thromboplastin time; FIB, fibrinogen; TT, thrombin time; DD, D-Dimer; ALT, alanine transaminase; AST, aspartate aminotransferase; GGT, γ-glutamyl transpeptidase; TBIL, total bilirubin; BUN, blood urea nitrogen; CR, complete remission.

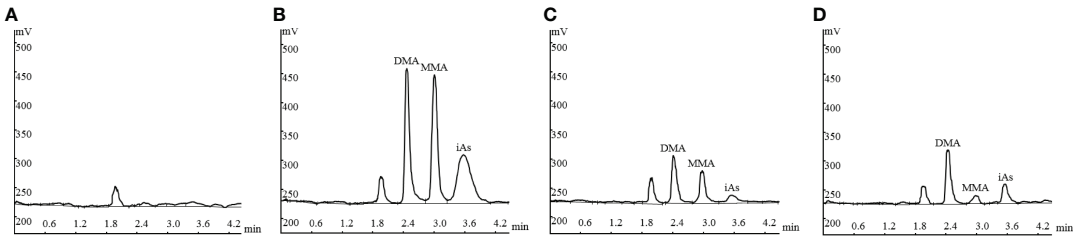

FIGURE 1 | Representative HPLC-HG-AFS chromatograms: drug-free plasma **(A)**; drug-free plasma spiked with standards of arsenic species **(B)**; plasma sample from a patient with APL **(C)**, and amniotic fluid sample from a patient with APL **(D)**. HPLC–HG–AFS: high-performance liquid chromatography–hydride generation–atomic fluorescence spectrometry; iAs: inorganic arsenic; MMA: monomethylarsonic acid; DMA: dimethylarsinic acid.

methylation index [PMI: primary methylation index (MMA/iAs); SMI: secondary methylation index (DMA/MMA)] of arsenic species in plasma from pregnant and non-pregnant women are summarized in **Table 2**. The mean arsenic C_{trough} in plasma from pregnant women (n = 3) was 17.31 ng/ml for iAs (range: 14.13–19.14 ng/ml), 24.01 ng/ml for DMA (range: 16.89–28.65 ng/ml), 23.42 ng/ml for MMA (range: 13.60–22.42 ng/ml), and 64.74 ng/ml for tAs (total arsenic, tAs = iAs + DMA + MMA) (range: 54.53–78.26 ng/ml). For non-pregnant women (n = 5), the mean arsenic C_{trough} in plasma was 16.53 ng/ml for iAs (range: 9.83–20.14 ng/ml), 18.19 ng/ml for DMA (range: 9.19–23.28 ng/ml), 18.41 ng/ml for MMA (range: 15.35–21.84 ng/ml), and 53.13 ng/ml for tAs (range: 44.67–58.87). There were higher arsenical concentrations in the plasma of pregnant women than that of non-pregnant women. However, no significant differences in C_{trough} levels of arsenic species, percentage (iAs%, DMA%, and MMA%), and methylation index (PMI and SMI) between the two sets were observed ($p > 0.05$).

Comparisons of Arsenic Species in AF With That in Maternal Blood

Arsenical concentrations in maternal plasma and AF of 2 pregnant patients at the time of delivery (4–6 days after the end of ATO treatment) were determined. The arsenic concentration of AF/maternal plasma ratio was calculated to reflect the AF penetration efficiency for arsenic compounds. The arsenic species concentrations, percentage, and methylation index in AF and maternal plasma and penetrations (AF concentration/maternal plasma concentration) in AF of pregnant patients are shown in **Table 3**. For the 2 pregnant patients, the mean iAs, DMA, MMA, and tAs concentrations of AF were 5.71 ng/ml, 8.98 ng/ml, 3.57 ng/ml, and 18.25 ng/ml, respectively. The overall concentration distribution trend in AF of the patients was DMA > iAs > MMA. The mean iAs, DMA, MMA, and tAs concentrations of AF/maternal plasma ratios were 2.09, 1.04, 0.49, and 0.98 after the end of induction therapy, respectively. The higher iAs levels in AF than that in maternal plasma from pregnant patients treated with ATO were observed. The iAs and DMA tended to exhibit higher penetrations into AF than MMA. The overall trend of penetration into AF of arsenic species in the 2 patients was iAs > DMA > MMA, which was different from the trend of DMA > MMA > iAs in maternal plasma.

Case Review

We performed a systematic retrospective review to analyze the outcomes reported for both mother and fetus when APL is diagnosed and treated with ATO during pregnancy. Literature

TABLE 2 | The C_{trough}, percentage, and methylation index of arsenic species in plasma from pregnant and non-pregnant women treated with arsenic trioxide (ATO), mean (range).

		iAs	DMA	MMA	tAs	PMI	SMI
Pregnant patients (n = 3)	**C_{trough}** (ng/ml)	17.31 (14.13–19.14)	24.01 (16.89–28.65)	23.4 2 (13.60–22.42)	64.74 (54.53–78.26)		
	Percentage (%)	26.74 (23.00–34.21)	37.08 (30.98–46.64)	36.18 (30.36–41.71)			
	Methylation index					1.35 (1.02–1.71)	1.02 (0.81–1.54)
Non-pregnant patients (n = 5)	**C_{trough}** (ng/ml)	16.53 (9.83–20.14)	18.19 (9.19–23.28)	18.41 (15.35–21.84)	53.13 (44.67–58.87)		
	Percentage (%)	31.11 (19.38–45.08)	34.24 (20.57–45.9)	34.65 (26.58–40.86)			
	Methylation index					1.11 (0.76–1.79)	0.99 (0.60–1.71)

C_{trough}, trough concentration; iAs, inorganic arsenic; MMA, monomethylarsonic acid; DMA, dimethylarsinic acid; tAs, total arsenic, tAs = iAs + DMA + MMA. Percentage (%). (Concentrations of arsenic species/Concentration of tAs) × 100%. PMI, primary methylation index (MMA/iAs); SMI, secondary methylation index (DMA/MMA).

TABLE 3 | Arsenic species in amniotic fluid (AF) and maternal plasma of APL patients treated with arsenic trioxide in pregnancy.

Patients	Sample time		Concentration (ng/ml)		Ratio(C_{AF}/C_{MP});
			Maternal plasma (C_{MP})	Amniotic fluid (C_{AF})	
P1	4 days after the end of induction therapy	iAs	3.56	5.81	1.63
		DMA	9.29	11.71	1.26
		MMA	8.07	4.79	0.59
		tAs	20.92	22.31	1.07
		PMI	2.27	0.82	/
		SMI	1.15	2.44	/
		iAs%	17.02	26.04	/
		DMA%	44.41	52.49	/
		MMA%	38.58	21.47	/
P2	6 days after the end of induction therapy	iAs	2.20	5.60	2.55
		DMA	7.68	6.25	0.81
		MMA	6.15	2.34	0.38
		tAs	16.03	14.19	0.89
		PMI	2.80	0.42	/
		SMI	1.25	2.67	/
		iAs%	13.72	39.46	/
		DMA%	47.91	44.05	/
		MMA%	38.37	16.49	/

C_{AF}/C_{MP}, AF concentration/maternal plasma concentration; iAs, inorganic arsenic; MMA, monomethylarsonic acid; DMA, dimethylarsinic acid; tAs, total arsenic, tAs = iAs + DMA + MMA. Percentage (%). (Concentrations of arsenic species/Concentration of tAs) × 100%. PMI, primary methylation index (MMA/iAs); SMI, secondary methylation index (DMA/MMA).

databases were systematically searched to identify studies reporting cases of ATO treatment during pregnancy. Eighteen published articles met the eligibility criteria. The extracted data from the selected articles are presented in **Table 4**. A total of 28 APL patients from literature were eligible for ATO therapy in pregnancy, with most of them being treated with ATO plus all-trans retinoic acid (ATRA) (n = 12, 43%) or ATO plus ATRA combined with chemotherapy (n = 15, 54%), while the remaining patients received ATO monotherapy (n = 1, 14%). All patients achieved CR during pregnancy or after delivery (100%). The age of women (n = 18) who experienced spontaneous or induced abortion was 27.8 ± 2.8 years, which was not significantly different from the age (28.0 ± 4.7 years) of women (n = 10) who delivered normal babies. The mean dose of ATO and duration of fetal exposure *in utero* to ATO of women who experience spontaneous or induced abortion were lower than that of women who delivered normal babies, 258 mg (n = 5) vs. 398 mg (n = 5) and 31.6 days (n = 17) vs. 40.2 days (n = 9), respectively. Evidently, apart from mother age, fetal viability is not related to dose of ATO and duration of fetal exposure *in utero* to ATO.

For the pregnant women diagnosed with APL in the first trimester, all of them (n = 10, 100%) experienced spontaneous or induced abortion. For the ones diagnosed with APL during the second trimester, 8 of 12 (67%) patients' gestation ended in abortion. The remaining 4 (33%) women who were diagnosed with APL during the second trimester continued gestation until delivery of healthy infants by vaginal delivery or cesarean section. For the APL patients during the third trimester, all pregnancies (n = 6, 100%) delivered normal babies. APL patients treated with ATO during the first trimester were more susceptible to spontaneous and induced abortion compared with those during the second trimester and the third trimester (100% vs. 67% and 100% vs. 0%) ($p < 0.0001$). Thus, gestational age at diagnosis was instead crucial in fetal outcomes. In these cases, an interesting case should be paid attention to (26). A 22-year-old woman was diagnosed with APL at only 14 weeks of gestation. The fetus received a total exposure to ATO of 93 days and 930 mg. A healthy infant was delivered at 40^{6+} weeks, and the mother achieved CR.

For the 3 patients in this study, information on APL risk score, gestational age at diagnosis, treatment program, dose of ATO, duration of fetal exposure *in utero* to ATO, therapy outcome of APL, gestational age at delivery/abortion, delivery method, and fetal outcome was also investigated. As presented in **Table 4**, 3 patients received ATO monotherapy (100%), which is different from that in previous reports. The gestation of 2 pregnant women diagnosed with APL during the second trimester ended in abortion. The APL patient during the third trimester delivered a normal baby. The fetal outcomes in the 3 cases seemed to be in accord with the above characteristics; that is to say, gestational age at diagnosis was instead crucial in fetal outcomes.

DISCUSSION

ATO has been successfully used for front-line treatment of APL (36). As a well-known poison, ATO treatment for APL during pregnancy is a significant challenge, which is associated with emergency treatment for APL, fetal exposure to arsenic, and pregnancy outcomes. Clinical trial is obviously impossible and no studies are available regarding the use of ATO in pregnant women. The only data available are from animal or environmental exposure studies. The current study is the first study to investigate the ATO and its metabolite concentrations in the plasma and AF from APL patients treated with ATO during pregnancy, which reflects the fetal exposure levels to arsenic

TABLE 4 | Clinical characteristics and maternal and fetal outcomes in pregnant women with APL treated with ATO in this study and literature.

	Case no.	Age, years	APL risk score	Gestational age at diagnosis, weeks	Treatment	Dose of ATO received	Fetal exposure *in utero* to ATO, days	Therapy outcome	Gestational age at delivery/abortion, weeks	Delivery method	Fetal outcome
Cases in this Study	1	29	Intermediate	17^{+5}	ATO monotherapy	0.17 mg/kg/day (10 mg/day)	28	CR	23^{+4}	TA (polyhydramnios)	Aborted fetus
	2	31	Low	20	ATO monotherapy	0.16 mg/kg/day (10 mg/day)	28	CR	24	TA	Aborted fetus
	3	34	Low	37	ATO monotherapy	0.16 mg/kg/day (10 mg/day)	15	CR	39^{+1}	Vaginal	Healthy infant
Cases in literature	1 (18)	30	\	2	ATO+ATRA +DNR	\	57	CR	10+1	TA	Aborted fetus
	2 (19)	25	Low/ Intermediate	5	ATO+ATRA +DNR	\	28	CR	9	SA	Aborted fetus
	3 (19)	28	Low/ Intermediate	5	ATO+ATRA +IDA	\	14	CR	7	TA	Aborted fetus
	4 (20)	25	High	8	ATO+ATRA +DNR	\	21	CR	11	TA	Aborted fetus
	5 (21)	32	Intermediate	9	ATO+ATRA	10 mg/day	21	CR	12	TA	Aborted fetus
	6 (22)	25	Low	9^{+5}	ATO+ATRA	10 mg/day	23	CR	13^{+1}	TA	Aborted fetus
	7 (23)	26	High	10	ATO+ATRA +DNR	\	21	CR	13	TA	Aborted fetus
	8 (19)	26	Low/ Intermediate	10	ATO+ATRA	\	35	CR	15	TA	Aborted fetus
	9 (24)	25	Low	11^{+3}	ATO+ATRA	0.15 mg/kg	14	CR	14^{+1}	TA	Aborted fetus
	10 (18)	31	\	12	ATO+ATRA +DNR	\	80	CR	23^{+3}	TA	Aborted fetus
	11 (25)	33	Low	12^{+4}	ATO+ATRA +IDA	10 mg/day	35	CR	17^{+4}	TA	Aborted fetus
	12 (18)	23	\	12^{+4}	ATO+ATRA +DNR	\	72	CR	23^{+6}	TA	Aborted fetus
	13 (19)	27	Low/ Intermediate	13	ATO+ATRA +DNR	\	28	CR	17	TA	Aborted fetus
	14 (26)	22	Intermediate	14	ATO+ATRA	0.15 mg/kg/day (10 mg/day)	93	CR	40^{+6}	Vaginal	Healthy infant
	15 (27)	28	Intermediate	23^{+4}	ATO+ATRA	\	25	CR	28	TA	Aborted fetus
	16 (24)	28	Intermediate	24^{+4}	ATO+ATRA	0.15 mg/kg	23	CR	29^{+4}	TA	Aborted fetus
	17 (22)	28	Intermediate	24^{+5}	ATO+ATRA	10 mg/day	30	CR	29	TA	Aborted fetus
	18 (28)	23	High	27	ATO+ATRA +IDA	0.15 mg/kg	35	CR	32	Cesarean	Healthy infant
	19 (29)	29	\	27	ATO + ATRA + DNR	\	\	CR	\	TA	Aborted fetus
	20 (30)	31	Intermediate	27	ATO monotherapy	10 mg/day	10	CR	29	ID+TA	Aborted fetus
	21 (30)	30	Intermediate	27^{+1}	ATO+ATRA +HHRT	10 mg/day	70	CR	37	Cesarean	Healthy infant
	22 (18)	33	\	28	ATO+ATRA	\	87	CR	40^{+3}	Vaginal	Healthy infant
	23 (31)	27	Intermediate	31^{+}	ATO+ATRA +DNR	10 mg/day	14	CR	33^{+}	Cesarean (fetal distress)	Healthy infant
	24 (32)	37	\	32	ATO+ATRA	\	20	CR	\	Cesarean	Healthy infant
	25 (33)	28	Intermediate	34^{+4}	ATO+ATRA +DNR	10 mg/day	16	CR	37^{+5}	Cesarean	Healthy infant
	26 (34)	23	Low	35	ATO+ATRA		21	CR	38	Vaginal	

(Continued)

TABLE 4 | Continued

Case no.	Age, years	APL risk score	Gestational age at diagnosis, weeks	Treatment	Dose of ATO received	Fetal exposure *in utero* to ATO, days	Therapy outcome	Gestational age at delivery/abortion, weeks	Delivery method	Fetal outcome
					0.15 mg/kg					Healthy infant
27 (35)	27	Low	36	ATO+ATRA	10 mg/day	6	CR	38	Cesarean	Healthy infant
28 (29)	30	\	36	ATO+ATRA +DNR	\	\	CR	\	Cesarean	Healthy infant

APL, acute promyelocytic leukemia; CR, complete remission; ATO, arsenic trioxide; ATRA, all-trans-retinoic acid; TA, therapeutic abortion; SA, spontaneous abortion; DNR, daunorubicin; IDA, idarubicin; HHRT, homoharringtonine; ID, Intrauterine death.

compounds during ATO treatment and the penetration efficiency of arsenic species into AF in the real world. The dose in these cases is much higher than in environmental studies, which is crucial to clinical treatments. In addition, the clinical cases on the application of ATO use during pregnancy in the literature were systematically searched and analyzed in this study. Our results may help medical teams make hard decisions in extremely complex clinical situations such as APL treatment during pregnancy.

Published reports and our preliminary results suggested that ATO is biotransformed into two types of major metabolites through oxidative methylation in human: MMA and DMA, which is catalyzed by arsenic methyltransferase (10, 11, 16, 17). As^V is a rare metabolite in the process (16). The prototype drug As^{III} and its metabolites are widely distributed throughout the body. The arsenic species can be detected in urine (11), plasma (16), red blood cells (17), leukocytes (37), granulocytes (37), and cerebrospinal fluid (CSF) (38) of APL patients treated with ATO, and in kidney (39), liver (39), and heart (39) of rat treated with ATO. In this study, the C_{trough}, percentage, and methylation index of arsenic species in plasma from pregnant and non-pregnant women treated with ATO were evaluated. As shown in **Table 2**, no significant differences between the two sets were observed. The reasons may be the small sample size or no significant influence of pregnancy on arsenic metabolism.

Another interesting finding of this study was the remarkable differences in the arsenic species levels in the plasma from those in our preliminary published report (16). Higher levels of DMA, iAs, MMA, and tAs were measured in the present study. The discrepancy might have resulted from the different sample preparation methods between the two studies. H_2O_2 was added to plasma during sample preparation to cleave the bonds between arsenic and plasma proteins. In this process, trivalent arsenicals (As^{III}, DMA^{III}, and MMA^{III}) were oxidized to pentavalent arsenicals (As^v, DMA^v, and MMA^v) by H_2O_2 (40). Based on our study (17) and previous reports (40), H_2O_2 at this concentration changed the oxidation state of arsenicals, but not the methylation status. Therefore, the detected arsenic species were the sum of unbound arsenicals and protein-bound arsenicals that were released and oxidized by H_2O_2.

Our published study showed that As^{III} and its metabolites have a limited ability to penetrate the blood–brain barrier into CSF (38). Arsenical concentration in CFS is much lower than that in plasma (38). In this study, our results showed that arsenic concentration in AF is much higher than that in maternal plasma, which suggested that As^{III} and its metabolites have a strong ability to penetrate the placental barrier into AF.

The overall concentration trend of arsenic species in AF of in the 2 APL patients was DMA > iAs > MMA during the drug-withdrawal period, which was different from that in maternal plasma (DMA > MMA > iAs). Our preliminary results indicated that the overall penetration into CSF of arsenic species was iAs > DMA^V > MMA^V (As^V was not detected in CSF) (38). It is interesting that a similar thing was observed in this study. Our results showed that the penetration into AF of iAs was higher than DMA and MMA, which suggested that the iAs may possess stronger placental barrier permeability and the MMA exhibited weaker placental barrier penetration efficiency. The results also implied higher iAs accumulation in the AF compared with DMA and MMA. Some reasons for this phenomenon can be traced as follows: (1) At middle and late gestation, fetal urine is produced, contributing to most of the volume and composition of the AF. DMA^V and As^{III} were the dominant arsenic compounds excreted from the urine (11). (2) Unbound arsenicals possess stronger barrier permeability than protein-bound arsenicals. The different placental barrier permeability of arsenic species probably comes from the different chemical structure or protein binding capacity. (3) The arsenic ingested by fetus could undergo fetal clearance by its metabolic pathways. Because of the lower metabolism of fetus, there is much higher level of un-metabolized As^{III} in AF than in maternal plasma. (4) There may be an increased penetration into and/or accumulation within AF or a decreased elimination out of AF. The exact reason is unknown and further explorations are needed.

Taken together, these data from our study indicated that maternally treated ATO (As^{III}) and its pharmacologically metabolites can easily pass through the placental barrier. Thus, *in utero*, the fetus could be simultaneously exposed to ATO and its metabolites by fetus swallowing AF. It has become clear that arsenic metabolites also possess cytotoxicity (13, 41). Previous studies have shown that trivalent methylated arsenicals (MMA^{III} and DMA^{III}) are much more toxic than iAs (13, 42). The concentration trend of DMA > iAs > MMA in AF suggests a higher fetal exposure to DMA. The higher permeability of the placental barrier and the lower affinity of fetal plasma proteins to the drugs could increase fetal exposure to the circulating drug and its metabolites. Our results also showed that there was a higher iAs level and a lower MMA level in the AF than those in

the maternal plasma. Furthermore, our data suggest that continuous fetal exposure to ATO and its metabolites *via* re-circulation of the AF could occur. The biological consequences of fetal exposure to maternally administered ATO and/or its metabolites *via* placental transfer and re-circulation of AF are yet to be determined. Further studies are needed to evaluate the effect(s) of iAs, DMA, and MMA on the neonatal outcome of infants exposed to the drug and its metabolites *in utero*.

The diagnosis and management of APL in pregnancy presents significant challenges. It is impossible to prospectively study the appropriate measures for the management of pregnant women with APL. A systematic review of the literature cases seems the best way to obtain evidence-based information to guide decision-making in clinical practice. To analyze the maternal and fetal outcomes of APL patients treated with ATO in pregnancy, a systematic literature review was performed for the first time in this study. The results suggested that all pregnant women with APL (n = 28) in literature reports achieved CR (CR rate was 100%). The correlation between fetal outcomes and age, dose of ATO, and duration of fetal exposure *in utero* to ATO was not observed. There was an abortion rate of 100%, 67%, and 0% in those diagnosed with APL during the first, second, or third trimester of pregnancy in 28 cases included, respectively. The results suggested that the chances of achieving CR for the pregnant women with APL remained very high by ATO treatment, regardless of gestational age at diagnosis. In other words, for the mother, gestational age has no significant influence on the probability of achieving CR. In contrast, fetal outcome is strongly related to gestational age. In these cases, polyhydramnios, jaundice, respiratory distress syndrome, and intrauterine death were observed during the perinatal period. However, teratogenic effects were not observed. Our results indicated that ATO and its metabolites can penetrate the placenta into AF. The concentration ratios of AF to maternal plasma highlighted a relatively high fetal exposure to arsenic compounds. Based on overall consideration, although teratogenic effects were not observed in this study, avoiding ATO during the early stage of pregnancy is recommended, due to its potential teratogenicity and other toxicity. Some reports support the proposal that the treatment of APL in pregnancy should give priority to an anthracycline, particularly daunorubicin (43, 44). More data and further exploration are needed to testify this. Comparing ATO treatment with daunorubicin or anthracycline treatment in a large sample is recommended. Our result suggested that ATO and chemotherapy seem to be reasonably safe when given to APL patients during the third trimester of pregnancy. Some reports indicated successful pregnancies after the end of ATO therapy for APL (4, 44–46). Even so, to avoid a fetal exposure to ATO, using this agent only after delivery is recommended.

Our study had some limitations. Acute leukemia in pregnancy has a low incidence (1 out of 100,000 pregnancies) (26). APL is a variant of acute myeloid leukemia (AML) with an incidence of approximately 2–3 per million. Then, APL during pregnancy is rather rare. In addition, obtaining AF is a prominent difficulty. Therefore, the small number of patients and AF samples included in our study poses a considerable shortcoming. Our findings do not allow for general conclusions on arsenic species concentrations in AF and maternal circulation within APL patients treated with ATO during pregnancy. Given that AF determinations were performed during delivery when ATO was withdrawn, drug concentrations of AF do not represent C_{trough} (trough levels), thus limiting the generalizability of the results. In our previous report (37), arsenic species could still be detected in blood cells at the time of drug withdrawal for 3–109 days. In this study, we collected the maternal blood samples and AF samples from 2 APL patients at 4 and 6 days after the treatment. Unfortunately, the samples from later time points were also not obtained due to the lack of clinical compliance or informed consent. Thus, arsenic metabolism and clearance after treatment in AF or maternal blood were not evaluated. Umbilical cord blood were not obtained. The conclusions on the correlation between maternal plasma concentration of arsenic species and cord blood levels were not made at this time. Besides that, further information about the long-term safety of arsenic compounds in terms of pregnancy outcomes and effects on fetus was lacking in our investigation. Further studies and follow-up are required.

Despite the above limitations, data from our *in vivo* study demonstrated the characteristics of intrauterine arsenic exposure and the permeability of placenta for ATO and its metabolites for the first time. The first safety assessment of ATO in pregnant women with APL was performed in this study. Our studies will enable further analysis of the possible effects of ATO and its metabolites on maternal and fetal outcomes.

CONCLUSIONS

In summary, ATO and its metabolites in AF and maternal plasma of pregnant APL patients treated with ATO were measured by HPLC–HG–AFS for the first time. There were no significant differences in C_{trough} levels of arsenic species, percentage (iAs%, DMA%, and MMA%), and methylation index (PMI and SMI) between pregnant women (n = 3) and non-pregnant women (n = 5) ($p > 0.05$), which may be due to the small size or no significant influence of pregnancy on arsenic metabolism. The overall concentration distribution trend in AF was DMA > iAs > MMA, which was different from that in the corresponding maternal plasma, DMA > MMA > iAs. These results suggested that arsenic compounds (iAs, DMA, and MMA) had the ability to easily cross the human placenta barrier and appear in AF, fetuses were exposed to relatively high levels of ATO and its metabolites *in utero* during maternal ATO treatment, and arsenic species exhibited different penetrations into AF (iAs> DMA > MMA); in other words, iAs possessed stronger placental barrier permeability and the MMA exhibited weaker placental barrier penetration efficiency, which was similar to that of arsenic penetration into CSF.

A systematic literature review about APL women in pregnancy treated with ATO was performed. Combined with the data of this study, the results indicated that mother age, the dose of ATO, and duration of fetal exposure *in utero* had no influences on fetal outcomes. Gestational age was closely related to fetal outcomes, but did not affect mother outcomes (CR rate,

100%). In brief, avoiding ATO treatment during the early stage of pregnancy should be emphasized, due to high fetal exposure to ATO and its metabolites *in utero*, ATO potential teratogenicity, and other toxicity.

These results may be beneficial for medical teams to assess maternal and fetal outcomes, preserve the obstetrical and fetal wellbeing, and make hard decisions such as ATO treatment for pregnant women with APL. Since this is the first report that analyzed the arsenical concentrations in maternal blood and AF and evaluated the permeability of the placenta barrier for arsenic species in pregnant APL patients receiving ATO, these findings need to be further investigated and should be corroborated using a larger sample population in multi-center studies.

DATA AVAILABILITY STATEMENT

The original contributions presented in the study are included in the article/supplementary material. Further inquiries can be directed to the corresponding author.

ETHICS STATEMENT

The studies involving human participants were reviewed and approved by the Ethics Committee of the First Affiliated Hospital of Harbin Medical University. The patients/participants provided their written informed consent to participate in this study.

AUTHOR CONTRIBUTIONS

MG and JL carried out experimental work, analyzed the data, and wrote the manuscript. XC collected the samples. MG, MW, and QZ contributed to the final preparation of this paper and submission. XH and XC revised the manuscript. XH designed and supervised this research. All authors contributed to the article and approved the submitted version.

FUNDING

This study was supported by the National Natural Science Foundation of China (No. 81700151), the Natural Science Foundation of Heilongjiang Province for Excellent Youths (No. YQ2019H016), the Excellent Youth Foundation of First Affiliated Hospital of Harbin Medical University (No. HYD2020JQ0018), the Heilongjiang Key R&D Program (No. GZ20210070), the Heilongjiang Postdoctoral Program (No. LBH-Q20031), and the Foundation of First Affiliated Hospital of Harbin Medical University (No. 2019M15).

REFERENCES

1. Wang QQ, Hua HY, Naranmandura H, Zhu HH. Balance Between the Toxicity and Anticancer Activity of Arsenic Trioxide in Treatment of Acute Promyelocytic Leukemia. *Toxicol Appl Pharmacol* (2020) 409:115299. doi: 10.1016/j.taap.2020.115299
2. Maimaitiyiming Y, Wang QQ, Yang C, Ogra Y, Lou Y, Smith CA, et al. Hyperthermia Selectively Destabilizes Oncogenic Fusion Proteins. *Blood Cancer Discov* (2021) 2:388–401. doi: 10.1158/2643-3230.BCD-20-0188
3. Ghavamzadeh A, Alimoghaddam K, Rostami S, Ghaffari SH, Jahani M, Iravani M, et al. Phase II Study of Single-Agent Arsenic Trioxide for the Front-Line Therapy of Acute Promyelocytic Leukemia. *J Clin Oncol* (2011) 29:2753–7. doi: 10.1200/JCO.2010.32.2107
4. Breccia M, Molica M, Efficace F, Minotti C, Latagliata R, Foà R, et al. Pregnancy in Acute Promyelocytic Leukaemia After Front-Line Therapy With Arsenic Trioxide and All-Trans Retinoic Acid. *Brit J Haematol* (2015) 167:428–30. doi: 10.1111/bjh.12995
5. Golub MS, Macintosh MS, Baumrind N. Developmental and Reproductive Toxicity of Inorganic Arsenic: Animal Studies and Human Concerns. *J Toxicol Env Heal B* (1998) 1:199–237. doi: 10.1080/10937409809524552
6. He W, Greenwell RJ, Brooks DM, Calderón-Garcidueñas L, Beall HD, Coffin JD. Arsenic Exposure in Pregnant Mice Disrupts Placental Vasculogenesis and Causes Spontaneous Abortion. *Toxicol Sci* (2007) 99:244–53. doi: 10.1093/toxsci/kfm162
7. Naujokas MF, Anderson B, Ahsan H, Aposhian HV, Graziano J, Thompson CL, et al. The Broad Scope of Health Effects From Chronic Arsenic Exposure: Update on a Worldwide Public Health Problem. *Environ Health Persp* (2013) 121:295–302. doi: 10.1289/ehp.1205875
8. Ahmad SA, Sayed MH, Barua S, Khan MH, Faruquee MH, Jalil A, et al. Arsenic in Drinking Water and Pregnancy Outcomes. *Environ Health Persp* (2001) 109:629–9. doi: 10.1289/ehp.01109629
9. Ahmed S, Mahabbat-e Khoda S, Rekha RS, Gardner RM, Ameer SS, Moore S, et al. Arsenic-Associated Oxidative Stress, Inflammation, and Immune Disruption in Human Placenta and Cord Blood. *Environ Health Persp* (2011) 119:258–64. doi: 10.2307/41000868
10. Rehman K, Naranmandura H. Arsenic Metabolism and Thioarsenicals. *Metallomics* (2012) 4:881–92. doi: 10.1039/c2mt00181k
11. Guo M, Li J, Fan S, Liu W, Wang B, Gao C, et al. Speciation Analysis of Arsenic in Urine Samples From APL Patients Treated With Single Agent As_2O_3 by HPLC-HG-AFS. *J Pharmaceut Biomed* (2019) 171:212–7. doi: 10.1016/j.jpba.2019.04.014
12. Maimaitiyiming Y, Zhu HH, Yang C, Naranmandura H. Biotransformation of Arsenic Trioxide by AS3MT Favors Eradication of Acute Promyelocytic Leukemia: Revealing the Hidden Facts. *Drug Metab Rev* (2020) 52:425–37. doi: 10.1080/03602532.2020.1791173
13. Moe B, Peng H, Lu X, Chen B, Chen LWL, Gabos S, et al. Comparative Cytotoxicity of Fourteen Trivalent and Pentavalent Arsenic Species Determined Using Real-Time Cell Sensing. *J Environ Sci China* (2016) 49:113–24. doi: 10.1016/j.jes.2016.10.004
14. Johnson J, Robinson S, Smeester L, Fry R, Boggess K, Vora N. Ubiquitous Identification of Inorganic Arsenic in a Cohort of Second Trimester Amniotic Fluid in Women With Preterm and Term Births. *Reprod Toxicol* (2019) 87:97–9. doi: 10.1016/j.reprotox.2019.05.061
15. Okabe K. Investigation Into Fetal Toxicity by Arsenic Exposure to Pregnant Women. *Placenta* (2017) 59:178. doi: 10.1016/j.placenta.2017.08.049
16. Guo M, Zhou J, Fan S, Li L, Chen H, Lin L, et al. Characteristics and ClinicalInfluence Factors of Arsenic Species in Plasma and Their Role of ArsenicSpecies as Predictors for Clinical Efficacy in Acute Promyelocytic Leukemia(APL) Patients Treated With Arsenic Trioxide. *Expert Rev Clin Phar* (2021) 14:503–12. doi: 10.1080/17512433.2021.1893940
17. Guo M, Wang B, Liu S, Wang W, Gao C, Hu S, et al. Time Course of Arsenic Species in Red Blood Cells of Acute Promyelocytic Leukemia (APL) Patients Treated With Single Agent Arsenic Trioxide. *Expert Rev Clin Phar* (2019) 12:378–8. doi: 10.1080/17512433.2019.1586532
18. Zhao J, Yang L, Hou L, Ge X, Kang J, Dong C, Dong C, et al.. Clinical Analysis of 13 Cases With Acute Lukemia During Pregnancy (in Chinese). *J Clin*

Hematol (China) (2015) 28:977–80. doi: 10.13201/j.issn.1004-2806.2015.11.016
19. Zhang X, Feng S, Zhou L, Liu H, Zhu W, Cai X, et al. Treatment and Prognosis Analysis of Acute Leukemia Patients During Pregnancy (in Chinese). *J Leuk Lymphoma (China)* (2021) 30:212–5. doi: 10.37601/cma.j.cn115356-20191111-00221
20. Yu J. The Treatment With Patients of Acute Promyelocytic Leukemia Complicating Pregnancy (in Chinese). *World Latest Med Inf (China)* (2014) 14:5–7. doi: 10.3969/j.issn.1671-3141.2014.21.001
21. Guan Y. PICC Catheterization and Nursing of a Patient With Acute Promyelocytic Leukemia Complicating Early Pregnancy, DIC, and Serious Thrombocytopenia (in Chinese). *Special Health* (2020) 33:204.
22. Yang R, Qian S, Chen C. Treatment of Acute Promyelocytic Leukemia During Pregnancy (in Chinese). *China J Hematol* (2019) 40:439–40. doi: 10.3760/cma.j.issn.0253-2727.2019.05.019
23. Xu Y. The Treatment Program of Acute Promyelocytic Leukemia Complicating Pregnancy (in Chinese). *J Clin Hematol (China)* (2013) 26:45–7. doi: 10.13201/j.issn.1004-2806.2013.01.016
24. Li YW, Xu YF, Hu W, Qian SX, Chen C. Acute Myeloid Leukemia During Pregnancy: A Aingle Institutional Experience With 17 Patients and Literature Review. *Int J Hematol* (2020) 112:487–95. doi: 10.1007/s12185-020-02938-2
25. Zhang Y, Ying S, Yang Q. A Case of Acute Promyelocytic Leukemia in Pregnancy (in Chinese). *Modern Pract Med (China)* (2018) 30:11141120. doi: 10.3969/j.issn.1671-0800.2018.08.072
26. Cochet C, Simonet M, Cattin J, Metz JP, Ana Berceanu A, Deconinck E, et al. Arsenic Trioxide Treatment During Pregnancy for Acute Promyelocytic Leukemia in a 22-Year-Old Woman. *Case Rep Hematol* (2020) 2020:3686584. doi: 10.1155/2020/3686584
27. Zhu M. Nursing Care of a Pregnant Woman With Acute Promyelocytic Leukemia (in Chinese). *Natl Med Front China* (2012) 7:84. doi: 10.3969/j.issn.1673-5552.2012.08.0055
28. Dang CC, Guan YK, Lau NS, Chan SY. Two Successful Deliveries of Healthy Children by a Young Woman Diagnosed and Treated During Induction and Relapsed Therapy for Acute Promyelocytic Leukemia. *J Oncol Pharm Pract* (2020) 26:2034–7. doi: 10.1177/1078155220915764
29. Su Y, Zhao W, Fan J. Clinical Analysis of 23 Cases of Acute Leukemia During Pregnancy (in Chinese). *Internal Med (China)* (2020) 15:759. doi: 10.16121/j.cnki.cn45-1347/r.2020.06.31
30. Zhu H. *Clinical Analysis and Literature Review of 26 Patients With Hematological Malignancies During Pregnancy (in Chinese)*. Ningxia: Ningxia Medical University (2021). doi: 10.27258/d.cnki.gnxyc.2021.000159
31. Meng X. *Clinical Analysis of 4 Patients With Leukaemia in Pregnancy (in Chinese)*. Dalian: Dalian Medical University (2014).
32. Pan D, Li Y. A Case of Successful Treatment of Acute Promyelocytic Leukemia in Pregnancy With All-trans Retinoic Acid and Arsenic Trioxide (in Chinese). *Chin J Pract Internal Med* (2007) S1:41. doi: 10.1007/s00404-017-4583-6
33. Niu J, Duan W, Cui X, Wei F, Fan X, Peng Y, et al. Analysis of Acute Promyelocytic Leukemia in Pregnancy With Arsenic Trioxide, All-trans Retinoic Acid and Chemotherapy (in Chinese). *J Pract Med Techniques.* (2013) 20:197–8. doi: 10.3969/j.issn.1671-5098.2013.02.055
34. Khosla H, Jain A, Tatawadiya S, Prasad P, Nagpal K, Chaudhry S, et al. First Report of Successful Management of Acute Promyelocytic Leukemia in a Pregnant Female With All-Trans-Retinoic Acid and Arsenic Trioxide-Based Induction Regimen. *Blood Cell Mol Dis* (2020) 85:102476. doi: 10.1016/j.bcmd.2020.102476
35. Bai L, Li C, Qi Y, Xu Y, Liu H, Wu G. A Case of Successful Full-Term Delivery of Acute Promyelocytic Leukemia in Pregnancy (in Chinese). *J Leuk Lymphoma (China)* (2012) 21:379–80. doi: 10.3760/cma.j.issn.1009-9921.2012.06.020
36. Wu HC, Rérolle D, de, Thé H. PML/RARA Destabilization by Hyperthermia: A New Model for Oncogenic Fusion Protein Degradation? *Blood Cancer Discovery* (2021) 2:300–1. doi: 10.1158/2643-3230.BCD-21-0071
37. Wang X, Qian Z, Li H, Chen H, Lin L, Guo M, et al. Evaluation of Arsenic Species in Leukocytes and Granulocytes of Acute Promyelocytic Leukemia Patients Treated With Arsenic Trioxide. *J Pharmaceut Biomed* (2021) 203:114201. doi: 10.1016/j.jpba.2021.114201
38. Guo M, Zhao Q, Fan S, Wu Z, Lin L, Chen H, et al. Characteristics of Arsenic Species in Cerebrospinal Fluid (CSF) of Acute Promyelocytic Leukemia (APL) Patients Treated With Arsenic Trioxide Plus Mannitol. *Brit J Clin Pharmaco* (2021) 87:4020–6. doi: 10.1111/bcp.14804
39. Liu W, Wang B, Zhao Y, Wu Z, Dong A, Chen H, et al. Pharmacokinetic Characteristics, Tissue Bioaccumulation and Toxicity Profiles of Oral Arsenic Trioxide in Rats: Implications for the Treatment and Risk Assessment of Acute Promyelocytic Leukemia. *Front Pharmacol* (2021) 12:647A87. doi: 10.3389/fphar.2021.647A87
40. Chen B, Lu X, Shen S, Arnold LL, Cohen SM, Le XC. Arsenic Speciation in the Blood of Arsenite-Treated F344 Rats. *Chem Res Toxicol* (2013) 26:952–62. doi: 10.1021/tx400123q
41. Chen GQ, Zhou L, Styblo M, Walton F, Jing Y, Weinberg R, et al. Methylated Metabolites of Arsenic Trioxide Are More Potent Than Arsenic Trioxide as Apoptotic But Not Differentiation Inducers in Leukemia and Lymphoma Cells. *Cancer Res* (2003) 63:1853–9. doi: 10.1016/S0165-4608(02)00840-3
42. Khairul I, Wang QQ, Jiang YH, Wang C, Naranmandura H. Metabolism, Toxicity and Anticancer Activities of Arsenic Compounds. *Oncotarget* (2017) 8:23905–26. doi: 10.18632/oncotarget.14733
43. Culligan DJ, Merriman L, Kell J, Parker J, Jovanovic JV, Smith N, et al. The Management of Acute Promyelocytic Leukemia Presenting During Pregnancy. *Clin Leuk* (2007) 1:183–91. doi: 10.3816/CLK.2007.n.006
44. Sanz MA, Grimwade D, Tallman MS, Lowenberg B, Fenaux P, Estey EH, et al. Management of Acute Promyelocytic Leukemia: Recommendations From An Expert Panel on Behalf of the European LeukemiaNet. *Blood* (2009) 113:1875–91. doi: 10.1051/0004-6361:20031716
45. Ammatuna E, Cavaliere A, Divona M, Amadori S, Scambia G, Lo-Coco F. Successful Pregnancy After Arsenic Trioxide Therapy for Relapsed Acute Promyelocytic Leukaemia. *Br J Haematol* (2009) 146:341. doi: 10.1111/j.1365-2141.2009.07756.x
46. Gupta S, Bagel B, Gujral S, Subramanian PG, Khattry N, Menon H, et al. Parenthood in Patients With Acute Promyelocytic Leukemia After Treatment With Arsenic Trioxide: A Case Series. *Leuk Lymphoma* (2012) 53:2192–4. doi: 10.3109/10428194.2012.679936

Conflict of Interest: The authors declare that the research was conducted in the absence of any commercial or financial relationships that could be construed as a potential conflict of interest.

frontiers | Frontiers in Pharmacology

ORIGINAL RESEARCH
published: 15 June 2022
doi: 10.3389/fphar.2022.912256

Myelodysplastic Syndrome/Acute Myeloid Leukemia Following the Use of Poly-ADP Ribose Polymerase (PARP) Inhibitors: A Real-World Analysis of Postmarketing Surveillance Data

Quanfeng Zhao[1], Pan Ma[1], Peishu Fu[1], Jiayu Wang[2,3], Kejing Wang[2,3], Lin Chen[2,3]* and Yang Yang[2,3]**

[1]Department of Pharmacy, The First Affiliated Hospital of Third Military Medical University (Army Medical University), Chongqing, China, [2]Department of Pharmacy, Women and Children's Hospital of Chongqing Medical University, Chongqing, China, [3]Department of Pharmacy, Chongqing Health Center for Women and Children, Chongqing, China

OPEN ACCESS

Edited by:
Yao Liu,
Daping Hospital, China

Reviewed by:
Dawid Sigorski,
University of Warmia and Mazury in Olsztyn, Poland
Jyothi Mahadevan,
University of Colorado Boulder, United States
Tarek El-hamoly,
Egyptian Atomic Energy Authority, Egypt

***Correspondence:**
Kejing Wang
wymwkj001@163.com
Lin Chen
cqfycl@126.com
Yang Yang
cqfyyy2020@163.com

Specialty section:
This article was submitted to Pharmacology of Anti-Cancer Drugs, a section of the journal Frontiers in Pharmacology

Received: 04 April 2022
Accepted: 27 May 2022
Published: 15 June 2022

Citation:
Zhao Q, Ma P, Fu P, Wang J, Wang K, Chen L and Yang Y (2022) Myelodysplastic Syndrome/Acute Myeloid Leukemia Following the Use of Poly-ADP Ribose Polymerase (PARP) Inhibitors: A Real-World Analysis of Postmarketing Surveillance Data. Front. Pharmacol. 13:912256. doi: 10.3389/fphar.2022.912256

Background and purpose: poly-ADP ribose polymerase (PARP) inhibitors show impressive efficacy in a range of tumors. However, concerns about rare and fatal adverse events, including myelodysplastic syndrome (MDS) and acute myelogenous leukemia (AML) have arisen. The aim of this study was to excavate and evaluate the risk of PARP inhibitors causing MDS and AML based on real-world data from two international pharmacovigilance databases.

Methods: We analyzed adverse event (AE) reports of four PARP inhibitors (olaparib, niraparib, rucaparib and talazoparib) associated with MDS and AML from the United States Food and Drug Administration (FDA) Adverse Event Reporting System (FAERS) and EudraVigilance (EV) databases between 1 October 2014, and 30 September 2021, including demographic characteristics, fatality and times to onset. Three different data mining algorithms were used to detect the signals of PARP inhibitors associated with MDS and AML.

Results: In total, 16,710 and 11,937 PARP inhibitor AE reports were found in the FAERS and EV databases, of which 332 and 349 were associated with MDS and AML, respectively. The median latencies of MDS and AML associated with PARP inhibitors were 211 [interquartile range (IQR) 93.5–491.25] days and 355 (IQR 72.00–483.50) days, respectively. The average fatality rates of MDS and AML caused by the four PARP inhibitors were 39.23 and 45.39%, respectively, in the FAERS database, while those in

Abbreviations: AE, adverse event; AML, Acute myeloid leukemia; BCPNN, Bayesian confidence propagation neural network; BRCA, breast cancer susceptibility protein; DNA, deoxyribonucleic acid; EV, EudraVigilance; EMA, European Medicines Agency; FDA, Food and Drug Administration; FAERS, FDA Adverse Event Reporting System; IQR, interquartile range; MedDRA, Medical Dictionary for Drug Regulatory Activities; MDS, Myelodysplastic syndrome; PARP, poly-ADP ribose polymerase; PRR, proportional reporting ratio; PT, preferred terms; RCT, randomized controlled trials; ROR, reporting odds ratio; WHO, World Health Organization.

the EV database were 32.32 and 34.94%, respectively. Based on the criteria used for the three algorithms, a significant disproportionate association was found between PARP inhibitors as a drug class and MDS/AML. Notably, the risk of MDS was much higher than that of AML. Olaparib appeared to have a stronger association with MDS and AML than did other PARP inhibitors.

Conclusion: In the real world, PARP inhibitors increase the risk of MDS and AML, which can result in high mortality and tend to occur during long-term use. Our findings provide objective evidence for the postmarketing safety of PARP inhibitors.

Keywords: PARP inhibitors, myelodysplastic syndrome, acute myeloid leukemia, pharmacovigilance, real-world

INTRODUCTION

In recent years, poly (ADP-ribose) polymerase (PARP) inhibitors, which rely on the mechanism of so-called synthetic sickness, have revolutionized the treatment of neoplasms, particularly in ovarian cancer (Lord and Ashworth, 2017). Four kinds of PARP inhibitors are approved by the Food and Drug Administration (FDA), including olaparib (Lynparza; AstraZeneca, initial FDA approval: December 2014), niraparib (Zejula, Tesaro, March 2017), rucaparib (Rubraca, Clovis Oncology, December 2016) and talazoparib (Talzenna, Pfizer, October 2018). A series of high-level evidence-based medical studies showed that PARP inhibitors have significant clinical benefits in patients with ovarian cancer (Coleman et al., 2017; Gonzalez-Martin et al., 2019; Ray-Coquard et al., 2019), breast cancer (Litton et al., 2018; Tutt et al., 2021), pancreatic cancer (Golan et al., 2019) and prostate cancer (Hussain et al., 2020).

However, with the increasing applications of PARP inhibitors, rare serious adverse reactions, especially myelodysplastic syndrome (MDS) and acute myeloid leukemia (AML), have become more prominent and are indicated by an FDA warning on the label. Although PARP inhibitors share the same mechanism of action, their specific toxicity profiles may vary considerably. Additionally, data from clinical trials showed low incidence rates of MDS and AML with PARP inhibitors, at between 0.5 and 1.4% (LaFargue et al., 2019). However, this measurement may be underestimated for assessing the association of PARP inhibitors with rare adverse events (AEs) because clinical trials have rigorous entry and exclusion criteria (such as excluding patients with higher burdens of comorbidities), relatively small sample sizes, and limited follow-up durations. Furthermore, the characteristics of MDS and AML caused by PARP inhibitors in the real world are poorly known. Therefore, the development of an understanding of their toxicity profiles by postmarketing pharmacovigilance is urgently needed.

The FDA Adverse Event Reporting System (FAERS) is the largest AE database in the world, containing more than 14 million reports. The FAERS database is considered the primary tool supporting the postmarketing safety surveillance of approved drugs and biologics. EudraVigilance (EV) is another public international spontaneously reported pharmacovigilance database for recording, managing and analyzing AEs in the European or non-European economic area and is maintained by the European Medicines Agency (EMA). Health care professionals, consumers, manufacturers and others can report AEs to the FAERS and EV databases. Analysis of the FAERS and EV databases provides a broader perspective for detecting AEs associated with newly approved drugs and rare AEs that occur in the real world (Pinheiro et al., 2016; Meng et al., 2019). The aim of this study was to characterize the association of PARP inhibitors (olaparib, rucaparib, niraparib, and talazoparib) with MDS/AML and to identify the signals of PARP inhibitor association with MDS/AML by utilizing real-world evidence.

METHODS

Data Sources

Four PARP inhibitors namely (generic name) olaparib, rucaparib, niraparib and talazoparib were selected as study drugs (AE reports were only included if a target drug was listed as the primary suspect). Data were retrieved from the public release of FAERS and EV database between 1 October 2014 (considering the FDA approved the first PARP inhibitors, olaparib on 19 December 2014) and the 30 September 2021. OpenVigil FDA, a pharmacovigilance tool, is a web-based user interface to the FAERS database for extraction and analysis of adverse event safety reports which has been successful verified by FDA(Bohm et al., 2021). For the present study, we used the OpenVigil FDA to analysis the data from FAERS. AE reports of PARP inhibitors from EV database are publicly available through the EMA website (www.adrreports.eu). In accordance with the pharmacovigilance legislation, FDA and EMA operate procedures that ensure the quality and integrity of data collected in FAERS and EV database the AE files from FDA and EMA were updated every quarter.

Definition of AEs

AEs are recoded using preferred terms (PTs) of the Medical Dictionary for Drug Regulatory Activities (MedDRA) terminology in FAERS and EV database. PT is a unique and clear expression in accordance with international standards for a single medical concept, and its specificity and description are strong. myelodysplastic syndrome (PT code: 10028533) and acute myeloid leukemia (PT code: 10000846) were selected as potential interest AEs for this study.

TABLE 1 | The characteristics of MDS reported by PARP inhibitors in FAERS and EV database.

	Olaparib		Niraparib		Rucaparib		Talazoparib		Total	
	FAERS	EV	FAERS	EV	FAERS	EV	FAERS	EV	FAERS	EV
Total cases	147	179	29	32	7	10	4	1	187	222
Age										
<18 y	0 (0)	0 (0)	0 (0)	0 (0)	0 (0)	0 (0)	0 (0)	0 (0)	0 (0)	0 (0)
18–64 y	50 (60.98)	75 (60.98)	8 (53.33)	8 (57.14)	1 (25.00)	4 (66.67)	1 (25.00)	0 (0)	60 (57.14)	87 (60.42)
65–85 y	31 (37.80)	47 (38.21)	7 (46.67)	6 (42.86)	3 (75.00)	2 (33.33)	3 (75.00)	1 (100.00)	44 (41.90)	56 (38.89)
>85 y	1 (1.22)	1 (0.81)	0 (0)	0 (0)	0 (0)	0 (0)	0 (0)	0 (0)	1 (0.95)	1 (0.69)
data available	82	123	15	14	4	6	4	1	105	144
Gender										
female	136 (99.27)	177 (99.44)	21 (95.45)	31 (96.88)	3 (75.00)	9 (90.00)	3 (75.00)	1 (100.00)	163 (97.60)	218 (98.64)
male	1 (0.73)	1 (0.56)	1 (4.55)	1 (3.13)	1 (25.00)	1 (10.00)	1 (25.00)	0 (0)	4 (2.40)	3 (1.36)
data available	137	178	22	32	4	10	4	1	167	221
Reporting region										
European Economic Area	68 (46.26)	89 (49.72)	11 (37.93)	18 (56.25)	4 (57.14)	3 (30.00)	3 (75.00)	1(100.00)	86(45.99)	111(50%)
Non-European Economic Area	79(53.74)	90(50.28)	18(62.07)	14(43.75)	3(42.86)	7(70.00)	1(25.00)	0(0)	101(54.01)	111(50%)
data available	147	179	29	32	7	10	4	1	187	222
Indication										
ovarian cancer	105(85.37)	134(93.06)	22(88.00)	18(90.00)	2(50.00)	3(75.00)	0(0)	0(0)	129(82.69)	155(91.72)
breast cancer	8(6.50)	5(3.47)	1(4.00)	1(5.00)	0(0)	0(0)	2(50.00)	1(100.00)	11(7.05)	7(4.14)
pancreatic carcinoma	2(1.63)	0(0)	0(0)	0(0)	0(0)	0(0)	0(0)	0(0)	2(1.28)	0(0)
prostate cancer	1(0.81)	0(0)	0(0)	0(0)	0(0)	0(0)	2(50.00)	0(0)	3(1.92)	0(0)
other malignant neoplasm	7(5.69)	5(3.47)	2(8.00)	1(5.00)	2(50.00)	1(25.00)	0(0)	0(0)	11(7.05)	7(4.14)
data available	123	144	25	20	4	4	4	1	156	169

In this study, the inclusion criteria for AE report were that PARP inhibitor as "primary suspected drug". Besides, we collected administrative and clinical characteristics of AE reports when data were available, including patient features (sex, age and country of origin), drug information (indication, concomitant drugs, therapy start dates and end dates), and final patient outcomes. We removed duplicated and aberrant reports (such as the date of adverse event occurrence is earlier than the start time of medication).

Statistical Analysis

Disproportionality analyses were commonly used to identify potential safety signals for AEs in the FAERS, including the established pharmacovigilance algorithms reporting odds ratio (ROR), proportional reporting ratio (PRR) and Bayesian confidence propagation neural network (BCPNN). Each method has its own characteristics, ROR or PRR algorithm has high sensitivity, but it is easy to produce false positive signals when the number of AE reports is not enough (Rothman et al., 2004). Bayesian algorithm has good stability, but the signal detection time is lagged (Bate, 2007). In order to reduce the bias caused by using a single algorithm as much as possible, three different data mining algorithms (ROR, PRR and BCPNN) were used for signal detection in this study. When all the three algorithms are positive, the signal is judged as suspicious AE signal. the equations and criteria for the three algorithms are shown in **Supplementary Table S2**, which is based on the fourfold table of disproportionality measurement (**Supplementary Table S1**).

Only FAERS can realize signal detection by using open database gratuitous, Therefore, we detected the signal value of PARP inhibitors associated with MDS and AML only in FAERS. Moreover, we summarized the time to onset for AEs of interest only in EV database due to data limitation and the analysis was conducted by GraphPad Prism (version 8.3.0).

RESULTS

Descriptive Analysis

During the study period, a total of 16,710 AE reports corresponding to PARP inhibitors were extracted from the FAERS database, including 5670 for olaparib, 8211 for niraparib, 2475 for rucaparib and 354 for talazoparib. Among these cases, the total numbers of MDS and AML AE cases were 187 and 145, respectively. In addition, the EV database presented a total of 11,937 events corresponding to PARP inhibitors, including 5493 for olaparib, 4854 for niraparib, 1428 for rucaparib and 198 for talazoparib. The total numbers of potential AEs of interest for PARP inhibitors were 222 and 127. The most frequently reported drug in the two databases was olaparib. **Table 1** shows the characteristics for MDS reported with PARP inhibitors in the two databases, and **Table 2** shows the same for AML. In these PARP associated with MDS/AML cases, we noted cases exposed to PARP inhibitors were similar between the European economic area and non-European economic area. More than 80% PARP inhibitors were used for ovarian cancer treatment(**Table 3**), and the patient gender of MDS and AML caused by the four PARP inhibitors were 97.6 and 91.73%, respectively, in the FAERS database, while those in EV database were 98.64 and 92.56%.

TABLE 2 | The characteristics of AML reported by PARP inhibitors in FAERS and EV database.

	Olaparib		Niraparib		Rucaparib		Talazoparib		Total	
	FAERS	EV	FAERS	EV	FAERS	EV	FAERS	EV	FAERS	EV
Total cases	110	103	30	19	4	5	1	0	145	127
Age										
<18 y	1(1.33)	1(1.47)	0(0)	0(0)	0(0)	0(0)	0(0)	0(0)	1(0.99)	1(1.20)
18–64 y	42(56.00)	29(42.65)	15(65.22)	9(69.23)	2(100.00)	0(0)	1(100.00)	0(0)	60(59.41)	38(45.78)
65–85 y	30(40.00)	36(52.94)	7(30.43)	4(30.77)	0(0)	2	0(0)	0(0)	37(36.63)	42(50.60)
>85 y	2(2.67)	2(2.94)	1(4.35)	0(0)	0(0)	0(0)	0(0)	0(0)	3(2.97)	2(2.41)
data available	75	68	23	13	2	2	1	0	101	83
Gender										
female	94(91.26)	95(93.14)	23(92.00)	12(85.71)	4(100.00)	5(100.00)	1(100.00)	0(0)	122(91.73)	112(92.56)
male	9(8.74)	7(6.86)	2(8.00)	2(14.29)	0(0)	0(0)	0(0)	0(0)	11(8.27)	9(7.44)
data available	103	102	25	14	4	5	1	0	133	121
Reporting region										
European Economic Area	53(48.18)	56(54.37)	17(56.67)	9(47.37)	1(25.00)	0(0)	1(100.00)	0(0)	72(49.66)	65(51.18)
Non-European Economic Area	57(51.82)	47(45.63)	13(43.33)	10(52.63)	3(75.00)	5(100.00)	0(0)	0(0)	73(50.34)	62(48.82)
data available	110	103	30	19	4	5	4	0	145	127
Indication										
ovarian cancer	77(81.05)	77(89.53)	18(90.00)	11(100.00)	2(100.00)	1(100.00)	0(0)	0(0)	97(82.20)	89(90.82)
breast cancer	3(3.16)	3(3.49)	0(0)	0(0)	0(0)	0(0)	1(100.00)	0(0)	4(3.39)	3(3.06)
prostate cancer	6(6.32)	6(6.98)	0(0)	0(0)	0(0)	0(0)	0(0)	0(0)	6(5.08)	6(6.12)
other malignant neoplasm	9(9.47)	0(0)	2(10.00)	0(0)	0(0)	0(0)	0(0)	0(0)	11(9.32)	0(0)
data available	95	86	20	11	2	1	1	0	118	98

TABLE 3 | Top 3 concomitant medications for PARP inhibitors associated with MDS and AML from FAERS and EV databases.

	Olaparib(N[a])		Niraparib(N)		Rucaparib(N)		Talazoparib(N)	
	FAERS	EV	FAERS	EV	FAERS	EV	FAERS	EV
MDS	Carboplatin (70)	Carboplatin (31)	Carboplatin (14)	Rivaroxaban (5)	Carboplatin (2)	Ondansetron (2)	—	—
	Paclitaxel (47)	Paclitaxel (26)	Doxorubicin (13)	Carboplatin (2)	paclitaxel (1)	Colecalciferol (2)	—	—
	Doxorubicin (26)	Bevacizumab (10)	Cisplatin (7)	Doxorubicin (2)	Gabapentin (1)	Bevacizumab (1)	—	—
AML	Carboplatin (28)	Carboplatin (32)	Acetaminophen (6)	Doxorubicin (4)	Acetaminophen (6)	Melatonin (1)	Enzalutamide (1)	—
	Paclitaxel (13)	Paclitaxel (23	Budesonide and formoterol fumarate (6)	Carboplatin (2)	Azacytidine (1)	—	—	—
	Bevacizumab (9)	Bevacizumab (15)	Calcium and vitamin D (4)	Cisplatin (1)	Binpcrit (1)	—	—	—

[a]*If the same number of cases are encountered, they are showed in alphabetical order.*

TABLE 4 | The serious outcome of MDS and AML reported by PARP inhibitors in FAERS and EV database[a].

	Olaparib		Niraparib		Rucaparib		Talazoparib		Total	
	MDS	AML	MDS	AML	MDS	AML	MDS	AML	MDS	AML
FAERS	147	110	29	30	7	4	4	1	187	145
death	36(41.38)	50(48.54)	10(33.33)	16(39.02)	3(42.86)	2(40.00)	2(33.33)	1(33.33)	51(39.23)	69(45.39)
life-threatening	26(29.89)	27(26.21)	11(36.67)	19(46.34)	1(14.86)	1(20.00)	1(16.67)	1(33.33)	39(30.00)	48(31.58)
hospital prolonged	23(26.44)	25(24.27)	7(23.33)	5(12.20)	3(42.86)	2(40.00)	3(50.00)	1(33.33)	36(27.69)	33(21.71)
disablity	2(2.30)	1(0.97)	2(6.67)	1(2.44)	0(0.00)	0(0.00)	0(0.00)	0(0.00)	4(3.07)	2(1.32)
data available	87	103	30	41	7	5	6	3	130	152
EV	179	103	32	19	10	5	4	1	222	127
death	27(36.49)	24(34.78)	4(19.05)	5(35.71)	1(33.33)	0(0.00)	0(0.00)	0(0.00)	32(32.32)	29(34.94)
life-threatening	25(33.78)	21(30.43)	7(33.33)	4(28.57)	0(0.00)	0(0.00)	0(0.00)	0(0.00)	32(32.32)	25(30.12)
hospital prolonged	18(24.32)	22(31.88)	9(42.86)	5(35.71)	2(66.67)	0(0.00)	1(100.00)	0(0.00)	30(30.30)	27(32.53)
disablity	4(5.41)	2(2.90)	1(4.76)	0(0.00)	0(0.00)	0(0.00)	0(0.00)	0(0.00)	5(5.51)	2(2.41)
data available	74	69	21	14	3	0	1	0	99	83

[a]*Multiple outcomes can be reported for the same report.*

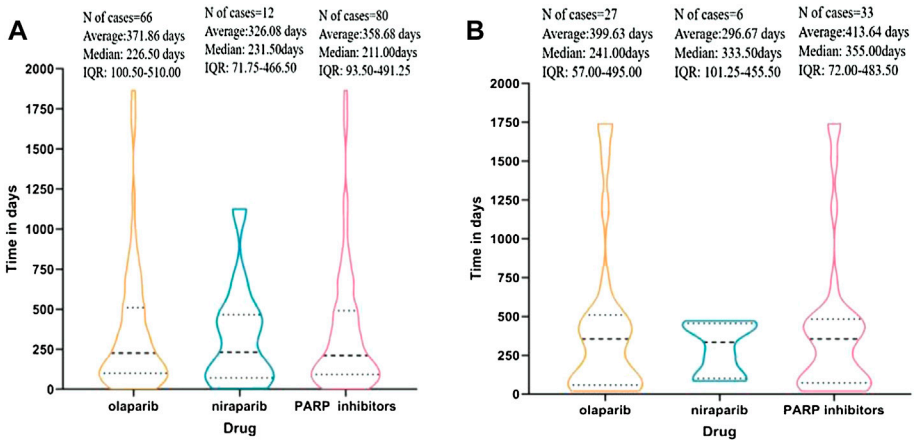

FIGURE 1 | (A) Time to event onset of myelodysplastic syndrome (MDS) following olaparib and niraparib. **(B)** Time to event onset of acute myeloid leukemia (AML) following olaparib and niraparib. Data on rucaparib and talazoparib are not available since the missing data (number of cases < 4).

Outcome of MDS and AML Reported By PARP Inhibitors in Two Databases

To determine the fatal risk, we measured the mortality rates of MDS and AML reported along with the four targeted PARP inhibitors in the two databases, and the generated results are shown in **Table 4**. We found that the mortality rate in the FAERS database was higher than that in the EV database; the universal mortality rates of MDS and AML caused by the four PARP inhibitors in the FAERS database were 39.23 and 45.39%, while those in the EV database were 32.32 and 34.94%, respectively.

Time to Onset of MDS and AML Reported By PARP Inhibitors in EV Databases

Overall, the median times to all PARP inhibitor-related MDS and AML events were 211 [interquartile range (IQR) 93.50–491.25] days and 355 (IQR 72.00–483.50) days, respectively. We display the time to onset of MDS/AML events for each PARP inhibitor in **Figures 1A,B**. The times to occurrence of MDS/AML ranged from the first days or weeks to 1 year or more after the start of therapy, with most times concentrated within 1 year. Because of the scantness of data, the times to MDS and AML event were not computed for rucaparib and talazoparib.

Disproportionality Analysis of MDS/AML Associated With PARP Inhibitors

Based on the criteria used for the three algorithms in the FAERS database, a significant disproportionate association was found between PARP inhibitors as a drug class and MDS and AML [**MDS**: 16.94 (14.66–19.57) for ROR, 16.76 (14.52–19.34) for PRR and 4.06 (3.51–4.69) for IC; **AML**: 12.85 (10.91–15.14) for ROR, 12.75 (10.84–14.99) for PRR and 3.66 (3.11–4.32) for IC]. For each PARP inhibitor, the association results are showed in **Figure 2**. The signal scores suggest that all four PARP inhibitors are associated with MDS. The relationship of olaparib with MDS was noteworthy due to having the highest ROR, PRR and BCPNN values [40.49 (34.3–47.78) for ROR, 39.46 (33.58–46.38) for PRR and 5.27 (4.54–6.12) for IC], whereas the signal values of rucaparib-related MDS were the weakest [4.22 (2.01–8.86) for ROR, 4.21 (2.01–8.82) for PRR and 2.07 (1.64–2.62) for IC]. Concerning AML, the signal scores suggest that only olaparib and niraparib are associated with AML, whereas no significant signals were detected for rucaparib (the 95% CI of ROR and PRR value is lower than 1) and talazoparib (the 95% CI of ROR and PRR value is lower than 1 and the cases of interest reported is lower than 3; the standard of signal detection are shown in **Supplementary Tables S1, S2**). Olaparib also had the highest signal values for AML [29.39 (24.29–35.55) for ROR, 28.84 (23.93–34.76) for PRR and 4.83 (4.15–5.6) for IC].

DISCUSSION

PARP inhibitors that are in the same category of drugs show some of the same toxic characteristics, but different drugs have different adverse reactions, and they vary in frequency and severity (Staropoli et al., 2018). Previous studies have shown that common toxicities among PARP inhibitors include hematological toxicity, gastrointestinal adverse reactions, nephrotoxicity, and fatigue, which usually occur during the first 3 months of treatment (LaFargue et al., 2019). However, a few randomized controlled trials (RCTs) have reported MDS and AML in patients using PARP inhibitors and indicated possible delayed toxicity of PARP inhibitor therapy (Mirza et al., 2016; Coleman et al., 2017).

To the best of our knowledge, this is the first pharmacovigilant analysis of MDS and AML adverse events associated with PARP inhibitors utilizing the FAERS and EV databases. Myelodysplastic syndrome and acute leukemia, these rare, serious and delayed adverse reactions, are the most concerning adverse reactions associated with PARP inhibitors therapy. Current literature

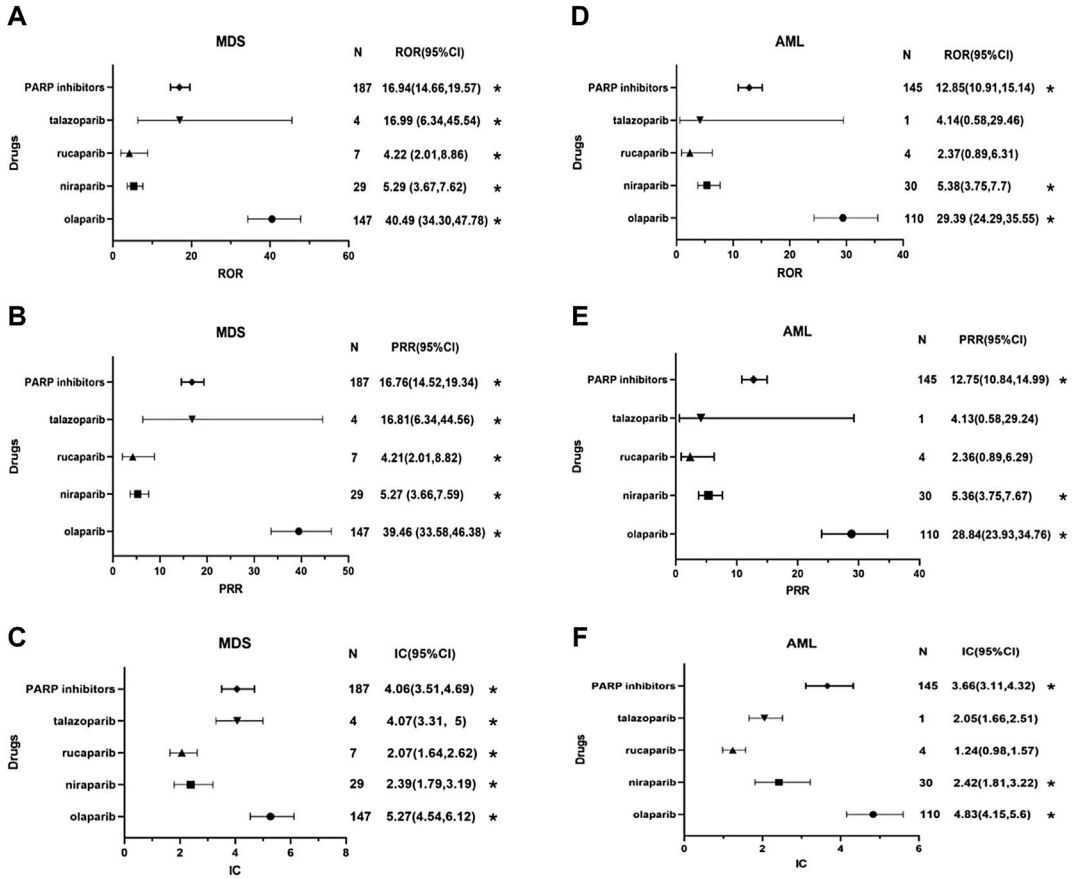

FIGURE 2 | Forest plots of disproportionality analysis of MDS/AML associated with PARP inhibitors. * Statistically significant disproportionality (the standard of signal detection in the **Supplementary Table S2**). Abbreviation: MDS, myelodysplastic syndrome; AML, acute myeloid leukemia; N, the number of reports of PARP-associated myelodysplastic syndrome or acute myeloid leukemia; CI, confidence interval; ROR, reporting odds ratio; PRR, proportional reporting ratio; IC, information component; PARP inhibitors, poly (ADP-ribose) polymerase inhibitors. **(A)** the reporting odds ratio (ROR) distribution of MDS reported by PARP inhibitors. **(B)** the proportional reporting ratio (PRR) distribution of MDS reported by PARP inhibitors. **(C)** the information component (IC) distribution of MDS reported by PARP inhibitors. **(D)** the reporting odds ratio (ROR) distribution of AML reported by PARP inhibitors. **(E)** the proportional reporting ratio (PRR) distribution of AML reported by PARP inhibitors. **(F)** the information component (IC) distribution of AML reported by PARP inhibitors.

reveals inconsistent conclusions about the associations of PARP inhibitors with MDS and AML. A meta-analysis of 5739 patients from 14 RCTs showed no significant association between PARP inhibitors and the incidence rates of MDS and AML (Nitecki et al., 2021). In some RCTs or meta-analyses, rare or delayed adverse events were not fully captured during short-term follow-up and may be affected by the size of the dataset. On the other hand, the final analysis of SOLO-2, which is the largest related long-term follow-up study that has been conducted, suggested that olaparib may cause MDS and AML (Poveda et al., 2021). A meta-analysis of 9099 patients from 28 RCTs and a retrospective study of the World Health Organization (WHO) pharmacovigilance database demonstrated that the combination of PARP inhibitors significantly increased the risk of MDS and AML (Peto OR 2.63 [95% CI 1·13–6·14], p = 0·026) (Morice et al., 2021). In another study, an increased risk of MDS/AML was observed in real-world patients who received PARP inhibitors (Ma et al., 2021; Matsuo et al., 2021). Our findings are consistent with the results of these epidemiological studies and meta-analyses. In addition, we have enumerated the following notable and interesting findings:

First, the risk of MDS related to PARP inhibitors was much higher than that of AML. MDS shares the clinical and pathological features of AML but shows a lower percentage of primitive cells in the peripheral blood and bone marrow (<20%) (Arber et al., 2016). Patients with MDS may develop symptomatic anemia, infection, and bleeding and may transition to having AML, and the incidence rates of MDS and AML are also different (Siegel et al., 2012; McQuilten et al., 2014). Our findings indicate that PARP inhibitors are associated with a higher risk of MDS than AML in a "real world" setting. According to the results of the meta-analysis involving several RCTs, there were no significant differences between the risks of MDS and AML associated with PARP inhibitors, which may account for differences between the real world and RCTs with rigorous study entry criteria (Morice et al., 2021). Indeed, a previous study showed that the power of RCTs to detect AEs was weak, especially for rarer AEs (Salem et al., 2021). Additional analysis is necessary based on the observed differences between RCTs and the "real world".

Second, MDS and AML signals were detected for PARP inhibitors as a drug class included in this study, suggesting that MDS and AML may be common AEs to PARP inhibitors. However, rucaparib and talazoparib-related AML showed no positive signals, which may be related to the short marketing time of these PARP inhibitors, and further studies on the risk of AEs associated with rucaparib and talazoparib are needed. Poly (ADP-ribose) polymerases are a family of enzymes that use the oxidized form of nicotinamide adenine dinucleotide to transfer ADP-ribose to other proteins (poly ADP-ribosylation). They are involved in deoxyribonucleic acid (DNA) damage response, regulation of apoptosis, and maintenance of genomic stability (Anderson et al., 2016). The anti-cancer mechanism of PARP inhibitors mainly includes two factors. PARP inhibitors can inhibit the activity of PARP enzymes and prevent DNA single-strand repair. PARP inhibitors can also stabilize the structure of DNA-PARP complexes and hinder their separation. This process, also known as trapping, results in long-term existence of DNA-PARP complexes that inhibit subsequent DNA repair processes (Murai et al., 2014). The exact mechanisms by which PARP inhibitor induces MDS and AML are unknown and may be multifaceted. Myeloid neoplasms, including MDS and AML, are heterogeneous diseases with multiple potential molecular abnormalities, characterized by high chromosomal instability, which is considered to be caused by the wrong DNA damage repair mechanism (Esposito and So, 2014). PARP family proteins play an important role in maintaining hematopoietic function, and the regulation of the expression of PARP family proteins differs between acute myelogenous leukemia cells and healthy cells (Gil-Kulik et al., 2020). PARP inhibitors can lead to acquired mutations with clonal hematopoiesis in the circulatory system through DNA-damaging reactions, thereby increasing the risk of MDS and AML. Additionally, PARP inhibitors may also cause off-target epigenetic changes that can result in MDS and AML through potential clonal hematopoietic transformations (Bolton et al., 2020). Besides, there were interactions between breast cancer susceptibility protein 1 or 2 (BRCA1 or BRCA 2) mutations and Fanconi Anemia proteins in the homologous recombination pathway. Some data suggest that BRCA deficiency may increase the risk of MDS/AML (Friedenson, 2007). These molecular studies might help explain some of the myeloid symptoms reported by patients using PARP inhibitors. Furthermore, concomitant medications should also be considered because the use of alkylating agents, topoisomerase inhibitors, platinum drugs, and bevacizumab has been reported to significantly increase the risk of MDS/AML (Shenolikar et al., 2018; Morton et al., 2019). According to information in the FAERS and EV databases, PARP inhibitors were mostly used for ovarian cancer treatment, and the common concomitant medications for PARP inhibitors were carboplatin and paclitaxel. Platinum-and-paclitaxel-based chemotherapy is the standard first-line chemotherapeutic regimen for ovarian cancer. Therefore, we cannot rule out the possibility that the combination of PARP inhibitors and chemotherapy drugs might increase the risk of MDS and AML. Overall, the mechanism of PARP inhibitors causing MDS/AML still needs to be further studied by relevant studies.

In addition, the results of the three signal mining methods showed that olaparib had the highest signal values for MDS and AML compared with those of other PARP inhibitors, indicating that olaparib had stronger associations with MDS and AML. it is difficult to explain the discrepancies between various PARP inhibitors, cases of olaparib-induced MDS have been noted in clinical practice (Moore et al., 2018). Some insights on the pharmacodynamic characteristics of PARP inhibitors have shown that olaparib among PARP inhibitors has a submifromolar potency on the PARP protein family (Thorsell et al., 2017), as increased PARP trapping has been proved to be associated with high myelosuppression (Hopkins et al., 2019). It remains to be further confirmed whether these characteristics of olaparib are likely to be highly correlated with MDS and AML, and the head-to-head comparison clinical studies are needed in the future.

Third, we observed that the prognoses of MDS and AML were not optimistic, leading to as high as 30% mortality and life-threatening rates, especially the universal mortality rates was 39.23 and 45.39% in the FAERS database. This result is similar to the finding reported in a recent study based on the WHO pharmacovigilance database (45.2%) (Morice et al., 2021). Even more worrisome, a SEER study reported that MDS/AML-related mortality can be as high as 78% (Morton et al., 2019). We should increase clinical vigilance regarding PARP inhibitor associations with MDS and AML. If the patient has persistent cytopenias, further investigations are recommended, including bone marrow analysis and blood samples for cytogenetics, and consideration of discontinuation of PARP inhibitors. If MDS or AML is confirmed, PARP inhibitors must be discontinued. American Society of Clinical Oncology guidelines also suggest that evaluations of treatment related MDS and AML should be initiated in patients with persistent cytopenia despite drug withdrawal (Tew et al., 2020).

Fourth, the timing of AE occurrence varies for each PARP inhibitor, and our study indicated that the risk of MDS/AML usually emerged after long-term treatment, which is in line with the results of previous studies (Mirza et al., 2016; Pujade-Lauraine et al., 2017). Care should be taken when prescribing these drugs for long-term use. Specifically, the first 1 year can be considered the "critical pharmacovigilance window" for olaparib and niraparib.

In this study, the detection signals of PARP inhibitor-related MDS and AML in two international pharmacovigilance databases were analyzed by the ROR, PRR and BCPNN methods, which can reflect the safety of drugs in the real world to a certain extent. However, we acknowledge several inherent limitations in our study. First, the incidence of adverse events could not be calculated due to the lack of overall drug use data. Second, although ROR, PRR and BCPNN are quantitative signal detection methods, they are only simple indicators of potential safety problems and can only indicate whether there is statistical correlation between drugs and AEs. Third, the spontaneous AE reports in the databases are arbitrary and biased and can include characteristics such as underreporting and missing information, which could also have affected the results.

Despite these limitations, the findings of this study indicate potential safety problems regarding the development of MDS and AML when using PARP inhibitors. Such adverse reactions are rare but lethal, and these results can provide a reference for clinical workers in the use of PARP inhibitors.

CONCLUSION

In this study, the results indicated that the use of PARP inhibitors may lead to MDS and AML toxicity, and the potential associations of olaparib were stronger. In addition, MDS and AML often occur in patients with long-term medication use, and their mortality rates are high. It was suggested that clinicians should pay more attention to the risk of MDS and AML when using PARP inhibitors. Our findings provide objective evidence for the postmarketing safety of PARP inhibitors.

DATA AVAILABILITY STATEMENT

The datasets presented in this study can be found in online repositories. The names of the repository/repositories and accession number(s) can be found below: http://openvigil.sourceforge.net/; https://www.adrreports.eu/.

ETHICS STATEMENT

This study uses public data to be identified without any form of ethical approval.

AUTHOR CONTRIBUTIONS

QZ took primary responsibility for conducting this study. YY and QZ drafted the manuscript with support from PM, PF, and GX. QZ, YY, LC, and KW contributed to conception and study design, and others authors participated in data collection, analyses, and interpretation, and approved the manuscript and approved the final version.

FUNDING

Natural Science Foundation Project of Chongqing Health Center for Women and Children (2020YJQN04 and 2021YJMS07). Chongqing Clinical Pharmacy Key Specialties Construction Project.

ACKNOWLEDGMENTS

This study was assisted by Doctor Ganfeng Xie, which come from Department of Oncology, Southwest Hospital, Third Military Medical University (Army Medical University). We hereby thank him for his help.

SUPPLEMENTARY MATERIAL

The Supplementary Material for this article can be found online at: https://www.frontiersin.org/articles/10.3389/fphar.2022.912256/full#supplementary-material

REFERENCES

Anderson, R. C., Makvandi, M., Xu, K., Lieberman, B. P., Zeng, C., Pryma, D. A., et al. (2016). Iodinated Benzimidazole PARP Radiotracer for Evaluating PARP1/2 Expression *In Vitro* and *In Vivo*. *Nucl. Med. Biol.* 43 (12), 752–758. doi:10.1016/j.nucmedbio.2016.08.007

Arber, D. A., Orazi, A., Hasserjian, R., Thiele, J., Borowitz, M. J., Le Beau, M. M., et al. (2016). The 2016 Revision to the World Health Organization Classification of Myeloid Neoplasms and Acute Leukemia. *Blood* 127 (20), 2391–2405. doi:10.1182/blood-2016-03-643544

Bate, A. (2007). Bayesian Confidence Propagation Neural Network. *Drug Saf.* 30 (7), 623–625. doi:10.2165/00002018-200730070-00011

Böhm, R., Bulin, C., Waetzig, V., Cascorbi, I., Klein, H. J., and Herdegen, T. (2021). Pharmacovigilance-based Drug Repurposing: The Search for Inverse Signals via OpenVigil Identifies Putative Drugs against Viral Respiratory Infections. *Br. J. Clin. Pharmacol.* 87 (11), 4421–4431. doi:10.1111/bcp.14868

Bolton, K. L., Moukarzel, L. A., Ptashkin, R., Gao, T., Patel, M., Caltabellotta, N., et al. (2020). The Impact of Poly ADP Ribose Polymerase (PARP) Inhibitors on Clonal Hematopoiesis. *J. Clin. Oncol.* 38 (15), 1513. doi:10.1200/JCO.2020.38.15_suppl.1513

Coleman, R. L., Oza, A. M., Lorusso, D., Aghajanian, C., Oaknin, A., Dean, A., et al. (2017). Rucaparib Maintenance Treatment for Recurrent Ovarian Carcinoma after Response to Platinum Therapy (ARIEL3): a Randomised, Double-Blind, Placebo-Controlled, Phase 3 Trial. *Lancet* 390 (10106), 1949–1961. doi:10.1016/S0140-6736(17)32440-6

Esposito, M. T., and So, C. W. (2014). DNA Damage Accumulation and Repair Defects in Acute Myeloid Leukemia: Implications for Pathogenesis, Disease Progression, and Chemotherapy Resistance. *Chromosoma* 123 (6), 545–561. doi:10.1007/s00412-014-0482-9

Friedenson, B. (2007). The BRCA1/2 Pathway Prevents Hematologic Cancers in Addition to Breast and Ovarian Cancers. *BMC Cancer* 7, 152. doi:10.1186/1471-2407-7-152

Gil-Kulik, P., Dudzińska, E., Radzikowska-Büchner, E., Wawer, J., Jojczuk, M., Nogalski, A., et al. (2020). Different Regulation of PARP1, PARP2, PARP3 and TRPM2 Genes Expression in Acute Myeloid Leukemia Cells. *BMC Cancer* 20 (1), 435. doi:10.1186/s12885-020-06903-4

Golan, T., Hammel, P., Reni, M., Van Cutsem, E., Macarulla, T., Hall, M. J., et al. (2019). Maintenance Olaparib for Germline BRCA-Mutated Metastatic Pancreatic Cancer. *N. Engl. J. Med.* 381 (4), 317–327. doi:10.1056/NEJMoa1903387

González-Martín, A., Pothuri, B., Vergote, I., DePont Christensen, R., Graybill, W., Mirza, M. R., et al. (2019). Niraparib in Patients with Newly Diagnosed Advanced Ovarian Cancer. *N. Engl. J. Med.* 381 (25), 2391–2402. doi:10.1056/NEJMoa1910962

Hopkins, T. A., Ainsworth, W. B., Ellis, P. A., Donawho, C. K., DiGiammarino, E. L., Panchal, S. C., et al. (2019). PARP1 Trapping by PARP Inhibitors Drives Cytotoxicity in Both Cancer Cells and Healthy Bone Marrow. *Mol. Cancer Res.* 17 (2), 409–419. doi:10.1158/1541-7786.Mcr-18-0138

Hussain, M., Mateo, J., Fizazi, K., Saad, F., Shore, N., Sandhu, S., et al. (2020). Survival with Olaparib in Metastatic Castration-Resistant Prostate Cancer. *N. Engl. J. Med.* 383 (22), 2345–2357. doi:10.1056/NEJMoa191144010.1056/NEJMoa2022485

LaFargue, C. J., Dal Molin, G. Z., Sood, A. K., and Coleman, R. L. (2019). Exploring and Comparing Adverse Events between PARP Inhibitors. *Lancet Oncol.* 20 (1), E15–E28. doi:10.1016/S1470-2045(18)30786-1

Litton, J. K., Rugo, H. S., Ettl, J., Hurvitz, S. A., Gonçalves, A., Lee, K. H., et al. (2018). Talazoparib in Patients with Advanced Breast Cancer and a Germline BRCA Mutation. *N. Engl. J. Med.* 379 (8), 753–763. doi:10.1056/NEJMoa1802905

Lord, C. J., and Ashworth, A. (2017). PARP Inhibitors: Synthetic Lethality in the Clinic. *Science* 355 (6330), 1152–1158. doi:10.1126/science.aam7344

Ma, Z., Sun, X. M., Lu, W. C., Zhao, Z. X., Xu, Z. M., Lyu, J. Y., et al. (2021). Poly(ADP-ribose) Polymerase Inhibitor-Associated Myelodysplastic Syndrome/acute Myeloid Leukemia: a Pharmacovigilance Analysis of the FAERS Database. *ESMO Open* 6 (1), 100033. doi:10.1016/j.esmoop.2020.100033

Matsuo, K., Klar, M., Mohrbacher, A. F., Roman, L. D., and Wright, J. D. (2021). Secondary Haematologic Malignancies in Women with Ovarian Cancer Receiving Poly-ADP Ribose Polymerase Inhibitor Therapy. *Eur. J. Cancer* 157, 59–62. doi:10.1016/j.ejca.2021.08.016

McQuilten, Z. K., Wood, E. M., Polizzotto, M. N., Campbell, L. J., Wall, M., Curtis, D. J., et al. (2014). Underestimation of Myelodysplastic Syndrome Incidence by Cancer Registries: Results from a Population-Based Data Linkage Study. *Cancer* 120 (11), 1686–1694. doi:10.1002/cncr.28641

Meng, L., Huang, J., Jia, Y., Huang, H., Qiu, F., and Sun, S. (2019). Assessing Fluoroquinolone-Associated Aortic Aneurysm and Dissection: Data Mining of the Public Version of the FDA Adverse Event Reporting System. *Int. J. Clin. Pract.* 73 (5), e13331. doi:10.1111/ijcp.13331

Mirza, M. R., Monk, B. J., Herrstedt, J., Oza, A. M., Mahner, S., Redondo, A., et al. (2016). Niraparib Maintenance Therapy in Platinum-Sensitive, Recurrent Ovarian Cancer. *N. Engl. J. Med.* 375 (22), 2154–2164. doi:10.1056/NEJMoa1611310

Moore, K., Colombo, N., Scambia, G., Kim, B. G., Oaknin, A., Friedlander, M., et al. (2018). Maintenance Olaparib in Patients with Newly Diagnosed Advanced Ovarian Cancer. *N. Engl. J. Med.* 379 (26), 2495–2505. doi:10.1056/NEJMoa1810858

Morice, P. M., Leary, A., Dolladille, C., Chrétien, B., Poulain, L., González-Martín, A., et al. (2021). Myelodysplastic Syndrome and Acute Myeloid Leukaemia in Patients Treated with PARP Inhibitors: a Safety Meta-Analysis of Randomised Controlled Trials and a Retrospective Study of the WHO Pharmacovigilance Database. *Lancet Haematol.* 8 (2), e122–e134. doi:10.1016/S2352-3026(20)30360-4

Morton, L. M., Dores, G. M., Schonfeld, S. J., Linet, M. S., Sigel, B. S., Lam, C. J. K., et al. (2019). Association of Chemotherapy for Solid Tumors with Development of Therapy-Related Myelodysplastic Syndrome or Acute Myeloid Leukemia in the Modern Era. *JAMA Oncol.* 5 (3), 318–325. doi:10.1001/jamaoncol.2018.5625

Murai, J., Huang, S. Y., Renaud, A., Zhang, Y., Ji, J., Takeda, S., et al. (2014). Stereospecific PARP Trapping by BMN 673 and Comparison with Olaparib and Rucaparib. *Mol. Cancer Ther.* 13 (2), 433–443. doi:10.1158/1535-7163.MCT-13-0803

Nitecki, R., Melamed, A., Gockley, A. A., Floyd, J., Krause, K. J., Coleman, R. L., et al. (2021). Incidence of Myelodysplastic Syndrome and Acute Myeloid Leukemia in Patients Receiving Poly-ADP Ribose Polymerase Inhibitors for the Treatment of Solid Tumors: A Meta-Analysis of Randomized Trials. *Gynecol. Oncol.* 161 (3), 653–659. doi:10.1016/j.ygyno.2021.03.011

Pinheiro, L., Blake, K., Januskiene, J., Yue, Q. Y., and Arlett, P. (2016). Geographical Variation in Reporting Interstitial Lung Disease as an Adverse Drug Reaction: Findings from an European Medicines Agency Analysis of Reports in EudraVigilance. *Pharmacoepidemiol Drug Saf.* 25 (6), 705–712. doi:10.1002/pds.3998

Poveda, A., Floquet, A., Ledermann, J. A., Asher, R., Penson, R. T., Oza, A. M., et al. (2021). Olaparib Tablets as Maintenance Therapy in Patients with Platinum-Sensitive Relapsed Ovarian Cancer and a BRCA1/2 Mutation (SOLO2/ENGOT-Ov21): a Final Analysis of a Double-Blind, Randomised, Placebo-Controlled, Phase 3 Trial. *Lancet Oncol.* 22 (5), 620–631. doi:10.1016/S1470-2045(21)00073-5

Pujade-Lauraine, E., Ledermann, J. A., Selle, F., Gebski, V., Penson, R. T., Oza, A. M., et al. (2017). Olaparib Tablets as Maintenance Therapy in Patients with Platinum-Sensitive, Relapsed Ovarian Cancer and a BRCA1/2 Mutation (SOLO2/ENGOT-Ov21): a Double-Blind, Randomised, Placebo-Controlled, Phase 3 Trial. *Lancet Oncol.* 18 (9), 1274–1284. doi:10.1016/S1470-2045(17)30469-2

Ray-Coquard, I., Pautier, P., Pignata, S., Pérol, D., González-Martín, A., Berger, R., et al. (2019). Olaparib Plus Bevacizumab as First-Line Maintenance in Ovarian Cancer. *N. Engl. J. Med.* 381 (25), 2416–2428. doi:10.1056/NEJMoa1911361

Rothman, K. J., Lanes, S., and Sacks, S. T. (2004). The Reporting Odds Ratio and its Advantages over the Proportional Reporting Ratio. *Pharmacoepidemiol Drug Saf.* 13 (8), 519–523. doi:10.1002/pds.1001

Salem, J. E., Nguyen, L. S., Moslehi, J. J., Ederhy, S., Lebrun-Vignes, B., Roden, D. M., et al. (2021). Anticancer Drug-Induced Life-Threatening Ventricular Arrhythmias: a World Health Organization Pharmacovigilance Study. *Eur. Heart J.* 42 (38), 3915–3928. doi:10.1093/eurheartj/ehab362

Shenolikar, R., Durden, E., Meyer, N., Lenhart, G., and Moore, K. (2018). Incidence of Secondary Myelodysplastic Syndrome (MDS) and Acute Myeloid Leukemia (AML) in Patients with Ovarian or Breast Cancer in a Real-World Setting in the United States. *Gynecol. Oncol.* 151 (2), 190–195. doi:10.1016/j.ygyno.2018.09.003

Siegel, R., Naishadham, D., and Jemal, A. (2012). Cancer Statistics, 2012. *CA Cancer J. Clin.* 62 (1), 10–29. doi:10.3322/caac.20138

Staropoli, N., Ciliberto, D., Del Giudice, T., Iuliano, E., Cucè, M., Grillone, F., et al. (2018). The Era of PARP Inhibitors in Ovarian Cancer: "Class Action" or Not? A Systematic Review and Meta-Analysis. *Crit. Rev. Oncol. Hematol.* 131, 83–89. doi:10.1016/j.critrevonc.2018.08.011

Tew, W. P., Lacchetti, C., Ellis, A., Maxian, K., Banerjee, S., Bookman, M., et al. (2020). PARP Inhibitors in the Management of Ovarian Cancer: ASCO Guideline. *J. Clin. Oncol.* 38 (30), 3468–3493. doi:10.1200/JCO.20.01924

Thorsell, A. G., Ekblad, T., Karlberg, T., Löw, M., Pinto, A. F., Trésaugues, L., et al. (2017). Structural Basis for Potency and Promiscuity in Poly(ADP-Ribose) Polymerase (PARP) and Tankyrase Inhibitors. *J. Med. Chem.* 60 (4), 1262–1271. doi:10.1021/acs.jmedchem.6b00990

Tutt, A. N. J., Garber, J. E., Kaufman, B., Viale, G., Fumagalli, D., Rastogi, P., et al. (2021). Adjuvant Olaparib for Patients with BRCA1- or BRCA2-Mutated Breast Cancer. *N. Engl. J. Med.* 384 (25), 2394–2405. doi:10.1056/NEJMoa2105215

Conflict of Interest: The authors declare that the research was conducted in the absence of any commercial or financial relationships that could be construed as a potential conflict of interest.

Publisher's Note: All claims expressed in this article are solely those of the authors and do not necessarily represent those of their affiliated organizations, or those of the publisher, the editors and the reviewers. Any product that may be evaluated in this article, or claim that may be made by its manufacturer, is not guaranteed or endorsed by the publisher.

frontiers | Frontiers in Pharmacology

ORIGINAL RESEARCH
published: 07 July 2022
doi: 10.3389/fphar.2022.835037

External Evaluation of Population Pharmacokinetic Models of Busulfan in Chinese Adult Hematopoietic Stem Cell Transplantation Recipients

Huiping Huang[1,2], Qingxia Liu[1,2], Xiaohan Zhang[3], Helin Xie[1], Maobai Liu[1], Nupur Chaphekar[4] and Xuemei Wu[1]**

[1]Department of Pharmacy, Fujian Medical University Union Hospital, Fuzhou, China, [2]School of Pharmacy, Fujian Medical University, Fuzhou, China, [3]College of Arts and Sciences, University of Virginia, Charlottesville, VA, United States, [4]Department of Pharmaceutical Sciences, School of Pharmacy, University of Pittsburgh, Pittsburgh, PA, United States

Objective: Busulfan (BU) is a bi-functional DNA-alkylating agent used in patients undergoing hematopoietic stem cell transplantation (HSCT). Over the last decades, several population pharmacokinetic (pop PK) models of BU have been established, but external evaluation has not been performed for almost all models. The purpose of the study was to evaluate the predictive performance of published pop PK models of intravenous BU in adults using an independent dataset from Chinese HSCT patients, and to identify the best model to guide personalized dosing.

Methods: The external evaluation methods included prediction-based diagnostics, simulation-based diagnostics, and Bayesian forecasting. In prediction-based diagnostics, the relative prediction error (PE%) was calculated by comparing the population predicted concentration (PRED) with the observations. Simulation-based diagnostics included the prediction- and variability-corrected visual predictive check (pvcVPC) and the normalized prediction distribution error (NPDE). Bayesian forecasting was executed by giving prior one to four observations. The factors influencing the model predictability, including the impact of structural models, were assessed.

Results: A total of 440 concentrations (110 patients) were obtained for analysis. Based on prediction-based diagnostics and Bayesian forecasting, preferable predictive performance was observed in the model developed by Huang et al. The median PE% was -1.44% which was closest to 0, and the maximum F_{20} of 57.27% and F_{30} of 72.73% were achieved. Bayesian forecasting demonstrated that prior concentrations remarkably improved the prediction precision and accuracy of all models, even with only one prior concentration.

Conclusion: This is the first study to comprehensively evaluate published pop PK models of BU. The model built by Huang et al. had satisfactory predictive performance, which can be used to guide individualized dosage adjustment of BU in Chinese patients.

Keywords: busulfan, population pharmacokinetic model, external evaluation, hematopoietic stem cell transplantation, precision medicine

OPEN ACCESS

Edited by:
Yao Liu,
Daping Hospital, China

Reviewed by:
Lujin Li,
Shanghai University, China
Linan Zeng,
McMaster University, Canada

****Correspondence:***
Xuemei Wu
wuxuemei@fjmu.edu.cn
Maobai Liu
liumaobai@126.com

Specialty section:
This article was submitted to Pharmacology of Anti-Cancer Drugs, a section of the journal Frontiers in Pharmacology

Received: *14 December 2021*
Accepted: *17 May 2022*
Published: *07 July 2022*

Citation:
Huang H, Liu Q, Zhang X, Xie H, Liu M, Chaphekar N and Wu X (2022) External Evaluation of Population Pharmacokinetic Models of Busulfan in Chinese Adult Hematopoietic Stem Cell Transplantation Recipients. Front. Pharmacol. 13:835037. doi: 10.3389/fphar.2022.835037

1 INTRODUCTION

Busulfan (BU) is a bi-functional DNA-alkylating agent used in conditional regimens in patients undergoing hematopoietic stem cell transplantation (HSCT) (Lawson et al., 2020). It is usually combined with other chemotherapeutic drugs, such as cyclophosphamide, cytarabine, and fludarabine (Chen et al., 2018; Khalil et al., 2018). It can dampen the immune system response to avoid graft rejection and provide conditions favorable for the implantation of normal hematopoietic stem cells.

Both the U.S. Food and Drug Administration (FDA) and European Medicines Agency (EMA) recommend an initial intravenous BU dose of 0.8 mg/kg for adults every 6 h for 4 days. The distribution of BU in adults is very rapid with an average half-life of 0.051 h (Hassan et al., 1994). BU is conjugated with glutathione (GSH) followed by intramolecular rearrangement to the GSH analog γ–glutamyl-dehydroalanyl-glycine (EdAG), which is mainly catalyzed by the enzyme glutathione S-transferase (GSTs) in the liver (Gibbs et al., 1996; Scian and Atkins, 2015). A high inter-individual variability is observed in the elimination half-life, varying from 0.97 to 7.2 h (Grochow et al., 1989). The excretion of unchanged drug into the urine is less (about 1–2%) (Ehrsson et al., 1983; Hassan et al., 1989).

BU has a narrow therapeutic window. Fifty percent inter- and intra-individual variability in pharmacokinetics (PK) has been reported in the literature (Hassan, 1999; Veal et al., 2012; Paci et al., 2014; Marsit et al., 2020). Studies have shown that area under the concentration-time curve (AUC_{ss}) or plasma concentration (C_{ss}) at steady-state is closely associated with the efficacy and toxicity (Bartelink et al., 2009; Ansari et al., 2014; Bartelink et al., 2016; Feng et al., 2020; Hill et al., 2020). Based on the plasma pharmacokinetics of BU, therapeutic drug monitoring (TDM) is recommended to improve engraftment (Kanda, 2018; Takachi et al., 2019). There is no recommended therapeutic window for BU in China now. FDA suggests that AUC of BU should be between 900–1,350 ± 5% μmol/L × min, while a therapeutic range of 900–1,500 μmol/L × min is recommended by EMA with every 6-h dosing (Nguyen et al., 2004; Palmer et al., 2016). The Practice Guidelines Committee of the American Society of Blood or Marrow Transplantation (ASBMT) also highlights the necessity for BU TDM (Bubalo et al., 2014; Tesfaye et al., 2014). It emphasizes that personalized BU dosing needs to be considered to minimize sinusoidal obstruction syndrome, lower graft rejection, and relapse rates (Bubalo et al., 2014). TDM guided BU dosing is routinely conducted in some institutions (Philippe et al., 2016; Shukla et al., 2020).

There are usually two ways to adjust dosing. First is the conventional PK-guided dose adjustment routinely performed in the clinical practice. AUC or Css can be calculated either by multiple pharmacokinetic samples (at least five samples) or a reliable limited sampling strategy (LSS) (Malär et al., 2011; Davis et al., 2019). Dosage can be adjusted by comparing the current AUC or Css with the target values. LSS has the advantage of predicting AUC with 2-4 samples (Huang et al., 2017; Teitelbaum et al., 2020). Recently, personalized dosing strategy based on population pharmacokinetic (pop PK) model coupled with Bayesian forecasting has become popular (Chaivichacharn et al., 2020; Gil Candel et al., 2020). It can obtain individual PK parameters with 1-2 concentrations per patient to get the individualized dosing via maximum a posteriori (Thomson and Whiting, 1992). It can overcome the inconvenience of multiple sampling. Many computer programs with built-in pop PK models have emerged (Felton et al., 2014; Ramos-Martin et al., 2017; Frymoyer et al., 2020; Kantasiripitak et al., 2020). These kind of computer-assisted decision tools usually have a user-friendly interface for application by physicians or pharmacologist.

Over the last decades, several pop PK models of BU have been developed (Nguyen et al., 2006; Salinger et al., 2010; Choe et al., 2012; Choi et al., 2015; Wang et al., 2015; Su et al., 2016; Wu et al., 2017; Huang et al., 2019; Sun et al., 2020), while differences exist between the various models. When these pop PK models are applied to guide individualized dosing in Chinese or other ethnic populations, the accuracy of their prediction needs to be explored and then only the fully validated model can be used to guide drug dosing. This study aimed to evaluate the predictive performance of the published intravenous BU pop PK models in adults. In order to identify which model is the best choice to guide personalized dosing in Chinese HSCT patients, the external predictability of the models was assessed using data obtained from Chinese adult patients undergoing HSCT in our center.

2 METHODS

2.1 Review of the Published Pop PK Studies

An extensive literature search was performed using PubMed, China National Knowledge Infrastructure (www.cnki.net), and Wanfang Data (www.wanfangdata.com.cn) for studies up to 31 October 2020, using the keywords “Busulfan” and “Population Pharmacokinetics”. Studies were included if they contained a pop PK model of intravenous BU in adults and were written in Chinese or English. The reference lists of the selected literatures should also be checked for additional studies. If the essential parameters of the pop PK models (typical value of CL, inter-individual variability of CL, etc.) were missing, the studies were excluded. On the occasions where studies were developed with overlapping data or cohorts, only the one with the largest study cohort was included. Published pop PK models were re-coded and the parameters were obtained from the final model in the literature.

2.2 Software

The external evaluation was conducted with non-linear mixed-effects modelling software package NONMEM version 7.5 (ICON Development Solutions, MD, United States), using Pirana 2.9.7 and Perl-speaks-NONMEM (PsN) Toolkit 4.8.1 as the modelling interface. Data handling, visualization and statistics were performed in R 4.0.0 (R Foundation for Statistical Computing, Vienna, Austria) and RStudio 1.2.5001 (RStudio Inc. Boston, MA, United States).

TABLE 1 | Demographics of external dataset.

	Mean ± SD/N (%)	Range
Demographic		
WT (kg)	62.6 ± 12.1	42.0–100
AIBW (kg)	59.0 ± 7.93	42.0–75.3
IBW (kg)	60.8 ± 5.94	47.5–73.7
BSA (m2)	1.69 ± 0.186	1.31–2.19
BMI (kg/m^2)	22.6 ± 3.74	14.04–33.80
Age (years)	34.8 ± 11.9	19–65
Gender (M/F)	60/50	—
Height (cm)	166.1 ± 8.12	147–183
Biochemistry		
Serum creatinine (μmol/L)	58.9 ± 16.8	25.0–117
Creatinine clearance (mL/min)	134 ± 36.1	62.9–245
Aspartate transaminase (IU/L)	27.7 ± 15.9	6–100
Alkaline phosphatase (IU/L)	62.0 ± 18.3	28.0–129
Gamma glutamyl transferase (IU/L)	38.2 ± 39.2	8.0–288
Serum albumin (g/L)	38.8 ± 5.19	28.0–49.7
Lactic dehydrogenase (IU/L)	229 ± 104	90.0–607
Total bilirubin (μmol/L)	13.27 ± 7.90	1.90–57.3
Alanine transaminase (IU/L)	38.3 ± 34.7	6.0–165
Genetic polymorphisms in GSTA$_1$[a,b]		
GG (^{a}A^{a}A)	58 (52.7%)	—
GA (^{a}A^{a}B)	14 (12.7%)	—
AA (^{a}B^{a}B)	0 (0%)	—
Diagnosis[b]		
Acute myeloid leukemia (AML)	44 (40.0%)	—
Acute lymphoblastic leukemia (ALL)	34 (30.9%)	—
Chronic myeloid leukemia (CML)	10 (0.09%)	—
Myelodysplastic syndrome (MDS)	10 (0.09%)	—
Miscellaneous	12 (10.9%)	—
Concomitant drug[b]		
Tropisetron	13 (11.8%)	—
Palonosetron	99 (90.0%)	—
Phenytoin (PHT)	98 (89.1%)	—
Micafungin sodium	19 (17.3%)	—
Voriconazole (VOR)	20 (18.2%)	—
Cyclosporine A (CSA)	67 (60.9%)	—

[a]*Thirty-eight patients in external dataset have no genetic polymorphisms information.*
[b]*The category variables such as genetic polymorphisms in GSTA$_1$, diagnosis, and concomitant drug are presented as n (%).*

2.3 Study Cohort of External Evaluation

2.3.1 External Dataset

The concentrations of 110 adult patients who received BU intravenously prior to HSCT at Fujian Medical University Union Hospital from March 2013 to May 2018 were collected as the external data. The study protocols were approved by the Ethics Committee of the Fujian Medical University Union Hospital and written informed consent was obtained from all the subjects. The demographic characteristics, biochemistry data, genetic polymorphisms information, and concomitant drugs are summarized in **Table 1**.

2.3.2 Dosing Regimen and Sampling

All patients received 0.8 mg/kg of BU every 6 h for 4 or 3 days, combined with other chemotherapeutic drugs (Cyclophosphamide, Fludarabine, etc.) as the conditional regimens prior to HSCT. Oral phenytoin (5–10 mg/kg/d) was given to prevent seizures. Cyclosporin was administered intravenously before transplantation. Anti-emetics and antifungal drugs were used during chemotherapy, depending on the actual clinical situation.

The dosage of BU with an infusion over 2 h was determined based on the adjusted ideal body weight (AIBW) which was calculated using the following formulas: IBW = height^2 × 22/10,000 and AIBW = IBW+0.25 × (ABW-IBW). If actual body weight (ABW) ≤ IBW, ABW would be equal to IBW (Wu et al., 2017). Intensive blood samples were collected from 28 patients at 0.5, 1, 2, 3, 4, 5 and 6 h after the start of the first dose infusion as well as pre-infusion of the fifth dose and 2 h after the start of the fifth dose infusion. Considering the convenience of clinical practice, a limited sampling strategy was conducted in the other 82 patients at 1, 3, and 5 h after the start of the first dose. A total of 440 concentrations were obtained for analysis. The plasma concentrations of BU were determined using high-performance liquid chromatography-mass spectrometry (HPLC-MS/MS). The calibration standards were linear over concentrations ranging from 0.05 to 2.5 μg/ml. The lower limit of detection was 3 ng/ml at which the signal level of BU reached at least 3 times the signal noise of the baseline. The single nucleotide polymorphism (SNPs) of GSTs were determined by matrix-assisted laser desorption/ionization-time of flight (MALDI-TOF-MS).

2.4 External Evaluation

2.4.1 Prediction-Based Diagnostics

The relative prediction error (PE%) was calculated by comparing the population predicted concentration (PRED) with the observations (OBS) using the **Eq. A**. If PEs% departed from the normal distribution, the median prediction error (MDPE, median PE%) was calculated to reflect accuracy. Meanwhile, the median absolute prediction error (MAPE, median |PE|%) was used to indicate precision. The percentage of PE% falling within the ±20% and ± 30% (F_{20}, F_{30}) were computed to represent combination index of accuracy and precision (Mao et al., 2018). The candidate model was considered to be clinically acceptable when the standards of MDPE≤±15%, MAPE≤30%, F_{20} > 35% and F_{30} > 50% were reached.

$$\mathrm{PE\%} = \left(\frac{\mathrm{PRED} - \mathrm{OBS}}{\mathrm{OBS}}\right) \times 100 \quad \text{Equation (A)} \tag{1}$$

2.4.2 Simulation-Based Diagnostics

The prediction- and variability-corrected visual predictive check (pvcVPC) and the normalized prediction distribution error (NPDE) were executed for the simulation-based diagnostics. The pvcVPCs were simulated by the PsN toolkit. The dataset was simulated for 2000 times (Zhao et al., 2016). The 95% confidence intervals (CI) for the median and the 5th and 95th percentiles of the simulations were calculated and compared with the prediction- and variability-corrected observations. NPDE contains four statistical tests (Wilcoxon signed rank test, Fisher test, Shapiro-Wilks test, and Global test) to verify whether NPDE follows a standard normal distribution N (0,1). The

TABLE 2 | Summary of published population pharmacokinetic studies of busulfan in adult hematopoietic stem cell transplantation recipients.

Study (publication year)	Country (single/ Multiple sites)	Number of Patients (Male/ Female)	Sampling schedule (number of samples)	Bioassay	Structural model	PK Parameters and formula	BSV(%)	Residual error
Choi et al. (2015)	Korean (Single)	36 (21/15)	IS(101)	HPLC/ MS/MS	1-CMT	CL = 11.0 × (BW/60) $^{0.843}$×e$^{(-0.161)\times GSTA1}$ (L/h)	14.7	15.3%
Choi et al. (2015)						V_d = 42.4 (L)	25.6	
Wang et al. (2015)	The U.S. (Multiple)	207(NA)	IS(2,454)	NA	1-CMT	CL = 7.74 × (BSA –2.0) + 12.7 (L/h)	13.7	8.65%
Wang et al. (2015)						V_d = 32.8 × (BSA –2.0) + 50.3 for male (L)	9.49	
						V_d = 32.8 × (BSA –2.0) + 46.3 for female (L)	—	
Choe et al. (2012)	Korean (Single)	60 (37/23)	IS(295)	LC/MS/MS	1-CMT	CL = 0.947 × ABW$^{0.5}$ (L/h)	16	6.3%
Choe et al. (2012)						V_d = 3.610 × ABW$^{0.5}$×(1 + SEX × 0.105) (L)	9	
Salinger et al. (2010) (Salinger et al., 2010)	The U.S. (Single)	37 (21/16)	IS(777)	GC/MS	1-CMT	CL = 0.179 (L/h/kg)	19.7	8.6%
						V_d = 0.723 (L/kg)	15.6	14.06 ng/ml
Huang et al. (2019) (Huang et al., 2019)	China (Single)	20 (11/9)	IS(280)	LC/MS/MS	1-CMT	CL = 12.02 (L/h)	15	20.3%
						V_d = 50.94 (L)	19	
Sun et al. (2020)	China (Single)	43 (32/11)	IS(488)	LC/MS/MS	1-CMT	CL = 14.2 × (1 + (-0.214)× GSTA1 (L/h)	14.6	-14.1%
Sun et al. (2020)						V_d = 64.1 (L)	16.7	
Su et al. (2016)	China (Single)	35 (23/12)	IS + LS(NA)	HPLC	2-CMT	CL = 8.11 × (WT/50)$^{0.726}$ × 1.39^{SEX} (L/h)	18.9	136.01 ng/ml
Su et al. (2016)						V_1 = 24.9×(CRE/53)$^{0.507}$×(WT/50)$^{1.35}$ (L)	31.1	
						Q = 22.2 (L/h)	69.2	
						V_2 = 28.1 (L)	43.3	

CRE, creatinine; WT/BW, body weight; BSA, body surface area; CL, clearance; ABW, actual body weight; 1-CMT, one-compartment model; 2-CMT, two-compartment model; HPLC, high performance liquid chromatography; LC/MS/MS, liquid chromatography tandem-mass spectrometry; GC, gas chromatography with mass selective detection; IS, intensive sampling; SS, sparse sampling; LS, limited sampling; BSV, between-subject variability; NA, not available.

results of NPDE were output by R software statistically and graphically.

2.4.3 Bayesian Forecasting

The Maximum a Posterior Bayesian (MAPB) forecasting was used to evaluate the effect of previous observations on model predictability (Zhang et al., 2019). A total of 107 patients with ≥3 observations were included in the evaluation. The individual predictions (IPRED) of observation for all patients were predicted by giving one to four prior observations, respectively. The individual PE% (IPE%) was computed by the following **Eq. B**. Similar to prediction-based diagnostics, median IPE% (MDIPE), median absolute IPE% (MAIPE), F_{20} and F_{30} of IPE% (IF_{20}, IF_{30}) were computed to reflect the overall prediction performance of the model.

$$\text{IPE\%} = \left(\frac{\text{IPRED} - \text{OBS}}{\text{OBS}}\right)\times 100 \quad \text{Equation (B)} \qquad (2)$$

2.5 Impact of Structural Model and Covariates

All structural models of the published studies had been generalized owing to the considerable effect on the prediction. Their impacts on the predictive performance were evaluated with or without major significant covariates. The covariates were screened using a stepwise method, which is consistent with the published pop PK studies. Three evaluation methods, the predication- and simulation-based diagnostics, and Bayesian forecasting, were applied.

3 RESULTS

3.1 Reviews of the Published Pop PK Analyses

A total of nine BU pop PK studies were published (Nguyen et al., 2006; Takama et al., 2006; Salinger et al., 2010; Choe et al., 2012; Choi et al., 2015; Wang et al., 2015; Su et al., 2016; Huang et al., 2019; Sun et al., 2020). Two studies were excluded. One was due to missing key parameters, another one involved inter-occasion variability but the sampling times were in the ninth and 13th dose, which is different from the external dataset (Nguyen et al., 2006; Takama et al., 2006). Seven studies were eventually retained for evaluation (Salinger et al., 2010; Choe et al., 2012; Choi et al., 2015; Wang et al., 2015; Su et al., 2016; Huang et al., 2019; Sun et al., 2020) and the details are listed in **Table 2**. Three of them were performed in China (Su et al., 2016; Huang et al., 2019; Sun et al., 2020), two in Korea (Choe et al., 2012; Choi et al., 2015), and

TABLE 3 | Results of prediction-based diagnostics.

Models	PE_{min} (%)	PE_{max} (%)	MDPE (%)	MAPE (%)	F_{20} (%)	F_{30} (%)
Published studies						
Choi et al. (2015)	−79.51	508.58	10.36	19.33	51.82	66.59
Wang et al. (2015)	−77.98	609.49	25.59	27.23	36.82	54.77
Choe et al. (2012)	−71.71	766.42	63.57	63.90	11.59	18.18
Salinger et al. (2010)	−64.59	943.19	−10.36	25.04	41.36	57.05
Huang et al. (2019)	−83.12	538.23	−1.44	16.25	57.27	72.73
Sun et al. (2020)	−86.24	409.11	−19.25	24.20	42.27	61.36
Su et al. (2016)	−80.37	480.88	−10.36	22.97	42.73	66.14
Impact of model structure						
1-CMT (Base Model)	−82.75	557.73	2.16	16.93	55.45	70.91
1-CMT+BSA	−82.68	511.25	0.78	15.74	57.73	71.59
2-CMT (Base Model)	−81.52	573.23	7.35	19.31	50.68	68.41
2-CMT+BSA	−81.41	519.43	5.47	17.54	55.68	70.45

PE_{min}, the minimal of prediction error; PE_{max}, the maximum of prediction error; MDPE (%), median prediction error; MDAE (%), median absolute prediction error; F_{20} (%) and F_{30} (%) the percentage of prediction error ≤ ±20% and ± 30%, respectively; 1-CMT, one-compartment model; 2-CMT, two-compartment model; BSA, body surface area.

two in the United States (Salinger et al., 2010; Wang et al., 2015). Only one study was a multicenter study (Wang et al., 2015). Six pop PK models were fitted with one compartmental model (1-CMT) (Salinger et al., 2010; Choe et al., 2012; Choi et al., 2015; Wang et al., 2015; Huang et al., 2019; Sun et al., 2020), and only one was fitted with two compartmental model (2-CMT) (Su et al., 2016). The covariates involved in the published final CL models were body weight (BW), body surface area (BSA), serum creatinine (Scr), $GSTA_1$ genotype, and gender (SEX). BW, as the most recognized covariate, was incorporated in three pop PK models (Choe et al., 2012; Choi et al., 2015; Su et al., 2016). There were two pop PK studies that found no covariates impacting CL (Salinger et al., 2010; Huang et al., 2019). In two studies, the relationship between $GSTA_1$ genotype and CL was taken into consideration, and $GSTA_1$ genotype was incorporated into their model (Choi et al., 2015; Sun et al., 2020). The typical CL and V of a 60–65 kg male varied from 7.3–14.2 L/h and 30.9–64.1 L, respectively. This discrepancy across the seven studies needs further investigations.

3.2 External Evaluation

3.2.1 Prediction-Based Diagnostics

The prediction-based diagnostic results were shown in **Table 3**. Five of seven models met all the criteria (MDPE ≤ ±20%, MAPE ≤30%, $F_{20} \geq 35\%$, and $F_{30} \geq 50\%$) (Salinger et al., 2010; Choi et al., 2015; Su et al., 2016; Huang et al., 2019; Sun et al., 2020). Taking both accuracy and precision into account, the model developed by Huang et al. (2019) showed preferable predictive performances compared to the others. The model yielded a MDPE of -1.44%, which was the closest to 0. The maximum F_{20} (57.27%) and F_{30} (72.73%) were also achieved.

3.2.2 Simulation-Based Diagnostics

Four models showed an un-ignorable difference between the observations and simulations in pvcVPC (Salinger et al., 2010; Choe et al., 2012; Wang et al., 2015; Sun et al., 2020). The model developed by Choi et al. (Choi et al., 2015) and Huang et al. (Huang et al., 2019) performed better than the other models in pvcVPC (**Figure 1**). Regarding the standard normal distribution of NPDE, NPDE plot of the model by Salinger et al. (Salinger et al., 2010) seemed to be better than other models as shown in **Figure 2**. However, **Supplementary Table S2** presented the results of four statistical tests, model built by Choi et al. passed Wilcoxon signed rank test and Fisher test, the other models only passed one statistical test ($p \geq 0.05$). No model satisfied all statistical test, which means all models failed in NPDE diagnostics.

3.2.3 Bayesian Forecasting

Figure 3 contains box plots of IPE% with Bayesian forecasting for seven published pop PK models in different scenarios (Salinger et al., 2010; Choe et al., 2012; Choi et al., 2015; Wang et al., 2015; Su et al., 2016; Huang et al., 2019; Sun et al., 2020). The results demonstrated that prior concentrations, even one prior concentration, improved the prediction precision and accuracy of all models, which was exhibited by the narrower range of IPEs, as well as the median of IPEs being closer to 0. Two or three prior concentrations could achieve better results. The IPRED of the model by Huang et al. (2019) demonstrated the most accurate result. With two prior concentrations, the IF_{20} and IF_{30} were 69 and 85%, respectively.

3.3 The Impact of Structural Models and Covariates

The structural models published included the 1-CMT and 2-CMT models. The above two covariate-free structural models were first developed and evaluated. The 1-CMT model fits well with the external dataset due to a small OFV value and low variability of the PK parameters. Covariates involved in the published pop PK studies (BSA, BW, Scr, $GSTA_1$ genotype, and SEX) were screened using a stepwise method. BSA was successfully included in the model based on a *p*-value of less than 0.05. Incorporation of other covariates in the model showed no significant amelioration. The results are summarized in **Figure 4**, **5**.

4 DISCUSSION

In our study, the external predictability of seven published intravenous BU pop PK models in adults (Salinger et al., 2010;

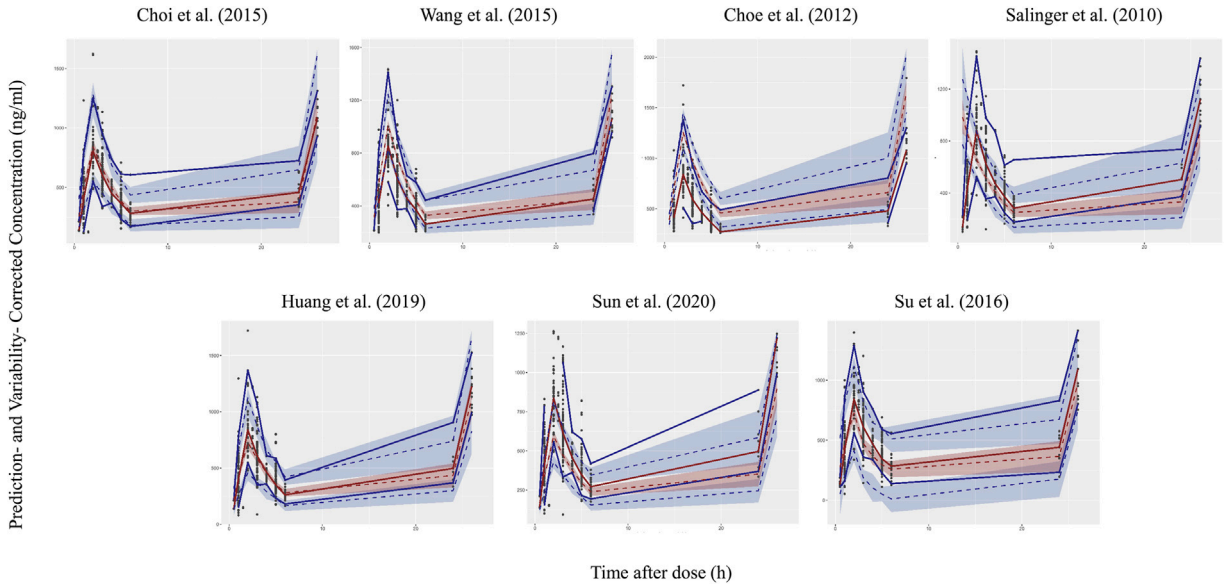

FIGURE 1 | Prediction- and variability-corrected visual predictive check (pvcVPC) plots of seven published population pharmacokinetic models (Salinger et al., 2010; Choe et al., 2012; Choi et al., 2015; Wang et al., 2015; Su et al., 2016; Huang et al., 2019; Sun et al., 2020). The middle dashed line represents the median prediction- and variability-corrected predictions. The middle semitransparent field represents a simulation-based 95% confidence interval (CI) for the median. Upper and lower dash lines represent the corrected observed 95th and fifth percentiles and semitransparent fields represent a simulation-based 95% CI for the corresponding model predicted percentiles. The solid lines represent the median, 95th and 5th percentiles of observations.

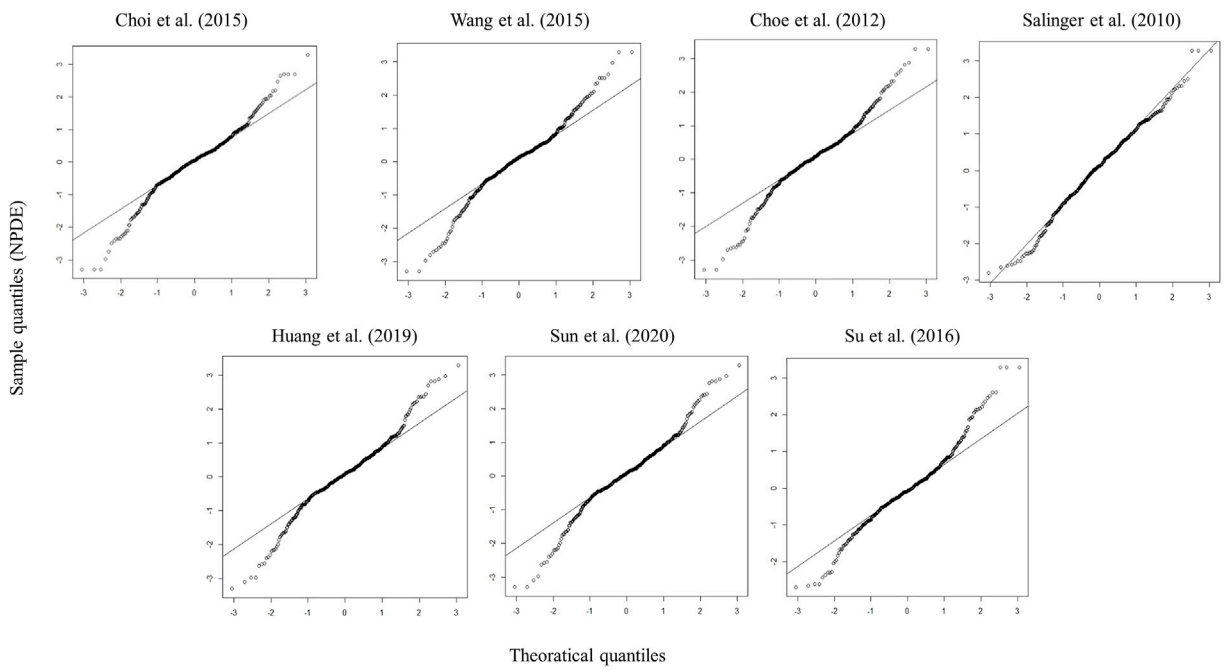

FIGURE 2 | Quantile–quantile plots (the distribution of the NPDE against theoretical distribution) of seven published population pharmacokinetic models (Salinger et al., 2010; Choe et al., 2012; Choi et al., 2015; Wang et al., 2015; Su et al., 2016; Huang et al., 2019; Sun et al., 2020).

Choe et al., 2012; Choi et al., 2015; Wang et al., 2015; Su et al., 2016; Huang et al., 2019; Sun et al., 2020) was explored using an independent dataset, which contained 110 patients with 440 observations. To the best of our knowledge, no similar research on BU has been published yet. All model has consistent performance in the statistical tests of NPDE.

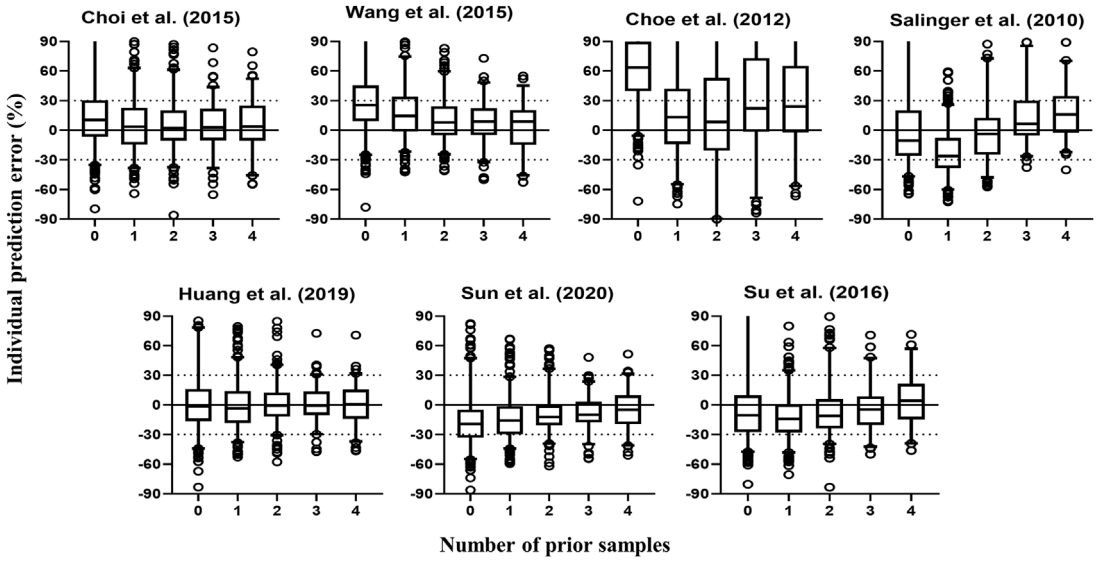

FIGURE 3 | Box plots of individual relative prediction error (IPE%) with Bayesian forecasting for seven published population pharmacokinetic models (Salinger et al., 2010; Choe et al., 2012; Choi et al., 2015; Wang et al., 2015; Su et al., 2016; Huang et al., 2019; Sun et al., 2020) in different scenarios (0 represents prediction without prior information and 1-4 represents with prior one to four observations, respectively). In scenario n, prior n observations were used to estimate the individual prediction and it was then compared with the corresponding observation.

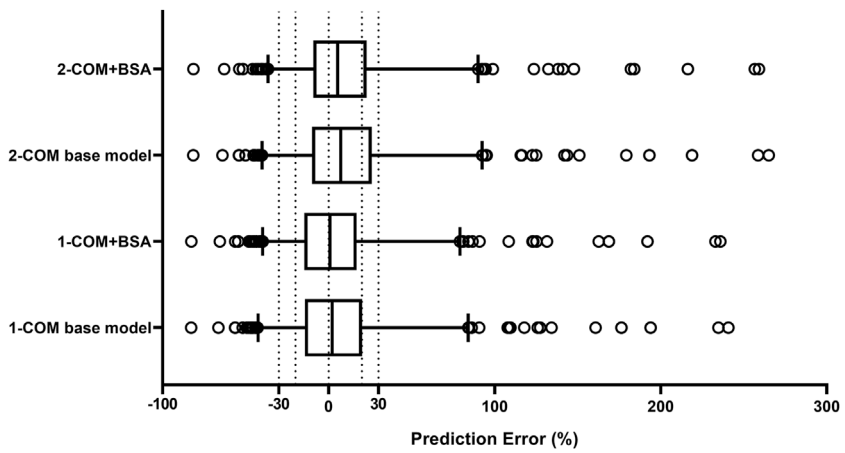

FIGURE 4 | Box plots of relative prediction error (PE%) for two structural models with or without covariates. Black solid line and dotted lines are reference lines indicating PE% of 0%, ±20% and ±30%, respectively. 1-COM, one compartmental model; 2-COM, two compartmental model; BSA, body surface area.

Overall, based on the results of prediction-based and Bayesian forecasting, the model built by Huang et al. (Huang et al., 2019) has satisfied predictive performance, which can be used to guide individualized dosing of BU in our center. Bayesian forecasting suggested that predictive accuracy would be improved by giving one or two prior concentrations, which indicated that the qualified published models can potentially guide personalized dosing in Chinese population.

With the progress of dose individualization, decision-making systems have been developed rapidly in recent years (Mould et al., 2016), with the characteristics of clinical compliance and predictive accuracy. The decision-making system can be designed by different forms, such as computer programs, web platforms, and applications (APPs) (Barrett et al., 2008; Hope et al., 2013; Shukla et al., 2020). They are easy to use and incorporate over 20 drugs, covering populations ranging from neonate to adult. For BU individualized dose adjustment, the computer programs BestDose (http://www.lapk.org/bestdose.php), DoseMe (https://doseme-rx.com/), and the web platform InsightRX (https://www.insight-rx.com/), NextDose (https://www.nextdose.org/) are available. All of them estimate parameters by Bayesian algorithm, but using different pop PK

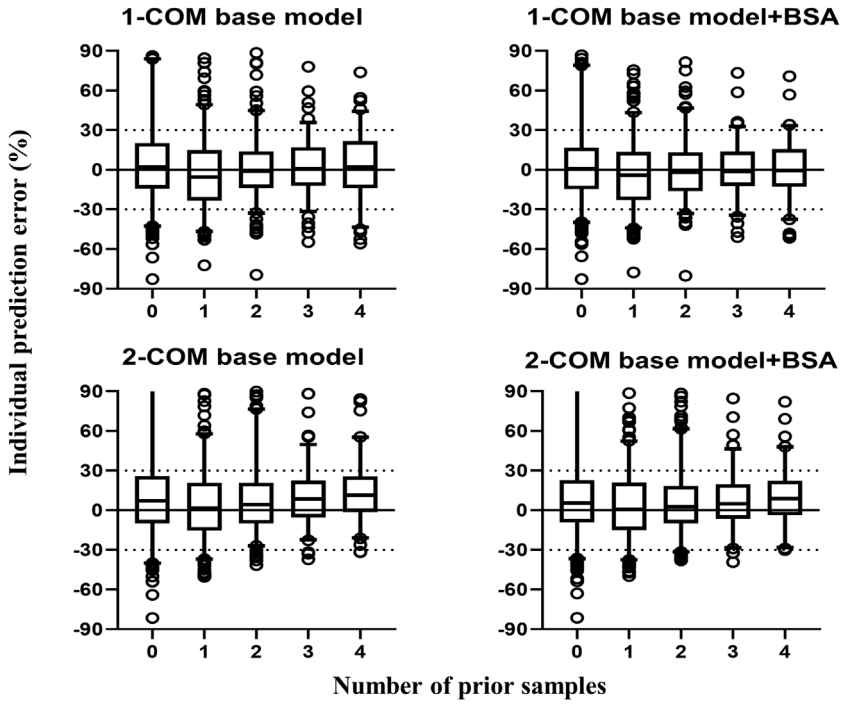

FIGURE 5 | Box plots of individual relative prediction error (IPE%) with Bayesian forecasting for two structural models with or without covariates in different scenarios (0 represents prediction without prior information and 1-4 represents with prior one to four observations, respectively). In scenario n, prior n observations were used to estimate the individual prediction and it was then compared with the corresponding observation. 1-COM, one compartmental model; 2-COM, two compartmental model; BSA, body surface area.

models. Before applying the pop PK model for BU in our center, it is necessary to externally validate the model based on institutional data.

BestDose choose a non-parametric population model of BU for individual patient therapeutic drug dose management. The model was developed in pediatric patients, using the Non-Parametric Adaptive Grid algorithm in the Pmetrics package for R. Therefore, we didn't include it in our study. A population pharmacokinetic model by (Long-Boyle et al., 2015) for children ≥12 kg was implemented in InsightRX and available. NextDose's recommendations use the model by (McCune et al., 2014). The above two models were built in patients ranged from infants to adults. The age range of our dataset was 19–65 years old. It may be more appropriated to evaluated them using pediatric patients. DoseMeRx supports a couple of drug models for BU. For adult, model built by (Salinger et al., 2010) is applied, which has been external evaluated in our study. However, it didn't show satisfactory predictive performance. This maybe explain by the differences between the model development dataset (White population) and the external evaluation dataset (Chinese population). Generally speaking, the models developed in a similar population might have a superior predictive performance with external dataset because of similar ethnic background with parallel genotypes, prescribing and dietary habits. This helps to explain the superiority of the model built by Huang et al., which was developed in Chinese population.

Three diagnostics are usually used to evaluate the predictive performance of the published pop PK models. Prediction-based diagnostics is a useful method to assess the correlation of observations and simulations. The criteria are typically set as MDPE ≤ ±20%, MAPE ≤30%, F_{20} ≥ 35% and F_{30} ≥ 50% in the literature (Deng et al., 2013; Zhao et al., 2016). Simulation-based diagnostics include pvcVPC and NPDE. Compared with traditional VPCs, pvcVPC is readily applicable to data from studies with a prior and a posteriori dose adaptation (Bergstrand et al., 2011). Both pvcVPC and NPDE could allow us to correctly detect a misspecification of the model. Bayesian forecasting is usually used to adjust dosage in clinical practice with prior observations (Bhattacharjee, 2014).

With these diagnostics, the pop PK models showed different predictive performance in Chinese HSCT patients. Several factors, such as the incorporated covariates, the incorporated ways of covariates, and the characteristics of participants, may impact the predictive ability of pop PK models. In the published pop PK studies of BU, the most recognized covariate impacting CL was body size. BW/IBW/adjusted ideal body weight (AIBW)/body surface area (BSA)/body mass index (BMI) can be classified as body size (Wang et al., 2015), but just one of them can be incorporated in the formula theoretically due to collinearity. Trame et al. suggested allometric BW model and BSA model as a preferred choice for BU dosing in children, which is consistent with the study of Anderson and Holford

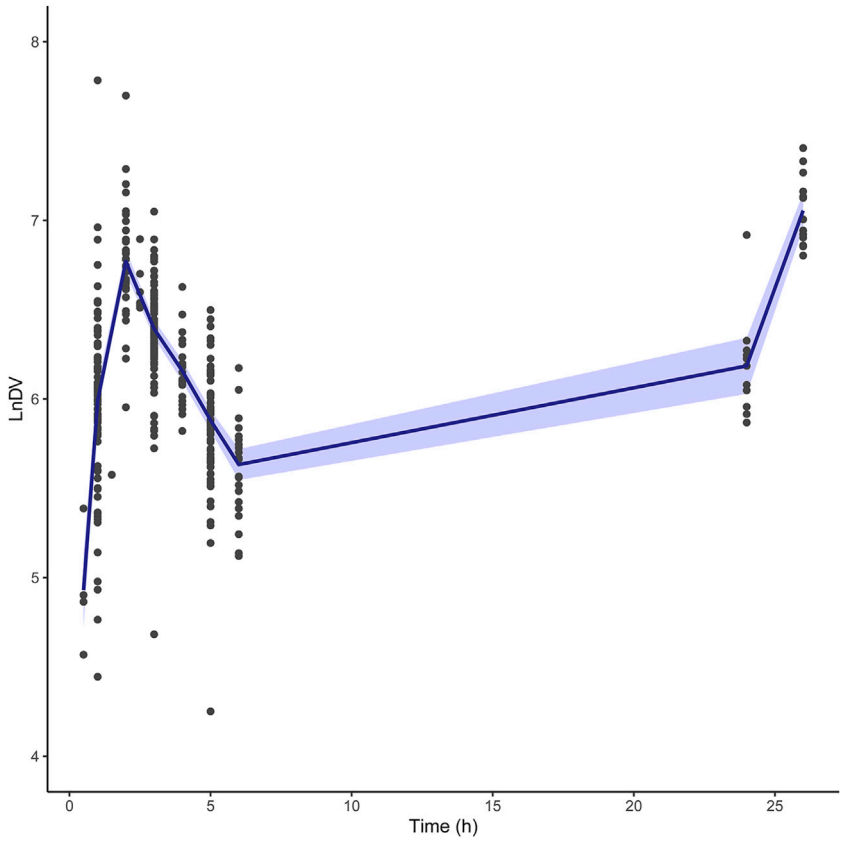

FIGURE 6 | The LnDV vs. Time plot for external dataset. The middle solid blue line represents the mean LnDV. The semitransparent fields represent a 90% confidence interval for the mean.

(Anderson and Holford, 2008; Trame et al., 2011). Commonly used dosing regimen maybe based on BSA because it is most frequently used by clinicians and pharmacists in pediatric oncology (Trame et al., 2011). With regards to the structural model, we found that adding BSA to the base model significantly improved the predictive ability, the final model was CL = 11.7 × (BSA/1.69)$^{1.05}$. This is consistent with the previous findings (Choe et al., 2012; Choi et al., 2015; Su et al., 2016). BU is mainly catalyzed by GSTs and $GSTA_1$ is the main GST isoenzyme. Most of studies focused on the relationship between $GSTA_1$ gene polymorphism and PK of BU, patients with the $GSTA_1$ *A/*B genotype had an 8–27% lower CL than $GSTA_1$ *A/*A group (Ansari et al., 2013; Yin et al., 2015; Ansari et al., 2016). However, some studies showed no association between BU exposure and $GSTA_1$ genotype (Zwaveling et al., 2008; Ansari et al., 2010; Yin et al., 2015), the results remain debatable. Therefore, pharmacogenomics-based dosing of BU was not recommended by the Practice Guidelines Committee of ASBMT (Bubalo et al., 2014). It should be noted that gender was incorporated as a covariate of CL in one pop PK study and as a covariate of volume of distribution (V_d) in two pop PK studies. According to Ansari et al. (2016), the relationship between $GSTA_1$ and first BU dose PK depended on sex and Pesaro risk classification. This result may be explained by the difference in cytosolic GST activity between females and males (Miyagi et al., 2009).

In the seven published pop PK models, only the one built by Su et al. was two-compartment model. This may due to differences in PK sampling times. Most pop PK studies sampled at 0.5 h after the end of the infusion with the possibility of missing the fast distribution phase, while the sampling schedule in Su et al. was 0.25, 0.5, 1, 2, 2.25, 2.5, 3, 4, and 6 h after the start of the infusion for dose 1 or 9. If sufficient samples are collected in the fast distribution phase, the pop PK model may be developed as a two-compartment model. Another PK study with a dense sampling scheme also confirmed that BU fits a two-compartment model with a very rapid distribution phase ($t_{1/2\alpha}$ = 0.05 h), (Hassan et al., 1994). Given that the first sampling time in the external dataset was 0.5 h after the end of infusion, one-compartment model fitted better with our dataset. The LnDV vs. TIME plot was showed in **Figure 6**. The disposition for most individuals were observed a single slope.

Although the model built by Huang et al. was established based on a small population (20 subjects) and incorporated no covariates, it showed good predictability with our dataset of 110 patients. The reason may be found in the structural model of our

dataset, in which the only incorporated covariate was BSA. However, the exponent for effect of BSA on CL was 1.05, much close to 1. In addition, the BSA range in Chinese patients is usually not wide. It can be considered that the impact of BSA on CL was not influential. Therefore, it could be accepted to guide individualized dosage adjustment of BU in Chinese patients because of the satisfied evaluation results.

It is important to explore the predictive ability of the published pop PK models in patients with extreme weight and specific $GSTA_1$ genotypes, because it is usually these subjects with these extreme characteristics that need to adjust the dose. We examined the predictive performance of the models using obese patients (BMI ≥ 24, 31 subjects) and patients with $GSTA_1$ *A/*B genotype (14 subjects). Similarly, the model built by Huang et al. showed better predictive performance than other models. For example, the MDPE was 6.21%, and the maximum F_{20} (64.57%) and F_{30} (77.35%) were also achieved in obese patients.

The Practice Guidelines Committee of ASBMT pointed that fludarabine, deferasirox, and metronidazole affected intravenous BU CL (Palmer et al., 2016). When BU was combined with oral or intravenous metronidazole, BU CL decreased by 46 and 57%, respectively (Gulbis et al., 2011; Chung et al., 2017). Fludarabine slightly affected the intravenous BU CL, with an average of 9.7% reduction (Yeh et al., 2012). However, others didn't get the same results (Russell et al., 2002; de Lima et al., 2004). Co-administration with deferasirox led to a 1.5 times higher AUC (Sweiss et al., 2012). Phenytoin was usually used to prevent seizures when conditioning. It is reported that phenytoin had a higher CL of oral BU, however, the effect of phenytoin upon intravenous BU is limited (Kangarloo et al., 2012; Beumer et al., 2014). The effect of the conditioning regimen on BU CL was investigated by Huang et al. during the model development, but no significant change was observed (Huang et al., 2019).

The application of the Bayesian approach for dosage individualization has proven to be of value in clinical practice for several drugs (Brooks et al., 2020; Guo et al., 2020). It has the advantage of minimizing the need for monitoring of plasma drug concentrations, such as patient blood loss, pain and the cost of determining plasma drug concentration of multiple samples. For Bayesian forecasting, it is important to choose the most appropriate pop PK models and optimal sampling times for dosage prediction (Brooks et al., 2016). Based on the results of Bayesian forecasting, model built by Huang et al. (Huang et al., 2019) had better predictive performance. It can be considered as a qualified model to guide individualized dosing in our center. It seems that two prior concentrations are enough because more prior concentrations no longer improve predictive accuracy. The precision of prediction with four prior observations was decreased in our results, which might be due to lack of adequate patients with ≥ 5 observations.

Based on the model built by Huang et al. (2019), the dosage adjustment strategy for Chinese HSCT patients will execute as follows. Firstly, the initial dose will be calculated by typical CL times AUC_{target}, which can be determined by physicians. Secondly, two blood samples will be collected randomly after the end of the first dose infusion and the measured concentrations will be used to get the individual CL (CL_{ind}) through Bayesian forecasting using NONMEM software. Lastly, the dosage will be adjusted by multiplying CL_{ind} by AUC_{target}.

The study has some limitations, including the lack of subjects with enough intensive samplings, as well as the fact that all the subjects came from the same center. A portion of the subjects had no genetic polymorphism information. Further studies are needed to increase the number of subjects and study centers, which would be helpful to get a more persuasive conclusion.

In conclusion, a total of seven published BU adult pop PK models were externally evaluated using an independent dataset from patients undergoing HSCT in our center. Based on prediction-based diagnostic and Bayesian forecasting, the model developed by Huang et al. (2019) showed accurate predictive performance. It can be built into computer programs to guide personalized dosing in our center. Further studies are needed to evaluate its performance in other centers in China. Bayesian forecasting indicated a potential application of quantified pop PK models to guide dosage adjustment. Based on the obvious differences between the adult model and the pediatric model, further external evaluation of pop PK models of BU in pediatrics is planned to be conducted.

DATA AVAILABILITY STATEMENT

The raw data supporting the conclusion of this article will be made available by the authors, without undue reservation.

ETHICS STATEMENT

The studies involving human participants were reviewed and approved by the Fujian Medical University Union Hospital. The patients/participants provided their written informed consent to participate in this study. Written informed consent was obtained from the individual(s) for the publication of any potentially identifiable images or data included in this article.

AUTHOR CONTRIBUTIONS

XW and ML were involved in the study design, method execution, data analysis and plotting, manuscript writing. HH, QL, and XZ analyzed the data and drafted the manuscript. HX was responsible for data collection. WH contributed to data analysis and plotting. NC revised the manuscript and polished the language. All authors approved the manuscript for submission.

FUNDING

This study was supported by the Joint Funds for the innovation of science and Technology, Fujian Province (2019Y9059).

ACKNOWLEDGMENTS

The authors thank Zheng Jiao (Department of Pharmacy, Shanghai Chest Hospital, Shanghai Jiao Tong University) for providing the study idea and useful papers. We would like to sincerely thank Dongho Lee and Sangmin Choe (Department of Clinical Pharmacology and Therapeutics, University of Ulsan College of Medicine, Asan Medical Center, Korean), Shantang Zhang (Department of Pharmacy, Anhui Provincial Hospital, Hefei) for providing the model code. We also wish to thank Xiao Zhu (School of Pharmacy, University of Otago, New Zealand) for providing the guide of VPC and NPC user guide.

SUPPLEMENTARY MATERIAL

The Supplementary Material for this article can be found online at: https://www.frontiersin.org/articles/10.3389/fphar.2022.835037/full#supplementary-material

REFERENCES

Anderson, B. J., and Holford, N. H. (2008). Mechanism-based Concepts of Size and Maturity in Pharmacokinetics. *Annu. Rev. Pharmacol. Toxicol.* 48, 303–332. doi:10.1146/annurev.pharmtox.48.113006.094708

Ansari, M., Huezo-Diaz, P., Rezgui, M. A., Marktel, S., Duval, M., Bittencourt, H., et al. (2016). Influence of Glutathione S-Transferase Gene Polymorphisms on Busulfan Pharmacokinetics and Outcome of Hematopoietic Stem-Cell Transplantation in Thalassemia Pediatric Patients. *Bone Marrow Transpl.* 51 (3), 377–383. doi:10.1038/bmt.2015.321

Ansari, M., Lauzon-Joset, J. F., Vachon, M. F., Duval, M., Théoret, Y., Champagne, M. A., et al. (2010). Influence of GST Gene Polymorphisms on Busulfan Pharmacokinetics in Children. *Bone Marrow Transpl.* 45 (2), 261–267. doi:10.1038/bmt.2009.143

Ansari, M., Rezgui, M. A., Théoret, Y., Uppugunduri, C. R., Mezziani, S., Vachon, M. F., et al. (2013). Glutathione S-Transferase Gene Variations Influence BU Pharmacokinetics and Outcome of Hematopoietic SCT in Pediatric Patients. *Bone Marrow Transpl.* 48 (7), 939–946. doi:10.1038/bmt.2012.265

Ansari, M., Théoret, Y., Rezgui, M. A., Peters, C., Mezziani, S., Desjean, C., et al. (2014). Association between Busulfan Exposure and Outcome in Children Receiving Intravenous Busulfan before Hematopoietic Stem Cell Transplantation. *Ther. Drug Monit.* 36 (1), 93–99. doi:10.1097/FTD.0b013e3182a04fc7

Barrett, J. S., Mondick, J. T., Narayan, M., Vijayakumar, K., and Vijayakumar, S. (2008). Integration of Modeling and Simulation into Hospital-Based Decision Support Systems Guiding Pediatric Pharmacotherapy. *BMC Med. Inf. Decis. Mak.* 8, 6. doi:10.1186/1472-6947-8-6

Bartelink, I. H., Bredius, R. G., Belitser, S. V., Suttorp, M. M., Bierings, M., Knibbe, C. A., et al. (2009). Association between Busulfan Exposure and Outcome in Children Receiving Intravenous Busulfan before Hematologic Stem Cell Transplantation. *Biol. Blood Marrow Transpl.* 15 (2), 231–241. doi:10.1016/j.bbmt.2008.11.022

Bartelink, I. H., Lalmohamed, A., van Reij, E. M., Dvorak, C. C., Savic, R. M., Zwaveling, J., et al. (2016). Association of Busulfan Exposure with Survival and Toxicity after Haemopoietic Cell Transplantation in Children and Young Adults: a Multicentre, Retrospective Cohort Analysis. *Lancet Haematol.* 3 (11), e526–e536. doi:10.1016/s2352-3026(16)30114-4

Bergstrand, M., Hooker, A. C., Wallin, J. E., and Karlsson, M. O. (2011). Prediction-corrected Visual Predictive Checks for Diagnosing Nonlinear Mixed-Effects Models. *AAPS J.* 13 (2), 143–151. doi:10.1208/s12248-011-9255-z

Beumer, J. H., Owzar, K., Lewis, L. D., Jiang, C., Holleran, J. L., Christner, S. M., et al. (2014). Effect of Age on the Pharmacokinetics of Busulfan in Patients Undergoing Hematopoietic Cell Transplantation; an Alliance Study (CALGB 10503, 19808, and 100103). *Cancer Chemother. Pharmacol.* 74 (5), 927–938. doi:10.1007/s00280-014-2571-0

Bhattacharjee, A. (2014). Application of Bayesian Approach in Cancer Clinical Trial. *World J. Oncol.* 5 (3), 109–112. doi:10.14740/wjon842e

Brooks, E., Tett, S. E., Isbel, N. M., McWhinney, B., and Staatz, C. E. (2020). Evaluation of Bayesian Forecasting Methods for Prediction of Tacrolimus Exposure Using Samples Taken on Two Occasions in Adult Kidney Transplant Recipients. *Ther. Drug Monit.* 42 (2), 238–246. doi:10.1097/FTD.0000000000000814

Brooks, E., Tett, S. E., Isbel, N. M., and Staatz, C. E. (2016). Population Pharmacokinetic Modelling and Bayesian Estimation of Tacrolimus Exposure: Is This Clinically Useful for Dosage Prediction yet? *Clin. Pharmacokinet.* 55 (11), 1295–1335. doi:10.1007/s40262-016-0396-1

Bubalo, J., Carpenter, P. A., Majhail, N., Perales, M. A., Marks, D. I., Shaughnessy, P., et al. (2014). Conditioning Chemotherapy Dose Adjustment in Obese Patients: a Review and Position Statement by the American Society for Blood and Marrow Transplantation Practice Guideline Committee. *Biol. Blood Marrow Transpl.* 20 (5), 600–616. doi:10.1016/j.bbmt.2014.01.019

Chaivichacharn, P., Avihingsanon, A., Manosuthi, W., Ubolyam, S., Tongkobpetch, S., Shotelersuk, V., et al. (2020). Dosage Optimization of Efavirenz Based on a Population Pharmacokinetic-Pharmacogenetic Model of HIV-Infected Patients in Thailand. *Clin. Ther.* 42 (7), 1234–1245. doi:10.1016/j.clinthera.2020.04.013

Chen, Y., Xu, L. P., Zhang, X. H., Chen, H., Wang, F. R., Liu, K. Y., et al. (2018). Busulfan, Fludarabine, and Cyclophosphamide (BFC) Conditioning Allowed Stable Engraftment after Haplo-Identical Allogeneic Stem Cell Transplantation in Children with Adrenoleukodystrophy and Mucopolysaccharidosis. *Bone Marrow Transpl.* 53 (6), 770–773. doi:10.1038/s41409-018-0175-8

Choe, S., Kim, G., Lim, H. S., Cho, S. H., Ghim, J. L., Jung, J. A., et al. (2012). A Simple Dosing Scheme for Intravenous Busulfan Based on Retrospective Population Pharmacokinetic Analysis in Korean Patients. *Korean J. Physiol. Pharmacol.* 16 (4), 273–280. doi:10.4196/kjpp.2012.16.4.273

Choi, B., Kim, M. G., Han, N., Kim, T., Ji, E., Park, S., et al. (2015). Population Pharmacokinetics and Pharmacodynamics of Busulfan with GSTA1 Polymorphisms in Patients Undergoing Allogeneic Hematopoietic Stem Cell Transplantation. *Pharmacogenomics* 16 (14), 1585–1594. doi:10.2217/pgs.15.98

Chung, H., Yu, K. S., Hong, K. T., Choi, J. Y., Hong, C. R., Kang, H. J., et al. (2017). A Significant Influence of Metronidazole on Busulfan Pharmacokinetics: A Case Report of Therapeutic Drug Monitoring. *Ther. Drug Monit.* 39 (3), 208–210. doi:10.1097/FTD.0000000000000395

Davis, J. M., Ivanova, A., Chung, Y., Shaw, J. R., Rao, K. V., Ptachcinski, J. R., et al. (2019). Evaluation of a Test Dose Strategy for Pharmacokinetically-Guided Busulfan Dosing for Hematopoietic Stem Cell Transplantation. *Biol. Blood Marrow Transpl.* 25 (2), 391–397. doi:10.1016/j.bbmt.2018.09.017

de Lima, M., Couriel, D., Thall, P. F., Wang, X., Madden, T., Jones, R., et al. (2004). Once-daily Intravenous Busulfan and Fludarabine: Clinical and Pharmacokinetic Results of a Myeloablative, Reduced-Toxicity Conditioning Regimen for Allogeneic Stem Cell Transplantation in AML and MDS. *Blood* 104 (3), 857–864. doi:10.1182/blood-2004-02-0414

Deng, C., Liu, T., Wu, K., Wang, S., Li, L., Lu, H., et al. (2013). Predictive Performance of Reported Population Pharmacokinetic Models of Vancomycin in Chinese Adult Patients. *J. Clin. Pharm. Ther.* 38 (6), 480–489. doi:10.1111/jcpt.12092

Ehrsson, H., Hassan, M., Ehrnebo, M., and Beran, M. (1983). Busulfan Kinetics. *Clin. Pharmacol. Ther.* 34 (1), 86–89. doi:10.1038/clpt.1983.134

Felton, T. W., Roberts, J. A., Lodise, T. P., Van Guilder, M., Boselli, E., Neely, M. N., et al. (2014). Individualization of Piperacillin Dosing for Critically Ill

Patients: Dosing Software to Optimize Antimicrobial Therapy. *Antimicrob. Agents Chemother.* 58 (7), 4094–4102. doi:10.1128/AAC.02664-14

Feng, X., Wu, Y., Zhang, J., Li, J., Zhu, G., Fan, D., et al. (2020). Busulfan Systemic Exposure and its Relationship with Efficacy and Safety in Hematopoietic Stem Cell Transplantation in Children: a Meta-Analysis. *BMC Pediatr.* 20 (1), 176. doi:10.1186/s12887-020-02028-6

Frymoyer, A., Schwenk, H. T., Zorn, Y., Bio, L., Moss, J. D., Chasmawala, B., et al. (2020). Model-Informed Precision Dosing of Vancomycin in Hospitalized Children: Implementation and Adoption at an Academic Children's Hospital. *Front. Pharmacol.* 11, 551. doi:10.3389/fphar.2020.00551

Gibbs, J. P., Czerwinski, M., and Slattery, J. T. (1996). Busulfan-glutathione Conjugation Catalyzed by Human Liver Cytosolic Glutathione S-Transferases. *Cancer Res.* 56 (16), 3678–3681.

Gil Candel, M., Gascón Cánovas, J. J., Gómez Espín, R., Nicolás de Prado, I., Rentero Redondo, L., Urbieta Sanz, E., et al. (2020). Usefulness of Population Pharmacokinetics to Optimize the Dosage Regimen of Infliximab in Inflammatory Bowel Disease Patients. *Rev. Esp. Enferm. Dig.* 112 (8), 590–597. doi:10.17235/reed.2020.6857/2020

Grochow, L. B., Jones, R. J., Brundrett, R. B., Braine, H. G., Chen, T. L., Saral, R., et al. (1989). Pharmacokinetics of Busulfan: Correlation with Veno-Occlusive Disease in Patients Undergoing Bone Marrow Transplantation. *Cancer Chemother. Pharmacol.* 25 (1), 55–61. doi:10.1007/BF00694339

Gulbis, A. M., Culotta, K. S., Jones, R. B., and Andersson, B. S. (2011). Busulfan and Metronidazole: an Often Forgotten but Significant Drug Interaction. *Ann. Pharmacother.* 45 (7-8), e39. doi:10.1345/aph.1Q087

Guo, T., van Hest, R. M., Zwep, L. B., Roggeveen, L. F., Fleuren, L. M., Bosman, R. J., et al. (2020). Optimizing Predictive Performance of Bayesian Forecasting for Vancomycin Concentration in Intensive Care Patients. *Pharm. Res.* 37 (9), 171. doi:10.1007/s11095-020-02908-7

Hassan, M., Ljungman, P., Bolme, P., Ringdén, O., Syrůcková, Z., Békàssy, A., et al. (1994). Busulfan Bioavailability. *Blood* 84 (7), 2144–2150. doi:10.1182/blood.v84.7.2144.bloodjournal8472144

Hassan, M., Oberg, G., Ehrsson, H., Ehrnebo, M., Wallin, I., Smedmyr, B., et al. (1989). Pharmacokinetic and Metabolic Studies of High-Dose Busulphan in Adults. *Eur. J. Clin. Pharmacol.* 36 (5), 525–530. doi:10.1007/BF00558081

Hassan, M. (1999). The Role of Busulfan in Bone Marrow Transplantation. *Med. Oncol.* 16 (3), 166–176. doi:10.1007/bf02906128

Hill, B. T., Rybicki, L. A., Urban, T. A., Lucena, M., Jagadeesh, D., Gerds, A. T., et al. (2020). Therapeutic Dose Monitoring of Busulfan Is Associated with Reduced Risk of Relapse in Non-hodgkin Lymphoma Patients Undergoing Autologous Stem Cell Transplantation. *Biol. Blood Marrow Transpl.* 26 (2), 262–271. doi:10.1016/j.bbmt.2019.09.033

Hope, W. W., Vanguilder, M., Donnelly, J. P., Blijlevens, N. M., Brüggemann, R. J., Jelliffe, R. W., et al. (2013). Software for Dosage Individualization of Voriconazole for Immunocompromised Patients. *Antimicrob. Agents Chemother.* 57 (4), 1888–1894. doi:10.1128/aac.02025-12

Huang, J., Li, Z., Liang, W., Chen, B., Hu, J., and Yang, W. (2019). Accurate Prediction of Initial Busulfan Exposure Using a Test Dose with 2- and 6-Hour Blood Sampling in Adult Patients Receiving a Twice-Daily Intravenous Busulfan-Based Conditioning Regimen. *J. Clin. Pharmacol.* 59 (5), 638–645. doi:10.1002/jcph.1354

Huang, J. J., Chen, B., Hu, J., and Yang, W. H. (2017). Limited Sampling Strategy for Predicting Busulfan Exposure in Hematopoietic Stem Cell Transplantation Recipients. *Int. J. Clin. Pharm.* 39 (4), 662–668. doi:10.1007/s11096-017-0481-z

Kanda, Y. (2018). Is Pharmacokinetic Guidance a Must in Busulfan Regimens? *Lancet Haematol.* 5 (11), e498–e499. doi:10.1016/S2352-3026(18)30171-6

Kangarloo, S. B., Naveed, F., Ng, E. S., Chaudhry, M. A., Wu, J., Bahlis, N. J., et al. (2012). Development and Validation of a Test Dose Strategy for Once-Daily i.V. Busulfan: Importance of Fixed Infusion Rate Dosing. *Biol. Blood Marrow Transpl.* 18 (2), 295–301. doi:10.1016/j.bbmt.2011.07.015

Kantasiripitak, W., Van Daele, R., Gijsen, M., Ferrante, M., Spriet, I., and Dreesen, E. (2020). Software Tools for Model-Informed Precision Dosing: How Well Do They Satisfy the Needs? *Front. Pharmacol.* 11, 620. doi:10.3389/fphar.2020.00620

Khalil, M. M. I., Messner, H. A., Lipton, J. H., Kim, D. D., Viswabandya, A., Thyagu, S., et al. (2018). Fludarabine and Busulfan Plus Low-Dose TBI as Reduced Intensity Conditioning in Older Patients Undergoing Allogeneic Hematopoietic Cell Transplant for Myeloid Malignancies. *Ann. Hematol.* 97 (10), 1975–1985. doi:10.1007/s00277-018-3391-9

Lawson, R., Staatz, C. E., Fraser, C. J., and Hennig, S. (2020). Review of the Pharmacokinetics and Pharmacodynamics of Intravenous Busulfan in Paediatric Patients. *Clin. Pharmacokinet.* 60 (1), 17–51. doi:10.1007/s40262-020-00947-2

Long-Boyle, J. R., Savic, R., Yan, S., Bartelink, I., Musick, L., French, D., et al. (2015). Population Pharmacokinetics of Busulfan in Pediatric and Young Adult Patients Undergoing Hematopoietic Cell Transplant: A Model-Based Dosing Algorithm for Personalized Therapy and Implementation Into Routine Clinical Use. *Ther. Drug Monit.* 37 (2), 236–245. doi:10.1097/FTD.0000000000000131

Malär, R., Sjöö, F., Rentsch, K., Hassan, M., and Güngör, T. (2011). Therapeutic Drug Monitoring Is Essential for Intravenous Busulfan Therapy in Pediatric Hematopoietic Stem Cell Recipients. *Pediatr. Transpl.* 15 (6), no. doi:10.1111/j.1399-3046.2011.01529.x

Mao, J. J., Jiao, Z., Yun, H. Y., Zhao, C. Y., Chen, H. C., Qiu, X. Y., et al. (2018). External Evaluation of Population Pharmacokinetic Models for Ciclosporin in Adult Renal Transplant Recipients. *Br. J. Clin. Pharmacol.* 84 (1), 153–171. doi:10.1111/bcp.13431

Marsit, H., Philippe, M., Neely, M., Rushing, T., Bertrand, Y., Ducher, M., et al. (2020). Intra-individual Pharmacokinetic Variability of Intravenous Busulfan in Hematopoietic Stem Cell-Transplanted Children. *Clin. Pharmacokinet.* 59 (8), 1049–1061. doi:10.1007/s40262-020-00877-z

McCune, J. S., Bemer, M. J., Barrett, J. S., Scott Baker, K., Gamis, A. S., and Holford, N. H. (2014). Busulfan in Infant to Adult Hematopoietic Cell Transplant Recipients: A Population Pharmacokinetic Model for Initial and Bayesian Dose Personalization. *Clin. Cancer Res.* 20 (3), 754–763. doi:10.1158/1078-0432.CCR-13-1960

Miyagi, S. J., Brown, I. W., Chock, J. M., and Collier, A. C. (2009). Developmental Changes in Hepatic Antioxidant Capacity Are Age-And Sex-dependent. *J. Pharmacol. Sci.* 111 (4), 440–445. doi:10.1254/jphs.09223sc

Mould, D. R., D'Haens, G., and Upton, R. N. (2016). Clinical Decision Support Tools: The Evolution of a Revolution. *Clin. Pharmacol. Ther.* 99 (4), 405–418. doi:10.1002/cpt.334

Nguyen, L., Fuller, D., Lennon, S., Leger, F., and Puozzo, C. (2004). I.V. Busulfan in Pediatrics: a Novel Dosing to Improve Safety/efficacy for Hematopoietic Progenitor Cell Transplantation Recipients. *Bone Marrow Transpl.* 33 (10), 979–987. doi:10.1038/sj.bmt.1704446

Nguyen, L., Leger, F., Lennon, S., and Puozzo, C. (2006). Intravenous Busulfan in Adults Prior to Haematopoietic Stem Cell Transplantation: a Population Pharmacokinetic Study. *Cancer Chemother. Pharmacol.* 57 (2), 191–198. doi:10.1007/s00280-005-0029-0

Paci, A., Veal, G., Bardin, C., Levêque, D., Widmer, N., Beijnen, J., et al. (2014). Review of Therapeutic Drug Monitoring of Anticancer Drugs Part 1--cytotoxics. *Eur. J. Cancer* 50 (12), 2010–2019. doi:10.1016/j.ejca.2014.04.014

Palmer, J., McCune, J. S., Perales, M. A., Marks, D., Bubalo, J., Mohty, M., et al. (2016). Personalizing Busulfan-Based Conditioning: Considerations from the American Society for Blood and Marrow Transplantation Practice Guidelines Committee. *Biol. Blood Marrow Transpl.* 22 (11), 1915–1925. doi:10.1016/j.bbmt.2016.07.013

Philippe, M., Goutelle, S., Guitton, J., Fonrose, X., Bergeron, C., Girard, P., et al. (2016). Should Busulfan Therapeutic Range Be Narrowed in Pediatrics? Experience from a Large Cohort of Hematopoietic Stem Cell Transplant Children. *Bone Marrow Transpl.* 51 (1), 72–78. doi:10.1038/bmt.2015.218

Ramos-Martín, V., Neely, M. N., Padmore, K., Peak, M., Beresford, M. W., Turner, M. A., et al. (2017). Tools for the Individualized Therapy of Teicoplanin for Neonates and Children. *Antimicrob. Agents Chemother.* 61 (10). doi:10.1128/AAC.00707-17

Russell, J. A., Tran, H. T., Quinlan, D., Chaudhry, A., Duggan, P., Brown, C., et al. (2002). Once-daily Intravenous Busulfan Given with Fludarabine as Conditioning for Allogeneic Stem Cell Transplantation: Study of Pharmacokinetics and Early Clinical Outcomes. *Biol. Blood Marrow Transpl.* 8 (9), 468–476. doi:10.1053/bbmt.2002.v8.pm12374451

Salinger, D. H., Vicini, P., Blough, D. K., O'Donnell, P. V., Pawlikowski, M. A., and McCune, J. S. (2010). Development of a Population Pharmacokinetics-Based Sampling Schedule to Target Daily Intravenous Busulfan for Outpatient Clinic Administration. *J. Clin. Pharmacol.* 50 (11), 1292–1300. doi:10.1177/0091270009357430

Scian, M., and Atkins, W. M. (2015). Supporting Data for Characterization of the Busulfan Metabolite EdAG and the Glutaredoxins that it Adducts. *Data Brief.* 5, 161–170. doi:10.1016/j.dib.2015.09.002

Shukla, P., Goswami, S., Keizer, R. J., Winger, B. A., Kharbanda, S., Dvorak, C. C., et al. (2020). Assessment of a Model-Informed Precision Dosing Platform Use in Routine Clinical Care for Personalized Busulfan Therapy in the Pediatric Hematopoietic Cell Transplantation (HCT) Population. *Front. Pharmacol.* 11, 888. doi:10.3389/fphar.2020.00888

Su, H., Zhang, S., Sun, Z., Tang, L., Fang, Y., Liu, H., et al. (2016). Population Pharmacokinetics of Intravenous Infusing Busulfan in Patients Undergoing Hematopoietic Stem Cell Transplantation. *Chin. Pharm. J.* 51 (21), 1860–1865. doi:10.11669/cpj.2016.21.007

Sun, Y., Huang, J., Hao, C., Li, Z., Liang, W., Zhang, W., et al. (2020). Population Pharmacokinetic Analysis of Intravenous Busulfan: GSTA1 Genotype Is Not a Predictive Factor of Initial Dose in Chinese Adult Patients Undergoing Hematopoietic Stem Cell Transplantation. *Cancer Chemother. Pharmacol.* 85 (2), 293–308. doi:10.1007/s00280-019-04001-2

Sweiss, K., Patel, P., and Rondelli, D. (2012). Deferasirox Increases BU Blood Concentrations. *Bone Marrow Transpl.* 47 (2), 315–316. doi:10.1038/bmt.2011.75

Takachi, T., Arakawa, Y., Nakamura, H., Watanabe, T., Aoki, Y., Ohshima, J., et al. (2019). Personalized Pharmacokinetic Targeting with Busulfan in Allogeneic Hematopoietic Stem Cell Transplantation in Infants with Acute Lymphoblastic Leukemia. *Int. J. Hematol.* 110 (3), 355–363. doi:10.1007/s12185-019-02684-0

Takama, H., Tanaka, H., Nakashima, D., Ueda, R., and Takaue, Y. (2006). Population Pharmacokinetics of Intravenous Busulfan in Patients Undergoing Hematopoietic Stem Cell Transplantation. *Bone Marrow Transpl.* 37 (4), 345–351. doi:10.1038/sj.bmt.1705252

Teitelbaum, Z., Nassar, L., Scherb, I., Fink, D., Ring, G., Lurie, Y., et al. (2020). Limited Sampling Strategies Supporting Individualized Dose Adjustment of Intravenous Busulfan in Children and Young Adults. *Ther. Drug Monit.* 42 (3), 427–434. doi:10.1097/FTD.0000000000000700

Tesfaye, H., Branova, R., Klapkova, E., Prusa, R., Janeckova, D., Riha, P., et al. (2014). The Importance of Therapeutic Drug Monitoring (TDM) for Parenteral Busulfan Dosing in Conditioning Regimen for Hematopoietic Stem Cell Transplantation (HSCT) in Children. *Ann. Transpl.* 19, 214–224. doi:10.12659/AOT.889933

Thomson, A. H., and Whiting, B. (1992). Bayesian Parameter Estimation and Population Pharmacokinetics. *Clin. Pharmacokinet.* 22 (6), 447–467. doi:10.2165/00003088-199222060-00004

Trame, M. N., Bergstrand, M., Karlsson, M. O., Boos, J., and Hempel, G. (2011). Population Pharmacokinetics of Busulfan in Children: Increased Evidence for Body Surface Area and Allometric Body Weight Dosing of Busulfan in Children. *Clin. Cancer Res.* 17 (21), 6867–6877. doi:10.1158/1078-0432.CCR-11-0074

Veal, G. J., Nguyen, L., Paci, A., Riggi, M., Amiel, M., Valteau-Couanet, D., et al. (2012). Busulfan Pharmacokinetics Following Intravenous and Oral Dosing Regimens in Children Receiving High-Dose Myeloablative Chemotherapy for High-Risk Neuroblastoma as Part of the HR-NBL-1/SIOPEN Trial. *Eur. J. Cancer* 48 (16), 3063–3072. doi:10.1016/j.ejca.2012.05.020

Wang, Y., Kato, K., Le Gallo, C., Armstrong, E., Rock, E., and Wang, X. (2015). Dosing Algorithm Revisit for Busulfan Following IV Infusion. *Cancer Chemother. Pharmacol.* 75 (3), 505–512. doi:10.1007/s00280-014-2660-0

Wu, X., Xie, H., Lin, W., Yang, T., Li, N., Lin, S., et al. (2017). Population Pharmacokinetics Analysis of Intravenous Busulfan in Chinese Patients Undergoing Hematopoietic Stem Cell Transplantation. *Clin. Exp. Pharmacol. Physiol.* 44 (5), 529–538. doi:10.1111/1440-1681.12735

Yeh, R. F., Pawlikowski, M. A., Blough, D. K., McDonald, G. B., O'Donnell, P. V., Rezvani, A., et al. (2012). Accurate Targeting of Daily Intravenous Busulfan with 8-hour Blood Sampling in Hospitalized Adult Hematopoietic Cell Transplant Recipients. *Biol. Blood Marrow Transpl.* 18 (2), 265–272. doi:10.1016/j.bbmt.2011.06.013

Yin, J., Xiao, Y., Zheng, H., and Zhang, Y. C. (2015). Once-daily i.V. BU-Based Conditioning Regimen before Allogeneic Hematopoietic SCT: a Study of Influence of GST Gene Polymorphisms on BU Pharmacokinetics and Clinical Outcomes in Chinese Patients. *Bone Marrow Transpl.* 50 (5), 696–705. doi:10.1038/bmt.2015.14

Zhang, H. X., Sheng, C. C., Liu, L. S., Luo, B., Fu, Q., Zhao, Q., et al. (2019). Systematic External Evaluation of Published Population Pharmacokinetic Models of Mycophenolate Mofetil in Adult Kidney Transplant Recipients Co-administered with Tacrolimus. *Br. J. Clin. Pharmacol.* 85 (4), 746–761. doi:10.1111/bcp.13850

Zhao, C. Y., Jiao, Z., Mao, J. J., and Qiu, X. Y. (2016). External Evaluation of Published Population Pharmacokinetic Models of Tacrolimus in Adult Renal Transplant Recipients. *Br. J. Clin. Pharmacol.* 81 (5), 891–907. doi:10.1111/bcp.12830

Zwaveling, J., Press, R. R., Bredius, R. G., van Derstraaten, T. R., den Hartigh, J., Bartelink, I. H., et al. (2008). Glutathione S-Transferase Polymorphisms Are Not Associated with Population Pharmacokinetic Parameters of Busulfan in Pediatric Patients. *Ther. Drug Monit.* 30 (4), 504–510. doi:10.1097/FTD.0b013e3181817428

Conflict of Interest: The authors declare that the research was conducted in the absence of any commercial or financial relationships that could be construed as a potential conflict of interest.

Publisher's Note: All claims expressed in this article are solely those of the authors and do not necessarily represent those of their affiliated organizations, or those of the publisher, the editors and the reviewers. Any product that may be evaluated in this article, or claim that may be made by its manufacturer, is not guaranteed or endorsed by the publisher.

Advantages of publishing in Frontiers

OPEN ACCESS
Articles are free to read for greatest visibility and readership

FAST PUBLICATION
Around 90 days from submission to decision

HIGH QUALITY PEER-REVIEW
Rigorous, collaborative, and constructive peer-review

TRANSPARENT PEER-REVIEW
Editors and reviewers acknowledged by name on published articles

Frontiers
Avenue du Tribunal-Fédéral 34
1005 Lausanne | Switzerland

Visit us: www.frontiersin.org
Contact us: frontiersin.org/about/contact

REPRODUCIBILITY OF RESEARCH
Support open data and methods to enhance research reproducibility

DIGITAL PUBLISHING
Articles designed for optimal readership across devices

FOLLOW US
@frontiersin

IMPACT METRICS
Advanced article metrics track visibility across digital media

EXTENSIVE PROMOTION
Marketing and promotion of impactful research

LOOP RESEARCH NETWORK
Our network increases your article's readership